

Particle Kinematics

E. Byckling

University of Jyväskylä, Finland

K. Kajantie

University of Helsinki, Finland

A Wiley-Interscience Publication

JOHN WILEY & SONS

London · New York · Sydney · Toronto

Preface

The purpose of this book is to give a systematic account of relativistic kinematics of particle reactions, with the emphasis on the practical needs of workers in the field of high energy physics.

The complexity of observed particle reactions has grown rapidly in recent years as the energy of particle accelerators has increased. Because of this a thorough knowledge of relativistic kinematics has become a necessary prerequisite for the understanding of essential dynamical features. Such a knowledge can not only help the physicist to avoid tedious calculations, but can often save him from incorrect interpretations of experimental effects; an appreciation of the simple and attractive structure of relativistic kinematics can lead both to practical and to conceptual simplifications. Recent developments in particle physics have produced a spate of papers on ways of choosing variables and plotting data in many-particle reactions, kinematical reflections, effects of peripherality, longitudinal phase space, kinematics of inclusive reactions, numerical methods (Monte Carlo techniques, in particular), etc. At present these are scattered through various scientific journals, and there is a growing need for a detailed and coherent treatment of kinematics related to these and other problems.

As prerequisites, this book assumes familiarity with the basic notions of elementary particle physics and special relativity. We hope that it will be useful for self-study and reference purposes and also as a text for a course in particle kinematics at the advanced undergraduate or graduate level.

To keep this book to a reasonable size we have been forced to limit the discussion to spinless particles. Problems connected with polarization and also questions related to the spin determination of systems of particles are not treated. The kinematics of spinless particles covered here constitutes an attractive, selfcontained whole and this book can be supplemented by other texts devoted to the theory and methodology of spin.

The authors are indebted to the Finnish National Research Council for financial support, to the Research Institute for Theoretical Physics at the University of Helsinki for the use of its facilities, and to Drs. Per Nyborg and M. L. Whippman for a critical reading of the manuscript.

Helsinki
April 27, 1972

E. BYCKLING
K. KAJANTIE

Contents

Preface	v
I Introduction	1
II Special Relativity	4
1. Lorentz transformations, four-vectors, rapidity and pseudospherical coordinates	4
2. Four-velocity and four-momentum	13
3. Units and conventions	17
4. Reference frames for collision processes	19
5. Lorentz transformations between centre-of-momentum, target and colliding beam systems	20
6. Energies and momenta in terms of the invariants	23
*7. Momenta and angles in terms of invariants	27
*8. Detailed treatment of the Lorentz transformation of a four-momentum vector	36
III Phase Space	47
1. Definition of phase space	47
2. Integration over phase space and cross-sections	49
3. The phase space integral	54
*4. Lorentz transformations of one-particle distributions	57
IV Two-Particle Final States	63
1. Two-particle phase space	63
*2. Distribution in opening angle	68
3. Two-particle scattering: relations between the CMS and TS	71
4. Invariant variables for $2 \rightarrow 2$ scattering	76
5. The physical region in s, t, u	82
6. Value of t in the forward direction	96
V Three-Particle Final States	102
1. Decay of one particle into three particles	102
2. Dalitz plot	106
3. Momentum configuration on the Dalitz plot	112
4. Scattering of two particles into three particles	115

5. Description in two invariants and two angles, Chew-Low plot	118
6. Jackson, Treiman-Yang, helicity and related angles	125
*7. Description in three invariants and one angle	128
*8. Azimuthal angles in invariant variables	134
*9. Description in four invariants	136
*10. Cyclic symmetry, the Toller angle	144
*11. Applications	149
VI Multiparticle Production	158
1. Introduction	158
2. Timelike recursion relations	159
**3. Spacelike recursion relations, Toller variables	167
4. Phase-space distributions	180
5. Transverse-cut phase space	188
6. Longitudinal phase space	192
**7. Physical region in invariant variables	202
**8. Phase space density in invariant variables	211
VII Inclusive Reactions	218
1. One-particle distributions	218
2. The sets (P, θ) and (q, r)	221
3. The sets (t, s_X) and (t, v)	227
4. The set (ζ, r)	233
5. Kinematics of scaling and fragmentation	238
6. Missing mass techniques	243
7. Higher order distributions, correlations	246
VIII Kinematical Reflections	251
1. General description	251
2. Effects of cuts in transverse momentum and invariant momentum transfer	252
3. Effects of resonances	257
IX Numerical Methods of Phase Space Integration	260
1. Introduction	260
2. Direct numerical integration	262
3. Principles of Monte Carlo integration	264
4. Reduction of the statistical error	269
5. Application of the Monte Carlo method to particle physics	273
**6. Statistical methods	281
Appendices	288
*A. Gram determinants	288
B. Spherical trigonometry	296

Contents	ix
Solutions to Exercises	299
References	306
List of Symbols	311
Index	315

I

Introduction

In this book particle kinematics is defined as the study of those aspects of elementary particle reactions which are understood in terms of special relativity. The theory of special relativity (see, for instance, Rindler, 1960) is one of the best established physical theories, and thus kinematics has a well defined structure with ample experimental support. In contrast, the dynamical properties of particle reactions are still largely unknown and, in fact, the purpose of most research in particle physics is to clarify these basic properties. Experimental results and dynamical laws are always expressed in terms of kinematic variables and are subject to kinematic constraints, so that a thorough understanding of particle kinematics is indispensable for the correct interpretation of the dynamics of particle reactions.

From the point of view of the material of this book, particles are completely characterized by their energy and momentum. These combine to give the four-momentum which transforms as a four-vector under Lorentz transformations. A basic property of four-momentum is that it is conserved: the sum of all four-momenta in the initial state is equal to the sum in the final state. These very simple facts are the foundation of particle kinematics. In spite of this concise and well-established theoretical basis, kinematical considerations may be extremely complicated if the number of particles involved is large.

One source of complexity is the fact that the components of the four-momenta of the particles are usually not the most suitable variables for the description of reactions, and dynamical effects show up most clearly in other variables. For example, one observes resonance peaks in invariant masses and peripherality in momentum transfers, etc. Furthermore, relativity implies that the description of a process must be Lorentz invariant, and thus invariant variables are often most appropriate. Still further sets of variables are introduced because measurements are done in a definite Lorentz frame but their interpretation may be more natural in some other frames.

In addition to energy and momentum, one-particle states are characterized by further quantum numbers like spin, parity, isospin, charge, baryon or lepton number, strangeness, etc. These quantum numbers are neglected in our treatment of particle kinematics. Among these quantities spin has a special role since it is connected (Halpern, 1968) with the properties of the

inhomogeneous Lorentz group (see below) and could be considered as part of our subject matter. In fact, we have neglected spin mainly to keep the text to a manageable length and to avoid introducing mathematical machinery more complicated and of quite different nature than that used in this book. We also do not consider the very important practical problems related to the angular momentum properties of systems of particles (Zemach, 1965; Werle, 1966; Koch, 1968).

To clarify the significance of the neglect of spin, we note for those familiar with group theory that mathematically spin arises (Halpern, 1968) when one considers the unitary representations of the Poincaré group, i.e. of the inhomogeneous Lorentz group (including translations). These representations are characterized by a definite mass and spin, the states within a representation are indexed by the momentum and the third component of spin. The transformation properties of the states are well defined but turn out to be rather complicated unless the spin is zero. By neglecting spin, we limit ourselves to representations corresponding to spin zero. Similarly, neglecting the angular momentum of systems of n particles involves working with reducible representations of the Poincaré group, and the spin analysis of this state is equivalent to separating the representation into irreducible components (Wick, 1962; Werle, 1966).

The only books on particle kinematics at present are those by Baldin, Goldanskii and Rozental (Baldin, 1961), Hagedorn (Hagedorn, 1964) and Kopylov (Kopylov, 1970). Kopylov's book deals mainly with the kinematics of resonances, and, incidentally, is a good source of references to many papers existing only in Russian, which are not included in our list of references. In addition to these texts, lectures on particle kinematics have been given at several physics schools (see, for instance, Czyzewski, 1968; Nyborg, 1967, 1969C, 1970C; Skjeggestad, 1964; Werbrouck, 1968).

The plan of this book is as follows. In Chapter II we review a number of the concepts and equations of special relativity which form the basis for the subsequent discussion. In particular, we define various Lorentz frames and study in detail the Lorentz transformations of physical quantities from one frame to another. In Section II.7 and in Appendix A we show that the most natural way to express the relation between invariant and non-invariant quantities is by use of Gram determinants, and this result will be applied throughout the book.

The four-momenta of a decay (or scattering process) are constrained by energy-momentum conservation $p_0 (= p_a + p_b) = p_1 + \dots + p_n$. For fixed initial state four-momentum this determines a finite $3n - 4$ dimensional region, the phase space, in the space of the final state momentum components. Points of phase space correspond to observed events of the reaction. In Chapter III we introduce the main problems of particle kinematics: parametrization of the phase space by different sets of variables, motivated by

experiment or theory, the relations between these sets, and the calculation of total or differential cross-sections which are integrals over phase space.

In Chapters IV–VI the general ideas are then applied in turn to the processes $1 \rightarrow 2$, $2 \rightarrow 2$, $1 \rightarrow 3$, $2 \rightarrow 3$, etc., where the notation refers to the number of particles in the initial or final states. This is a sequence of increasing complexity in which successive elements are closely related to each other (Section III.1). In Chapter VII we discuss inclusive experiments, in which the final state is only partly identified. Chapter VIII contains a brief characterization of kinematic reflections. Sometimes in a multiply integrated differential cross-section a conspicuous feature may not be a dynamical effect in the observed variable at all but a kinematic reflection from another dynamical feature. Finally, numerical methods of phase-space integration are reviewed in Chapter IX, with particular emphasis on Monte Carlo techniques. Most chapters contain a set of exercises, the solutions of which are collected at the end of the book. A number of the exercises and solutions contain supplementary material which was not included in the text.

The different sections vary considerably in difficulty. The following sections contain the material for a basic course in kinematics both for experimentalists and theorists: II.1–6, III.1–3, IV.1, 3–6, V.1–6, VI.1–2, 4–6, VII.1–7, VIII.1–3, IX.1–5, Appendix B. On the next higher level, it is very useful to have an understanding of the properties and use of Gram determinants (considered and applied in Sections II.7, V.7–11, Appendix A) and of momentum space ellipsoids (Sections II.8, III.4). The sections at this level are denoted in the table of contents by one star. Note also that parts of some sections listed for the basic course make use of the one-star material and these subsections can be omitted in a shorter basic course. The most difficult parts of the text (denoted by two stars) are Sections VI.3, on Toller variables, VI.7–8, on invariant variables, and IX.6, on statistical methods.

As to conventions we note that chapters are referred to by a Roman numeral, sections by a combination of a Roman and Arabic numeral (chapter, section) and equations or figures by a combination of a Roman and two Arabic numerals (chapter, section, equation). However, when referring to a section, equation or figure within a given chapter, the Roman numeral corresponding to this chapter is omitted. References to a publication contain the name of the first author and the year of publication. All notational conventions are collected in a list of symbols at the end of the book.

II

Special Relativity

1. Lorentz transformations, four-vectors, rapidity and pseudospherical coordinates

A general and systematic treatment of the principles of special relativity can be found in many text-books (see, for example, Rindler, 1960). In this section we review a few special topics which will be needed later: (a) Lorentz transformations, (b) four vectors, (c) rapidity, (d) spherical and pseudo-spherical coordinates.

(a) Lorentz transformations

Consider a point in space-time defined by its coordinates t, x, y, z in a given frame S . According to the theory of special relativity the relationship between the coordinates of the point in S and its coordinates t', x', y', z' in a second inertial frame S' is given by a *Lorentz transformation*. Assume that S' moves with a constant velocity v in S . To obtain a simple expression for the transformation, one chooses the z axis of S and the z' axis of S' along the relative velocity v and the corresponding coordinate planes parallel (Figure 1.1). If

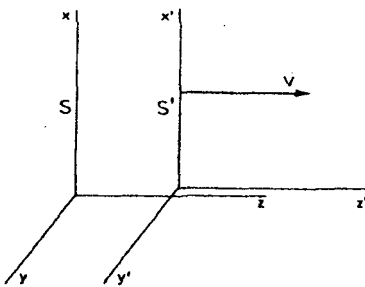


Figure II.1.1

one further assumes that the origins of the coordinate systems coincide at $t = t' = 0$, the Lorentz transformation and its inverse are given by

$$\begin{aligned}
 x' &= x & x &= x' \\
 y' &= y & y &= y' \\
 z' &= \gamma(z - vt) & z &= \gamma(z' + vt') \\
 t' &= \gamma(t - vz/c^2) & t &= \gamma(t' + vz'/c^2)
 \end{aligned} \tag{1.1}$$

where

$$\gamma = \gamma(v) = (1 - v^2/c^2)^{-\frac{1}{2}} \tag{1.2}$$

is the *Lorentz factor*. The components x and y , perpendicular to the velocity v , remain unchanged. The inverse of a transform is obtained simply by changing the sign of v .

When v approaches zero, the velocity of light, c , disappears from equations (1.1) and they approach the nonrelativistic Galilean transformation. On the macroscopic scale only some astronomical phenomena involve velocities so large that equations (1.1) need be applied. The velocities in particle physics are mostly so close to c that deviations from the Galilean transformation are large. In fact, particle physics offers numerous opportunities to verify the validity of equations (1.1).

If the relative velocity v of the frames S' and S is not parallel to the z and z' axes, equations (1.1) will be modified. However, since the standard expressions for these modified transformation equations will not be needed here, we leave their derivation (see, for example, Hagedorn, 1964) to an exercise (Exercise II.2).

(b) Four-vectors

Equations (1.1) form a special class of Lorentz transformations. The most general Lorentz transformation equations have the simplest form, both technically and conceptually, in the four-dimensional space of vectors $\mathbf{x} = (x^0, x^1, x^2, x^3) = (x^0, \mathbf{x}) = (ct, \mathbf{x}, y, z)$. In general, a *four-vector* $a = (a^0, \mathbf{a})$ is an object which transforms like \mathbf{x} . (When indexing spatial components we use interchangeably a^1 or a_x , a^2 or a_y , a^3 or a_z .) Thus under a Lorentz transformation between frames in the configuration of Figure 1.1 the four-vector a transforms as follows:

$$\begin{aligned}
 a'^0 &= \gamma(a^0 - va^3/c) \\
 a'^1 &= a^1 \\
 a'^2 &= a^2 \\
 a'^3 &= \gamma(a^3 - va^0/c).
 \end{aligned} \tag{1.3}$$

$$x = (ct, x_1, x_2, x_3) = (ct, x, y, z)$$

6 $x_\mu = (ct, -x_1, -x_2, -x_3) = (ct, -x, -y, -z)$ 11. Special Relativity

To define a general Lorentz transformation,

$$a' = La, \quad (1.4)$$

$$a'^\mu = \sum_0^3 L_\nu^\mu a^\nu,$$

where L is a real matrix, we introduce the *metric tensor*

$$\begin{aligned} g &= (g_{\mu\nu}) \\ &= (g^{\mu\nu}) \\ &= \begin{bmatrix} 1 & 0 & 0 & 0 \\ 0 & -1 & 0 & 0 \\ 0 & 0 & -1 & 0 \\ 0 & 0 & 0 & -1 \end{bmatrix} \quad (1.5) \\ &= g^{-1} \end{aligned}$$

and the *scalar product* $a \cdot b$ of two four-vectors a and b :

$$\begin{aligned} a \cdot b &= \sum_\mu a_\mu b^\mu \\ &= \sum_{\mu, \nu} g_{\mu\nu} a^\mu b^\nu \\ &= a^0 b^0 - \mathbf{ab} \quad (1.6) \end{aligned}$$

A general Lorentz transformation is then defined as a linear transformation leaving the scalar product $x \cdot y$ *invariant*. This implies that the matrix L in equation (1.4) has to satisfy

$$gL^{-1}g = L^T. \quad (1.7)$$

Thus the inverse of L is obtained by transposing L and changing the sign of the components $L_{i0}, L_{0i}, i = 1, 2, 3$. A general Lorentz transformation can be expressed as a *boost* (1.3) (see comments after equation (1.22)) followed by a three-dimensional rotation.

In particle kinematics the transformations (1.4) are mostly *proper orthochronous* Lorentz transformations. In addition to preserving the scalar product (1.6), these satisfy the following two conditions:

$\det L = +1$, i.e. spatial reflections are excluded

$L_0^0 \geq 1$, the sign of the 0 component of a time-like vector is invariant.

(c) Rapidity

The Lorentz transformations form a group, that is, the product of two Lorentz transformations is again a Lorentz transformation. If one performs consecutively two Lorentz transformations of the special type (1.3) with

parameters v_1 and v_2 the combined result is seen to be equivalent to a single transformation with parameters

$$\begin{aligned} v_3 &= (v_1 + v_2)/(1 + v_1 v_2/c^2), \\ \gamma_3 &= \gamma_1 \gamma_2 (1 + v_1 v_2/c^2). \end{aligned} \quad (1.8)$$

To see this more clearly, replace v by a new parameter ξ called *rapidity* through the equations

$$v/c = \tanh \xi, \quad \gamma = \cosh \xi, \quad \gamma v/c = \sinh \xi, \quad (1.9)$$

which map the velocity range $-1 \leq v/c \leq 1$ into the rapidity range $-\infty < \xi < \infty$. Equation (1.8) then implies that the rapidities satisfy

$$\begin{aligned} v_3 &= c \tanh \xi_3 = \frac{c(\tanh \xi_1 + \tanh \xi_2)}{(1 + \tanh \xi_1 \tanh \xi_2)} \\ &= c \tanh (\xi_1 + \xi_2), \end{aligned} \quad (1.10)$$

or that $\xi_3 = \xi_1 + \xi_2$. Thus one sees that *rapidities are additive under parallel Lorentz transformations*. In more detail, if v is replaced by ξ in equation (1.3), one obtains for the inverted equations

$$\begin{aligned} a^0 &= a'^0 \cosh \xi + a'^3 \sinh \xi \\ a^3 &= a'^0 \sinh \xi + a'^3 \cosh \xi \end{aligned} \quad (1.11)$$

The transformation (1.11) clearly leaves the hyperbolas $(a^0)^2 - (a^3)^2 =$ constant (Figure 1.2) invariant. Apart from the minus sign in this invariant

$$\begin{aligned} x^\mu x_\mu &= x'^\mu x'_\mu \\ x^\mu x_\mu &= \Lambda^\mu_\nu x^\nu \Lambda_\mu^\alpha x^\alpha \\ g_{\mu\nu} x^\mu x^\nu &= \Lambda^\beta_\mu g_{\beta\nu} \Lambda^\alpha_\nu x^\mu x^\nu \end{aligned}$$

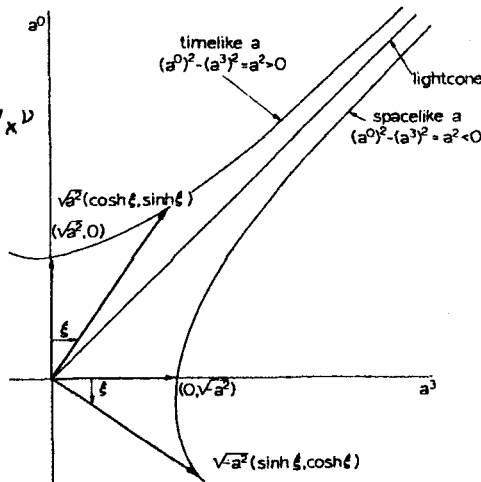


Figure 1.1.2 The rapidity $\xi = \tanh(v/c)$ parametrizes all vectors a which are obtainable from the standard vectors $(\sqrt{(a^2)}, 0)$ and $(0, \sqrt{(-a^2)})$

form the situation is analogous to a rotation in a two-dimensional Euclidean plane. The rapidity ξ thus corresponds to the rotation angle, and one sometimes refers to equations (1.11) as an imaginary rotation because of the relations $\cos i\xi = \cosh \xi$ and $\sin i\xi = i \sinh \xi$. The analogy with rotations also clarifies the additivity property of rapidities. If the Lorentz transformations involved are not parallel, both equations (1.8) and (1.10) have to be replaced by more complicated formulas (see, for example, Rindler, 1960, p. 39; Werle, 1966, pp. 342–348). We do not give them here; they are implicitly contained in equations (1.26–27) below.

(d) Spherical and pseudospherical coordinates

For later use we shall now investigate various parametrizations of four-vectors. These considerations are not indispensable for the understanding of the main parts of the book and may be omitted at first reading.

A four-vector a belongs to one of the following four classes

timelike,	$a^2 > 0$	(1.12)
lightlike,	$a^2 = 0$	
spacelike,	$a^2 < 0$	
zero,	$a = 0$.	

For simplicity, we shall assume that the 0-component of a timelike or lightlike vector is positive. By a suitable Lorentz transformation the four-vector a can then be transformed to one of the *standard forms*

$$\begin{aligned} a &= (+\sqrt{(a^2)}, 0, 0, 0) && a \text{ timelike} \\ a &= (1, 0, 0, 1) && a \text{ lightlike} \\ a &= (0, 0, 0, \sqrt{(-a^2)}) && a \text{ spacelike.} \end{aligned} \quad (1.13)$$

if a is timelike, the frame in which equation (1.13) is valid is called the rest frame $R(a)$ of a , if a is spacelike, we shall refer to this frame as the standard frame $S(a)$ of a .

An arbitrary four-vector will now be parametrized by the parameters of the Lorentz transformation which relates it to the appropriate standard form (1.13). The situation is analogous to the use of three-dimensional spherical coordinates (Appendix B and Figure 1.3), in terms of which we write

$$a = A(\sin \theta \cos \phi, \sin \theta \sin \phi, \cos \theta), \quad (1.14)$$

where $A = |a|$. In this case the parametrization is generated by applying to the standard vector

$$a = (0, 0, A) \quad (1.15)$$

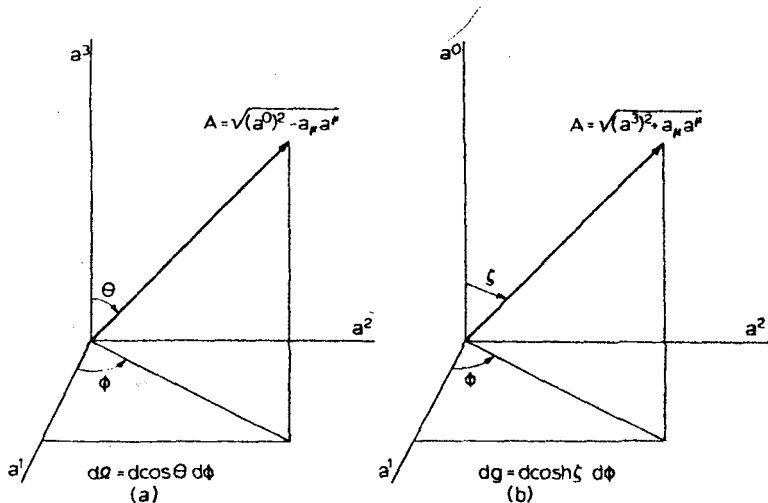


Figure II.1.3 Spherical and pseudospherical coordinates in spaces with invariant forms $A^2 = a_1^2 + a_2^2 + a_3^2$ (a) and $A^2 = a_0^2 - a_1^2 - a_2^2$ (b). The parameters $\Omega = (\cos \theta, \phi)$ and $g = (\cosh \zeta, \phi)$ parametrize Lorentz transformations leaving a_0 and a_3 invariant, respectively. There is no difference between spacelike and timelike a

the two consecutive rotations (Figure 1.3(a))

$$R_z(\phi)R_y(\theta) = \begin{bmatrix} \cos \phi & -\sin \phi & 0 \\ \sin \phi & \cos \phi & 0 \\ 0 & 0 & 1 \end{bmatrix} \begin{bmatrix} \cos \theta & 0 & \sin \theta \\ 0 & 1 & 0 \\ -\sin \theta & 0 & \cos \theta \end{bmatrix}, \quad (1.16)$$

in an obvious notation. Note that the rotations (1.16) are to be interpreted in an *active sense*: for instance, $R_y(\theta)$ turns a vector about the y axis through the angle θ , but the coordinate axes through the angle $-\theta$.

In four-dimensional Lorentz space we shall introduce the analogous **pseudospherical coordinates**. These can be defined in several ways, of which the following parametrizations in terms of the two sets (ξ, θ, ϕ) and (ξ, ζ, ϕ) will be of use later. If a is timelike, we write

$$a = \sqrt{(a^2)}(\cosh \xi, \sinh \xi \sin \theta \cos \phi, \sinh \xi \sin \theta \sin \phi, \sinh \xi \cos \theta) \quad (1.17)$$

or

$$a = \sqrt{(a^2)}(\cosh \xi \cosh \zeta, \cosh \xi \sinh \zeta \cos \phi, \cosh \xi \sinh \zeta \sin \phi, \sinh \xi). \quad (1.18)$$

If a is spacelike, we write instead

$$a = \sqrt{(-a^2)}(\sinh \xi, \cosh \xi \sin \theta \cos \phi, \cosh \xi \sin \theta \sin \phi, \cosh \xi \cos \theta) \quad (1.19)$$

or

$$a = \sqrt{(-a^2)}(\sinh \xi \cosh \zeta, \sinh \xi \sinh \zeta \cos \phi, \sinh \xi \sinh \zeta \sin \phi, \cosh \xi). \quad (1.20)$$

The natural ranges of the angular variables are $0 \leq \theta \leq \pi$, $0 \leq \phi < 2\pi$. To obtain each four-vector a only once, the ranges of the other variables must then be $-\infty < \xi < \infty$, $0 \leq \zeta < \infty$, except that in (1.17) one has $0 \leq \xi < \infty$. All the forms (1.17)–(1.20) clearly satisfy $a_\mu a^\mu = (a^0)^2 - a^2 = a^2$.

Note that the choice of the standard form $(0, 0, 0, \sqrt{(-a^2)})$ implies in equation (1.20) that the direction of the z axis is fixed by a . Thus when $\xi \rightarrow 0$ ($a^0 \rightarrow 0$) in equation (1.20), the vector a becomes parallel to the z axis. A vector of the form, say, $(0, 0, \sqrt{(-a^2)}, 0)$ cannot be obtained with any values of ξ, ζ, ϕ . The parametrization (1.20) will be used only in Section VI.3, and it is sufficiently general for the purpose stated there.

In order to motivate equations (1.17)–(1.20) we shall establish the Lorentz transformations which lead from the standard forms (1.13) to the general forms (1.17)–(1.20). In this way we give an operational definition of the sets (ξ, θ, ϕ) or (ξ, ζ, ϕ) . Consider first the parameter ξ , which is just the rapidity in equation (1.9). To analyze it, assume either $\theta = 0$ or $\zeta = 0$, the value of ϕ being irrelevant. Then

$$\begin{aligned} a &= \sqrt{(a^2)}(\cosh \xi, 0, 0, \sinh \xi), & a^2 > 0, \\ &= \sqrt{(-a^2)}(\sinh \xi, 0, 0, \cosh \xi), & a^2 < 0. \end{aligned} \quad (1.21)$$

It is immediately obvious that these forms are obtained from the standard forms (1.13) by the Lorentz transformation (1.11). In explicit matrix form this transformation is

$$L_z(\xi) = \begin{bmatrix} \cosh \xi & 0 & 0 & \sinh \xi \\ 0 & 1 & 0 & 0 \\ 0 & 0 & 1 & 0 \\ \sinh \xi & 0 & 0 & \cosh \xi \end{bmatrix}. \quad (1.22)$$

For instance, if $L_z(\xi)$ is applied to the timelike vector $\sqrt{(a^2)}(1, 0, 0, 0)$ one obtains the vector $\sqrt{(a^2)}(\cosh \xi, 0, 0, \sinh \xi)$, i.e. $L_z(\xi)$ gives to the rest frame form of a , $a = 0$, a nonzero value a directed along z axis. Because of this the transformation (1.22) or (1.11) is called a *boost along z axis with parameter ξ* . Note that as in equation (1.16) $L_z(\xi)$ is to be interpreted in an active sense: when applied on a rest frame vector, $\xi > 0$ gives this vector a positive z

component but gives the new frame a velocity directed along the negative z axis.

The role of the remaining pairs of variables (θ, ϕ) in equations (1.17) and (1.19) and (ζ, ϕ) in equations (1.18) and (1.20) is now clear. Consider first θ and ϕ which are the standard spherical coordinates in three-dimensional Euclidean space. The forms (1.17) and (1.19) are clearly obtained from equation (1.21) by first rotating about the y axis through an angle θ and then about the new z axis through an angle ϕ (Figure 1.3(a) and equation (1.16)). These transformations are elements of the group $O(3)$ of three-dimensional Euclidian rotations and they leave the 0 component a^0 of a four-vector invariant. Natural parameters within this group are the coordinates $\Omega = (\cos \theta, \phi)$.

The pair (ζ, ϕ) presents more novel features. The forms (1.18) and (1.20) are obtained from equation (1.21) by first performing a boost in the x direction with parameter ζ . Equivalently, this may be called a hyperrotation through ζ in the 01 plane, given as in equation (1.11). Finally one performs a rotation ϕ about the 0 axis in the 12 plane and ends up with a situation shown in Figure 1.3(b). These transformations leave the component a^3 of a four-vector unchanged. They are elements of the group $O(1, 2)$ which leaves the quadratic form

$$A^2 = (a^0)^2 - (a^1)^2 - (a^2)^2 \quad (1.23)$$

invariant. In terms of A we have

$$\begin{aligned} a^0 &= A \cosh \zeta \\ a^1 &= A \sinh \zeta \cos \phi \\ a^2 &= A \sinh \zeta \sin \phi. \end{aligned} \quad (1.24)$$

These elements of the group $O(1, 2)$ are parametrized by

$$g \equiv (\cosh \zeta, \phi). \quad (1.25)$$

The operational interpretation of the sets (ξ, θ, ϕ) and (ξ, ζ, ϕ) can be given most concrete formulation if we write down explicitly the matrices corresponding to the transformations from equations (1.13) to (1.17)–(1.20). Taking the rotation matrices from equation (1.16) and the boost from equation (1.22) one finds that

$$L(\xi, \theta, \phi) = R_z(\phi)R_y(\theta)L_x(\xi) \quad (1.26)$$

$$= \begin{bmatrix} \cosh \xi & 0 & 0 & \sinh \xi \\ \sinh \xi \sin \theta \cos \phi & \cos \theta \cos \phi & -\sin \phi & \cosh \xi \sin \theta \cos \phi \\ \sinh \xi \sin \theta \sin \phi & \cos \theta \sin \phi & \cos \phi & \cosh \xi \sin \theta \sin \phi \\ \sinh \xi \cos \theta & -\sin \theta & 0 & \cosh \xi \cos \theta \end{bmatrix}.$$

Similarly,

$$L(\xi, \zeta, \phi) = R_z(\phi)L_x(\zeta)L_z(\xi) \quad (1.27)$$

$$= \begin{bmatrix} \cosh \xi \cosh \zeta & \sinh \zeta & 0 & \sinh \xi \cosh \zeta \\ \cosh \xi \sinh \zeta \cos \phi & \cosh \zeta \cos \phi & -\sin \phi & \sinh \xi \sinh \zeta \cos \phi \\ \cosh \xi \sinh \zeta \sin \phi & \cosh \zeta \sin \phi & \cos \phi & \sinh \xi \sinh \zeta \sin \phi \\ \sinh \xi & 0 & 0 & \cosh \xi \end{bmatrix}.$$

When $L(\xi, \theta, \phi)$ is applied to the vectors $\sqrt{(a^2)}(1, 0, 0, 0)$ or $\sqrt{(-a^2)}(0, 0, 0, 1)$ one obtains vectors proportional to the first and last columns of equation (1.26). These are just the forms (1.17) and (1.19). In practice, we shall need $L(\xi, \theta, \phi)$ and $L(\xi, \zeta, \phi)$ to Lorentz transform general four-vectors specified in the standard frames $R(a)$ and $S(a)$ to other frames. The inverses of equations (1.26) and (1.27) are obtained from equation (1.7). We also note that equations (1.26) and (1.27) are combined boosts and rotations. A pure boost with parameter ξ in θ, ϕ direction is given by

$$L = R_z(\phi)R_y(-\theta)L_z(\xi)R_y(-\theta)R_z(-\phi). \quad (1.28)$$

For $a = (a^0, \mathbf{0})$ one has, of course, $R_y(-\theta)R_z(-\phi)a = a$.

The differential volume element corresponding to the spherical coordinates in equation (1.14) is given by

$$\begin{aligned} da^1 da^2 da^3 &= A^2 dA d\Omega \\ &= A^2 dA d\cos \theta d\phi. \end{aligned} \quad (1.29)$$

Correspondingly, in a Lorentz space with one time and two space coordinates we have, according to equation (1.24),

$$\begin{aligned} da^0 da^1 da^2 &= A^2 dA dg \\ &= A^2 dA d\cosh \xi d\phi. \end{aligned} \quad (1.30)$$

The total surface $\int d\Omega = 4\pi$ is finite but $\int dg$ is clearly infinite. To find the volume element in the full four-dimensional Lorentz space we calculate from equations (1.17–20) that

$$d^4a = da^0 da^1 da^2 da^3 = (\sqrt{(a^2)})^3 \sinh^2 \xi \sin \theta d(\sqrt{(a^2)}) d\xi d\theta d\phi \quad (a^2 > 0) \quad (1.31)$$

$$= (\sqrt{(a^2)})^3 \cosh^2 \xi \sinh \zeta d(\sqrt{(a^2)}) d\xi d\zeta d\phi \quad (a^2 > 0) \quad (1.32)$$

$$= (\sqrt{(-a^2)})^3 \cosh^2 \xi \sin \theta d(\sqrt{(-a^2)}) d\xi d\theta d\phi \quad (a^2 < 0) \quad (1.33)$$

$$= (\sqrt{(-a^2)})^3 \sinh^2 \xi \sinh \zeta d(\sqrt{(-a^2)}) d\xi d\zeta d\phi \quad (a^2 < 0). \quad (1.34)$$

If we take $A = |\mathbf{a}|$ as a variable instead of ξ in equations (1.31) and (1.33), we obtain in both cases

$$\begin{aligned} d^4a &= d(a^2) \frac{A^2 dA d\Omega}{2a^0} \\ &= d(a^2) \frac{da^1 da^2 da^3}{2a^0}. \end{aligned} \quad (1.35)$$

Alternatively, if A from equation (1.23) is used as a variable in equations (1.32) and (1.34) we obtain

$$\begin{aligned} d^4a &= d(a^2) \frac{A^2 dA dg}{2a^3} \\ &= d(a^2) \frac{da^0 da^1 da^2}{2a^3}. \end{aligned} \quad (1.36)$$

The differential d^4a is, of course, Lorentz invariant.

2. Four-velocity and four-momentum

The three-velocity \mathbf{v} is defined by $v = dx/dt$. Because t is not an invariant variable, \mathbf{v} does not transform like the space component of a four-vector. To construct a *velocity four-vector*, one must take the derivative of $x = (x^\mu)$ with respect to some invariant variable related to time. A natural choice is the proper time τ defined by

$$\begin{aligned} d\tau^2 &= c^{-2} dx^2 \\ &= c^{-2}(c^2 dt^2 - dx_1^2 - dx_2^2 - dx_3^2). \end{aligned} \quad (2.1)$$

Here $dx^2 = dx_\mu dx^\mu$ is evidently an invariant so that $d\tau$ is invariant. We can further write equation (2.1) as

$$\begin{aligned} d\tau &= dt \left\{ 1 - c^{-2} \left(\frac{dx}{dt} \right)^2 \right\}^{1/2} \\ &= dt/\gamma(v). \end{aligned} \quad (2.2)$$

In the rest frame, defined by $v = 0$, the times t and τ are equal which explains the term proper time. The factor γ in equation (2.2) causes time dilatation.

The *four-velocity* $u = (u^\mu)$ will thus be defined by

$$\begin{aligned} u^\mu &= \frac{dx^\mu}{d\tau} = \frac{dx^\mu}{dt} \cdot \frac{dt}{d\tau} \\ &= \gamma(v) \frac{dx^\mu}{dt} \end{aligned} \quad (2.3)$$

and it has the components

$$u = \gamma(v)(c, \mathbf{v}). \quad (2.4)$$

The space component of u differs from \mathbf{v} by the Lorentz factor γ . In the rest frame $v = 0$ the space component vanishes, $u = (c, \mathbf{0})$. Since u is a four-vector, u^2 is an invariant. In fact, equation (2.4) gives $u^2 = c^2$ so that the four-velocity is timelike.

The basic four-vector in particle kinematics is the *four-momentum* defined by

$$\begin{aligned} p &= mu \\ &= m\gamma(v)(c, \mathbf{v}) \\ &= \left(\frac{E}{c}, \mathbf{p} \right), \end{aligned} \quad (2.5)$$

where m is the *rest mass* of the particle considered. The equivalence of the two last forms of p in equation (2.5) implies that the energy, rest mass and velocity of a particle are related by

$$E = m\gamma(v)c^2.$$

Since $u^2 = c^2$ one has

$$\begin{aligned} p^2 &= m^2c^2 \\ &= (E/c)^2 - \mathbf{p}^2 \end{aligned}$$

or equivalently,

$$E^2 = c^2\mathbf{p}^2 + (mc^2)^2. \quad (2.6)$$

According to equation (2.5), the velocity and γ factor of a particle are related to its energy and momentum by the equations

$$\mathbf{v} = c^2\mathbf{p}/E, \quad \gamma(v) = E/mc^2, \quad \mathbf{v}\gamma(v) = \mathbf{p}/m. \quad (2.7)$$

By comparing equations (2.5) and (1.1) one finds that E and the components of \mathbf{p} transform as follows:

$$\begin{aligned} p'_x &= p_x, & p'_y &= p_y, \\ p'_z &= \gamma(p_z - vE/c^2) \\ E' &= \gamma(E - vp_z). \end{aligned} \quad (2.8)$$

It is useful to visualize equation (2.7) for fixed p_x and p_y in the form shown in Figure 2.1. If the relative velocity \mathbf{v} of the two frames S' and S has an arbitrary direction, the transformation equations are (Hagedorn, 1964, Exercise II.2)

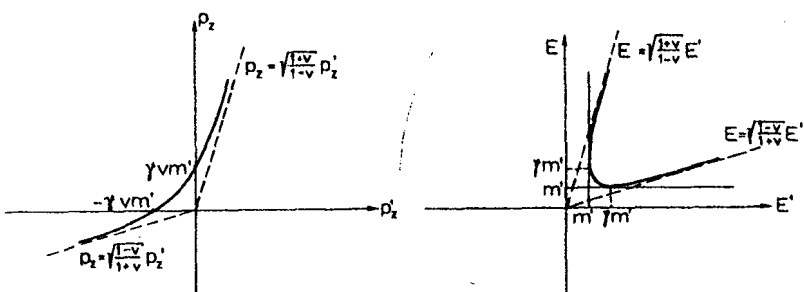


Figure II.2.1 Mapping between p_z and p'_z and E and E' for fixed $m' = (p_x^2 + p_y^2 + m^2)^{1/2}$

$$\begin{aligned} p' &= p + \gamma v \left(\frac{\gamma v \cdot p}{\gamma + 1} - E \right) c^{-2} \\ E' &= \gamma(E - v \cdot p). \end{aligned} \quad (2.9)$$

The inverses of equations (2.7–8) are obtained by changing v to $-v$ and by interchanging primed and unprimed variables.

In equation (2.8) one can further replace v by the rapidity ξ . The relation between v and ξ is given by equation (1.9) or, conversely, by

$$\begin{aligned} \xi &= \log(v + \gamma v) \\ &= \frac{1}{2} \log \{(1 + v)/(1 - v)\}. \end{aligned} \quad (2.10)$$

Due to its simple additivity property (equation (1.10)), ξ is sometimes more convenient than v . Examples of this are given in Chapter VII.

Physically p is always forward timelike, $E > 0$, but we shall also for formal purposes consider backward timelike four-momenta. If $p = (E/c, \mathbf{p})$ is backward timelike, the four-vector $-p = (-E/c, -\mathbf{p})$ is the four momentum of a physical particle.

If we have a set of four-momenta, p_1, p_2, \dots , one can form three types of *invariants* from them, and any invariant can then be expressed in terms of these. These types of invariants are listed in (a)–(c) below.

(a) The *scalar products*

$$p_i \cdot p_j = E_i E_j / c^2 - \mathbf{p}_i \cdot \mathbf{p}_j, \quad i, j = 1, 2, \dots \quad (2.11)$$

are invariant, by definition. Instead of, for example, $p_1 \cdot p_2$ one commonly uses the *two particle invariant mass squared*

$$\begin{aligned} s_{12} &= (p_1 + p_2)^2 / c^2 \\ &= m_1^2 + m_2^2 + 2p_1 \cdot p_2 / c^2 \end{aligned} \quad (2.12)$$

or the *invariant momentum transfer squared*

$$\begin{aligned} t_{12} &= (p_1 - p_2)^2 \\ &= m_1^2 c^2 + m_2^2 c^2 - 2 p_1 \cdot p_2 \end{aligned} \quad (2.13)$$

When m_1 and m_2 are constants, s_{12} , t_{12} and $p_1 \cdot p_2$ attain extremum value simultaneously. With fixed p_1 , this happens when

$$\begin{aligned} \frac{\partial(p_1 \cdot p_2)}{\partial p_2} &= E_1 \frac{\mathbf{p}_2}{E_2} - \mathbf{p}_1 \\ &= 0, \end{aligned} \quad (2.14)$$

or from equation (2.7), when $\mathbf{v}_1 = \mathbf{v}_2$. Equal velocities are equal in any frame (Exercise II.10), and this is thus a Lorentz invariant condition, as it must be. The extremum value is found directly by going to the frame $\mathbf{v}_1 = \mathbf{v}_2 = 0$, and one finds

$$p_1 \cdot p_2 \geq m_1 m_2 c^2. \quad (2.15)$$

Correspondingly,

$$\begin{aligned} s_{12} &\geq (m_1 + m_2)^2 \\ t_{12} &\leq (m_1 - m_2)^2 c^2, \end{aligned} \quad (2.16)$$

where, and this is important, the equality signs correspond to $\mathbf{v}_1 = \mathbf{v}_2$ in any frame. If either one of p_1 and p_2 is backward and the other forward timelike, equation (2.15) should be replaced by $p_1 \cdot p_2 \leq -m_1 m_2 c^2 (\leq 0)$.

(b) The signs of the energy components of timelike four-vectors are invariant, since one only deals with orthochronous Lorentz transformations.

(c) If there are four or more vectors, the quantity ϵ defined by

$$\begin{aligned} \epsilon &\equiv \epsilon(p_i, p_j, p_k, p_l) \\ &= \epsilon_{\kappa\lambda\mu\nu} p_i^\kappa p_j^\lambda p_k^\mu p_l^\nu, \end{aligned} \quad (2.17)$$

is invariant. Here $\epsilon_{\kappa\lambda\mu\nu}$ is the totally antisymmetric four-dimensional tensor (equation (A.15)). Equivalently, $\epsilon(p_i, p_j, p_k, p_l)$ is the 4×4 determinant formed of the components of the four-vectors in the argument. To prove the invariance of ϵ one carries out a proper orthochronous Lorentz transformation determined by the matrix L_v^μ , $\det L = +1$, $gL^{-1}g = L^T$, $L_0^0 > 0$. One sees immediately that

$$\epsilon(Lp_i, Lp_j, Lp_k, Lp_l) = \det L \cdot \epsilon(p_i, p_j, p_k, p_l) \quad (2.18)$$

so that ϵ is invariant. It is further simple to prove (Appendix A, equation (A.23)) that

$$|\epsilon(p_i, p_j, p_k, p_l)|^2 = -\det(p_m \cdot p_n), \quad m, n = i, j, k, l \quad (2.19)$$

Since the absolute value of ε is determined by the scalar products, the new invariant quantity brought in by ε is just the *sign of ε* . Under a space reflection, $(E, \mathbf{p}) \rightarrow (E, -\mathbf{p})$, ε changes sign but the other invariants remain unchanged.

3. Units and conventions

To facilitate the transition from special relativity to particle kinematics the light velocity c has so far been explicitly written in all formulas. From here on we shall everywhere set $c = 1$, as is customary in particle physics. This is just a formal simplification and simply means choosing c as the unit of velocity.

According to the relation $E = mc^2 = m$, the rest mass is equivalent to energy and thus mass is expressed in energy units. The basic energy unit is $J = \text{Nm} = \text{kgm}^2/\text{s}^2$, but in high energy physics the electron volt (eV) is more common:

$$\begin{aligned} 1 \text{ GeV} &= 10^3 \text{ MeV} \\ &= 10^9 \text{ eV} \\ &= 1.602 \times 10^{-10} \text{ J} \end{aligned} \tag{3.1}$$

The inverse relation is

$$\begin{aligned} 1 \text{ erg} &= 10^{-7} \text{ J} \\ &= 624 \text{ GeV} \\ &= 624 \times 10^9 \text{ eV.} \end{aligned}$$

Accelerators with energies in the 100 GeV range give macroscopic energies (\approx erg) to microscopic particles. The conversion factor between kg and GeV is obtained by solving $1 \text{ GeV} = mc^2 = m$ for m . The result is

$$1 \text{ GeV} = 1.7827 \times 10^{-27} \text{ kg.} \tag{3.2}$$

For instance, the proton mass $m_p = 1.673 \times 10^{-27} \text{ kg}$ is 0.938 GeV in eV units.

The energies of accelerated particle beams are always expressed in eV units. The choice of the energy variable is not unique and the following alternatives are in use.

1. Kinetic energy of the particle, $T = E - m$, is mostly used in the domain where the rest energy is larger than the kinetic energy. T is the normal variable in nuclear physics.
2. Total energy E of the particles is used in the high energy domain ($E \geq 1 \text{ GeV}$).
3. Momentum P of the particles (in units of MeV/c or GeV/c) is normally used to express the energy of an experiment. The separators producing

monoenergetic particle beams separate most directly in momentum and not in energy. Note the convention of writing the unit in the form GeV/c to indicate a momentum.

All these variables are, of course, equivalent. They become asymptotically equal when $E \gg m$, that is for $E \gg 1 \text{ GeV}$ for hadrons, $E \gg 1 \text{ MeV}$ for electrons and always for photons.

A convention analogous to $c = 1$ is $\hbar = 1$. This is not relevant to pure kinematics where only momentum vectors appear. It is convenient when one calculates lengths (cross-sections) or lifetimes. Previously $E = mc^2 = m$ permitted one to express mass in kg or GeV. The relations

$$\begin{aligned}\lambda &= \frac{\hbar}{mc} \\ &= \frac{1}{m}\end{aligned}\quad (3.3)$$

and

$$\begin{aligned}\frac{\lambda}{c} &= \frac{\hbar}{mc^2} \\ &= \frac{1}{m}\end{aligned}\quad (3.4)$$

can now be used to express length (metre) and time (sec.) in $1/\text{GeV}$. To calculate the conversion factors, the value of m in kg corresponding to 1 GeV from equation (3.2) is inserted in equations (3.3) and (3.4), together with the known values of \hbar and c . The results are

$$\begin{aligned}1/\text{GeV} &= 0.19733 \text{ fm} \\ &= 0.19733 \times 10^{-15} \text{ m}\end{aligned}\quad (3.5)$$

$$1/\text{GeV} = 6.5822 \times 10^{-25} \text{ sec.} \quad (3.6)$$

In harmony with these relations one often tabulates $\hbar c$ and \hbar as follows

$$\hbar c = 197.33 \text{ MeV} \times \text{fm}$$

$$\hbar = 6.5822 \times 10^{-22} \text{ MeV sec.}$$

Length in particle physics is mostly needed in connection with areas or cross-sections. The normal unit of cross-section is the millibarn = mb = $10^{-31} (\text{metre})^2 = 0.1 \text{ fm}^2$. From equation (3.5) one then obtains the very practical relation

$$\begin{aligned}\left(\frac{1}{\text{GeV}}\right)^2 &= 0.38939 \text{ mb} \\ &= \frac{1}{2.568} \text{ mb.}\end{aligned}\quad (3.7)$$

With the known values of proton and pion masses m_p and m_π one has, equivalently

$$\frac{1}{m_p^2} = 0.44232 \text{ mb}$$

$$\frac{1}{m_\pi^2} = 19.987 \text{ mb.}$$

4. Reference frames for collision processes

We have so far considered general properties of Lorentz transformations. In this section, a set of reference frames, defined by the properties of the initial state of a collision process, is introduced. Later on, several frames depending on the reaction products will also be considered.

In a two-particle collision process, two particles a and b with four-momenta $p_a = (E_a, \mathbf{p}_a)$ and $p_b = (E_b, \mathbf{p}_b)$ collide. The values of p_a and p_b are normally fixed by experimental conditions up to some experimental errors. Different frames can be defined by requiring \mathbf{p}_a or \mathbf{p}_b to have some special values. The following are most frequently used.

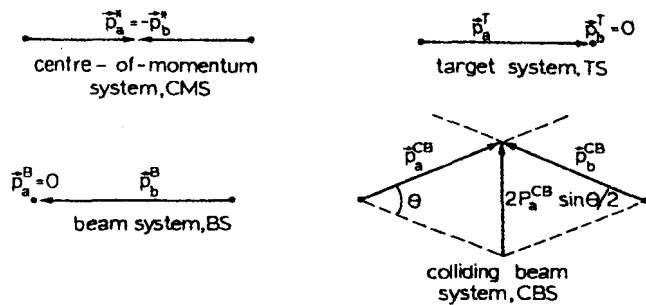


Figure II.4.1 Definition of several common frames

1. **Laboratory system (LS)** is defined as the system in which the experiment is carried out and all energies and momenta measured. It is fixed by the experimental set up, which may involve either a beam of particles hitting a stationary target or colliding beams (see below). The LS is, in a sense, the primary system. From this the momenta and energies are then transformed to other systems. We shall denote LS quantities by an index L: E^L, \mathbf{p}^L .

2. **Centre-of-momentum system (CMS)** is defined as the system in which

$$\mathbf{p}_a^* + \mathbf{p}_b^* = 0. \quad (4.1)$$

The CMS quantities will be denoted by an asterisk.

3. **Target system (TS)** is defined as a system in which

$$\mathbf{p}_b^T = \mathbf{0}. \quad (4.2)$$

Most experiments are carried out on stationary targets and for all these the TS coincides with the LS. In fact, in standard terminology our TS is called the laboratory system. However, for colliding beam experiments TS and LS do not coincide and we have preferred to keep the terminology unambiguous.

4. **Beam system (BS)** is defined by

$$\mathbf{p}_a^B = \mathbf{0}.$$

From a kinematical point of view the BS and TS are equivalent.

5. **Colliding beam system (CBS)** is defined as the frame in which two particles of equal mass and equal absolute value of momentum ($P_a^{CB} = P_b^{CB}$) collide so that their momenta form an angle $\pi - \theta$, as shown in Figure 4.1. For colliding beam experiments the CBS coincides with the LS, and for $\theta = 0$ it even coincides with the CMS. Being completely general, one could even let the masses and absolute values of momenta be different.

In practice Lorentz transformations between the systems defined above are frequently needed. In the following sections we shall show that these transformations can be carried out either by applying the explicit transformation equations (1.3) or even more simply by using invariants.

5. Lorentz transformations between centre-of-momentum, target and colliding beam systems

Consider first Lorentz transformations between the CMS and the TS. The two vectors p_a and p_b of the initial state $p_a + p_b$ of a collision can be expressed in the CMS and the TS as follows:

$$\begin{aligned} p_a^* &= (E_a^*, 0, 0, P_a^*), & p_a^T &= (E_a^T, 0, 0, P_a^T) \\ p_b^* &= (E_b^*, 0, 0, -P_a^*), & p_b^T &= (m_b^T, 0, 0, 0), \end{aligned} \quad (5.1)$$

where the direction of motion has been chosen as the z axis. The systems then move relative to each other as shown in Figure 5.1. CMS and TS

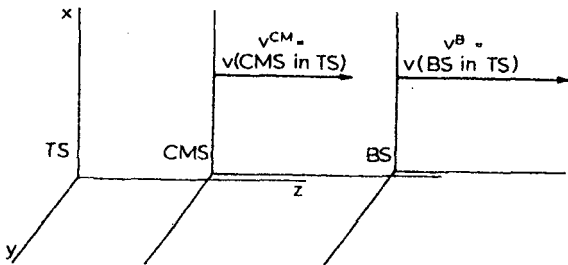


Figure II.5.1

quantities are, of course, related by Lorentz transformations. We shall carry them out explicitly, and later on it will be shown that it is often more convenient to carry them out implicitly by the use of invariants.

The Lorentz transformation equations (1.3) are now

$$\begin{aligned} P_a^* &= \gamma^{CM}(p_a^T - v^{CM}E_a^T) \\ E_a^* &= \gamma^{CM}(E_a^T - v^{CM}p_a^T), \end{aligned} \quad (5.2)$$

where v^{CM} is the velocity of the CMS in the TS. To determine v^{CM} we proceed as follows. If the total energy and momentum of a group of particles (consisting of one or more particles) are E and \mathbf{p} in some reference frame, according to equation (2.9) the velocity \mathbf{v} of the group in the frame in question is given by

$$\begin{aligned} \mathbf{v} &= \mathbf{p}/E \\ \gamma &= E/m \\ \gamma\mathbf{v} &= \mathbf{p}/m, \end{aligned} \quad (5.3)$$

where $m = (E^2 - \mathbf{p}^2)^{\frac{1}{2}}$ is the *invariant mass of the group of particles*. Now we have, for the two-particle system $p_a + p_b$, that the velocity of the CMS in the TS is given by

$$\begin{aligned} v^{CM} &= \left| \frac{\mathbf{p}_a + \mathbf{p}_b}{E_a + E_b} \right|_{\mathbf{p}_b=0} \\ &= \frac{P_a^T}{E_a^T + m_b}. \end{aligned} \quad (5.4)$$

Similarly,

$$\begin{aligned} \gamma^{CM} &= (E_a^T + m_b)/\sqrt{s} \\ v^{CM}\gamma^{CM} &= P_a^T/\sqrt{s}, \end{aligned} \quad (5.5)$$

where the invariant mass \sqrt{s} of the system $p_a + p_b$ is defined by

$$\begin{aligned} s &\equiv s_{ab} \\ &= (p_a + p_b)^2 \\ &= (E_a + E_b)^2 - (\mathbf{p}_a + \mathbf{p}_b)^2. \end{aligned} \quad (5.6)$$

It has the same value in all frames and thus one has, in particular,

$$s = (E_a^* + E_b^*)^2 \quad (5.7)$$

$$\begin{aligned} &= (E_a^T + m_b)^2 - (P_a^T)^2 \\ &= m_a^2 + m_b^2 + 2m_bE_a^T. \end{aligned} \quad (5.8)$$

Inserting equations (5.4–5) into equation (5.2) one finds

$$\begin{aligned} P_a^* &= m_a P_a^T / \sqrt{s} \\ E_a^* &= (m_a^2 + m_b E_a^T) / \sqrt{s}. \end{aligned} \quad (5.9)$$

Similarly, applying equation (5.2) to p_b ,

$$\begin{aligned} P_b^* &= m_b P_b^T / \sqrt{s} \\ &= P_a^* (-) \\ E_b^* &= m_b (E_b^T + m_b) / \sqrt{s}. \end{aligned} \quad (5.10)$$

Carrying out the Lorentz transformation in this explicit way is a completely mechanical procedure, but it becomes tedious in more complicated cases. The idea for a simpler method can be seen from equations (5.6–8). They relate all noncovariant quantities relevant to the state $p_a + p_b$ to the invariant s . In order to compute relations between the different quantities, it is thus sufficient to evaluate s in terms of each of them. We shall return to this approach in the following section.

Consider now Lorentz transformations between the colliding beam system (CBS) and the CMS. The introduction of the CBS has become useful now that one is able to carry out experiments with colliding beams. For instance, our definition of the CBS (Figure 4.1) describes directly the experimental situation in the CERN Intersecting Storage Rings (ISR), if the two colliding proton beams have equal momenta. For unequal momenta slight and obvious modifications are necessary. In the ISR the maximum momenta are 28 GeV/c and the angle of the intersection is $\theta = 14.77^\circ \approx 0.2578$ rad.

One should again emphasize that for colliding beam experiments of the ISR type the CBS coincides with the laboratory system. From the CBS one may then Lorentz transform the measured momenta and energies to any frame, for instance to the CMS or target system (which in pre-ISR times was mostly called the laboratory system). We shall in the following only consider the transformation to the CMS.

For the transformation to the CMS one needs the velocity of the CMS in the CBS ($=$ LS). As the velocity of the CMS in any frame is $(p_a + p_b)/(E_a + E_b)$, the velocity v^{CB} of the CMS in CBS is according to Figure 4.1 given by

$$v^{CB} = v_a \sin \frac{\theta}{2}, \quad (5.11)$$

where v_a ($= v_b$) is the velocity of particle a in the laboratory frame. Correspondingly, the Lorentz factors are related by

$$\gamma^{CB} = \frac{\gamma_a}{\left(\sin^2 \frac{\theta}{2} + \gamma_a^2 \cos^2 \frac{\theta}{2} \right)^{\frac{1}{2}}}. \quad (5.12)$$

The velocity is oriented along $\mathbf{p}_a + \mathbf{p}_b$ as shown in Figure 4.1 and the Lorentz transformation is easy to carry out by choosing the z axis parallel to the velocity. The momentum in the CMS is simply the projection of P_a^{CB} :

$$P_a^* = P_a^{\text{CB}} \cos \frac{\theta}{2}. \quad (5.13)$$

6. Energies and momenta in terms of the invariants

We shall here work out the connection between the invariants s , m_a and m_b and the noninvariant variables E_a , \mathbf{p}_a and E_b , \mathbf{p}_b separately for the TS, CMS and CBS. The results for the beam system are obtained from those for the target system by interchanging particles a and b.

(a) Target system

To begin with, we have for the TS, $\mathbf{p}_b^T = 0$ and $E_b^T = m_b$. From equation (5.8) we have also

$$E_a^T = (s - m_a^2 - m_b^2)/2m_b \quad (6.1)$$

and consequently

$$\begin{aligned} (P_a^T)^2 &= (E_a^T)^2 - m_a^2 \\ &= \{(s - m_a^2 - m_b^2)^2 - 4m_a^2m_b^2\}/4m_b^2. \end{aligned}$$

We write this result in the form

$$P_a^T = \lambda^{\frac{1}{2}}(s, m_a^2, m_b^2)/2m_b \quad (6.2)$$

by introducing the kinematical function

$$\lambda(x, y, z) = (x - y - z)^2 - 4yz \quad (6.3)$$

$$= x^2 + y^2 + z^2 - 2xy - 2yz - 2zx \quad (6.4)$$

$$= \{x - (\sqrt{y} + \sqrt{z})^2\}\{x - (\sqrt{y} - \sqrt{z})^2\} \quad (6.5)$$

$$= (\sqrt{x} - \sqrt{y} - \sqrt{z})(\sqrt{x} + \sqrt{y} + \sqrt{z}) \quad (6.6)$$

$$\cdot (\sqrt{x} - \sqrt{y} + \sqrt{z})(\sqrt{x} + \sqrt{y} - \sqrt{z}) \quad (6.6)$$

$$= x^2 - 2(y + z)x + (y - z)^2. \quad (6.7)$$

Special cases of interest are

$$\lambda(x, y, y) = x(x - 4y) \quad (6.8)$$

$$\lambda(x, y, 0) = (x - y)^2. \quad (6.9)$$

From equation (6.4) it is seen that λ is invariant under all permutations of its

arguments. The basic motivation for the introduction of λ will be clarified in Section 7. Sometimes λ is called the *triangle function* since $\frac{1}{4}\{-\lambda(x, y, z)\}^{\frac{1}{2}}$ is the area of a triangle with sides \sqrt{x} , \sqrt{y} and \sqrt{z} .

According to equation (6.5) we have

$$\lambda(s, m_a^2, m_b^2) = \{s - (m_a + m_b)^2\} \{s - (m_a - m_b)^2\}. \quad (6.10)$$

Thus p_a^T in equation (6.2) is real if

$$\sqrt{s} \geq m_a + m_b. \quad (6.11)$$

The threshold value $m_a + m_b$ is the smallest value \sqrt{s} can attain and, as shown at the end of Section 2, this happens when the velocities of particles a and b are equal. The threshold $m_a + m_b$ also appears if one writes the kinetic energy T_a of a particle a in TS in terms of s :

$$T_a = E_a^T - m_a = \{s - (m_a + m_b)^2\}/2m_b.$$

The 'pseudothreshold' value $m_a - m_b$ will be important for some kinematical considerations later on.

(b) Centre-of-momentum system

In the CMS, $p_a^* + p_b^* = 0$ implies

$$P_a^* = P_b^* = P^*. \quad (6.12)$$

According to equation (5.7), one has

$$\sqrt{s} = E_a^* + E_b^*. \quad (6.13)$$

The invariant energy is thus equal to the total energy in the CMS. Inserting equation (6.12) in equation (6.13) one obtains

$$\sqrt{s} = \{(P^*)^2 + m_a^2\}^{\frac{1}{2}} + \{(P^*)^2 + m_b^2\}^{\frac{1}{2}}.$$

Squaring once this gives

$$E_a^* = (s + m_a^2 - m_b^2)/2\sqrt{s}. \quad (6.14)$$

Squaring a second time results in

$$P^* = \lambda^{\frac{1}{2}}(s, m_a^2, m_b^2)/2\sqrt{s}. \quad (6.15)$$

The remaining energy E_b^* is then obtained from $E_b^* = \sqrt{s} - E_a^*$:

$$E_b^* = (s - m_a^2 + m_b^2)/2\sqrt{s}. \quad (6.16)$$

Note as a mnemonic rule that, in equations (6.14) and (6.16), E_i^* has in the numerator a plus sign in front of the mass m_i^2 .

It is easy to verify that the expressions so obtained for TS and CMS quantities satisfy the relations (5.9) and (5.10) obtained by explicit Lorentz transformations.

(c) Colliding beam system

For a colliding beam experiment the invariant s is given by

$$\begin{aligned}s &= (E_a + E_b)^2 - |\mathbf{p}_a + \mathbf{p}_b|^2 \\ &= 4m^2 + 4\left(P_{\text{CB}}^{\text{CB}} \cos \frac{\theta}{2}\right)^2,\end{aligned}\quad (6.17)$$

where $P_{\text{CB}}^{\text{CB}} = P_a^{\text{CB}} = P_b^{\text{CB}}$ is the laboratory momentum of the particles a and b and $m_a = m_b = m$. To second order in θ this is

$$s \approx 2E^{\text{CB}}(1 - \theta^2/8), \quad (6.18)$$

where E^{CB} is the laboratory energy of the particles a and b and the approximation $P^{\text{CB}} \approx E^{\text{CB}}$ has been used. Since $\theta^2/8 \approx 0.0083$ for the ISR, the correction to the total CMS energy \sqrt{s} arising from the fact that the two beams intersect at an angle θ is numerically very small. Inverting equation (6.17) we have, finally,

$$\begin{aligned}P_{\text{CB}}^{\text{CB}} &= \frac{(s - 4m^2)^{\frac{1}{2}}}{2 \cos \frac{\theta}{2}} \\ E^{\text{CB}} &= \left(s - 4m^2 \sin^2 \frac{\theta}{2}\right)^{\frac{1}{2}} / 2 \cos \frac{\theta}{2}.\end{aligned}\quad (6.19)$$

Example 1: It is useful to have an idea of the numerical magnitudes of various kinematical quantities for normal experiments, which are characterized by the value P_a^T of the incident momentum. When the momenta involved are sufficiently large, for instance, $P_a^T \geq 5 \text{ GeV}/c$, one may neglect the rest masses and assume that $E = P$. Then equation (5.8) gives $s \approx 2m_b P_a^T$. If one takes into account that the target is—practically without exception—a nucleon ($m_b = 1 \text{ GeV}$) one may estimate

$$s \approx 2P_a^T \quad (\text{in GeV units}). \quad (6.20)$$

For the CMS quantities one has similarly

$$E_a^* \approx E_b^* \approx P_a^* \approx P_b^* \approx \frac{1}{2}\sqrt{s} \approx \sqrt{(P_a^T/2)}. \quad (6.21)$$

For a pp initial state with $P_a^T = 19 \text{ GeV}/c$ the exact values are $E_a^* = E_b^* = 3.06 \text{ GeV}$, $P_a^* = P_b^* = 2.91 \text{ GeV}/c$, $s = 37.45 \text{ GeV}^2$, while the approximation (6.21) would give $\sqrt{(P_a^T/2)} = 3.08 \text{ GeV}$, $s = 38 \text{ GeV}^2$. For qualitative purposes the accuracy is adequate.

Example 2: According to equation (6.20) the useful energy \sqrt{s} of an accelerator behaves like $\sqrt{s} \approx \sqrt{(2P_a^T)}$. Increasing the incident momentum of a particle hitting a stationary target by a factor, for instance, four will increase the useful energy \sqrt{s} only by a factor two. The rest will go to the useless energy of

the motion of the centre of mass. This simple consideration is the motivation for constructing colliding beams. If two beams with particles of momentum P^{CB} collide head on in the laboratory, the total energy \sqrt{s} will be approximately equal to $2P^{CB}$. According to equation (6.20) this corresponds to an effective momentum P_{eff}^T of a beam hitting a stationary target given by

$$P_{\text{eff}}^T \simeq 2(P^{CB})^2 \quad (6.22)$$

For $P^{CB} = 28 \text{ GeV}/c$, the effective momentum would be $P_{\text{eff}}^T \simeq 1570 \text{ GeV}/c$. The gain is impressive.

Using the formulas derived in this and the previous section we can write down the Lorentz transformation parameters v and γ between the three standard systems BS, CMS and TS in terms of s , m_a and m_b . We shall also list the limiting forms valid for $s \rightarrow \infty$. With our conventions (equations (5.1–2)) the frames move relative to each other as shown in Figure 5.1. Using $v = p/E$, $\gamma = E/m$ we then have for transformations between the CMS and the TS,

$$\begin{aligned} v^{CM} &\equiv v(\text{CMS in TS}) \\ &= P_a^T/(E_a^T + m_b) \\ &= \lambda^{\frac{1}{2}}(s, m_a^2, m_b^2)/(s - m_a^2 + m_b^2) \\ &\simeq 1 - 2m_b^2/s, \end{aligned} \quad (6.23)$$

$$\begin{aligned} \gamma^{CM} &= (s - m_a^2 + m_b^2)/2m_b\sqrt{s} \\ &\simeq \sqrt{s}/2m_b, \end{aligned} \quad (6.24)$$

for transformations between BS and TS,

$$\begin{aligned} v^B &\equiv v(\text{BS in TS}) \\ &= P_a^T/E_a^T \\ &= \lambda^{\frac{1}{2}}(s, m_a^2, m_b^2)/(s - m_a^2 - m_b^2) \\ &\simeq 1 - 2m_a^2m_b^2/s^2, \end{aligned} \quad (6.25)$$

$$\begin{aligned} \gamma^B &= p_a \cdot p_b / m_a m_b \\ &= (s - m_a^2 - m_b^2)/2m_a m_b \\ &\simeq s/2m_a m_b, \end{aligned} \quad (6.26)$$

and for transformations between BS and CMS

$$\begin{aligned} v^{B,CM} &\equiv v(\text{BS in CMS}) \\ &= P_b^B/(E_b^B + m_a) \\ &= \lambda^{\frac{1}{2}}(s, m_a^2, m_b^2)/(s + m_a^2 - m_b^2) \\ &\simeq 1 - 2m_a^2/s. \end{aligned} \quad (6.27)$$

$$\gamma^{B,CM} = (s + m_a^2 - m_b^2)/2m_a\sqrt{s} \quad (6.28)$$

$$\approx \sqrt{s}/2m_a.$$

Of course, any two of the velocities or γ -factors above give the third one by using equation (1.8) with the correct signs for the velocities. The relative velocities may finally be replaced by relative rapidities ζ according to the formula (2.10):

$$\zeta = \log(\gamma + \gamma v). \quad (6.29)$$

Then $\zeta^B = \zeta^{CM} + \zeta^{B,CM}$, etc. These formulas will be given explicitly in Section VII.4.

7. Momenta and angles in terms of invariants

A momentum configuration p_1, \dots, p_n can be described either in terms of geometric or invariant variables. The former are angles, rapidities, absolute values of three-momenta, etc. and they are defined in a definite Lorentz frame. The possible types of invariant variables were listed in Section 2.

In the preceding sections we saw simple examples of how momenta can be written in terms of invariant variables. Here we extend the analysis to angles and rapidities. Besides their obvious use to relate geometric and invariant quantities the resulting equations have another important application. To write a non-invariant quantity in a given frame in terms of quantities in some other frame, it is often simplest to first write the quantity in terms of invariants and then to express the result in the geometric variables of the second frame.

From a technical point of view we shall find that in writing geometric quantities in terms of invariants one is very naturally lead to the use of Gram determinants (Appendix A). Similarly, when later on we treat the kinematics of particle reactions, it will be seen that if invariants are used, the kinematics of a particle reaction involving $n + 1$ particles (for instance, a $2 \rightarrow n - 1$ process) will be determined by Gram determinants up to order n (one four-momentum is eliminated by energy-momentum conservation). The important advantage of Gram determinants is that they combine considerable algebraic complexity with great conceptual simplicity. Their use shortens kinematic calculations significantly and often permits one to write the answer almost automatically. There will be ample proof of this in later sections.

Consider a set of four-vectors p_1, p_2, p_3 and p_4 and assume first that p_1 is *timelike*, the type of the other vectors being irrelevant. The four-vector p_1 then defines a frame in which $p_1 = (m_1, \mathbf{0})$, the rest frame $R(p_1)$ of p_1 . We shall consider in this frame the following geometric quantities, written in order of

increasing complexity :

the length P_2 of \mathbf{p}_2

the angle θ_{23} between \mathbf{p}_2 and \mathbf{p}_3

the angle ϕ between the planes spanned by $\mathbf{p}_2, \mathbf{p}_3$ and $\mathbf{p}_2, \mathbf{p}_4$.

These variables are precisely the spherical coordinates of equation (1.17). To make this explicit, we introduce a coordinate system in $R(p_1)$ so that \mathbf{p}_2 is parallel to z axis and \mathbf{p}_3 lies in the xz plane with $p_{3x} \geq 0$ (Figure 7.1). In this

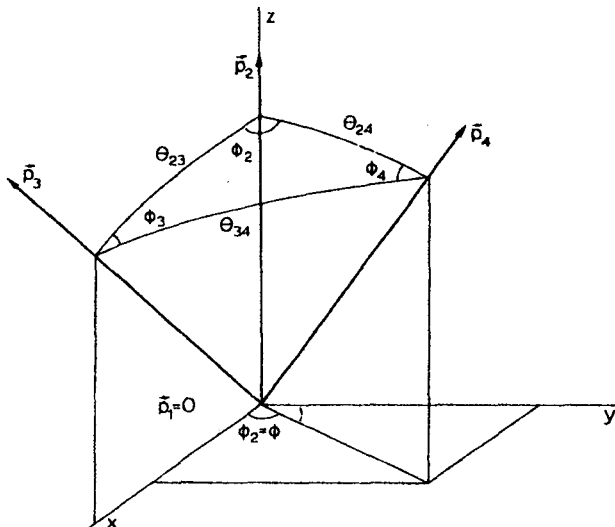


Figure II.7.1

frame, called $R(p_1, p_2, p_3)$, the following representations are valid :

$$p_1 = (m_1, 0, 0, 0)$$

$$p_2 = (E_2, 0, 0, P_2)$$

$$p_3 = (E_3, P_3 \sin \theta_{23}, 0, P_3 \cos \theta_{23}) \quad (7.1)$$

$$p_4 = (E_4, P_4 \sin \theta_{24} \cos \phi, P_4 \sin \theta_{24} \sin \phi, P_4 \cos \theta_{24}).$$

The energies are, of course, given by $E_i^2 = P_i^2 + p_i^2$. The ranges of the angles are $0 \leq \theta \leq \pi$, $0 \leq \phi < 2\pi$. If p_i ($i = 2, 3, 4$) is timelike equation (1.17) implies that $0 \leq P_i < \infty$, $m_i \leq |E_i| < \infty$, and if p_i is spacelike equation (1.19) gives $\sqrt{(-t_i)} \leq |P_i| < \infty$ and $-\infty < E_i < \infty$. We now solve the problem of writing the components in equation (7.1) in terms of invariants ; the answer is written down in the form (7.1) later in equations (VI.7.31).

(a) Length of three-momentum

Since $\mathbf{p}_1 = 0$, one has $p_1 \cdot p_2 = m_1 E_2$ and

$$\begin{aligned} E_2 &= p_1 \cdot p_2 / m_1 \\ P_2^2 &= m_1^2 (p_1 \cdot p_2)^2 - p_2^2. \end{aligned} \quad (7.2)$$

Here E_2 , P_2 have been written in terms of invariants in a fixed frame. Equation (7.2) can be further modified into a standard form:

$$\begin{aligned} P_2^2 &= \{(p_1 \cdot p_2)^2 - p_1^2 p_2^2\} / p_1^2 \\ &= -\frac{1}{p_1^2} \begin{vmatrix} p_1 \cdot p_1 & p_1 \cdot p_2 \\ p_2 \cdot p_1 & p_2 \cdot p_2 \end{vmatrix} \\ &\equiv -\frac{1}{p_1^2} \Delta_2(p_1, p_2). \end{aligned} \quad (7.3)$$

The symmetric Gram determinant $\Delta_2(p_1, p_2)$ of p_1 and p_2 (Appendix A) has been introduced here. Since $(p_1 \cdot p_2)^2 \geq m_1^2 m_2^2$ (equation (2.18)) one has $\Delta_2 < 0$ and thus $P_2^2 > 0$. Taking into account equation (6.3) we get

$$\begin{aligned} \Delta_2(p_1, p_2) &= p_1^2 p_2^2 - \frac{1}{4} \{(p_1 + p_2)^2 - p_1^2 - p_2^2\}^2 \\ &= -\frac{1}{4} \lambda \{(p_1 + p_2)^2, p_1^2, p_2^2\}. \end{aligned} \quad (7.4)$$

This equation shows the true significance of the λ function: it is an expanded form of Δ_2 , which is the more fundamental quantity. One may thus call λ the basic three-particle kinematic function. The number three here follows from the fact that Δ_2 is relevant for a reaction in which the total number of four-momenta is three (a $1 \rightarrow 2$ decay, for example).

Example 1: For the initial state $a + b$ we want to find P_a^* in the frame $p_a + p_b = (\sqrt{s}, \mathbf{0})$. Equation (7.3) with $p_1 \rightarrow p_a + p_b$, $p_2 \rightarrow p_a$ gives

$$P_a^{*2} = -\frac{1}{s} \Delta_2(p_a + p_b, p_a).$$

Equation (A.6) in Appendix A, which follows from general properties of determinants, implies

$$\begin{aligned} P_a^{*2} &= -\frac{1}{s} \Delta_2(p_b, p_a) \\ &= \frac{1}{4s} \lambda(s, m_a^2, m_b^2). \end{aligned}$$

This agrees with equation (6.15).

(b) Angle between two momenta

We now consider the *polar angle* θ_{23} between two vectors \mathbf{p}_2 and \mathbf{p}_3 in the frame $\mathbf{p}_1 = (m_1, \mathbf{0})$. We should thus write an invariant expression formed from $\mathbf{p}_1, \mathbf{p}_2, \mathbf{p}_3$ which involves θ_{23} in the frame $\mathbf{p}_1 = \mathbf{0}$. This is clearly $\mathbf{p}_2 \cdot \mathbf{p}_3$:

$$\begin{aligned} \mathbf{p}_2 \cdot \mathbf{p}_3 &= E_2 E_3 - P_2 P_3 \cos \theta_{23} \\ &= \frac{\mathbf{p}_1 \cdot \mathbf{p}_2}{\mathbf{p}_1^2} \frac{\mathbf{p}_1 \cdot \mathbf{p}_3}{\mathbf{p}_1^2} - \frac{\{\Delta_2(\mathbf{p}_1, \mathbf{p}_2) \quad \Delta_2(\mathbf{p}_1, \mathbf{p}_3)\}^{\frac{1}{2}}}{\mathbf{p}_1^2} \cos \theta_{23}. \end{aligned} \quad (7.5)$$

The second line follows from equations (7.2) and (7.3). The required angle is then given by

$$\cos \theta_{23} = \frac{\mathbf{p}_1 \cdot \mathbf{p}_2}{\{\Delta_2(\mathbf{p}_1, \mathbf{p}_2) \quad \Delta_2(\mathbf{p}_1, \mathbf{p}_3)\}^{\frac{1}{2}}}. \quad (7.6)$$

Except for the sign, the numerator equals the *unsymmetric Gram determinant*

$$G\begin{pmatrix} \mathbf{p}_1, \mathbf{p}_2 \\ \mathbf{p}_1, \mathbf{p}_3 \end{pmatrix} = \begin{vmatrix} \mathbf{p}_1 \cdot \mathbf{p}_1 & \mathbf{p}_1 \cdot \mathbf{p}_3 \\ \mathbf{p}_2 \cdot \mathbf{p}_1 & \mathbf{p}_2 \cdot \mathbf{p}_3 \end{vmatrix}. \quad (7.7)$$

The basic relation for angles between momenta is thus

$$\cos \theta_{23} = -\frac{G\begin{pmatrix} \mathbf{p}_1, \mathbf{p}_2 \\ \mathbf{p}_1, \mathbf{p}_3 \end{pmatrix}}{\{\Delta_2(\mathbf{p}_1, \mathbf{p}_2) \quad \Delta_2(\mathbf{p}_1, \mathbf{p}_3)\}^{\frac{1}{2}}}. \quad (7.8)$$

One can also write $\sin \theta_{23}$ as an elegant expression in the invariants. Starting from $\sin^2 \theta = 1 - \cos^2 \theta$ and equation (7.8), it is not easy to find this simple expression. Anticipating the result we consider the 3×3 symmetric Gram determinant

$$\Delta_3(\mathbf{p}_1, \mathbf{p}_2, \mathbf{p}_3) = \begin{vmatrix} \mathbf{p}_1^2 & \mathbf{p}_1 \cdot \mathbf{p}_2 & \mathbf{p}_1 \cdot \mathbf{p}_3 \\ \mathbf{p}_2 \cdot \mathbf{p}_1 & \mathbf{p}_2^2 & \mathbf{p}_2 \cdot \mathbf{p}_3 \\ \mathbf{p}_3 \cdot \mathbf{p}_1 & \mathbf{p}_3 \cdot \mathbf{p}_2 & \mathbf{p}_3^2 \end{vmatrix}.$$

In the rest frame of \mathbf{p}_1 , it becomes

$$\begin{aligned} \Delta_3(\mathbf{p}_1, \mathbf{p}_2, \mathbf{p}_3) &= \begin{vmatrix} m_1^2 & m_1 E_2 & m_1 E_3 \\ m_1 E_2 & \mathbf{p}_2^2 & \mathbf{p}_2 \cdot \mathbf{p}_3 \\ m_1 E_3 & \mathbf{p}_2 \cdot \mathbf{p}_3 & \mathbf{p}_3^2 \end{vmatrix} \\ &= m_1^2 \begin{vmatrix} 1 & E_2 & E_3 \\ 0 & -\mathbf{p}_2^2 & -\mathbf{p}_2 \cdot \mathbf{p}_3 \\ 0 & -\mathbf{p}_2 \cdot \mathbf{p}_3 & -\mathbf{p}_3^2 \end{vmatrix} \\ &= m_1^2 |\mathbf{p}_2 \times \mathbf{p}_3|^2 \\ &= m_1^2 D^2 D^2 \sin^2 \theta \end{aligned} \quad (7.9)$$

The determinant has been simplified by multiplying the first row by E_2/m_1 or by E_3/m_1 , and by then subtracting it from the second or the third row, respectively. Using equation (7.3) and writing $\Delta_1(p_1) = p_1^2 = m_1^2$ one gets

$$\sin^2 \theta_{23} = \frac{\Delta_1(p_1)\Delta_3(p_1, p_2, p_3)}{\Delta_2(p_1, p_2)\Delta_2(p_1, p_3)}. \quad (7.10)$$

A difference between equations (7.8) and (7.10) is that Δ_3 in equation (7.10) gives two values of the angle: θ and $\pi - \theta$, while equation (7.8) fixes θ unambiguously.

(c) Angle between two planes

The polar angle θ_{23} was defined above by giving two vectors p_2 and p_3 in the frame $p_1 = (m_1, \mathbf{0})$. One may generalize this further to *azimuthal angles* or *angles between two planes* by inducing a fourth vector p_4 . The three vectors p_2, p_3 and p_4 define a spherical triangle as shown in Figure 7.1. All the sides θ_{23}, θ_{34} and θ_{42} involve only three four-vectors and can be written as functions of invariants as shown previously. The angles ϕ_2, ϕ_3 and ϕ_4 involve four four-vectors and we shall next write them in terms of invariants. As the problem has an obvious cyclic symmetry, we shall only consider $\phi = \phi_2$.

It is easy to see that in vector form

$$\cos \phi = \frac{(\mathbf{p}_2 \times \mathbf{p}_3) \cdot (\mathbf{p}_2 \times \mathbf{p}_4)}{|\mathbf{p}_2 \times \mathbf{p}_3| |\mathbf{p}_2 \times \mathbf{p}_4|} \Big|_{\mathbf{p}_1=0} \quad (7.11)$$

$$\sin \phi = \frac{P_2(\mathbf{p}_2 \cdot \mathbf{p}_3 \times \mathbf{p}_4)}{|\mathbf{p}_2 \times \mathbf{p}_3| |\mathbf{p}_2 \times \mathbf{p}_4|} \Big|_{\mathbf{p}_1=0}. \quad (7.12)$$

Equation (7.11) expresses the fact that ϕ is the angle between the normals to the two planes spanned by $\mathbf{p}_2, \mathbf{p}_3$ and by $\mathbf{p}_2, \mathbf{p}_4$. Since ϕ varies between 0 and 2π one needs both sine and cosine to give it uniquely. The ambiguities inherent in defining an azimuthal angle are considered in detail at the end of this section.

The solution of the problem of writing $\cos \phi$ in invariant form is similar to the derivation of equation (7.8). Let us consider (equation (A.1)), $G\begin{pmatrix} p_1, p_2, p_3 \\ p_1, p_2, p_4 \end{pmatrix}$ in the frame $\mathbf{p}_1 = \mathbf{0}$, and copy the steps in the reduction (7.9):

$$\begin{aligned} G\begin{pmatrix} p_1, p_2, p_3 \\ p_1, p_2, p_4 \end{pmatrix} &= \begin{vmatrix} m_1^2 & m_1 E_2 & m_1 E_4 \\ m_1 E_2 & p_2^2 & p_2 \cdot p_4 \\ m_1 E_3 & p_2 \cdot p_3 & p_3 \cdot p_4 \end{vmatrix} \\ &= m_1^2 \begin{vmatrix} 1 & E_2 & E_4 \\ 0 & -p_2^2 & -p_2 \cdot p_4 \\ 0 & -p_2 \cdot p_3 & -p_3 \cdot p_4 \end{vmatrix} \\ &= m_1^2 (\mathbf{p}_2 \times \mathbf{p}_3) \cdot (\mathbf{p}_2 \times \mathbf{p}_4) \quad (7.13) \\ &= m_1^2 P_2^2 P_3 P_4 \sin \theta_{23} \sin \theta_{34} \cos \phi. \quad (7.14) \end{aligned}$$

Combining equation (7.14) with equation (7.10) gives

$$\cos \phi = \frac{G(p_1, p_2, p_3)}{\{ \Delta_3(p_1, p_2, p_3) \Delta_3(p_1, p_2, p_4) \}^{\frac{1}{2}}}. \quad (7.15)$$

The relation between ϕ and an invariant variable $p_i \cdot p_j$ in equation (7.15) is in general fairly complicated. An exception is $p_3 \cdot p_4$. This appears in equation (7.15) only as a single element of G , and, therefore, $\cos \phi$ and $p_3 \cdot p_4$ are linearly related. An expansion of G in cofactors is

$$G(p_1, p_2, p_3) = p_3 \cdot p_4 \Delta_2(p_1, p_2) + p_1 \cdot p_3 G(p_1, p_2) - p_2 \cdot p_3 G(p_1, p_2). \quad (7.15)$$

Solving for $p_3 \cdot p_4$ from this and equation (7.15) results in

$$p_3 \cdot p_4 = \frac{p_1 \cdot p_3 G(p_1, p_2) - p_2 \cdot p_3 G(p_1, p_2)}{-\Delta_2(p_1, p_2)} - \frac{\{ \Delta_3(p_1, p_2, p_3) \Delta_3(p_1, p_2, p_4) \}^{\frac{1}{2}}}{-\Delta_2(p_1, p_2)} \cos \phi. \quad (7.16)$$

Of course, $p_3 \cdot p_4$ is also linearly related to the cosine of the angle θ_{34} between \mathbf{p}_3 and \mathbf{p}_4 (equation (7.5) and Figure 7.1); equation (7.16) follows also if θ_{34} is replaced by ϕ according to the law of cosines for sides in spherical trigonometry (equation (B.4)).

To obtain $\sin \phi$ in invariants we shall again use the reduction process with the result

$$\begin{aligned} \Delta_4(p_1, p_2, p_3, p_4) &= m_1^2 \begin{vmatrix} 1 & E_2 & E_3 & E_4 \\ 0 & -\mathbf{p}_2^2 & -\mathbf{p}_2 \cdot \mathbf{p}_3 & -\mathbf{p}_2 \cdot \mathbf{p}_4 \\ 0 & -\mathbf{p}_2 \cdot \mathbf{p}_3 & -\mathbf{p}_3^2 & -\mathbf{p}_3 \cdot \mathbf{p}_4 \\ 0 & -\mathbf{p}_2 \cdot \mathbf{p}_4 & -\mathbf{p}_3 \cdot \mathbf{p}_4 & -\mathbf{p}_4^2 \end{vmatrix} \\ &= -m_1^2 \{ \mathbf{p}_2 \cdot (\mathbf{p}_3 \times \mathbf{p}_4) \}^2 \\ &= -m_1^2 P_2^2 P_3^2 P_4^2 \sin^2 \theta_{23} \sin^2 \theta_{24} \sin^2 \phi \end{aligned} \quad (7.17)$$

in the frame $p_1 = (m_1, \mathbf{0})$. Combining with equations (7.3) and (7.10) one has

$$\sin^2 \phi = \frac{\Delta_2(p_1, p_2) \Delta_4(p_1, p_2, p_3, p_4)}{\Delta_3(p_1, p_2, p_3) \Delta_3(p_1, p_2, p_4)}. \quad (7.18)$$

The compatibility of equations (7.15) and (7.18) is equivalent to a certain property of determinants (equation (A.32)).

(d) **Solid angle**

The relations derived above also allow one to write the differential

$$d\Omega_4 = d \cos \theta_{24} d\phi, \quad (7.19)$$

defined in the frame $R(p_1, p_2, p_3)$, in invariant form. Equation (7.5) relates $\cos \theta_{24}$ simply to $p_2 \cdot p_4$ and equation (7.16) $\cos \phi$ to $p_3 \cdot p_4$. Taking differentials we have

$$\begin{aligned} d(p_2 \cdot p_4) &= -d \cos \theta_{24} \frac{1}{m_1^2} \{\Delta_2(p_1, p_2) \Delta_2(p_1, p_4)\}^{\frac{1}{2}} \\ d(p_3 \cdot p_4) &= \sin \phi \, d\phi \frac{1}{-\Delta_2(p_1, p_2)} \{\Delta_3(p_1, p_2, p_3) \Delta_3(p_1, p_2, p_4)\}^{\frac{1}{2}} \quad (7.20) \\ &= d\phi \{-\Delta_4(p_1, p_2, p_3, p_4)\}^{\frac{1}{2}} \{-\Delta_2(p_1, p_2)\}^{-\frac{1}{2}} \end{aligned}$$

where we have taken $\sin \phi$ from equation (7.18). The signs of the arguments of the square roots follow from the fact that, according to equations (7.3), (7.10) and (7.17), physical four-vectors imply $\Delta_2 \leq 0$, $\Delta_3 \geq 0$, $\Delta_4 \leq 0$. Note that in equation (7.16) $p_3 \cdot p_4$ varies between its minimum and maximum values when $\cos \phi$ varies between -1 and $+1$ or ϕ between π and 0 . However, since ϕ is an azimuthal angle, its whole range of variation is $0 \leq \phi < 2\pi$. Thus two values of ϕ (ϕ and $2\pi - \phi$), corresponding to a reflection of p_4 with respect to the xz plane in Figure 7.1., are obtained for each value of $p_3 \cdot p_4$. Taking into account this double-valuedness we have, from equation (7.20):

$$\begin{aligned} d\Omega_4 &= d \cos \theta_{24} d\phi \\ &= \frac{2m_1^2}{\{-\Delta_2(p_1, p_4)\}^{\frac{1}{2}}} \frac{d(p_2 \cdot p_4) d(p_3 \cdot p_4)}{\{-\Delta_4(p_1, p_2, p_3, p_4)\}^{\frac{1}{2}}}. \quad (7.21) \end{aligned}$$

The range of integration in $p_2 \cdot p_4$ and $p_3 \cdot p_4$ follows from equations (7.5) and (7.16). Within this range one has $\Delta_2 < 0$, $\Delta_4 < 0$.

In the previous subsections (a)–(d) p_1 was assumed to be timelike. The case of spacelike p_1 will be needed for more theoretically oriented purposes in section VI.3. The standard frame $S(p_1)$ is now the frame in which $p_1 = (0, 0, 0, \sqrt{(-t_1)})$ and the results derived above for timelike p_1 are to be modified in a way analogous to the transition from Figure 1.3(a) to Figure 1.3(b). This transition is fairly straightforward and we shall limit ourselves to mentioning the main results. If the coordinate axes are chosen as above in terms of p_2 and p_3 , the geometric variables are defined by the following

representation (Figure 7.2)

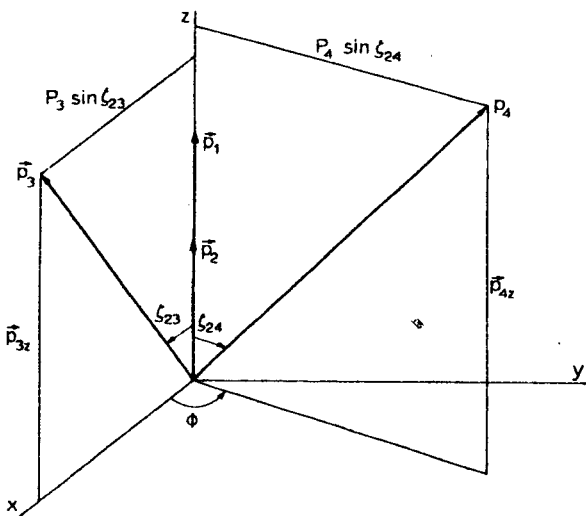


Figure II.7.2 Pseudospherical coordinates for p_4 in $S(p_1, p_2, p_3)$. The four-vector p_1 is spacelike and its 0-component vanishes in this frame. The variables P_i are defined as $P_i^2 = p_{ix}^2 + p_i^2$

$$p_1 = (0, 0, 0, \sqrt{(-t_1)})$$

$$p_2 = (P_2, 0, 0, p_{2z}) \quad (7.22)$$

$$p_3 = (P_3 \cosh \zeta_{23}, P_3 \sinh \zeta_{23}, 0, p_{3z})$$

$$p_4 = (P_4 \cosh \zeta_{24}, P_4 \sinh \zeta_{24} \cos \phi, P_4 \sinh \zeta_{24} \sin \phi, p_{4z})$$

with $p_{iz}^2 = P_i^2 - p_i^2$. Instead of P_i , θ_{2i} and ϕ (Figure 7.1), the geometric variables are now P_i , ζ_{2i} and ϕ (Figure 7.2). Their ranges follow from comparison with equations (1.18) and (1.20): $0 \leq \phi < 2\pi$, $0 \leq \zeta < \infty$, and for $p_i^2 > 0$, $m_i \leq P_i < \infty$. For $p_i^2 < 0$ the situation is slightly more complicated because one has to parametrize separately the branches $p_{iz}^2 + p_i^2 < 0$ and $p_{iz}^2 + p_i^2 > 0$; we do not write down these cases here. The required expressions for P_2 , ζ_{23} and ϕ follow directly from the following Gram determinant

reductions in the frame $S(p_1, p_2, p_3)$ defined by equation (7.22):

$$\Delta_1(p_1) = t_1$$

$$\Delta_2(p_1, p_2) = \begin{vmatrix} t_1 & \sqrt{(-t_1)} & P_{2z} \\ \sqrt{(-t_1)} & P_{2z} & p_2^2 \end{vmatrix}$$

$$= -t_1 \begin{vmatrix} -1 & P_{2z} \\ 0 & P_2^2 \end{vmatrix}$$

$$= t_1 P_2^2$$

$$\Delta_3(p_1, p_2, p_3) = \begin{vmatrix} t_1 & \sqrt{(-t_1)p_{2z}} & \sqrt{(-t_1)p_{3z}} \\ \sqrt{-t_1 p_{2z}} & p_2^2 & P_2 P_3 \cosh \zeta_{23} - p_{2z} p_{3z} \\ \sqrt{-t_1 p_{3z}} & P_2 P_3 \cosh \zeta_{23} & p_3^2 \\ & -p_{2z} p_{3z} & \end{vmatrix}$$

$$= -t_1 \begin{vmatrix} -1 & p_{2z} & p_{3z} \\ 0 & P_2^2 & P_2 P_3 \cosh \zeta_{23} \\ 0 & P_2 P_3 \cosh \zeta_{23} & P_3^2 \end{vmatrix}$$

$$= t_1 P_2^2 P_3^2 \sin^2 \zeta_{23}$$

$$\Delta_4(p_1, p_2, p_3, p_4) = t_1 P_2^2 P_3^2 P_4^2 \sinh^2 \zeta_{23} \sinh^2 \zeta_{24} \sin^2 \phi.$$

The unsymmetric Gram determinants are evaluated in Appendix A. Finally one finds that

$$dg_4 = d \cosh \zeta_{24} d\phi \quad (7.24)$$

is in invariant form given by exactly the same expression (7.21) as $d\Omega_4$ (with $m_1^2 = t_1$).

Finally, we shall consider the ambiguities occurring in the definition of azimuthal angles, equations (7.11–12). In practical cases one often has to fix the signs and order of the vectors p_2 , p_3 and p_4 by convention. Keeping $+p_2$ as the direction of the axis, and choosing different signs and orderings will lead to azimuthal angles differing by multiples of π or by sign. If one denotes the set defining ϕ as in equations (7.11–12) by $(p_2; p_3, p_4)$ so that

$$(p_2; p_3, p_4) \rightarrow \phi,$$

(see also equation (V.6.8) later) it is easy to see that

$$\begin{array}{ll}
 (-\mathbf{p}_2; \mathbf{p}_3, \mathbf{p}_4) \rightarrow 2\pi - \phi & (\mathbf{p}_2; -\mathbf{p}_3, \mathbf{p}_4) \rightarrow \pi + \phi \\
 (\mathbf{p}_2; \mathbf{p}_3, -\mathbf{p}_4) \rightarrow \pi + \phi & (-\mathbf{p}_2; -\mathbf{p}_3, \mathbf{p}_4) \rightarrow \pi + \phi \\
 (-\mathbf{p}_2; \mathbf{p}_3, -\mathbf{p}_4) \rightarrow \pi - \phi & (\mathbf{p}_2; -\mathbf{p}_3, -\mathbf{p}_4) \rightarrow \phi \\
 (-\mathbf{p}_2; -\mathbf{p}_3, -\mathbf{p}_4) \rightarrow 2\pi - \phi & (\mathbf{p}_2; \mathbf{p}_4, \mathbf{p}_3) \rightarrow 2\pi - \phi.
 \end{array} \quad (7.25)$$

8. Detailed treatment of the Lorentz transformation of a four-momentum vector

Consider now the transformation of an arbitrary four-momentum p , $p^2 = m^2$ from a frame in which it has the form $p = (E^*, \mathbf{p}^*)$ to a frame in which it has the form $p = (E, \mathbf{p})$. As the notation implies, we shall for simplicity refer to the two frames as the centre-of-momentum and target systems, but the treatment, of course, applies to any two frames. The vector p is most often the four-momentum of one of the final state particles of a collision or decay.

Depending on the purpose, the spatial component \mathbf{p} can be expressed either in Cartesian or polar coordinates:

$$\mathbf{p} = (p_x, p_y, p_z) \quad (8.1)$$

$$= P(\sin \theta \cos \phi, \sin \theta \sin \phi, \cos \theta), \quad (8.2)$$

and similarly for \mathbf{p}^* . We shall choose the direction of motion of the CMS in the TS both as the positive z axis and as the polar axis. Accordingly, the z -component of \mathbf{p} is also called the longitudinal component q of \mathbf{p} :

$$q = p_z = P \cos \theta. \quad (8.3)$$

Similarly, the transverse component r of \mathbf{p} is defined by

$$\begin{aligned}
 r &= (p_x^2 + p_y^2)^{\frac{1}{2}} \\
 &= P \sin \theta.
 \end{aligned} \quad (8.4)$$

The problem will normally have cylindrical symmetry around the z axis and only the value of r and not that of p_x, p_y separately is relevant.

If v is the velocity of the TS in the CMS, and $\gamma = (1 - v^2)^{-\frac{1}{2}}$, the basic Lorentz transformation equations (2.8) in Cartesian form give the following relations:

$$p_x = p_x^*, p_y = p_y^* \quad (8.5)$$

$$p_z = \gamma p_z^* + \gamma v E^* \quad (8.6)$$

$$E = \gamma p_z^* + \gamma E^*. \quad (8.7)$$

If the inverse relations are put into polar coordinates we have:

$$P^* \sin \theta^* = P \sin \theta \quad (8.8)$$

$$P^* \cos \theta^* = \gamma P \cos \theta - \gamma v E \quad (8.9)$$

$$E^* = -\gamma v P \cos \theta + \gamma E \quad (8.10)$$

Equations (8.5–7) or (8.8–10) contain everything necessary and our goal now is to analyse them in detail (Baldin, 1961; Dedrick, 1962; Hagedorn, 1964).

It is convenient to start from the variables P^* and E^* which are independent of the orientation of \mathbf{p}^* , i.e. to consider the transformation of the CMS sphere (Figure 8.1)

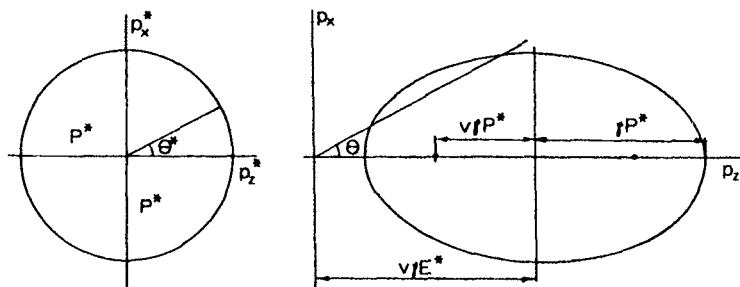


Figure II.8.1 The momentum sphere $P^* = \text{constant}$ before and after the Lorentz transformation

$$\begin{aligned} p^{*2} &= P^{*2} \\ &= p_x^{*2} + p_y^{*2} + p_z^{*2} \\ &= \text{constant}. \end{aligned} \quad (8.11)$$

Later on we shall often be able to compute P^* and E^* in terms of some other input quantities like the mass of a decaying particle, but for the moment they are just some fixed quantities related by $E^{*2} = P^{*2} + m^2$. Since the problem has cylindrical symmetry, it is sufficient to discuss how the circle of intersection of the sphere (8.11) with the xz plane (Figure 8.1) transforms. We shall for clarity divide the analysis into several different parts.

(a) Transformation of the azimuthal angle

From equation (8.5) we have

$$\begin{aligned} \operatorname{tg} \phi &= \frac{p_y}{p_x} = \frac{p_y^*}{p_x^*} \\ &= \operatorname{tg} \phi^* \end{aligned}$$

so that

$$\phi = \phi^*. \quad (8.12)$$

This is a very useful result, which can be expressed in the general form as follows: the azimuthal angle around an axis is invariant under Lorentz transformation along this axis.

(b) Transformation of the sphere (8.11) in Cartesian coordinates

In order to express equation (8.11) in terms of p_x, p_y, p_z we write equation (8.6) as

$$p_z^* = \frac{1}{\gamma} p_z - v E^*. \quad (8.13)$$

Note that one has to use p_z^* in terms of p_z and the constant quantity E^* . Introducing equations (8.5) and (8.13) in equation (8.11) we find that the sphere (8.11) is transformed into an ellipsoid (Blatón, 1950) (Figure 8.1)

$$\frac{p_x^2 + p_y^2}{a^2} + \frac{(p_z - h)^2}{b^2} = 1 \quad (8.14)$$

with

$$\begin{aligned} a &= P^* \\ b &= \gamma P^* \\ h &= \gamma v E^*. \end{aligned} \quad (8.15)$$

The distance l between the focus and the centre of the ellipsoid and its eccentricity ε are thus given by

$$\begin{aligned} l &= (b^2 - a^2)^{\frac{1}{2}} = \gamma v P^* \\ \varepsilon &= l/b = v. \end{aligned} \quad (8.16)$$

These results are easy to understand qualitatively. Under the Lorentz transformation the transverse dimensions of the sphere (8.11) have remained unchanged while longitudinally it has been dilated by γ and translated by $\gamma v E^*$.

The intercepts of the ellipsoid (8.14) with the z axis are given by the Lorentz transforms of the two CMS momentum vectors lying parallel and antiparallel to the z axis (Figure 8.2). Equation (8.6) gives immediately

$$\begin{aligned} -P^* &\rightarrow \gamma(-P^* + vE^*) = \gamma E^*(v - v^*) \\ P^* &\rightarrow \gamma(P^* + vE^*) = \gamma E^*(v + v^*) \end{aligned} \quad (8.17)$$

where $v^* = P^*/E^*$ is the CMS velocity of the particle. We see that the ellipsoids can be divided in different classes (Figure 8.3) depending on the relative magnitude of v and v^* .

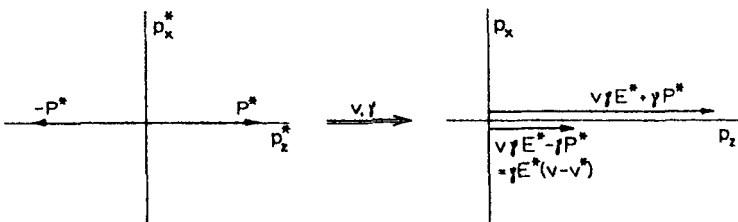


Figure II.8.2 Transformation of momenta parallel to z axis. This figure refers to the case $v > v^*$

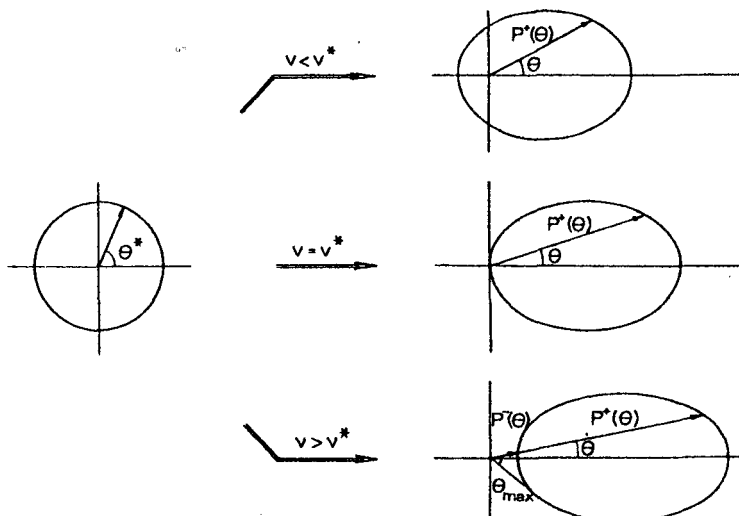


Figure II.8.3 Classification of transformed momentum ellipsoids. The CMS velocity of the particle is $v^* = P^*/E^*$ and v is the velocity parameter of the transformation (velocity of the TS in the CMS)

Class 1: $v < v^*$, the origin lies inside the ellipsoid.

Class 2: $v = v^*$, the origin lies on the ellipsoid.

Class 3: $v > v^*$, the origin lies outside the ellipsoid.

That the classification depends on the velocities is natural. Suppose a particle is moving in the negative z direction with a velocity $v^* = P^*/E^*$. In order to change from the negative to the positive z direction one clearly has to go to a frame which moves in the CMS antiparallel to the particle with a velocity v larger than v^* . The classification also implies, as is obvious from Figure 8.3, that in Class 3 the correspondence between θ and θ^* is two-to-one and that there exists a maximum angle θ_{\max} . These properties are most conveniently analysed in polar coordinates.

The separation into the different classes has practical implications, since a Class 1 particle can go in all directions in the laboratory (or TS) while Class 3 particles only go into the forward hemisphere. The smaller the mass of a particle, the larger its v^* and the more likely it is to belong to Class 1. In particular, zero mass particles like photons always belong to Class 1.

(c) Transformation of the sphere (8.11) in polar coordinates

Thus subsection is technically more complicated than subsection (b), though conceptually it just repeats the same things in different form. In CMS polar coordinates the sphere (8.11) is simply $P^* = \text{const.}$, i.e. P^* does not depend on θ^* . On the other hand, the corresponding P depends on θ (Figure 8.1). This dependence can most simply be found from equation (8.10) by writing it in the form

$$E^* + v\gamma P \cos \theta = \gamma(P^2 + m^2)^{\frac{1}{2}}, \quad (8.18)$$

squaring, and solving for $P = P(\theta)$. The choice of equation (8.10) is dictated by the fact that one needs an equation in which only P , $\cos \theta$ and some constant quantities appear. After some algebraic manipulations one finds from equation (8.18) that

$$\frac{P^\pm}{P^*} = \frac{\cos \theta(g^* \pm \sqrt{D})}{\gamma(1 - v^2 \cos^2 \theta)} \quad (8.19)$$

or

$$\frac{P^\pm}{m} = \frac{v\gamma^* \cos \theta \pm (v^{*2}\gamma^{*2} - v^2\gamma^2 \sin^2 \theta)^{\frac{1}{2}}}{\gamma(1 - v^2 \cos^2 \theta)}, \quad (8.20)$$

where

$$\begin{aligned} D &= 1 + \gamma^2(1 - g^{*2})tg^2 \theta \\ &= \frac{v^{*2}\gamma^{*2} - v^2\gamma^2 \sin^2 \theta}{v^{*2}\gamma^{*2} \cos^2 \theta} \end{aligned} \quad (8.21)$$

and, as previously defined,

$$v^* = P^*/E^*, \quad \gamma^* = E^*/m, \quad v^*\gamma^* = P^*/m,$$

v = velocity of the CMS in the TS, $\gamma = (1 - v^2)^{-\frac{1}{2}}$.

We have also introduced the quantity (Dedrick, 1962)

$$\begin{aligned} g^* &= \frac{v}{P^*/E^*} \\ &= \frac{v}{v^*} \\ &= \frac{\text{velocity of TS in CMS}}{\text{velocity of the particle in CMS}}. \end{aligned} \quad (8.22)$$

The values $g^* < 1$, $g^* = 1$, $g^* > 1$ correspond to the classes 1, 2 and 3.

Equivalently, $E^2 = P^2 + m^2$ is given as a function of θ by

$$\frac{E^\pm}{E^*} = \frac{(1 \pm vv^* \cos^2 \theta \sqrt{D})}{\gamma(1 - v^2 \cos^2 \theta)} \quad (8.23)$$

or

$$\frac{E^\pm}{m} = \frac{\gamma^* \pm v \cos \theta (v^{*2} \gamma^{*2} - v^2 \gamma^2 \sin^2 \theta)^{\frac{1}{2}}}{\gamma(1 - v^2 \cos^2 \theta)}. \quad (8.24)$$

The equations for P^\pm and E^\pm contain, for instance, the well-known equations expressing the scattering angle dependence of the momentum or energy of a final state particle in a $2 \rightarrow 2$ collision process (see later equations (IV.3.8-9)).

The existence of two solutions P^\pm is related to the occurrence of the previously distinguished three cases. From equation (8.19) and Figure 8.4 we

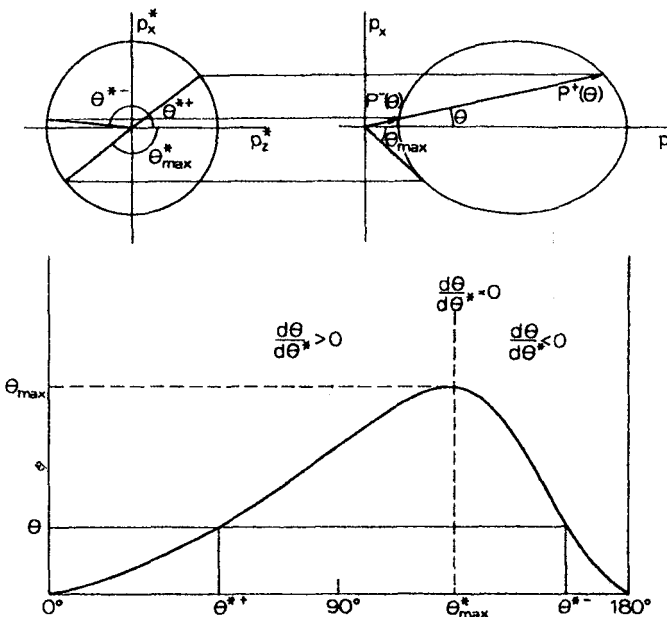


Figure II.8.4 Correspondence between the polar angles θ and θ^* in the two frames. The maximum value of θ is given by $\tan \theta_{\max} = 1/\gamma(g^{*2} - 1)^{\frac{1}{2}}$ and the resulting θ^* by $\cos \theta_{\max}^* = -1/g^*$. The figure relates to case 3, $v > v^*$.

see that the maximum value θ_{\max} of θ is obtained when the two roots coincide or $D = 0$. According to equation (8.21) this gives

$$\tan \theta_{\max} = \gamma^{-1}(g^{*2} - 1)^{-\frac{1}{2}} \quad (8.25)$$

or

$$\sin \theta_{\max} = \gamma^* v^*/\gamma v. \quad (8.26)$$

Substitution of this in equation (8.24) gives

$$E/m = \gamma/\gamma^* \quad \text{at } \theta = \theta_{\max}. \quad (8.27)$$

The maximum only exists when $g^* \geq 1$, $v \geq v^*$, that is in Classes 3 and 2 (Figure 8.3). In Class 2, $g^* = 1$, $v = v^*$, the maximum is 90° . From equation (8.21) one also finds

$$g^{*2} - D = (g^{*2} - 1)(1 + \gamma^2 \operatorname{tg}^2 \theta)$$

so that $g^* - \sqrt{D}$ or P^- has the sign of $g^{*2} - 1$. It is thus negative when $g^* < 1$ and only P^+ corresponds to a physical solution in Case 1.

When $m = 0$, the equations (8.20) and (8.24) are not directly applicable. After some modifications they reduce to the simple relation

$$P = E = \frac{P^*}{\gamma(1 - v \cos \theta)}. \quad (8.28)$$

If the wavelength of a zero-mass particle (photon) is introduced through $E = h(c/\lambda) = 2\pi/\lambda$ one has equivalently

$$\frac{\lambda}{\lambda^*} = \gamma(1 - v \cos \theta). \quad (8.29)$$

As a simple example suppose the photon is emitted towards the Earth by a celestial body receding away from the Earth with a velocity v . Then $\cos \theta = -1$ in equation (8.29) and

$$\frac{\lambda}{\lambda^*} = \sqrt{\left(\frac{1+v}{1-v}\right)} > 1.$$

This is the relativistic Doppler formula.

(d) Transformation of polar angle

The transformation equation for the polar angle θ is obtained immediately by dividing equation (8.8) by the inverse of equation (8.9), $P \cos \theta = \gamma P^* \cos \theta^* + \gamma v E^*$:

$$\operatorname{tg} \theta = \frac{\sin \theta^*}{\gamma(\cos \theta^* + g^*)}. \quad (8.30)$$

This is a simple equation, since $g^* = v/v^*$ does not depend on θ^* . In order to invert equation (8.30), one can divide equation (8.8) by equation (8.9) and obtain

$$\operatorname{tg} \theta^{*\pm} = \frac{\sin \theta}{\gamma \{\cos \theta - v/(P^\pm/E^\pm)\}}. \quad (8.31)$$

Here one has to remember that the velocity P^\pm/E^\pm of the particle in the target system also depends on θ through equations (8.19) and (8.23). It is thus more convenient to invert equation (8.30) directly by solving for $\cos \theta^*$:

$$\cos \theta^{*\pm} = \frac{-g^* \gamma^2 \operatorname{tg}^2 \theta \pm \sqrt{D}}{1 + \gamma^2 \operatorname{tg}^2 \theta}, \quad (8.32)$$

where D was given in (8.21) and where, for comparison with equations (8.19) and (8.23), it may be useful to apply the identity

$$1 + \gamma^2 \operatorname{tg}^2 \theta = \frac{\gamma^2}{\cos^2 \theta} (1 - v^2 \cos^2 \theta). \quad (8.33)$$

The CMS angle $\theta^*(\theta_{\max})$, corresponding to the maximum TS angle in Class 3, is, according to equations (8.25) and (8.32), given by

$$\begin{aligned} \cos \theta^*(\theta_{\max}) &= -1/g^* \\ &= -v^*/v. \end{aligned} \quad (8.34)$$

Again this is physical only for $g^* \geq 1$.

The behaviour of the solutions (8.30) and (8.32) in the $\theta^* \theta$ plane is shown qualitatively in Figure 8.5 for the three cases and in detail for Class 3 in Figure 8.4. These figures should be consulted in parallel with Figure 8.3.

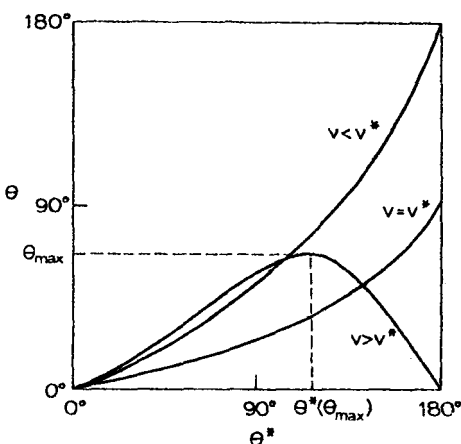


Figure II.8.5 Qualitative dependence of θ on θ^* in the three cases $v < v^*$, $v = v^*$ and $v > v^*$

Exercises

- II.1. The Stanford linear electron accelerator is 3 km long and accelerates the electrons to an energy of $E = 20 \text{ GeV}$. The energy of the electron is linearly proportional to the distance covered. What is the total length of the accelerator seen by the electron?
- II.2. Derive a Lorentz transformation formula generalizing equation (1.1) to a case in which the velocity of S' in S has an arbitrary direction. Use the fact that the components of \mathbf{x} perpendicular to \mathbf{v} are unchanged while the parallel components transform as z in equation (1.1).
- II.3. (a) What are the maximum values of v and γ if one wants to write $E = m + p^2/2m$ so that the error is less than $\epsilon \cdot p^2/2m$?
 (b) What are the minimum values of v and γ , if one wants to write $E \cong p$ so that the error is less than $\epsilon \cdot p$? Formulate the conditions for the validity of the non-relativistic and relativistic approximations if $\epsilon = 1$ per cent.
- II.4. An electron, a pion and a proton have each a momentum $1 \text{ GeV}/c$. What are the times these particles need to cover a distance of 3 m?
- II.5. The four-acceleration a^μ is defined by the equation
- $$a^\mu = du^\mu/d\tau.$$
- (a) Determine a^0 and \mathbf{a} ,
 (b) Prove that $a \cdot u = 0$,
 (c) Evaluate the invariant $a \cdot a$ if the particle to which a^μ refers follows a straight path.
- II.6. In a proton-proton experiment at $19 \text{ GeV}/c$ ($\sqrt{s} = 6.12 \text{ GeV}$) one observes in the final state a proton with a momentum $4 \text{ GeV}/c$ at an angle 30° relative to the beam axis. What are the energy and momentum of the produced proton in the centre-of-momentum system?
- II.7. Suppose a proton-proton experiment is done at a fixed incident momentum P_s^T , and consider a momentum vector of a final state particle which is perpendicular to the beam direction in the centre-of-momentum system. If its length varies between zero and its maximum value (determine this maximum), how does the corresponding momentum vector vary in the target system? Draw a figure with the numerical values of Problem II.6.
- II.8. Check the correctness of the calculations in Problems II.6 and II.7 by computing the magnitude of the transformed momentum vector both from $P = (p_x^2 + p_y^2 + p_z^2)^{\frac{1}{2}}$ and from $P = (E^2 - m^2)^{\frac{1}{2}}$.

- II.9. Consider a Lorentz transformation of a four-momentum between S' and S (S' moves in S with velocity v parallel to $+z$ axis) and divide the four-momentum into transverse ($r = (p_x^2 + p_y^2)^{\frac{1}{2}}$) and longitudinal ($q = p_z$) components.
- What are the transforms of the vectors in S' with $q' = \text{constant}$ in S , that is how does the plane $q' = \text{constant}$ transform?
 - What are the transforms of the vectors $r' = \text{constant}$, that is how does the cylinder $r' = \text{constant}$ transform?
- II.10. Suppose two particles have equal velocities (in magnitude and direction) in some Lorentz system. How are their velocities in any other Lorentz frame related? What if velocities are replaced by three-momenta?
- II.11. Show that for $m = 0$ the relation (8.32) giving θ^* in terms of θ can be written as
- $$\cos \theta^* = \frac{\cos \theta - v}{1 - v \cos \theta}.$$
- II.12. (a) The width of the η -meson is $\Gamma_\eta \simeq 2.6 \text{ keV}$. What is the lifetime of the η ?
- (b) The lifetime of the π^0 is $T_{\pi^0} \simeq 0.89 \times 10^{-16} \text{ sec}$. What is the width of the π^0 ?
- II.13. Derive the Lorentz transformation formula for three-velocity \mathbf{v} by (a) using the definition of $\mathbf{v} = dx/dt$ and the transformation properties of x^μ , (b) using the transformation properties of four-velocity.
- II.14. Consider the transformation from the target system TS ($\mathbf{p}_b = 0$) to the beam system BS ($\mathbf{p}_a = 0$). What are the transformation parameters? How is the velocity v_a^T of a particle a in TS related to the velocity v_b^B of particle b in BS?
- II.15. Equation (7.10) gives $\sin^2 \theta_{23}$ and equation (7.8) $\cos \theta_{23}$ in terms of invariants. Show by direct computation that these results are compatible.
- II.16. Show by explicit calculation of the components in the frame $\mathbf{p}_1 = 0$ that the scalar product of two vectors of type $c_v = \epsilon_{\kappa\lambda\mu\nu} p_1^\kappa p_2^\lambda p_3^\mu$ in equation (A.16) in Appendix A gives $G \begin{pmatrix} p_1 & p_2 & p_3 \\ p_1 & p_4 & p_5 \end{pmatrix}$ in equation (A.30).
- II.17. Let A be the 4×4 matrix formed by the components of the four-vectors p_1, p_2, p_3, p_4 , and $g = (g^{\mu\nu})$ be the metric tensor. Show that

$$\begin{aligned}\Delta_4 &= \text{Det}(AgA^T) \\ &= -(\text{Det } A)^2.\end{aligned}$$

- II.18. Show that if the momenta \mathbf{p}_a and \mathbf{p}_b are parallel, then $E_a P_b - P_a E_b$ is invariant under boosts along \mathbf{p}_a , and its value is

$$\begin{aligned} E_a P_b - P_a E_b &= \{-\Delta_2(p_a, p_b)\}^{\frac{1}{2}} \\ &= \frac{1}{2}\lambda^{\frac{1}{2}}(s, m_a^2, m_b^2). \end{aligned}$$

Note that the velocity difference $v_b - v_a$ is not invariant under these transformations but $E_a E_b(v_b - v_a)$ is.

- II.19. Let \mathbf{w} and \mathbf{w}' be the values of a velocity in frames S and S' , \mathbf{v} the relative velocity of S and S' , and assume that the angles between \mathbf{w} and \mathbf{v} and between \mathbf{w}' and \mathbf{v} are θ , and θ' . Denote the rapidities corresponding to \mathbf{v} , \mathbf{w} and \mathbf{w}' by ξ , ζ , ζ' , respectively. Prove the transformation equations

$$\gamma(w') = \gamma(v)\gamma(w)(1 - \mathbf{v} \cdot \mathbf{w}/c^2),$$

$$\cosh \zeta' = \cosh \xi \cosh \zeta - \sinh \xi \sinh \zeta \cos \theta,$$

$$\operatorname{tg} \theta' = \frac{\sinh \zeta \sin \theta}{\cosh \xi \sinh \zeta \cos \theta - \sinh \xi \cosh \zeta}.$$

Show also that if the rapidities are interpreted as imaginary angles, these formulas are equivalent to equations (B.4) and (B.10) in Appendix B. The rapidities ξ , ζ , ζ' can be regarded as the sides of a triangle on the pseudosphere $u^2 = c^2$ (Werle, 1966, pp. 342–348).

III

Phase Space

1. Definition of phase space

So far we have essentially considered only properties of the initial state of a scattering process and Lorentz transformations of unconstrained final state momentum vectors. Turning now to the complete particle reaction $p_a + p_b \rightarrow p_1 + \dots + p_n$ (Figure 1.1(a)) we have to impose the condition of four-momentum conservation on the final state momentum vectors:

$$\begin{aligned} E_a + E_b &= \sum_{i=1}^n E_i \\ \mathbf{p}_a + \mathbf{p}_b &= \sum_{i=1}^n \mathbf{p}_i \end{aligned} \tag{1.1}$$

with

$$E_i^2 = \mathbf{p}_i^2 + m_i^2, \quad i = a, b, 1, \dots, n.$$

The m_i are fixed particle masses. Due to four-momentum conservation the n momentum vectors \mathbf{p}_i cannot vary arbitrarily for a fixed initial state, but have to satisfy the four conditions (1.1). We shall call the $3n$ dimensional space of the unconstrained final state momentum vectors \mathbf{p}_i the *momentum space*. The conditions (1.1) define in this space a $3n - 4$ dimensional surface which will be called the *phase space*. Sometimes the terms momentum space and phase space are used synonymously for the $3n$ dimensional space, and the $3n - 4$ dimensional space is called a surface of constant energy and momentum. We have adopted the definitions above in order to fix a concise and unique terminology. In terms of momenta, the structure of the momentum space is simple, while the structure of the phase space is more complicated.

In studying the dynamics of particle processes, the momentum vectors \mathbf{p}_i are rarely useful variables. To exhibit interesting features of data or to formulate theoretical models, one needs variables, such as invariant masses or momentum transfers, in terms of which the description of phase space often turns out to be extremely complex. A large part of our subsequent effort will go to parametrizing phase space using various sets of variables motivated by dynamics.

Both kinematically and dynamically it is important to distinguish between two different types of experiments: measurement of exclusive or inclusive reactions. An *exclusive* reaction (Figure 1.1(a)) is one in which all particles and their momenta are known, as in a completely identified bubble chamber event. In an *inclusive* reaction (Figure 1.1(b)) only some of the particles and their momenta are known so that the final state is not completely identified. An experimental realization is a counter experiment with m spectrometer arms. We also note that in an exclusive reaction the reaction channel is fixed while an inclusive experiment involves a sum over different exclusive channels and multiplicities. Exclusive processes will be discussed in Chapters IV–VI, inclusive processes in Chapter VII.

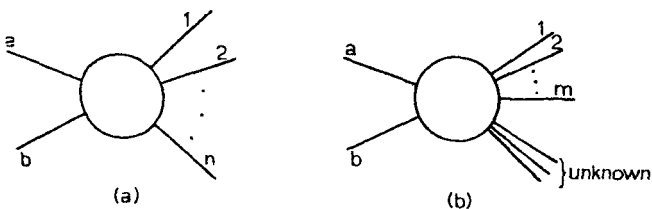


Figure III.1.1 An exclusive (a) and inclusive (b) reaction

Two types of exclusive process are encountered in practice: **a particle decay**.

$$p_0 \rightarrow p_1 + p_2 + \dots + p_m, \quad (1.2)$$

and a **collision of two particles**,

$$p_a + p_b \rightarrow p_1 + p_2 + \dots + p_n. \quad (1.3)$$

For conciseness, the first is called a $1 \rightarrow m$ process, the latter a $2 \rightarrow n$ process. When computing the number of essential variables for these processes spin will be neglected, as is done everywhere in this book. In equation (1.2), the number of variables p_1, \dots, p_m , constrained by four-momentum conservation, is $3m - 4$. However, absence of spin implies that in the rest frame of the decaying particle the orientation of the momentum configuration is irrelevant. This means that three variables are trivial and there remain $3m - 7$ **essential variables**. All the masses m_0, m_1, \dots, m_m are here regarded as fixed. In equation (1.3) there are $3n - 4$ **final state variables**. The beam axis (direction of p_a in the TS or CMS) defines a direction in space, and there is just one trivial variable ϕ , corresponding to rotation around the beam axis. In this case there are thus $3n - 5$ **essential final state variables**. If one now also takes the initial state of equation (1.3) into consideration, there is one further essential variable, the total energy squared s , and there are in all $3n - 4$

essential variables. These numbers are presented in Table III.1 together with some examples of sets of variables.

If we put $m = n + 1$, $p_a = p_0$, $p_b = -p_m$, it is seen that equations (1.2) and (1.3) are related by crossing, that is equation (1.3) is obtained from (1.2) by moving one particle from the final to the initial state (Section IV.4). In this case the total number of essential variables $3n - 4 = 3m - 7$ is the same for equations (1.2) and (1.3). There is a much deeper connection between the kinematics of processes related by crossing; it will be shown in Sections VI.7–8 that in invariant variables the physical regions of two such processes are given by the same equations and that the phase space density $\rho(\Phi)$ (defined in equation (2.14) below) is the same for both.

In summary, we see that the phase spaces for processes $1 \rightarrow n$ and $2 \rightarrow n$, with $m_0^2 = s$, are the same $3n - 4$ dimensional regions. In the latter there is one specified space direction, the beam axis, and thus in addition to identical parametrizations of the phase space for the two processes, there are some which are more complex for $2 \rightarrow n$ than for $1 \rightarrow n$. Regardless of this, the identity of the phase spaces implies a definite type of equivalence of the reactions $1 \rightarrow n$ and $2 \rightarrow n$. On the other hand, the processes $1 \rightarrow n + 1$ and $2 \rightarrow n$ are related by crossing, and this causes a different type of equivalence which is especially evident when invariant variables are used. In the chain $1 \rightarrow 2$, $2 \rightarrow 2$, $1 \rightarrow 3$, $2 \rightarrow 3$, ..., the neighbouring processes are thus close relatives. This fact determines to a great extent the logical structure of this book.

Table III.1. Different ways of counting variables in the absence of spin, with illustrations for processes $1 \rightarrow 3$ and $2 \rightarrow 2$. The variables quoted are defined in Chapters IV and V, ϕ is everywhere an angle describing rotations around the beam axis ($2 \rightarrow n$) or some axis

	\Leftrightarrow	($1 \rightarrow m$)		
Number of Variables for $1 \rightarrow m$			Number of Variables for $2 \rightarrow n$	Example for $2 \rightarrow 2$
All Variables	—	—	$3n - 3$	s, t, ϕ
Essential Variables	—	—	$3n - 4$	s, t
Final State Variables	$3m - 4$	$s_1, s_2, \theta_1,$ ϕ_1, ϕ	$3n - 4$	t, ϕ
Essential Final State Variables	$3m - 7$	s_1, s_2	$3n - 5$	t

2. Integration over phase space and cross-sections

According to the usual formalism for the dynamics of particle reactions, the transition probability from an initial state $p_a + p_b$ to a final state with

definite momenta \mathbf{p}_i is obtained from a matrix element

$$\langle \mathbf{p}_1, \dots, \mathbf{p}_n | A | \mathbf{p}_a, \mathbf{p}_b \rangle \equiv A(\mathbf{p}_i). \quad (2.1)$$

The purpose of experiments is to clarify the structure of $A(\mathbf{p}_i)$, and the conclusions are theoretically described in the form of different dynamical models specifying $A(\mathbf{p}_i)$. Later on we shall present some general properties that $A(\mathbf{p}_i)$ is known to satisfy, but for the moment it is sufficient to consider it as some unknown function of the \mathbf{p}_i .

In order to obtain measurable quantities (for $n > 2$), the square $|A(\mathbf{p}_i)|^2$ of the matrix element (2.1), which will be denoted by $T(\mathbf{p}_i)$ or simply by T , has to be integrated over a set of allowed values of the \mathbf{p}_i . The **total reaction cross-section** is obtained when the integration is over all possible values of the \mathbf{p}_i , that is over the entire $3n - 4$ dimensional phase space. The corresponding quantity for decay is the **lifetime**. If the integration is restricted to a subset of the phase space, a **differential cross-section** or, if the absolute magnitude is inessential, a **distribution** is obtained. How exactly $T(\mathbf{p}_i)$ and the cross-sections are related, depends on some normalization conventions. The derivations can be found in textbooks on high energy physics (for instance, Källén, 1964). For our purposes it is sufficient just to state the results.

(a) Total reaction cross-section

Denoting the total reaction cross-section of a fixed channel by $\sigma_n \equiv \sigma_n(s; m_i)$ we have

$$\sigma_n = \frac{1}{F} I_n(s), \quad (2.2)$$

where

$$F = 2\lambda^4(s, m_a^2, m_b^2)(2\pi)^{3n-4} \quad (2.3)$$

is the **flux factor** (we include the powers of 2π in the definition) and

$$I_n(s) = \int \prod_{i=1}^n \frac{d^3 p_i}{2E_i} \delta^4 \left(p_a + p_b - \sum_i p_i \right) T(\mathbf{p}_i) \quad (2.4)$$

contains the integration over the phase space. The conservation of four-momentum has been accounted for by including a four-dimensional δ function, which is a product of four δ functions corresponding to the four components p^μ . The dependence on m_i is suppressed in the notation. We shall presently discuss the reasons for including the factors of $2E$ in the definition of $I_n(s)$. It is important to emphasize that equation (2.2) defines the normalization of $A(\mathbf{p}_i)$, that is what constants and s dependent factors are

attached to $A(\mathbf{p}_i)$ by convention. In this sense the derivation of equation (2.2) is not essential; it can be understood as a definition.

(b) Lifetime

The formula for the lifetime τ for the decay of an unstable particle of mass m to a fixed final state is very much similar to equation (2.2):

$$\frac{1}{\tau} = \frac{1}{2m} \frac{1}{(2\pi)^{3n-4}} I_n(m^2), \quad (2.5)$$

where $I_n(m^2)$ is given by

$$I_n(m^2) = \int \prod_{i=1}^n \frac{d^3 p_i}{2E_i} \delta^4 \left(p - \sum p_i \right) |\langle \mathbf{p}_1, \dots, \mathbf{p}_n | A | \mathbf{p} \rangle|^2. \quad (2.6)$$

(c) Differential cross-section

If $x = x(\mathbf{p}_i)$ is any variable depending on the \mathbf{p}_i , the differential cross-section $d\sigma_n/dx$ is obtained by transforming the integral in equation (2.4) so that x appears as a variable and then omitting the integration over x . In practice, this can be most simply carried out by inserting the constraint $x = x(\mathbf{p}_i)$ in the integrand as a δ function so that

$$\frac{d\sigma_n}{dx} = \frac{1}{F} \int \prod_{i=1}^n \frac{d^3 p_i}{2E_i} \delta^4 \left(p_a + p_b - \sum_i p_i \right) \delta(x - x(\mathbf{p}_i)) T(\mathbf{p}_i) \quad (2.7)$$

This trivially satisfies $\int dx \cdot (d\sigma_n/dx) = \sigma_n$. Equation (2.7) is very convenient and will be used frequently. Higher-order differential cross-sections $d^2\sigma/dx dy$, etc., are obtained similarly by inserting more δ functions.

(d) Distribution

If $d\sigma/dx$ is a differential cross-section, the corresponding distribution $w(x)$ is defined by

$$w(x) = \frac{1}{\sigma} \frac{d\sigma}{dx}. \quad (2.8)$$

This is clearly normalized to unity:

$$\int dx w(x) = \frac{1}{\sigma} \int dx \frac{d\sigma}{dx} = 1.$$

Distributions $w(x, y)$, $w(x, y, z)$, etc. depending on more variables are defined similarly in terms of higher order differential cross-sections.

(e) Change of variables in distributions

Consider for example a three-variable distribution $w(x, y, z)$. If x, y and z are related to x', y' and z' in a one-to-one fashion, we see from the generalization of equation (2.8), using a basic theorem of differential calculus, that the new three-variable distribution is

$$\begin{aligned} w'(x', y', z') &= \frac{1}{\sigma} \frac{d^3\sigma}{dx' dy' dz'} \\ &= \frac{1}{\sigma} \frac{d^3\sigma}{dx dy dz} \frac{\partial(x, y, z)}{\partial(x', y', z')} \\ &= \frac{\partial(x, y, z)}{\partial(x', y', z')} w(x, y, z). \end{aligned} \quad (2.9)$$

Equation (2.9) is strictly valid if the correspondence between x, y, z and x', y', z' is one-to-one; if this is not true each of the regions corresponding to one region of the other set must be carefully accounted for. It is then sufficient to calculate the Jacobian $\partial(x, y, z)/\partial(x', y', z')$ of the transformation of variables. When the transformation equations between primed and unprimed variables are known this is just a technical problem. The Jacobian is, by definition, always positive. Equation (2.9) will find several applications in Sections 4 and VII.1. In particular, it has to be used when Lorentz transforming distributions from one frame to another.

Consider now in more detail the integral $I_n(s)$. In its definition (2.4) we have included the factor $\prod_i (2E_i)^{-1}$, where E_i means $(p_i^2 + m_i^2)^{\frac{1}{2}}$, in the integration over the p_i . This factor could, in principle, be included in A , but it is kept separate since the quantity $d^3p/2E$ is invariant under Lorentz transformations. The invariance of d^3p/E follows immediately from equation (II.1.35). One can also prove it directly by differentiating the transformation formulas (II.8.5–7) for four-momentum. One finds that

$$\begin{aligned} dp_x &= dp'_x \\ dp_y &= dp'_y \\ dp_z &= \gamma(dp'_z + v dE') \\ &= \gamma dp'_z(1 + vp'_z/E') \\ &= dp'_z E'/E, \end{aligned}$$

since $dE'/dp'_z = p'_z/E'$ and $E = \gamma(E' + vp'_z)$. The volume element $d^3p = dp_x dp_y dp_z$ thus satisfies

$$d^3p'/E' = d^3p/E \quad (2.10)$$

so that the combination d^3p/E is invariant.

Written in an integral form equation (II.1.35) implies for a timelike p that

$$\frac{d^3 p}{2E} = \int d^4 p \delta(p^2 - m^2) \Theta(p^0), \quad (2.11)$$

where the second integral is extended over all values of the components p^μ , $\mu = 0, \dots, 3$. The *step function* $\Theta(p^0)$ is zero for $p^0 < 0$ and 1 for $p^0 > 0$. It is also invariant under the orthochronous Lorentz transformations considered here. Writing $p^2 = (p^0)^2 - \mathbf{p}^2$ and $E^2 = \mathbf{p}^2 + m^2$ and using the following property of the δ function integrations:

$$\begin{aligned} \delta(f(x)) &= \frac{1}{|f'(x_0)|} \delta(x - x_0) \\ f(x_0) &= 0, \end{aligned} \quad (2.12)$$

one can easily prove equation (2.11) directly. Equation (2.11) also explains the factor 2 added conventionally to the invariant $d^3 p/E$. Formula (2.11) is often used to write the integrals (2.4), (2.6) and (2.7) in other equivalent forms, e.g.

$$I_n(s) = \int \prod_{i=1}^n d^4 p_i \delta(p_i^2 - m_i^2) \Theta(p_i^0) \delta^4(p_a + p_b - \sum_i p_i) T(\mathbf{p}_i) \quad (2.13)$$

Here the Θ function is usually not written explicitly.

For applications, the integral (2.4), which is written in terms of momenta, usually has to be transformed into some other set of variables. This may be required because T is expressed in terms of some definite set of dynamically motivated variables or because some of the required differential cross-sections $d\sigma/dx$ involve x_s which are not momentum variables. Furthermore, the δ function in equation (2.4) is a singular function. Thus for many purposes it has to be eliminated, for instance if one wants to calculate equation (2.4) numerically. After the elimination one has $3n - 4$ variables which are only constrained by limits of integration and not by any singular constraints. Calling this set of variables Φ we shall write (2.4) in the form

$$I_n(s) = \int d\Phi \rho_n(\Phi) T(\Phi) \quad (2.14)$$

where $d\Phi$ is a volume element in the $3n - 4$ dimensional phase space and the *phase space density* $\rho_n(\Phi)$ contains all factors arising from transforming from the \mathbf{p}_i in equation (2.4) to the variables Φ . These include factors arising from integrations over the δ functions according to equation (2.12) and a Jacobian. The exact relation between equations (2.4) and (2.14) will be more transparent after we have given concrete examples.

When $\mathbf{p}_1, \dots, \mathbf{p}_n$ vary over the whole phase space, the set Φ varies over a $3n - 4$ dimensional region which is the *physical region of Φ* . Similarly, if x

is any single kinematical variable, the *physical region in x* is defined as the range of variation of x as p_1, \dots, p_n varies over phase space. Analogously one defines the two-dimensional physical region in a pair of variables (x, y) , and also physical regions in several variables. If x, \dots, z are included among the variables in Φ , the physical region in x, \dots, z is a projection of the $3n - 4$ dimensional physical region of Φ on the x, \dots, z subspace. One may also consider the *physical region in x for fixed values of some other variables* (see Section V.4).

3. The phase space integral

If the matrix element squared T is identically 1, the integral $I_n(s)$ defined in equation (2.4) is called the *phase space integral*. Denoting I_n in this case by R_n , we have

$$R_n(s) = \int \prod_{i=1}^n \frac{d^3 p_i}{2E_i} \delta^4(p - \sum p_i), \quad (3.1)$$

where $s = p^2$. There is no deep theoretical reason for giving $A \equiv 1$ a special treatment; it is just the simplest possible choice. In fact, experimentally one knows that at high energies A may vary considerably over phase space. If R_n is used for I_n in equations (2.2) or (2.5), the total cross-section or lifetime is said to be given by *phase space*. Similarly, all distributions $d\sigma/dx, d^2\sigma/dx dy$, etc. derived from equation (2.7) under the assumption $A \equiv 1$ are called *phase space distributions*. In general, the experimentally measured distributions tend to deviate from phase space predictions more and more as the energy increases.

Historically, phase space distributions have played a significant role as resonance backgrounds in connection with a search for resonances. The assumption was made that $A \equiv 1$ somehow gives the consequences of pure kinematics and any deviation from this denotes a dynamical effect, for instance, a resonance. This works at lower energies where the matrix element really is rather constant, but at higher energies the separation of kinematical and dynamical effects becomes involved. This question will be discussed later on in connection with kinematical reflections (Chapter VIII).

R_n has one technically very important use. If I_n is transformed to new variables Φ as in equation (2.14), the phase space density $\rho_n(\Phi)$ is, of course, independent of the matrix element. Similarly, the physical region of Φ does not depend on A . This also applies to any projections of the physical region, such as the boundaries of the physical region in the variable x , or in the xy plane, etc. The specification of the physical region only involves four-momentum conservation and the form of A does not enter. Thus we see that both of these central problems, determination of the range of Φ and calculation of the weight function $\rho_n(\Phi)$ for a given set Φ , can be solved considering

just R_n . In the next chapters a large part of the discussion will deal with transformations of R_n to various physically motivated sets Φ . These expressions will then give I_n , σ or any $d\sigma/dx$, etc., simply by just inserting $|A|^2$ inside the integral.

Other special choices of A may also be given a special treatment. One example is the *non-covariant phase space integral* $R_n(p^\mu)$, defined by

$$R_n(p^\mu) = \int \prod_{i=1}^n d^3 p_i \delta^4(p - \sum p_i) \quad (3.2)$$

or by choosing $T = \prod_i (2E_i)$. For many purposes equation (3.2) would be as convenient as equation (3.1), but due to its noncovariance it is far more difficult to handle (Lepore, 1954; Block, 1956; Cerulus, 1958).

Turning now to another aspect of phase space integration, we point out that there is a direct formal analogy between phase space in statistical physics and that in particle physics. This is due to the fact that both in relativistic quantum statistics and in the study of final states of particle collisions a state is determined by a set of four-momenta p_1, \dots, p_n . In order to discuss this connection we shall mention here some concepts of statistical mechanics (Huang, 1967). The following remarks are not needed for the understanding of the rest of this book.

To make the momentum spectrum discrete, one assumes in quantum mechanics that particles are enclosed in a box of volume V . Then the volume element $d^3 p$ of momentum space contains $(V/(2\pi)^3) d^3 p$ states. For a relativistic particle, the number of states is (see equation (2.11))

$$\begin{aligned} dN &= V \frac{m}{E} \frac{d^3 p}{(2\pi)^3} \\ &= 2mV \frac{d^4 p}{(2\pi)^3} \delta(p^2 - m^2). \end{aligned} \quad (3.3)$$

The factor $y^{-1} = m/E$ corresponds to the fact that the box, as seen by the particle, is Lorentz contracted. The quantity (3.3) is clearly invariant.

In particle physics one calculates total cross-sections, in statistical physics partition functions. Both are sums over all states that are allowed by external constraints. One very common constraint is to require total energy and momentum and the particle number (number of particles of each type) to have fixed values. The sum over states is then

$$I_n = \frac{1}{(2\pi)^{3n-4}} \int \prod_{i=1}^n d^4 p_i \delta(p_i^2 - m_i^2) \delta^4(p_{\text{tot}} - \sum p_i) T_n. \quad (3.4)$$

The factor $(2\pi)^{-4}$ is due to the normalization of $\delta^4(\dots)$, and the function T_n depends on the process.

The standard expression (3.4) for the integral over phase space differs from a direct sum over states in that the factor $2mV$ in equation (3.3) has been omitted. As a result the number of states will not be a dimensionless quantity, and the dimensions of equation (3.4) will depend on n . Because the difference amounts only to a redefinition of T_n , we here adhere to the usual convention (3.4).

Taking $T_n \equiv 1$ we see that the phase space integral R_n is identical to the partition function of a relativistic ideal gas. More exactly, it is the microcanonical partition function taken in the microcanonical ensemble in which the total energy and momentum and the number of particles of each type are fixed.

Now one may make use of the result from statistical physics that the thermodynamic functions of different ensembles differ only by terms which are of order $N^{-\frac{1}{2}}$ where N is the number of degrees of freedom of the system. Suppose we take the canonical ensemble in which temperature T is fixed and energy can vary. The canonical partition of the relativistic ideal gas is

$$Q_n = \frac{1}{(2\pi)^{3n-4}} \int \prod_{i=1}^n \{d^4 p_i \delta(p_i^2 - m_i^2) e^{-\beta \cdot p_i}\}. \quad (3.5)$$

The four-vector β is a generalized inverse temperature, and its length is $|\beta| = 1/T$ (see Section IX.6). The quantity (3.5) without the four-fold δ function is much easier to evaluate than the corresponding equation (3.4). The error $(Q_n - R_n)/R_n$ is proportional to $N^{-\frac{1}{2}} \approx (3n)^{-\frac{1}{2}}$ (Lurçat, 1964). Due to $n \simeq 10^{24}$, in statistical physics the different partition functions give identical thermodynamics. In particle physics one can also use equation (3.5) to calculate the complicated phase space integral (3.4) (cross-section) of a multiparticle process. This statistical method is the subject of Section IX.6.

If the constraint on particle number is relaxed, the appropriate ensemble is the grand canonical one. In this the particle number is replaced by its complementary variable, fugacity. This situation occurs for total cross-sections and for inclusive processes where sums over different channels are involved.

If A is not constant, particle collisions have a formal analogy to an interacting relativistic gas. Because $|A|^2$ and the corresponding $e^{-\beta U}$, where U is interaction potential, have very different forms, the analogy is not very direct. However, many of the statistical concepts are useful here. Thus, for example, cluster expansions of statistical physics (Huang, 1963) also express relations between correlation functions of inclusive processes (Section VII.7). One can even carry the analogy to the level of thermodynamics (Hagedorn, 1965) or hydrodynamics (Landau, 1953). It is essential to realize that although the analogy at the level of statistics, based on the large number of degrees of freedom, is complete, the derived quantities have a completely different

physical origin and interpretation. Thus arguments based on usual thermodynamics are not applicable as such; the laws of 'thermodynamics' of particle processes must be based directly on the properties of I_n and its derivatives.

4. Lorentz transformations of one-particle distributions

We shall now treat in some detail Lorentz transformation properties of *one-particle distributions*. This section may be omitted at first reading; it is just an application of equation (2.9):

A one-particle distribution or *spectrum* is obtained either from an inclusive reaction (Chapter VII)



where X denotes an unknown system of particles, or from an exclusive reaction. In either case one, in principle, counts the number of particles of a certain type arriving in a solid angle $d\Omega$ at Ω within a momentum interval dP at P . The distribution measured is then

$$w(P, \cos \theta, \phi) \equiv w(P, \Omega) = \frac{1}{\sigma} \frac{d^3\sigma}{dP d\Omega}. \quad (4.2)$$

If the situation is cylindrically symmetric around the beam direction (z axis), $w(P, \Omega)$ does not depend on ϕ and one actually measures

$$w(P, \cos \theta) = \frac{1}{\sigma} \frac{d^2\sigma}{dP d\cos \theta}. \quad (4.3)$$

If no momentum analysis is carried out one effectively integrates over P in equation (4.3) and measures

$$\begin{aligned} w(\cos \theta) &= \frac{1}{\sigma} \frac{d\sigma}{d \cos \theta} \\ &= \frac{2\pi}{\sigma} \frac{d\sigma}{d\Omega} \end{aligned} \quad (4.4)$$

or

$$\begin{aligned} w(\theta) &= \frac{1}{\sigma} \frac{d\sigma}{d\theta} \\ &= \sin \theta w(\cos \theta). \end{aligned} \quad (4.5)$$

For two-particle final states at fixed total energy the magnitude P is determined by θ so that the integration over P is trivial.

The set of variables in equations (4.2–5) is not unique; other choices are treated in detail in Chapter VII. Here we shall only consider how the

distributions (4.2–5) are transformed when going from one Lorentz system to another. These transformation equations follow directly from equation (2.9) and the results of Section II.8.

(a) Transformation of one-dimensional one-particle distributions

When reading this subsection it is useful to keep Figure II.8.4 in mind. Considering first the transformation of $w(\theta)$ or $w(\cos \theta)$, we have according to equation (2.9)

$$w(\theta) = \sum_{\pm} \frac{d\theta^{*\pm}}{d\theta} w^*(\theta^{*\pm}). \quad (4.6)$$

Note that we have to face the fact that in Class 3 (Section II.8) a single value of θ ($\leq \theta_{\max}$) corresponds to two values of $\theta^{*\pm}$ (Figure II.8.4). However, if the detector is able to separate the two branches P^\pm by momentum analysis we may write

$$w(\theta) = \frac{d\theta^*}{d\theta} w(\theta^*). \quad (4.7)$$

This also applies in Classes 1 and 2 where only P^+ is to be considered. The transformation properties of $w(\cos \theta)$ follow from those of $w(\theta)$, since

$$\begin{aligned} \frac{d\Omega^*}{d\Omega} &= \frac{d \cos \theta^*}{d \cos \theta} \\ &= \frac{\sin \theta^*}{\sin \theta} \frac{d\theta^*}{d\theta} \\ &= \frac{P}{P^*} \frac{d\theta^*}{d\theta}. \end{aligned} \quad (4.8)$$

By differentiating equation (II.8.30) one finds after some algebra

$$\frac{d\theta}{d\theta^*} = \frac{\cos^2 \theta (1 + g^* \cos \theta^*)}{\gamma(g^* + \cos \theta^*)^2}. \quad (4.9)$$

This can now be expressed either in terms of CMS or TS variables. In CMS variables, inserting $\cos^2 \theta$ from equation (II.8.30), one gets

$$\frac{d\theta}{d\theta^*} = \frac{\gamma(1 + g^* \cos \theta^*)}{\gamma^2(g^* + \cos \theta^*)^2 + \sin^2 \theta^*}. \quad (4.10)$$

To calculate $d\cos \theta^*/d\cos \theta$ it is simplest to use equations (II.8.6) and (II.8.8) to obtain

$$\begin{aligned} \frac{P^2}{P^{*2}} &= \frac{(P \cos \theta)^2 + (P \sin \theta)^2}{P^{*2}} \\ &= \gamma^2(g^* + \cos \theta^*)^2 + \sin^2 \theta^*. \end{aligned} \quad (4.11)$$

This gives, using equation (4.8)

$$\frac{d \cos \theta}{d \cos \theta^*} = \frac{\gamma(1 + g^* \cos \theta^*)}{\{\gamma^2(g^* + \cos \theta^*)^2 + \sin^2 \theta^*\}^{\frac{1}{2}}}. \quad (4.12)$$

From these equations one sees that the derivative $d\theta^*/d\theta$ vanishes when $\cos \theta = -1/g^*$, as shown earlier in equation (II.8.34). For smaller θ^* the derivative is positive, for larger θ^* it is negative (Figure II.8.4).

In TS variables, which are to be used if one wants to construct $w(\theta)$ from $w(\theta^*)$, one again has to give attention to the double-valuedness of the Class 3 solution (II.8.32) giving $\cos \theta^{*\pm}$ in terms of θ . Inserting equation (II.8.32) in equation (4.9) one has

$$\begin{aligned} \frac{d\theta^{*\pm}}{d\theta} &= \frac{1}{\gamma(1 - v^2 \cos^2 \theta)} \frac{g^* \pm \sqrt{D}}{(\pm \sqrt{D})} \\ &= \frac{P^\pm}{P^*} \frac{1}{(\pm \cos \theta \sqrt{D})}, \end{aligned} \quad (4.13)$$

where $D = 1 + \gamma^2(1 - g^{*2})/g^2 \theta$, and $P^\pm(\theta)$ is given in equation (II.8.19). Similarly,

$$\begin{aligned} \frac{d \cos \theta^{*\pm}}{d \cos \theta} &= \frac{\cos \theta}{\gamma^2(1 - v^2 \cos^2 \theta)^2} \frac{(g^* \pm \sqrt{D})^2}{(\pm \sqrt{D})} \\ &= \left(\frac{P^\pm}{P^*} \right)^2 \frac{1}{(\pm \cos \theta \sqrt{D})}. \end{aligned} \quad (4.14)$$

Note that we can use equations (II.8.19) and (II.8.23) to prove that

$$\pm \cos \theta \sqrt{D} = \gamma(P^\pm - E^\pm v \cos \theta)/P^*. \quad (4.15)$$

Equation (4.14) can thus also be written in the form

$$\frac{d \cos \theta^{*\pm}}{d \cos \theta} = \frac{(P^\pm)^2}{\gamma P^*(P^\pm - E^\pm v \cos \theta)}. \quad (4.16)$$

We shall rediscover this relation later on in connection with the two-particle phase integral.

Summarizing, if one knows $w^*(\cos \theta^*)$ or $d\sigma/d\Omega^*$ then to find $w(\cos \theta)$ or $d\sigma/d\Omega$ one has to use equation (4.14) for the Jacobian and equation (II.8.30) to express θ in terms of θ^* . For the inverse operation the Jacobian is obtained from equation (4.12) and θ^* in terms of θ from equation (II.8.32). In both cases one has to pay proper attention to the possible double-valuedness of the relation between θ^* and θ . In practice, however, the simplest way to carry out these transformations is to use the invariant momentum transfer t and $d\sigma/dt$ (Section IV.6) instead of $\cos \theta$ and $d\sigma/d\Omega$.

Example 1: Consider an isotropic decay in the CMS so that the distribution $w^*(\cos \theta^*)$ in the cosine of the decay angle θ^* is constant:

$$w^*(\cos \theta^*) = \frac{1}{2}, \quad (4.17)$$

where the normalization is carried over the whole range $0 \leq \theta^* \leq \pi$. Equivalently

$$w^*(\theta^*) = \frac{1}{2} \sin \theta^*. \quad (4.18)$$

Assume, for example, that the decaying particle is moving in the laboratory with a velocity v which is equal to the velocity v^* of the decay product in the CMS. Then $g^* = 1$ and equation (4.14) give for the angular distribution $w(\cos \theta)$ in the laboratory

$$w(\cos \theta) = 2 \cos \theta^{-2} (1 - v^2 \cos^2 \theta)^{-2}. \quad (4.19)$$

It is easy to see that this distribution is peaked in the forward direction, the value at $\theta = 0^\circ$ increasing as $2y^2$. Note that the range of θ is now $0 \leq \theta \leq \pi/2$.

(b) Transformation of two-dimensional one-particle distributions

The transformation equations are in this case actually simpler than those for one-dimensional distributions. The Jacobian needed to apply equation (2.9) has already been evaluated in equation (2.10):

$$\frac{\partial(p_x^*, p_y^*, p_z^*)}{\partial(p_x, p_y, p_z)} = \frac{d^3 p^*}{d^3 p} = \frac{E^*}{E}. \quad (4.20)$$

This implies that

$$Ew(p_x, p_y, p_z) = E \frac{1}{\sigma} \frac{d^3 \sigma}{d^3 p} \quad (4.21)$$

is an invariant, so that

$$w(p_x, p_y, p_z) = \frac{E^*}{E} w(p_x^*, p_y^*, p_z^*). \quad (4.22)$$

This is the basic result and the transformation rule for distributions in other variables is obtained by transforming from the Cartesian components p_x, p_y, p_z to these other variables. Equation (4.22) looks so simple since it has been written in terms of quantities defined in different frames. In a more explicit form one may write, for instance

$$w(p_x, p_y, p_z) = \gamma E^{-1} (E - vp_z) w^* \{p_x, p_y, \gamma(p_z - vE)\}, \quad (4.23)$$

which gives the TS distribution w in TS variables corresponding to a given CMS distribution w^* .

Other variables replacing p_x, p_y, p_z will be considered in detail in Chapter VII. Here we shall only illustrate the general idea by the important cases (P, Ω) and $(q, r) \equiv (P \cos \theta, P \sin \theta)$. The relevant Jacobians are obtained from equations (II.8.1-4) by mechanical calculations:

$$\frac{\partial(p_x, p_y, p_z)}{\partial(P, \cos \theta, \phi)} = P^2 \quad (4.24)$$

$$\begin{aligned} \frac{\partial(P, \cos \theta)}{\partial(q, r)} &= \frac{\sin \theta}{P} \\ &= \frac{r}{P^2}. \end{aligned} \quad (4.25)$$

These equations imply that

$$\begin{aligned} w(P, \Omega) &= w(P, \cos \theta) \\ &= P^2 w(p_x, p_y, p_z) \end{aligned} \quad (4.26)$$

$$w(q, r) = r w(p_x, p_y, p_z). \quad (4.27)$$

Combining them with equation (4.22) one has

$$w(P, \Omega) = (P^2 E^*/P^{*2} E) w(P^*, \Omega^*) \quad (4.28)$$

and, taking into account that $r = r^*$,

$$w(q, r) = (E^*/E) w(q^*, r), \quad (4.29)$$

Example 2: Assume we have a model for one-particle spectra implying that

$$\frac{d^2\sigma}{dq^* dr} = f(r),$$

where f is some function, and we want to find out what this predicts for the experimentally measured quantity $d^3\sigma/dP d\Omega$. Using equations (4.25) and (4.29) the answer is

$$\begin{aligned} d^3\sigma/dP d\Omega &= (P^2/2\pi r)(d^2\sigma/dq dr) \\ &= (P^2/2\pi r)(E^*/E)(d^2\sigma/dq^* dr) \\ &= (P^2/2\pi r)(1 - vP \cos \theta/E)f(r) \end{aligned}$$

The distribution $d^2\sigma/dq dr$ now depends on $q = P \cos \theta$.

Exercises

- III.1. (a) What are the dimensions of the n -particle production amplitude $A(p_i)$ if σ is to have the dimensions of mb?
 (b) What are the dimensions of the phase space integral R_n ?

- III.2. Evaluate the non-relativistic phase space integral $I(E)$ defined by

$$I(E) = \int \prod_{i=1}^n d^3 p_i \delta\left(E - \sum_i \frac{p_i^2}{2m}\right)$$

in terms of the Euler gamma function.

- III.3. Why does an isotropic distribution imply that $w(\cos \theta) = \text{constant}$ and not that $w(\theta) = \text{constant}$?
- III.4. Verify the normalization of equation (4.19).
- III.5. Rederive equation (4.19) by starting from $w^*(\theta^*) = \frac{1}{2} \sin \theta^*$ and using an appropriate formula for $d\theta^*/d\theta$.

IV

Two-Particle Final States

1. Two-particle phase space

In this section we consider the simplest possible process: one particle going into two. We thus study the two-particle final state without any reference to the initial state besides four-momentum conservation. The properties of the initial state may thus be compressed into its total four-momentum $p = (E, \mathbf{p})$. In applications p may either be the four-momentum p_0 of a decaying particle or the total four-momentum $p_a + p_b$ of an initial collision state.

The *two-particle phase space integral* is needed in connection with cross-section and lifetime formulas and in developing sets of convenient variables for n particle final states. According to the definition of R_n it is

$$R_2(p; m_1^2, m_2^2) = \int d^4 p_1 d^4 p_2 \delta(p_1^2 - m_1^2) \delta(p_2^2 - m_2^2) \delta^4(p - p_1 - p_2). \quad (1.1)$$

The constants m_1^2 and m_2^2 can be of either sign; for simplicity we have denoted them by masses squared. By Lorentz invariance R_2 is known to be only a function of

$$\begin{aligned} s &= p^2 \\ &= E^2 - \mathbf{p}^2 \end{aligned} \quad (1.2)$$

and of m_1^2 and m_2^2 . We shall evaluate equation (1.1) separately for the cases p timelike, spacelike and lightlike.

(a) *p timelike*

To begin with, let us give the simple standard derivation of R_2 for p timelike; the rest of this section may then be omitted at first reading. Integrate in equation (1.1) first over p_2 by using the four-dimensional δ function and go then to the frame $p = (\sqrt{s}, \mathbf{0})$:

$$R_2(s) = \int d^4 p_1 \delta(p_1^2 - m_1^2) \delta((p - p_1)^2 - m_2^2) \quad (1.3)$$

$$= \int \frac{d^3 p_1}{2E_1} \delta(s - 2\sqrt{s}E_1^* + m_1^2 - m_2^2) \quad (1.4)$$

$$= \frac{1}{2} \int d\Omega_1^* dE_1^* \delta(s - 2\sqrt{s}E_1^* + m_1^2 - m_2^2), \quad (1.5)$$

where the solid angle Ω_1^* describes the orientation of \mathbf{p}_1 in the rest frame of p . The δ function fixes the magnitudes of the *decay momenta* to be

$$\begin{aligned} P_1^* &= P_2^* \\ &= \frac{\lambda^{\frac{1}{2}}(s, m_1^2, m_2^2)}{2\sqrt{s}}. \end{aligned} \quad (1.6)$$

The values of these decay momenta are tabulated in the Elementary Particle Tables for different observed resonances and their two-particle decay modes. Integrating in equation (1.5) over E_1^* by using equation (2.12) one finds

$$R_2(s) = \frac{P_1^*}{4\sqrt{s}} \int d\Omega_1^* \quad (1.7)$$

$$= \frac{\lambda^{\frac{1}{2}}(s, m_1^2, m_2^2)}{8s} \int d\Omega_1^*. \quad (1.8)$$

At this stage only the integrations over the δ functions in equation (1.1) have been carried out; $R_2(s)$ will later on often be needed in this form, since the introduction of a matrix element $A(\mathbf{p}_1, \mathbf{p}_2)$ to equations (1.7-8) is trivial. Now that the matrix element is unity one can immediately integrate over Ω_1^* in equations (1.7-8):

$$\begin{aligned} R_2(s) &= \frac{\pi P_1^*}{\sqrt{s}} \\ &= \frac{\pi \lambda^{\frac{1}{2}}(s, m_1^2, m_2^2)}{2s}. \end{aligned} \quad (1.9)$$

All the equations for R_2 should actually contain a Θ function $\Theta(\sqrt{s} - m_1 - m_2)$ specifying that R_2 vanish below threshold. Formally this threshold Θ function arises from the Θ function $\Theta(p_0)$ in equation (III.2.11).

After this simple derivation, we wish, for comparison with earlier results, to be more general and eliminate the δ functions in equation (1.1) in an arbitrary frame, $p = (E, \mathbf{p})$. Integrating in (1.1) first over p_1^0 and p_2^0 using the mass shell constraints one has

$$R_2(E, \mathbf{p}) = \int \frac{d^3 p_1}{2E_1} \frac{d^3 p_2}{2E_2} \delta(E - E_1 - E_2) \delta^3(\mathbf{p} - \mathbf{p}_1 - \mathbf{p}_2).$$

Then the integral over \mathbf{p}_2 in the second δ function gives

$$R_2(E, \mathbf{p}) = \int d\Omega_1 \int \frac{dP_1 P_1^2}{4E_1(E - E_1)} \delta\{f(P_1)\}. \quad (1.10)$$

The solid angle $\Omega_1 = (\cos \theta_1, \phi_1)$ defines the orientation of \mathbf{p}_1 with respect to \mathbf{p} (Figure 1.1) and we have introduced

$$f(P_1) = E - E_1 - (P^2 + P_1^2 - 2PP_1 \cos \theta_1 + m_2^2)^{\frac{1}{2}}. \quad (1.11)$$

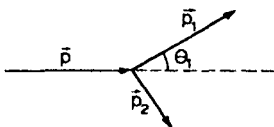


Figure IV.1.1 The decay angle θ_1 is the angle between \bar{p} and \bar{p}_1 , the angle ϕ_1 (not shown) describes the azimuthal orientation of \bar{p}_1 around \bar{p}

The constraint $f(P_1) = 0$ defines the length of \bar{p}_1 as a function of $\cos \theta_1$, i.e. of the angle between \bar{p} and \bar{p}_1 . The two-valued solution $P_1 = P_1^\pm$ is, not unexpectedly, given by our old result equations (II.8.19–20). The properties of P_1^\pm were analyzed in detail in Section II.8. Since the integral over P_1 goes from 0 to ∞ , only the positive solutions contribute. In Classes 1 and 2 ($v \leq v^*$) the value of P_1^- was always negative while in Class 3 ($v > v^*$) one found $P_1^\pm > 0$ for $0 \leq \theta_1 \leq \theta_{1,\max}$. Calculating $f'(P)$ from (1.10)

$$f'(P_1) = \frac{P_1 E - PE_1 \cos \theta_1}{E_1(E - E_1)}$$

and using the integration formula (2.12) one has, finally

$$R_2(E, \bar{p}) = \frac{1}{2} \int d\Omega_1 \sum_{\pm} (P_1^\pm)^2 (EP_1^\pm - PE_1^\pm \cos \theta_1)^{-1}. \quad (1.12)$$

Equation (1.12) is complicated but by relativistic invariance we now know that if equation (1.12) were integrated over $\cos \theta_1$ we would obtain the result (1.9) with $s = E^2 - \bar{p}^2$. Since we have integrated only over the δ functions, equation (1.12) is also valid if one introduces a matrix element $A(\bar{p}_1, \bar{p}_2)$. Due to the δ functions only the dependence of A on angular variables enters into equation (1.12). The integrand in equation (1.12) is essentially the differential cross-section $d\sigma_2/d\Omega_1$ in an arbitrary system. When $\bar{p} = (\sqrt{s}, 0)$, equation (1.12) reduces to equation (1.7), of course.

By comparing equations (1.12) and (1.7) one finds, in differential form, that

$$\frac{d\Omega_1^*}{d\Omega_1^\pm} = \frac{\sqrt{s(P_1^\pm)^2}}{P_1^*(EP_1^\pm - PE_1^\pm \cos \theta_1)}. \quad (1.13)$$

The two values of \bar{p}_1 , which in Class 3 correspond to a single value of θ_1 , are treated separately. Equation (1.13) is nothing but our old result in equation (III.4.16) for a Lorentz transformation of a differential cross-section $d\sigma/d\Omega$, if we write $\gamma = E/\sqrt{s}$ for the γ factor of the motion of the CMS in the TS. Here the result was obtained very simply by using Lorentz invariance of R_2 .

(b) p spacelike

To find R_2 for spacelike p , first integrate over \bar{p}_2 in equation (1.1) with the result (1.3). Now that p is spacelike we can go to the frame $p = (0, 0, 0, \sqrt{-t})$

to evaluate equation (1.3). Then the second δ function fixes the z component of p_1 to be

$$p_{1z} = \frac{-t - m_1^2 + m_2^2}{2\sqrt{-t}}.$$

An integration over p_{1z} then gives

$$R_2(p; m_1^2, m_2^2) = \int dE_1 dp_{1x} dp_{1y} (2\sqrt{-t})^{-1} \delta(p_1^2 - m_1^2). \quad (1.14)$$

The remaining integral is most naturally carried out by using the pseudo-spherical coordinates introduced in Figure II.7.2 and equations (II.1.19–20). In terms of these one has (see equation (II.1.36))

$$dE_1 dp_{1x} dp_{1y} = P_1^2 dP_1 dg_1, \quad (1.15)$$

where

$$\begin{aligned} P_1^2 &= E_1^2 - p_{1x}^2 - p_{1y}^2 \\ &= m_1^2 + p_{1z}^2 \\ &= \frac{\lambda(t, m_1^2, m_2^2)}{-4t} \end{aligned} \quad (1.16)$$

$$dg_1 = d\cosh \zeta_1 d\phi_1. \quad (1.17)$$

We use P_1 both for the variable of integration and for its value fixed by the δ function. It is now simple to integrate over dP_1 by using the remaining δ function in equation (1.14). The result is

$$\begin{aligned} R_2(p; m_1^2, m_2^2) &= \frac{P_1}{4\sqrt{-t}} \int dg_1 \\ &= \frac{\lambda^{\frac{1}{2}}(t, m_1^2, m_2^2)}{-8t} \int dg_1. \end{aligned} \quad (1.18)$$

This equation is completely analogous to equations (1.7) and (1.8); only now the total volume is infinite. In practical applications of equation (1.18) there will be some additional conditions which limit the range of ζ_1 and make the integral finite.

(c) p lightlike

Finally, in the lightlike case we must evaluate equation (1.12) with $p^2 = 0$. The corresponding standard frame is (equation (II.1.13)) $p = (\omega, 0, 0, \omega)$. The proper parametrization of p_1 is given by

$$\begin{aligned} p_1 &= (E_1, p_{1x}, p_{1y}, p_{1z}) \\ &= \left\{ \frac{1}{2}(\lambda_+ + \lambda_-), p_{1x}, p_{1y}, \frac{1}{2}(\lambda_+ - \lambda_-) \right\}, \end{aligned} \quad (1.19)$$

i.e. we choose as new variables $\lambda_{\pm} = E_1 \pm p_{1z}$. These variables are sometimes called *light-cone variables*. Then

$$\begin{aligned} R_2(p; m_1^2, m_2^2) &= \frac{1}{2} \int d\lambda_+ d\lambda_- d^2 r_1 \delta(\lambda_+ \lambda_- - r_1^2 - m_1^2) \delta(m_1^2 - m_2^2 - 2\omega \lambda_-) \\ &= \frac{1}{2(m_1^2 - m_2^2)} \int d^2 r_1, \end{aligned} \quad (1.20)$$

where $r_1 = (p_{1x}, p_{1y})$ is the transverse momentum of p_1 .

In all cases R_2 has thus been reduced to an integral over the *little group* (see, for example, Halpern, 1968) of the corresponding standard vector. When $p^2 > 0$, $p^2 < 0$, $p^2 = 0$ the little groups are $O(3)$, $O(1, 2)$, $E(2)$, respectively ($E(2)$ is the group of rotations and translations in the two-dimensional Euclidean plane). The corresponding volume elements are $d\Omega$ (1.8), dg (1.18) and d^2r (1.20).

From equations (1.8) and (1.18) we see that a necessary condition for the process $p \rightarrow p_1 + p_2$ to be physical is

$$\begin{aligned} \lambda(p^2, p_1^2, p_2^2) &= \{p^2 - (\sqrt{p_1^2} + \sqrt{p_2^2})^2\} \{p^2 - (\sqrt{p_1^2} - \sqrt{p_2^2})^2\} \\ &= \{p^2 + (\sqrt{-p_1^2} + \sqrt{-p_2^2})^2\} \{p^2 + (\sqrt{-p_1^2} - \sqrt{-p_2^2})^2\} \quad (1.21) \\ &\geq 0. \end{aligned}$$

This is always satisfied unless all three vectors are spacelike or all timelike. If all are timelike, equation (1.21) requires

$$\sqrt{p^2} \geq m_1 + m_2 = \text{threshold} \quad (1.22)$$

or

$$\sqrt{p^2} \leq |m_1 - m_2| = \text{pseudothreshold}. \quad (1.23)$$

The former is a natural condition for a decay; the latter is appropriate if p is a momentum transfer. Equations (1.22) and (1.23) should be compared with equation (II.2.19).

The condition (1.21) can be written in a more symmetric form by using the Gram determinant $\Delta_2(p_1, p_2)$ of p_1 and p_2 introduced in equation (II.7.3). We can then state that the process $p \rightarrow p_1 + p_2$ is physical if

$$\Delta_2(p_1, p_2) \leq 0. \quad (1.24)$$

In particular, the *boundary of the physical region in terms of invariants* is given by $\Delta_2(p_1, p_2) = 0$. This case of two independent four-vectors is almost trivial, but for larger particle numbers the use of Gram determinants is indispensable, as we shall later show in detail.

2. Distribution in opening angle

The distribution $w(\cos \theta_1)$ appearing inside the integral in equation (1.12) is the distribution in the *decay angle* (Figure 1.1), the angle θ_1 between the

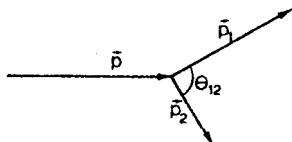


Figure IV.2.1 The opening angle θ_{12} is the angle between \bar{p}_1 and \bar{p}_2

momenta of the decaying particle and of one of the decay products. We shall now determine the distribution in the *opening angle* θ_{12} , defined in Figure 2.1 as the angle between the momenta of the two decay products. Note the qualitative difference between these two: the decay angle distribution relates the initial and final states while the opening angle distribution only refers to the final state. The difference can also be made apparent in the rest frame of the decaying particle: there $w(\cos \theta_1)$ is some regular function of $\cos \theta_1$, but $w(\cos \theta_{12})$ is a δ function peaked at π since by momentum conservation $\cos \theta_{12} = \pi$.

The distribution in $\cos \theta_{12}$ can be derived by starting from the known distribution $w^*(\cos \theta_1^*)$, finding the relation between the angles $\theta_{12} = \theta_1 + \theta_2$ and θ_1^* , and calculating

$$w(\cos \theta_{12}) = \frac{d \cos \theta_1^*}{d \cos \theta_{12}} w^*(\cos \theta_1^*). \quad (2.1)$$

The angles θ_1 and θ_2 can be expressed in terms of the components of \bar{p}_1 and \bar{p}_2 , and these again in terms of the CMS quantities $P_1^* = P_2^*, \theta_1^* = \pi - \theta_2^*$, and the transformation parameters from CMS to the present frame: $v = P/E$, $\gamma = E/\sqrt{s}$. The CMS velocities of 1 and 2 are $v_i^* = P_i^*/E_i^*$, $i = 1, 2$. Using now $\cos \theta_{12} = \cos \theta_1 \cos \theta_2 - \sin \theta_1 \sin \theta_2$, one obtains

$$\cos \theta_{12} = \{\gamma^2 v^2 - v_1^* v_2^* + \gamma^2 v(v_1^* - v_2^*) \cos \theta_1^* - \gamma^2 v^2 v_1^* v_2^* \cos^2 \theta_1^*\}/h_1 h_2 \quad (2.2)$$

with

$$h_1^2 = \gamma^2 v^2 + v_1^{*2} + 2\gamma^2 v v_1^* \cos \theta_1^* + \gamma^2 v^2 v_1^{*2} \cos^2 \theta_1^*$$

$$h_2^2 = \gamma^2 v^2 + v_2^{*2} - 2\gamma^2 v v_2^* \cos \theta_1^* + \gamma^2 v^2 v_2^{*2} \cos^2 \theta_1^*.$$

The general case is obviously very complicated. Instead of proceeding further we shall later use a different method to find $w(\cos \theta_{12})$ for arbitrary masses. We only note that for equal masses, $m_1 = m_2$, $v_1^* = v_2^*$, it is possible to solve for $\cos^2 \theta_1^*$ from equation (2.2), and to find an explicit expression for $w(\cos \theta_{12})$. The result is so lengthy that we do not reproduce it here.

Only if the masses vanish, equation (2.2) simplifies so much that it will lead to a compact result. Examples of processes of this type are $\pi^0 \rightarrow \gamma\gamma$ and $e^+e^- \rightarrow \gamma\gamma$. In the latter the matrix element has a $\cos \theta_1^*$ dependence given by quantum electrodynamics. Putting $m_1 = m_2 = 0$, or $v_1^* = v_2^* = 1$ in equation (2.2) gives

$$\cos \theta_{12} = \frac{2v^2 - 1 - v^2 \cos^2 \theta_1^*}{1 - v^2 \cos^2 \theta_1^*}. \quad (2.3)$$

From this $\cos \theta_1^*$ is obtained as

$$\cos \theta_1^* = \frac{\{v^2 - \cos^2(\theta_{12}/2)\}^{\frac{1}{2}}}{v \sin(\theta_{12}/2)}. \quad (2.4)$$

Substitution in equation (2.1) yields the result (see also Källén, 1964, p. 32)

$$w(\cos \theta_{12}) = \frac{w^*(\cos \theta_1^*)}{4\gamma^2 v \sin^3(\theta_{12}/2) \{v^2 - \cos^2(\theta_{12}/2)\}^{\frac{1}{2}}}. \quad (2.5)$$

The distribution $w(\theta_{12}) = \sin \theta_{12} w(\cos \theta_{12})$ is plotted in Figure 2.2 in the case $w^*(\cos \theta_1^*) = \text{constant}$ for some values of v . Note that equation (2.5) implies the existence of a minimum opening angle (Exercises IV.2 and IV.6).

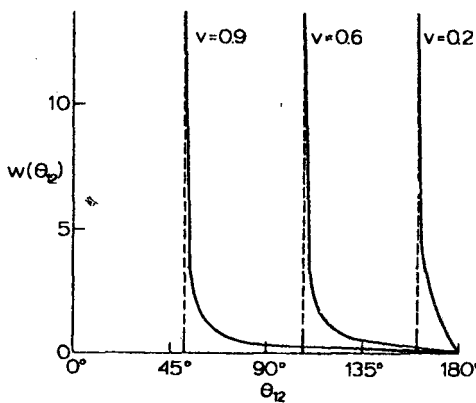


Figure IV.2.2 Distribution in the opening angle of a decay to two zero-mass particles for some values of the velocity of the decaying particle

We now derive $w(\cos \theta_{12})$ in a different way for arbitrary masses. Set first $x = \cos \theta_{12} = \mathbf{p}_1 \cdot \mathbf{p}_2 / P_1 P_2$ in the general formula (III.2.7) for the differential cross-section. We shall also assume that the matrix element is constant, i.e. $w^*(\cos \theta_1^*) = \text{constant}$. Otherwise the final result will just be multiplied by $w^*(\cos \theta_1^*)$, where θ_1^* is expressed in terms of θ_{12} , equation (2.2). Now,

we note that the cross-section and R_2 differ only by a constant factor and we thus have

$$\begin{aligned} w(\cos \theta_{12}) &= \frac{R_2^{-1} dR_2}{d \cos \theta_{12}} \\ &= R_2^{-1} \int d^3 p_1 d^3 p_2 (4E_1 E_2)^{-1} \delta^4(p - p_1 - p_2) \\ &\quad \times \delta(\cos \theta_{12} - \mathbf{p}_1 \cdot \mathbf{p}_2 / P_1 P_2). \end{aligned} \quad (2.6)$$

R_2 is given by equation (1.9). Writing $d^3 p_2 = 2E_2 \delta(p_2^2 - m_2^2) d^4 p_2$, we integrate over $d^4 p_2$, and get

$$\begin{aligned} \frac{dR_2}{d \cos \theta_{12}} &= \int d^3 p_1 (2E_1)^{-1} \delta((p - p_1)^2 - m_1^2) \delta(\cos \theta_{12} - \mathbf{p}_1 \cdot (\mathbf{p} - \mathbf{p}_1) / P_1 P_2) \\ &= \int_0^\infty dP_1 P_1^2 (2E_1)^{-1} \\ &\quad \times \int d\phi_1 d \cos \theta_1 \delta(s + m_1^2 - m_2^2 - 2EE_1 + 2PP_1 \cos \theta_1) \\ &\quad \times \delta(\cos \theta_{12} - (P \cos \theta_1 - P_1) / P_2), \end{aligned}$$

where θ_1 is the angle between \mathbf{p} and \mathbf{p}_1 . The integration over ϕ_1 is trivial and the integration over $\cos \theta_1$ can be carried out by using the first δ function. Writing $P_1 dP_1 = E_1 dE_1$ we have

$$\frac{dR_2}{d \cos \theta_{12}} = \left(\frac{\pi}{2P} \right) \int_{m_1}^\infty dE_1 \delta \left(\cos \theta_{12} - \frac{2EE_1 - 2E_1^2 - s + m_1^2 + m_2^2}{2(E_1^2 - m_1^2)^{\frac{1}{2}} \{(E - E_1)^2 - m_2^2\}^{\frac{1}{2}}} \right), \quad (2.7)$$

where the dependence on the integration variable E_1 has been stated explicitly. To integrate over the δ function in equation (2.7), we need the derivative of the argument $f(E_1)$ of the δ function:

$$f'(E_1) = \frac{E_2 - E_1 - \frac{1}{2}(2E_1 E_2 - s + m_1^2 + m_2^2)(E_1 P_1^{-2} - E_2 P_2^{-2})}{P_1 P_2}.$$

Then putting the results from equations (2.7) and (1.9) into equation (2.6) one gets the final expression (see, for instance, Werbrouck, 1968)

$$\begin{aligned} w(\cos \theta_{12}) &= sP_1 P_2 P^{-1} \lambda^{-\frac{1}{2}}(s, m_1^2, m_2^2) \\ &\quad \times \{E_2 - E_1 - \frac{1}{2}(2E_1 E_2 - s + m_1^2 + m_2^2)(E_1 P_1^{-2} - E_2 P_2^{-2})\}^{-\frac{1}{2}} \end{aligned} \quad (2.8)$$

Because P_1 , P_2 , E_1 , E_2 are complicated functions of $\cos \theta_{12}$, it is not easy to uncover the actual θ_{12} dependence of $w(\cos \theta_{12})$ in equation (2.8). Thus

either of the two equivalent results (2.1–2) and (2.8) leads to a useful result only when evaluated numerically.

3. Two-particle scattering: relations between the CMS and TS

We shall now proceed to treat the reaction $p_a + p_b \rightarrow p_1 + p_2$ ($2 \rightarrow 2$ scattering). The notation has been chosen so that it can be easily generalized to higher multiplicities. The phase space (defined for s fixed) is now two dimensional and is parametrized, for example, by the scattering angle θ and one angular variable ϕ describing rotations around the beam axis. The latter is trivial leaving one essential final state variable in the present case. The total number of essential variables is two: one fixes the total energy, the other the scattering angle. Energy-type variables (for instance, E_a, P_a, \sqrt{s}) have already been treated in detail (Chapter II). As frame-dependent, angle-type variables we shall use the angle between p_a and p_1 either in the CMS (Figure 3.1) or in the TS (Figure 3.2):

$$\begin{aligned}\theta_1^* &\equiv \theta_{a1}^* \\ &= \pi - \theta_{a2}^*\end{aligned}\quad (3.1)$$

$$\theta_1 \equiv \theta_{a1}^T. \quad (3.2)$$

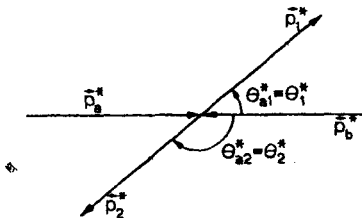


Figure IV.3.1 The scattering angles θ_1^* and $\theta_2^* = \pi - \theta_1^*$

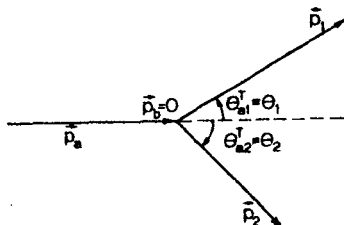


Figure IV.3.2 The scattering angles θ_1 and θ_2 in the TS. Now θ_1 and θ_2 are related in a complicated manner

The index T will be omitted in this section since only CMS and TS quantities will be considered. By definition, one calls scattering near $\theta_1^* = 0$ forward scattering and scattering near $\theta_1^* = \pi$ backward scattering. Note that θ_1 and $\theta_2 = \theta_{a2}^*$ are related in a complicated manner. The invariant angle-type variable will be the invariant momentum transfer

$$\begin{aligned} t &\equiv t_{a1} \\ &= (p_a - p_1)^2 \\ &= m_a^2 + m_1^2 - 2E_a E_1 + 2P_a P_1 \cos \theta_{a1}. \end{aligned} \quad (3.3)$$

The treatment of $2 \rightarrow 2$ scattering in terms of invariants s and t is important for theoretical purposes and will be considered in detail in the following section. This section will be devoted to relations between quantities in the CMS and in the TS, keeping in mind especially their relevance for experiments.

In the CMS, $2 \rightarrow 2$ scattering is kinematically extremely simple, since energy- and angle-dependences are completely decoupled. In fact, according to equation (II.6.15), the momenta are

$$\begin{aligned} P_a^* &= P_b^* \\ &= \frac{\lambda^{\frac{1}{2}}(s, m_a^2, m_b^2)}{2\sqrt{s}}, \\ P_1^* &= P_2^* \\ &= \frac{\lambda^{\frac{1}{2}}(s, m_1^2, m_2^2)}{2\sqrt{s}}, \end{aligned} \quad (3.4)$$

while θ_1^* gives all other angles as shown in Figure 3.1. The TS relations are more involved. Let us assume that \sqrt{s} is fixed so that the initial state $p_a + p_b$ in Figure 3.2 is fixed. Then any one of the four final state variables P_1 , θ_1 , P_2 , θ_2 will determine the remaining three. The most interesting relations are those relating (a) P_1 to θ_1 and P_2 to θ_2 , (b) θ_1 to θ_2 .

(a) Dependence of P_i on θ_i

Because all results for P_2 can be obtained from those of P_1 by interchanging 1 and 2, it is enough to treat $P_1 = P_1(\theta_1)$. This dependence can, of course, be calculated directly (see Exercise IV.8) but, in order to understand the situation completely, it is much better to apply the results of Section II.8. There it was seen how the sphere $P_1^* = \text{constant}$ transforms in going to the TS. We now have to specialize the general equations to the present case by finding the values of the parameters v and v_1^* .

The parameters for the Lorentz transformation between the CMS and TS have already been calculated in equations (II.6.23–24):

$$\begin{aligned} v &= \frac{P_s}{E_a + m_b} \\ &= \frac{\lambda^{\frac{1}{2}}(s, m_a^2, m_b^2)}{s - m_a^2 + m_b^2} \\ \gamma &= \frac{E_a + m_b}{\sqrt{s}} \\ &= \frac{s - m_a^2 + m_b^2}{2m_b\sqrt{s}}. \end{aligned} \tag{3.5}$$

The velocity of particle 1 and its γ parameter in the CMS are

$$\begin{aligned} v_1^* &= \frac{P_1^*}{E_1^*} \\ &= \frac{\lambda^{\frac{1}{2}}(s, m_1^2, m_2^2)}{s + m_1^2 - m_2^2} \\ \gamma_1^* &= \frac{E_1^*}{m_1} \\ &= \frac{s + m_1^2 - m_2^2}{2m_1\sqrt{s}}. \end{aligned} \tag{3.6}$$

The basic parameter g_1^* (equation (II.8.22)) is thus given by

$$\begin{aligned} g_1^* &= \frac{v}{v_1^*} \\ &= \frac{s + m_1^2 - m_2^2}{s - m_a^2 + m_b^2} \frac{\lambda^{\frac{1}{2}}(s, m_a^2, m_b^2)}{\lambda^{\frac{1}{2}}(s, m_1^2, m_2^2)}. \end{aligned} \tag{3.7}$$

Depending on whether $g_1^* < 1$ or $g_1^* \geq 1$ particle p_1 can be emitted in any direction ($0 < \theta_1 < 180^\circ$) or only into the forward hemisphere ($0 < \theta_1 < \theta_1^{\max} \leq 90^\circ$) in the TS as shown by the detailed analysis of Section II.8. The change of g_1^* as a function of \sqrt{s} depends on the relative magnitude of the masses. One can distinguish between ten qualitatively different cases (Dedrick, 1962).

Inserting equations (3.5–7) into equations (II.8.20) and (II.8.24) and expressing everything in terms of the masses and of E_a and P_s , the energy and

momentum of the beam particle in TS, one can derive the following results:

$$\begin{aligned} P_1^\pm &= [P_a \{m_b E_a + \frac{1}{2}(m_a^2 + m_b^2 + m_1^2 - m_2^2)\} \cos \theta_1 \\ &\quad \pm (E_a + m_b) [\{m_b E_a + \frac{1}{2}(m_a^2 + m_b^2 - m_1^2 - m_2^2)\}^2 \\ &\quad - m_1^2 m_2^2 - m_1^2 P_a^2 \sin^2 \theta_1]^{\frac{1}{2}}] \{(E_a + m_b)^2 - P_a^2 \cos^2 \theta_1\}^{-1}, \end{aligned} \quad (3.8)$$

$$\begin{aligned} E_1^\pm &= [(E_a + m_b) \{m_b E_a + \frac{1}{2}(m_a^2 + m_b^2 + m_1^2 - m_2^2)\} \\ &\quad \pm P_a \cos \theta_1 [\{m_b E_a + \frac{1}{2}(m_a^2 + m_b^2 - m_1^2 - m_2^2)\}^2 \\ &\quad - m_1^2 m_2^2 - m_1^2 P_a^2 \sin^2 \theta_1]^{\frac{1}{2}}] \{(E_a + m_b)^2 - P_a^2 \cos^2 \theta_1\}^{-1}. \end{aligned} \quad (3.9)$$

Equation (3.8) represents a rotational ellipsoid in momentum space, now parametrized in terms of the four masses and the incident energy.

(b) Relation between θ_1 and θ_2

In many experimental situations of coincidence type, it is important to know θ_2 when the value of θ_1 is given. There are many ways of deriving this relation. For instance, one may use the CMS equation $\theta_2^* = \pi - \theta_1^*$ (θ_1 is counted anticlockwise and θ_2 clockwise). Then (equation II.8.30)

$$\begin{aligned} \operatorname{tg} \theta_1 &= \frac{\sin \theta_1^*}{\gamma(\cos \theta_1^* + g_1^*)} \\ \operatorname{tg} \theta_2 &= \frac{\sin \theta_1^*}{\gamma(-\cos \theta_1^* + g_2^*)}, \end{aligned} \quad (3.10)$$

where γ and g_1^* are given by equations (3.5) and (3.7) and g_2^* by interchanging 1 and 2 in equation (3.7). It is easy to eliminate θ_1^* from these equations (use equation (II.8.32)) and obtain a relation between θ_1 and θ_2 . The general relation is not very transparent and in practice it has to be evaluated numerically. Instead of writing it down we exhibit in Figure 3.3 how θ_1 and θ_2 depend on each other for various combinations of g_1^* and g_2^* .

Example 1: As an example we shall consider the case of elastic scattering with masses $\mu m \rightarrow \mu m$ (m is the target mass m_b and we assume that $\mu \leq m$). For the basic parameters g_1^* and g_2^* one obtains from equation (3.7):

$$\begin{aligned} g_1^* &= \frac{s + \mu^2 - m^2}{s - \mu^2 + m^2} \\ &= \frac{E_a + \mu^2/m}{E_a + m} \\ &\leq 1 \end{aligned} \quad (3.11)$$

and

$$g_2^* = 1. \quad (3.12)$$

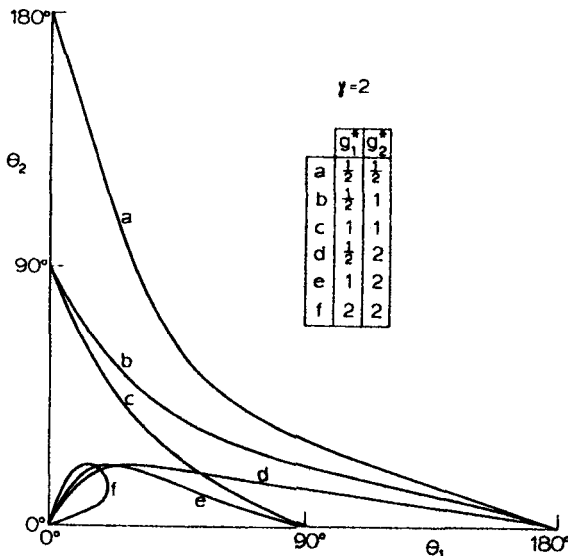


Figure IV.3.3 The relation between θ_1 and θ_2 for different values of g_1^* and g_2^*

As noted after equation (3.7), $g_2^* = 1$ implies that the recoil particle p_2 moves in the forward hemisphere in the TS ($0 \leq \theta_2 \leq \pi/2$). On the other hand, the beam particle can be emitted in any direction unless the masses are equal, $\mu = m$, in which case also $\theta_1 \leq \pi/2$.

In this special case, equations (3.8) and (3.9) are

$$\begin{aligned} P_1 &= \frac{(mE_a + \mu^2) \cos \theta_1 + (E_a + m)(m^2 - \mu^2 \sin^2 \theta_1)^{\frac{1}{2}}}{(E_a + m)^2 - P_a^2 \cos^2 \theta_1} P_a \\ E_1 &= \frac{(mE_a + \mu^2)(E_a + m) + P_a^2 \cos \theta_1(m^2 - \mu^2 \sin^2 \theta_1)^{\frac{1}{2}}}{(E_a + m)^2 - P_a^2 \cos^2 \theta_1} \end{aligned} \quad (3.13)$$

and

$$\begin{aligned} P_2 &= \frac{2m(E_a + m)P_a \cos \theta_2}{(E_a + m)^2 - P_a^2 \cos^2 \theta_2}, \\ E_2 &= \frac{(E_a + m)^2 + P_a^2 \cos^2 \theta_2}{(E_a + m)^2 - P_a^2 \cos^2 \theta_2} m. \end{aligned} \quad (3.14)$$

The equations simplify further if $\mu = m$ (for instance, proton-proton scattering) or $\mu = 0$ (for instance, Compton scattering or electron-proton scattering at high energies). These cases are left as an exercise (Exercise IV.9). The relation between θ_1 and θ_2 is also simple in these cases (Exercise IV.10).

4. Invariant variables for $2 \rightarrow 2$ scattering

The invariant treatment of $2 \rightarrow 2$ scattering is a basic kinematical topic of particle physics and it can be found in one form or another in virtually any book in this field. We have already used the invariant s extensively and mentioned the invariant t in passing. For reasons related to *crossing* one introduces a third variable, u . The definitions of the invariants for $p_a + p_b \rightarrow p_1 + p_2$ can thus be summarized as follows (Figure 4.1):

$$\begin{aligned} s &= (p_a + p_b)^2 \\ &= (p_1 + p_2)^2 \\ &= (E_a^* + E_b^*)^2 \\ &= (E_1^* + E_2^*)^2 \\ &= m_a^2 + m_b^2 + 2m_b E_a^T \end{aligned} \tag{4.1}$$

$$\begin{aligned} t &= (p_a - p_1)^2 \\ &= (p_b - p_2)^2 \\ &= m_a^2 + m_1^2 - 2E_a E_1 + 2P_a P_1 \cos \theta_{a1} \quad \text{CMS or TS} \\ &= m_b^2 + m_2^2 - 2m_b E_2^T \end{aligned} \tag{4.2}$$

$$\begin{aligned} u &= (p_a - p_2)^2 \\ &= (p_b - p_1)^2 \\ &= m_a^2 + m_2^2 - 2E_a E_2 + 2P_a P_2 \cos \theta_{a2} \quad \text{CMS or TS} \\ &= m_b^2 + m_1^2 - 2m_b E_1^T. \end{aligned} \tag{4.3}$$

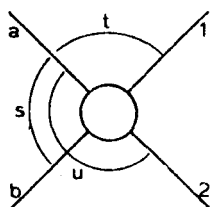


Figure IV.3.1 Invariant variables for $p_a + p_b \rightarrow p_1 + p_2$

There are two independent variables, and thus s, t, u must be related. In fact, there is the linear relation

$$\begin{aligned} s + t + u &= (p_a + p_b)^2 + (p_a - p_1)^2 + (p_b - p_2)^2 \\ &= p_a^2 + p_b^2 + p_1^2 + (p_a + p_b - p_1 - p_2)^2 \\ &= m_a^2 + m_b^2 + m_1^2 + m_2^2. \end{aligned} \tag{4.4}$$

The reason for introducing three dependent variables is based on the concept of crossing. Crossing is extremely important in dynamics, but in kinematics it is almost trivial. We have so far treated the reaction $p_a + p_b \rightarrow p_1 + p_2$ assuming that all energies are positive: $p = (E, \mathbf{p})$ with $E = +(\mathbf{p}^2 + m^2)^{\frac{1}{2}} \geq m \geq 0$. But the four-momentum conservation equation is, as an analytic relation, also valid if any P is timelike with negative 0-component: $p = (E, \mathbf{p})$ with $E = -(\mathbf{p}^2 + m^2)^{\frac{1}{2}}$. One may then write four-momentum conservation in the following alternate forms:

$$\begin{aligned} p_a + p_b &= p_1 + p_2 \\ p_a + (-p_1) &= (-p_b) + p_2 \\ p_a + (-p_2) &= p_1 + (-p_b), \end{aligned} \quad (4.5)$$

where in the second form p_1 and p_b have negative E , and in the third form p_2 and p_b . But these forms may be interpreted as four-momentum conservation equations for the reactions (Figure 4.2)

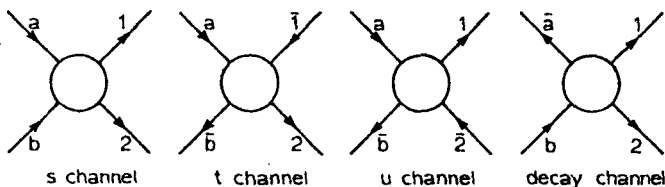


Figure IV.4.2 Various channels for $p_a + p_b \rightarrow p_1 + p_2$. The decay channel shown is physical if $m_b > m_1 + m_2 + m_a$

s channel	$p_a + p_b \rightarrow p_1 + p_2$
t channel	$p_a + p_{\bar{b}} \rightarrow p_1 + p_2$
u channel	$p_a + p_{\bar{b}} \rightarrow p_1 + p_{\bar{2}}$

(4.6)

where a bar denotes the antiparticle of the particle in question and where all four-momenta now have positive E . From the kinematical point of view it is unnecessary to talk about antiparticles, but when dynamic properties are taken into account particle-antiparticle conjugation has to be carried out when a particle is moved from the initial to the final state and vice versa. The three **channels** in equation (4.6) are denoted by the variable which is positive (or of energy type) in the channel in question. The two remaining ones are then invariant momentum transfers. For instance, t is always defined by $t = (p_a - p_1)^2$. But in the t -channel p_1 has a negative E_1 so that in the frame $\mathbf{p}_a - \mathbf{p}_1 = \mathbf{p}_a + \mathbf{p}_{\bar{1}} = 0$ (t -channel CMS) the energy variable is $t = (E_a - E_1)^2 = (E_a + |E_1|)^2 \geq (m_a + m_1)^2$. Similarly, one sees that s and u are momentum transfers in the t -channel.

In addition to the scattering channels (4.6) there may also exist **decay channels**. For instance, if $m_b > m_a + m_1 + m_2$ (Figure 4.2), the decay

$$p_b \rightarrow p_{\bar{a}} + p_1 + p_2 \quad (4.7)$$

can take place. There are thus four possible decay channels.

In dynamics, the different channels may look completely different and by going from one channel to another, which is carried out by using the assumed **analyticity of the scattering amplitude**, one may obtain much useful information. Kinematically, the relations between channels involve only a trivial change of sign and thus they are very simple. In fact, if one works out the kinematics of one channel in s, t, u , one automatically obtains its consequences for all other channels. Thus when we refer to $p_a + p_b \rightarrow p_1 + p_2$ and the st plane in the following it is implied that the treatment is *crossing symmetric*, that is treats all channels on an equal footing, in spite of its unsymmetric appearance.

The relations between s, t and u and frame-dependent quantities are very important in practice. We shall give some of them, always referring to s -channel frames. We also relate the invariant cross-section $d\sigma/dt$ to the amplitude.

(a) Relations between s, t, u and CMS quantities

The relations between s and CMS energies and momenta are very simple since no angles are involved. These relations have been worked out earlier (Sections II.6 and IV.1) and are collected here for easier reference:

$$\begin{aligned} P_{\bar{a}}^* &= P_b^* \\ &= \frac{\lambda^{\frac{1}{2}}(s, m_a^2, m_b^2)}{2\sqrt{s}} \\ P_1^* &= P_2^* \\ &= \frac{\lambda^{\frac{1}{2}}(s, m_1^2, m_2^2)}{2\sqrt{s}} \\ E_{\bar{a}}^* &= \frac{s + m_a^2 - m_b^2}{2\sqrt{s}} \\ E_b^* &= \frac{s + m_b^2 - m_a^2}{2\sqrt{s}} \\ E_1^* &= \frac{s + m_1^2 - m_2^2}{2\sqrt{s}} \\ E_2^* &= \frac{s + m_2^2 - m_1^2}{2\sqrt{s}} \end{aligned} \quad (4.8)$$

The first two equations imply that $s \geq \max\{(m_a + m_b)^2, (m_1 + m_2)^2\}$. Introducing equations (4.8) in the relation (4.2) between t and $\cos \theta_{a1}^*$ we have, by solving for $\cos \theta_{a1}^*$,

$$\begin{aligned}\cos \theta_{a1}^* &= \frac{t - m_a^2 - m_1^2 + 2E_a^* E_1^*}{2P_a^* P_1^*} \\&= \frac{2s(t - m_a^2 - m_1^2) + (s + m_a^2 - m_b^2)(s + m_1^2 - m_2^2)}{\lambda^4(s, m_a^2, m_b^2)\lambda^4(s, m_1^2, m_2^2)} \\&= \frac{s^2 + s(2t - m_a^2 - m_b^2 - m_1^2 - m_2^2) + (m_a^2 - m_b^2)(m_1^2 - m_2^2)}{\lambda^4(s, m_a^2, m_b^2)\lambda^4(s, m_1^2, m_2^2)} \\&= \frac{s(t - u) + (m_a^2 - m_b^2)(m_1^2 - m_2^2)}{\lambda^4(s, m_a^2, m_b^2)\lambda^4(s, m_1^2, m_2^2)}.\end{aligned}\quad (4.9)$$

We shall in the following section give an independent derivation for $\sin \theta_{a1}^*$, based on the results of Section II.7. The other angles are then obtained from θ_{a1}^* , for instance, $\theta_{a2}^* = \pi - \theta_{a1}^*$, etc. It is also instructive to derive equation (4.9) by applying the rule stated in equation (II.7.8) (Exercise IV.13).

(b) Relations between s, t, u and TS quantities

For the initial-state quantities we have already derived the equations

$$\begin{aligned}p_a &= \left(\frac{s - m_a^2 - m_b^2}{2m_b}, 0, 0, \frac{\lambda^4(s, m_a^2, m_b^2)}{2m_b} \right) \\p_b &= (m_b, 0, 0, 0).\end{aligned}\quad (4.10)$$

In the final state we have to determine two energies (E_1^T, E_2^T), momenta (P_1^T, P_2^T) and angles ($\theta_{a1}^T, \theta_{a2}^T$), (Figure 3.2). The energies are now most simply related to momentum transfers. For instance, from equation (4.2) one has directly

$$E_2^T = \frac{m_b^2 + m_2^2 - t}{2m_b} \quad (4.11)$$

so that

$$P_2^T = \frac{\lambda^4(t, m_b^2, m_2^2)}{2m_b}. \quad (4.12)$$

Similarly, from equation (4.3),

$$E_1^T = \frac{m_b^2 + m_1^2 - u}{2m_b} \quad (4.13)$$

and

$$P_1^T = \frac{\lambda^4(u, m_b^2, m_1^2)}{2m_b}. \quad (4.14)$$

Note how equations (4.12) and (4.14) require the validity of the pseudothreshold condition (1.23): $t \leq (m_b - m_2)^2$, $u \leq (m_b - m_1)^2$. From similar equations in the beam system one infers that $t \leq (m_a - m_1)^2$, $u \leq (m_a - m_2)^2$. The angles θ_{a1}^T and θ_{a2}^T are finally obtained from $t = (p_a - p_1)^2$ and $u = (p_a - p_2)^2$ with the result

$$\cos \theta_{a1}^T = \frac{(s - m_a^2 - m_b^2)(m_b^2 + m_1^2 - u) + 2m_b^2(t - m_a^2 - m_1^2)}{\lambda^1(s, m_a^2, m_b^2)\lambda^1(u, m_b^2, m_1^2)} \quad (4.15)$$

and

$$\cos \theta_{a2}^T = \frac{(s - m_a^2 - m_b^2)(m_b^2 + m_2^2 - t) + 2m_b^2(u - m_a^2 - m_2^2)}{\lambda^1(s, m_a^2, m_b^2)\lambda^1(t, m_b^2, m_2^2)}. \quad (4.16)$$

The relations (4.8–16) refer to the s channel frames. For many theoretical purposes it is important to be able to express noncovariant quantities in t and u channel frames in terms of s , t and u . But these relations are obtained from equations (4.8–16) by a simple permutation of indices. To go from the s to the t channel one interchanges 1 and b ($s \leftrightarrow t$, u unchanged), to go from s to u channel 2 and b ($s \leftrightarrow u$, t unchanged). For instance, the t channel CMS scattering angle is given by

$$\cos \theta_{ab}^{*(t)} = \frac{t(s - u) + (m_a^2 - m_1^2)(m_b^2 - m_2^2)}{\lambda^1(t, m_a^2, m_1^2)\lambda^1(t, m_b^2, m_2^2)}. \quad (4.17)$$

(c) Cross-section formulas

With the normalization convention (III.2.2–4) the reaction cross-section for $p_a + p_b \rightarrow p_1 + p_2$ is

$$\sigma(s) = \frac{1}{8\pi^2 \lambda^1(s, m_a^2, m_b^2)} \int \frac{d^3 p_1}{2E_1} \frac{d^3 p_2}{2E_2} \delta^4(p_a + p_b - p_1 - p_2) |A|^2. \quad (4.18)$$

The matrix element A depends on two independent variables. If a differential cross-section $d\sigma/dx$ is computed, there is no further integration over A , since there is only one nontrivial integration in equation (4.18).

The integral (4.18) was already treated in Section IV.1. On the basis of equations (1.7) and (1.12) one may immediately write in the CMS and TS:

$$\frac{d\sigma}{d\Omega_1^*} = \frac{1}{64\pi^2 s} \frac{P_1^*}{P_a^*} |A|^2 \quad (4.19)$$

$$\frac{d\sigma}{d\Omega_1^T} = \frac{1}{64\pi^2 m_b P_a^*} \frac{(P_1^T)^2}{(E_a^T + m_b)P_1^T - P_a^T E_1^T \cos \theta_{a1}^T} |A|^2. \quad (4.20)$$

In equation (4.20) P_1^T depends on θ_{a1}^T according to equation (3.8). Similar formulas for $d\sigma/d\Omega_2^*$ and $d\sigma/d\Omega_2^T$ are obtained by interchanging $1 \leftrightarrow 2$. Equations (4.19–20) simplify in some special cases (see Exercise IV.12).

Instead of the non-covariant cross-sections (4.19–20) it is mostly more convenient to use the invariant cross-section $d\sigma/dt$ (for instance, for data presentation). This can be obtained directly from equation (4.19). According to equation (4.2)

$$\begin{aligned} dt &= 2P_a^* P_1^* d \cos \theta_{a1}^* \\ &= \frac{1}{\pi} P_a^* P_1^* d\Omega_1^*. \end{aligned} \quad (4.21)$$

Then

$$\begin{aligned} \frac{d\sigma}{dt} &= \frac{d\sigma}{d\Omega_1^*} \frac{d\Omega_1^*}{dt} \\ &= \frac{|A|^2}{64\pi s P_a^{*2}} \\ &= \frac{|A|^2}{16\pi \lambda(s, m_a^2, m_b^2)}. \end{aligned} \quad (4.22)$$

It is very useful to give a direct derivation of equation (4.22). For this we have to evaluate the integral

$$\frac{dR_2}{dt} = \int \frac{d^3 p_1}{2E_1} \frac{d^3 p_2}{2E_2} \delta^4(p_a + p_b - p_1 - p_2) \delta\{t - (p_a - p_1)^2\}. \quad (4.23)$$

$A(s, t)$ could be included in the integrand, since it is a constant in the integration (s and t are constants). Using first equation (III.2.11) and integrating over $d^4 p_2$ one has

$$\frac{dR_2}{dt} = \int \left(\frac{d^3 p_1}{2E_1} \right) \delta\{(p_a + p_b - p_1)^2 - m_2^2\} \delta\{t - (p_a - p_1)^2\}.$$

Then going to CMS: $p_a + p_b = 0$, and using

$$\begin{aligned} \frac{d^3 p_1}{2E_1} &= \frac{P_1^2 dP_1 d\Omega_1}{2E_1} \\ &= \pi P_1 dE_1 d \cos \theta_{a1} \end{aligned}$$

one obtains

$$\begin{aligned} \frac{dR_2}{dt} &= \pi P_1^* \int_{m_1}^{\infty} dE_1^* \int_{-1}^1 d \cos \theta_{a1}^* \delta(s - 2E_1^* \sqrt{s + m_1^2 - m_2^2}) \\ &\quad \times \delta(t - m_a^2 - m_1^2 - 2E_a^* E_1^* + 2P_a^* P_1^* \cos \theta_{a1}^*). \end{aligned}$$

The integral over E_1^* is carried out by using the first δ function (integral nonzero if $m_1 \leq E_1^* < \infty$) and that over $\cos \theta_{a1}^*$ by using the second δ

function (integral nonzero if $-1 \leq \cos \theta_{a1}^* \leq 1$). Putting all factors together one obtains a result which we, for later reference, write in integral form:

$$R_2(s) = \frac{1}{4} \lambda^{-\frac{1}{2}}(s, m_a^2, m_b^2) \int d\phi_1 dt \Theta(1 - \cos^2 \theta_{a1}^*) \Theta(E_1^* - m_1). \quad (4.24)$$

The integrand is nonvanishing only if $E_1^* \geq m_1$, $-1 \leq \cos \theta_{a1}^* \leq 1$. When expressed in terms of s and t these requirements define the physical region in the st plane, which will be considered in the following section. Including the flux factor F defined by $F^{-1} = 8\pi^2 \lambda^{\frac{1}{2}}(s, m_a^2, m_b^2)$ again gives equation (4.22).

The reaction cross-section can now be computed from

$$\sigma(s) = \frac{1}{16\pi \lambda(s, m_a^2, m_b^2)} \int_{t^-}^{t^+} dt |A(s, t)|^2, \quad (4.25)$$

where $t^\pm = t^\pm(s; m_i^2)$ are the limits on t for fixed s determined in the following section (equation (5.31)).

The total cross-section for $p_a + p_b \rightarrow$ anything is given by the optical theorem (Källén, 1964) in terms of the forward scattering amplitude of an elastic process with masses $\mu m \rightarrow \mu m$ as follows:

$$\text{Im } A(s, t = 0) = \lambda^{\frac{1}{2}}(s, m^2, \mu^2) \sigma_T(s). \quad (4.26)$$

Later on we shall show that for elastic scattering the forward direction corresponds to $t = 0$ (equation (5.8)). Combining equations (4.26) and (4.22) one may compute the real part of the forward amplitude:

$$\{\text{Re } A(s, t = 0)\}^2 = \lambda(s, m^2, \mu^2) \left\{ 16\pi \frac{d\sigma}{dt} \Big|_{t=0} - \sigma_T^2(s) \right\}. \quad (4.27)$$

This is a positive quantity so that

$$\frac{d\sigma}{dt} \Big|_{t=0} \geq \frac{1}{16\pi} \sigma_T^2(s). \quad (4.28)$$

The value of $d\sigma/dt|_{t=0}$ corresponding to the equality sign is called the optical point. When applying equation (4.28) and all equations relating $d\sigma/dt$ and $\sigma^2(s)$ one must remember that their dimensions are $\text{mb}/(\text{GeV}/c)^2$ and mb^2 . The numerical value involved is $1/\text{GeV}^2 = 0.389 \text{ mb}$ (equation (II.3.7)).

5. The physical region in s, t, u

When the reaction $p_a + p_b \rightarrow p_1 + p_2$ is described, for instance, in terms of the variables E_1^* and θ_{a1}^* having an immediate physical significance, the s -channel physical region is easily determined: $E_1^* \geq m_1$, $-1 \geq \cos \theta_{a1}^* \geq 1$. In other words, the reaction $p_a + p_b \rightarrow p_1 + p_2$ can be experimentally measured at any point within this region. The problem now is to map this

region in the st plane. The complexity of the solution depends on the values of the masses. We shall first work out the case of elastic scattering and then deal with the general case.

Example 1: Assume the reaction $p_a + p_b \rightarrow p_1 + p_2$ is a process with $m_a = m_1 = \mu$ and $m_b = m_2 = m$, where one may choose $\mu \leq m$. This includes elastic scattering (e.g. $\pi^- p \rightarrow \pi^- p$) and, in practice, related charge exchange processes (e.g. $\pi^- p \rightarrow \pi^0 n$). Since this case is so important we shall here summarize the simplified forms of kinematical relations between s, t, u and some s channel CMS quantities. For energies and momenta we have from equation (4.8):

$$\begin{aligned} E_a^* &= E_1^* \\ &= \frac{s + \mu^2 - m^2}{2\sqrt{s}} \\ E_b^* &= E_2^* \\ &= \frac{s - m^2 + \mu^2}{2\sqrt{s}} \\ P_a^* &= P_b^* = P_1^* = P_2^* \\ &\equiv P^* \\ &= \frac{\lambda(s, m^2, \mu^2)}{2\sqrt{s}} \end{aligned} \quad (5.1)$$

and for the scattering angle θ_{a1}^* from equation (4.9):

$$\cos \theta_{a1}^* = 1 + \frac{2st}{\lambda(s, m^2, \mu^2)} \quad (5.2)$$

or, conversely,

$$\begin{aligned} t &= -\frac{\lambda(s, m^2, \mu^2)}{2s}(1 - \cos \theta_{a1}^*) \\ &= -2P^{*2}(1 - \cos \theta_{a1}^*) \\ &= -4P^{*2} \sin^2 \frac{1}{2}\theta_{a1}^*. \end{aligned} \quad (5.3)$$

Notice, in particular, the simple form of equation (5.3) (Exercise IV.14). For the relation between u and $\cos \theta_{a1}^*$ one obtains from

$$s + t + u = 2m^2 + 2\mu^2 \quad (5.4)$$

that

$$u = \frac{(m^2 - \mu^2)^2}{s} - \frac{\lambda(s, m^2, \mu^2)}{2s}(1 + \cos \theta_{a1}^*). \quad (5.5)$$

Compared with equation (5.3) there is an important extra term in equation (5.5) which implies that in the backward direction

$$u(\theta_{a1}^* = \pi) = \frac{(m^2 - \mu^2)^2}{s} \quad (5.6)$$

while in the forward region

$$t(\theta_{a1}^* = 0) = 0. \quad (5.7)$$

This extra term will be analysed in detail in Section 6.

The boundary of the physical region can now be obtained from the requirement $-1 \leq \cos \theta_{a1}^* \leq 1$ for $\cos \theta_{a1}^*$ in equation (5.2). The upper limit of t is attained when

$$\begin{aligned} t &= 0 \\ u &= 2m^2 + 2\mu^2 - s \end{aligned} \quad (\cos \theta_{a1}^* = 1) \quad (5.8)$$

and the lower limit when

$$\begin{aligned} t &= -\frac{\lambda(s, m^2, \mu^2)}{s} \\ u &= \frac{(m^2 - \mu^2)^2}{s}. \end{aligned} \quad (\cos \theta_{a1}^* = -1) \quad (5.9)$$

In the st plane equation (5.8) is a straight line and equation (5.9) is a hyperbola with the asymptotes

$$\begin{aligned} s &= 0 \\ u &= 0 \quad \text{or} \quad t = -s + 2m^2 + 2\mu^2 \end{aligned} \quad (5.10)$$

(Figure 5.1). The curves (5.8) and (5.9) intersect at $s = (m \pm \mu)^2$. The value $s = (m + \mu)^2$ corresponds to the threshold ($P^* = 0$) of the reaction $p_a + p_b \rightarrow p_1 + p_2$. For each larger value $s \geq (m + \mu)^2$ the vertical straight line between the curves (5.8–9) corresponds to the complete range of values $-1 \leq \cos \theta_{a1}^* \leq 1$. Note that the threshold condition was automatically included in the angular condition (5.9). The physical region in the st plane for $p_a + p_b \rightarrow p_1 + p_2$ has thus been determined.

Although we only used the s channel angle θ_{a1}^* in the derivation, equations (5.8–9) also give the u channel ($u \geq (m + \mu)^2$) and t channel ($t \geq 4m^2$) physical regions. These are also shown in Figure 5.1.

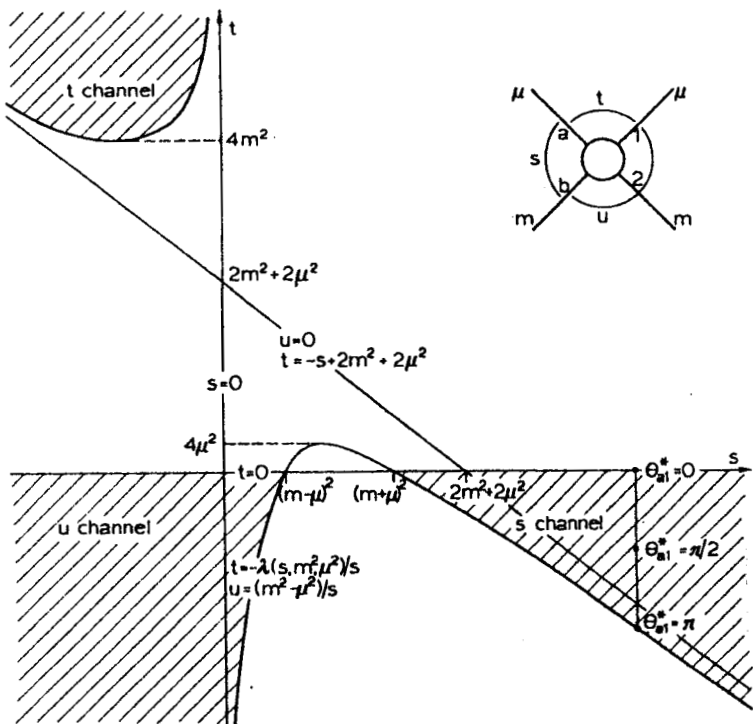


Figure IV.5.1 Physical region on st plane for masses $\mu m \rightarrow \mu m$

We can now return to the case of arbitrary masses. By considering a decay $p \rightarrow p_i + p_j$ we proved earlier that

$$\Delta_2(p_i, p_j) = p_i^2 p_j^2 - (p_i \cdot p_j)^2 \leq 0. \quad (5.11)$$

Equivalently, the invariant $(p_i + p_j)^2$ must satisfy

$$(p_i + p_j)^2 \geq (m_i + m_j)^2$$

or

$$(p_i + p_j)^2 \leq (m_i - m_j)^2.$$

In $p_a + p_b \rightarrow p_1 + p_2$, $s = (p_a + p_b)^2 = (p_1 + p_2)^2$ thus has to be larger than both $(m_a + m_b)^2$ and $(m_1 + m_2)^2$ or smaller than both $(m_a - m_b)^2$ and $(m_1 - m_2)^2$. Since the same is valid for all invariants, one sees that in the

scattering channels physical s , t and u have to satisfy

$$s \geq \max \{(m_a + m_b)^2, (m_1 + m_2)^2\}$$

or

$$s \leq \min \{(m_a - m_b)^2, (m_1 - m_2)^2\},$$

$$t \geq \max \{(m_a + m_1)^2, (m_b + m_2)^2\}$$

or

$$t \leq \min \{(m_a - m_1)^2, (m_b - m_2)^2\},$$

$$u \geq \max \{(m_a + m_2)^2, (m_b + m_1)^2\}$$

(5.12)

or

$$u \leq \min \{(m_a - m_2)^2, (m_b - m_1)^2\}.$$

In the decay channels (we first consider $p_b \rightarrow p_{\bar{a}} + p_1 + p_2$) one must remember that in the equation $p_a + p_b = p_1 + p_2$, p_a now has a negative energy. To give p_a a positive energy we replace $p_a \rightarrow -p_a$, and therefore $s = (p_b - p_a)^2 = (p_1 + p_2)^2$ satisfies $(m_1 + m_2)^2 \leq s \leq (m_b - m_a)^2$. Applying the same to $t = (p_a + p_1)^2 = (p_b - p_2)^2$ and $u = (p_b - p_1)^2 = (p_a + p_2)^2$ one finds

$$\begin{aligned} (m_1 + m_2)^2 &\leq s \leq (m_b - m_a)^2 \\ (m_a + m_1)^2 &\leq t \leq (m_b - m_2)^2 \\ (m_a + m_2)^2 &\leq u \leq (m_b - m_1)^2. \end{aligned} \quad (5.13)$$

These inequalities can obviously be satisfied only if $m_b \geq m_1 + m_2 + m_a$. If instead m_a , m_1 or m_2 is larger than the sum of the remaining masses, one obtains a similar set of inequalities for each case. Together with equations (5.12) and (5.13) these exhaust all conditions of the type $\Delta_2 \leq 0$, expressed in terms of s , t and u .

In addition to equation (5.12) one must impose the condition $|\cos \theta_{a1}^*| \leq 1$, which will be shown to lead to a condition of the type $\Delta_3 \geq 0$ and which obviously restricts s and t simultaneously. In fact, by inserting $\cos \theta_{a1}^* = \pm 1$ in equation (4.9) and using equation (4.8) to write energies and momenta in terms of s we have simply

$$\begin{aligned} t^\pm &= m_a^2 + m_1^2 - 2E_a^* E_1^* \pm 2P_a^* P_1^* \\ &= m_a^2 + m_1^2 - \frac{1}{2s} \{(s + m_a^2 - m_b^2)(s + m_1^2 - m_2^2) \\ &\quad \mp \lambda^4(s, m_a^2, m_b^2) \lambda^4(s, m_1^2, m_2^2)\} \end{aligned} \quad (5.14)$$

where the \pm indices in t^\pm refer to the two values $\cos \theta_{s1}^* = \pm 1$. In particular, t^+ (often called $|t|^{min}$) is the value of t in the forward direction (Section 6). For elastic scattering equation (5.14) reduces to equations (5.8–9). In general, equation (5.14) gives the boundary of the physical region for $2 \rightarrow 2$ scattering in the st plane. An example is given in Figure 5.2; further examples are found in Figures 5.6 and 5.7.

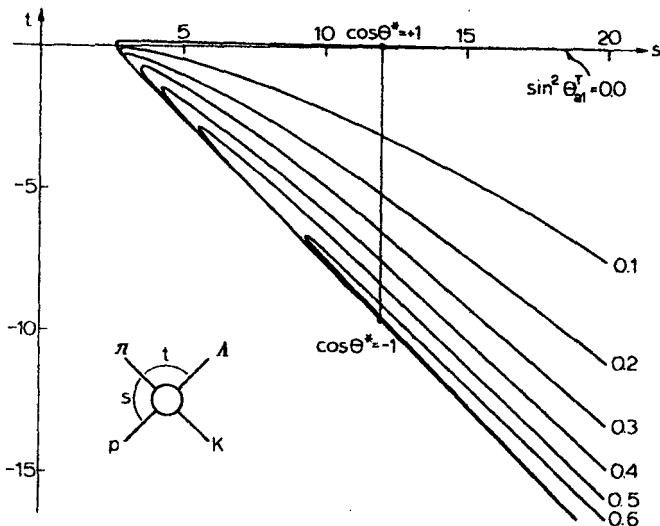


Figure IV.5.2 Physical region of $\pi p \rightarrow \Lambda K$ in the st plane. Curves of constant target system scattering angle θ_{s1}^* are also shown

Equation (5.14) actually gives the physical region in all possible channels, although this is not obvious from the derivation. To see the symmetries between the various channels and to obtain the result in a compact form it is simplest to determine the boundary not from $\cos \theta_{s1}^* = \pm 1$ but from the equivalent single condition $\sin^2 \theta_{s1}^* = 0$ (Kibble, 1960). To compute $\sin \theta_{s1}^*$ it is inconvenient to start from equation (4.9), and the most elegant method is to write $\sin \theta_{s1}^*$ in terms of invariants, as shown in Section II.7. We know that θ_{s1}^* is the angle between p_s and p_1 in the frame $p_s + p_b = 0$. Then equation (II.7.9) permits us to write

$$\begin{aligned} s P_s^{*2} P_1^{*2} \sin^2 \theta_{s1}^* &= \Delta_3(p_s + p_b, p_s, p_1) \\ &= \Delta_3(p_s, p_b, p_1) \end{aligned} \quad (5.15)$$

where equation (A.6) was used. The Gram determinant Δ_3 is the following

function of s, t and the masses:

$$\Delta_3(p_a, p_b, p_1) = \begin{vmatrix} p_a^2 & p_a \cdot p_b & p_a \cdot p_1 \\ p_a \cdot p_b & p_b^2 & p_b \cdot p_1 \\ p_a \cdot p_1 & p_b \cdot p_1 & p_1^2 \end{vmatrix} \quad (5.16)$$

$$= \frac{1}{8} \begin{vmatrix} 2m_a^2 & s - m_a^2 - m_b^2 & m_a^2 + m_1^2 - t \\ s - m_a^2 - m_b^2 & 2m_b^2 & m_b^2 + m_1^2 - u \\ m_a^2 + m_1^2 - t & m_b^2 + m_1^2 - u & 2m_1^2 \end{vmatrix}.$$

When the determinant on the right hand side of equation (5.16) is expanded, one obtains the basic four-particle kinematic function $G(x, y, z, u, v, w)$ (Nyborg, 1965a), which corresponds to Δ_3 in the same way as $\lambda(x, y, z)$ corresponds to Δ_2 (equation (II.7.4)):

$$\begin{aligned} \Delta_3(p_a, p_b, p_1) &= -\frac{1}{4}G\{(p_a + p_b)^2, (p_a - p_1)^2, (p_a + p_b - p_1)^2, p_a^2, p_b^2, p_1^2\} \\ &= -\frac{1}{4}G(s, t, m_2^2, m_a^2, m_b^2, m_1^2). \end{aligned} \quad (5.17)$$

The properties of G will presently be analyzed in great detail. In terms of it we may write equation (5.15) in the form

$$\sin^2 \theta_{a1}^* = -4s \frac{G(s, t, m_2^2, m_a^2, m_b^2, m_1^2)}{\lambda(s, m_a^2, m_b^2)\lambda(s, m_1^2, m_2^2)}. \quad (5.18)$$

The physical region for $2 \rightarrow 2$ scattering in the st plane thus has to satisfy, in addition to conditions of the type (5.12) or (5.13), the requirement

$$\Delta_3 \geq 0, \quad (5.19)$$

where the arguments may be any three linearly independent combinations of p_a, p_b, p_1 and p_2 , or the equivalent requirement

$$G(s, t, m_2^2, m_a^2, m_b^2, m_1^2) \leq 0. \quad (5.20)$$

Note, in particular, that equation (5.20) applies even if any of the p_i is not the four-momentum of a single particle but of a group of particles. Then m_i is the invariant mass of the group. Equation (5.20) is, therefore, very general and it is useful to remember it in the form of a mnemonic rule shown in Figure 5.3.



Figure IV.5.3

To derive equation (5.20) one may equally well use the target system scattering angle θ_{a1}^T . In order to find θ_{a1}^T in terms of invariants, we use the rule (II.7.9) for the angle between p_a and p_1 in the frame $p_b = 0$:

$$\begin{aligned} m_b^2 (P_a^T P_1^T)^2 \sin^2 \theta_{a1}^T &= \Delta_3(p_b, p_a, p_1) \\ &= \Delta_3(p_a, p_b, p_1). \end{aligned}$$

Using the definition of G , equations (4.10) and (4.14), one has

$$\sin^2 \theta_{a1}^T = -4 \frac{m_b^2 G(s, t, m_2^2, m_a^2, m_b^2, m_1^2)}{\lambda(s, m_a^2, m_b^2) \lambda(u, m_b^2, m_1^2)}. \quad (5.21)$$

By dividing equation (5.18) by (5.21) and using equations (4.8) and (4.14) one sees that

$$\frac{\sin \theta_{a1}^*}{\sin \theta_{a1}^T} = \frac{P_1^T}{P_1^*}, \quad (5.22)$$

as we expect.

We shall now consider the properties of G . Since G is connected with the Gram determinant Δ_3 , it satisfies a number of symmetry relations and possesses a number of simple algebraic properties. These are analogous to the relations (II.6.3-7) for $\lambda(x, y, z)$.

(a) Algebraic expression for $G(x, y, z, u, v, w)$

Since one may replace p_a , p_b and p_1 in equation (5.16) by any of their linearly independent combinations, the determinantal representation of Δ_3 can be put in many not manifestly equal representations. All these lead upon expansion to a single universal function G given by

$$\begin{aligned} G(x, y, z, u, v, w) &= x^2y + xy^2 + z^2u + zu^2 + v^2w + vw^2 + xzw + xuv \\ &\quad + yzw + yuw - xy(z + u + v + w) \\ &\quad - zu(x + y + v + w) - vw(x + y + z + u). \end{aligned} \quad (5.23)$$

From equation (A.13) it is seen that G can also be expressed as a Cayley determinant

$$G(x, y, z, u, v, w) = -\frac{1}{2} \begin{vmatrix} 0 & 1 & 1 & 1 & 1 \\ 1 & 0 & v & x & z \\ 1 & v & 0 & u & y \\ 1 & x & u & 0 & w \\ 1 & z & y & w & 0 \end{vmatrix} \quad (5.24)$$

If the masses are given by $m_a = m_1 = \mu$, $m_b = m_2 = m$, the G function in equation (5.20) is needed in the simplified form

$$G(x, y, z, u, v, w) = y\{xy + \lambda(x, z, u)\}. \quad (5.25)$$

Equation (5.18) then gives

$$\sin \theta_{*1}^* = \frac{2}{\lambda(s, m^2, \mu^2)} [-st\{st + \lambda(s, m^2, \mu^2)\}]^{\frac{1}{2}} \quad (5.26)$$

and one has rediscovered the boundary equations (5.8–9) for $\mu m \rightarrow \mu m$. It is easy to see that equations (5.2) and (5.26) are compatible.

(b) Interpretation of G

Exactly as $\lambda(x, y, z)$ was related to the area of a triangle, one can see (Exercise IV.17) that

$$G(x, y, z, u, v, w) = (-144) \times (\text{squared volume of a tetrahedron with pairwise opposite sides } \sqrt{x}, \sqrt{y}; \sqrt{z}, \sqrt{u}; \sqrt{v}, \sqrt{w}) \quad (5.27)$$

The ordering of the sides is indicated in Figure 5.4. Due to this interpretation one may call G the tetrahedron function.

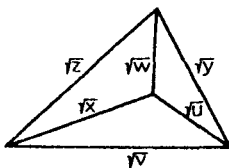


Figure IV.5.4

(c) Symmetry properties of G

G is invariant under certain permutations of its six arguments. What these permutations are can be most easily seen from the interpretation of G as the volume of the tetrahedron in Figure 5.4. This volume is clearly invariant under any permutations of the four faces (or vertices) of the tetrahedron. These $4! = 24$ transformations of the faces induce a set of transformations on the sides x, y, z, u, v, w . This set can be generated as follows. Group the arguments of G in three groups xy, zy, vw corresponding to the opposite sides of the tetrahedron. Then G is invariant under

- (i) any permutation of these groups
 - (ii) any simultaneous interchange of arguments inside two groups
- Transformations (i) give six orderings and to each of these one may apply three transformations of type (ii) leading to a total of $6 + 6 \times 3 = 24$ transformations. In the language of group theory, the invariance group

$G(x, y, z, u, v, w)$ is a subgroup of the group of permutations of six objects. It is generated by (i) and (ii) and is isomorphic to the group permutations of four objects.

(d) *Algebraic properties*

G is often needed as a function of two variables, for instance, of s and t in equation (5.20). Due to the symmetry properties there are only two essentially different cases, and the two variables can be chosen to be either xy or xz . The curve $G = 0$ is of third order in x, y and of second order in x, z . To plot $G = 0$ in the xy or xz plane one has to solve $G = 0$ for x, y and z . The solutions of these second-degree equations are:

$$\begin{aligned}x^{\pm} &= z + w - \frac{1}{2y} \{(y + z - v)(y + w - u) \mp \lambda^{\frac{1}{2}}(y, z, v)\lambda^{\frac{1}{2}}(y, u, w)\} \\&= u + v - \frac{1}{2y} \{(y - z + v)(y - w + u) \mp \lambda^{\frac{1}{2}}(y, z, v)\lambda^{\frac{1}{2}}(y, u, w)\} \\y^{\pm} &= u + w - \frac{1}{2x} \{(x + u - v)(x + w - z) \mp \lambda^{\frac{1}{2}}(x, u, v)\lambda^{\frac{1}{2}}(x, w, z)\} \\z^{\pm} &= x + w - \frac{1}{2u} \{(u + x - v)(u + w - y) \pm \lambda^{\frac{1}{2}}(u, x, v)\lambda^{\frac{1}{2}}(u, w, y)\}. \end{aligned}\quad (5.28)$$

The solutions for y and z are obtained from x^{\pm} by the permutations $x \leftrightarrow y$, $z \leftrightarrow u$ and $x \leftrightarrow z$, $u \leftrightarrow y$, respectively, but since they are so often needed we give the solutions corresponding to the first form of x^{\pm} explicitly. We always want $x^+ \geq x^-$ and the signs above are written for $y > 0$.

The λ s in equation (5.28) are clearly related to areas of the faces of the tetrahedron in Figure 5.4. G can now be also expressed in terms of its roots as follows:

$$\begin{aligned}G(x, y, z, u, v, w) &= y(x - x^+)(x - x^-) \\&= x(y - y^+)(y - y^-) \\&= u(z - z^+)(z - z^-),\end{aligned}\quad (5.29)$$

where the coefficients of the quadratic terms were found from equation (5.23).

The form of the equations (5.28) can be understood by noting that they are the analogues of equation (II.7.5) evaluated for $\cos \theta_{23} = \pm 1$. G or Δ_3 vanishes when some $\sin^2 = 0$; the \pm signs in equation (5.28) corresponding to putting the corresponding cosine equal to ± 1 . This cosine is evaluated in the rest frame of the variable dividing the brackets in equation (5.28); if, for instance, $y = s$, the frame is the CMS. The λ s in equation (5.28) are related to momenta and the two first factors within the brackets to energies in this frame.

These conclusions are also obvious if we use equation (5.28) to plot the physical region boundary (5.20) for $p_a + p_b \rightarrow p_1 + p_2$ in the st plane. We can either solve for s in terms of t :

$$s^\pm = m_a^2 + m_b^2 - \frac{1}{2t} \{(t + m_b^2 - m_2^2)(t + m_a^2 - m_1^2) \\ \pm \lambda^{\frac{1}{4}}(t, m_b^2, m_2^2)\lambda^{\frac{1}{4}}(t, m_a^2, m_1^2)\} \quad (5.30)$$

or for t in terms of s :

$$t^\pm = m_a^2 + m_1^2 - \frac{1}{2s} \{(s + m_a^2 - m_b^2)(s + m_1^2 - m_2^2) \\ \mp \lambda^{\frac{1}{4}}(s, m_a^2, m_b^2)\lambda^{\frac{1}{4}}(s, m_1^2, m_2^2)\} \quad (5.31)$$

Equation (5.31) is, of course, the same as equation (5.14), which was directly derived by setting $\cos \theta_{a1} = \pm 1$. If one applies the second form of x^\pm (or the analogous one for y^\pm) to solve for t , one sees that it corresponds to setting $\cos \theta_{b2}^* = \cos \theta_{a1}^* = \pm 1$ in $t = (p_b - p_2)^2 = (p_a - p_1)^2$:

$$t^\pm = m_b^2 + m_2^2 - 2E_b^*E_2^* \pm 2P_b^*P_2^*. \quad (5.32)$$

Similarly, the \pm signs in equation (5.30) correspond to putting the cosine of the t channel CMS scattering angle equal to ± 1 .

(e) Symmetric representation of G

Equations (5.30–31) can be used to plot the physical regions in all the channels, although they are not manifestly symmetric. In order to treat the boundary in a more symmetric way we shall write G in a form which shows explicitly the symmetry between s, t and u channels (Kibble, 1960). The relevant identity is

$$- G(s, t, m_2^2, m_a^2, m_b^2, m_1^2) \equiv \Phi(s, t) \\ = stu - (\alpha s + \beta t + \gamma u), \quad (5.33)$$

where

$$\begin{aligned} K\alpha &= (m_a^2 m_b^2 - m_1^2 m_2^2)(m_a^2 + m_b^2 - m_1^2 - m_2^2) \\ K\beta &= (m_a^2 m_1^2 - m_b^2 m_2^2)(m_a^2 + m_1^2 - m_b^2 - m_2^2) \\ K\gamma &= (m_a^2 m_2^2 - m_b^2 m_1^2)(m_a^2 + m_2^2 - m_b^2 - m_1^2) \end{aligned} \quad (5.34)$$

with

$$\begin{aligned} K &= m_a^2 + m_b^2 + m_1^2 + m_2^2 \\ &= s + t + u. \end{aligned}$$

It is also convenient to use, instead of Cartesian s, t coordinates, triangular coordinates. The axes are three lines intersecting at 60° , and s, t, u are the distances from the corresponding axes (Figure 5.5). When the height of the triangle between the lines is $\sum m_i^2$, the condition $s + t + u = \sum m_i^2$ is automatically satisfied.

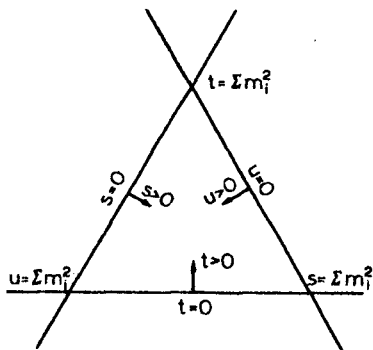


Figure IV.5.5 Triangular coordinates for s, t, u

It is easy to see that the cubic curve $\Phi(s, t) = 0$ has the following properties:

1. The asymptotes are $s = 0, t = 0, u = 0$

2. The curve $\Phi(s, t) = 0$ intersects the asymptotes in the following three points on the line $\alpha s + \beta t + \gamma u = 0$:

$$s = 0: \quad t = -\frac{\gamma K}{\beta - \gamma} \quad u = \frac{\beta K}{\beta - \gamma}$$

$$t = 0: \quad s = -\frac{\gamma K}{\alpha - \gamma} \quad u = \frac{\alpha K}{\alpha - \gamma}$$

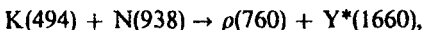
$$u = 0: \quad s = -\frac{\beta K}{\alpha - \beta} \quad t = \frac{\alpha K}{\alpha - \beta}$$

3. The tangents of $\Phi(s, t) = 0$ parallel to the three coordinate axes are the following twelve lines at the threshold and pseudothreshold of the three channels:

$$\begin{aligned} s &= (m_a \pm m_b)^2, & s &= (m_1 \pm m_2)^2 \\ t &= (m_a \pm m_1)^2, & t &= (m_b \pm m_2)^2 \\ u &= (m_a \pm m_2)^2, & u &= (m_b \pm m_1)^2. \end{aligned} \tag{5.35}$$

For different sets of masses the curves $\Phi = 0$ fall into 14 different types. We do not here attempt a general classification of them. This has been carried out by Kotanski (Kotanski, 1968; see also Sakmar, 1967). We shall limit ourselves to presenting the 'normal' case, in which all masses are nonzero and satisfy no special relationships, in addition to the elastic case treated previously.

Consider first the reaction



the physical region of which is plotted in Figure 5.6 by using equation (5.31). Now $m_a + m_b < m_1 + m_2$ so that the s channel threshold is $m_1 + m_2 = m_\rho + m_{Y^*}$. In the s channel t remains negative while u may attain the value $(m_b - m_1)^2 = (m_N - m_\rho)^2$ in the backward direction. The t channel is $K\bar{\rho} \rightarrow$

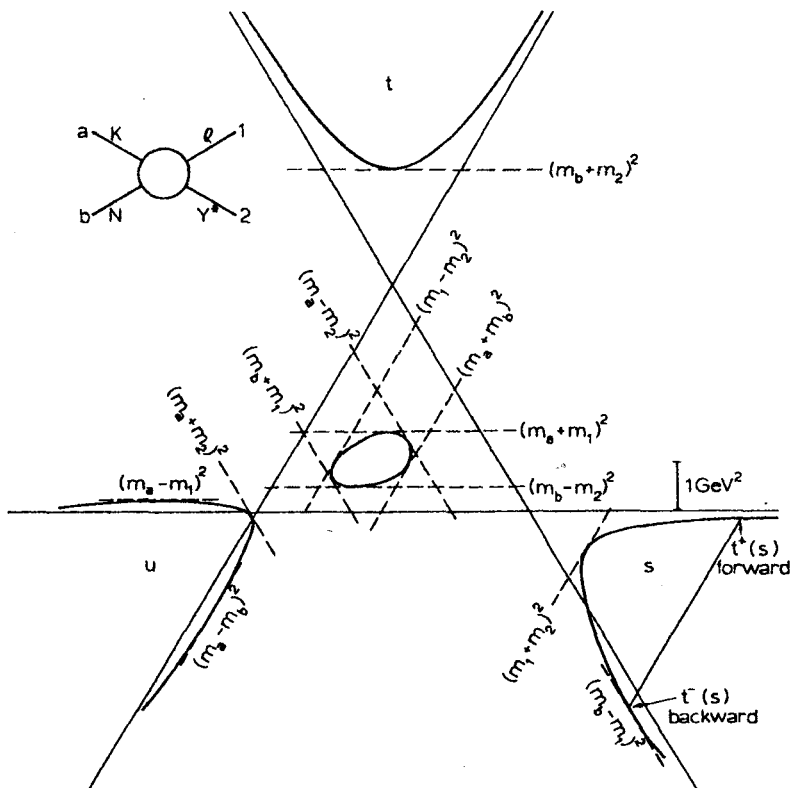


Figure IV.5.6 Physical regions for the reaction $KN \rightarrow \rho Y^*$. The central region is not physical in this case. The boundaries for the s and u channels have been slightly distorted to show the tangents clearly. The expressions for $t^\pm(s)$ are given in equation (5.31)

$\bar{N}Y^*$ so that its threshold is $m_b + m_2 = m_N + m_{Y^*}$. Both s and u remain negative. The threshold of the u channel $K\bar{Y}^* \rightarrow \rho\bar{N}$ is $m_a + m_2 = m_K + m_{Y^*}$, and t reaches the value $(m_a - m_1)^2 = (m_K - m_\rho)^2$, and s the value $(m_a - m_b)^2 = (m_K - m_N)^2$. The remaining three thresholds and three pseudothresholds are tangent to a connected *central region*, which lies in the region where s, t and u are all positive. In the present case no mass is larger than the sum of the remaining three. This implies that all thresholds tangent to the central region are larger than the parallel pseudothresholds, e.g. $(m_a + m_1)^2 > (m_b - m_2)^2$. Thus no decay can take place and the central region is unphysical. In other words, the central region satisfies $\Delta_3 \geq 0$ but not $\Delta_2 \leq 0$.

If one instead considers the reaction (Figure 5.7)

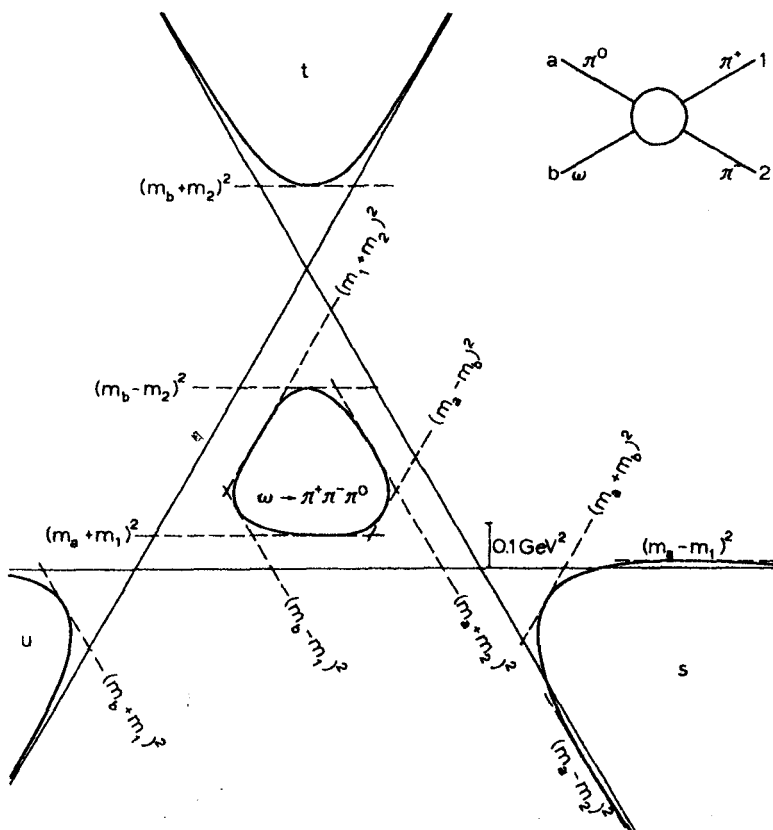
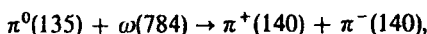


Figure IV.5.7 Physical regions of the reaction $\pi^0\omega \rightarrow \pi^+\pi^-$. The central region is now physical (Dalitz plot). The s channel boundary is distorted as in Figure 5.6

the central region is physical since the decay $\omega \rightarrow \pi^+ \pi^- \pi^0$ is possible. One sees explicitly how the inequalities (5.13) are satisfied. When the central region is physical it will be called the *Dalitz plot*. This is treated in detail in Chapter V.

(f) Formal relation between G and λ

As a final remark, we note as a curiosity that the G function can be related to the λ function as follows. Assume three three-vectors satisfy $\mathbf{p}_1 + \mathbf{p}_2 + \mathbf{p}_3 = 0$. Then it follows from the fact that λ is related to the area of a triangle (see remark after equation (II.6.9)) that

$$\begin{aligned} |\mathbf{p}_1 \times \mathbf{p}_2|^2 &= |\mathbf{p}_2 \times \mathbf{p}_3|^2 \\ &= |\mathbf{p}_3 \times \mathbf{p}_1|^2 \\ &= -\frac{1}{4}\lambda(P_1^2, P_2^2, P_3^2) \end{aligned} \quad (5.36)$$

Apply this to $p_a + p_b \rightarrow p_1 + p_2$ in the TS: $\mathbf{p}_b = 0$, $\mathbf{p}_a - \mathbf{p}_1 - \mathbf{p}_2 = 0$. Then we may write

$$|\mathbf{p}_a \times \mathbf{p}_1|^2 = -\frac{1}{4}\lambda\{(P_a^T)^2, (P_1^T)^2, (P_2^T)^2\}. \quad (5.37)$$

On the other hand, the rule (II.7.9) implies

$$\begin{aligned} m_b^2|\mathbf{p}_a \times \mathbf{p}_1|^2 &= \Delta_3(p_a, p_b, p_1) \\ &= -\frac{1}{4}G(s, t, m_2^2, m_a^2, m_b^2, m_1^2). \end{aligned} \quad (5.38)$$

By equating equations (5.37) and (5.38) and by replacing the momenta in equation (5.37) by invariants according to equations (4.10–14) we find the identity

$$G(s, t, m_2^2, m_a^2, m_b^2, m_1^2) = \lambda\{\lambda(s, m_a^2, m_b^2), \lambda(t, m_b^2, m_2^2), \lambda(u, m_b^2, m_1^2)\}/16m_b^2. \quad (5.39)$$

From a practical point of view this identity is not very useful.

6. Value of t in the forward direction

We have seen that for $\mu m \rightarrow \mu m$ the value of t in the forward direction (t^+) is zero but that in the backward direction $u = (m^2 - \mu^2)^2/s > 0$. In general, the value of t^+ , as given by equation (5.14), (either positive or negative) is non-zero, but approaches zero when $s \rightarrow \infty$. However, equation (5.14) gives the small number t^+ as a difference of two large numbers and the magnitude of t^+ is not obvious. For large s one may cancel the large terms by expanding as follows (Pilkuhn, 1967).

Introduce expansion parameters

$$\begin{aligned}\varepsilon_{ab} &= \frac{m_a m_b}{s - m_a^2 - m_b^2}, \\ \varepsilon_{12} &= \frac{m_1 m_2}{s - m_1^2 - m_2^2}.\end{aligned}\quad (6.1)$$

This is convenient because then expansions of $\lambda^\frac{1}{2}(s, m_a^2, m_b^2)$ and $\lambda^\frac{1}{2}(s, m_1^2, m_2^2)$ go as powers of ε^2 :

$$\begin{aligned}\lambda^\frac{1}{2}(s, m_a^2, m_b^2) &= \{(s - m_a^2 - m_b^2) - 4m_a^2 m_b^2\}^\frac{1}{2} \\ &= (s - m_a^2 - m_b^2)(1 - 4\varepsilon_{ab}^2)^\frac{1}{2} \\ &= (s - m_a^2 - m_b^2)(1 - 2\varepsilon_{ab}^2 - 2\varepsilon_{ab}^4 + \dots),\end{aligned}\quad (6.2)$$

and similarly for the other λ . When this is inserted in equation (5.14), the terms proportional to s and the constant terms cancel and the expansion starts as follows:

$$\begin{aligned}t^+ &= -\frac{1}{s}(m_a^2 - m_1^2)(m_b^2 - m_2^2) - \frac{1}{s^2}(m_a^2 + m_b^2 - m_1^2 - m_2^2) \\ &\quad \times (m_a^2 m_b^2 - m_1^2 m_2^2) + \dots\end{aligned}\quad (6.3)$$

If $m_a \neq m_1$ and $m_b \neq m_2$ one sees that t^+ is proportional to $1/s$:

$$t^+ \simeq -(m_a^2 - m_1^2)(m_b^2 - m_2^2)/s \quad (m_a m_b \rightarrow m_1 m_2) \quad (6.4)$$

Thus t^+ is positive if $m_a < m_1$, $m_b > m_2$ or $m_a > m_1$, $m_b < m_2$. For instance, for $\mu m \rightarrow \mu \mu (m_a = m_2 = \mu, m_b = m_1 = m)$,

$$t^+ \simeq (m^2 - \mu^2)^2/s \quad (\mu m \rightarrow \mu \mu) \quad (6.5)$$

happens to be exactly the old result for the backward value of u in $\mu m \rightarrow \mu m$, which corresponds to the forward value of t in $\mu m \rightarrow \mu \mu$.

If $m_a = m_1$ or $m_b = m_2$, or both, t^+ is proportional to $1/s^2$. An example of this is resonance production with masses $\mu m \rightarrow \mu m^*, m^* > m$. Then

$$t^+ \simeq -\mu^2(m^{*2} - m^2)^2/s^2 \quad (\mu m \rightarrow \mu m^*) \quad (6.6)$$

Now t^+ is always negative.

Exercises

- IV.1. Consider a decay $p \rightarrow p_1 + p_2$ to two zero-mass particles ($m_1 = m_2 = 0$) in a frame $p = (E, \mathbf{p})$. Compute the angle θ_{12} between \mathbf{p}_1 and \mathbf{p}_2 in terms of the angle θ_1 between \mathbf{p}_1 and \mathbf{p} .

- IV.2. For the decay $p \rightarrow p_1 + p_2$ with $m_1 = m_2 = 0$ derive the relation

$$\sin \frac{1}{2}\theta_{12} = \frac{m}{2\sqrt{(E_1 E_2)}}$$

and show from this that the minimum opening angle θ_{12}^{\min} is obtained in the symmetric situation $\theta_1 = \theta_2$. What is $\sin \frac{1}{2}\theta_{12}^{\min}$?

- IV.3. The existence of a minimum opening angle can be used for the mass determination of a neutral particle with a $\gamma\gamma$ decay mode (for instance π^0 or η) as follows. Assume the neutral particle p_2 is produced in the reaction $p_a + p_b \rightarrow p_1 + p_2$. Observe the $\gamma\gamma$ decays of p_2 and find out what the minimum opening angle is in the CMS of the whole reaction. If this angle is α , the mass of p_1 is m_1 and the total energy is \sqrt{s} , what is m_2 ?
- IV.4. Show that equation (2.8) gives the distribution (2.5) if the masses are $m_1 = m_2 = 0$.
- IV.5. Compute in a $1 \rightarrow 2$ decay the transverse momentum distribution $w(r_1)$ in terms of the distribution $w(\cos \theta_1^*)$.
- IV.6. For a decay $p \rightarrow p_1 + p_2$ assume you can compute the quantity

$$T_2 = \frac{1}{2s+1} \sum |A|^2,$$

where s is the spin of p , the sum goes over the final spin states and A is the matrix element of the decay. What is the lifetime τ of p ? What are the dimensions of T_2 ? For the decay $K_s^0 \rightarrow \pi^+ \pi^-$, assume that $T = f_\kappa = \text{constant}$. Determine f_κ from $\tau_{K^0} = 0.86 \times 10^{-10} \text{ sec}$.

- IV.7. For the decay $\rho \rightarrow \pi\pi$ one conventionally writes $A = f_{\rho\pi\pi} \varepsilon \cdot (p_1 - p_2)$, where ε is the polarization vector of the ρ . Then, if T_2 is defined as in Exercise 6, one finds

$$T_2 = \frac{4}{3} p_\pi^{*2}.$$

(Can you compute this?) What is the lifetime τ_ρ of the ρ in terms of $f_{\rho\pi\pi}$? What is $f_{\rho\pi\pi}^2/4\pi$ if $\Gamma_\rho = 0.125 \text{ GeV}$?

- IV.8. Calculate the dependence of P_1 on the scattering angle θ_1 in the TS ($p_b = 0$) by evaluating the equation $p_2^2 = (p_a + p_b - p_1)^2$ in the TS and solving for P_1 .
- IV.9. Find how the momenta of the scattered (p_1) and recoil (p_2) particles in the reaction $p_a + p_b = p_1 + p_2$ depend on the corresponding target system scattering angles when the incident energy is E_a and all masses are equal ($= m$). What are the relations if $m_a = m_1 = 0$ and $m_b = m_2 = m$?

- IV.10. What is the relation between the two target system scattering angles θ_1 and θ_2 in $p_a + p_b \rightarrow p_1 + p_2$ when (a) all masses are equal ($= m$), (b) $m_a = m_1 = 0, m_b = m_2 = m$? Plot the curves when $\gamma^2 = 10$ and compare with Figure 3.3.
- IV.11. What are the maximum and the minimum values of the momenta of (a) the scattered particle (p_1), (b) the recoil particle in an elastic scattering process $p_a + p_b \rightarrow p_1 + p_2$?
- IV.12. Show that for electron-proton scattering at high energies ($m_a = m_1 = 0, m_b = m_2 = m$) in the target system

$$\frac{dR_2}{d\Omega_1} = \frac{E_1^2}{4mE_a}, \quad \frac{dR_2}{d\Omega_2} = \frac{P_2(E_2 + m)}{m(E_a + m)}.$$

- IV.13. Equations (4.9) give $\cos \theta_{ai}^*$ in terms of invariants. Rederive the same equations by using the rule (II.7.8) and the fact that θ_{ai}^* is the angle between the vectors \mathbf{p}_a and \mathbf{p}_1 in the frame $\mathbf{p}_a + \mathbf{p}_b = 0$.
- IV.14. For what masses in $p_a + p_b \rightarrow p_1 + p_2$ is the relation $t = -2P^{*2}(1 - \cos \theta_{ai}^*)$ valid?
- IV.15. Find the physical region in the st plane in the equal mass case, $m_a = m_b = m_1 = m_2 = m$.
- IV.16. Show that

$$G(x, y, z, u, v, w) = -\frac{1}{2} \begin{vmatrix} 2u & x+u-v & u+w-y \\ x+u-v & 2x & x-z+w \\ u+w-y & x-z+w & 2w \end{vmatrix}$$

- IV.17. Prove that $G(x, y, z, u, v, w)$ is equal to -144 times the squared volume of a tetrahedron with sides $\sqrt{x}, \sqrt{y}, \sqrt{z}, \sqrt{u}, \sqrt{v}, \sqrt{w}$ as shown in Figure 5.4.
- IV.18. Show that the roots y^\pm (equation 5.28) of $G(x, y, z, u, v, w) = 0$ satisfy

$$-2x\lambda^{\frac{1}{2}}(y^\pm, z, v) = (-x+u-v)\lambda^{\frac{1}{2}}(x, z, w) \\ \pm (x+z-w)\lambda^{\frac{1}{2}}(x, u, v)$$

How is this physically interpreted when applied, for instance, to the boundary $G(s, t, m_2^2, m_a^2, m_b^2, m_1^2) = 0$ of a $2 \rightarrow 2$ reaction?

- IV.19. This is a more extensive exercise which requires the knowledge of how to handle spin $\frac{1}{2}$ particles. A standard form for the invariant amplitude of $0^{-\frac{1}{2}+} \rightarrow 0^{-\frac{1}{2}+}$ scattering is $T = \bar{u}(p_2)\{A + \frac{1}{2}(p_a +$

$P_1)B\}u(p_1)$, where A and B are some functions of s and t . Show then that the result of summing over spins can be written in the form

$$2m_b m_2 \sum_{\text{spins}} |T|^2 = |A'|^2 \{(m_b + m_2)^2 - t\} \\ + \frac{4|B|^2}{(m_b + m_2)^2 - t} \Delta_3(p_a, p_b, p_1)$$

where Δ_3 is the Gram determinant of p_a, p_b, p_1 and where

$$A' = A + \lambda B$$

with

$$\lambda = - \frac{(m_b + m_2)(s - u) + (m_b - m_2)(m_a^2 - m_1^2)}{2\{(m_b + m_2)^2 - t\}}$$

This form is useful since one can use the known properties of Δ_3 to write the coefficient of the spin flip term in many different forms, all vanishing at the boundary ($\Delta_3 = 0$). Show, for instance, that

$$\Delta_3(p_a, p_b, p_1) = \frac{1}{4}s(t^+ - t)(t - t^-) \\ = \frac{1}{4}s(u^+ - u)(u - u^-) \\ = m_b^2(P_a^T P_1^T)^2 \sin^2 \theta_{al}^T$$

where t^\pm (u^\pm) are the maximum and the minimum values of t (of u). What is the result for elastic scattering?

- IV.20. What is the analogue of the central region for $KN \rightarrow \rho Y^*$ in Figure 5.6 for the elastic case $\mu m \rightarrow \mu m$?
- IV.21. Compute the value of t^+ for (a) $\pi p \rightarrow \pi \Delta$ (b) $\pi p \rightarrow \rho \Delta$ at $p_{\text{lab}} = 10 \text{ GeV}/c$.
- IV.22. Assume $t^+ > 0$. What is the value of θ_{al}^* corresponding to $t^+ = 0$ for large s ? What is the value of θ_{al}^* corresponding to $u = 0$ in elastic scattering? For what scattering angle of $\pi N \rightarrow \pi N$ at $p_{\text{lab}} = 10 \text{ GeV}/c$ is $u = 0$?
- IV.23. Assume you have a detector spanning a constant $d\Omega$ in the laboratory and with which you measure the counting rate of $p_a + p_b \rightarrow p_1 + p_2$ as a function of θ_{al} . How do you transform this counting rate to $d\sigma/dt$ (unnormalized)?
- IV.24. Compute $\sigma(s)$ for an elastic scattering process $\mu m \rightarrow \mu m$ if the matrix element squared is $|A|^2 = \beta(s) e^{2at}$ ($\beta(s)$ is some dimensionless function of s , a is a constant).

- IV.25. Assume measurements have given the following data for proton-proton scattering:

$$\sigma_T(s) = 40 \text{ mb}$$

$$\frac{d\sigma}{dt} = 100 e^{9t} \frac{1}{(\text{GeV}/c)^2}$$

$$\sigma(s) = 11 \text{ mb},$$

independent of s . Fit these data with

$$A(s, t) = (-\Phi + i\beta) e^{at} \frac{s}{s_0},$$

where $\Phi > 0$, β , a and $s_0 = 1 \text{ GeV}^2$ are constants.

- IV.26. The differential cross-section for electron-proton scattering (treating the proton as a Dirac point particle) can be written in the target system (laboratory) in the form

$$\frac{d\sigma}{d\Omega_1} = \frac{\alpha^2}{4E_s^2} \frac{\cos^2 \frac{1}{2}\theta_1}{\sin^4 \frac{1}{2}\theta_1} \frac{1 + \frac{2E_s E_1}{M^2} \cos^2 \frac{1}{2}\theta_1}{1 + \frac{2E_s}{M} \sin^2 \frac{1}{2}\theta_1},$$

where α is the fine-structure constant, E_s is the incident laboratory energy, E_1 the recoil electron energy, θ_1 the scattering angle, M the proton mass and $m_{\text{electron}} \approx 0$. What is $d\sigma/dt$?

- IV.27. Determine the curves of constant target system scattering angle (θ_{μ}^T) in the st plane for proton-proton elastic scattering.
- IV.28. Show that if $(m_a - m_1)(m_b - m_2) \geq 0$ then t is always negative.
- IV.29. Evaluate the integrals

$$I_\mu = \int dR_2 p_{1\mu}, \quad I_{\mu\nu} = \int dR_2 p_{1\mu} p_{1\nu},$$

where

$$dR_2 = d^4 p_1 d^4 p_2 \delta(p_1^2 - m_1^2) \delta(p_2^2 - m_2^2) \delta^4(p - p_1 - p_2).$$

V

Three-Particle Final States

1. Decay of one particle into three particles

Kinematically a decay process $p \rightarrow p_1 + p_2 + p_3$ (Figure 1.1) depends on

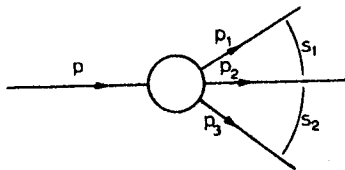


Figure V.1.1 Three-particle decay $p \rightarrow p_1 + p_2 + p_3$ with invariant variables s_1 and s_2

two independent variables (the particles are spinless). It is related by crossing to $2 \rightarrow 2$ scattering (e.g. $p + p_1 \rightarrow p_2 + p_3$) and the number of invariant variables must, of course, be the same. Alternatively, one may argue that the three final state three-vectors or nine variables are constrained by four energy-momentum conservation equations. In addition, the initial state is isotropic in the rest frame of p so that the final state cannot depend on three angles describing its orientation as a whole. This leaves two independent variables (Table III.1). In this section we consider separately invariant and non-invariant variables for the process $1 \rightarrow 3$.

(a) Invariant variables

As invariant variables it is convenient to choose s, t and u as in $2 \rightarrow 2$ scattering. As these are all positive in the decay channel we shall take, with a slight change in notation,

$$\begin{aligned}s_{12} &\equiv s_1 = (p_1 + p_2)^2 = (p - p_3)^2, \\ s_{23} &\equiv s_2 = (p_2 + p_3)^2 = (p - p_1)^2, \\ s_{31} &\equiv s_3 = (p_3 + p_1)^2 = (p - p_2)^2,\end{aligned}\tag{1.1}$$

as invariant variables. The condition (IV.4.4) relating these is then

$$s_1 + s_2 + s_3 = s + m_1^2 + m_2^2 + m_3^2.\tag{1.2}$$

In Sections 1–3 we denote the mass of the decaying particle by \sqrt{s} . This is done so that the formulae will later apply unchanged in the case of $2 \rightarrow 3$ scattering.

(b) **Non-invariant variables**

Non-invariant variables are three-momenta and angles. To define these one has to specify a Lorentz frame. The frames introduced below correspond to the centre-of-mass and target systems in $2 \rightarrow 2$ scattering.

The rest frame of the decaying system or overall CMS is defined as the frame in which $\mathbf{p} = \mathbf{p}_1 + \mathbf{p}_2 + \mathbf{p}_3 = 0$ (Figure 1.2). This is the analogue of

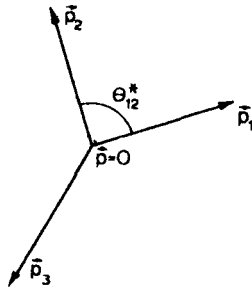


Figure V.1.2 Rest frame of the decaying system ($\mathbf{p} = 0$)

the target (or beam) system in $2 \rightarrow 2$ scattering in the sense that one of the external momenta in the diagram of Figure 1.1 is taken to be at rest. Quantities in this frame are denoted by an asterisk.

We may derive expressions for energies and momenta immediately by expanding the latter parts of the definitions (1.1) in the frame $\mathbf{p} = (\sqrt{s}, 0)$:

$$\begin{aligned} E_1^* &= \frac{s + m_1^2 - s_2}{2\sqrt{s}} \\ E_2^* &= \frac{s + m_2^2 - s_3}{2\sqrt{s}} \\ E_3^* &= \frac{s + m_3^2 - s_1}{2\sqrt{s}} \\ P_1^* &= \frac{\lambda^{\frac{1}{2}}(s, m_1^2, s_2)}{2\sqrt{s}} \\ P_2^* &= \frac{\lambda^{\frac{1}{2}}(s, m_2^2, s_3)}{2\sqrt{s}} \\ P_3^* &= \frac{\lambda^{\frac{1}{2}}(s, m_3^2, s_1)}{2\sqrt{s}}. \end{aligned} \quad (1.3)$$

Note the rule applied here: E_1^* is obtained by considering the two-particle decay $p \rightarrow p_1 + (p_2 + p_3)$ with final state masses m_1 and $\sqrt{s_2}$. The angles between the momentum vectors follow from the definitions (1.1) by expanding the squares and inserting equations (1.3). Equivalently, one may use the rules of Section II.7. We have, for instance, for the angle θ_{12}^* between \mathbf{p}_1 and \mathbf{p}_2 (Figure 1.2)

$$s_1 = (p_1 + p_2)^2 = m_1^2 + m_2^2 + 2E_1^*E_2^* - 2P_1^*P_2^* \cos \theta_{12}^*$$

from which

$$\begin{aligned} \cos \theta_{12}^* &= \frac{\mathbf{p}_1 \cdot \mathbf{p}_2}{P_1 P_2} \Big|_{\mathbf{p}=0} \\ &= \frac{(s + m_1^2 - s_2)(s + m_2^2 - s_3) + 2s(m_1^2 + m_2^2 - s_1)}{\lambda^1(s, m_1^2, s_2)\lambda^1(s, m_2^2, s_3)}. \end{aligned} \quad (1.4)$$

This is obtained also from equation (II.7.6) with $p_1, p_2, p_3 \rightarrow p, -p_1, p_2$. Similarly equation (II.7.10) gives

$$\begin{aligned} \sin^2 \theta_{12}^* &= \frac{|\mathbf{p}_1 \times \mathbf{p}_2|^2}{P_1^* P_2^2} \Big|_{\mathbf{p}=0} \\ &= \frac{\Delta_3(p, -p_1, p_2)}{s P_1^{*2} P_2^{*2}} \\ &= \frac{-4sG(s_1, s_2, s, m_2^2, m_1^2, m_3^2)}{\lambda(s, m_1^2, s_2)\lambda(s, m_2^2, s_3)}. \end{aligned} \quad (1.5)$$

There are three possible *rest frames of a produced two-particle system* (Figure 1.3), corresponding to s , t and u channel centre of momentum-

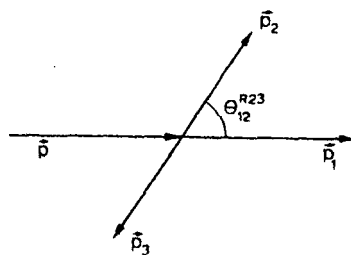


Figure V.1.3 Rest frame of the system formed by the particles 2 and 3 ($\mathbf{p}_2 + \mathbf{p}_3 = 0$)

systems in $2 \rightarrow 2$ scattering. These are the following:

$$\begin{aligned} p_1 + p_2 &= p - p_3 = 0, \\ p_2 + p_3 &= p - p_1 = 0, \\ p_3 + p_1 &= p - p_2 = 0. \end{aligned} \quad (1.6)$$

We shall denote quantities defined in these frames, often called Gottfried-Jackson frames, by the superscripts R12, R23, R31, respectively (R for rest). When no confusion can arise, these superscripts may be omitted. It is also sufficient to consider one of these, say R23, since equations referring to other frames are obtained from those referring to R23 by a cyclic permutation of indices.

In order to write energies and momenta in R23 in terms of invariants we expand $s_2 = (p_2 + p_3)^2$ in R23, i.e. in the frame $p_2 + p_3 = (\sqrt{s_2}, \mathbf{0})$. This leads to the following formulae:

$$\begin{aligned} E^{\text{R23}} &= \frac{s + s_2 - m_1^2}{2\sqrt{s_2}} \\ E_1^{\text{R23}} &= \frac{s - s_2 - m_1^2}{2\sqrt{s_2}} \\ E_2^{\text{R23}} &= \frac{s_2 + m_2^2 - m_3^2}{2\sqrt{s_2}} \\ E_3^{\text{R23}} &= \frac{s_2 + m_3^2 - m_2^2}{2\sqrt{s_2}} \\ p^{\text{R23}} = P_1^{\text{R23}} &= \frac{\lambda^{\frac{1}{2}}(s, s_2, m_1^2)}{2\sqrt{s_2}} \\ P_2^{\text{R23}} = P_3^{\text{R23}} &= \frac{\lambda^{\frac{1}{2}}(s_2, m_2^2, m_3^2)}{2\sqrt{s_2}}. \end{aligned} \quad (1.7)$$

Only one angle in R23 is essential for a decay, namely θ_{12}^{R23} (Figure 1.3). In connection with $2 \rightarrow 3$ processes this angle will be called the **helicity polar angle** (see Section V.6, where one actually uses $\pi - \theta_{12}^{\text{R23}}$). For θ_{12}^{R23} we find by using equations (1.7) that

$$\begin{aligned} s_1 &= (p_1 + p_2)^2 \\ &= m_1^2 + m_2^2 + 2E_1^{\text{R23}}E_2^{\text{R23}} - 2P_1^{\text{R23}}P_2^{\text{R23}} \cos \theta_{12}^{\text{R23}} \\ &= m_1^2 + m_2^2 + \frac{1}{2s_2}(s - s_2 - m_1^2)(s_2 + m_2^2 - m_3^2) \\ &\quad - \frac{1}{2s_2} \cos \theta_{12}^{\text{R23}} \lambda^{\frac{1}{2}}(s, s_2, m_1^2) \lambda^{\frac{1}{2}}(s_2, m_2^2, m_3^2) \end{aligned} \quad (1.8)$$

or that

$$\cos \theta_{12}^{R23} = \frac{(s - s_2 - m_1^2)(s_2 + m_2^2 - m_3^2) + 2s_2(m_1^2 + m_2^2 - s_1)}{\lambda^{\frac{1}{2}}(s, s_2, m_1^2)\lambda^{\frac{1}{2}}(s_2, m_2^2, m_3^2)} \quad (1.9)$$

The corresponding sine follows most simply from equation (II.7.10), with $p_1, p_2, p_3 \rightarrow p_2 + p_3, p_1, p_2$:

$$\begin{aligned} \sin^2 \theta_{12}^{R23} &= \left. \frac{|\mathbf{p}_1 \times \mathbf{p}_2|^2}{P_1^2 P_2^2} \right|_{\mathbf{p}_2 = -\mathbf{p}_3} \\ &= \frac{\Delta_3(p_2 + p_3, p_1, p_2)}{s_2(P_1^{R23} P_2^{R23})^2} \\ &= \frac{-4s_2 G(s_1, s_2, s, m_2^2, m_1^2, m_3^2)}{\lambda(s, s_2, m_1^2)\lambda(s_2, m_2^2, m_3^2)} \end{aligned} \quad (1.10)$$

Note the great similarity of equations (1.10) and (1.5) (Exercise V.1).

Equations (1.8-9) show that s_1 depends linearly on $\cos \theta_{12}^{R23}$, exactly as t depended on $\cos \theta_{\text{al}}^*$ in $2 \rightarrow 2$ scattering. On the other hand, the relation (1.4) between s_1 and $\cos \theta_{12}^*$ is a more complicated algebraic function, because s_3 depends on s_1 and s_2 (equation (1.2)). For many purposes kinematics is simpler in the frames R12, R23, R31 than in the total CMS. The reason is that the role of the frames R12, R23, R31 in $1 \rightarrow 3$ decay is the same as that of CMS in $2 \rightarrow 2$ scattering.

2. Dalitz plot

The *Dalitz plot* (Dalitz, 1953; Fabri, 1954) is defined as the physical region of $p \rightarrow p_1 + p_2 + p_3$ in the $s_1 s_2$ plane. More generally, it can be defined as the physical region in terms of any variables related to s_1, s_2 by a linear transformation with constant Jacobian. Examples of these are: (a) any pair $s_i, s_j, i, j = 1, 2, 3$; (b) any pair E^*, E_j^* ; (c) any pair of kinetic energies ($T = E - m$) T_i, T_j .

The equation determining the Dalitz plot is obtained quite automatically by applying the mnemonic rule of Figure IV.5.3. To this end one writes the diagram in Figure 1.1 in the form shown in Figure 2.1, compares with the

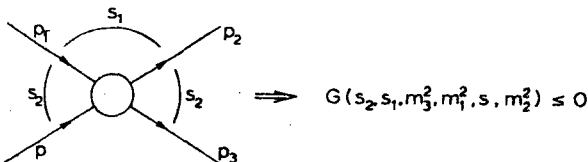


Figure V.2.1 A direct procedure giving the physical region in the $s_1 s_2$ plane

mnemonic rule of Figure IV.5.3 and finds that physical values of s_1 and s_2 have to satisfy

$$G(s_2, s_1, m_3^2, m_1^2, s, m_2^2) \leq 0.$$

By the symmetry properties of G (Section IV.5(c)) this is equivalent to

$$G(s_1, s_2, s, m_2^2, m_1^2, m_3^2) \leq 0. \quad (2.1)$$

The G function here is the same as that appearing in equations (1.5) and (1.10). The equality sign gives the boundary of the Dalitz plot. To plot it in the $s_1 s_2$ plane one solves for s_1 in terms of s_2 by using equation (IV.5.28):

$$\begin{aligned} s_1^\pm &= m_1^2 + m_2^2 - \frac{1}{2s_2} \{(s_2 - s + m_1^2)(s_2 + m_2^2 - m_3^2) \\ &\quad \mp \lambda^4(s_2, s, m_1^2) \lambda^4(s_2, m_2^2, m_3^2)\}. \end{aligned} \quad (2.2)$$

One sees that this is precisely equation (1.8) with $\cos \theta_{12}^{R23} = \pm 1$. The equation giving s_2 in terms of s_1 is obtained from equation (2.2) by the transformation $p_1 \leftrightarrow p_3$; p, p_2 unchanged. They represent, of course, the same curve, but for numerical purposes it may be convenient to use both equations. By requiring the square roots in equation (2.2) to be real one gets the physical region in s_2 . By cyclic symmetry one further deduces that s_1, s_2 and s_3 have to satisfy

$$\begin{aligned} (m_1 + m_2)^2 &\leq s_1 \leq (\sqrt{s} - m_3)^2 \\ (m_2 + m_3)^2 &\leq s_2 \leq (\sqrt{s} - m_1)^2 \\ (m_1 + m_3)^2 &\leq s_3 \leq (\sqrt{s} - m_2)^2. \end{aligned} \quad (2.3)$$

In order to give a direct derivation of equation (2.1) and to determine the phase space density of the Dalitz plot, consider the phase space integral

$$R_3(s) = \int \prod_{i=1}^3 \frac{d^3 p_i}{2E_i} \delta^3(\mathbf{p} - \mathbf{p}_1 - \mathbf{p}_2 - \mathbf{p}_3) \delta(\sqrt{s} - E_1 - E_2 - E_3) \quad (2.4)$$

For any practical purposes one should integrate over the δ functions so that the integrand becomes nonsingular (see equation (III.2.14)). We shall ultimately present a number of choices of variables for the remaining integrations. The following form is most convenient for the analysis of the Dalitz plot.

Integrate first over \mathbf{p}_2 in the rest frame $\mathbf{p} = 0$:

$$R_3(s) = \int \frac{d^3 p_1 d^3 p_3}{8E_1 E_2 E_3} \delta(\sqrt{s} - E_1 - E_2 - E_3), \quad (2.5)$$

where

$$\begin{aligned} E_2^2 &= |\mathbf{p}_1 + \mathbf{p}_3|^2 + m_2^2 \\ &= P_1^2 + P_3^2 + 2P_1 P_3 \cos \theta_{13} + m_2^2, \end{aligned} \quad (2.6)$$

The asterisks have been omitted for brevity. Write further

$$\begin{aligned} d^3 p_1 d^3 p_3 &= P_1^2 dP_1 d\Omega_1 P_3^2 dP_3 d\Omega_3 \\ &= P_1 E_1 dE_1 d\Omega_1 P_3 E_3 dE_3 d\cos \theta_{13} d\phi_3, \end{aligned}$$

where $\Omega_3 = (\cos \theta_{13}, \phi_3)$ describes the orientation of \mathbf{p}_3 with respect to \mathbf{p}_1 , and Ω_1 the orientation of \mathbf{p}_1 with respect to some axis. In the decay case at hand there is no preferred direction in space, and Ω_1 could be integrated to give 4π and ϕ_3 to give 2π , but we keep $d\Omega_1 d\phi_3$ as such for later use. The energy δ function can be used to integrate over $\cos \theta_{13}$ ($dE_2/d\cos \theta_{13} = P_1 P_3/E_2$) with the result

$$\begin{aligned} R_3(s) &= \int \frac{dE_1 dE_3 d\Omega_1 d\phi_3 P_1 E_1 P_3 E_3}{8E_1 E_2 E_3 (P_1 P_3/E_2)} \Theta(1 - \cos^2 \theta_{13}) \\ &= \frac{1}{8} \int dE_1 dE_3 d\Omega_1 d\phi_3 \Theta(1 - \cos^2 \theta_{13}). \end{aligned} \quad (2.7)$$

Here the Θ function restricts $\cos \theta_{13}$ to physical values. The values $\cos \theta_{13} = \pm 1$ correspond to the boundary of the physical region in the $E_1 E_3$ plane, that is the Dalitz plot. According to equation (2.6) the equation of the boundary is

$$\begin{aligned} (\sqrt{s} - E_1 - E_3)^2 &= P_1^2 + P_3^2 \pm 2P_1 P_3 + m_2^2 \\ &= |P_1 \pm P_3|^2 + m_2^2 \\ &= E_1^2 - m_1^2 + E_3^2 - m_3^2 \pm 2\{(E_1^2 - m_1^2)(E_3^2 - m_3^2)\}^{1/2} + m_2^2 \end{aligned} \quad (2.8)$$

or

$$4(E_1^2 - m_1^2)(E_3^2 - m_3^2) = \{2E_1 E_3 - 2\sqrt{s}(E_1 + E_3) + s + m_1^2 - m_2^2 + m_3^2\}^2. \quad (2.9)$$

Note that in squaring equation (2.8) one loses track of the sign of the momenta. Knowledge of the sign would be important in the $2 \rightarrow 3$ case. To restore it one may consider plots in longitudinal momenta (Section VI.6).

The variables E_1 and E_3 in equation (2.9) are linearly connected to s_1 and s_2 by equation (1.3) with the Jacobian $\partial(E_1, E_3)/\partial(s_1, s_2) = 1/4s$. If equation (1.3) is used in equation (2.9) one sees after some algebra that the boundary equation becomes the G function equation (2.1) written down previously. We then have

$$R_3(s) = \frac{1}{32s} \int ds_1 ds_2 d\Omega_1 d\phi_3 \Theta\{-G(s_1, s_2, s, m_2^2, m_1^2, m_3^2)\}. \quad (2.10)$$

The solid angle Ω_1 describes the orientation of \mathbf{p}_1 in the CMS; for the decay problem $\int d\Omega_1 = 4\pi$. Similarly, ϕ_3 describes the rotation of the entire momentum configuration about some axis. Equation (2.10) is one of the standard forms of $R_3(s)$. Analogous forms of $R_3(s)$ with the pairs E_1, E_2 and s_2, s_3 , or E_2, E_3 and s_1, s_3 , as variables are obtained from equations (2.7) and (2.10) by cyclic permutations of indices.

Equation (2.8) implies that at the boundary $P_2 = P_1 \pm P_3$, by cyclic permutations it is evident that also $P_3 = P_2 \pm P_1$, $P_1 = P_3 \pm P_2$. These conditions can be combined in a concise and symmetric form by stating that at the boundary

$$\lambda(P_1^2, P_2^2, P_3^2) = 0 \quad (2.11)$$

or that the area of the triangle formed by the momenta vanishes. Here the momenta still have to be replaced by the two energy-type variables in terms of which one has chosen to draw the Dalitz plot. For instance, introducing E_1 and E_3 leads to equation (2.9); introducing s_1 and s_2 leads to the G function condition (2.1). These results are, of course, analogous to those in equations (IV.5.36–39) for $2 \rightarrow 2$ scattering.

We shall next consider the boundary of the Dalitz plot for some special values of masses.

(a) **All masses equal**

If the three decay particles have equal masses (as in $K \rightarrow 3\pi$, $\eta \rightarrow 3\pi$), it is convenient to make this symmetry explicit by using all three energies simultaneously and by plotting in triangular coordinates (Figure IV.5.5). This is actually the representation employed originally by Dalitz (Dalitz, 1953; see also Fabri, 1954). This symmetric representation is described elsewhere in detail (Hagedorn, 1964; Källén, 1964); we shall only go through the main properties here. If the three CMS kinetic energies $T_i = E_i - m$ are used as variables they satisfy $T_1 + T_2 + T_3 = \sqrt{s} - 3m = Q$, where Q is the energy released. One should, therefore, use an equilateral triangle of height Q . Any point within the triangle satisfies energy conservation. To find the boundary of the physical region, introduce polar coordinates (r, ϕ) measured relative to the centre of the triangle ($T_1 = T_2 = T_3 = Q/3$) by the equations

$$\begin{aligned} T_1 &= \frac{Q}{3}(1 + r \cos \phi) \\ T_2 &= \frac{Q}{3} \left\{ 1 + r \cos \left(\phi + \frac{2\pi}{3} \right) \right\} \\ T_3 &= \frac{Q}{3} \left\{ 1 + r \cos \left(\phi - \frac{2\pi}{3} \right) \right\}. \end{aligned} \quad (2.12)$$

The curve bounding the kinematically accessible region is then obtained by inserting equation (2.12) in equation (2.9) with the result

$$1 = (1 + x)r^2 + xr^3 \cos 3\phi, \quad (2.13)$$

where $x = 2c/(2 - c)^2$ and $c = Q/\sqrt{s}$. It is seen that c characterizes the curve completely; its value for $K, \eta, \omega \rightarrow 3\pi$ decays is 0.17, 0.23 and 0.47, respectively.

(b) **Two or three masses vanish**

There are three distinct cases: $m_2 = m_3 = 0$, $m_1 = m_3 = 0$ and $m_1 = m_2 = m_3 = 0$; the case $m_1 = m_2 = 0$ follows by symmetry. We find from equation (IV.5.23) that the condition (2.1) then simplifies to the forms

$$\begin{aligned} G(s_1, s_2, s, 0, m_1^2, 0) &= s_2\{s_1(s_1 + s_2 - s) - m_1^2(s_1 - s)\} \leq 0, \\ G(s_1, s_2, s, m_2^2, 0, 0) &= (s_1 s_2 - s m_2^2)(s_1 + s_2 - s - m_2^2) \leq 0, \\ G(s_1, s_2, s, 0, 0, 0) &= s_1 s_2(s_1 + s_2 - s) \\ &= -s_1 s_2 s_3 \leq 0, \end{aligned} \quad (2.14)$$

respectively. As the equations of the boundary curves factorize, the Dalitz plots are easy to draw (Figure 2.2). The results hold approximately if the masses put to zero in Figure 2.2 are small compared with \sqrt{s} . In particular, when $s \rightarrow \infty$, the Dalitz plot approaches a triangle.

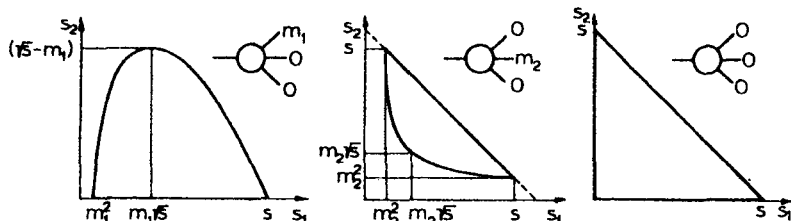


Figure V.2.2 The schematic Dalitz plots for the special mass values shown in the figure

There is one feature of equation (2.10) which has played a special role in the development of the techniques of plotting data. The **phase space distribution**

$$\frac{d^2 R_3}{ds_1 ds_2} = \frac{\pi^2}{4s} \quad (2.15)$$

is **constant** at fixed s . In other words, if the data of a three-particle decay are

plotted as points on the Dalitz plot, the density of the points is proportional to the matrix element squared. Any structure is then apparent at a glance. Actually, the non-constant phase space density of other plots will not make it more difficult to study the structure as long as the density is fairly uniform. Note also that it is only in the decay $p \rightarrow p_1 + p_2 + p_3$ that the Dalitz plot distribution gives directly the matrix element. In other cases, like $p_a + p_b \rightarrow p_1 + p_2 + p_3$, the matrix element depends on more than two variables and the Dalitz plot distribution gives the integral of the squared matrix element over these unshown variables. Inferring something about the matrix element itself from this integral will evidently require both further assumptions and caution (Chapter VIII).

Starting from equation (2.10) it is very simple to carry out one further integration. We have, for instance,

$$\begin{aligned} \frac{dR_3}{ds_2} &= \frac{\pi^2}{4s} \int_{s_1^-}^{s_1^+} ds_1 \\ &= \frac{\pi^2}{4ss_2} \lambda^{\frac{1}{2}}(s_2, s, m_1^2) \lambda^{\frac{1}{2}}(s_2, m_2^2, m_3^2), \end{aligned} \quad (2.16)$$

where s_1^{\pm} were taken from equation (2.2). Equation (2.16) gives the projection of the Dalitz plot on one of the coordinate axes. For the total volume of the three-particle phase space one further obtains

$$R_3(s) = \frac{\pi^2}{4s} \int_{(m_1+m_3)^2}^{(\sqrt{s}-m_1)^2} \frac{ds_2}{s_2} \lambda^{\frac{1}{2}}(s_2, s, m_1^2) \lambda^{\frac{1}{2}}(s_2, m_2^2, m_3^2). \quad (2.17)$$

The factor under the square root is a fourth-order polynomial in s_2 and equation (2.17) leads, in general, to elliptic functions (Kopylov, 1960; Almgren, 1968). Only for some special cases can equation (2.17) be integrated in closed form (Exercise V.4). Particularly interesting are the limiting cases $s \rightarrow \infty$ (extremely relativistic, ER) or $s \rightarrow \text{threshold} = (m_1 + m_2 + m_3)^2$ (non-relativistic, NR). The first limiting form is obtained from equation (2.17) by putting all $m_i = 0$:

$$R_3^{\text{ER}}(s) = \frac{\pi^2}{8}s. \quad (2.18)$$

For the second limiting form one has to expand R_3 in powers of $\sqrt{s} - m_1 - m_2 - m_3$. The result for general R_n^{NR} is given later in equation (VI.2.19); when applied to R_3 it gives

$$R^{\text{NR}}(s) = \frac{\pi^3}{2} \frac{(m_1 m_2 m_3)^{\frac{1}{2}}}{(m_1 + m_2 + m_3)^{\frac{3}{2}}} (\sqrt{s} - m_1 - m_2 - m_3)^2. \quad (2.19)$$

Example 1: Consider the decays $K^+ \rightarrow \pi^+ \pi^+ \pi^-$ and $K^+ \rightarrow \pi^+ \pi^0 \pi^0$. Even if the matrix elements for these were the same, the mass difference $m_{\pi^{\pm}} \neq m_{\pi^0}$.

will cause a difference in available phase space and decay rates. Since $\sqrt{s} - \sum m_i$ is small, one may use the approximation (2.19) and obtain for the ratio of the phase space volumes, in an obvious notation,

$$\frac{R_3(+00)}{R_3(+-+)} \approx \frac{m_{\pi^0}}{m_{\pi^+}} \left(\frac{m_K - m_{\pi^+} - 2m_{\pi^0}}{m_K - 3m_{\pi^+}} \right)^2 \\ \approx 1.261.$$

A more complicated approximation is used in (Källén, 1964).

3. Momentum configuration on the Dalitz plot

As was seen previously, the final state momentum vectors $\mathbf{p}_1, \mathbf{p}_2, \mathbf{p}_3$ are collinear on the boundary of the Dalitz plot. We shall next investigate in more detail how the momentum configuration varies as one moves within the Dalitz plot. Momentum vectors in the overall CMS ($\mathbf{p}_1 + \mathbf{p}_2 + \mathbf{p}_3 = 0$) and in R23 ($\mathbf{p}_2 + \mathbf{p}_3 = 0$) will be treated separately.

Consider first CMS momenta, omitting the asterisks. To see how the configuration varies, let us look at the points in which s_{12}, s_{23}, s_{31} attain their minima and maxima given by equation (2.3). In this section we use the two indices in s_{ij} for clarity. The minimum of s_{12} , $s_{12} = (m_1 + m_2)^2$, is reached when $\mathbf{p}_1 \cdot \mathbf{p}_2 = m_1 m_2$ or when (Section II.2) the velocities of particles 1 and 2 are equal: $v_1 = v_2$ or $E_2 \mathbf{p}_1 = E_1 \mathbf{p}_2$. Physically the equality of the velocities implies that the particles really move together as a lump of matter in any frame (see Exercise II.10). When the velocities are equal the momenta are in the ratio $P_1/P_2 = m_1/m_2$. For instance, when a pion and nucleon move together their momenta satisfy $P_\pi/P_N = m_\pi/m_N \approx \frac{1}{7}$. That this ratio is so different from one will have practical implications. When s_{12} is as small as possible one sees from equation (1.3) that E_3 and P_3 are as large as possible:

$$E_3 = E_3^{\max} \\ = \frac{s + m_3^2 - (m_1 + m_2)^2}{2\sqrt{s}}, \quad (3.1)$$

similarly for P_3 . This characterizes the momentum configuration at the point $s_{12} = (m_1 + m_2)^2$ completely, disregarding, of course, the overall rotation of all momenta. It is shown as point A_1 in Figure 3.1. The other coordinate s_{23} is obtained directly from equation (2.2):

$$s_{23}^\pm \{s_{12} = (m_1 + m_2)^2\} = \frac{m_2 s + m_1(m_3^2 - m_2^2 - m_1 m_2)}{m_1 + m_2}. \quad (3.2)$$

For $s_{12} = (m_1 + m_2)^2$ one has $\lambda(s_{12}, m_1^2, m_2^2) = 0$ and the two roots s_{23}^+ and s_{23}^- coincide.

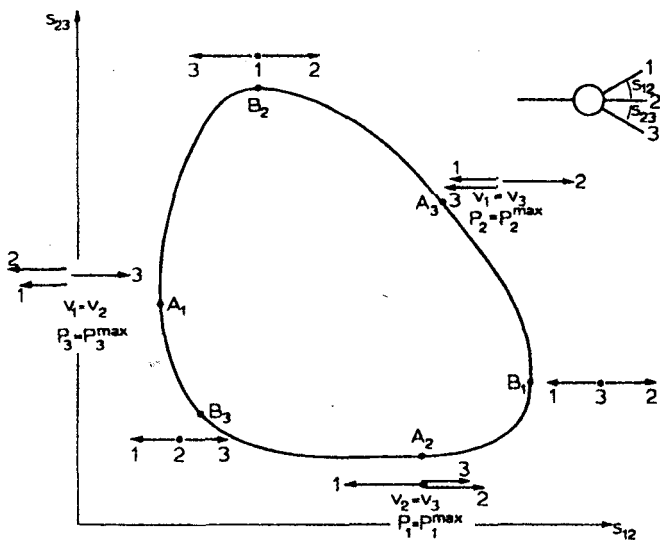


Figure V.3.1 Configurations of momentum vectors in overall CMS on the boundary of the Dalitz plot

The points A_2 and A_3 in which s_{23} and s_{31} have their minimum values $(m_2 + m_3)^2$ and $(m_1 + m_3)^2$ have an analogous interpretation. At the point $s_{ij} = s_{ij}^{\min} = (m_i + m_j)^2$ particles i and j move in one direction with equal velocities and the third particle k in the opposite direction with the largest CMS momentum it can attain for the reaction in question.

Turning then to the maximum value of s_{12} , $s_{12} = s_{12}^{\max} = (\sqrt{s} - m_3)^2$, one sees from equation (1.3) that this corresponds to $P_3 = 0$, $E_3 = m_3$. Thus particle 3 is at rest in CMS and particles 1 and 2 move in opposite directions with equal momenta: $\mathbf{p}_1 = -\mathbf{p}_2$ (point B_1 in Figure 3.1). This corresponds to the intuitive idea of having particles 1 and 2 as far apart as possible when s_{12} is as large as possible. The maximum values of s_{23} and s_{31} are realized similarly (points B_2 and B_3 in Figure 3.1). For $s_{12} = (\sqrt{s} - m_3)^2$ the two roots in equation (2.2) again coincide and the corresponding value of s_{23} is

$$s_{23}^{\pm}\{s_{12} = (\sqrt{s} - m_3)^2\} = \frac{m_3(s - m_1^2) + (m_2^2 - m_3^2)\sqrt{s}}{\sqrt{s} - m_3}; \quad (3.3)$$

similarly for points B_2 and B_3 .

Interpolating between the six points A_i and B_i one can now trace how the CMS momentum configuration varies as one moves around the boundary. To get to the inside one must relax the condition $\cos \theta_{ij} = \pm 1$, $i, j = 1, 2, 3$.

The value of θ_{12} corresponding to a point s_1, s_2 can be found from equations (1.4–5).

If we consider the momentum configuration in the frame R23 (Figure 3.2), the analysis is actually simpler than in the overall CMS. The reason for this is that a fixed value of s_{23} determines the magnitudes of all momenta. For instance, at the point A_2 , with $s_{23} = (m_2 + m_3)^2$, in Figure 3.2 one has

$$P_2^{R23} = P_3^{R23} = 0,$$

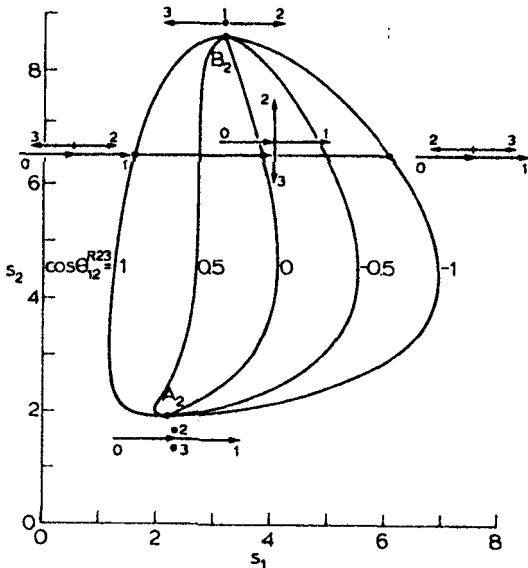


Figure V.3.2 Configurations of momentum vectors in R23 ($p_2 + p_3 = 0$) on the Dalitz plot. Curves of constant $\cos \theta_{12}^{R23}$ are also shown. Numbers refer to $p\bar{p} \rightarrow p\pi\Delta$ at 7 GeV/c

and at the point B_2 with $s_{23} = (\sqrt{s} - m_1)^2$

$$P_2^{R23} = P_3^{R23} = 0.$$

At any intermediate s_{23} all momenta are nonzero. As one moves along a line $s_{23} = \text{constant}$ from boundary to boundary, $\cos \theta_{12}^{R23}$ varies linearly from $+1$ to -1 (Figure 3.2). This follows directly from equations (1.8) and (2.2). Therefore, the distribution in the helicity polar angle is obtained if one only knows the distribution in the Dalitz plot.

4. Scattering of two particles into three particles

The initial state of $2 \rightarrow 3$ scattering, $p_a + p_b \rightarrow p_1 + p_2 + p_3$, contains in the CMS a preferred direction, the direction of the incoming beam $\mathbf{p}_a^* = -\mathbf{p}_b^*$. The total number of variables is $3 \times 3 - 4 = 5$. Of these, the rotation around the beam axis is trivial for spinless particles and the number of essential final state variables is 4 (Table III.1). Now it is no longer possible to present data and predictions in a fully differential form, which would require showing intensity versus four dimensions. At best one can plot in two dimensions. To compare with data, one must then integrate over the remaining variables either over their whole range or over different intervals in them. The integration may obscure essential features in the matrix element. To avoid erroneous conclusions one must be fully conscious of the difficulties in the presentation of data in several variables. The simplest reaction in which these complications appear in fully developed form is $2 \rightarrow 3$ scattering. Thus in addition to the intrinsic interest, it is instructive to study $2 \rightarrow 3$ scattering in detail in order to understand some problems of general multi-particle kinematics.

In our analysis of $2 \rightarrow 3$ reactions, we shall introduce several different sets of four variables to describe the phase space. For each of these the phase space density and physical region boundaries will be calculated. The situation was very simple for $2 \rightarrow 2$ scattering; there the physical region for fixed s was the one-dimensional range $t^- \leq t \leq t^+$ (equation (IV.5.14)) and the phase space distribution was constant (equation (IV.4.24)). Now one can distinguish between physical regions of different types and dimensionalities. Calling the four variables x, y, z and u , the various possibilities for s fixed are obviously as follows (physical region = PR):

$$\text{PR in } xyzu \quad (4.1)$$

$$\text{PR in } xyz \quad (4.2a)$$

$$\ddots \quad \text{PR in } xyz \text{ for } u \text{ fixed} \quad (4.2b)$$

$$\text{PR in } xy \text{ (xy plot)} \quad (4.3a)$$

$$\text{PR in } xy \text{ for } z \text{ fixed} \quad (4.3b)$$

$$\text{PR in } xy \text{ for } z, u \text{ fixed} \quad (4.3c)$$

$$\text{PR in } x \text{ ('range of } x) \quad (4.4a)$$

$$\text{PR in } x \text{ for } y \text{ fixed} \quad (4.4b)$$

$$\text{PR in } x \text{ for } y, z \text{ fixed} \quad (4.4c)$$

$$\text{PR in } x \text{ for } y, z, u \text{ fixed.} \quad (4.4d)$$

Note that one goes, for instance, from (4.3b) to (4.3a) by integrating over z .

Thus (4.3b) always lies within (4.3a). We have already had an example of a set of four variables: in equation (2.10) $x = s_1$, $y = s_2$, $(z, u) = \Omega_1$. Then (4.3a) is the Dalitz plot obtained by integrating over Ω_1 . This integration is nontrivial in the $2 \rightarrow 3$ case.

Our procedure of constructing sets of variables will be to start from the original form of $R_3(s)$, in which only momentum vectors appear, to integrate over the δ functions, and then to replace stage by stage the remaining four noninvariant variables by invariant variables. The sets of variables can thus be conveniently characterized by the number of invariants included. For instance, the set of variables in equation (2.7), E_1^*, E_3^*, Ω_1^* , does not contain any invariants while the set s_1, s_2, Ω_1^* in equation (2.10) contains two.

The angular variables which will be used, like the Jackson, Treiman-Yang, helicity, Toller, etc., angles, are very important in practice. For their definition one has to specify a frame and orientations of coordinate axes. This may lead to confusion unless one is very specific about the conventions. We shall introduce these in later sections. On the other hand, the invariant variables can be defined very simply and once for all. We shall use as the standard set the five invariants obtained by joining adjacent particles in the diagram of Figure 4.1:

$$\begin{aligned}
 s_1 &\equiv s_{12} \\
 &= (p_1 + p_2)^2 \\
 &= (p_a + p_b - p_3)^2, \\
 s_2 &\equiv s_{23} \\
 &= (p_2 + p_3)^2 \\
 &= (p_a + p_b - p_1)^2, \\
 t_1 &\equiv t_{a1} \\
 &= (p_a - p_1)^2 \\
 &= (p_2 + p_3 - p_b)^2, \\
 t_2 &\equiv t_{b3} \\
 &= (p_b - p_3)^2 \\
 &= (p_1 + p_2 - p_a)^2, \\
 s &\equiv s_{ab} \\
 &= (p_a + p_b)^2 \\
 &= (p_1 + p_2 + p_3)^2.
 \end{aligned} \tag{4.5}$$

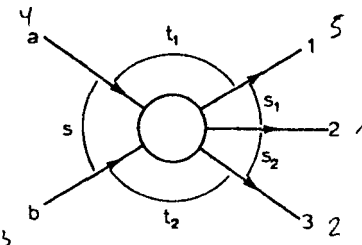


Figure V.4.1

In the phase space of the channel $p_a + p_b \rightarrow p_1 + p_2 + p_3$, s is fixed and only four invariants vary. However, when this condition is relaxed s has by crossing exactly the same variable status as the other invariants. In fact, the set (4.5) has an obvious cyclic symmetry and we shall in the following find the cyclic transformation

$$-p_a \rightarrow p_1 \rightarrow p_2 \rightarrow p_3 \rightarrow -p_b \rightarrow -p_a \quad (4.6)$$

implying

$$s \rightarrow t_1 \rightarrow s_1 \rightarrow s_2 \rightarrow t_2 \rightarrow s \quad (4.7)$$

very useful. Note that this simple and symmetric choice of invariant variables is possible only for $2 \rightarrow 3$ reactions. Already for $2 \rightarrow 4$ reactions there are invariants containing three particles which are not equal to two-particle invariants (compare set (4.5)).

In addition to set (4.5) one can define five further invariants by joining particles not adjacent in Figure 4.1. These are linearly dependent on the set (4.5). The relation between t_{b2} , say, and the set (4.5) is most easily obtained by drawing the diagram in Figure 4.2 and applying the relation $s + t + u = \sum m_i^2$ to the $2 \rightarrow 2$ scattering at the lower vertex. Applying this rule to all possibilities one obtains the relations

$$\begin{aligned} t_{a2} &= (p_a - p_2)^2 \\ &= t_2 - t_1 - s_1 + m_a^2 + m_1^2 + m_2^2, \\ t_{b2} &= (p_b - p_2)^2 \\ &= t_1 - t_2 - s_2 + m_b^2 + m_2^2 + m_3^2, \\ t_{a3} &= (p_a - p_3)^2 \\ &= s_1 - s - t_2 + m_a^2 + m_b^2 + m_3^2, \\ t_{b1} &= (p_b - p_1)^2 \\ &= s_2 - s - t_1 + m_b^2 + m_a^2 + m_1^2, \\ s_{13} &= (p_1 + p_3)^2 \\ &= s - s_1 - s_2 + m_1^2 + m_2^2 + m_3^2. \end{aligned} \quad (4.8)$$

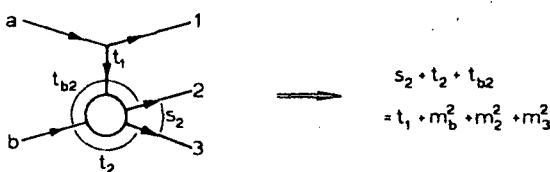


Figure V.4.2 Derivation of the relation between t_{b2} and the standard invariants

With the aid of sets (4.5) and (4.8) it is also easy to express all ten scalar products $p_i \cdot p_j$ in terms of the standard set of invariant quantities:

$$\begin{array}{ll} 2p_a \cdot p_b = s - m_a^2 - m_b^2 & 2p_b \cdot p_2 = s_2 + t_2 - t_1 - m_3^2 \\ 2p_a \cdot p_1 = m_a^2 + m_1^2 - t_1 & 2p_b \cdot p_3 = m_b^2 + m_3^2 - t_2 \\ 2p_a \cdot p_2 = s_1 + t_1 - t_2 - m_1^2 & 2p_1 \cdot p_2 = s_1 - m_1^2 - m_2^2 \\ 2p_a \cdot p_3 = s - s_1 + t_2 - m_b^2 & 2p_1 \cdot p_3 = s - s_1 - s_2 + m_2^2 \\ 2p_b \cdot p_1 = s - s_2 + t_1 - m_a^2 & 2p_2 \cdot p_3 = s_2 - m_2^2 - m_3^2. \end{array} \quad (4.9)$$

If one investigates a fixed channel, for instance $K p \rightarrow K \pi p$, one still has to choose the permutation of particles which corresponds to the order 1, 2, 3. This question has to be resolved on grounds of maximum applicability of formulas derived later.

5. Description in two invariants and two angles, Chew-Low plot

The detailed treatment of the $2 \rightarrow 3$ process in Sections 5-8 will be based on the factorization of the phase space integral into two processes $2 \rightarrow 2$ and $1 \rightarrow 2$. For definiteness we choose the two-particle intermediate system to be $p_2 + p_3$ (see Figure 5.1); other cases are discussed in Section 10. Apart from the rotation ϕ around the beam axis, both the production of the system

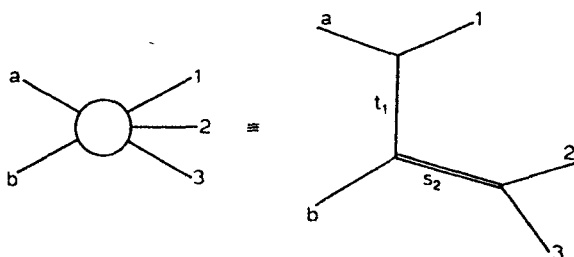


Figure V.5.1

$2 + 3$ and its decay are described by two variables. In this and the next section, the first two are taken to be invariants, and the latter two are decay angles in the rest frame of $2 + 3$.

We start from

$$R_3(s) = \int \frac{d^3 p_1}{2E_1} \frac{d^3 p_2}{2E_2} \frac{d^3 p_3}{2E_3} \delta^4(p_a + p_b - p_1 - p_2 - p_3). \quad (5.1)$$

To have the intermediate system included explicitly, the identity

$$1 = \int ds_2 \int \frac{d^3 p_{23}}{2E_{23}} \delta^4(p_{23} - p_2 - p_3)$$

with $E_{23}^2 = p_{23}^2 + s_2$, is inserted in equation (5.1) with the result

$$\begin{aligned} R_3 &= \int ds_2 \left\{ \int \frac{d^3 p_1}{2E_1} \frac{d^3 p_{23}}{2E_{23}} \delta^4(p_a + p_b - p_1 - p_{23}) \right\} \\ &\times \left\{ \int \frac{d^3 p_2}{2E_2} \frac{d^3 p_3}{2E_3} \delta^4(p_{23} - p_2 - p_3) \right\}. \end{aligned} \quad (5.2)$$

This is the mathematical equivalent of Figure 5.1; in concise form it is

$$R_3(s) = \int ds_2 R_2(s; m_1^2, s_2) R_2(s_2; m_2^2, m_3^2). \quad (5.3)$$

Insertion of any expressions for the two factors R_2 in equation (5.3), as given in Sections IV.1 and IV.4, results in an expression for R_3 in terms of variables which are related to Figure 5.1. Here we choose equation (IV.4.24) for the first R_2 in equation (5.3), and equation (IV.1.7) in the rest frame of $2 + 3$ for the second R_2 , and get

$$R_3 = \frac{1}{8\sqrt{s}P_a^*} \int_0^{2\pi} d\phi \int dt_1 ds_2 \frac{P_3^{R23}}{4\sqrt{s_2}} \int d\Omega_3^{R23} \quad (5.4)$$

From equation (1.7) we obtain

$$P_2^{R23} = P_3^{R23} = \frac{\lambda^4(s_2, m_2^2, m_3^2)}{2\sqrt{s_2}} \quad (5.5)$$

and consequently

$$R_3 = \frac{1}{8\sqrt{s}P_a^*} \int_0^{2\pi} d\phi \int dt_1 ds_2 \frac{\lambda^4(s_2, m_2^2, m_3^2)}{8s_2} \int d\Omega_3^{R23}. \quad (5.6)$$

We shall next analyze the region of integration in the variables t_1, s_2 and specify it exactly in equation (5.16). The specification of the solid angle $\Omega_3^{R23} = (\cos \theta_3^{R23}, \phi_3^{R23})$ is carried out in Section 6.

The invariants s_2, t_1 are given in the CMS by

$$\begin{aligned}s_2 &= s + m_1^2 - 2\sqrt{s}E_1^*, \\ t_1 &= m_a^2 + m_b^2 - 2E_a^*E_b^* + 2P_a^*P_b^* \cos\theta_1^*.\end{aligned}\quad (5.7)$$

The physical region of the process $m_a + m_b \rightarrow m_1 + \sqrt{s_2}$ can be found from equation (5.7) by requiring

$$E_1^* \geq m_1 \text{ and } \sqrt{s_2} \geq m_2 + m_3,$$

i.e.

$$m_2 + m_3 \leq \sqrt{s_2} \leq \sqrt{s} - m_1, \quad (5.8)$$

and requiring that $|\cos\theta_1^*| \leq 1$. The latter condition, however, has already been considered for $2 \rightarrow 2$ scattering and using the rule in Figure IV.5.3 we find in Figure 5.2 that it is

$$G(s, t_1, s_2, m_a^2, m_b^2, m_1^2) \leq 0. \quad (5.9)$$

Equations (5.8) and (5.9) specify the integration region in equation (5.6).

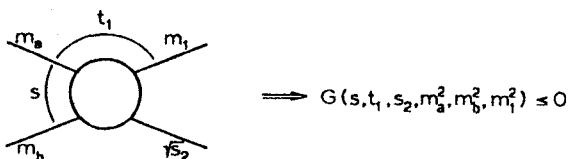


Figure V.5.2

The region (5.9) in the $t_1 s_2$ plane is called the *Chew-Low plot* (Chew, 1959). To plot the boundary one can solve either for t_1 in terms of s_2 , or vice versa,

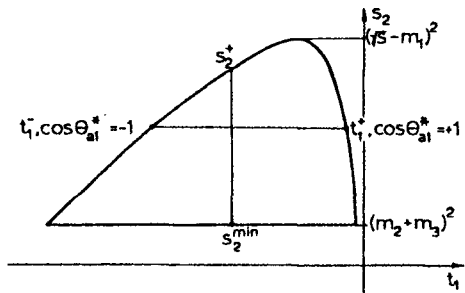


Figure V.5.3 The Chew-Low plot. The quantities t_1^\pm and s_2^\pm are given in equations (5.10-11). In this case the hyperbola $G = 0$ reaches the value $t_1 = (m_a - m_1)^2$ outside the physical region

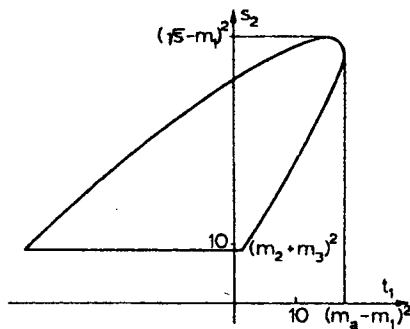


Figure V.5.4 The Chew-Low plot for the case $m_b = m_2 = m_1 = 1$, $m_3 = 2$, $m_a = 5$, $s = 60$. The value $t = (m_a - m_1)^2$ is now physical

by using equation (IV.5.28):

$$t_1^\pm = m_a^2 + m_1^2 - \frac{1}{2s} \{(s + m_a^2 - m_b^2)(s - s_2 + m_1^2) \\ \mp \lambda^\frac{1}{2}(s, m_a^2, m_b^2) \lambda^\frac{1}{2}(s, s_2, m_1^2)\} \quad (5.10)$$

$$s_2^\pm = s + m_1^2 - \frac{1}{2m_a^2} \{(s + m_a^2 - m_b^2)(m_a^2 + m_1^2 - t_1) \\ \mp \lambda^\frac{1}{2}(s, m_a^2, m_b^2) \lambda^\frac{1}{2}(t_1, m_a^2, m_1^2)\} \quad (5.11)$$

Two examples are given in Figures 5.3–4. These curves are of second order in t_1 and s_2 : the boundary curve is a branch of a hyperbola. Equation (5.10) is clearly equation (5.7) for $\cos \theta_1^\pm = \pm 1$. Equation (5.7) shows that when a point with fixed s_2 moves across the Chew-Low plot, t_1 varies linearly with $\cos \theta_{b1}^\pm$. On the other hand, equation (5.11) is obtained by evaluating s_2 in the beam system $p_a = 0$:

$$s_2 = (p_a + p_b - p_1)^2 \\ = s + m_1^2 - 2E_1(m_a + E_b) + 2P_b P_1 \cos \theta_{b1} \quad (5.12)$$

and setting $\cos \theta_{b1} = \pm 1$. In the BS, fixed $t_1 = m_a^2 + m_1^2 - 2m_a E_1$ means fixed E_1 and P_1 , and equation (5.12) shows that s_2 is linear in $\cos \theta_{b1}$.

Since equation (5.10) is also obtained from equation (IV.5.31) by replacing m_2^2 by s_2 , we can use the results for t^{\max} derived in Section IV.6. When considered as functions of s_2 , the approximations for t^{\max} derived there are also approximations for boundary of the Chew-Low plot for s larger than all the masses, in particular, for $s \gg s_2$.

The condition (5.8) limits the Chew-Low plot between two horizontal lines in the $t_1 s_2$ plane. The upper branch of the hyperbola is eliminated by $s_2 \leq (\sqrt{s} - m_1)^2$, and $s_2 \geq (m_2 + m_3)^2$ limits a finite region from the lower region $G \leq 0$. These conditions can be expressed as

$$\begin{aligned}\lambda(s, s_2, m_1^2) &\geq 0 \\ \lambda(s_2, m_2^2, m_3^2) &\geq 0,\end{aligned}\tag{5.13}$$

which state that the two processes $s \rightarrow m_1 + \sqrt{s_2}$ and $\sqrt{s_2} \rightarrow m_2 + m_3$ must be physical.

Substituting $t_1 = (m_a - m_1)^2$ in equation (5.11) gives $s_2^+ = s_2^-$, which shows that the line $t_1 = (m_a - m_1)^2$ is tangent to the hyperbola $G = 0$. This is the maximum value that t_1 may attain and corresponds to the situation in which the velocities of the particles a and 1 are equal. However, if the corresponding value of s_2 is below the threshold, as in Figure 5.3, this t_1 value is not in the physical region. To find when $t_1 = (m_a - m_1)^2$ is attained, we find the value of s_2 at $t_1 = (m_a - m_1)^2$ from equation (5.11) and require it to be larger than the threshold $(m_2 + m_3)^2$:

$$\begin{aligned}s_2^\pm \{t_1 = (m_a - m_1)^2\} &= \frac{1}{m_a} \{s(m_a - m_1) - m_1(m_a^2 - m_b^2) + m_a m_1^2\} \\ &\geq (m_2 + m_3)^2.\end{aligned}\tag{5.14}$$

To get a more transparent condition, we separate four cases: $m_a + m_b \gtrless m_1 + m_2 + m_3$, $m_a \gtrless m_1$. Then $t_1 = (m_a - m_1)^2$ is attained only in one of the following three situations:

- (a) $m_a + m_b > m_1 + m_2 + m_3$
and

$$m_a > m_1$$

- (b) $m_a + m_b > m_1 + m_2 + m_3$,

$$m_a < m_1$$

and

$$\begin{aligned}s &\leq (m_a + m_b)^2 + \frac{m_a}{m_1 - m_a} (m_a + m_b - m_1 - m_2 - m_3) \\ &\quad \times (m_a + m_b - m_1 + m_2 + m_3)\end{aligned}\tag{5.15}$$

- (c) $m_a + m_b < m_1 + m_2 + m_3$,

$$m_a > m_1$$

and

$$s > (m_1 + m_2 + m_3)^2 + \frac{m_1}{m_a - m_1} (m_1 + m_2 + m_3 - m_a - m_b) \\ \times (m_b - m_a + m_1 + m_2 + m_3)$$

We now return to equation (5.6) and state the limits of integration explicitly. This leads to the following important formula:

$$R_3 = \frac{1}{4\lambda^{\frac{1}{2}}(s, m_a^2, m_b^2)} \int_0^{2\pi} d\phi dt_1 ds_2 \Theta\{-G(s, t_1, s_2, m_a^2, m_b^2, m_1^2)\} \\ \times \Theta\{\lambda(s, m_1^2, s_2)\} \Theta\{\lambda(s_2, m_2^2, m_3^2)\} \frac{\lambda^{\frac{1}{2}}(s_2, m_2^2, m_3^2)}{8s_2} \int d\Omega_3^{R^{23}} \quad (5.16)$$

There are several comments one can make about the use and consequences of equation (5.16):

(a) Equation (5.16) implies that the phase space density on the Chew-Low plot is given by

$$\frac{d^2 R_3}{ds_2 dt_1} = \frac{\pi^2}{4\lambda^{\frac{1}{2}}(s, m_a^2, m_b^2)} \frac{\lambda^{\frac{1}{2}}(s_2, m_2^2, m_3^2)}{s_2}. \quad (5.17)$$

This is constant in t_1 , but varies with s_2 . However, it is easy to replace s_2 by another variable r so that phase space density in t_1 and r is constant (Exercise V.3).

(b) In equation (5.17) one can further integrate over either s_2 or t_1 . Since the integrand is independent of t_1 , the integration over t_1 gives the length $t_1^+ - t_1^-$ of the range of integration (equation (5.10)). The result for dR_3/ds_2 is, of course, the same as equation (2.16) obtained from the Dalitz plot. For dR_3/dt_1 we have

$$\frac{dR_3}{dt_1} = \frac{\pi^2}{4\lambda^{\frac{1}{2}}(s, m_a^2, m_b^2)} \int_{s_2^{\min}}^{s_2^{\max}} ds_2 \frac{\lambda^{\frac{1}{2}}(s_2, m_2^2, m_3^2)}{s_2} \quad (5.18)$$

where

$$s_2^{\min} = \max\{s_2^-, (m_2 + m_3)^2\}$$

and s_2^{\pm} are given by equation (5.11). The integral in equation (5.18) is evaluated in closed form in Exercise V.2. An interesting property of equation (5.18) is that it shows how dR_3/dt_1 vanishes near $t_1 = t_{1\max}$ or $t_{1\min}$, due to the vanishing of the range of integration. The situation is different for dR_2/dt (equation (IV.4.24)).

(c) If we abbreviate $\Omega_3^{R^{23}} = \Omega = (\cos \theta, \phi)$, equation (5.16) implies that the distribution $w(\cos \theta, \phi)$ in Ω at fixed s is proportional to

$$w(\cos \theta, \phi) \propto \int dt_1 ds_2 \frac{\lambda^{\frac{1}{2}}(s_2, m_2^2, m_3^2)}{8s_2} T(s_2, t_1, \Omega), \quad (5.19)$$

where $T(p_i) = T(s_2, t_1, \Omega)$ is the matrix element squared for $p_a + p_b \rightarrow p_1 + p_2 + p_3$. In particular, if $T = T(s_2, t_1)$ only depends on s_2 and t_1 , $w(\cos \theta, \phi)$ is constant. Conversely, any experimentally detected variation in $w(\cos \theta, \phi)$ is purely due to a dependence of T on Ω . In practice, if one has some idea of which spin state the 23 system is produced in, it is customary to parametrize $w(\cos \theta, \phi)$ by **density matrix elements** (see, for example, Koch, 1968).

Example 1: As an illustration of a dynamical model, assume one wants to describe the production of a resonance of spin l in the 23 system of the reaction $p_a + p_b \rightarrow p_1 + p_2 + p_3$ by the simple experimentally motivated matrix element squared

$$T = e^{at_1} F(s_2) \frac{2l+1}{4\pi} \{P_l(\cos \theta)\}^2, \quad (5.20)$$

where $a > 0$ is a constant, $F(s_2)$ is some function of s_2 (e.g. the Breit–Wigner function), and P_l is a Legendre polynomial. The axis from which $\cos \theta$ is measured is specified in the next section to be $-p_b$. According to equation (5.19) the distribution in $\cos \theta$ will be proportional to $\{P_l(\cos \theta)\}^2$ – as it should be for a pure resonance of spin l – and the distribution in ϕ will be constant. According to equation (5.16) one finds, after carrying out a simple integral over t_1 , that

$$\frac{d\sigma}{ds_2} = \frac{1}{(4\pi)^4 4\lambda(s, m_a^2, m_b^2)} F(s_2) \frac{\lambda^4(s_2, m_2^2, m_3^2)}{s_2} \frac{1}{a} (e^{at_1^+} - e^{at_1^-}), \quad (5.21)$$

where $t_1^\pm = t_1^\pm(s_2)$ is given in equation (5.10). Thus the distribution in s_2 consists of the input factor $F(s_2)$ modified by the phase space factor $\lambda^4(s_2, m_2^2, m_3^2)/s_2$, which makes $d\sigma/ds_2$ vanish at $s_2 = s_2^{\min} = (m_2 + m_3)^2$, and the last factor, which makes $d\sigma/ds_2$ vanish at $s_2 = s_2^{\max} = (\sqrt{s} - m_1)^2$. We shall return to equation (5.21) when discussing kinematic reflections in Section VIII.2.

Example 2: As a second illustration, consider exchange models of the type

$$T_3 = F(t_1) |A(s_2, \cos \theta; t_1, m_b^2, m_2^2, m_3^2)|^2, \quad (5.22)$$

where $F(t_1)$ is some function of t_1 and A is the amplitude for the $2 \rightarrow 2$ process $(p_a - p_1) + p_b \rightarrow p_2 + p_3$ in which one of the external masses squared is t_1 (Figure 5.1). A simple example is the unmodified one-pion exchange model in which $F(t_1) = g_{NN\pi} t_1 / (t_1 - m_\pi^2)^2$ and in which A is the continuation of the πN scattering amplitude off the pion mass shell. Equation (5.16) is convenient for the integration of an amplitude of the form (5.22) (Exercise V.5) if one makes the assumption that the continuation leaves A unchanged, i.e. one may replace t_1 in A in equation (5.22) by a constant positive mass. This is actually the context in which the Chew–Low plot originally arose (Chew 1959).

6. Jackson, Treiman-Yang, helicity and related angles

We shall now consider the solid angle Ω_3^{R23} in equation (5.6), which in the decay $\sqrt{s}_2 \rightarrow m_2 + m_3$ specifies the orientation of \vec{p}_3 in the frame $\vec{p}_2 + \vec{p}_3 = \vec{p}_a + \vec{p}_b - \vec{p}_1 = \mathbf{0}$ (Figure 6.1). In this frame the vectors $\vec{p}_a, \vec{p}_b, \vec{p}_1$

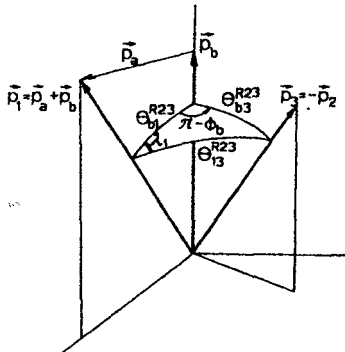


Figure V.6.1 Definition of the Treiman-Yang angle ϕ_b and the helicity angle λ_1 in the frame
 $\vec{p}_2 + \vec{p}_3 = \mathbf{0}$

define a plane, the production plane, which by convention is chosen as the xz plane. The configuration of these vectors depends only on t_1 and s_2 (and on s and the masses). In fact, by applying equations (II.7.10) and (IV.5.17) with the replacement $p_1 \rightarrow p_2 + p_3, p_2 \rightarrow p_b$, and $p_3 \rightarrow p_1$ one finds that the angle θ_{b1}^{R23} between \vec{p}_b and \vec{p}_1 in the frame R23 is given by

$$\sin^2 \theta_{b1}^{R23} = -\frac{4s_2 G(s, t_1, s_2, m_a^2, m_b^2, m_1^2)}{\lambda(s_2, m_b^2, t_1)\lambda(s, s_2, m_1^2)}. \quad (6.1)$$

Other angles are determined similarly.

To define the orientation of \vec{p}_3 we shall choose as the polar axis either \vec{p}_b or \vec{p}_1 . If \vec{p}_b is the axis, one speaks about the Jackson frame, if \vec{p}_1 is the axis, about the helicity frame. Accordingly, the angle θ_{b1}^{R23} in equation (6.1) is called the angle between the Jackson and helicity frames. Note that the word frame refers here only to different choices of axes in the same Lorentz system. The polar and azimuthal angles in the Jackson and helicity frames are defined as follows.

(a) The Jackson frame

Since \vec{p}_b is the axis the polar angle or the Jackson angle (Jackson, 1964) is defined by

$$\cos \theta_{b3}^{R23} = \left. \frac{\vec{p}_b \cdot \vec{p}_3}{P_b P_3} \right|_{\vec{p}_2 = -\vec{p}_3}. \quad (6.2)$$

A polar angle varies between 0 and π , so that its cosine defines it uniquely. Note that $\theta_{b3}^{R23} = \theta_{2-1,2}^{R23}$ is the CMS scattering angle for the subprocess $(p_a - p_1) + p_b \rightarrow p_2 + p_3$. This also explains why p_3 and not p_2 is chosen to define the decay angles of $(p_2 + p_3) \rightarrow p_2 + p_3$ in Figure 6.1. Any resonance structure in the 23 system will directly reflect itself in the Jackson angle distribution.

The azimuthal angle in the Jackson frame is called the *Treiman–Yang angle*, and is defined by

$$\begin{aligned}\cos \phi_b &= -\frac{(\mathbf{p}_b \times \mathbf{p}_1) \cdot (\mathbf{p}_b \times \mathbf{p}_3)}{|\mathbf{p}_b \times \mathbf{p}_1| |\mathbf{p}_b \times \mathbf{p}_3|} \Big|_{\mathbf{p}_2 = -\mathbf{p}_3} \\ \sin \phi_b &= \frac{P_b(-\mathbf{p}_b \cdot \mathbf{p}_1 \times \mathbf{p}_3)}{|\mathbf{p}_b \times \mathbf{p}_1| |\mathbf{p}_b \times \mathbf{p}_3|} \Big|_{\mathbf{p}_2 = -\mathbf{p}_3}\end{aligned}\quad (6.3)$$

The Treiman–Yang angle ϕ_b is essentially the angle between the production plane $\mathbf{p}_b, \mathbf{p}_1$ and the *decay plane* $\mathbf{p}_b, \mathbf{p}_3$, see Figure 6.1. The subscript b underlines the fact that the polar axis is \mathbf{p}_b ; we omit the superscript R23 from azimuthal angles.

Note the minus sign in $\cos \phi_b$ in equation (6.3). This makes our definition coincide with the one in common use. It implies that the angle in Figure 6.1 defined by $\mathbf{p}_b, \mathbf{p}_1, \mathbf{p}_3$ is actually $\pi - \phi_b$ and not ϕ_b , so that for $p_{2y} \approx 0$, $p_{2x} > 0$, i.e. \mathbf{p}_2 ‘close’ to \mathbf{p}_1 ($p_{1x} > 0$), the angle ϕ_b is close to zero. Secondly, note that a reflection in the production plane will change ϕ_b into $2\pi - \phi_b$. If in the initial state there is nothing to distinguish the two sides of the plane, the distribution in ϕ_b will be symmetric around π .

(b) The helicity frame

In the helicity frame \mathbf{p}_1 is the polar axis and the polar angle, called here the *helicity polar angle*, is defined by

$$\cos \theta_{13}^{R23} = \frac{\mathbf{p}_1 \cdot \mathbf{p}_3}{P_1 P_3} \Big|_{\mathbf{p}_2 = -\mathbf{p}_3} \quad (6.4)$$

The angle $\theta_{12}^{R23} = \pi - \theta_{13}^{R23}$ has already been treated in Section 1 (equations 1.9–10). As was shown earlier, the distribution on the Dalitz plot gives directly the distribution in the helicity polar angle (see comments at the end of Section 3).

The corresponding azimuthal angle λ_1 is called the *helicity angle* and is defined by

$$\begin{aligned}\cos \lambda_1 &= \frac{(\mathbf{p}_1 \times \mathbf{p}_b) \cdot (\mathbf{p}_1 \times \mathbf{p}_3)}{|\mathbf{p}_1 \times \mathbf{p}_b| |\mathbf{p}_1 \times \mathbf{p}_3|} \Big|_{\mathbf{p}_2 = -\mathbf{p}_3} \\ \sin \lambda_1 &= \frac{P_1 \mathbf{p}_1 \cdot \mathbf{p}_b \times \mathbf{p}_3}{|\mathbf{p}_1 \times \mathbf{p}_b| |\mathbf{p}_1 \times \mathbf{p}_3|} \Big|_{\mathbf{p}_2 = -\mathbf{p}_3}\end{aligned}\quad (6.5)$$

Thus λ_1 is the angle between the production plane $\mathbf{p}_1, \mathbf{p}_b$ and the plane $\mathbf{p}_1, \mathbf{p}_3$ with $\mathbf{p}_a + \mathbf{p}_b = \mathbf{p}_1$ as the axis (see Figure 6.1). As with ϕ_b , the distribution is usually symmetric around $\lambda_1 = \pi$.

According to equations (5.16) and (5.19), the phase space distributions in Jackson, Treiman-Yang, helicity polar and helicity angles are uniform.

The definitions (6.3) and (6.5) of ϕ_b and λ_1 can be put in several different but equivalent forms. There are two types of modifications. For the first one may, still remaining in the frame R23, use the equations $\mathbf{p}_a = \mathbf{p}_1 - \mathbf{p}_b$, $\mathbf{p}_2 = -\mathbf{p}_3$ to replace some of the vectors in equations (6.3) and (6.5) by other vectors. One of the forms so obtained is rather interesting (Exercise V.6). Less trivial modifications are possible due to the fact that an azimuthal angle is invariant under Lorentz transformations parallel to the polar axis. Thus ϕ_b is invariant under transformations along

$$\mathbf{p}_b = \mathbf{p}_1 - \mathbf{p}_a \quad (6.6)$$

and λ_1 under transformations along

$$\mathbf{p}_1 = \mathbf{p}_a + \mathbf{p}_b. \quad (6.7)$$

These transformations lead to different frames and it is only in R23 that ϕ_b and λ_1 can be simultaneously defined.

To exhibit some alternative definitions in other frames, we shall adopt the following notation, used in equation (II.7.25):

$$\mathbf{p}_1 = \mathbf{0}, \quad (\mathbf{p}_2; \mathbf{p}_3, \mathbf{p}_4) \rightarrow \phi \quad (6.8)$$

means

$$\cos \phi = \frac{(\mathbf{p}_2 \times \mathbf{p}_3) \cdot (\mathbf{p}_2 \times \mathbf{p}_4)}{|\mathbf{p}_2 \times \mathbf{p}_3| |\mathbf{p}_2 \times \mathbf{p}_4|},$$

$$\sin \phi = \frac{\mathbf{P}_2(\mathbf{p}_2 \cdot \mathbf{p}_3 \times \mathbf{p}_4)}{|\mathbf{p}_2 \times \mathbf{p}_3| |\mathbf{p}_2 \times \mathbf{p}_4|}.$$

Thus ϕ is the azimuthal angle of \mathbf{p}_4 in the frame $\mathbf{p}_1 = \mathbf{0}$ with \mathbf{p}_2 parallel to z axis and $p_{3y} = 0$, $p_{3x} \geq 0$ (Figure II.7.1). Then equations (6.3) and (6.5) are

$$\mathbf{p}_2 + \mathbf{p}_3 = \mathbf{0}, \quad (\mathbf{p}_b; \mathbf{p}_1, \mathbf{p}_3) \rightarrow \pi - \phi_b \quad (6.9)$$

$$\mathbf{p}_2 + \mathbf{p}_3 = \mathbf{0}, \quad (\mathbf{p}_1; \mathbf{p}_b, \mathbf{p}_3) \rightarrow \lambda_1. \quad (6.10)$$

From equation (6.6) it is seen that the Treiman-Yang angle ϕ_b has a simple definition also in the frames $\mathbf{p}_b = \mathbf{0}$ (the target system) or $\mathbf{p}_a - \mathbf{p}_1 = \mathbf{0}$. To be able to transform to $\mathbf{p}_b = \mathbf{0}$ equation (6.9) must be written so that \mathbf{p}_b is absent. In R23 \mathbf{p}_b equals $\mathbf{p}_1 - \mathbf{p}_a$ which implies

$$\mathbf{p}_2 + \mathbf{p}_3 = \mathbf{0}, \quad (\mathbf{p}_1 - \mathbf{p}_a; \mathbf{p}_1, \mathbf{p}_3) \rightarrow \pi - \phi_b.$$

Now also in $\mathbf{p}_b = \mathbf{0}$ the angle between $\mathbf{p}_1 - \mathbf{p}_a, \mathbf{p}_1$ and $\mathbf{p}_1 - \mathbf{p}_a, \mathbf{p}_3$ is $\pi - \phi_b$.

To modify the result slightly, the equality $\mathbf{p}_1 - \mathbf{p}_a = -\mathbf{p}_2 - \mathbf{p}_3$, valid in $\mathbf{p}_b = \mathbf{0}$, is used to get

$$\mathbf{p}_b = \mathbf{0}, \quad (-\mathbf{p}_2 - \mathbf{p}_3; \mathbf{p}_1, \mathbf{p}_3) \rightarrow \pi - \phi_b.$$

According to equation (II.7.25) this is equivalent to

$$\mathbf{p}_b = \mathbf{0}, \quad (\mathbf{p}_2 + \mathbf{p}_3; \mathbf{p}_1, \mathbf{p}_2) \rightarrow \phi_b. \quad (6.11)$$

Equation (6.11) is essentially the original definition by Treiman and Yang (Treiman, 1962).

Since $\mathbf{p}_a - \mathbf{p}_1$ does not appear in equation (6.11), it could be used to define ϕ_b in the frame $\mathbf{p}_a - \mathbf{p}_1 = \mathbf{0}$. However, because $\mathbf{p}_a - \mathbf{p}_1$ is usually spacelike, this frame does not always exist. The appropriate frame is then $\mathbf{p}_a - \mathbf{p}_1 = (0, 0, 0, \sqrt{(-t_1)})$, and equation (6.11) is valid there as such. For elastic upper vertex, $m_a = m_1$, this is the Breit frame: $E_a = E_1$, $\mathbf{p}_a = -\mathbf{p}_1$.

The helicity angle can similarly be seen to allow the definitions

$$\mathbf{p}_1 = \mathbf{0}, \quad (\mathbf{p}_a + \mathbf{p}_b; \mathbf{p}_b, \mathbf{p}_3) \rightarrow \lambda_1, \quad (6.12)$$

$$\mathbf{p}_a + \mathbf{p}_b = \mathbf{0}, \quad (\mathbf{p}_1; \mathbf{p}_b, \mathbf{p}_3) \rightarrow \lambda_1. \quad (6.13)$$

7. Description in three invariants and one angle

Specifying the orientation of \mathbf{p}_3 in the Jackson or helicity frame we have in equation (5.16)

$$d\Omega_3^{R23} = d \cos \theta_{b3}^{R23} d\phi_b, \quad (7.1)$$

$$\begin{aligned} d\Omega_3^{R23} &= d \cos \theta_{13}^{R23} d\lambda_1 \\ &= -d \cos \theta_{12}^{R23} d\lambda_1. \end{aligned} \quad (7.2)$$

The purpose of this section is to show how to replace either $\cos \theta_{b3}^{R23}$ in equation (7.1) by $t_2 = t_{b3}$ or $\cos \theta_{13}^{R23}$ in equation (7.2) by $s_1 = s_{12}$ and in this way write equation (5.16) for $R_3(s)$ in terms of three invariants and one angle.

The relations between t_2 and s_1 and the angles can be derived in many ways. Proceeding in a very pedestrian manner we have for t_2

$$\begin{aligned} t_2 &= (\mathbf{p}_b - \mathbf{p}_3)^2 \\ &= m_b^2 + m_3^2 - 2E_b^{R23}E_3^{R23} + 2P_b^{R23}P_3^{R23} \cos \theta_{b3}^{R23}. \end{aligned} \quad (7.3)$$

To write this in invariant variables the list given in equation (1.7) must be supplemented by E_a and E_b , which were not defined for a decay. One can

directly write down the following equations:

$$\begin{aligned} E_a^{R23} &= \frac{s_2 + m_a^2 - t_{b1}}{2\sqrt{s_2}} \\ &= \frac{s + t_1 - m_b^2 - m_1^2}{2\sqrt{s_2}}, \\ E_b^{R23} &= \frac{s_2 + m_b^2 - t_1}{2\sqrt{s_2}}, \\ P_a^{R23} &= \frac{\lambda^{\frac{1}{2}}(s_2, m_a^2, t_{b1})}{2\sqrt{s_2}}, \\ P_b^{R23} &= \frac{\lambda^{\frac{1}{2}}(s_2, m_b^2, t_1)}{2\sqrt{s_2}}. \end{aligned} \quad (7.4)$$

The linear relation between t_2 and $\cos \theta_{b3}^{R23}$ is, therefore,

$$\begin{aligned} t_2 &= m_b^2 + m_3^2 - \frac{1}{2s_2}(s_2 + m_b^2 - t_1)(s_2 + m_3^2 - m_2^2) \\ &\quad + \cos \theta_{b3}^{R23} \frac{1}{2s_2} \lambda^{\frac{1}{2}}(s_2, m_b^2, t_1) \lambda^{\frac{1}{2}}(s_2, m_3^2, m_2^2). \end{aligned} \quad (7.5)$$

By putting $\cos \theta_{b3}^{R23} = \pm 1$ we obviously obtain the range of t_2 for fixed values of s_2 and t_1 . Remembering that θ_{b3}^{R23} is the CMS scattering angle of $(p_a - p_1) + p_b \rightarrow p_2 + p_3$ and by applying the rule of Figure IV.5.3 to this reaction (Figure 7.1) one obtains this range in the form

$$G(s_2, t_2, m_3^2, t_1, m_b^2, m_2^2) \leq 0. \quad (7.6)$$

The linear relation between s_1 and $\cos \theta_{13}^{R23}$ has already been given in equation (1.8), since $\cos \theta_{12}^{R23} = -\cos \theta_{13}^{R23}$. Putting in this equation $\cos \theta_{13}^{R23} = \pm 1$ one obtains the range of s_1 for fixed values of s and s_2 . Letting s_2 vary this leads, of course, to the boundary of the Dalitz plot. In G function form the condition of physical $\cos \theta_{13}^{R23}$ is given by equation (2.1) (Figure 7.1).

It is now a simple task to replace the polar angle in equation (7.1) by t_2 and in equation (7.2) by s_1 . Inserting the results into equation (5.16) one obtains the following forms of $R_3(s)$:

$$\begin{aligned} R_3(s) &= \frac{\pi}{2\lambda^{\frac{1}{2}}(s, m_a^2, m_b^2)} \int dt_1 ds_2 \frac{\Theta\{-G(s, t_1, s_2, m_a^2, m_b^2, m_1^2)\}}{4\lambda^{\frac{1}{2}}(s_2, m_b^2, t_1)} \\ &\quad \times \int dt_2 \Theta\{-G(s_2, t_2, m_3^2, t_1, m_b^2, m_2^2)\} \int_0^{2\pi} d\phi_b, \end{aligned}$$

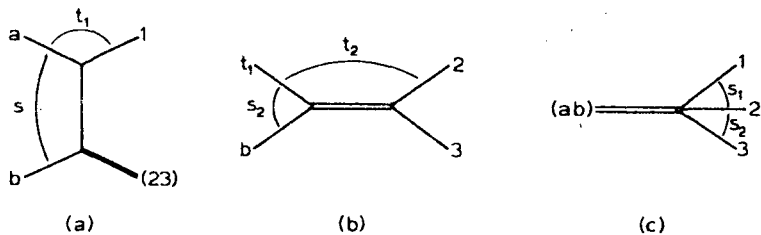


Figure V.7.1 Three subprocesses of the reaction $a + b \rightarrow 1 + 2 + 3$. The physical regions are specified by the following inequalities:

$$(a) \Delta_3(p_2 + p_3, p_b, p_1) = \Delta_3(p_2 + p_3, p_b, p_a + p_b) \geq 0,$$

$$G(s, t_1, s_2, m_a^2, m_b^2, m_1^2) \leq 0,$$

$$(b) \Delta_3(p_a - p_1, p_b, p_2) = \Delta_3(p_2 + p_3, p_b, p_3) \geq 0,$$

$$G(s_2, t_2, m_3^2, t_1, m_b^2, m_2^2) \leq 0,$$

$$(c) \Delta_3(p_2, p_1, p_3) = \Delta_3(p_2 + p_3, p_a + p_b, p_3) \geq 0,$$

$$G(s_1, s_2, s, m_2^2, m_1^2, m_3^2) \leq 0.$$

$$R_3(s) = \frac{\pi}{2\lambda^3(s, m_a^2, m_b^2)} \int dt_1 ds_2 \frac{\Theta\{-G(s, t_1, s_2, m_a^2, m_b^2, m_1^2)\}}{4\lambda^3(s, s_2, m_1^2)} \\ \times \int ds_1 \Theta\{-G(s_1, s_2, s, m_2^2, m_1^2, m_3^2)\} \int_0^{2\pi} d\lambda_1. \quad (7.8)$$

These forms of $R_3(s)$ are evidently useful if the matrix element squared is of the form $T = f(t_1, s_2, t_2, \phi_b)$ or $T = f(t_1, s_2, s_1, \lambda_1)$.

Example 1: If the matrix element squared is of the form

$$T = F(t_1, s_2) e^{bt_2}, \quad (7.9)$$

according to equation (7.7) and (III.2.2), the distribution on the Chew-Low plot is given by

$$\frac{d^2\sigma}{dt_1 ds_2} = \frac{1}{(4\pi)^3 \lambda(s, m_a^2, m_b^2)} \frac{F(t_1, s_2)}{4\lambda^3(s_2, m_b^2, t_1)} \frac{1}{b} (e^{bt_1^+} - e^{bt_1^-}), \quad (7.10)$$

where

$$e^{bt_1^+} - e^{bt_1^-} = 2 \exp \left[b \left\{ m_b^2 + m_3^2 - \frac{1}{2s_2} (s_2 + m_b^2 - t_1)(s_2 + m_3^2 - m_2^2) \right\} \right] \\ \times \sinh \left\{ \frac{b}{2s_2} \lambda^{\frac{1}{2}}(s_2, m_b^2, t_1) \lambda^{\frac{1}{2}}(s_2, m_3^2, m_2^2) \right\}.$$

Further integrations have to be carried out numerically.

Equation (7.8) implies (Nybørg, 1970a, 1970c) that the physical region in $t_1 s_1 s_2$ is determined by the conditions

$$\begin{aligned} G(s, t_1, s_2, m_a^2, m_b^2, m_1^2) &\leq 0, \\ G(s_1, s_2, s, m_2^2, m_1^2, m_3^2) &\leq 0. \end{aligned} \quad (7.11)$$

Since the G functions here only contain two variable invariants ($t_1 s_2$ and $s_1 s_2$, respectively), they represent cylinders in the space of t_1, s_1 and s_2 and the physical region is the common interior of these two cylinders. Figure 7.2

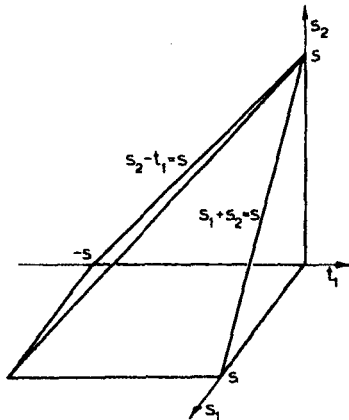


Figure V.7.2 Physical region in $s_1 s_2 t_1$ for zero masses is the intersection of two prisms (cylinders for $m_i \neq 0$)

shows what this three-dimensional region looks like if all masses vanish or s is very large. The projections of this region on $s_1 s_2$ and $s_2 t_1$ planes are the Dalitz plot and the Chew-Low plots, respectively. The projection on the $t_1 s_1$ plane gives the $t_1 s_1$ plot. From Figure 7.2 one sees that for large s the $t_1 s_1$ plot approaches a square.

Similarly, equation (7.7) implies that the physical region in $t_1 s_2 t_2$ satisfies (Nybørg, 1970a, 1970c)

$$\begin{aligned} G(s, t_1, s_2, m_a^2, m_b^2, m_1^2) &\leq 0, \\ G(s_2, t_2, m_3^2, t_1, m_b^2, m_2^2) &\leq 0. \end{aligned} \quad (7.12)$$

Now the second G function contains all three variable invariants, and the physical region is thus the common interior of the cylinder defined by the first G function and the three-dimensional surface defined by the second G function. Figure 7.3 shows the physical region for zero masses. The projections

on the coordinate planes are the $t_1 s_2$ Chew-Low plot, the $t_2 s_2$ plot and the $t_1 t_2$ plot. From Figure 7.3 one sees that the $t_1 t_2$ plot also approaches a square as s increases.

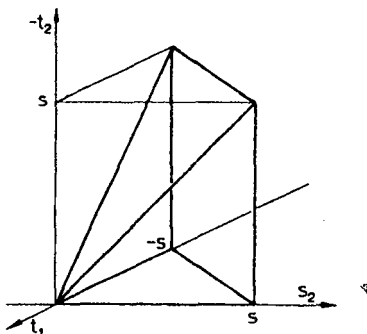


Figure V.7.3 Physical region in $t_1 s_2 t_2$ for zero masses

The exact boundary curves of $t_1 s_1$ (or $t_2 s_2$) and $t_1 t_2$ plots are much more complicated than those of the Dalitz ($s_1 s_2$) or Chew-Low ($t_1 s_2$ or $t_2 s_1$) plots. The reason for this is as follows. To obtain the Chew-Low plot one integrates in equation (7.7) over t_2 and to obtain the Dalitz plot in equation (7.8) over t_1 . In both cases the integration variable occurs in one G function, which gives the limits of integration, the other G function being constant in the integration and giving the boundary. However, to obtain the $t_1 t_2$ plot one has to integrate in equation (7.7) over s_2 , which appears in *both* G functions. The determination of the boundary, therefore, has to be carried out by different means. Instead of carrying out an extensive treatment (Kajantie, 1968b) we illustrate the properties of the $t_1 t_2$ plot by an example.

Example 2: If the masses are given by $m_a = m_1 = m_2 = 0$, $m_b = m_3 = m$ ($\pi N \rightarrow \pi\pi N$ with $m_\pi \simeq 0$) the $t_1 t_2$ plot (Figure 7.4) is bounded by parts of

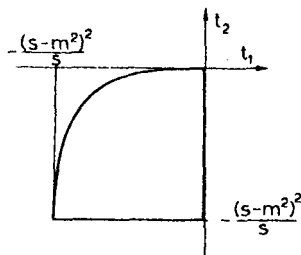


Figure V.7.4 The $t_1 t_2$ plot for $m_a = m_1 = m_2 = 0, m_b = m_3 = m$

the curves

$$t_1 = 0,$$

$$t_2 = \frac{-m^2 t_1^2}{(s - m^2)(s - m^2 + t_1)}, \quad (7.13)$$

$$t_2 = \frac{-(s - m^2)^2}{s},$$

and the phase-space distribution is

$$\frac{d^2 R_3}{dt_1 dt_2} = \frac{\pi^2}{4(s - m^2)} \log \left[\frac{s - m^2}{m^2} \cdot \frac{t_2 + \{t_2(t_2 - 4m^2)\}^{1/2}}{|t_1 - t_2| - t_1 - t_2} \right]. \quad (7.14)$$

The phase-space distribution has a peak at small values of t_1 and t_2 and vanishes at the boundary. In the limit $m \rightarrow 0$ the $t_1 t_2$ plot becomes a square.

The significant qualitative difference observed above between the $t_1 s_1$ and $t_1 t_2$ plots, and the Dalitz ($s_1 s_2$) and Chew-Low ($t_1 s_2$) plots can be characterized as follows. In the latter the three invariants involved (s included) are not all adjacent in the sense of Figure 7.5. The process is then

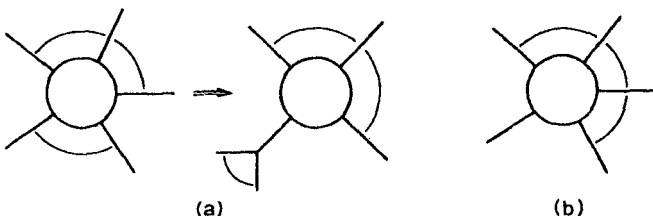


Figure V.7.5 Definition of (a) three non-adjacent, (b) three adjacent invariants. In the case (a), the $2 \rightarrow 3$ reaction can be reduced to a $2 \rightarrow 2$ reaction

effectively a $2 \rightarrow 2$ process in which the mass squared of one of the external particles equals the separate invariant (s for Dalitz plot, s_2 for Chew-Low plot). But in $t_1 t_2$ and $t_1 s_1$ plots all three invariants (t_2 , s , t_1 and s , t_1 , s_1) are adjacent and there is no way of reducing the process to a $2 \rightarrow 2$ subprocess. Accordingly, the boundary is not given by a single G function.

Physical regions in two invariants when a third invariant is fixed (in addition to s and the masses) are also directly given by equations (7.11–12): they are intersections of the three-dimensional regions (7.11–12) with a plane. For instance, the physical region in $t_1 t_2$ when s_2 is fixed is plotted by first drawing in the $t_1 t_2$ plane the hyperbola defined by the second G function in equation (7.12) (given in solved form by equation (7.5)), and by separating from this hyperbola with two straight lines $t_1 = \text{constant}$ given by equation (5.10) a

region satisfying also the first G function. When $s_2 \rightarrow (m_2 + m_3)^2$ the region so obtained approaches a part of the straight line

$$(m_2 + m_3)t_2 = m_3 t_1 + m_2(m_b^2 - m_3^2 - m_2 m_3), \quad (7.15)$$

as is directly seen by inserting $s_2 = (m_2 + m_3)^2$ into equation (7.5).

8. Azimuthal angles in invariant variables

The remaining non-invariant variables in equations (7.7) and (7.8) are the Treiman-Yang angle ϕ_b in equation (7.7) and the helicity angle λ_1 in equation (7.8). We shall now show that there exists a *linear relationship* between s_1 and $\cos \phi_b$ (when s_2, t_1, t_2 are fixed) and between t_2 and $\cos \lambda_1$ (when s_1, s_2, t_1 are fixed). These relations give ϕ_b and λ_1 in terms of invariants. The dependence of ϕ_b on all other invariants but s_1 is more complicated; similarly for λ_1 .

That s_1 and ϕ_b are simply related follows qualitatively by comparing Figures 6.1 and II.7.1. If an azimuthal angle is defined as in Figure II.7.1 by

$$\mathbf{p}_1 = 0, \quad (\mathbf{p}_2, \mathbf{p}_3, \mathbf{p}_4) \rightarrow \phi, \quad (8.1)$$

then according to equation (II.7.16) $\cos \phi$ will depend linearly on $p_3 \cdot p_4$. Similarly, the cosine of the angle ϕ_b in Figure 6.1 will depend linearly on the invariant 'connecting' \mathbf{p}_1 and $\mathbf{p}_2 (= -\mathbf{p}_3)$. This invariant is $s_1 \equiv s_{12}$. Applying the same argument to λ_1 one infers that $\cos \lambda_1$ and t_2 are linearly related.

(a) Relation between s_1 and the Treiman-Yang angle ϕ_b

Applying equation (II.7.15) to equation (6.11) one finds

$$\cos \phi_b = \frac{G(p_b, p_2 + p_3, p_1)}{\Delta_3(p_b, p_2 + p_3, p_1)\Delta_3(p_b, p_2 + p_3, p_2)} \quad (8.2)$$

In equation (8.2) the determinants Δ_3 are easily written in terms of invariants by drawing pictures of the subprocesses involved, as shown in Figure 7.1. The numerator is evaluated by substituting the scalar products from equation (4.9). In order to get a more symmetric expression, however, we first use equations (A.5) and (A.3) to write

$$G(p_b, p_2 + p_3, p_1) = -G(p_b, p_2 + p_3, p_4 + p_b). \quad (8.3)$$

Then equation (4.9) and Figure 7.1 imply

$$\cos \phi_b = - \frac{\begin{vmatrix} 2m_b^2 & s_2 - t_1 + m_b^2 & m_b^2 + m_3^2 - t_2 \\ s_2 - t_1 + m_b^2 & 2s_2 & s_2 - m_2^2 + m_3^2 \\ s - m_a^2 + m_b^2 & s + s_2 - m_1^2 & s - s_1 + m_3^2 \end{vmatrix}}{2\{G(s, t_1, s_2, m_a^2, m_b^2, m_1^2)G(s_2, t_2, m_3^2, t_1, m_b^2, m_2^2)\}^{\frac{1}{2}}} \quad (8.4)$$

Equation (8.4) gives two solutions, ϕ_b and $2\pi - \phi_b$. The corresponding two momentum configurations are mirror images of each other, the reflection being in the p_b, p_1 plane in Figure 6.1, and the set s_1, s_2, t_1, t_2 is the same for both configurations.

The inverse relation of equation (8.4) follows after simple algebra as

$$s_1 = s + m_3^2 - \frac{1}{\lambda(s_2, t_1, m_b^2)} \left[\begin{vmatrix} 2m_b^2 & s_2 - t_1 + m_b^2 & m_b^2 + m_3^2 - t_2 \\ s_2 - t_1 + m_b^2 & 2s_2 & s_2 - m_2^2 + m_3^2 \\ s - m_a^2 + m_b^2 & s + s_2 - m_1^2 & 0 \end{vmatrix} + 2\{G(s, t_1, s_2, m_a^2, m_b^2, m_1^2)G(s_2, t_2, m_3^2, t_1, m_b^2, m_2^2)\}^{\frac{1}{2}} \cos \phi_b \right]. \quad (8.5)$$

(b) Relation between t_2 and the helicity angle λ_1

The helicity angle λ_1 is according to equations (6.13) and (II.7.15) given by

$$\cos \lambda_1 = \frac{G\left(\begin{matrix} p_a + p_b, p_1, p_b \\ p_a + p_b, p_1, p_3 \end{matrix}\right)}{\{\Delta_3(p_a + p_b, p_1, p_b)\Delta_3(p_a + p_b, p_1, p_3)\}^{\frac{1}{2}}}. \quad (8.6)$$

The two Δ_3 s are again written in G function form as shown in Figure 7.1. The numerator is modified slightly,

$$G\left(\begin{matrix} p_a + p_b, p_1, p_b \\ p_a + p_b, p_1, p_3 \end{matrix}\right) = G\left(\begin{matrix} p_a + p_b, p_2 + p_3, p_b \\ p_a + p_b, p_2 + p_3, p_3 \end{matrix}\right), \quad (8.7)$$

and the scalar products are replaced by standard invariants using equation (4.9). Then $\cos \lambda_1$ becomes

$$\cos \lambda_1 = \frac{\begin{vmatrix} 2s & s + s_2 - m_1^2 & s - s_1 + m_3^2 \\ s + s_2 - m_1^2 & 2s_2 & s_2 - m_2^2 + m_3^2 \\ s - m_a^2 + m_b^2 & s_2 - t_1 + m_b^2 & m_b^2 + m_3^2 - t_2 \end{vmatrix}}{2\{G(s, t_1, s_2, m_a^2, m_b^2, m_1^2)G(s_1, s_2, s, m_2^2, m_1^2, m_3^2)\}^{\frac{1}{2}}} \quad (8.8)$$

The explicit expression for t_2 in terms of $\cos \lambda_1$ is

$$t_2 = m_b^2 + m_3^2 + \frac{1}{\lambda(s, s_2, m_1^2)} \left[- \begin{vmatrix} 2s & s + s_2 - m_1^2 & s - s_1 + m_3^2 \\ s + s_2 - m_1^2 & 2s_2 & s_2 - m_2^2 + m_3^2 \\ s - m_1^2 + m_b^2 & s_2 - t_1 + m_b^2 & 0 \end{vmatrix} + 2\{G(s, t_1, s_2, m_a^2, m_b^2, m_1^2)G(s_1, s_2, s, m_2^2, m_1^2, m_3^2)\}^{\frac{1}{2}} \cos \lambda_1 \right]^{(8.9)}$$

The above derivations may appear somewhat formal, and we indicate briefly how the above results are obtained directly from geometric arguments. Expanding t_2 in the frame R23 ($p_2 + p_3 = 0$) one has the relation equation (7.3). According to the cosine theorem of spherical trigonometry (equation (B.4) and Figures B.1. and 6.1), $\cos \theta_{b3} = \cos \theta_{b1} \cos \theta_{13} + \sin \theta_{b1} \sin \theta_{13} \cos \lambda_1$, one finds

$$t_2 = m_b^2 + m_3^2 - 2E_b E_3 + 2P_b P_3 \cos \theta_{b1} \cos \theta_{13} + 2P_b P_3 \sin \theta_{b1} \sin \theta_{13} \cos \lambda_1. \quad (8.10)$$

All angles, energies and momenta are here expressed in R23. When they are written in invariant form by using equations (1.7), (7.4), (6.1) and (1.8) one rediscovers equation (8.9). Equation (8.5) is found similarly by evaluating $s_1 = (p_a + p_b - p_3)^2$ in R23.

Equations (8.5) and (8.9) also clarify the dynamic significance of the angles ϕ_b and λ_1 (Lyons, 1970). From equations (7.7-8) it clearly follows that a uniform distribution in ϕ_b or λ_1 implies an amplitude of the form $T_3(t_1, s_2, t_2)$ or $T_3(t_1, s_2, s_1)$, respectively. Equations (8.5), (8.9) show how a dependence on s_1 or t_2 correlates with a dependence on ϕ_b or λ_1 . If there is any dependence on s_1 , there will be a dependence on ϕ_b . In particular, since s_1 is proportional to $-\cos \phi_b$ an amplitude favouring large values of s_1 will also favour values of ϕ_b near π . This is the case if $T \simeq s_1^{2\alpha_1}$, $\alpha_1 \leq 1$, as is assumed in models of Regge type. The smaller α_1 is, the less peaking near $\phi_b \simeq \pi$ should there be. Similarly since t_2 is proportional to $+\cos \lambda_1$, an amplitude favouring small values of $|t_2|$ will peak the distribution near $\lambda_1 \simeq 0$.

9. Description in four invariants

The form of the phase space integral in the space of all four invariants is obtained either from equation (7.7) by replacing ϕ_b by s_1 , from equation (7.9) by replacing λ_1 by t_2 , or directly from equation (5.16) by using the formula (II.7.21) expressing $d\Omega_3^{R23}$ in invariant variables. Choosing the latter

way we have

$$\begin{aligned} d\Omega_3^{R23} &= \frac{2s_2}{\{-\Delta_2(p_2 + p_3, p_3)\}^{\frac{1}{2}}} \frac{d(p_b \cdot p_3) d(p_1 \cdot p_3)}{\{-\Delta_4(p_a, p_b, p_1, p_3)\}^{\frac{1}{2}}} \\ &= \frac{s_2 dt_2 ds_1}{\lambda^{\frac{1}{2}}(s_2, m_2^2, m_3^2)(-\Delta_4)^{\frac{1}{2}}} \end{aligned} \quad (9.1)$$

so that

$$R_3(s) = \frac{\pi}{16\lambda^{\frac{1}{2}}(s, m_a^2, m_b^2)} \int \frac{dt_1 ds_2 dt_2 ds_1}{(-\Delta_4)^{\frac{1}{2}}}. \quad (9.2)$$

Here Δ_4 is the 4×4 symmetric Gram determinant of any four independent vectors formed out of p_a, p_b, p_1, p_2, p_3 . Due to this freedom of choice we shall in the notation often omit the arguments from Δ_4 . Remember that the factor 2 in equation (9.1) arose from the fact that two momentum configurations corresponding to azimuthal angles ϕ and $2\pi - \phi$ lead to the same invariants.

The range of integration in equation (9.2) is the physical region in $t_1 s_2 t_2 s_1$ for the channel $p_a + p_b \rightarrow p_1 + p_2 + p_3$ for fixed s . We see that the physical region in these variables (equation (4.1)) has to satisfy

$$\Delta_4 \leq 0. \quad (9.3)$$

The boundary is given by the equality sign. Physical regions of lower dimensionalities are obtained by integrating over one or more variables (these have already been treated) or by holding one or more variables fixed (see equations (4.2b), (4.3c) and (4.4d)). Thus, for instance, the physical region in $t_1 s_1 s_2$ for t_2 fixed is simply bounded by the surface $\Delta_4 = 0$ taken for t_2 fixed. This physical region will lie within the physical region which is obtained by integrating over all values of t_2 and which is shown in Figure 7.2 for zero masses. Similarly, for instance, the physical region in $t_1 t_2$ for s_1, s_2 fixed is bounded by the curve $\Delta_4 = 0$ drawn on $t_1 t_2$ plane for s_1, s_2 fixed. This curve will be within the $t_1 t_2$ plot.

In terms of the standard set of five invariants and five masses Δ_4 is given by

$$\begin{aligned} \Delta_4 &= \Delta_4(p_a, p_b, p_1, p_2) \\ &\equiv -\frac{1}{16} B(s, t_1, s_1, s_2, t_2; m_a^2, m_b^2, m_3^2, m_b^2, m_1^2) \\ &= \frac{1}{16} \begin{vmatrix} 2m_a^2 & 2p_a \cdot p_b & 2p_a \cdot p_1 & 2p_a \cdot p_3 \\ 2p_a \cdot p_b & 2m_b^2 & 2p_b \cdot p_1 & 2p_b \cdot p_3 \\ 2p_a \cdot p_1 & 2p_b \cdot p_1 & 2m_1^2 & 2p_1 \cdot p_3 \\ 2p_a \cdot p_3 & 2p_b \cdot p_3 & 2p_1 \cdot p_3 & 2m_3^2 \end{vmatrix} \end{aligned}$$

$$= \frac{1}{16} \begin{vmatrix} 2m_a^2 & s - m_a^2 - m_b^2 & m_a^2 + m_1^2 - t_1 & s - s_1 + t_2 - m_b^2 \\ s - m_a^2 - m_b^2 & 2m_b^2 & s - s_2 + t_1 - m_a^2 & m_b^2 + m_3^2 - t_2 \\ m_a^2 + m_1^2 - t_1 & s - s_2 + t_1 - m_a^2 & 2m_1^2 & s - s_1 - s_2 + m_2^2 \\ s - s_1 + t_2 - m_b^2 & m_b^2 + m_3^2 - t_2 & s - s_1 - s_2 + m_2^2 & 2m_3^2 \end{vmatrix}$$

A more useful form is obtained if the arguments are modified as follows:

$$\Delta_4 = \Delta_4(p_2 + p_3, p_b, p_a + p_b, p_3) \quad (9.4)$$

$$= \frac{1}{16} \begin{vmatrix} 2s_2 & s_2 - t_1 + m_b^2 & s + s_2 - m_1^2 & s_2 - m_2^2 + m_3^2 \\ s_2 - t_1 + m_b^2 & 2m_b^2 & s - m_a^2 + m_b^2 & m_b^2 + m_3^2 - t_2 \\ s + s_2 - m_1^2 & s - m_a^2 + m_b^2 & 2s & s - s_1 + m_3^2 \\ s_2 - m_2^2 + m_3^2 & m_b^2 + m_3^2 - t_2 & s - s_1 + m_3^2 & 2m_3^2 \end{vmatrix}$$

In this form the invariants t_1 , s_2 and t_2 occur only in two symmetrically situated positions. The unsymmetric Gram determinant in equation (8.4) is the minor of the element $(p_a + p_b) \cdot p_3 = \frac{1}{2}(s - s_1 + m_3^2)$ in equation (9.4), and it is immediately seen that $\cos \phi_b$ is linear in s_1 . Similarly $\cos \lambda_1$ is seen to be linear in t_2 . The purpose of the modifications (8.3) and (8.7) was to establish the connection with the form (9.4). The choice of arguments in equation (9.4) is motivated in a general form in Figure 9.1.

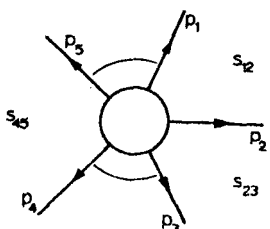


Figure V.9.1 Choosing the arguments of Δ_4 so that $\Delta_4 = \Delta_4(p_2 + p_1, p_5, p_4, p_3 + p_4)$ gives a determinant in which s_{12} , s_{23} and s_{45} appear only in two symmetrically situated positions

Finally, a form exhibiting the symmetries most clearly is obtained from the Cayley representation (A.13):

$$B = \begin{vmatrix} 0 & m_2^2 & s_2 & t_1 & m_1^2 & 1 \\ m_2^2 & 0 & m_3^2 & t_2 & s_1 & 1 \\ s_2 & m_3^2 & 0 & m_b^2 & s & 1 \\ t_1 & t_2 & m_b^2 & 0 & m_a^2 & 1 \\ m_1^2 & s_1 & s & m_a^2 & 0 & 1 \\ 1 & 1 & 1 & 1 & 1 & 0 \end{vmatrix} \quad (9.5)$$

The preceding equations determine B as *the basic five-particle kinematic function*. It is related to Δ_4 exactly as λ was related to Δ_2 and G to Δ_3 . Its explicit form (Nyborg, 1965a) can be computed by evaluating any of the above determinants. This explicit form is not needed in practice; for numerical purposes one may as well use the determinantal representations. We shall use B when it is useful to emphasize that it has ten arguments as in equation (9.5); otherwise we shall talk about Δ_4 .

The properties of B and Δ_4 are in many respects parallel to those of G and Δ_3 . We do not attempt a detailed analysis but just list some important points:

(a) Symmetries of Δ_4

Let $(1 \dots 5) \rightarrow (i_1 \dots i_5)$ be any permutation, and apply this permutation both to the first five rows and first five columns of the determinant in equation (9.5). This gives a permutation of the ten arguments of B , which preserves B unchanged. The symmetry group of B contains $5! = 120$ permutations. In general these interchange one-particle and two-particle masses, but there are ten permutations under which this does not happen. These are generated by the cyclic transformations of particles $1 \rightarrow 2 \rightarrow 3 \rightarrow 4 \rightarrow 5$ and the reflection $1 \leftrightarrow 5, 2 \leftrightarrow 4, 3$ unchanged.

The symmetry properties of B are most clearly seen in the notation

$$x_{ij} = \{(p_i + \dots + p_5) - (p_j + \dots + p_5)\}^2, \quad i, j = 1, \dots, 5.$$

The quantities x_{ij} satisfy $x_{ij} = x_{ji}$ and $x_{ii} = 0$. The correspondence between x_{ij} and usual invariants is seen from Figure 9.2. Then the 120 index permutations $(1 \dots 5) \rightarrow (i_1 \dots i_5)$ give the permutations of $\{x_{ij}\}$ under which $B(\{x_{ij}\})$ is invariant. Analogously with G , B can be related to the volume of a hyper-tetrahedron with five vertices $1, \dots, 5$ and ten sides x_{ij} in a four-dimensional space.

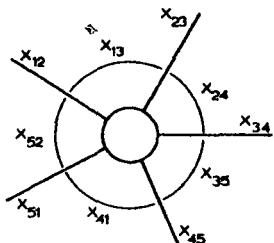


Figure V.9.2 Symmetric variables in Δ_4

(b) Δ_4 as a function of one variable

B is a homogeneous polynomial of order four in its arguments and quadratic in any one of them. Thus the equation $\Delta_4 = 0$ is a quadratic equation and has two solutions. These solutions are already known since Δ_4 vanishes,

for instance, for $\sin^2 \lambda_1 = 0$ or $\cos \lambda_1 = \pm 1$. Thus the two roots t_2^\pm of the equation

$$\begin{aligned} 16\Delta_4 &\equiv Pt_2^2 + 2Qt_2 + R \\ &= 0 \end{aligned} \quad (9.6)$$

can be read directly from equation (8.9):

$$t_2 = t_2^\pm$$

corresponding to

$$\cos \lambda_1 = \pm 1 \quad (9.7)$$

in equation (8.9).

It is easy to see from equations (9.4) or (9.5) that $P = \lambda(s, s_2, m_1^2)$. Conversely, one can infer that if Δ_4 is written in the form of equation (9.6) the parameters P , Q and R are

$$\begin{aligned} P &= \lambda(s, s_2, m_1^2), \\ Q^2 - PR &= 4G(s, t_1, s_2, m_a^2, m_b^2, m_1^2)G(s_1, s_2, s, m_2^2, m_1^2, m_3^2), \\ Q &= \begin{vmatrix} 2s_2 & s + s_2 - m_1^2 & s_2 - t_1 + m_b^2 \\ s + s_2 - m_1^2 & 2s & s - m_a^2 + m_b^2 \\ s_2 - m_2^2 + m_3^2 & s - s_1 + m_3^2 & m_b^2 + m_3^2 \end{vmatrix}, \\ R &= 16\Delta_4 \text{ evaluated for } t_2 = 0. \end{aligned} \quad (9.8)$$

The corresponding quantities for any other invariant are obtained by a cyclic transformation of particles. It is useful to understand equation (9.8) in terms of the pictorial interpretation in Figure 9.3. Finally, Δ_4 can obviously

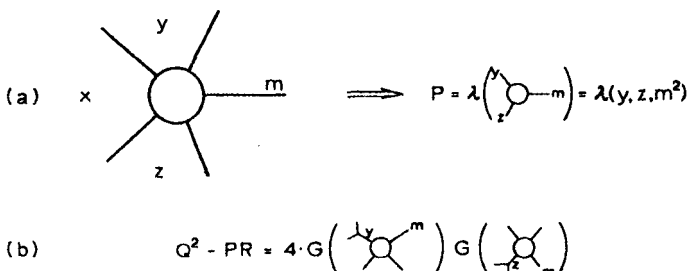


Figure V.9.3 If Δ_4 is written in the form $16\Delta_4 = Px^2 + 2Qx + R$ (x is any invariant), the coefficient P is given by (a) (y and z are adjacent invariants and m is the opposite mass). The discriminant $Q^2 - PR$ is obtained from (b); it is four times the product of the two G functions which correspond to $2 \rightarrow 2$ processes in which the adjacent two-particle systems are taken as single particles of mass squared y and z , respectively

be written in the form

$$16\Delta_4 = \lambda(s, s_2, m_b^2)(t_2 - t_2^+)(t_2 - t_2^-), \quad (9.9)$$

where t_2^\pm are given by equation (9.7). Again, cyclic symmetry leads to similar relations for other variables.

Example 1: We can now retrace some steps backwards from equation (9.2). To integrate first over s_1 one uses equation (9.9) cyclically permuted to give $16\Delta_4 = \lambda(s_2, t_1, m_b^2)(s_1 - s_1^+)(s_1 - s_1^-)$, where s_1^\pm are given by equation (8.5) with $\cos \phi_b = \mp 1$. The integration itself is very simple (Exercise V.2):

$$\int_{s_1^-}^{s_1^+} ds_1 (-\Delta_4)^{\frac{1}{2}} = 4\pi \lambda^{-\frac{1}{2}}(s_2, t_1, m_b^2),$$

but the expressions for s_1^\pm are real only if the two G functions in equation (8.5) are simultaneously negative. We are thus back to equation (7.7) with the ϕ_b integration carried out. Alternatively, one may start by integrating over any of the other three invariants. After the first integration, performed as above, one is always back to equations (7.7), (7.8) or to equations obtained from these by the transformation $p_a \leftrightarrow p_b$, $p_1 \leftrightarrow p_3$, $p_2 \leftrightarrow p_2$.

(c) Δ_4 as a function of two variables

If Δ_4 is considered as a function of two invariants (Morrow, 1966), it is of second order in invariants which are not adjacent (these are the pairs $ss_1, t_1s_2, s_1t_2, s_2s, t_1t_2$) and quadratic in adjacent invariants (the pairs $st_1, t_1s_1, s_1s_2, s_2t_2, t_2s$). This is immediately seen from the Cayley representation (9.5), in which non-adjacent invariants occur in the same row or column. Also one sees explicitly from equation (8.5), which for $\cos \phi_b = \pm 1$ gives the curve $\Delta_4 = 0$ solved for s_1 , that the non-adjacent invariants s and t_2 appear in only one G function while s_2 and t_1 appear in both. The curve $\Delta_4 = 0$ when plotted in the plane of any two invariants x and y is thus a conic section (x, y non-adjacent) or a curve of fourth order (x, y adjacent). We again emphasize the difference between this curve and the xy -plot; the latter is the 'shadow' of the surface $\Delta_4 = 0$ in the xy plane containing all physical values of the two remaining invariants z and u , while the former is drawn for fixed values of z and u (s is always fixed). The curve $\Delta_4 = 0$ thus always lies within the xy plot.

Next we shall consider in some detail the case of nonadjacent invariants choosing t_1 and t_2 for definiteness. Write first Δ_4 in the form

$$16\Delta_4 = At_1^2 + 2Ct_1t_2 + Bt_2^2 + 2A't_1 + 2B't_2 + D \quad (9.10)$$

where $A = \lambda(s, s_1, m_3^2)$,

$$B = \lambda(s, s_2, m_1^2),$$

$$C = -s(s - s_1 - s_2 - m_1^2 + 2m_2^2 - m_3^2) + (s_2 - m_1^2)(s_1 - m_3^2), \quad (9.11)$$

$B' = Q$ in equation (9.8) evaluated for $t_1 = 0$,

$A' = B'$ after the transformation $p_a \leftrightarrow p_b, p_1 \leftrightarrow p_3, p_2 \leftrightarrow p_2$, and

$D = 16\Delta_4$ evaluated for $t_1 = t_2 = 0$.

The type of the conic section is determined by the determinant

$$\Delta = \begin{vmatrix} A & C \\ C & B \end{vmatrix} = -4sG(s_1, s_2, s, m_2^2, m_1^2, m_3^2). \quad (9.12)$$

Here and later the parameters describing equation (9.10) are very complicated to derive by mechanical insertion of equations (9.11). Instead, one can infer them from known properties of the roots of $\Delta_4 = 0$ and $\Delta_3 = 0$. Since $G < 0$ and $s > 0$ one has $\Delta > 0$ and the conic section is an ellipse (Figure 9.4). To plot it one simply takes $t_2 = t_2^\pm(t_1; s, s_1, s_2)$ from equation (8.9)

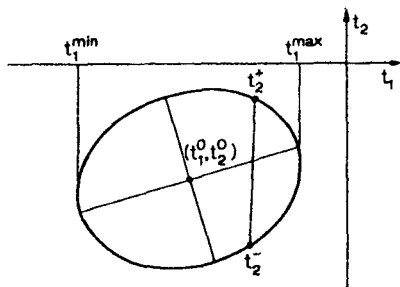


Figure V.9.4 The curve $\Delta_4 = 0$ on $t_1 t_2$ plane. The curve is plotted by taking the solution t_2^\pm with respect to t_1 from equation (8.9). The limits $t_1^{\max, \min}$ are given in equation (9.13). Formulae for t_1^\pm and $t_2^{\max, \min}$ are obtained by the transformation

$$p_a \leftrightarrow p_b, p_1 \leftrightarrow p_3, p_2 \leftrightarrow p_2$$

with $\cos \lambda_1 = \pm 1$. By considering the difference $t_2^+ - t_2^-$ one is easily led to equation (9.12). The limiting values of t_1, t_1^{\max} and t_1^{\min} are obtained when the two roots t_2^\pm coincide. According to equation (8.9) this happens when $G(s, t_1, s_2, m_a^2, m_b^2, m_1^2) = 0$. Thus

$$t_1^{\max} = t_1^+, \quad t_1^{\min} = t_1^-, \quad (9.13)$$

where t_1^\pm are given in equation (5.10).

The quadratic form of equation (9.10) can be diagonalized by standard methods. First, the centre of the ellipse is given by

$$\begin{aligned} t_1^{(0)} &= \begin{vmatrix} C & A' \\ B & B' \end{vmatrix} / \Delta = \frac{1}{2}(t_1^{\max} + t_1^{\min}) \\ &= m_a^2 + m_b^2 - \frac{1}{2s}(s + m_a^2 - m_b^2)(s + m_b^2 - s_2), \\ t_2^{(0)} &= m_b^2 + m_3^2 - \frac{1}{2s}(s - m_a^2 + m_b^2)(s + m_3^2 - s_1) \end{aligned} \quad (9.14)$$

After rotating the coordinates around the new origin $(t_1^{(0)}, t_2^{(0)})$ by an angle determined by $\tan 2\alpha = 2C/(A - B)$ one finds

$$16\Delta_4 = \lambda_1 t_1'^2 + \lambda_2 t_2'^2 + U, \quad (9.15)$$

where

$$\begin{aligned} 2\lambda_{1,2} &= \lambda(s, s_2, m_1^2) + \lambda(s, s_1, m_3^2) \pm [\{\lambda(s, s_2, m_1^2) + \lambda(s, s_1, m_3^2)\}^2 \\ &\quad + 16sG(s_1, s_2, s, m_2^2, m_1^2, m_3^2)]^{\frac{1}{2}} \end{aligned} \quad (9.16)$$

and where

$$U = \frac{1}{\Delta} \begin{vmatrix} A & C & A' \\ C & B & B' \\ A' & B' & D \end{vmatrix} \quad (9.17)$$

satisfies

$$(-U/\Delta)^{\frac{1}{2}} = \frac{\lambda^{\frac{1}{2}}(s, m_a^2, m_b^2)}{2s}. \quad (9.18)$$

Equation (9.18) follows simply from $t_1^{\max} - t_1^{\min} = 2(-CU/\Delta)^{\frac{1}{2}}$ and equation (9.13).

The cyclic transformation (4.6) gives the curves $\Delta_4 = 0$ in the $s_1 t_2, ss_2$, $t_1 s_2$ and ss_1 planes. Note that s in the formula (9.12) for Δ is the invariant between the invariants considered. Thus it becomes s_2 or s_1 in the $s_1 t_2$ and $s_2 t_1$ planes so that $\Delta > 0$ and the curves are ellipses. In the ss_1 or ss_2 planes it becomes t_1 or t_2 so that $\Delta < 0$, i.e. the curve is hyperbola, if $t_1 < 0$ or $t_2 < 0$ (see Figure 10.4).

(d) Δ_4 for vanishing masses

When $m_i = 0$ one finds from equation (9.4) that

$$16\Delta_4 = (st_1 - t_1 s_1 + s_1 s_2 - s_2 t_2 + t_2 s)^2 - 4s(s - s_1 - s_2)t_1 t_2. \quad (9.19)$$

The terms within the first parenthesis are just the five pairs of adjacent invariants in which Δ_4 is of fourth order. The simple form of equation (9.19) is often useful if one wants to estimate various effects qualitatively.

10. Cyclic symmetry, the Toller angle

All the discussion in Sections 5–8 concerning invariants and angles was based on the definite factorization of R_3 shown in Figure 5.1. We now generalize the situation by allowing the two particle intermediate state to be any pair of adjacent particles. For a symmetric treatment we take all momenta to be outgoing (Figure 10.1) and use for invariants a notation with double

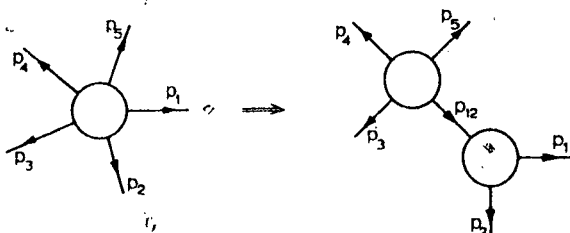


Figure V.10.1

subscripts. The $2 \rightarrow 2$ scattering in the decomposition of Figure 10.1 involves the invariants s_{34}, s_{45} . The $1 \rightarrow 2$ decay shown there is described in terms of angles θ, ϕ of p_1 with respect to a coordinate system fixed by p_3, p_4 , and p_5 , in addition to the invariant mass s_{12} of the system. Alternatively, the orientation of p_1, p_2 with respect to p_3, p_4, p_5 is fixed by the invariants s_{51} and s_{23} , or by a mixture of one angle and one invariant.

Assume first that $s_{12} > 0$, so that one can go to the frame $p_1 + p_2 = 0$. We take the z axis parallel to p_5 and choose the x axis so that $p_{4y} = 0$, $p_{4x} \geq 0$. The polar and azimuthal angles of p_1 are defined through (see equation (6.8))

$$\cos \theta = \frac{c_\theta p_1 \cdot p_5}{P_1 P_5}, \quad (10.1)$$

$$\begin{aligned} p_1 + p_2 &= 0, \\ (p_5; p_4, e_\phi p_1) &\rightarrow \phi. \end{aligned} \quad (10.2)$$

The sign factors $c_\theta, e_\phi = \pm 1$ are included so that we can later obtain common definitions of certain angles. The procedure of writing angles in terms of invariants is familiar by now, and θ and ϕ turn out to be given by

$$\cos \theta = -c_\theta \frac{\{(s_{12} + m_1^2 - m_2^2)(s_{12} - s_{34} + m_5^2) - 2(m_1^2 + m_5^2)s_{12}\} + 2s_{12}s_{51}}{\{\lambda(s_{34}, s_{12}, m_5^2)\lambda(s_{12}, m_1^2, m_2^2)\}^{\frac{1}{2}}}. \quad (10.3)$$

$$\cos \phi = \varepsilon_\phi G \left(\begin{array}{l} p_1 + p_2, \quad p_5, \quad p_1 \\ p_1 + p_2, \quad p_5, \quad p_4 + p_5 \end{array} \right) \times \{ \Delta_3(p_1 + p_2, p_5, p_1) \Delta_3(p_1 + p_2, p_5, p_4) \}^{-\frac{1}{2}} \quad (10.4)$$

$$= \varepsilon_\phi \frac{\begin{vmatrix} 2s_{12} & s_{34} - s_{12} - m_5^2 & s_{12} + m_1^2 - m_2^2 \\ s_{34} - s_{12} - m_5^2 & 2m_3^2 & s_{51} - m_5^2 - m_1^2 \\ m_3^2 - s_{12} - s_{45} & s_{45} - m_4^2 + m_5^2 & s_{23} - s_{45} - m_1^2 \end{vmatrix}}{2 \{ G(s_{34}, m_1^2, s_{15}, s_{12}, m_5^2, m_2^2) \} \times G(s_{34}, s_{45}, m_4^2, s_{12}, m_5^2, m_3^2)^{\frac{1}{2}}}$$

For each cyclic permutation of indices, equations (10.3) and (10.4) define angles which are useful for the study of the process $2 \rightarrow 3$. In Table 1 we list these angles, together with the sign factors $\varepsilon_\theta, \varepsilon_\phi$ which correspond to the commonly used definitions. The appropriate invariants in equations (10.3) and (10.4) are found by replacing 12345 by a permutation of ba123 as shown

Table V.1. Angles (or rapidities) related to the scattering process $a + b \rightarrow 1 + 2 + 3$. In polar angles the superscripts give the frame in which the angle is defined (R12 is the frame $p_1 + p_2 = 0$, (a1) is a spacelike or timelike frame $R(p_a - p_1)$ or $S(p_a - p_1)$, equation (II.1.13), depending on whether $t_1 > 0$ or $t_1 < 0$) and the subscripts give the vectors defining the angle. In azimuthal angles the subscript gives the polar axis. Each azimuthal angle is defined in two different frames. In order to write any of the angles in terms of invariants, apply equations (10.3-4) by carrying out the permutation shown in the first column and insert the phase factors ε_θ and ε_ϕ

Permutation of 12345 To Be

Applied To

Equation (10.3-4)	Name of the Polar Angle (or Rapidity)	ε_θ	Name of the Azimuthal Angle	ε_ϕ
a b 3 2 1	θ_{st}^* CMS scattering angle	-1	λ_1 , helicity azimuthal angle in R23	-1
1 a b 3 2	$\theta_{12}^{(a1)} = i\zeta_{12}^{(a1)}$	-1	$\omega_2 = \omega$ Toller angle	-1
2 1 a b 3	$\theta_{23}^{(12)}$ helicity polar angle in R12	+1	λ_3 , helicity azimuthal angle in R12	-1
3 2 1 a b	$\theta_{b3}^{(33)}$ Jackson angle in R23	-1	ϕ_b Treiman-Yang angle in R23	+1
b 3 2 1 a	$\theta_{ab}^{(b3)} = i\zeta_{ab}^{(b3)}$	-1	ϕ_4 Treiman-Yang angle in R12	+1
b a 1 2 3	θ_{b3}^* CMS scattering angle	-1	λ_3	-1
3 b a 1 2	$\theta_{23}^{(b3)} = i\zeta_{23}^{(b3)}$	-1	ω_2	-1
2 3 b a 1	$\theta_{12}^{(23)}$ helicity polar angle in R23	+1	λ_1	as above
1 2 3 b a	$\theta_{a1}^{(12)}$ Jackson angle in R12	-1	ϕ_a	
a 1 2 3 b	$\theta_{ab}^{(a1)} = i\zeta_{ab}^{(a1)}$	-1	ϕ_b	+1

in the table and making the corresponding substitution of s, t_1, s_1, s_2, t_2 in place of $s_{12}, s_{23}, s_{34}, s_{45}, s_{51}$. For instance, to write $\cos \lambda_1$ in invariant form (equation (8.8)) one simply permutes 12345 \rightarrow 23ba1 in equation (10.4).

Assume secondly that $s_{12} < 0$ so that instead of the frame $p_1 + p_2 = 0$, one must use the frame $p_1 + p_2 = (0, 0, 0, \sqrt{(-s_{12})})$. The orientation of the frame is fixed so that $p_{5x} = p_{5y} = p_{4y} = 0, p_{5z} > 0, p_{4x} > 0$. Then writing p_1 in pseudospherical coordinates P, ζ, ϕ (equation (II.7.22)) and using equation (A.29) one finds

$$\cosh \zeta = -\varepsilon_\zeta \frac{\{(s_{12} + m_1^2 - m_2^2)(s_{12} - s_{34} + m_5^2) - 2(m_1^2 + m_5^2)s_{12}\} + 2s_{12}s_{15}}{\{\lambda(s_{34}, s_{12}, m_5^2)\lambda(s_{12}, m_1^2, m_5^2)\}^{\frac{1}{2}}}, \quad (10.5)$$

where $\varepsilon_\zeta = +1$ if $E_1 E_5 > 0$ and $\varepsilon_\zeta = -1$ if $E_1 E_5 < 0$. Thus $\cosh \zeta$ depends on invariants in the same way as $\cos \theta$, and one can formally identify the rapidity ζ as an imaginary angle, $\zeta = -i\theta$. For $s_{12} > 0$, θ is real, for $s_{12} < 0$ ζ is real. The expression (10.4) for ϕ remains the same when s_{12} becomes negative.

Any of the permutations in Table 1 gives rise to an expression for the phase space integral R_3 (Byckling, 1972a). The angles θ, ϕ very often have fixed limits: $0 \leq \theta < \pi, 0 \leq \phi < 2\pi$. The rapidity variables ζ do not vary over the natural interval $0, \infty$, but have limits depending on other variables and s . The set $t_1, t_2, \zeta_{12}^{(a1)}, \zeta_{23}^{(b3)}, \omega$ are the **Toller variables** for a $2 \rightarrow 3$ process (Section VI.3).

In equation (10.4) $\cos \phi$ is linearly related to one of the invariants, namely s_{23} . Thus each of the basic invariants s, t_1, s_1, s_2, t_2 is linear in the cosine of one azimuthal angle, and the pairs are as follows:

- $s_1 \rightarrow$ Treiman-Yang angle ϕ_b ,
- $s_2 \rightarrow$ Treiman-Yang angle ϕ_a ,
- $t_1 \rightarrow$ helicity angle λ_3 ,
- $t_2 \rightarrow$ helicity angle λ_1 , and
- $s \rightarrow$ Toller angle $\omega \equiv \omega_2$.

The first and fourth of these relations are given explicitly in equations (8.5) and (8.9). The permutation $p_a \leftrightarrow p_b, p_1 \leftrightarrow p_3, p_2 \leftrightarrow p_4$ gives the relations for s_2 and t_1 . A new quantity is the **Toller angle** ω , which is kinematically defined as the angle the **cosine of which is linearly related to s** (Bali, 1967a; Chan, 1967a; Morrow, 1968, 1969, 1970b). Replacing p_1, p_2, p_3, p_4, p_5 by $p_3, -p_b, -p_a, p_1, p_2$ in equation (10.2) we obtain the definition of the Toller angle in the form

$$p_1 - p_b = 0, \quad (p_2; p_1, -p_3) \rightarrow \omega. \quad (10.7)$$

Because this frame does not generally exist, we first put $\mathbf{p}_2 = \mathbf{p}_a - \mathbf{p}_1$ in equation (10.7) and then go to the frame $\mathbf{p}_2 = 0$:

$$\mathbf{p}_2 = 0, \quad (\mathbf{p}_a - \mathbf{p}_1; \mathbf{p}_1, -\mathbf{p}_3) \rightarrow \omega. \quad (10.8)$$

In the frame $\mathbf{p}_2 = 0$ (Figure 10.2), in which $\mathbf{p}_1 - \mathbf{p}_a = \mathbf{p}_b - \mathbf{p}_3$, one sees that

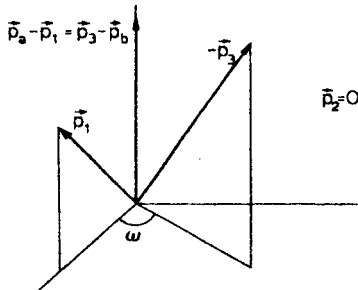


Figure V.10.2 Geometric definition of the Toller angle ω in the frame $\mathbf{p}_2 = 0$

the $\mathbf{p}_1 - \mathbf{p}_a, -\mathbf{p}_1$ plane is the $\mathbf{p}_a, \mathbf{p}_1$ plane and the $\mathbf{p}_1 - \mathbf{p}_a, \mathbf{p}_3$ plane is the $\mathbf{p}_b, \mathbf{p}_3$ plane. Thus ω is the angle between the planes $\mathbf{p}_a, \mathbf{p}_1$ and $\mathbf{p}_b, \mathbf{p}_3$:

$$\cos \omega = \frac{(\mathbf{p}_a \times \mathbf{p}_1) \cdot (\mathbf{p}_b \times \mathbf{p}_3)}{|\mathbf{p}_a \times \mathbf{p}_1| |\mathbf{p}_b \times \mathbf{p}_3|} \Big|_{\mathbf{p}_2=0}. \quad (10.9)$$

This is the standard definition of the Toller angle (see also Exercise V.6).

From equation (10.4) or from equation (10.8) and the general rule (II.7.15) it is easy to derive the following linear relation between s and $\cos \omega$:

$$\begin{aligned} s &= s(s_1, s_2, t_1, t_2, \omega) \\ &= m_a^2 + m_b^2 + \frac{1}{\lambda(t_1, t_2, m_2^2)} \begin{bmatrix} 2t_1 & m_2^2 - t_1 - t_2 & m_a^2 - m_1^2 + t_1 \\ m_2^2 - t_1 - t_2 & 2t_2 & s_1 - t_2 - m_a^2 \\ s_2 - t_1 - m_b^2 & m_b^2 - m_3^2 + t_2 & 0 \end{bmatrix} \\ &\quad - 2 \cos \omega \{ G(t_1, s_1, t_2, m_1^2, m_a^2, m_2^2) G(s_2, t_2, t_1, m_3^2, m_2^2, m_b^2) \}^{\frac{1}{2}}. \end{aligned} \quad (10.10)$$

The $2 \rightarrow 2$ subprocesses corresponding to the G functions in equation (10.10) are shown in Figure 10.3. Since s is normally fixed, ω is not an independent

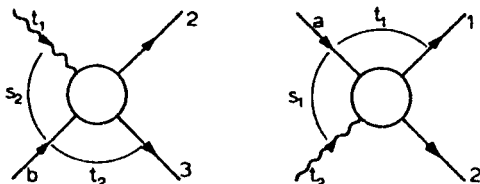


Figure V.10.3 The $2 \rightarrow 2$ subprocesses involved in the definition of ω

variable in the sense of ϕ_b or λ_1 . Fixing its value means setting up a relation between the other final state variables. To illustrate this, Figure 10.4 shows

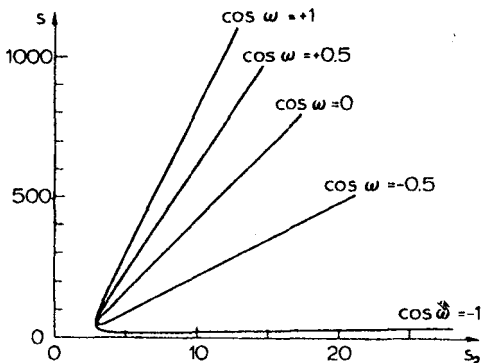


Figure V.10.4 Curves of constant value of the Toller angle ω in the ss_2 plane. The fixed invariants have the values $s_1 = 8$, $t_1 = -4$, $t_2 = -5$ and the reaction is $pp \rightarrow p\pi\Delta$

some curves $\cos \omega = \text{constant}$ in the ss_2 plane. We also note that the phase space distributions in ϕ_b and λ_1 were constant, but that the phase space distribution in ω is peaked near 180° , the peaking increasing with increasing s .

Because ω is linearly related to s , replacing the set p_1, p_2, p_3, p_4 by $p_2, p_2 - p_1, p_1, -p_3$ (see Figure II.7.1 and equation (10.8)), equation (II.7.20) immediately gives the relation

$$\frac{ds}{2(-\Delta_4)^{\frac{1}{2}}} = \frac{d\omega}{\lambda^{\frac{1}{2}}(t_1, t_2, m_2^2)}. \quad (10.11)$$

An integral of $R_3(s)$ over s can thus very simply be transformed to an integral over ω (Morrow, 1968). The full range $0 \leq \omega < 2\pi$ corresponds to an interval in s , and equation (10.11) is not of much practical use. However, we can apply it formally by inserting the identity

$$1 = \int ds \delta\{s - s(s_1, s_2, t_1, t_2, \omega)\}, \quad (10.12)$$

in equation (9.2), where s is given in equation (10.10) and by transforming ds in equation (10.12) to $d\omega$ by using equation (10.11). The result is

$$R_3(s) = \frac{\pi}{8} \lambda^{-\frac{1}{2}}(s, m_a^2, m_b^2) \int dt_1 dt_2 ds_1 ds_2 d\omega \lambda^{-\frac{1}{2}}(t_1, t_2, m_2^2) \times \delta\{s - s(s_1, s_2, t_1, t_2, \omega)\} \quad (10.13)$$

The integrand looks now very simple, but all the complexities of equation (9.2) are hidden in the δ function. This δ function defines the domain of integration in equation (10.13) as a four-dimensional surface $s = \text{constant}$ in the space of the five variables of integration. The main interest in equation (10.13) lies in its behaviour at large s (Section 11) and in its generalizations to arbitrary n (Section VI.3).

11. Applications

(a) Integration with matrix element $\exp(\frac{1}{2}at_1 + \frac{1}{2}bt_2)$

We know already that $T = 1$ allows one to reduce equation (9.2) to a single integration (equation (2.17)). We shall now show that the integration over t_1 and t_2 , which physically amounts to calculation of the distribution on the Dalitz plot, can be carried out in closed form if T depends on t_1, t_2 through a factor $\exp(at_1 + bt_2)$, where a and b do not depend on t_1, t_2 (Chan, 1967a, 1967b). This *doubly peripheral* form of the matrix element squared is in many cases suggested both by experimental evidence and theoretical ideas.

According to the results of the previous section, the region of integration is an ellipse in the t_1, t_2 plane. We therefore have to establish a general formula for the integral

$$I = \int \frac{dx dy}{\{-H(x, y)\}^{\frac{1}{2}}} e^{ax+by} \quad (11.1)$$

in which

$$H(x, y) = Ax^2 + By^2 + 2Cxy + 2A'x + 2B'y + D,$$

$A > 0$, $B > 0$, $\Delta = AB - C^2 \geq 0$ and U , defined in equation (9.17), is negative. The last condition implies that H is negative within the ellipse. The case $\Delta = 0$ in which the ellipse becomes a parabola also occurs in practice as the limit $\Delta \rightarrow 0$. Note that by taking derivatives with respect to a and b , equation (11.1) will lead to integration formulas having positive integer powers of x and y in the integrand.

Taking first $\Delta > 0$, the integrations in equation (11.1) are carried out by first integrating over y by using the formula

$$\int_{y^-}^{y^+} dy \frac{e^{by}}{\{(y^+ - y)(y - y^-)\}^{\frac{1}{2}}} = \pi \exp\left\{\frac{1}{2}b(y^+ + y^-)\right\} I_0\left\{\frac{1}{2}b(y^+ - y^-)\right\}, \quad (11.2)$$

where I_0 is the modified Bessel function of zeroth order (Abramowitz, 1965), and then over x by the formula

$$\begin{aligned} & \int_{x^-}^{x^+} dx e^{\mu x} I_0[v\{(x^+ - x)(x - x^-)\}^{\frac{1}{2}}] \\ &= \exp\left\{\frac{1}{2}\mu(x^+ + x^-)\right\} 2(\mu^2 + v^2)^{-\frac{1}{2}} \sinh\left\{\frac{1}{2}(x^+ - x^-)(\mu^2 + v^2)^{\frac{1}{2}}\right\}. \end{aligned} \quad (11.3)$$

Expressing the roots in terms of the coefficients of the quadratic form H one finds

$$I = \frac{2\pi e^{ax_0 + by_0}}{(Ba^2 + Ab^2 - 2Cab)^{\frac{1}{4}}} \sinh \{(-U/\Delta)^{\frac{1}{4}}(Ba^2 + Ab^2 - 2Cab)^{\frac{1}{4}}\}, \quad (11.4)$$

where

$$(x_0, y_0) = \left(\frac{1}{\Delta} \begin{vmatrix} C & A' \\ B & B' \end{vmatrix}, \frac{1}{\Delta} \begin{vmatrix} A' & A \\ B' & C \end{vmatrix} \right)$$

is the centre of the ellipse and Δ and U are defined in equations (9.12) and (9.17).

In the case $\Delta = 0$, one of limits in the second integration over x goes to infinity: either $x^+ \rightarrow +\infty$ or $x^- \rightarrow -\infty$, depending on the sign of μ . Equation (11.3) then has to be replaced by ($\mu > 0$)

$$\int_{x^-}^{\infty} dx e^{-\mu x} I_0\{v\sqrt{(x - x^-)}\} = \frac{1}{\mu} \exp \left(\frac{v^2}{4\mu} - \mu x^- \right). \quad (11.5)$$

Expressing again the roots in terms of the coefficients one finds

$$I = \frac{\pi}{\sqrt{C} \left| a - \frac{bC}{B} \right|} \exp \left\{ \frac{a^2(BD - B'^2) + b^2(AD - A'^2) - 2ab(CD - A'B')}{2 \left(a - \frac{bC}{B} \right) (CB' - BA')} \right\}, \quad (11.6)$$

where $AC = B^2$.

According to equations (9.2) and (III.2.2) we now have for $T = f(s_1, s_2)$ $\exp(at_1 + bt_2)$:

$$\frac{d^2\sigma}{ds_1 ds_2} = \frac{f(s_1, s_2)}{(4\pi)^4 4\lambda(s, m_a^2, m_b^2)} \int \frac{dt_1 dt_2}{(-\Delta_4)^{\frac{1}{4}}} e^{at_1 + bt_2}. \quad (11.7)$$

The integration is carried out immediately by using equations (9.10) and (11.4):

$$\begin{aligned} \frac{d^2\sigma}{ds_1 ds_2} &= \frac{f(s_1, s_2)}{(4\pi)^4 \lambda(s, m_a^2, m_b^2)} \cdot \frac{2\pi e^{at_1^{(0)} + bt_2^{(0)}}}{(Ba^2 + Ab^2 - 2Cab)^{\frac{1}{4}}} \\ &\times \sinh \left\{ \frac{1}{2s} \lambda^{\frac{1}{4}}(s, m_a^2, m_b^2) (Ba^2 + Ab^2 - 2Cab)^{\frac{1}{4}} \right\} \end{aligned} \quad (11.8)$$

where $t_1^{(0)}$ and $t_2^{(0)}$ are given in equation (9.14), and A , B and C in equation (9.11). No further integrations can be carried out in closed form. Note that formula (11.4) could also be used to integrate over t_1 and s_2 or t_2 and s_1 , but in these cases there is no motivation to include an exponential dependence on s_1 or s_2 .

(b) Unitarity relation with a two-particle intermediate state, box diagram

The condition between $2 \rightarrow 3$ reactions and the formulation of the unitarity relation (Källén, 1964) in the approximation of including only two particles in the intermediate state is dynamically very distant, but kinematically they are closely related, since both involve four independent four-vectors. In particular, this leads to a natural inclusion of Δ_4 in the formulation.

Omitting all dynamical explanations, the **two-particle unitarity relation** reads as follows:

$$\text{Im } A(s, t_{a1}) = \frac{1}{8\pi^2} \int \frac{d^3 p_3}{2E_3} \frac{d^3 p_4}{2E_4} \delta^4(p_a + p_b - p_1 - p_2) A_1(s, t_{a3}) A_2^*(s, t_{13}). \quad (11.9)$$

Here $A(s, t_{a1})$, $A_1(s, t_{a3})$ and $A_2(s, t_{13})$ are the amplitudes for the $2 \rightarrow 2$ reactions shown in Figure 11.1, which also defines the notation and variables. The imaginary part of $A(s, t_{a1})$ is thus calculated by integrating over all possible two-particle intermediate states in Figure 11.1. A similar integration

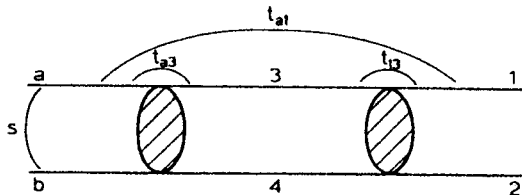


Figure V.11.1 Two-particle unitarity relation. The diagram here is a box diagram: two particles interact twice by some mechanism

always appears when one is calculating a **box diagram** of the type in Figure 11.1. Using previous results (equation IV.1.7) concerning two-particle phase space integration, equation (11.9) leads to

$$\text{Im } A(s, t_{a1}) = \frac{1}{8\pi^2} \frac{P_3^*}{4\sqrt{s}} \int d\Omega_3 A_1(s, t_{a3}) A_2^*(s, t_{13}), \quad (11.10)$$

where $P_3^* = \lambda^4(s, m_3^2, m_4^2)/2\sqrt{s}$ and Ω_3 describes the orientation of p_3 with respect to the fixed vectors p_a and p_1 as shown in Figure 11.2.

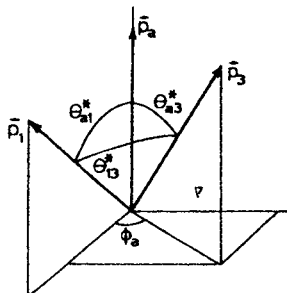


Figure V.11.2

We can now write

$$\begin{aligned} d\Omega_3 &= d \cos \theta_{a3} d\phi_a \\ &= \frac{d \cos \theta_{a3}^* d \cos \theta_{13}^*}{K^4(\cos \theta_{a1}^*, \cos \theta_{a3}^*, \cos \theta_{13}^*)} \end{aligned} \quad (11.11)$$

with $K(x, y, z) = 1 - x^2 - y^2 - z^2 + 2xyz$ (see equation (B.12)). Alternatively, using equation (II.7.21) with the identification $p_1 \rightarrow p_a + p_b, p_2 \rightarrow p_a, p_3 \rightarrow p_1, p_4 \rightarrow p_3$, we also find

$$\begin{aligned} d\Omega_3 &= \frac{2s d(p_b \cdot p_3) d(p_1 \cdot p_3)}{\{-\Delta_2(p_a + p_b, p_3)\}^{\frac{1}{2}} \{-\Delta_4(p_a + p_b, p_a, p_1, p_3)\}^{\frac{1}{2}}} \\ &= \frac{\sqrt{s}}{2P_3^*} \frac{dt_{a3} dt_{13}}{(-\Delta_4)^{\frac{1}{2}}}. \end{aligned} \quad (11.12)$$

Inserting equation (11.12) in equation (11.10) we discover the invariant form of the two-particle unitarity relation (Kibble, 1960):

$$\text{Im } A(s, t_{a1}) = \frac{1}{64\pi^2} \int \frac{dt_{a3} dt_{13}}{(-\Delta_4)^{\frac{1}{2}}} A_1(s, t_{a3}) A_2^*(s, t_{13}), \quad (11.13)$$

where Δ_4 is a function of four invariants and six masses given, for instance, by the symmetric determinant

$$\begin{aligned} \Delta_4 &= \Delta_4(s, t_{a1}, t_{a3}, t_{13}; m_a^2, m_b^2, m_1^2, m_2^2, m_3^2, m_4^2) \\ &= \Delta_4(p_a + p_b, p_a, p_1, p_3) \end{aligned} \quad (11.14)$$

$$\Delta_4 = \frac{1}{16} \begin{vmatrix} 2s & s + m_a^2 - m_b^2 & s + m_1^2 - m_2^2 & s + m_3^2 - m_4^2 \\ s + m_a^2 - m_b^2 & 2m_a^2 & m_a^2 + m_1^2 - t_{a1} & m_a^2 + m_3^2 - t_{a3} \\ s + m_1^2 - m_2^2 & m_a^2 + m_1^2 - t_{a1} & 2m_1^2 & m_1^2 + m_3^2 - t_{13} \\ s + m_3^2 - m_4^2 & m_a^2 + m_3^2 - t_{a3} & m_1^2 + m_3^2 - t_{13} & 2m_3^2 \end{vmatrix}.$$

The matrix elements in equation (11.14) are determined by the relation $p_a + p_b = p_1 + p_2 = p_3 + p_4$. This is different from $2 \rightarrow 3$ reactions satisfying $p_a + p_b = p_1 + p_2 + p_3$ so that the Δ_4 's, although their vector arguments are identical, look different in terms of invariant variables. However, by a simple comparison one sees that equation (11.14) is obtained if the following transformation is carried out in $\Delta_4(p_a + p_b, p_a, p_1, p_3)$ evaluated for $p_a + p_b \rightarrow p_1 + p_2 + p_3$:

$$s_2 \rightarrow m_2^2, \quad s_1 \rightarrow m_3^2, \quad m_3^2 \rightarrow m_4^2, \quad m_2^2 \rightarrow t_{13}, \quad t_2 \rightarrow t_{a3}, \quad (11.15)$$

the other variables remaining unchanged. The transformation equation (11.15) is, of course, not unique. One also sees clearly how equation (11.15)

leads outside the physical region of $2 \rightarrow 3$ scattering. If one considers elastic unitarity defined by $m_a = m_1 = m_3 = \mu$ and $m_b = m_2 = m_4 = m$, equation (10.14) simplifies considerably. In fact, one finds that in this case

$$16\Delta_4 = \lambda(s, \mu^2, m^2)\lambda(t_{a1}, t_{a3}, t_{13}) - 4st_{a1}t_{a3}t_{13}. \quad (11.16)$$

Note how the coefficient of s^2 in equation (11.16) follows by the transformation (11.15) from the known coefficient $\lambda(t_1, t_2, m_2^2)$ of s^2 in Δ_4 for $2 \rightarrow 3$ scattering (Figure 9.3).

If the $2 \rightarrow 2$ amplitudes A_1 and A_2 in equation (11.13) are assumed to depend on t_{a3} and t_{13} exponentially, the integrals in equation (11.13) can be done in closed form by using the formula (11.4). Let us for illustration consider the case of elastic unitarity in the limit of large s , so that we can neglect the masses and the last term in equation (11.16). Writing $A_1 = f_1 \exp(at_{a3})$, $A_2 = f_2 \exp(bt_{13})$, the unitarity relation reads

$$\text{Im } A(s, t_{a1}) = \frac{f_1 f_2}{16\pi^2 s} \cdot K$$

with

$$K \equiv \int \frac{dt_{a3} dt_{13}}{\{-\lambda(t_{a1}, t_{a3}, t_{13})\}^{\frac{1}{2}}} e^{at_{a3} + bt_{13}}. \quad (11.17)$$

This integral occurs very frequently in many theories involving the box diagram of Figure 11.1, since it is in the spirit of these theories to work within the approximation of including only leading powers of s . The range of integration in equation (11.17) is the inside of the parabola $\lambda(t_{a1}, t_{a3}, t_{13}) = 0$, which implies $\Delta = 0$ in equation (11.4), and one has to apply equation (11.6). A brief calculation leads to

$$K = \frac{\pi}{a+b} \exp\left(\frac{ab}{a+b} t_{a1}\right). \quad (11.18)$$

(c) Behaviour of $R_3(s)$ in the double Regge limit

From a theoretical point of view there is some interest in the **double Regge limit** (Bali, 1967a, 1967b; Chan, 1967a, 1967b; Lipes, 1970), defined by

$$s \rightarrow \infty$$

$$s_1, s_2 \gg |t_1|, |t_2|, m_i^2 \quad (11.19)$$

$$s_1 s_2 / s \text{ finite.}$$

In addition to assuming that the kinematic configuration is doubly peripheral (t_1 and t_2 small) one thus assumes that the two-particle subenergies s_1 and s_2 are large. The last condition in equation (11.19) is necessary, since otherwise the conditions s_1, s_2 large, t_1, t_2 small are not compatible (equation (11.23)).

The properties of the kinematic configuration (11.19) are simply obtained from the condition $\Delta_4 < 0$. After some algebraic manipulations one sees that Δ_4 , as given by equation (9.4), reduces in the limit (11.19) to the very simple form

$$16\Delta_4 \simeq s^2 \lambda(m_2^2 - s_1 s_2/s, t_1, t_2). \quad (11.20)$$

In this limit, the curve $\Delta_4 = 0$ in the $t_1 t_2$ plane (Figure 11.3) is thus a parabola

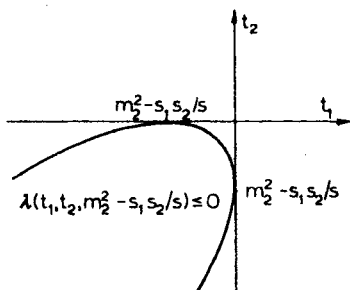


Figure V.11.3. The physical region on $t_1 t_2$ plane in the double Regge limit is the inside of the parabola

with axis $t_1 = t_2$ and tangent to the coordinate axes in the points t_1 (or t_2) = 0, t_2 (or t_1) = $m_2^2 - s_1 s_2/s < 0$. The physical region is the inside of this parabola ; this is the limit of the ellipsoid in Figure 9.4 when one only considers a neighbourhood of the origin. One can further simplify the boundary by writing

$$\begin{aligned} \lambda(m_2^2 - s_1 s_2/s, t_1, t_2) \\ = [m_2^2 - s_1 s_2/s + \{\sqrt{(-t_1)} - \sqrt{(-t_2)}\}^2] \\ \times [m_2^2 - s_1 s_2/s + \{\sqrt{(-t_1)} + \sqrt{(-t_2)}\}^2] \leq 0. \end{aligned} \quad (11.21)$$

The two factors in equation (11.21) only differ by the sign of $\sqrt{(t_1 t_2)}$ and represent the same curve in the $t_1 t_2$ plane. The product has to be negative and this can clearly only happen if the first factor is negative and the second positive. Thus the kinematic configuration in the limit (11.19) satisfies

$$\{\sqrt{(-t_1)} - \sqrt{(-t_2)}\}^2 \leq s_1 s_2/s - m_2^2 \quad (11.22)$$

$$\{\sqrt{(-t_1)} + \sqrt{(-t_2)}\}^2 \geq s_1 s_2/s - m_2^2. \quad (11.23)$$

The first condition specifies that t_1 and t_2 must not be too different, while the second one gives a lower limit for the magnitudes of t_1 and t_2 . This has important practical consequences (Chapter VIII).

Let us again assume $T = f(s_1, s_2) \exp(at_1 + bt_2)$. With the simplified form of equation (11.20) we can now, in the limit (11.19), in place of equation (11.7) write

$$\frac{d^2\sigma}{ds_1 ds_2} = \frac{f(s_1, s_2)}{(4\pi)^4 s^3} \int \frac{dt_1 dt_2 \exp(at_1 + bt_2)}{\{-\lambda(m_2^2 - s_1 s_2/s, t_1, t_2)\}^4}. \quad (11.24)$$

The integral over t_1 and t_2 is exactly the same as that in equation (11.17), and we obtain immediately (Kajantie, 1968a)

$$\frac{d^2\sigma}{ds_1 ds_2} = \frac{f(s_1, s_2)}{(4\pi)^4 s^3} \cdot \frac{\pi}{(a+b)} \exp \left\{ \frac{ab}{a+b} \left(m_2^2 - \frac{s_1 s_2}{s} \right) \right\}. \quad (11.25)$$

This result, of course, also follows from the exact result (11.8) in the limit (11.19). We shall return to equation (11.25) in Chapter VIII.

It is also interesting to consider the Toller angle ω in the limit (11.19) (Chan, 1967a). Applying this limit to equation (10.10) one obtains after some calculations that

$$s = \frac{s_1 s_2}{\lambda(t_1, t_2, m_2^2)} (m_2^2 - t_1 - t_2 + 2\sqrt{(t_1 t_2) \cos \omega}), \quad (11.26)$$

or, solving for $\cos \omega$,

$$\cos \omega = \frac{(s/s_1 s_2) \lambda(t_1, t_2, m_2^2) - (m_2^2 - t_1 - t_2)}{2\sqrt{(t_1 t_2)}}. \quad (11.27)$$

The corresponding sine is, of course, proportional to $\sqrt{(-\Delta_4)}$:

$$\sin^2 \omega = \frac{-\lambda(t_1, t_2, m_2^2) \lambda(m_2^2 - s_1 s_2/s, t_1 t_2)}{4(s_1 s_2/s)^2 t_1 t_2}. \quad (11.28)$$

Starting from equation (11.27) it is easy to verify that

$$\begin{aligned} & 2(s_1 s_2/s) \sqrt{(t_1 t_2)} (1 \pm \cos \omega) \\ &= \pm [m_2^2 + \{\sqrt{(-t_1)} \mp \sqrt{(-t_2)}\}^2] \\ & \quad \times [m_2^2 - s_1 s_2/s + \{\sqrt{(-t_1)} \pm \sqrt{(-t_2)}\}^2]. \end{aligned} \quad (11.29)$$

Multiplication of the two relations in equation (11.29) leads to equation (11.28). We can now interpret equation (11.22) as demanding that $\cos \omega < 1$ and equation (11.23) as demanding that $\cos \omega > -1$. The boundary near the origin is thus defined by $\cos \omega = -1$ (Figure 11.3). As we have assumed that $-t_1$ and $-t_2$ remain small, one can infer that ω lies mostly near 180° . This result is to be compared with our earlier statement according to which even the phase space distribution of ω is peaked near 180° . In fact, adding peripherality to phase space decreases the peaking near 180° , but leaves it qualitatively unchanged. It is very complicated to give an analytic proof of

this statement, since the calculation of the distribution in ω always involves four nontrivial integrations. However, it can be very simply justified by standard Monte Carlo programs (Chapter IX).

Exercises

- V.1. Compute the ratio $\sin \theta_{12}^*/\sin \theta_{12}^{R23}$ from equations (1.5) and (1.10). How is the result interpreted?
- V.2. Evaluate the integrals

$$I_1 = \int \frac{dx}{\lambda^{\frac{1}{2}}(x, a, b)},$$

$$I_2 = \int dx \frac{\lambda^{\frac{1}{2}}(x, a, b)}{x},$$

$$I_3 = \int dx \lambda^{\frac{1}{2}}(x, a, b),$$

$$K = \int_{x^-}^{x^+} \frac{dx}{(ax^2 + bx + c)^{\frac{1}{2}}}.$$

In K , x^\pm are the roots of $ax^2 + bx + c = 0$ and $a < 0$.

- V.3. Show that if instead of s_2 one uses in equation (5.17) the variable

$$r(s_2) = \int_{(m_2 + m_3)^2}^{s_2} dx \lambda^{\frac{1}{2}}(x, m_2^2, m_3^2)/x,$$

the phase space density in r, t_1 is constant. Find this constant.

- V.4. Compute the volume $R_3(s)$ of the three-particle phase space when one of the final-state masses vanish, $m_3 = 0$. What does one obtain by further specializing to (a) $m_1 = m_2 = m, m_3 = 0$; (b) $m_1 = m_2 = m_3 = 0$?
- V.5. Compute $d^2\sigma_3/dt_1 ds_2$ for $\pi N \rightarrow \pi\pi N$ from the one-pion exchange model of equation (5.22) by assuming that the continuation to the pion pole leaves A unchanged and by obtaining A from the measured πN cross-sections.

- V.6. Show that the definition

$$\cos \phi_b = \frac{(\mathbf{p}_a \times \mathbf{p}_1) \cdot (\mathbf{p}_b \times \mathbf{p}_3)}{|\mathbf{p}_a \times \mathbf{p}_1| |\mathbf{p}_b \times \mathbf{p}_3|} \Big|_{\mathbf{p}_2 = -\mathbf{p}_1}$$

of the Treiman-Yang angle is equivalent to equation (6.3). Show also that this same formula when evaluated in the frame R12, $\mathbf{p}_2 = -\mathbf{p}_1$, gives the Treiman-Yang angle ϕ_a in the frame R12.

- V.7. What is the distribution in the Jackson angle θ_{b3}^{R23} of $p_a + p_b \rightarrow p_1 + p_2 + p_3$ if the matrix element squared is $T = e^{bt}$? Integrate the result in the case $m_t = 0$.
- V.8. Derive the alternative definitions (6.9) and (6.11) of the Treiman-Yang angle and (6.12) and (6.13) of the helicity angle by using the invariant forms of equations (8.2) and (8.6).
- V.9. Find the effective mass distribution dR_3/dM_{12} of particles 1 and 2 in a three-particle final state, if particles 2 and 3 form a resonance of mass M and zero width.
- V.10. The channel $pp \rightarrow p\pi^0 p$ can be separated from other channels by measuring the momenta p_1, p_3 of the protons and requiring

$$m_2^2 = (p_a + p_b - p_1 - p_3)^2 = m_{\pi^0}^2$$

Determine the surface of allowed values of p_3 for a given fixed p_1 .

VI

Multiparticle Production

1. Introduction

As we saw in Chapter III (Table III.1), the process

$$p_a + p_b \rightarrow p_1 + \dots + p_n \quad (1.1)$$

depends on $3n - 4$ essential independent variables. In Chapter V we introduced many different sets of variables to describe $2 \rightarrow 3$ reactions and it is obvious that further sets can be constructed at will. It is then easy to understand that for $2 \rightarrow n$ processes an even larger variety of different descriptions have been used. In fact, the choice of appropriate variables for the description of a multiparticle amplitude has been a long-standing problem in particle physics.

At present experimental observations on a process such as reaction (1.1) are usually interpreted in terms of a matrix element. It is possible that there exists a set of variables in terms of which the matrix elements of all the various reactions are particularly simple. However, so far no clear choice has emerged, and it rather seems that there is no privileged set of variables. Instead, different sets are motivated by different considerations and one set may be useful for one purpose and useless for another.

The main goal in this chapter will be to introduce different sets Φ of $3n - 4$ variables to describe a point in phase space. Once a set Φ has been chosen, there are three main questions to settle. One has to determine

1. the physical region in the variables Φ , that is the range of integration in

$$\begin{aligned} R_n(p^2; p_1^2, \dots, p_n^2) &= \int \prod_1^n \frac{d^3 p_i}{2E_i} \delta^4 \left(p - \sum_i p_i \right) \\ &= \int d\Phi \rho_n(\Phi). \end{aligned} \quad (1.2)$$

2. the phase space factor $\rho_n(\Phi)$. This factor gives the density of points in phase space, expressed in variables Φ .
3. the relation of this set Φ to other sets, especially to the momentum configuration p_1, \dots, p_n .

2. Timelike recursion relations

It is possible to visualize a multiparticle reaction as taking place via resonance formation and decay (Figure 2.1). In the intermediate state there

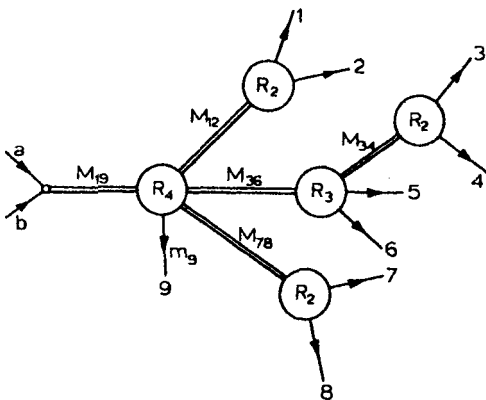


Figure VI.2.1 Example of cascade decay. Double lines denote systems of particles. Total energy is fixed. In this figure $M_{19}^2 = (p_1 + p_2 + \dots + p_9)^2$, etc.

are unstable particles which then successively decay to others and eventually form the final state particles. Alternatively, one often uses a multiperipheral mechanism, implying the dominance of a diagram of the type exhibited in Figure 2.2. Now, regardless of the actual validity of such dynamical ideas, we shall prove that kinematically an n -particle final state can always be subdivided into simpler processes. More concretely (considering $2 \rightarrow n$ reactions),

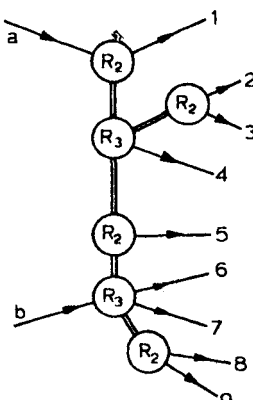


Figure VI.2.2 A diagram in which total energy is not fixed by one intermediate mass

suppose one draws an arbitrary *tree diagram* with $n + 2$ external legs, that is a diagram without closed loops of the type in Figures 2.1–2. We shall then see that corresponding to every such tree diagram there exists a set of $3n - 4$ phase space variables Φ , which define a form of R_n and of the phase space density $\rho_n(\Phi)$. This form of R_n expresses it recursively in terms of R_l , $l < n$. It is important to separate two cases. In the first one (Srivastava, 1958; Byckling, 1969a, 1969d), represented by Figure 2.1, one internal line in the graph has the total incoming energy \sqrt{s} , and this then decays to lower mass systems and finally to outgoing particles. All the intermediate systems occurring have, as a consequence, timelike total four-momenta, and one can go to their rest frames and parametrize vectors by spherical angles. In the second case (Toller, 1965; Bali, 1967a), represented by Figure 2.2, particles a and b do not join to the graph at the same vertex but at some separate vertices, and there is at least one line which is connected to one initial and one final state four-momentum. Starting at one incoming momentum, the total energy s can only be fixed when one has reached the other initial state momentum in the graph. This imposes a constraint on the variables between p_a and p_b and makes the second case more complicated. Also the intermediate state momenta may now be spacelike, for which the standard frames (equation (II.1.13)) are of the type $(0, 0, 0, \sqrt{(-t)})$ and some of the appropriate variables are boosts instead of polar angles. In the second case the variables may include the so-called *Toller variables*. With regard to the first difficulty, the two cases become equivalent if one relaxes the condition $s = \text{constant}$. They are also related by crossing; going to the channel with the initial state $a + \bar{1}$ in Figure 2.2 obviously gives a tree diagram in which the decay chain beginning with $a + \bar{1}$ allows one to fix the total energy very simply.

It is also important to realize that a tree diagram only fixes the squares of the intermediate four-momenta as variables. All the $3l - 4$ variables in each intermediate R_l are still left unspecified. This leaves one with a considerable freedom of choice, which, when properly exploited, will lead to useful results.

In this section we shall only consider the first case leaving the second one to Section 3.

The simplest possible recursion relation is based on the physical picture of sequential decay, exhibited in Figure 2.3 (Srivastava, 1958). Grouping

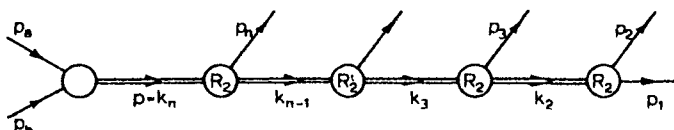


Figure VI.2.3 The reaction $p_a + p_b \rightarrow p_1 + \dots + p_n$ expressed as a sequence of two-particle decays

together the factors in equation (III.3.1) which refer to the system $1, \dots, n-1$ results in

$$R_n(p) = \iint \frac{d^3 p_n}{2E_n} \prod_{i=1}^{n-1} \frac{d^3 p_i}{2E_i} \delta^4 \left\{ (p - p_n) - \sum_{i=1}^{n-1} p_i \right\} \quad (2.3)$$

$$= \int \frac{d^3 p_n}{2E_n} R_{n-1}(p - p_n). \quad (2.4)$$

Here R_n is, by Lorentz invariance, a function of $p^2 \equiv M_n^2 = s$. The dependence on masses is written down explicitly only when needed. Similarly, R_{n-1} is only a function of

$$\begin{aligned} M_{n-1}^2 &= (p - p_n)^2 \\ &= (p_1 + p_2 + \dots + p_{n-1})^2 \\ &\equiv k_{n-1}^2, \end{aligned} \quad (2.5)$$

where we have introduced the four-vector

$$k_i = p_1 + \dots + p_i. \quad (2.6)$$

One clearly has $k_n = p$. As the notation implies, M_{n-1} is the invariant mass of the system formed by particles $1, \dots, n-1$.

Since R_{n-1} is a function of only one variable, it is natural to take this as a variable of integration in equation (2.4). Let us insert in the integrand in equation (2.4)

$$1 = \int dM_{n-1}^2 \delta(M_{n-1}^2 - k_{n-1}^2) \quad (2.7)$$

$$1 = \int d^4 k_{n-1} \delta^4(p - p_n - k_{n-1}). \quad (2.8)$$

Then

$$\begin{aligned} R_n(M_n^2) &= \int dM_{n-1}^2 \int d^4 k_{n-1} \int d^4 p_n \delta(k_{n-1}^2 - M_{n-1}^2) \delta(p_n^2 - m_n^2) \\ &\times \delta^4(p - p_n - k_{n-1}) R_{n-1}(M_{n-1}^2). \end{aligned} \quad (2.9)$$

Recalling the definition of R_2 this is simply

$$R_n(M_n^2) = \int_{\mu_{n-1}}^{(M_n - m_n)^2} dM_{n-1}^2 R_2(k_n; k_{n-1}^2, p_n^2) R_{n-1}(M_{n-1}^2) \quad (2.10)$$

$$= \int_{\mu_{n-1}}^{(M_n - m_n)^2} dM_{n-1}^2 \int d\Omega_{n-1} \frac{\lambda^4(M_n^2, M_{n-1}^2, m_n^2)}{8M_n^2} R_{n-1}(M_{n-1}^2), \quad (2.11)$$

where the explicit form (IV.1.8) of R_2 was used and μ_i is defined in equation (2.13). Equations (2.10) and (2.11) express R_n as a product of R_2 describing the

decay $p \rightarrow p_n + k_{n-1}$, and R_{n-1} describing the decay $k_{n-1} \rightarrow p_1 + \dots + p_{n-1}$, integrated over all possible values of the invariant mass M_{n-1} . This is the first step from the left in the chain in Figure 2.3. For $n = 3$ equation (2.10) leads directly to the formula (V.2.17) for $R_3(M_n^2)$ derived previously.

As stated in equation (2.10), the limits on M_{n-1}^2 are

$$\mu_{n-1} \leq M_{n-1} \leq M_n - m_n \quad (2.12)$$

with the notation

$$\mu_i = m_1 + \dots + m_i. \quad (2.13)$$

The lower limit follows since R_{n-1} vanishes below threshold $M_{n-1} = \mu_{n-1}$. Similarly R_2 in equation (2.10) is nonvanishing only if M_n is above threshold, $M_n \geq M_{n-1} + m_n$, which gives the upper limit of M_{n-1} .

To proceed further we iterate equation (2.10) or equation (2.11) to obtain a relation corresponding to the entire chain in Figure 2.3. Let us take M_i instead of M_i^2 as a variable. We obtain

$$R_n(M_n^2) = \frac{1}{2M_n} \int_{\mu_{n-1}}^{M_n - m_n} dM_{n-1} d\Omega_{n-1} \frac{1}{2} P_n \dots \int_{\mu_2}^{M_3 - m_3} dM_2 d\Omega_2 \frac{1}{2} P_3 \int d\Omega_1 \frac{1}{2} P_2 \quad (2.14)$$

where P_i is

$$P_i = \frac{\lambda^{\frac{1}{4}}(M_i^2, M_{i-1}^2, m_i^2)}{2M_i}. \quad (2.15)$$

The $3n - 4$ variables Φ in equation (1.2) now consist of two types:

$n - 2$ invariant masses M_i , $M_i^2 = k_i^2$, defined as the masses of the intermediate particles in Figure 2.3.

$2(n - 1)$ angles θ_i, ϕ_i in $\Omega_i = (\cos \theta_i, \phi_i)$, $i = 1, \dots, n - 1$. These define the direction of $\vec{k}_i = -\vec{p}_{i+1}$ in the rest frame $\vec{k}_{i+1} = 0$ of the decay $k_{i+1} \rightarrow p_{i+1} + k_i$ (Figure 2.4).

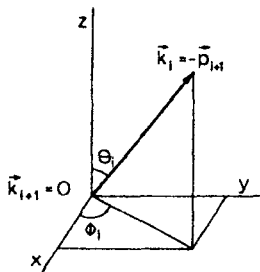


Figure VI.2.4 Definition of $\Omega_i = (\cos \theta_i, \phi_i)$. The orientation of coordinate axes can be chosen arbitrarily. To obtain the recursion relation (2.27) with multiperipheral momentum transfers, one chooses \vec{p}_n as the z-axis and replaces $\cos \theta_i$ by the corresponding momentum transfer

The density function $\rho_n(\Phi)$ in equation (1.2) corresponding to equation (2.14) is given by

$$\rho_n(\Phi) = \frac{1}{2^n M_n} \prod_{i=2}^n P_i. \quad (2.16)$$

The set of variables in equation (2.14) actually gives the simplest description of n -particle phase space. For this reason it is used in many applications, for instance, as a basis of Monte Carlo techniques (Chapter IX). Equation (2.14) is also a good starting point for numerical evaluation of R_n for small values of n (Almgren, 1968; Block, 1956; Kopylov, 1960; Milburn, 1955).

As an application of equation (2.14) consider the case where all m_i are zero, which also gives the asymptotic limit of $R_n(M_n^2)$ when $M_n \rightarrow \infty$ (extremely relativistic case). We claim that

$$\begin{aligned} R_n^{ER}(M_n^2) &= R_n(M_n^2; m_i^2 = 0) \\ &= \frac{(\pi/2)^{n-1}}{(n-1)!(n-2)!} M_n^{2n-4}. \end{aligned} \quad (2.17)$$

This is true for $n = 2$, since $R_2^{ER} = \pi/2$ given by equation (2.17) is correct. Further, an elementary calculation shows that equation (2.17) satisfies the recursion relation

$$R_n(M_n^2) = \frac{\pi}{2M_n} \int_0^{M_n} dM_{n-1}^2 (M_n^2 - M_{n-1}^2) R_{n-1}(M_{n-1}^2), \quad (2.18)$$

following from equation (2.10) when $m_i = 0$. According to equation (2.17) the total volume of phase space grows very rapidly, proportionally to M_n^{2n-4} , for large M_n . In the nonrelativistic case $M_n \rightarrow \mu_n = \sum m_i$ one can similarly derive (Exercise VI.2)

$$R_n^{NR}(M_n^2) = \frac{(2\pi^3)^{(n-1)/2}}{2\Gamma\left\{\frac{3}{2}(n-1)\right\}} \frac{(\Pi m_i)^{\frac{1}{2}}}{(\Sigma m_i)^{\frac{3}{2}}} (M_n - \Sigma m_i)^{(3n-5)/2}. \quad (2.19)$$

A slightly more complicated relation giving R_n is obtained if instead of separating one particle at a time, one starts by dividing the final state particles into two groups, one containing particles $1, \dots, l$, the other particles $l+1, \dots, n$ (Figure 2.5). This is realized formally by inserting

$$1 = \int dM_l^2 \delta(M_l^2 - k_l^2) \quad (2.20)$$

$$1 = \int d^4 k_l \delta^4(p_1 + \dots + p_l - k_l)$$

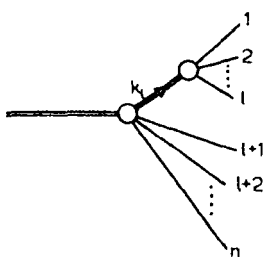


Figure VI.2.5 Physical picture of the splitting relation (2.21)

in the definition of R_n . Then one obtains the *splitting relation*

$$\begin{aligned}
 R_n(M_n^2) &= \int dM_l^2 \int d^4k_l d^4p_{l+1} \dots d^4p_n \delta(k_l^2 - M_l^2) \delta(p_{l+1}^2 - m_{l+1}^2) \\
 &\quad \dots \delta(p_n^2 - m_n^2) \delta^4\left(p - k_l - \sum_{i=l+1}^n p_i\right) \\
 &\quad \times \int d^4p_1 \dots d^4p_l \delta(p_1^2 - m_1^2) \dots \delta(p_l^2 - m_l^2) \delta^4(k_l - \sum p_i) \\
 &= \int_{\mu_l^2}^{(M_n - \mu_n + \mu_l)^2} dM_l^2 R_{n-l+1}(M_n^2; M_l^2, m_{l+1}^2, \dots, m_n^2) R_l(M_l^2; m_1^2, \dots, m_l^2),
 \end{aligned} \tag{2.21}$$

where $l = 2, 3, \dots, n-1$. For $l = n-1$ one obtains the previously derived relations (2.10). The upper and lower limits of M_l^2 in equation (2.21) again follow by considering the thresholds for $p \rightarrow k_l + p_{l+1} + \dots + p_n$ and of $k_l \rightarrow p_1 + \dots + p_l$, respectively.

The splitting relation (2.21) can now be iterated by applying it to arbitrary further splittings of both R_{n-l+1} and R_l . Proceeding in this way one obtains a tree graph, for instance that in Figure 2.1, depicting the final state as arising from successive cascade decays. The number of possible topologically different tree diagrams obviously increases rapidly with n . We do not attempt to analyse them more comprehensively, since, given any tree diagram, it is easy to find the associated forms of R_n , Φ , and $\rho_n(\Phi)$. Consider, for example, the diagram in Figure 2.1. For $n = 9$ there are $3 \times 9 - 4 = 23$ variables in Φ . There are 8 in R_4 , 5 in R_3 , 3 × 2 in the three R_2 s, and the four intermediate masses. We can immediately write in the notation of Figure 2.1:

$$\begin{aligned}
 R_9(M_{19}^2) &= \int dM_{12}^2 dM_{36}^2 dM_{78}^2 R_4(M_{19}^2; M_{12}^2, M_{36}^2, M_{78}^2, m_9^2) \\
 &\quad \times R_2(M_{12}^2; m_1^2, m_2^2) R_2(M_{78}^2; m_7^2, m_8^2) \\
 &\quad \times \int dM_{34}^2 R_3(M_{36}^2; M_{34}^2, m_5^2, m_6^2) R_2(M_{34}^2; m_3^2, m_4^2).
 \end{aligned} \tag{2.22}$$

As emphasized earlier this form still leaves the variables in R_2 , R_3 and R_4 unspecified.

As an example of how the freedom of choosing the variables in the intermediate R_i s of a tree diagram can be exploited, we shall consider the following case (Byckling, 1969a). In equation (2.11) the axes with respect to which Ω_{n-1} is measured are arbitrary (see also Figure 2.4). A very useful result is obtained, if the direction of p_a is chosen as the z axis. Then the angle θ_{n-1} is the scattering angle of the process $p_a + p_b \rightarrow k_{n-1} + p_n$ (Figure 2.6) and

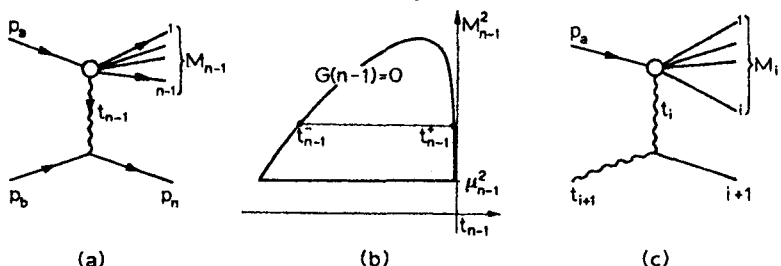


Figure VI.2.6 (a) The basic process when p_a is chosen as z axis in the frame $k_n \equiv p_a + p_b = 0$; (b) the range of variation of t_{n-1} is given by the M_{n-1}^2 , t_{n-1} Chew-Low plot; (c) the basic process at stage i of the iteration

one can replace it by the corresponding momentum transfer

$$\begin{aligned} t_{n-1} &= (p_a - p_1 - \dots - p_{n-1})^2 \\ &= (p_a - k_{n-1})^2 \\ &= m_a^2 + M_{n-1}^2 - 2E_a k_{n-1}^0 + 2P_a K_{n-1} \cos \theta_{n-1}, \end{aligned} \quad (2.23)$$

where

$$\begin{aligned} P_a &\equiv P_a^{(n)} = \frac{\lambda^{\frac{1}{2}}(M_n^2, m_a^2, m_b^2)}{2M_n}, \\ K_{n-1} &= \frac{\lambda^{\frac{1}{2}}(M_n^2, M_{n-1}^2, m_n^2)}{2M_n}. \end{aligned} \quad (2.24)$$

When $\cos \theta_{n-1}$ is replaced by t_{n-1} , the range $-1 \leq \cos \theta_{n-1} \leq 1$ is transformed to a M_{n-1} -dependent range $t_{n-1}^- \leq t_{n-1} \leq t_{n-1}^+$ (Figure 2.6(b)), where according to earlier results (Figure IV.5.3) t_{n-1}^\pm follow from

$$\begin{aligned} G(n-1) &\equiv G(s, t_{n-1}, m_n^2, m_a^2, m_b^2, M_{n-1}^2) \\ &= 0. \end{aligned} \quad (2.25)$$

In terms of t_{n-1} the recursion relation (2.11) reads

$$R_n(M_n^2) = \int_{\mu_{n-1}^2}^{(M_n - m_n)^2} dM_{n-1}^2 \int_{t_{n-1}}^{t_{n-1}^\pm} dt_{n-1} \int_0^{2\pi} d\phi_{n-1} \frac{R_{n-1}(M_{n-1}^2; t_{n-1})}{4\lambda^4(M_n^2, m_a^2, m_b^2)}, \quad (2.26)$$

where R_{n-1} also has to be regarded as a function of t_{n-1} , since t_{n-1} is the mass squared of one of the initial particles leading to R_{n-1} (Figure 2.6(a)).

In order to iterate equation (2.26) we must apply the same equation to R_{n-1} . Now one only has to remember that $m_b^2 \equiv t_n$ is to be replaced by t_{n-1} . If we also take M_n instead of M_n^2 as a variable we finally obtain (Byckling, 1969a)

$$R_n(M_n^2) = \frac{1}{2M_n} \cdot \frac{1}{4P_a^{(n)}} \int_{\mu_n}^{M_n - m_n} dM_{n-1} \int_{t_{n-1}}^{t_{n-1}^\pm} dt_{n-1} \int_0^{2\pi} d\phi_{n-1} \dots \\ \dots \frac{1}{4P_a^{(3)}} \int_{\mu_2}^{M_3 - m_3} dM_3 \int_{t_2}^{t_2^\pm} dt_2 \int_0^{2\pi} d\phi_2 \frac{1}{4P_a^{(2)}} \int_{t_1}^{t_1^\pm} dt_1 \int_0^{2\pi} d\phi_1, \quad (2.27)$$

where

$$P_a^{(i)} = \frac{\lambda^4(M_i^2, t_i, m_a^2)}{2M_i} \quad (2.28)$$

and

$$t_i = q_i^2, \quad (2.29)$$

$$q_i = p_a - p_1 - \dots - p_i \\ = p_a - k_i. \quad (2.30)$$

The limits t_i^\pm are the physical region boundaries of the $2 \rightarrow 2$ reaction shown in Figure 2.6(c). Equation (2.27) is obtained directly from equation (2.14) by choosing in each of the frames $k_{i+1} = 0$ the direction of p_a as the z axis and by replacing the corresponding polar angle $\cos \theta_i$ by t_i . The tree diagram corresponding to equation (2.27) is thus still that of Figure 2.3.

In equation (2.27) we have a form of R_n in which the ***multiperipheral momentum transfers*** t_i (Figure 2.7) appear as variables. As the t_i occur in many places, equation (2.27) is often more useful than the original form of equation (2.14). For instance, equation (2.27) forms the starting point of an efficient Monte Carlo method (Section IX.5). By choosing the z axes differently it is also easy to derive a representation of R_n in which instead of the t_i the ***two-particle subenergies*** s_i (Figure 2.7) appear as variables (Exercise VI.4). Further, one may also use the techniques of Section II.7 to replace the azimuthal angles ϕ_i in equation (2.27) by invariant variables, which, in fact, turn out to be just the two-particle subenergies s_i (Byckling, 1969d). This

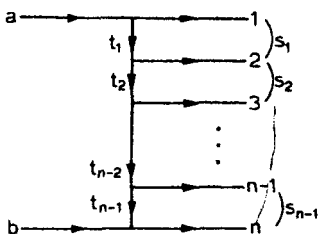


Figure VI.2.7 The multiperipheral momentum transfers
 $t_i = (p_1 - p_2 - \dots - p_i)^2$ and
 two-particle subenergies
 $s_i = (p_i + p_{i+1})^2$

gives one a form of R_n in which, in addition to M_i^2 , all the multi-Regge variables of Figure 2.7 appear as variables. If the M_i finally are replaced by certain azimuthal angles by a relation which is analogous to that (equation V.10.10) relating s and the Toller angle ω , one obtains a form of R_n (equation (3.36)) which we actually shall later derive by using spacelike recursion relations.

The points made above emphasize the fact that, starting from a single tree diagram (that in Figure 2.3) by judiciously choosing the variables in the R_2 s one can obtain many different sets of variables in R_n . It is obvious how the same procedure is to be extended to the general tree diagrams (see Figure 2.1 and equation (2.22)). It is easy to write down more examples (see, for instance, Nyborg, 1970b) but only the sets given above have so far been motivated by theoretical ideas. For explicit treatments of some small values of n see (Nyborg, 1965b; McNeil, 1969) for $1 \rightarrow 5$ reactions and (Nyborg, 1966a) for $1 \rightarrow 6$ reactions.

3. Spacelike recursion relations, Toller variables

Consider now the tree diagram in Figure 3.1 and compare it with Figure 2.3. In the former the first process is $p_b \rightarrow p_n + (-q_{n-1}) = p_n + (p_1 + \dots + p_{n-1} - p_a)$ while in the latter it is $(p_n + p_b) \rightarrow p_n + k_{n-1} = p_n + (p_1 + \dots + p_{n-1})$. In the former one continues by separating p_{n-1}, p_{n-2} , etc., and meets

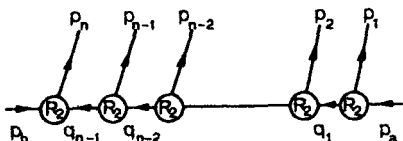


Figure VI.3.1

p_a only at the end, while in the latter both p_b and p_a are known from the beginning. As a consequence, the intermediate systems in Figure 3.1 can be and mostly are spacelike. We shall now establish the form of the phase space integral corresponding to Figure 3.1 (Bali, 1967a; Chew, 1969).

In order to emphasize the different roles of p_b and p_a we define the integral

$$R_i(-q_i, p_a) = \int \prod_{i=1}^l \frac{d^3 p_i}{2E_i} \delta^4(-q_i - p_l - p_{l-1} - \dots - p_1 + p_a). \quad (3.1)$$

Note that in analogy with Figure 2.3 the index i runs from n to 1 and therefore the q_i s defined by equation (2.30) have minus signs in equation (3.1). The complete phase space integral R_n is obtained by setting $i = n$ and $q_n = -p_b$:

$$R_n = R_n(p_b, p_a) \quad (3.2)$$

and it, of course, only depends on $p_a + p_b$. $R_i(-q_i, p_a)$ clearly satisfies the recursion relation

$$R_i(-q_i, p_a) = \int \frac{d^3 p_i}{2E_i} R_{i-1}(-q_{i-1}, p_a). \quad (3.3)$$

In particular, at the beginning of the chain

$$R_n(p_b, p_a) = \int \frac{d^3 p_n}{2E_n} R_{n-1}(-q_{n-1}, p_a)$$

and at the end of the chain

$$R_1(-q_1, p_a) = \int \frac{d^3 p_1}{2E_1} \delta^4(-q_1 - p_1 + p_a). \quad (3.5)$$

Formally we may thus write $R_0(-q_0, p_a) = \delta^4(-q_0 + p_a)$.

Equation (3.3) is obviously the analogue of equation (2.4) and its further treatment will also be similar. Introduce in equation (3.3) the identities

$$\begin{aligned} 1 &= \int dt_{i-1} \delta(t_{i-1} - q_{i-1}^2) \\ 1 &= \int d^4 q_{i-1} \delta^4(q_{i-1} - p_i - q_i) \end{aligned} \quad (3.6)$$

Then equation (3.3) is equivalent to

$$\begin{aligned} R_i(-q_i, p_a) &= \int dt_{i-1} d^4 q_{i-1} d^4 p_i \delta(q_{i-1}^2 - t_{i-1}) \delta(p_i^2 - m_i^2) \\ &\quad \times \delta^4(-q_i - p_i + q_{i-1}) R_{i-1}(-q_{i-1}, p_a) \\ &= \int dt_{i-1} R_2(-q_i; p_i^2, q_{i-1}^2) R_{i-1}(-q_{i-1}, p_a) \end{aligned} \quad (3.7)$$

This result is analogous to equation (2.10): R_2 describes the decay $-q_i \rightarrow p_i + (-q_{i-1})$, R_{i-1} the decay $-q_{i-1} \rightarrow p_{i-1} + \dots + p_1 - p_a$, and all possible intermediate masses t_{i-1} are integrated over. The further treatment of R_2 depends on the type of q_i (equations (IV.1.8), (IV.1.18) and (IV.1.20)). As the q_i are mostly spacelike and for certain mass combinations occurring in practice always spacelike, we shall in the following only consider this case with the understanding that for $q_i^2 \geq 0$ the results have to be appropriately modified. For $q_i^2 = t_i < 0$ the explicit form of R_2 is given in equation (IV.1.18), and we may write for R_2 in equation (3.7):

$$R_2(-q_i; p_i^2, q_{i-1}^2) = \frac{\lambda^{\frac{1}{2}}(t_i, t_{i-1}, m_i^2)}{-8t_i} \int dg_{i-1}, \quad (3.8)$$

where $dg_{i-1} = d\cosh \zeta_i d\omega_{i+1}$ describes the orientation of q_{i-1} in the standard frame $S(q_i)$ of q_i , $q_i = (0, 0, 0, \sqrt{(-t_i)})$ (Figure II.1.3(b)). The choice of indices in ζ_i and ω_{i+1} will be explained presently. At the first stage, however, $q_n = -p_b$ is timelike and equation (IV.1.8) for R_2 applies. Instead of g_{n-1} in equation (3.8) we then have Ω_{n-1} describing the orientation of q_{n-1} in the frame $p_b = (m_b, 0)$. The ranges of the variables in equations (3.7–8) will be specified later.

Applying equations (3.7) and (3.8) repeatedly to equation (3.4) we obtain

$$\begin{aligned} R_n(p_b, p_a) &= \int dt_{n-1} d\Omega_{n-1} \frac{\lambda^{\frac{1}{2}}(m_b^2, t_{n-1}, m_n^2)}{8m_b^2} \times \dots \\ &\quad \times \int dt_{i-1} dg_{i-1} \frac{\lambda^{\frac{1}{2}}(t_i, t_{i-1}, m_i^2)}{-8t_i} \times \dots \\ &\quad \times \int dt_1 dg_1 \frac{\lambda^{\frac{1}{2}}(t_2, t_1, m_2^2)}{-8t_2} \times \dots \\ &\quad \times \int dt_0 dg_0 \frac{\lambda^{\frac{1}{2}}(t_1, t_0, m_1^2)}{-8t_1} \delta^4(-q_0 + p_a). \end{aligned} \quad (3.9)$$

This equation is the most general form of R_n corresponding to the tree diagram of Figure 3.1. It is the analogue of equation (2.14). A new feature is the appearance of the four-dimensional δ function $\delta^4(-q_0 + p_a)$ in equation (3.9). It reduces the number of variables to $3n - 4$. As we shall see, the values of $\cos \theta_{n-1}$, ω_n and t_0 are fixed by the δ function constraint. This leaves one essential δ function, the argument of which is a complicated function of $t_1, \dots, t_{n-1}, \zeta_1, \dots, \zeta_{n-1}, \omega_2, \dots, \omega_{n-1}$, and which is seen to determine the total energy. This δ function also defines the domain of integration in equation (3.9) to be a $3n - 4$ dimensional surface in the space of the $3n - 3$ variables $t_i, \zeta_i, \omega_j, \phi_{n+1}$. The trivial variable ϕ_{n+1} describes rotations around the beam axis and is not fixed by the energy constraint. Equation (3.9) is rederived in a slightly different manner in equations (3.22–23) below.

The orientations of the coordinate axes of the frames $S(q_i)$ can be specified in many ways. This freedom can be exploited to introduce variables that are of some required type. We shall now present a choice that includes the two-particle energies s_i in Figure 2.7 among the variables.

Consider step i , $2 \leq i \leq n - 2$, in equation (3.9). The differences of the successive q_i 's in Figure 3.2 give

$$\begin{aligned}(q_{i-1} - q_i)^2 &= p_i^2 \\ &= m_i^2\end{aligned}\quad (3.10)$$

$$\begin{aligned}(q_{i-1} - q_{i+1})^2 &= (p_i + p_{i+1})^2 \\ &= s_i\end{aligned}\quad (3.11)$$

$$(q_{i-1} - q_{i+2})^2 = (p_i + p_{i+1} + p_{i+2})^2. \quad (3.12)$$

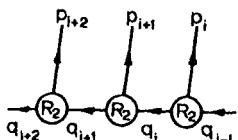


Figure VI.3.2

Thus if the orientation of q_{i-1} is specified with respect to q_i , q_{i+1} and q_{i+2} , the geometric variables involved are related to the invariants (3.10)–(3.12).

This relation can be made explicit by writing q_{i-1} in pseudospherical coordinates (II.7.22) in the standard frame $S(q_i, q_{i+1}, q_{i+2})$:

$$\begin{aligned}q_{i+2} &= (E_{i+2}, x_{i+2}, 0, z_{i+2}) \\ q_{i+1} &= \sqrt{(-t_{i+1})}(-\sinh \eta_{i+1}, 0, 0, \cosh \eta_{i+1}) \\ q_i &= (0, 0, 0, \sqrt{(-t_i)}) \\ q_{i-1} &= \sqrt{(-t_{i-1})}(\sinh \eta_i \cosh \zeta_i, \sinh \eta_i \sinh \zeta_i \cos \omega_{i+1}, \\ &\quad \sinh \eta_i \sinh \zeta_i \sin \omega_{i+1}, \cosh \eta_i) \\ &\equiv L(\eta_i, \zeta_i, \omega_{i+1})(0, 0, 0, \sqrt{(-t_{i-1})}).\end{aligned}\quad (3.13)$$

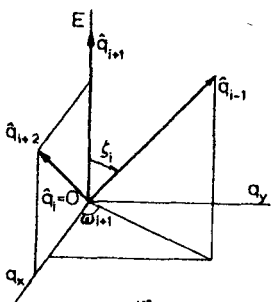


Figure VI.3.3 Specification of the coordinate axes in the frame $S(q_i)$ defined by $q_i = (0, 0, 0, \sqrt{(-t_i)})$ or by $\hat{q}_i = 0$ if \hat{q}_j denotes the three components of q_j in the $E_{q_x}q_j$ subspace, i.e. $q_j = \{\hat{q}_j, \sqrt{(\hat{q}_j^2 - t_j)}\}$. The frame is now called $S(q_i, q_{i+1}, q_{i+2})$.

The Lorentz transformation $L(\eta, \zeta, \omega)$ is given explicitly in equation (II.1.27). The minus sign in $\sinh \eta_{i+1}$ is due to the fact that if η_{i+1} is the rapidity of q_i in $S(q_{i+1})$, then the rapidity of q_{i+1} in $S(q_i)$ is $-\eta_{i+1}$.

The values of the parameters in equation (3.13) are found taking scalar products with q_{i-1} . First one has

$$\begin{aligned} -q_{i-1} \cdot q_i &= \sqrt{(-t_{i-1})} \sqrt{(-t_i)} \cosh \eta_i \\ &= \frac{1}{2}(m_i^2 - t_{i-1} - t_i), \end{aligned} \quad (3.14)$$

$$\sqrt{(-t_{i-1})} \sqrt{(-t_i)} \sinh \eta_i = \pm \frac{1}{2} \lambda^{\frac{1}{2}}(m_i^2, t_{i-1}, t_i).$$

The value of ζ_i is connected to s_i :

$$\begin{aligned} q_{i-1} \cdot q_{i+1} &= \sqrt{(-t_{i-1})} \sqrt{(-t_i)} (\cosh \eta_{i-1} \cosh \eta_i + \sinh \eta_{i-1} \sinh \eta_i \cosh \zeta_i) \\ &= \frac{1}{2}(t_{i-1} + t_{i+1} - s_i). \end{aligned} \quad (3.15)$$

The relation between $\cosh \zeta_i$ and s_i could also be found from equation (A.29). Equation (3.15) implies that at fixed t_j ,

$$ds_i = 2\sqrt{(-t_{i-1})} \sqrt{(-t_i)} \sinh \eta_{i-1} \sinh \eta_i d \cosh \zeta_i. \quad (3.16)$$

The angle ω_{i+1} could be expressed in terms of equation (3.12), but this is not generally done. Figure 3.4 shows how the vectors (3.13) look in the

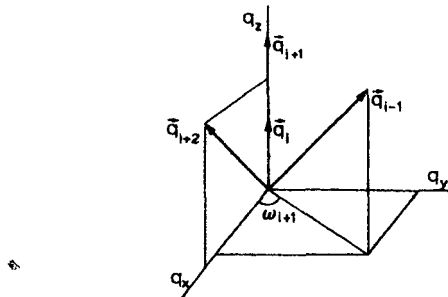


Figure VI.3.4 The vectors (3.13)
in the xyz subspace

xyz subspace. The angle ω_{i+1} remains invariant under Lorentz transformations parallel to the z axis. Thus we may, for instance, transform to the frame $q_i = q_{i+1}$ or $p_{i+1} = 0$. Thus ω_{i+1} can be defined in the rest frame of particle $i+1$ by the equation

$$\begin{aligned} \cos \omega_{i+1} &= \frac{(q_{i+1} \times q_{i+2}) \cdot (q_i \times q_{i-1})}{|q_{i+1} \times q_{i+2}| |q_i \times q_{i-1}|} \Big|_{p_{i+1}=0} \\ &= \frac{(-q_{i+2} \times p_{i+2}) \cdot (q_{i-1} \times p_i)}{|q_{i+2} \times p_{i+2}| |q_{i-1} \times p_i|} \Big|_{p_{i+1}=0} \end{aligned} \quad (3.17)$$

For $i = 1$ and $n = 3$ this is seen to be identical with equation (V.10.9). The angles ω_i are thus Toller angles of the $2 \rightarrow 3$ subprocesses shown in Figure 3.2.

As it stands the parametrization (3.13) only applies to $2 \leq i \leq n - 2$. In the frame $S(q_{n-1})$ there is no vector to fix the E_{q_x} plane so that the angle ω_n is at this stage undetermined. Otherwise equations (3.13)–(3.17) apply, if one inserts $q_n = -p_b$, $t_n = m_b^2$. Further, since $q_n = -p_b$ is timelike, we must work in the frame $R(q_n)$:

$$q_n = (-m_b, 0, 0, 0)$$

$$q_{n-1} = \sqrt{(-t_{n-1})}(\sinh \eta_n, \cosh \eta_n \sin \theta_n \cos \phi_{n+1},$$

$$\cosh \eta_n \sin \theta_n \sin \phi_{n+1}, \cosh \eta_n \cos \theta_n), \quad (3.18)$$

where the parametrization of q_{n-1} is that given in equation (II.1.19). This form is obtained from the standard frame form $(0, 0, 0, \sqrt{(-t_{n-1})})$ of q_{n-1} by the Lorentz transformation $L(\eta_n, \theta_n, \phi_{n+1})$ given explicitly in equation (II.1.26). The scalar product $q_n \cdot q_{n-1}$ now picks out the energy component of q_{n-1} and we find

$$\begin{aligned} E_{n-1} &= \sqrt{(-t_{n-1})} \sinh \eta_n \\ &= \frac{m_n^2 - m_b^2 - t_{n-1}}{2m_b} \\ Q_{n-1} &= \sqrt{(-t_{n-1})} \cosh \eta_n \\ &= \frac{\lambda^3(m_n^2, m_b^2, t_{n-1})}{2m_b}. \end{aligned} \quad (3.19)$$

The angles θ_n and ϕ_{n+1} are, for the moment, undetermined.

At the other end of the chain, $q_0 = p_a$ is parametrized in $S(q_1)$ by

$$q_0 = L(\eta_1, \zeta_1, \omega_2)(m_a, 0, 0, 0), \quad (3.20)$$

where $L(\eta, \zeta, \omega)$ is given in equation (II.1.27). Computation of $q_0 \cdot q_1$ results in

$$\begin{aligned} z_0 &= m_a \sinh \eta_1 \\ &= \frac{m_1^2 - m_a^2 - t_1}{2\sqrt{(-t_1)}} \end{aligned} \quad (3.21)$$

$$\begin{aligned} Q_0 &= m_a \cosh \eta_1 \\ &= \frac{\lambda^3(m_1^2, m_a^2, t_1)}{2\sqrt{(-t_1)}}. \end{aligned}$$

With the aid of equation (3.13) it is simple to rederive equation (3.9). Take first $q_{n-1} = p_n - p_b$, $q_{n-2} = p_{n-1} + q_{n-1}$, etc., as new variables in the phase

...

space integral:

$$R_n(p_b, p_a) = \int \prod_{i=1}^n [d^4 q_{i-1} \delta\{(q_{i-1} - q_i)^2 - m_i^2\}] \delta^4(-q_0 + p_a), \quad (3.22)$$

where the δ^4 function expresses four-momentum conservation in the new variables. Taking into account equation (II.1.34) for $d^4 q_{i-1}$, and equation (3.13) for q_i and q_{i-1} , one can write

$$\begin{aligned} & \int d^4 q_{i-1} \delta\{(q_{i-1} - q_i)^2 - m_i^2\} \\ &= \frac{1}{2} \int dt_{i-1} d\eta_i dg_{i-1} t_{i-1} \sinh^2 \eta_{i-1} \\ & \quad \times \delta\{t_{i-1} + t_i - m_i^2 + 2\sqrt{(t_i t_{i-1})} \cosh \eta_i\} \end{aligned} \quad (3.23)$$

for $i \leq n-1$. For $i=n$ one uses $d^4 q_{n-1} = \frac{1}{2} dt_{n-1} d\eta_n d\Omega_{n-1} t_{n-1} \sinh^2 \eta_n$. Integration over η_i leads immediately to equation (3.9) again.

Next we shall use the parametrization (3.13), (3.18), (3.20) to investigate the constraint $q_0 = p_a$ required by the δ -function $\delta^4(p_a - q_0)$ in equation (3.9). Because $p_a^2 > 0$, the standard form of q_0 , in frame $R(q_0)$, is $q_0 = (\sqrt{t_0}, 0)$. In frames $S(q_1), \dots, S(q_{n-1}), R(q_n)$, q_0 is obtained by successive Lorentz transformations by the matrices $L(\eta, \zeta, \omega)$. Proceeding through the chain we get its value in $R(q_n)$:

$$q_0 = L(\eta_n, 0_n, \phi_{n+1}) L(\eta_{n-1}, \zeta_{n-1}, \omega_n) \times \dots \times L(\eta_1, \zeta_1, \omega_2)(\sqrt{t_0}, 0, 0, 0) \quad (3.24)$$

The orientation of the frame $R(q_n)$ is so far undetermined. It is natural to choose it so that $R(q_n)$ becomes the target system, in which $-q_n = p_b = (m_b, 0)$ and

$$\begin{aligned} p_a &= ((s - m_a^2 - m_b^2)/2m_b, 0, 0, \lambda^{\frac{1}{2}}(s, m_a^2, m_b^2)/2m_b) \\ &\equiv m_a(\cosh \eta_{ab}, 0, 0, \sinh \eta_{ab}). \end{aligned} \quad (3.25)$$

The constraint $\delta^4(q_0 - p_a)$ then implies that the four components of equation (3.24) must equal those in equation (3.25).

Writing $q_0 = (E_0, \mathbf{q}_0)$ and using $\delta(P_a - Q_0) = 2P_a \delta(t_0 - m_a^2), \delta(p_a - p_0) = P_a^{-2} \delta(P_a - Q_0) \delta(\Omega_a - \Omega_0)$ and $E_a \delta(P_a - Q_0) = P_a \delta(E_a - E_0)$,

$$\begin{aligned} \int dt_0 \delta^4(p_a - q_0) &= \int dt_0 \delta(E_a - E_0) \delta^3(p_a - p_0) \\ &= \int dt_0 \delta(E_a - E_0) P_a^{-2} \delta(P_a - Q_0) \delta^2(\Omega_a - \Omega_0) \\ &= \frac{2}{P_a} \delta(E_a - E_0) \delta^2(\Omega_a - \Omega_0). \end{aligned} \quad (3.26)$$

The next step is to satisfy the orientation condition $\Omega_0 = \Omega_a$ in equation (3.26) for the vectors (3.24) and (3.25). Factorizing the leftmost terms in equation (3.24) as in equations (II.1.26–27) we can write

$$q_0 = R_z(\phi_{n+1})R_y(\theta_n)L_z(\eta_n)R_z(\omega_n)\tilde{q}_0, \quad (3.27)$$

where \tilde{q}_0 is fixed once the variables with index $i \leq n - 1$ are fixed. Now it is clear that for any \tilde{q}_0 , ω_n can be chosen to put q_0 in the xz plane, $L_z(\eta_n)$ keeps it there and θ_n can be chosen to put q_0 parallel to z axis. Then one has $\Omega_0 = \Omega_a$ irrespective of ϕ_{n+1} . Thus we can evaluate part of equation (3.9) as

$$\int d\Omega_{n-1} d\omega_n \delta^2(\Omega_a - \Omega_0) = \int d\phi_{n+1}. \quad (3.28)$$

Here $\delta^2(\Omega_a - \Omega_0)$ gives θ_n and ω_n some fixed values, which are some complicated functions of the parameters of the Lorentz transformations in equation (3.24). As shown presently, these functions are not needed in explicit form.

The single remaining δ function in equation (3.26)

$$2P_a^{-1} \delta(E_a - E_0) = 4m_b P_a^{-1} \delta(s - m_a^2 - m_b^2 - 2m_b E_0), \quad (3.29)$$

fixes E_0 in terms of the total energy squared s . E_0 is the energy component of the four-vector (3.24) and it may formally be projected out by multiplying equation (3.24) from the left by the vector $(1, 0, 0, 0)$. By using the explicit representations of equations (II.1.26–27) of the L -matrices it is easy to verify that

$$\begin{aligned} & (1, 0, 0, 0) L(\eta_n, \theta_n, \phi_{n+1}) L(\eta_{n-1}, \zeta_{n-1}, \omega_n) \\ &= (\cosh \eta_n \cosh \eta_{n-1} \cosh \zeta_{n-1} + \sinh \eta_n \sinh \eta_{n-1}, \cosh \eta_n \sinh \zeta_{n-1}, \\ & \quad 0, \cosh \eta_n \sinh \eta_{n-1} \cosh \zeta_{n-1} + \sinh \eta_n \cosh \eta_{n-1}) \end{aligned} \quad (3.30)$$

Thus the energy constraint does not depend on the fixed values of θ_n and ω_n nor on the undetermined value of ϕ_{n+1} . By combining equation (3.30) with equations (3.29) and (3.24) one can calculate s as a complicated function

$$s = s(t_1, \dots, t_{n-1}; \zeta_1, \dots, \zeta_{n-1}; \omega_2, \dots, \omega_{n-2}) \quad (3.31)$$

of $3n - 4$ arguments. This will later be written down explicitly for $n = 3$ and also in the limit $s \rightarrow \infty$. Inserting equations (3.26), (3.28) and (3.29) in equation (3.9), one obtains the result

$$\begin{aligned} R_n(p_b, p_a) &= \frac{8m_b^2}{\lambda^{\frac{1}{2}}(s, m_a^2, m_b^2)} \int d\phi_{n+1} dt_1 \dots dt_{n-1} d \cosh \zeta_1 \dots d \cosh \zeta_{n-1} \\ & \times d\omega_2 \dots d\omega_{n-2} \frac{\lambda^{\frac{1}{2}}(m_b^2, t_{n-1}, m_n^2)}{8m_b^2} \prod_{j=2}^{n-1} \frac{\lambda^{\frac{1}{2}}(t_j, t_{j-1}, m_j^2)}{-8t_j} \\ & \times \frac{\lambda^{\frac{1}{2}}(t_1, m_a^2, m_1^2)}{-8t_1} \delta\{s - s(t_i, \zeta_i, \omega_j)\}. \end{aligned} \quad (3.32)$$

As the derivation implies, the rapidities and angles have simple limits

$$0 \leq \zeta_i < \infty, \quad 0 \leq \omega_i < 2\pi, \quad 0 \leq \phi_{n+1} < 2\pi. \quad (3.33)$$

The ranges of t_1, \dots, t_{n-1} depend on the masses m_i and they are coupled. In equations (3.21), (3.14) and (3.19) the rapidities vary in the interval $-\infty < \eta_i < \infty$, $i = 1, \dots, n$. Substitution of fixed values for any set of $n - 1$ variables η_i determines t_1, \dots, t_{n-1} and also the value of the one remaining η_i . In this way the range of variation of the set t_1, \dots, t_{n-1} can be found. Finally, from the $3n - 3$ dimensional region defined by the range of t_1, \dots, t_{n-1} , and by equation (3.33), the condition (3.31) cuts a $3n - 4$ dimensional subspace of finite volume which is the physical region in Toller variables.

If the masses $m_a, m_b, m_1, \dots, m_n$ have appropriate magnitudes, some t_i take on positive values, and ζ_i will be replaced by angular variables. An example of a case when all t_i are always negative is elastic outer vertices, $m_a = m_1, m_b = m_n$. Then because t_i is the momentum transfer of the process $m_a + m_b \rightarrow (m_1 + \dots + m_i) + (m_{i+1} + \dots + m_n)$, according to Exercise IV.30 it cannot be positive.

The result (3.33) can be further modified by replacing the non-invariant variables ζ_i and ω_j by corresponding invariants. We could apply the results of Section II.7 to Figure 3.3, but one also obtains directly from equation (3.15):

$$s_i = t_{i-1} + t_{i+1} - \frac{1}{2t_i} \{(m_{i+1} - t_{i+1} - t_i)(m_i^2 - t_i - t_{i-1}) \\ + \cosh \zeta_i \lambda^{\frac{1}{4}}(t_{i+1}, t_i, m_{i+1}^2) \lambda^{\frac{1}{4}}(t_i, t_{i-1}, m_i^2)\}. \quad (3.34)$$

This form of s_i is also obtained by equating the G function corresponding to the process $t_{i-1} + t_{i+1} \rightarrow m_i^2 + m_{i+1}^2$ with zero:

$$G(s_i, t_i, m_i^2, t_{i+1}, t_{i-1}, m_{i+1}^2) = 0, \quad (3.35)$$

using the solutions (IV.5.31) and replacing the \pm sign there by $\cosh \zeta_i$. If we inserted cosine in place of \cosh in equation (3.34), this cosine would be the t channel scattering angle of the process $t_{i-1} + t_{i+1} \rightarrow m_i^2 + m_{i+1}^2$. As is well known, this cosine is linearly related to the t channel momentum s_i . However, now we are in the s channel, where the cosine of the t channel scattering angle is > 1 or < -1 so that, to obtain a real quantity, it is replaced by a \cosh .

The use of equations (3.16) and (3.14) in equation (3.32) leads to

$$R_n(p_b, p_a) = \frac{1}{4} \lambda^{-\frac{1}{4}}(s, m_a^2, m_b^2) \int d\phi_{n+1} dt_{n-1} \dots dt_1 ds_{n-1} \dots ds_1 d\omega_{n-1} \dots d\omega_2 \\ \times \prod_{j=2}^{n-1} \{ \frac{1}{4} \lambda^{-\frac{1}{4}}(t_j, t_{j-1}, m_j^2) \} \delta\{s - s(t_i, s_i, \omega_j)\}. \quad (3.36)$$

In order to obtain more insight into this result we shall treat in more detail the case $n = 3$ and the case $s \rightarrow \infty$.

(a) $n = 3$

To formulate the energy constraint we first calculate from equations (3.24) and (3.30) that

$$\begin{aligned} \frac{E_0}{m_a} &= \frac{s - m_a^2 - m_b^2}{2m_a m_b} \\ &= \cosh \eta_3 \cosh \eta_2 \cosh \eta_1 \cosh \zeta_2 \cosh \zeta_1 \\ &\quad + \sinh \eta_2 (\cosh \eta_3 \sinh \eta_1 \cosh \zeta_2 + \sinh \eta_3 \cosh \eta_1 \cosh \zeta_1) \quad (3.37) \\ &\quad + \sinh \eta_3 \cosh \eta_2 \sinh \eta_1 \\ &\quad + \cos \omega_2 (\cosh \eta_3 \cosh \eta_1 \sinh \zeta_2 \sinh \zeta_1), \end{aligned}$$

where, according to equations (3.19), (3.14) and (3.21),

$$\begin{aligned} \cosh \eta_3 &= \frac{\lambda^{\frac{1}{2}}(t_2, m_3^2, m_b^2)}{2m_b \sqrt{(-t_2)}} \\ \sinh \eta_3 &= \frac{m_3^2 - m_b^2 - t_2}{2m_b \sqrt{(-t_2)}} \\ \cosh \eta_2 &= \frac{m_2^2 - t_1 - t_2}{2\sqrt{(t_1 t_2)}} \quad (3.38) \\ \sinh \eta_2 &= \frac{\lambda^{\frac{1}{2}}(t_2, t_1, m_2^2)}{2\sqrt{(t_1 t_2)}} \\ \cosh \eta_1 &= \frac{\lambda^{\frac{1}{2}}(t_1, m_1^2, m_a^2)}{2m_a \sqrt{(-t_1)}} \\ \sinh \eta_1 &= \frac{m_1^2 - m_a^2 - t_1}{2m_a \sqrt{(-t_1)}}. \end{aligned}$$

Further, ζ_2 and ζ_1 are related to s_2 and s_1 by the equations

$$\cosh \zeta_2 = \frac{-2t_2(s_2 - t_1 - m_b^2) - (m_3^2 - m_b^2 - t_2)(m_2^2 - t_2 - t_1)}{\lambda^{\frac{1}{2}}(t_2, m_b^2, m_3^2) \lambda^{\frac{1}{2}}(t_1, t_2, m_2^2)}, \quad (3.39)$$

$$\cosh \zeta_1 = \frac{-2t_1(s_1 - t_2 - m_a^2) - (m_1^2 - m_a^2 - t_1)(m_2^2 - t_2 - t_1)}{\lambda^{\frac{1}{2}}(t_1, m_a^2, m_1^2) \lambda^{\frac{1}{2}}(t_1, t_2, m_2^2)}. \quad (3.40)$$

As pointed out after equation (3.35), $\cosh \zeta_2$ and $\cosh \zeta_1$ are the cosines of the t channel scattering angles of the two $2 \rightarrow 2$ processes associated with $\cos \omega$ and shown in Figure V.10.3. The quantities $\sinh \zeta_2$ and $\sinh \zeta_1$ can

thus be expressed in terms of the G functions associated with the processes in Figure V.10.3 (these are the G functions in Equation (V.10.10)). If ζ_2 and ζ_1 are replaced by s_2 and s_1 in equation (3.37) one, of course, obtains the relation $s = s(s_1, s_2, t_1, t_2, \cos \omega)$ given previously in equation (V.10.10).

The two associated forms of R_3 are obtained from equations (3.32) and (3.36):

$$R_3 = \frac{\pi}{32} \lambda^{-\frac{1}{2}}(s, m_a^2, m_b^2) \int dt_2 dt_1 d \cosh \zeta_2 d \cosh \zeta_1 d\omega_2 \lambda^{\frac{1}{2}}(m_b^2, t_2, m_3^2) \\ \times \lambda^{\frac{1}{2}}(t_2, t_1, m_2^2) \lambda^{\frac{1}{2}}(t_1, m_a^2, m_1^2) (t_1 t_2)^{-1} \delta\{s - s(t_2, t_1, \zeta_2, \zeta_1, \omega_2)\} \quad (3.41)$$

$$= \frac{\pi}{8} \lambda^{-\frac{1}{2}}(s, m_a^2, m_b^2) \int dt_2 dt_1 ds_2 ds_1 d\omega_2 \lambda^{-\frac{1}{2}}(t_2, t_1, m_2^2) \\ \times \delta\{s - s(t_2, t_1, s_2, s_1, \omega)\}, \quad (3.42)$$

where the integration over ϕ_{n+1} has been carried out. Again, equation (3.42) is seen to be the same as equation (V.10.13). We can thus use equation (V.10.11) to replace $d\omega_2$ by ds . After this the trivial integration over s leads back to equation (V.9.2).

(b) Behaviour of $R_n(s)$ in the multi-Regge limit

As a generalization of equation (V.11.19) we shall define the **multi-Regge limit** as the kinematic configuration satisfying

$$s \rightarrow \infty$$

$$s_1, s_2, \dots, s_{n-1} \gg |t_1|, \dots, |t_{n-1}|, m_i^2, \quad (3.43)$$

$$s_1 \dots s_{n-1}/s \text{ finite.}$$

The last condition is needed for compatibility of s_i large with $|t_i|$ small (Exercise VI.5). It is important to realize that equation (3.43) represents an extremely small part of phase space. In particular, **multiperipherality** only requires the $|t_i|$ to be small, which is valid in a much larger part of the phase space than equation (3.43). The appropriate form of R_n in the multiperipheral case has already been derived in equation (2.27). Now we add further assumptions and the result simplifies at the expense of decreasing generality (Bali, 1967b; Chew, 1968; Finkelstein, 1968).

In the previous analysis of $n = 3$ it was found that in the limit (3.43) the complicated energy constraint (3.37) or (V.10.10) reduces to the simple form (V.11.26). The same significant simplification will be seen to take place for arbitrary n , too. The reason for this is the assumption s_i large. This implies that the ζ_i are large, too. Thus we can make the approximation $\cosh \zeta_i \simeq \sinh \zeta_i \gg 1$ and the transformations L_i in equation (3.24) simplify. Starting

from $L_1 \equiv L(\eta_1, \zeta_1, \omega_2)$ one finds

$$L_1 \begin{pmatrix} 1 \\ 0 \\ 0 \\ 0 \end{pmatrix} \simeq \cosh \zeta_1 \cosh \eta_1 \begin{pmatrix} 1 \\ \cos \omega_2 \\ \sin \omega_2 \\ 0 \end{pmatrix}, \quad (3.44)$$

$$L_2 L_1 \begin{pmatrix} 1 \\ 0 \\ 0 \\ 0 \end{pmatrix} = \cosh \zeta_2 (\cosh \eta_2 + \cos \omega_2) \cosh \zeta_1 \cosh \eta_1 \begin{pmatrix} 1 \\ \cos \omega_3 \\ \sin \omega_3 \\ 0 \end{pmatrix},$$

etc. At the end of the sequence, equation (3.30) implies

$$(1, 0, 0, 0) L_n L_{n-1} = \cosh \zeta_{n-1} \cosh \eta_n (\cosh \eta_{n-1}, 1, 0, \sinh \eta_{n-1}). \quad (3.45)$$

Putting everything together gives

$$\frac{E_0}{m_a} \simeq \frac{s}{2m_a m_b} \simeq \prod_{i=1}^{n-1} (\cosh \zeta_i) \cosh \eta_n \prod_{j=2}^{n-1} (\cosh \eta_j + \cos \omega_j) \cosh \eta_1 \quad (3.46)$$

or, inserting η_i explicitly from equations (3.14), (3.19) and (3.21),

$$s \simeq \lambda^{\frac{1}{2}}(t_1, m_a^2, m_1^2) \lambda^{\frac{1}{2}}(t_{n-1}, m_b^2, m_n^2) \prod_{i=1}^{n-1} \left\{ (-2t_i)^{-1} \cosh \zeta_i \right\} \times \prod_{j=2}^{n-1} (m_j^2 - t_j - t_{j-1} + 2\sqrt{(t_j t_{j-1}) \cos \omega_j}). \quad (3.47)$$

Finally, within the approximation (3.43), we have from equation (3.34):

$$\cosh \zeta_i \simeq \frac{-2t_i s_i}{\lambda^{\frac{1}{2}}(t_{i+1}, t_i, m_{i+1}^2) \lambda^{\frac{1}{2}}(t_i, t_{i-1}, m_i^2)}, \quad (3.48)$$

so that equation (3.47) is transformed to

$$s \simeq \left(\prod_{i=1}^{n-1} s_i \right) \prod_{j=2}^{n-1} \left\{ \lambda^{-1}(t_j, t_{j-1}, m_j^2) (m_j^2 - t_j - t_{j-1} + 2\sqrt{(t_j t_{j-1}) \cos \omega_j}) \right\}. \quad (3.49)$$

This result is a generalization of equation (V.11.26) derived for $n = 3$. Equation (3.49) can also be used to generalize the condition (V.11.23) to arbitrary n (Exercise VI.5).

The forms of R_n valid in the multi-Regge limit are obtained either when equation (3.47) is inserted in equations (3.32) or (3.49) in equation (3.36).

No further simplifications take place, but it is convenient to take either ζ_i or $\log s_i$ as variables instead of $\cosh \zeta_i$ or s_i . Using the relation $\delta(x - a) = \delta\{\log(x/a)/x$ one has after some calculations in the multi-Regge limit (Bali, 1967b)

$$R_n = \frac{1}{4s} \int dt_{n-1} \dots dt_1 d\omega_{n-1} \dots d\omega_2 d\zeta_{n-1} \dots d\zeta_1 \\ \times \prod_{j=2}^{n-1} \frac{\lambda^{\frac{1}{2}}(t_j, t_{j-1}, m_j^2)}{4(m_j^2 - t_j - t_{j-1} + 2\sqrt{(t_j t_{j-1}) \cos \omega_j})} \delta \left\{ \sum_{i=1}^{n-1} \zeta_i - \zeta^+(s, t_i, \omega_j) \right\}, \quad (3.50)$$

where ζ^+ is defined by

$$e^{\zeta^+} = \frac{s \cdot \prod_{i=1}^{n-1} (-4t_i)}{\lambda^{\frac{1}{2}}(t_1, m_a^2, m_1^2) \lambda^{\frac{1}{2}}(m_b^2, t_{n-1}, m_n^2) \prod_{j=2}^{n-1} (m_j^2 - t_j - t_{j-1} + 2(t_j t_{j-1}) \cos \omega_j)}. \quad (3.51)$$

For $\log s_i$ one has $d\zeta_i = d\log s_i$ and the δ -function requires the logarithm of the right hand side of equation (3.49) to equal logs. The energy constraint given by equation (3.49) is now written in an elegant form requiring the sum of the rapidities ζ_i to equal ζ^+ , but ζ^+ is still a function of t_i and ω_j and the integration over t_i and ω_j is impossible to carry out explicitly. The integration over ζ_i is formally simpler since the limits of integration depend on t_i and ω_j . However, in the asymptotic limit $s \rightarrow \infty$ the limits simplify. In the multi-Regge limit the t_i are small and vary essentially between some negative constant and zero. By extending our previous analysis of ω_2 in $2 \rightarrow 3$ reactions to $2 \rightarrow n$ reactions one can see that the ω_j vary between 0 and 2π in the limit $s \rightarrow \infty$. Then the limits of ζ_i -integrations are only determined by the δ function. For instance, if the integrand or the matrix element squared is of the form

$$T = f(t_j) \prod_{i=1}^{n-1} s_i^{2\alpha} \\ = g(t_j) \prod_{i=1}^{n-1} e^{2\alpha \zeta_i}, \quad (3.52)$$

where $f(t_j)$ and $g(t_j)$ are some functions of the t_j , related in a way that follows from equation (3.48), we may use the relation

$$\int d\zeta_{n-1} \dots d\zeta_1 \prod_{i=1}^n e^{2\alpha \zeta_i} \delta \left(\sum_{i=1}^{n-1} \zeta_i - \zeta^+ \right) = \frac{(\zeta^+)^{n-2}}{(n-2)!} e^{2\alpha \zeta^+} \quad (3.53)$$

to integrate over ζ_i . The remaining integral over t_i and ω_j is then energy-independent.

4. Phase-space distributions

In this section we shall present examples of phase space distributions in some kinematical variables. One knows that the assumption $T = 1$ is not at all valid in high energy reactions because of the observed strong cut in transverse momentum (Section 5). Phase space predictions are thus meaningful mainly if the total energy is not too large, for example, provided that in the channel studied the momentum of each produced particle in CMS is on the average well below $1 \text{ GeV}/c$.

(a) Distributions in one invariant mass

Consider the invariant mass $M_l, M_l^2 = (p_1 + \dots + p_l)^2$, of the group formed by particles p_1, \dots, p_l (Figure 2.5). It is clear that choosing this set of indices does not decrease the generality of the argument. The phase space distribution $w(M_l)$ is immediately obtained from equation (2.21), according to which

$$\begin{aligned} w(M_l) &= R_n^{-1} \frac{dR_n}{dM_l} \\ &= 2M_l \frac{R_l(M_l^2; m_1^2, \dots, m_l^2) R_{n-l+1}(s; M_l^2, m_{l+1}^2, \dots, m_n^2)}{R_n(s; m_1^2, \dots, m_n^2)}. \end{aligned} \quad (4.1)$$

Here R_n^{-1} normalizes the distribution. Equation (4.1) is given for the special case $n = 3, l = 2$ in equation (V.2.16).

To analyze the shape of equation (4.1) we note that it is nonzero only if

$$m_1 + \dots + m_l = M_{l,\min} \leq M_l \leq M_{l,\max}'' = \sqrt{s - (m_{l+1} + \dots + m_n)}. \quad (4.2)$$

The lower limit corresponds to the threshold of R_l , that is the situation in which particles p_1, \dots, p_l are at rest in their CMS so that they move with the same velocity in any frame. The upper limit corresponds to the threshold of R_{n-l+1} , that is the situation in which particles p_{l+1}, \dots, p_n are at rest in the overall CMS of the final state p_1, \dots, p_n . More quantitatively, when $M_l \rightarrow M_{l,\min}$ or $M_l \rightarrow M_{l,\max}''$ the distribution (4.1) vanishes according to equation (2.19) as follows:

$$M_l \simeq M_{l,\min}: \quad w(M_l) = \text{constant} \times (M_l - M_{l,\min})^{\frac{1}{2}l - \frac{3}{2}}, \quad (4.3)$$

$$M_l \simeq M_{l,\max}'': \quad w(M_l) = \text{constant} \times (M_{l,\max}'' - M_l)^{\frac{1}{2}(n-l) - 1}. \quad (4.4)$$

The general shape of $w(M_l)$ largely depends on its behaviour at $M_{l,\min}$ and $M_{l,\max}''$. As seen from equations (4.3) and (4.4), the distribution has a vertical tangent at $M_{l,\min}$ for $l = 2$ and at $M_{l,\max}''$ for $l = n - 1$; otherwise the slope vanishes at $M_{l,\min}$ and $M_{l,\max}''$. The qualitatively different possibilities are displayed in Figure 4.1.

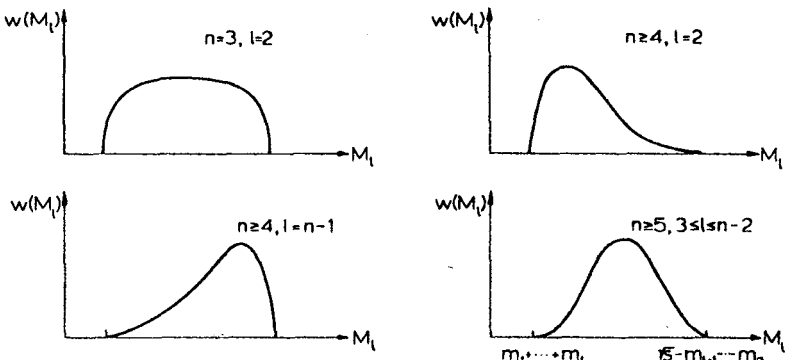


Figure VI.4.1 Qualitatively different types of phase space distribution $w(M_l)$ in invariant mass $M_l^2 = (p_1 + \dots + p_l)^2$ in the final state p_1, \dots, p_n

The behaviour (4.3–4) at the limits dominates the general shape of $w(M_l)$ so strongly that one can even approximate $w(M_l)$ by a product of the two limiting expressions (4.3) and (4.4) (Kopylov, 1963). If one normalizes this product to 1, and uses the dimensionless variable

$$x = \frac{M_l - m_1 - \dots - m_l}{\sqrt{s} - m_1 - \dots - m_n}, \quad (4.5)$$

the approximation is

$$w_{n,l}(x) = \frac{\Gamma(\frac{3}{2}n - \frac{3}{2})}{\Gamma(\frac{3}{2}l - \frac{3}{2})\Gamma(\frac{3}{2}n - \frac{3}{2}l)} x^{\frac{3}{2}l - \frac{3}{2}} (1-x)^{\frac{3}{2}(n-l)-1}. \quad (4.6)$$

The shape of the function (4.6) is independent of the masses m_i . It is easily seen that $w_{n,l}(x)$ has a maximum at $x = (3l - 5)/(3n - 7)$. In Figure 4.2 $w_{5,2}(x)$ and $w_{5,3}(x)$ are compared with the exact $w(M_l)$ for some mass combinations.

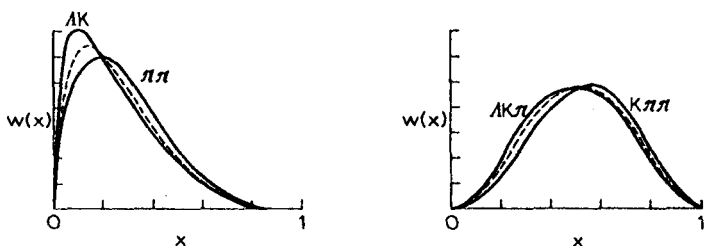
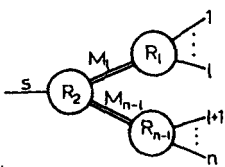


Figure VI.4.2 Distribution in ΛK , $\pi\pi$, $\Lambda K\pi$ and $K\pi\pi$ effective mass in the reaction $\pi^- p \rightarrow \Lambda K\pi$ at 7 GeV/c, compared with the approximation (4.6) (dotted line)

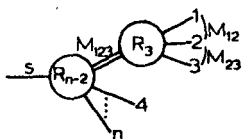
(b) Distributions in two invariant masses

The form of the distributions in two invariant masses can always be obtained by using the results of Section VI.2. There are many qualitatively different cases, and instead of attempting a general classification, we consider some examples to give an idea of how one should proceed in an arbitrary situation.

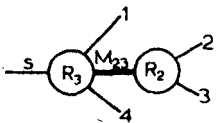
Assume first that one has split the final state of $p \rightarrow p_1 + \dots + p_n$ into two groups of invariant mass squared $M_i^2 = (p_1 + \dots + p_i)^2$, $M_{n-i}^2 = (p_{i+1} + \dots + p_n)^2$. By drawing the tree diagram shown in Figure 4.3(a) one can



(a)



(b)



(c)

Figure VI.4.3 Tree diagrams

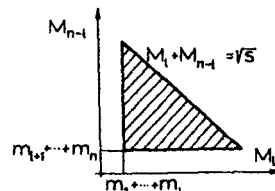
immediately write the associated form of $R_n(s)$ as

$$R_n(s) = \int dM_1^2 dM_{n-1}^2 R_2(s; M_1^2, M_{n-1}^2) R_l(M_l^2; m_1^2, \dots, m_l^2) \times R_{n-l}(M_{n-l}^2; m_{l+1}^2, \dots, m_n^2) \quad (4.7)$$

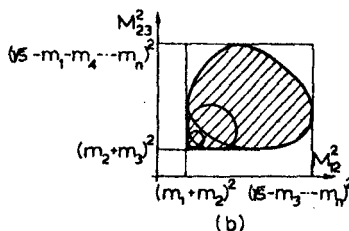
By considering the thresholds of the R_s in equation (4.7) one sees that the domain of integration or the physical region in the $M_i M_{n-i}$ plane is a triangle (Figure 4.4) satisfying

$$\begin{aligned} M_i &\geq m_1 + \dots + m_i \\ M_{n-i} &\geq m_{i+1} + \dots + m_n \\ M_i + M_{n-i} &\leq s. \end{aligned} \quad (4.8)$$

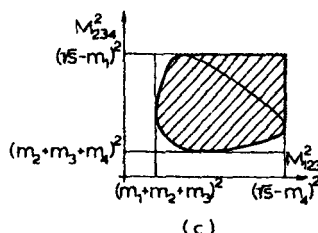
This region is called the **Goldhaber plot** (Goldhaber, 1963). The phase space density on it is given by the integrand of equation (4.7) (multiplied by $4M_i M_{n-i}$).



(a)



(b)



(c)

Figure VI.4.4 Physical regions in the invariants

(a) $M_i = \{(p_1 + \dots + p_i)^2\}^{\frac{1}{2}}$,
 $M_{n-i} = \{(p_{i+1} + \dots + p_n)^2\}^{\frac{1}{2}}$,

(b) M_{12}^2, M_{23}^2 ,

(c) M_{123}^2, M_{234}^2 .

In (a) and (b) the final state has n particles, in (c) four

In particular, for $n = 4$ and $l = 2$ with the notation $M_1 = M_{12}$, $M_{n-1} = M_{34}$ one has by using the explicit forms (IV.1.7-8) of R_2 that

$$\frac{d^2 R_4}{dM_{12} dM_{34}} = \frac{\pi^3}{2s M_{12} M_{34}} \lambda^4(s, M_{12}^2, M_{34}^2) \lambda^4(M_{12}^2, m_1^2, m_2^2) \lambda^4(M_{34}^2, m_3^2, m_4^2) \quad (4.9)$$

$$= \frac{4\pi^3}{\sqrt{s}} P_{12}^* P_1^{R12} P_3^{R34}, \quad (4.10)$$

where P_{12}^* , P_1^{R12} and P_3^{R34} are the decay momenta in the rest frames of the three decays in Figure 4.3(a).

If the two invariant masses are either disjoint (as M_{12} , M_{34}) or overlap completely (for instance, $M_{123} = (p_1 + p_2 + p_3)^2$, $M_{12} = (p_1 + p_2)^2$) one can always draw a tree diagram in which only these masses appear in intermediate states. Then one can immediately write the associated form of R_n , which both gives the phase space density and determines the physical region. In other cases one has to proceed in a slightly more complicated way, which we illustrate by the following examples.

Assume one wants to determine the distribution in the $M_{12} M_{23}$ plane ($M_{ij} = (p_i + p_j)^2$) for an n -particle final state. Then one must start from the tree diagram of Figure 4.3(b), which leads to the following form of R_n :

$$R_n(s) = \int dM_{123}^2 R_{n-2}(s; M_{123}^2, m_4^2, \dots, m_n^2) R_3(M_{123}^2; m_1^2, m_2^2, m_3^2). \quad (4.11)$$

The representation (V.2.10) then permits one to express R_3 in terms of M_{12} and M_{23} with the result

$$R_n(s) = \frac{\pi^2}{4} \int dM_{12}^2 dM_{23}^2 \int dM_{123}^2 M_{123}^{-2} R_{n-2}(s; M_{123}^2, m_4^2, \dots, m_n^2) \times \Theta\{-G(M_{12}^2, M_{23}^2, M_{123}^2, m_2^2, m_1^2, m_3^2)\}. \quad (4.12)$$

The physical region in the $M_{12}^2 M_{23}^2$ plane is thus the superposition of Dalitz plots for all possible values of M_{123} , which satisfy

$$m_1 + m_2 + m_3 \leq M_{123} \leq \sqrt{s} - m_4 - \dots - m_n. \quad (4.13)$$

Using the results of Section V.2 the physical region comes out to be of the form shown in Figure 4.4(b). The density is given in equation (4.12) by the integral over M_{123}^2 in which the integration interval in M_{123}^2 is determined by $G \leq 0$.

As a second example, consider the invariants M_{123} and M_{234} of a four-particle final state. Starting from the tree diagram of Figure 4.3(c) one writes

$$R_4(s) = \int dM_{23}^2 R_3(s; m_1^2, M_{23}^2, m_4^2) R_2(M_{23}^2; m_2^2, m_3^2) \quad (4.14)$$

and inserts the representation (V.2.10) of R_3 in terms of M_{123}^2 and M_{234}^2 :

$$R_4(s) = \frac{\pi^2}{4s} \int dM_{123}^2 dM_{234}^2 \int dM_{23}^2 R_2(M_{23}^2; m_2^2, m_3^2) \\ \times \Theta\{-G(M_{123}^2, M_{234}^2, s, M_{23}^2, m_1^2, m_4^2)\}. \quad (4.15)$$

Now the physical region in the $M_{123}^2 M_{234}^2$ plane (Figure 4.4(c)) is obtained by superposing Dalitz plots of all allowed masses M_{23} , i.e.

$$m_2 + m_3 \leq M_{23} \leq \sqrt{s} - m_1 - m_4. \quad (4.16)$$

The density is the integral over M_{23}^2 in equation (4.15).

(c) Distribution on the Chew-Low plot

We shall here generalize the results of Section V.5, concerning the Chew-Low plot of a $2 \rightarrow 3$ reaction, to $2 \rightarrow n$ reactions. Consider the invariant momentum transfer $t = (p_a - p_1)^2$ for the process $a + b \rightarrow 1 + \dots + n$.

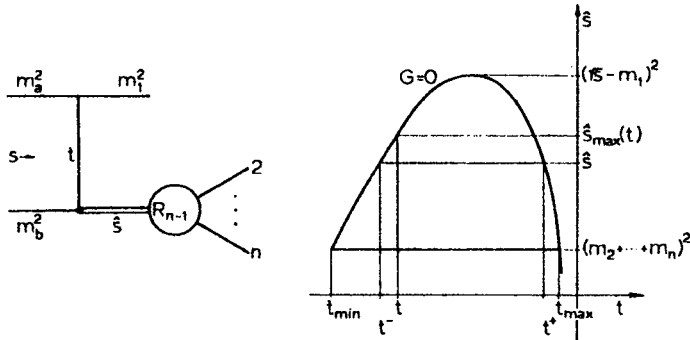


Figure VI.4.5 Physical region in the $\hat{s}\hat{t}$ plane of the process $a + b \rightarrow 1 + \dots + n$, where $t = (p_a - p_1)^2$, $\hat{s} = (p_a + p_b - p_1)^2 = (p_2 + \dots + p_n)^2$

Grouping $2, \dots, n$ together into a system of mass $\sqrt{\hat{s}}$, $\hat{s} = (p_a + p_b - p_1)^2 = (p_2 + \dots + p_n)^2$, we get from equation (2.10)

$$R_n(s) = \int d\hat{s} R_2(s; \hat{s}, m_1^2) R_{n-1}(\hat{s}; m_2^2, \dots, m_n^2). \quad (4.17)$$

If we now write R_2 in terms of an integral over t , as shown by equation (IV.4.24), we find that the phase space distribution over the $\hat{s}\hat{t}$ Chew-Low plot is given by

$$\frac{d^2 R_n(s)}{dt d\hat{s}} = \frac{1}{2} \pi \lambda^{-\frac{1}{2}}(s, m_a^2, m_b^2) R_{n-1}(\hat{s}; m_2^2, \dots, m_n^2) \Theta(-G). \quad (4.18)$$

This can be compared with equation (V.5.17). The boundary of the Chew-Low plot is obtained from

$$G = G(s, t, \hat{s}, m_a^2, m_b^2, m_1^2) \leq 0 \quad (4.19)$$

(compare equation (V.5.9)). The distribution (4.18) is independent of t . It increases with \hat{s} and the rate of this growth increases with n . A further integration over \hat{s} gives the t -distribution

$$\frac{dR_n(s)}{dt} = \frac{1}{2}\pi\lambda^{-\frac{1}{2}}(s, m_a^2, m_b^2) \int_{\hat{s}_{\min}}^{\hat{s}_{\max}} d\hat{s} R_{n-1}(\hat{s}) \Theta\{-G(s, t, \hat{s}, m_a^2, m_b^2, m_1^2)\} \quad (4.20)$$

where

$$\hat{s}_{\max} = \hat{s}^+(t) \quad (4.21)$$

$$\hat{s}_{\min} = \max \{\hat{s}^-(t), (m_2 + \dots + m_n)^2\} \quad (4.22)$$

and s^\pm are given by equation (V.5.11),

$$\begin{aligned} \hat{s}^\pm(t) &= s + m_1^2 - (2m_2^2)^{-1} \{(s + m_a^2 - m_b^2)(m_a^2 + m_1^2 - t) \\ &\quad \mp \lambda^{\frac{1}{4}}(s, m_a^2, m_b^2) \lambda^{\frac{1}{4}}(t_1, m_a^2, m_1^2)\}. \end{aligned} \quad (4.23)$$

Equation (4.20) is a generalization of equation (V.5.18). The lower limit of \hat{s} depends on whether the maximum value $t = (m_a - m_1)^2$ (corresponding to $v_a = v_1$ in any frame) really is attained or not (Figures V.5.3–4). This question was already analyzed exhaustively in connection with $2 \rightarrow 3$ reactions in Section V.5 and to generalize the results obtained there we just have to replace s_2 by \hat{s} and $m_2 + m_3$ by $m_2 + \dots + m_n$. Figure 4.5 is drawn for the case in which $t = (m_a - m_1)^2$ is not attained because the corresponding value of \hat{s} lies below threshold $(m_2 + \dots + m_n)^2$.

The Chew-Low plot is useful in the analysis of dynamics of quasi two-body reactions. If there is a strong resonance at some fixed value of \hat{s} , one can read from the \hat{s} -t Chew-Low plot the t -dependence of the production mechanism of this resonance. In doing this one often measures t not by starting from $t = 0$, but, instead, from the boundary of the plot. The appropriate variable is then $t' = t - t^+$ where the \hat{s} -dependent value of t^+ is given by equation (V.5.11) with $s_2 \rightarrow \hat{s}$.

An application of equation (4.18) is the $F(t)$ -method (Bialkowski, 1967). If one assumes that the matrix element squared of the reaction $a + b \rightarrow 1 + 2 + \dots + n$ depends only on t , say as $F(t)$, then the t -distribution (up to a constant) is $w(t) = F(t) dR_n(s)/dt$. The function $F(t)$ may thus be determined by plotting

$$F(t) = \frac{w(t)}{\frac{dR_n}{dt}}, \quad (4.25)$$

where $w(t)$ is the observed t -distribution. Experimental t -distributions go to zero when $t \rightarrow t_{\max}$, but this is a purely kinematic effect because then $dR_n/dt \rightarrow 0$. To isolate the dynamical mechanism one has to divide out the phase space as in equation (4.25). If the matrix element squared T also depends on other variables, $F(t)$ is the average of T integrated over these other variables.

We shall return to the Chew-Low plot in connection with inclusive reactions (Section VII.3). In particular, we shall determine the relation of \hat{s} and t to the components of \mathbf{p}_1 .

(d) One-particle distributions

Choosing particle p_1 from the final state p_1, \dots, p_n , the phase space distribution in its momentum is given by

$$\frac{d^3 R_n}{d^3 p_1} = \frac{1}{2E_1} R_{n-1}\{(p - p_1)^2; m_2, \dots, m_n\}, \quad (4.26)$$

with $(p - p_1)^2 = \hat{s} = (p_2 + \dots + p_n)^2$. This distribution is frame-dependent. Using standard methods of changing variables one may further modify equation (4.26) to give the distribution in any set of independent variables which specify the vector \mathbf{p}_1 . For instance, introducing t and \hat{s} and integrating over rotations around the beam axis will lead back to equation (4.18). These results for one-particle distributions for exclusive reactions are important in practice, but since they are essentially the same as those for inclusive reactions we shall present them in detail only in Chapter VII.

(e) Two-particle distributions

Choosing particles p_1 and p_2 from the final state p_1, p_2, \dots, p_n , we have in analogy with equation (4.26):

$$\frac{d^6 R_n}{d^3 p_1 d^3 p_2} = \frac{1}{4E_1 E_2} R_{n-2}\{(p - p_1 - p_2)^2; m_3, \dots, m_n\}, \quad (4.27)$$

where

$$\begin{aligned} (p - p_1 - p_2)^2 &= M_{3\dots n}^2 \\ &= (p_3 + \dots + p_n)^2. \end{aligned} \quad (4.28)$$

Again it is straightforward to introduce other sets of variables to describe the six components of \mathbf{p}_1 and \mathbf{p}_2 . The distribution (4.27) is six-dimensional and several complicated integrations are needed to obtain the distribution in some interesting variable. As an example we quote the result (Nyborg, 1967, Exercise VI.9) for the distribution in the cosine of the CMS angle θ_{12} between \mathbf{p}_1 and \mathbf{p}_2 . This is

$$\frac{dR_n(s)}{d \cos \theta_{12}} = \pi^2 \int dM_{3\dots n}^2 dP_1 \frac{P_1^2 P_2^2 R_{n-2}(M_{3\dots n}^2; m_3, \dots, m_n)}{E_1 \{(\sqrt{s} - E_1)P_2 + P_1 E_2 \cos \theta_{12}\}}, \quad (4.29)$$

where $P_2 = P_2(\cos \theta_{12})$ is the solution of

$$\sqrt{s} = (P_1^2 + m_1^2)^{\frac{1}{2}} + (P_2^2 + m_2^2)^{\frac{1}{2}} + (P_1^2 + P_2^2 + 2P_1 P_2 \cos \theta_{12} + M_{3...n}^2)^{\frac{1}{2}}. \quad (4.30)$$

A particularly interesting property of equation (4.27) is that it predicts that there are correlations between \mathbf{p}_1 and \mathbf{p}_2 , which are purely kinematic. Thus equation (4.27) is not a product of two one-particle distributions (4.26). These correlations will be analysed in more detail in Section VII.7.

5. Transverse-cut phase space

A three-momentum \mathbf{p}_i can be split into the component q_i parallel to the incident beam, the longitudinal component, and the component \mathbf{r}_i perpendicular to the incident beam, the transverse component:

$$\mathbf{p}_i = (E_i, q_i, \mathbf{r}_i), \quad (5.1)$$

$$E_i^2 = q_i^2 + m_i'^2, \quad (5.2)$$

$$m_i'^2 = \mathbf{r}_i^2 + m_i^2. \quad (5.3)$$

Here \mathbf{r}_i is a two-dimensional vector in a plane perpendicular to the beam and is invariant under all longitudinal Lorentz transformations (Lorentz transformations parallel to the beam). In equation (5.3) and in the following, quantities obtained by separating the longitudinally invariant part (m_i') from a Lorentz invariant quantity (m_i) are denoted by a prime. The vector q_i is one-dimensional and one has to specify in which one of the standard frames it is defined: q_i^*, q_i^T or q_i^B in the CMS, TS or BS, respectively.

An outstanding feature of multiparticle processes is that the average transverse momentum $\langle r_i \rangle$ of a produced particle is of the order of 0.3 to 0.4 GeV/c and almost independent of the type and number of particles and of the incident energy. In fact, the r_i -distributions are fairly well represented by functions of the form

$$w(r) = \frac{b^{a+1} r^a e^{-br}}{\Gamma(a+1)}, \quad (5.4)$$

with $a \geq 1, b \approx 5$, leading to

$$\begin{aligned} \langle r \rangle &= \int_0^\infty dr r w(r) \\ &= \frac{\Gamma(a+2)}{b\Gamma(a+1)} \simeq 0.4 \text{ GeV/c}. \end{aligned} \quad (5.5)$$

The dynamical origin of this general cut in transverse momenta is not yet understood.

On the other hand, longitudinal momenta q_i of produced particles depend strongly on the incident energy and the type and multiplicity of the particles. At any energy, the observed values of q_i are distributed over a sizable part of the kinematically allowed q_i -interval (e.g. $-\frac{1}{2}\sqrt{s} \leq q_i^* \leq \frac{1}{2}\sqrt{s}$), and thus the distribution in q_i is markedly different from the r_i -distribution which is limited to the small interval $r_i \lesssim 1 \text{ GeV}/c$. The region actually populated by final state momenta of a $2 \rightarrow n$ reaction is thus not spherical, as would follow from phase space, but rather resembles a cigar. We shall refer to the corresponding subregion of the $3n - 4$ dimensional phase space as the *transverse-cut phase space*. When the incident energy increases, the $2n - 2$ transverse dimensions of this region remain constant while its $n - 2$ longitudinal CMS dimensions increase as \sqrt{s} . The region can be regarded as an $n - 2$ dimensional surface in the $3n - 4$ dimensional space, which has a thickness of the order of $0.5 \text{ GeV}/c$ in $2n - 2$ dimensions. The thickness is almost constant with increasing energy. In contrast, the size of the $n - 2$ dimensional surface increases with increasing incident energy.

At low energy, more accurately when \sqrt{s}/n is small enough, the momenta of emitted particles are so small that the transverse cut has no effect. The transition in \sqrt{s} or in n from the low energy region where the whole phase space is important to the region where the transverse cut is important is gradual and vaguely defined.

As the behaviour in transverse and longitudinal directions is so drastically different at high energy, it is evident that in kinematical analysis one should separate transverse and longitudinal degrees of freedom. Using equations (5.1-3) and $d^3 p_i = d^2 r_i dq_i$, the phase space integral takes the form

$$\begin{aligned} R_n(s) &= R_n(E, q, \mathbf{r}; m_i) \\ &= \int \prod_1^n (d^2 r_i) \delta^2(\Sigma \mathbf{r}_i - \mathbf{r}) \int \prod_1^n \frac{dq_i}{2E_i} \delta(\Sigma q_i - q) \delta(\Sigma E_i - E) \quad (5.6) \\ &= \int \prod_1^n (d^2 r_i) \delta^2(\Sigma \mathbf{r}_i - \mathbf{r}) L_n(E, q; r_i^2 + m_i^2). \end{aligned}$$

Here

$$\begin{aligned} L_n(s) &= L_n(E, q; m_i) \\ &= \int \prod_1^n \frac{dq_i}{2E_i} \delta(\Sigma q_i - q) \delta(\Sigma E_i - E), \quad (5.7) \end{aligned}$$

with the definitions (5.2) and (5.3), is the *longitudinal phase space integral* (Huang, 1967). L_n is thus the phase space integral in a space with one space and one time dimension. Due to the Lorentz invariance, it is a function only

Tu ma byæ str 190

Tu ma byæ str 191

$L_2(s') \simeq 1/s'$ as given by equation (5.12) and then iterate this by equation (5.14). One has to be careful in picking out the dominant terms, and we leave the details to an exercise (Exercise VI.15). The answer comes out to be

$$L_n^{\text{ER}}(s') = \frac{n(n-1)}{2^{n-1}} \cdot \frac{1}{s'} (\log s')^{n-2} \left\{ 1 + O\left(\frac{n}{\log s'}\right) \right\} \quad (5.17)$$

Since equation (5.17) is valid for $\log s' \gg n$, the scale of s' in the logarithm is irrelevant. The origin of the logarithms is easy to understand: they come from the $1/q_i$ -factors and the power is $n - 2$ since there are $n - 2$ independent q_i 's.

To determine the volume of the $n - 2$ dimensional surface we note that it is longitudinally invariant and take $(E, q, r) = (\sqrt{s}, 0, \mathbf{0})$ in equation (5.6) so that $s = s'$. Secondly, the limit in equation (5.17) does not depend on m'_i so that asymptotically L_n^{ER} comes outside of the integral in equation (5.6). Putting in a matrix element describing the cut this leaves us with the integral

$$I = \int \prod_{i=1}^n (d^2 r_i) \delta^2(\sum r_i) T_n(r_1, \dots, r_n) \quad (5.18)$$

taken over the transverse dimensions of the surface. We could describe the transverse cut by introducing cut-off functions of the type $\Theta(a_i - r_i)$ or $\exp(-a_i r_i)$ or $\exp(-a_i r_i^2)$ in equation (5.18) (Exercise VI.16), where, in a first approximation, the a_i are energy-independent. However, the main point is that equation (5.18) is energy-independent provided that the transverse cut is. We can thus write

$$\text{ER volume of transverse-cut phase space} = \text{constant} \times (1/s)(\log s)^{n-2} \quad (5.19)$$

where the n -dependent constant can be read from equations (5.17–18). The volume thus goes down when s increases. This may sound contradictory as the size of the surface evidently increases. The explanation is that the average value of the factor $\prod_i (2E_i)^{-1}$ in the integrand decreases.

6. Longitudinal phase space

As defined earlier, the $n - 2$ dimensional longitudinal phase space (LPS) is determined by imposing the conditions

$$\sum_{i=1}^n q_i = 0 \quad (6.1)$$

$$\begin{aligned} \sum_{i=1}^n E_i &= \sum_{i=1}^n (q_i^2 + m_i'^2)^{\frac{1}{2}} \\ &= \sqrt{s} \end{aligned} \quad (6.2)$$

on the n Euclidian coordinates q_i . Following the original treatment (Van Hove, 1969), we analyse the structure of LPS in this section. To understand the treatment of arbitrary n , it may be convenient to follow in parallel the case $n = 3$ presented below. Only the situation in the CMS will be discussed (for arbitrary frames, see Kajantie, 1972b), and we omit the asterisks from the q_i^* 's.

By imposing equations (6.1–2) successively one may define the following spaces.

1. The n dimensional Euclidian space S_n of the n vectors q_i . This is the analogue of the $3n$ dimensional momentum space of the vectors p_i .
2. The $n - 1$ dimensional space Q_{n-1} of the vectors q_i satisfying $\sum q_i = q (= 0)$.
3. The $n - 2$ dimensional space L_{n-2} of the vectors q_i satisfying $\sum q_i = q (= 0)$ and $\sum E_i = E (= \sqrt{s})$. The condition $\sum E_i = E$ depends on m'_i , that is on the fixed values of r_i . We shall call this space the longitudinal phase space in analogy with our convention of calling the $3n - 4$ dimensional space of the vectors p_i satisfying $\sum p_i = p$ the phase space (Section III.1). Note that it is Q_{n-1} which is called LPS in (Van Hove, 1969).

The condition (6.1) is symmetric with respect to the q_i and it is natural to take it into account in a symmetric way. This may be done by carrying out an orthogonal transformation in S_n so that one of the new coordinates becomes proportional to $\sum q_i$. Thus we write

$$q_i = \sum_{j=1}^n O_{ij} k_j, \quad (6.3)$$

$$k_i = \sum_{j=1}^n O_{ji} q_j, \quad (6.4)$$

where O is a real orthogonal matrix satisfying

$$\sum_{l=1}^n O_{il} O_{lk} = \delta_{jk}, \quad j, k = 1, \dots, n. \quad (6.5)$$

If we demand that k_n is proportional to $\sum q_i$ we must write

$$k_n = n^{-\frac{1}{2}} \sum_{i=1}^n q_i, \quad (6.6)$$

so that

$$O_{in} = n^{-\frac{1}{2}}, \quad i = 1, \dots, n \quad (6.7)$$

satisfy equation (6.5) for $j = k = n$. The remaining elements of O can be

chosen in many different ways, but the following choice is common:

$$O = \begin{bmatrix} \frac{1}{\sqrt{2}} & \frac{1}{\sqrt{6}} & \cdots & \frac{1}{\sqrt{\{(n-1)(n-2)\}}} & \frac{1}{\sqrt{\{n(n-1)\}}} & \frac{1}{\sqrt{n}} \\ -\frac{1}{\sqrt{2}} & \frac{1}{\sqrt{6}} & \cdots & \frac{1}{\sqrt{\{(n-1)(n-2)\}}} & \frac{1}{\sqrt{\{n(n-1)\}}} & \frac{1}{\sqrt{n}} \\ 0 & \frac{-2}{\sqrt{6}} & \cdots & \vdots & \vdots & \vdots \\ \vdots & \vdots & & & & \\ 0 & \cdots & 0 & \cdots & \frac{1}{\sqrt{\{(n-1)(n-2)\}}} & \frac{1}{\sqrt{\{n(n-1)\}}} & \frac{1}{\sqrt{n}} \\ 0 & \cdots & 0 & \cdots & \frac{-(n-2)}{\sqrt{\{(n-1)(n-2)\}}} & \frac{1}{\sqrt{\{n(n-1)\}}} & \frac{1}{\sqrt{n}} \\ 0 & \cdots & 0 & \cdots & 0 & \frac{-(n-1)}{\sqrt{\{n(n-1)\}}} & \frac{1}{\sqrt{n}} \end{bmatrix}. \quad (6.8)$$

Other equally useful forms can be obtained by permuting any of the n rows or any of the first $n-1$ columns or by multiplying by -1 any of the first $n-1$ columns. The Jacobian of the transformation from the q_i to the k_i is unity and integrating over k_n we find from equation (5.7) that $k_n = 0$ in equation (6.6) and that

$$L_n(s) = n^{-\frac{1}{2}} \int dk_1 \dots dk_{n-1} \prod_{i=1}^n (2E_i)^{-1} \delta(\sum E_i - \sqrt{s}). \quad (6.9)$$

The vectors k_1, \dots, k_{n-1} form an orthogonal basis in the space Q_{n-1} .

To dispose of the remaining δ function one introduces spherical coordinates in Q_{n-1} . These are defined by generalizing the well-known three-dimensional case as follows:

$$\begin{aligned} k_1 &= \rho \sin \theta_1 \sin \theta_2 \dots \dots & \sin \theta_{n-3} \cos \theta_{n-2} &= \rho \beta_1 \\ k_2 &= \rho \sin \theta_1 \sin \theta_2 \dots \dots & \sin \theta_{n-3} \sin \theta_{n-2} &= \rho \beta_2 \\ k_3 &= \rho \sin \theta_1 \sin \theta_2 \dots \sin \theta_{n-2} \cos \theta_{n-3} & &= \rho \beta_3 \\ &\vdots & & \\ k_i &= \rho \sin \theta_1 \sin \theta_2 \dots \sin \theta_{n-i+1} \cos \theta_{n-i} & &= \rho \beta_i \\ &\vdots & & \\ k_{n-1} &= \rho \cos \theta_1 & &= \rho \beta_{n-1}, \end{aligned} \quad (6.10)$$

where $0 \leq \rho < \infty$ and $0 \leq \theta_i < \pi$, $0 \leq \theta_{n-2} < 2\pi$ and $\sum_{i=1}^{n-1} \beta_i^2 = 1$. Since

the Jacobian is given by

$$\frac{\partial(k_1, \dots, k_{n-1})}{\partial(\rho, \theta_1, \dots, \theta_{n-2})} = \rho^{n-2} (\sin \theta_1)^{n-3} (\sin \theta_2)^{n-2} \dots \sin \theta_{n-3}, \quad (6.11)$$

we may write

$$dk_1 \dots dk_{n-1} = \rho^{n-2} dq dS_{n-1} \quad (6.12)$$

where

$$dS_{n-1} = d\theta_1 \dots d\theta_{n-2} (\sin \theta_1)^{n-3} \dots \sin \theta_{n-3} \quad (6.13)$$

is the surface element on the unit sphere in an $n - 1$ dimensional Euclidian space. It is easy to compute (Exercise VI.17) that the integral $\int dS_m$ over the sphere is

$$S_m = \frac{2\pi^{m/2}}{\Gamma\left(\frac{m}{2}\right)}. \quad (6.14)$$

Introducing equations (6.10) into equation (6.3) one finds the q_i in terms of ρ and β_i :

$$\begin{aligned} q_i &= \rho \gamma_i, \\ \gamma_i &= \sum_{j=1}^{n-1} O_{ij} \beta_j, \\ \sum_1^n \gamma_i^2 &= 1, \\ \gamma_n &= 0. \end{aligned} \quad (6.15)$$

The condition $\sum E_i = E$ or

$$\sum_{i=1}^n (\rho^2 \gamma_i^2 + m_i'^2)^\frac{1}{2} = \sqrt{s} \quad (6.16)$$

then determines ρ as a function of $\theta_1, \dots, \theta_{n-2}$:

$$\rho = \rho(\theta_1, \dots, \theta_{n-2}). \quad (6.17)$$

Carrying out the integration over ρ by the standard rule (III.2.12) and using the derivative of equation (6.16),

$$\frac{d}{d\rho} \sum_{i=1}^n E_i = \rho \sum_{i=1}^n \gamma_i^2 E_i^{-1},$$

gives L_n in the form

$$L_n(s) = n^{-\frac{1}{2}} \int dS_{n-1} \frac{\rho^{n-3}}{\prod_{i=1}^n (2E_i) \sum_{i=1}^n (\gamma_i^2/E_i)}. \quad (6.18)$$

The δ functions have now been eliminated, but the result is very complicated and further evaluation of L_n has to be done numerically. However, if one now restricts attention to the range of variation of the variables, that is to the geometry of LPS, useful results are obtained for $n = 3$ and 4.

(a) *The case $n = 3$*

When $n = 3$, LPS is one-dimensional, and (setting $\theta_1 = \omega$)

$$\begin{aligned} k_1 &= \rho \cos \omega, \\ k_2 &= \rho \sin \omega. \end{aligned} \quad (6.19)$$

To conform with the conventions of (Van Hove, 1969) we make suitable permutations and one multiplication by -1 in the matrix O in equation (6.8) and transform it to the form

$$O = \begin{bmatrix} 0 & \frac{2}{\sqrt{6}} & \frac{1}{\sqrt{3}} \\ -\frac{1}{\sqrt{2}} & -\frac{1}{\sqrt{6}} & \frac{1}{\sqrt{3}} \\ \frac{1}{\sqrt{2}} & -\frac{1}{\sqrt{6}} & \frac{1}{\sqrt{3}} \end{bmatrix}. \quad (6.20)$$

According to equation (6.3) we then have

$$\begin{aligned} q_1 &= \frac{2}{\sqrt{6}} k_2 \\ q_2 &= -\frac{1}{\sqrt{2}} k_1 - \frac{1}{\sqrt{6}} k_2 \\ q_3 &= \frac{1}{\sqrt{2}} k_1 - \frac{1}{\sqrt{6}} k_2. \end{aligned} \quad (6.21)$$

The Cartesian coordinates k_1, k_2 , or the polar coordinates q, ω in equation (6.19), give a parametrization of the points q_1, q_2, q_3 on the plane $\Sigma q_i = 0$. The values q_i on this plane are described symmetrically in triangular coordinates (Figure 6.1). The LPS region is now a curve determined by solving for $\rho = \rho(\omega)$ from

$$(\rho^2 \gamma_1^2 + m_1^2)^{\frac{1}{2}} + (\rho^2 \gamma_2^2 + m_2^2)^{\frac{1}{2}} + (\rho^2 \gamma_3^2 + m_3^2)^{\frac{1}{2}} = \sqrt{s}, \quad (6.22)$$

where

$$\begin{aligned}\gamma_1 &= \frac{2}{\sqrt{6}} \sin \omega \\ \gamma_2 &= -\frac{1}{\sqrt{2}} \cos \omega - \frac{1}{\sqrt{6}} \sin \omega \\ \gamma_3 &= \frac{1}{\sqrt{2}} \cos \omega - \frac{1}{\sqrt{6}} \sin \omega.\end{aligned}\quad (6.23)$$

A qualitative idea of the behaviour of $\rho(\omega)$ is obtained by assuming $m'_t = 0$ so that equation (6.22) implies

$$|q_1| + |q_2| + |q_3| = \sqrt{s}. \quad (6.24)$$

By considering different combinations of signs, one sees that equation (6.24) is a hexagon in the $k_1 k_2$ plane (Figure 6.1). When m'_t increases, $\rho(\omega)$ decreases

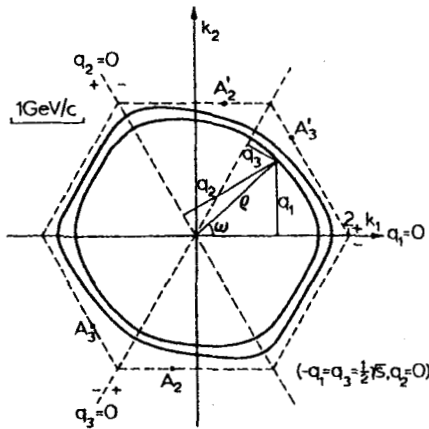


Figure VI.6.1 LPS for $n = 3$. The outer curve shows the boundary of the LPS plot for $\pi N \rightarrow \pi\pi N$ at $\sqrt{s} = 4$ GeV, i.e. $\rho = \rho(\omega)$ for $r_t = 0$. The inner curve corresponds to $r_1 = r_2 = 0.4, r_3 = 0.5$ GeV/c

monotonically. The outermost curve or the boundary of a *LPS plot* is obtained when all transverse momenta vanish, $m'_t = m_t$ (Figure 6.1). When s increases, this curve approaches the hexagon. The experimental events will lie inside this curve. Due to the limitation in transverse momenta they will be concentrated near the boundary. When \sqrt{s} increases, the linear dimensions of the LPS plot in CMS longitudinal momenta increase proportionally to \sqrt{s} , but the width of the populated region is expected to be nearly constant.

This effective one-dimensionality was just the starting point of LPS analysis. The density of events along the one-dimensional LPS is a characteristic of the specific reaction channel.

The LPS density for pure phase space, defined as usual by assuming $T = 1$, is found from equation (6.18) to be

$$\frac{dL_3}{d\omega} = \{8\sqrt{3}(\gamma_1^2 E_2 E_3 + \gamma_2^2 E_1 E_3 + \gamma_3^2 E_1 E_2)\}^{-1}, \quad (6.25)$$

where γ_i are given in equation (6.23) and $E_i^2 = q_i^2 + m_i'^2$ are functions of ω through equations (6.21–22). This equation is valid for fixed transverse momenta. When experimental events of all r_i are plotted as functions of ω , the phase space density is the integral over all r_i with a suitable transverse-cut function $f(r)$:

$$\frac{dR_3}{d\omega} = \int d^2 r_1 d^2 r_2 d^2 r_3 \delta^2(\mathbf{r}_1 + \mathbf{r}_2 + \mathbf{r}_3) \left(\frac{dL_3}{d\omega} \right) \prod_1^3 f(r_i). \quad (6.26)$$

For practical purposes one normally approximates equation (6.26) by equation (6.25). The qualitative behaviour of $dL_3/d\omega$ is again inferred by putting $m'_i = 0$ in equation (6.25). Then $E_i \approx |q_i| \approx \rho |\gamma_i|$ so that

$$\frac{dL_3}{d\omega} = \frac{\rho^2(\omega)}{8\sqrt{(3s)|q_1 q_2 q_3|}}, \quad (6.27)$$

where $\rho(\omega)$ is the radius vector to the hexagon in Figure 6.1. The distribution in ω has strong peaks at $q_i = 0$, arising mainly from the factor $1/\Pi E_i$ in the definition of L_n . The asymptotic singularities at $q_i = 0$ show that a LPS plot is not a convenient tool for investigating events having one slow particle in CMS.

For many purposes it is important to know how other commonly used variables (Chapter V) behave as functions of ω at fixed r_i . We shall consider s_1, s_2, t_1 and t_2 . The qualitative behaviour of these is again seen clearly by putting $m'_i = 0$. In the CMS one has

$$\begin{aligned} s_1 &= m_1^2 + m_2^2 + 2E_1 E_2 - 2q_1 q_2 - 2\mathbf{r}_1 \cdot \mathbf{r}_2 \\ &\simeq 2(|q_1| |q_2| - q_1 q_2) \\ s_2 &\simeq 2(|q_2| |q_3| - q_2 q_3) \\ t_1 &= m_1^2 + m_2^2 - 2E_1 E_2 + 2q_1 q_2 \\ &\simeq -\sqrt{s}(|q_1| - q_1) \\ t_2 &\simeq -\sqrt{s}(|q_3| + q_3). \end{aligned} \quad (6.28)$$

For $m'_i = 0$ the q_i are practically linear functions of ω , which leads to the pattern shown in Figure 6.2. With $m'_i \neq 0$ the corners would be rounded off.

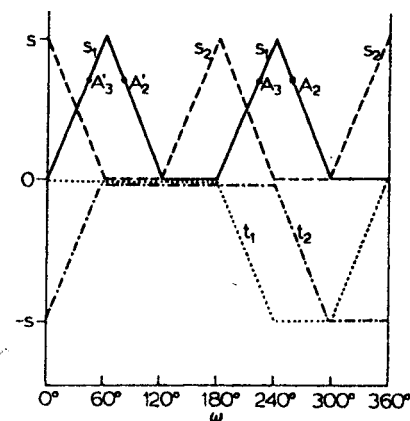


Figure VI.6.2 Behaviour of s_1, s_2, t_1, t_2 as functions of ω when $m'_i = 0$. The linear shape of the curves is only approximate

The regions in which the invariants are near zero can be characterized as follows.

$s_1 \approx 0$: Particles 1 and 2 both move forward or both backward. Since $m'_i = 0$ their velocities are equal (velocity of light) and since the velocities are equal, s_1 attains its threshold value = 0 (equation (II.2.16)). The region $s_2 \approx 0$ is interpreted similarly.

$t_1 \approx 0$: Particle 1 moves forward with the same velocity (velocity of light) as particle a.

$t_2 \approx 0$: Particle 3 moves backward with the same velocity (= velocity of light) as particle b.

One may also see that one value of s_1 corresponds to four values of ω . The points A_2 and A'_2 , and similarly A_3 and A'_3 , in Figure 6.2 lead to the same s_1 since s_1 does not change when forward and backward directions are exchanged. These points are indicated in Figure 6.1. The points A_2, A'_2 correspond to one point A_2 on the boundary of the Dalitz plot in Figure V.3.1, and A_3, A'_3 to the other point A_3 with the same value s_1 .

With the aid of Figures 6.2 and 6.1 we may now also investigate the relation between transverse-momentum and multiperipheral cuts (equations (5.9–10) for $n = 3$). The cut in transverse momentum leads to an essentially one-dimensional distribution of constant width lying near the boundary in Figure 6.1. If the doubly peripheral cut is of the form

$$\exp(at_1 + bt_2), \quad (6.29)$$

and requires both t_1 and t_2 to be small, one sees from Figure 6.2 that this requires $60^\circ < \omega < 180^\circ$. This doubly peripheral cut therefore populates only a part of LPS lying around $\omega = 120^\circ$. By considering all possible permutations of final state particles it appears that one can impose the six doubly peripheral cuts shown in Figure 6.3.

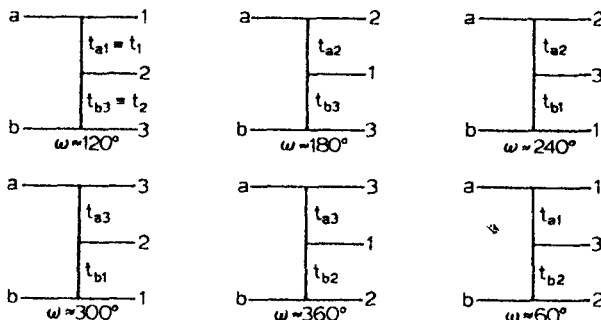


Figure VI.6.3 The six possible doubly peripheral cuts for a $2 \rightarrow 2$ process: the two momentum transfers shown are demanded to be small in absolute value. Each cut populates a region of LPS centred around the value of ω shown

Each cut populates a region of LPS which is centred around the value of ω corresponding to a point of LPS at which the central particle of the diagram in Figure 6.3 has zero longitudinal momentum, and the topmost particle positive longitudinal momentum, and the region extends about 60° to both sides. The cuts, therefore, overlap considerably (Exercise VI.18).

(b) **The case $n = 4$**

When $n = 4$ we write

$$\begin{aligned} k_1 &= \rho \sin \theta_1 \cos \theta_2 \\ k_2 &= \rho \sin \theta_1 \sin \theta_2 \\ k_3 &= \rho \cos \theta_1. \end{aligned} \tag{6.30}$$

Since equation (6.8) is now

$$O = \begin{bmatrix} \frac{1}{\sqrt{2}} & \frac{1}{\sqrt{6}} & \frac{1}{\sqrt{12}} & \frac{1}{2} \\ -\frac{1}{\sqrt{2}} & \frac{1}{\sqrt{6}} & \frac{1}{\sqrt{12}} & \frac{1}{2} \\ 0 & -\frac{2}{\sqrt{6}} & \frac{1}{\sqrt{12}} & \frac{1}{2} \\ 0 & 0 & -\frac{3}{\sqrt{12}} & \frac{1}{2} \end{bmatrix} \tag{6.31}$$

and since one has $k_4 = \sum q_i = 0$, the four q_i are expressed in terms of the three k_i by the equations

$$\begin{aligned} q_1 &= \frac{1}{\sqrt{2}}k_1 + \frac{1}{\sqrt{6}}k_2 + \frac{1}{\sqrt{12}}k_3 \\ q_2 &= -\frac{1}{\sqrt{2}}k_1 + \frac{1}{\sqrt{6}}k_2 + \frac{1}{\sqrt{12}}k_3 \\ q_3 &= -\frac{2}{\sqrt{6}}k_2 + \frac{1}{\sqrt{12}}k_3 \\ q_4 &= -\frac{3}{\sqrt{12}}k_3. \end{aligned} \quad (6.32)$$

The quantities $\gamma_1, \gamma_2, \gamma_3$ and γ_4 are found from $q_i = \rho\gamma_i$ by inserting equation (6.30) in equation (6.32).

As a generalization of Figure 6.1 the four q_i satisfying $q_1 + q_2 + q_3 + q_4 = 0$ are now represented in a symmetric way (Figure 6.4) by identifying the q_i with the distances of a point from four planes $q_i = 0$ in a three-dimensional space. The normals \mathbf{n}_i to these planes are defined by the three first columns of equation (6.31). For instance, one has $\mathbf{n}_1 = (1/\sqrt{2}, 1/\sqrt{6}, 1/\sqrt{12})$, etc., and the \mathbf{n}_i satisfy $\mathbf{n}_i \cdot \mathbf{n}_j = \delta_{ij} - \frac{1}{4}$. The planes are parallel to the sides of a regular tetrahedron.

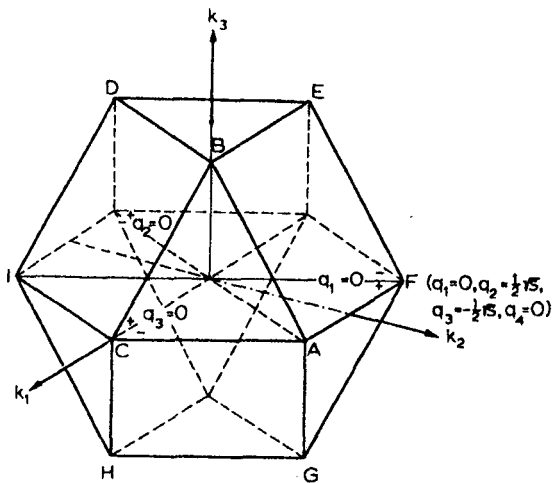


Figure VI.6.4 Coordinate system for $q_1 + q_2 + q_3 + q_4 = 0$. The plane CAF corresponds to $q_4 = 0$, CBE to $q_3 = 0$, ABD to $q_2 = 0$, DEF to $q_1 = 0$. The specifications of the axes on the figure refer to the hexagon CAF.

To see qualitatively what the two-dimensional LPS looks like, we again consider the set of points satisfying energy conservation for $m'_i = 0$:

$$|q_1| + |q_2| + |q_3| + |q_4| = \sqrt{s}. \quad (6.33)$$

It is obvious that the resulting surface must cut a hexagon of each of the planes $q_i = 0$, $i = 1, \dots, 4$. These hexagons are shown in Figure 6.4. If none of the q_i vanishes, one chooses definite signs for them. For instance, if $q_1 > 0$ and $q_2, q_3, q_4 < 0$, equations (6.33) and $\Sigma q_i = 0$ imply that

$$\begin{aligned} q_1 &= \frac{1}{2}\sqrt{s} \\ q_2 + q_3 + q_4 &= -\frac{1}{2}\sqrt{s}. \end{aligned} \quad (6.34)$$

One remains within this part of the surface unless either q_2, q_3 or q_4 vanishes. It is thus the triangle ABC, parallel to the hexagon DEFGHI in Figure 6.4. If $q_1, q_2 > 0$ and $q_3, q_4 < 0$, one has

$$\begin{aligned} q_1 + q_2 &= \frac{1}{2}\sqrt{s} \\ q_3 + q_4 &= -\frac{1}{2}\sqrt{s}. \end{aligned} \quad (6.35)$$

This part of the surface is bounded by a line on which one of the q_i changes sign. There are four possible q_i and the part of the plane obtained is the rectangle ABEF in Figure 6.4. By considering all possibilities one obtains the *cuboctahedron* in Figure 6.4.

When $m'_i > 0$, LPS is obviously a surface lying inside the cuboctahedron. With $s \rightarrow \infty$ this approaches the cuboctahedron. Experimental events with predominantly small transverse momenta will lie near the surface of the cuboctahedron forming an effectively two-dimensional distribution. The question of analysing this two-dimensional distribution is treated in specialized literature, and we do not pursue it further. As a curiosity one might add that the hexagon and cuboctahedron of Figures 6.1 and 6.4, as well as their generalizations, have earlier been met in physics as the weight diagrams of the groups $SU(n)$. For instance, the well-known basic octet or nonet representation of $SU(3)$ is displayed as in Figure 6.1.

7. Physical region in invariant variables

We have seen in earlier chapters how $2 \rightarrow 2$ and $2 \rightarrow 3$ reactions (or, equivalently, $1 \rightarrow 3$ and $1 \rightarrow 4$ decays) can be treated in terms of invariants. We shall now address ourselves to the $1 \rightarrow n$ decay and its crossed channels and formulate a completely Lorentz invariant description of these (Asribekov, 1962a–1962c; Byckling, 1972b; Byers, 1964; Frenkel, 1964; Jacobson, 1966; Kumar, 1969, 1970; McNeil, 1969; Michael, 1966; Morrow, 1966, 1970a; Poon, 1970; Rohrlich, 1965a–1965b; Tarski, 1960). In this section we determine the physical region in terms of invariant variables and in Section 8

the phase space density for some sets of variables. The results in these two sections will be much more mathematical in nature than elsewhere in this book, although the proofs are by no means rigorous. For an alternative more rigorous discussion see (Byers, 1964).

(a) *Physical region for the process $l \rightarrow n$ in invariant variables*

We assume

$$0 \rightarrow 1 + 2 + \dots + n \quad (7.1)$$

to be a real physical decay with non-vanishing masses m_i , so that the p_i are forward timelike, $p_i^2 = m_i^2 > 0$ and $E_i (\geq m_i) > 0$, $i = 1, \dots, n$. A natural set of invariant variables is the set of scalar products

$$x_{ij} = p_i \cdot p_j = m_i m_j \cosh \zeta_{ij}, \quad 1 \leq i \leq j \leq n. \quad (7.2)$$

This equation also defines the variables ζ_{ij} : they are the relative rapidities of particles i and j . The x_{ij} are linearly related to two particle invariant masses by

$$s_{ij} = m_i^2 + m_j^2 + 2x_{ij}. \quad (7.3)$$

The invariant masses $s_{i_1 \dots i_k} = (p_{i_1} + p_{i_2} + \dots + p_{i_k})^2$ of three or more particles are also linear combinations of the x_{ij} , and the same is true for any momentum transfers.

The set (7.2) contains $\frac{1}{2}n(n - 1)$ quantities x_{ij} . They are clearly not independent for $n \geq 4$. There are $3n - 7$ free invariant variables, and thus there must be $\frac{1}{2}(n^2 - n) - (3n - 7) = \frac{1}{2}(n^2 - 7n + 14)$ relations between the x_{ij} . One of these is the invariant equation due to four-momentum conservation, $m_0^2 = (\sum p_i)^2$ or

$$\sum_{1 \leq i < j \leq n} x_{ij} = \frac{1}{2} \left(m_0^2 - \sum_1^n m_i^2 \right) \equiv K. \quad (7.4)$$

The remaining $\frac{1}{2}(n - 3)(n - 4)$ equations are Gram determinant conditions expressing the fact that in a four-dimensional space five or more vectors are always linearly dependent (see the discussion below equation (A.8)).

In part (a) of this section we shall determine the necessary and sufficient conditions that the variables x_{ij} have to satisfy to correspond to a set of physical momenta p_1, \dots, p_n . By physical we mean that the components p_i^μ are real and one has $p_i^2 = m_i^2$, $i = 1, \dots, n$. To do this it is useful to define the matrix of the components p_i^μ :

$$A = \begin{bmatrix} p_1^0 & p_2^0 & \dots & p_n^0 \\ p_1^1 & p_2^1 & \dots & p_n^1 \\ p_1^2 & p_2^2 & \dots & p_n^2 \\ p_1^3 & p_2^3 & \dots & p_n^3 \end{bmatrix}. \quad (7.5)$$

If A^T is the transpose of A , we have

$$A^T g A = X \quad (7.6)$$

where g is the metric matrix of equation (II.1.5) and X is the matrix of the scalar products x_{ij} :

$$X = (x_{ij}) = \begin{bmatrix} p_1^2 & p_1 \cdot p_2 & \cdots & p_1 \cdot p_n \\ p_2 \cdot p_1 & p_2^2 & \cdots & p_2 \cdot p_n \\ \vdots & \vdots & \ddots & \vdots \\ p_n \cdot p_1 & p_n \cdot p_2 & \cdots & p_n^2 \end{bmatrix}. \quad (7.7)$$

$\text{Det } X$ is the Gram determinant $\Delta_n(p_1, \dots, p_n)$.

Now, because X is symmetric there exists an orthogonal matrix U which diagonalizes X . The elements of the diagonal matrix $Y = UXU^T$ are

$$\begin{aligned} y_{ij} &= \sum_{k,l} u_{ik} u_{jl} x_{kl} \\ &= \left(\sum_k u_{ik} p_k \right) \cdot \left(\sum_l u_{jl} p_l \right) \\ &\equiv q_i \cdot q_j. \end{aligned} \quad (7.8)$$

where the q_i are orthogonal four-vectors related to p_i by

$$q_i = \sum_k u_{ik} p_k, \quad i = 1, \dots, n. \quad (7.9)$$

Since U is orthogonal, these equations may be solved to give

$$p_i = \sum_k u_{ki} q_k, \quad i = 1, \dots, n. \quad (7.10)$$

Equations (7.9–10) show that the sets p_1, \dots, p_n and q_1, \dots, q_n span the same space. If this is the Lorentz-space, so that four of the q_i are linearly independent, then one of these four must be timelike and three must be spacelike. The remaining $n - 4$ q_i can be orthogonal to all four basis vectors only by being zero-vectors. Choosing an appropriate ordering of indices of the eigenvalues or diagonal elements λ_i of Y , we get

$$q_i \cdot q_j = \lambda_{i-1} \delta_{ij} \quad (7.11)$$

$$\begin{aligned} \lambda_0 &> 0, & \lambda_1 &< 0, & \lambda_2 &< 0, & \lambda_3 &< 0, \\ \lambda_4 &= \dots = \lambda_{n-1} = 0. \end{aligned} \quad (7.12)$$

Because U is orthogonal, $\lambda_0, \dots, \lambda_{n-1}$ are also eigenvalues of X .

It is clear that there is a frame Q in which the q_i are given by

$$\begin{aligned} q_1 &= (\sqrt{\lambda_0}, 0, 0, 0) \\ q_2 &= (0, \sqrt{(-\lambda_1)}, 0, 0) \\ q_3 &= (0, 0, \sqrt{(-\lambda_2)}, 0) \\ q_4 &= (0, 0, 0, \sqrt{(-\lambda_3)}) \\ q_i &= (0, \dots, 0), \quad i = 5, \dots, n. \end{aligned} \tag{7.13}$$

Just as A in equation (7.5) is formed from the components of the p_i , we may define a matrix B formed from the q_i :

$$B = \begin{bmatrix} \sqrt{\lambda_0} & 0 & 0 & 0 & \dots & 0 \\ 0 & \sqrt{(-\lambda_1)} & 0 & 0 & \dots & 0 \\ 0 & 0 & \sqrt{(-\lambda_2)} & 0 & \dots & 0 \\ 0 & 0 & 0 & \sqrt{(-\lambda_3)} & \dots & 0 \end{bmatrix}. \tag{7.14}$$

Any set q_i satisfying equation (7.11) can be obtained by a Lorentz transformation L from equation (7.13). Thus equation (7.10) implies

$$A = LBU. \tag{7.15}$$

We have shown that if p_1, \dots, p_n are physical, the eigenvalues of $X = (x_{ij})$ satisfy equation (7.12). Conversely, if the eigenvalues of the matrix X of scalar products satisfy equation (7.12), then $A = BU$ (where B is defined in equation (7.14) and U is a matrix that diagonalizes X) gives an explicit realization p_1, \dots, p_n of X . We will later show that this configuration is essentially unique by constructing p_1, \dots, p_n explicitly (see equations (7.31) and (7.33)). Thus we have the following theorem (Byers, 1964):

Theorem 1. There exists a physical momentum configuration p_1, \dots, p_n , if and only if the matrix $X = (x_{ij})$ has 1 positive, 3 negative and $n - 4$ zero eigenvalues. This configuration is unique, apart from an overall space reflection and a proper orthochronous Lorentz transformation.

To apply Theorem 1, it is useful to introduce the equation that determines the eigenvalues of X , the characteristic equation of X . By some algebraic manipulations one sees that this is given by

$$\lambda^n - \bar{\Delta}_1 \lambda^{n-1} - \dots - \bar{\Delta}_{d+1} \lambda^{n-d-1} - \bar{\Delta}_{d+2} \lambda^{n-d-2} - \dots - \bar{\Delta}_n = 0, \tag{7.16}$$

where

$$\bar{\Delta}_l = (-1)^{l-1} \sum \Delta_l(p_{i_1}, p_{i_2}, \dots, p_{i_l}) \tag{7.17}$$

is the sum of all $l \times l$ diagonal minors of $\text{Det } X$. The terms of equation (7.17) are symmetric Gram determinants (equation (A.2)),

$$\Delta(p_{i_1}, \dots, p_{i_l}) = \text{Det}(x_{ij}) \quad i, j = i_1, \dots, i_l, \quad (7.18)$$

where i_1, \dots, i_l is a subset of the indices $1, \dots, n$. Special cases of $\bar{\Delta}_l$ are

$$\begin{aligned} \bar{\Delta}_1 &= \sum m_i^2 = \text{Tr } X, \\ \bar{\Delta}_n &= (-1)^{n-1} \Delta_n(p_1, \dots, p_n) = (-1)^{n-1} \text{Det } X. \end{aligned} \quad (7.19)$$

The quantity $\bar{\Delta}_l$ is an l th degree polynomial in the variables x_{ij} and is of second degree in any one of the x_{ij} .

According to Theorem 1, equation (7.16) must have $n - 4$ zero eigenvalues. From equation (7.16) this is seen to imply \diamond

$$\bar{\Delta}_5 = 0, \dots, \bar{\Delta}_n = 0. \quad (7.20)$$

When equation (7.20) is satisfied, $\mu = 1/\lambda$ satisfies

$$\bar{\Delta}_4\mu^4 + \bar{\Delta}_3\mu^3 + \bar{\Delta}_2\mu^2 + \bar{\Delta}_1\mu - 1 = 0. \quad (7.21)$$

It is easy to see by drawing the curve (7.21) and by considering its value at $\mu = 0$ and derivative for $\mu > 0$ that equation (7.21) has one positive and three negative solutions if

$$\bar{\Delta}_1 > 0, \quad \bar{\Delta}_2 > 0, \quad \bar{\Delta}_3 > 0, \quad \bar{\Delta}_4 > 0. \quad (7.22)$$

The necessity of equations (7.20) and (7.22) follows by a simple argument, and we have obtained (Byers, 1964):

Theorem 2. The necessary and sufficient condition for X to correspond to a physical set p_1, \dots, p_n is given by equations (7.20) and (7.22).

We conclude part (a) of this section with a few remarks:

- (1) We saw after equation (7.4) that the x_{ij} must be related by $\frac{1}{2}(n-3)(n-4)$ Gram determinant conditions while the number of equations in equation (7.20) is only $n - 4$. When these equations are supplemented by the requirement that all x_{ij} be real, however, then the system (7.20) leaves only the required number of free parameters. As a trivial example of an analogous situation, $x^2 + y^2 + z^2 = 3$ and $xyz = 1$ have a one parameter set of solutions. However, if x, y, z must be real, only $x^2 = y^2 = z^2 = 1$ is a solution, because the two surfaces only touch at a point. Because the solutions of equation (7.20) are similarly singular points, the application of equation (7.20) is difficult in practice. Another problem is that, for large n , the number of terms in equation (7.17) is very large ($n!/(n-l)!l!$).

- (2) The elements of X are $x_{ij} = m_i m_j \cosh \zeta_{ij}$ where ζ_{ij} is the relative rapidity. By making the transformation

$$x_{ij} = m_i m_j \gamma_{ij}, \quad (7.23)$$

where the Lorentz factors

$$\begin{aligned}\gamma_{ij} &= \cosh \zeta_{ij} \\ &= u_i \cdot u_j\end{aligned} \quad (7.24)$$

are scalar products of velocity four-vectors, the masses can be eliminated. We define

$$\begin{aligned}X' &= (\gamma_{ij}) \\ \Delta'_i &= \Delta_i(u_{i_1}, \dots, u_{i_i}) \\ \bar{\Delta}'_i &= (-1)^{i-1} \sum \Delta'_i(u_{i_1}, \dots, u_{i_i}).\end{aligned} \quad (7.25)$$

From equation (A.4) it follows that

$$\Delta_i = \prod m_i^2 \Delta'_i \quad (7.26)$$

and therefore $\bar{\Delta}_i = 0$ is equivalent to $\bar{\Delta}'_i = 0$. In Theorems 1 and 2, $X = (x_{ij})$ can thus be replaced by $X' = (\gamma_{ij})$. Because the γ_{ij} do not depend on masses, the physical regions defined by Δ'_i are *universal*, valid for any nonvanishing masses.

- (3) We defined U as the matrix which diagonalizes $X = A^T g A$. Similarly, the equation

$$\begin{aligned}AA^T g &= LB U U^T B^T L^T g \\ &= L(BB^T g)L^{-1}\end{aligned} \quad (7.27)$$

(see equation (II.1.7)), shows that L^{-1} is the Lorentz transformation which diagonalizes $AA^T g$. This L specifies a definite Lorentz frame: the frame which is obtained from the original one by making the Lorentz transformation L^{-1} . In the new frame the components of the four-momentum vectors are the elements of the matrix.

$$L^{-1} A = B U, \quad (7.28)$$

where we have used equation (7.15). The matrix $B U$ has the property that

$$B U (B U)^T = B B^T \quad (7.29)$$

is diagonal with diagonal elements $|\lambda_\mu|$. Thus in this frame the rows of the matrix of momentum components,

$$a^\mu = (p_1^\mu, \dots, p_n^\mu) \quad \mu = 0, 1, 2, 3, \quad (7.30)$$

are orthogonal in the Euclidian metric of an n -dimensional space. This frame is easily seen to be the frame Q defined in equation (7.13).

Example 1: Let p_1 and p_2 be two two-vectors, $p_i = (E_i, P_i)$. If ζ is the relative rapidity of 1 and 2, the matrix X is

$$X = \begin{bmatrix} m_1^2 & m_1 m_2 \cosh \zeta \\ m_1 m_2 \cosh \zeta & m_2^2 \end{bmatrix}.$$

The roots of the eigenvalue equation $\lambda^2 - (m_1^2 + m_2^2)\lambda - m_1^2 m_2^2 \sinh^2 \zeta = 0$ are

$$\lambda_{0,1} = \frac{1}{2}(m_1^2 + m_2^2) \left[1 \pm \sqrt{1 + \frac{(2m_1 m_2)^2}{(m_1^2 + m_2^2)^2} \sinh^2 \zeta} \right].$$

The eigenvalue λ_0 is always positive; λ_1 is negative and vanishes at the boundary of the physical region, $\zeta = 0$. The vectors in the frame Q are

$$\begin{aligned} p_1 &= (\sqrt{\lambda_0} \cos \frac{1}{2}\alpha, -\sqrt{(-\lambda_1)} \sin \frac{1}{2}\alpha), \\ p_2 &= (\sqrt{\lambda_0} \sin \frac{1}{2}\alpha, \sqrt{(-\lambda_1)} \cos \frac{1}{2}\alpha). \end{aligned}$$

with α given by $\cos \alpha = |m_1^2 - m_2^2|/(\lambda_0 - \lambda_1)$. For equal masses one has $\alpha = \pi/2$, $P_1 = -P_2$, and the frame Q , defined in equation (7.13), coincides with the CMS.

(b) Unsymmetric sets of invariants

The complexity of equations (7.20) and the singular nature of their solutions forces one to search for simpler invariant descriptions. These can be obtained at the cost of giving up symmetry in the particle indices. Various choices of invariant variables are given in (Asribekov, 1962a–1962c; Frenkel, 1964; Rohrlich, 1965a–1965b).

Assume that p_1, p_2, p_3, p_4 are physical. In the frame $R(1, 2, 3)$, Figure II.7.1, the set is of the form given in equations (II.7.1). Using equations (7.3), (7.8), (7.10), (7.15) and (7.18) of Chapter II, equations (II.7.1) become

$$p_1 = [\{\Delta_1(p_1)\}^{\frac{1}{4}}, 0, 0, 0]$$

$$\begin{aligned} p_2 &= \left[\frac{G(p_1)}{\{\Delta_1(p_1)\}^{\frac{1}{4}}}, 0, 0, \sqrt{\frac{-\Delta_2(p_1, p_2)}{\Delta_1(p_1)}} \right] \\ p_3 &= \left[\frac{G(p_1)}{\{\Delta_1(p_1)\}^{\frac{1}{4}}}, \sqrt{\frac{\Delta_3(p_1, p_2, p_3)}{-\Delta_2(p_1, p_2)}} \right]^{\frac{1}{4}}, 0, \frac{-G(p_1, p_2)}{\{\Delta_1(p_1)\Delta_2(p_1, p_2)\}^{\frac{1}{4}}}, \\ p_4 &= \left[\frac{G(p_1)}{\{\Delta_1(p_1)\}^{\frac{1}{4}}}, \frac{G(p_1, p_2, p_3)}{\{\Delta_1(p_1)\Delta_2(p_1, p_2)\}^{\frac{1}{4}}}, \right. \\ &\quad \left. \pm \sqrt{\frac{-\Delta_4(p_1, p_2, p_3, p_4)}{\Delta_3(p_1, p_2, p_3)}} \right]^{\frac{1}{4}}, \frac{-G(p_1, p_2)}{\{\Delta_1(p_1)\Delta_2(p_1, p_2)\}^{\frac{1}{4}}} \end{aligned} \quad (7.31)$$

The components are real provided that

$$\begin{aligned}\Delta_1(p_1) &> 0, \\ \Delta_2(p_1, p_2) &< 0, \\ \Delta_3(p_1, p_2, p_3) &> 0, \\ \Delta_4(p_1, p_2, p_3, p_4) &< 0.\end{aligned}\tag{7.32}$$

The necessity of these conditions follows from equation (7.22), since $(-1)^{l-1} \Delta_l = \bar{\Delta}_l > 0$ for physical p_1, \dots, p_l ($l = 1, 2, 3, 4$). Conversely if equations (7.32) are valid for a set $X = (x_{ij})$, equations (7.31) give an explicit realization p_1, \dots, p_4 .

If there are more than four vectors, one can write p_i , $i = 5, \dots, n$, in $R(1, 2, 3)$ in a form similar to p_4 in the last equation (7.31):

$$p_i = \left[\frac{G\begin{pmatrix} p_1 \\ p_i \end{pmatrix}}{\{\Delta_1(p_1)\}^{\frac{1}{2}}, \{-\Delta_2(p_1, p_2)\Delta_3(p_1, p_2, p_3)\}^{\frac{1}{2}}}, \frac{G\begin{pmatrix} p_1, & p_2, & p_3 \\ p_1, & p_2, & p_i \end{pmatrix}}{\{\Delta_1(p_1)\}^{\frac{1}{2}}, \{-\Delta_2(p_1, p_2)\Delta_3(p_1, p_2, p_3)\}^{\frac{1}{2}}}, \right. \\ \left. \pm \frac{-\Delta_4(p_1, p_2, p_3, p_i)}{\Delta_3(p_1, p_2, p_3)} \right]^{\frac{1}{2}}, \frac{-G\begin{pmatrix} p_1, & p_2 \\ p_1, & p_i \end{pmatrix}}{\{-\Delta_1(p_1)\Delta_2(p_1, p_2)\}^{\frac{1}{2}}}, \tag{7.33}$$

provided that

$$\Delta_4(p_1, p_2, p_3, p_i) \leq 0, \quad i = 5, \dots, n. \tag{7.34}$$

As an explicit set of $3n - 6$ invariant variables one may now choose the scalar products

$$\begin{aligned}x_{12}, x_{13}, x_{23}, \\ x_{1i}, x_{2i}, x_{3i},\end{aligned} \quad i = 4, \dots, n. \tag{7.35}$$

Apart from the signs of p_{ij} , the set p_1, \dots, p_n in $R(1, 2, 3)$ is fixed uniquely by inserting these $3n - 6$ quantities in equations (7.31) and (7.33). The mapping from equation (7.35) to equations (7.31) and (7.33) is thus one-to- 2^{n-3} . If, in addition, x_{45}, \dots, x_{4n} are given, they fix the signs of p_5, \dots, p_n . To obtain real momentum components, equations (7.32) and (7.34) must be satisfied, and thus they define the physical region.

If one starts from the set of all $\frac{1}{2}n(n-1)x_{ij}$ s, one must first eliminate the scalar products not included in equation (7.35) by using the $\frac{1}{2}(n-3)(n-4)$ Gram determinant conditions mentioned after equation (7.4). These conditions can be written as (Asribekov, 1962a–1962c)

$$\Delta_5(p_1, p_2, p_3, p_4, p_i) = 0 \quad i = 5, \dots, n \tag{7.36}$$

$$G\begin{pmatrix} p_1, p_2, p_3, p_4, p_i \\ p_1, p_2, p_3, p_4, p_j \end{pmatrix} = 0 \quad 5 \leq i < j \leq n. \tag{7.37}$$

The $\frac{1}{2}(n-4)(n-5)$ equations (7.37) are linear in x_{ij} , $5 \leq i < j \leq n$. The $n-4$ equations (7.36) are quadratic in x_{45}, \dots, x_{4n} and the two solutions give the two signs of p_i^y in equation (7.33). We thus have the following.

Theorem 3. A set $X = (x_{ij})$ with $x_{ij} = x_{ji}$, $x_{ii} = m_i^2 > 0$, $i, j = 1, \dots, n$, corresponds to a physical four-momentum configuration p_1, \dots, p_n , with scalar products $p_i \cdot p_j = x_{ij}$, if and only if there is a permutation of the indices i such that equations (7.32), (7.34) and (7.36–37) are satisfied.

Up to now only final state momenta p_1, \dots, p_n have been considered. Four-momentum conservation allows us to include $x_{0i} = p_0 \cdot p_i$ or any momentum transfers $(p_0 - p_{t_1} - \dots - p_{t_n})^2$ among the variables. Multiplying $p_0 = \sum_i^n p_i$ by p_i one obtains

$$x_{0i} = \sum_{j=1}^n x_{ij} \quad i = 1, \dots, n. \quad (7.38)$$

(c) Physical region for the process $2 \rightarrow n - 1$

The decay (7.1) is related by crossing to a number of other processes. The energies of outgoing and incoming particles (forward and backward timelike vectors) have opposite signs. For a pair of particles, the sign of $x_{ij} = p_i \cdot p_j$ ($= \pm m_i E_j$ in rest frame of i) distinguishes the two cases:

$$x_{ij} \geq m_i m_j$$

$$s_{ij} = (p_i + p_j)^2 \geq (m_i + m_j)^2, \quad (7.39)$$

$$x_{ij} \leq -m_i m_j$$

$$s_{ij} = (p_i + p_j)^2 \leq (m_i - m_j)^2. \quad (7.40)$$

Thus in the space of the x_{ij} ($i, j = 1, \dots, n$), the different physical regions related by crossing are disconnected. The transformation $p_i \rightarrow -p_i$ changes the sign of x_{ij} , and amounts to a transformation from one channel to another. However, changing the signs of all the p_i does not change the matrix X . This means that $0 + \dots + m \rightarrow (m+1) + \dots + n$ and $(m+1) + \dots + n \rightarrow 0 + \dots + m$ have the same physical region in x_{ij} . Thus in the space of invariants there are in all 2^{n-1} disconnected physical regions related by crossing.

According to equations (A.4) and (A.3), $\Delta(p_1, \dots, p_n)$ remains unchanged when an argument p_i changes sign, and an unsymmetric Gram determinant G only changes sign. Thus all the 2^{n-1} physical regions are defined by the same set of conditions (7.32), (7.34) and (7.36–37). To distinguish the reactions the signs of $n-1$ scalar products, (e.g. x_{12}, \dots, x_{1n}) must be fixed. In particular, the physical region for the reaction

$$0 + \bar{n} \rightarrow 1 + \dots + (n-1) \quad (7.41)$$

is specified by Theorem 1, 2 or 3, together with the constraint (7.4) and the conditions $x_{12}, \dots, x_{1,n-1} > 0, x_{1n} < 0$.

Example 2: If we take $n = 3$, the reaction is of the type $0 \rightarrow 1 + 2 + 3$ or $0 + 3 \rightarrow 1 + 2$. The variables are $s = m_1^2 + m_2^2 + 2x_{12}$, $t = m_2^2 + m_3^2 + 2x_{23}$ and $u = m_1^2 + m_3^2 + 2x_{13}$. Equation (7.4) becomes $s + t + u = m_0^2 + m_1^2 + m_2^2 + m_3^2$. The condition $\Delta_3(1, 2, 3) > 0$ defines four physical regions as in Figure IV.5.6. Further, there must be a pair i, j such that $\Delta_2(i, j) < 0$, i.e. $\lambda(s_{ij}, m_i^2, m_j^2) = \{s_{ij} - (m_i + m_j)^2\} \{s_{ij} - (m_i - m_j)^2\} > 0$. This implies

$$s_{ij} > (m_i + m_j)^2$$

or

(7.42)

$$s_{ij} < (m_i - m_j)^2.$$

Comparing this with equations (7.39) and (7.40), these two cases are seen to correspond to different reactions. With the masses of Figure IV.5.6, the central region is forbidden by equation (7.42) and only the s, t, u channels are physical. In Figure IV.5.7 the decay process also satisfies $\Delta_3 > 0, \Delta_2 < 0$.

(d) Decay into four particles

For $1 \rightarrow 4$ there are five independent variables. The set $x_{ij}, 1 \leq i < j \leq 4$, contains six quantities and they are related by equation (7.4). An alternative set is formed by $s_{ij} = m_i^2 + m_j^2 + 2x_{ij}$ which are related by

$$\sum_{i < j} s_{ij} = m_0^2 + 2 \sum_1^4 m_i^2. \quad (7.43)$$

The four three-particle invariant masses are linearly related to s_{ij} :

$$s_{ijk} = s_{ij} + s_{ik} + s_{jk} - m_i^2 - m_j^2 - m_k^2. \quad (7.44)$$

There are many ways to choose five independent variables from the x_{ij}, s_{ij}, s_{ijk} , etc. However, because any two such sets are linearly related, the Jacobian of the transformation from one to the other is simply a constant. Thus, apart from such a trivial linear transformation, the choice of invariant variables is unique here.

The process $1 \rightarrow 4$ is related by crossing to the process $2 \rightarrow 3$. Their invariant descriptions are equivalent; as for $2 \rightarrow 3$, convenient variables for $1 \rightarrow 4$ are often the cyclically symmetric ones: $t_{01} = s_{234}, s_{12}, s_{23}, s_{34}, t_{40} = s_{123}$. The physical region is given by equation (7.32), and can be written in terms of the kinematic functions λ, G , and B .

8. Phase space density in invariant variables

In order to write I_n in terms of a set Φ of invariant variables, one needs the phase space density $\rho_n(\Phi)$ defined in equation (1.2). Integrating over p_n

in R_n gives

$$R_n = \int \prod_{i=1}^{n-1} d^4 p_i \delta(p_i^2 - m_i^2) \delta((p_0 - p_1 - \dots - p_{n-1})^2 - m_n^2). \quad (8.1)$$

Expansion of the argument of the δ function and the use of equation (7.38) show that the last δ function is equal to one half of

$$\begin{aligned} \delta(\xi) &\equiv \delta\left(\sum_{1 \leq i < j \leq n} x_{ij} - K\right) \\ &= \delta\left(\sum_{1 \leq i < j \leq n-1} x_{ij} - \sum_{i=1}^{n-1} x_{0i} - K + m_0^2 - m_n^2\right), \end{aligned} \quad (8.2)$$

with K defined in equation (7.4). Thus we have

$$R_n = \frac{1}{2} \int \prod_{i=1}^{n-1} \frac{d^3 p_i}{2E_i} \delta(\xi). \quad (8.3)$$

We shall now consider $n \leq 4$ and $n > 4$ separately, because the latter involves the difficult constraints (7.20).

(a) The case $n \leq 4$

To write p_i explicitly a Lorentz frame must be defined. As the first step we take rest frame of p_0 . From $x_{01} = m_0 E_1$ we get $\partial x_{01}/\partial P_1 = m_0 P_1/E_1$ and equation (II.7.3) gives

$$\begin{aligned} \int \frac{d^3 p_1}{2E_1} &= 4\pi \int \frac{dP_1 P_1^2}{2E_1} \\ &= 2\pi m_0^{-2} \int dx_{01} \{-\Delta_2(p_0, p_1)\}^{\frac{1}{2}}. \end{aligned} \quad (8.4)$$

Next we take the direction of p_1 as the z axis. The Jacobian

$$\frac{\partial(x_{02}, x_{12})}{\partial(P_2, \cos \theta_{12})} = \frac{m_0 P_1 P_2^2}{E_2} \quad (8.5)$$

and equations (II.7.3) give

$$\begin{aligned} \int \frac{d^3 p_2}{2E_2} &= 2\pi \int \frac{dP_2 P_2^2 d\cos \theta_{12}}{2E_2} \\ &= \pi \int dx_{02} dx_{12} \{-\Delta_2(p_0, p_1)\}^{-\frac{1}{2}}. \end{aligned} \quad (8.6)$$

We now consider $d^3 p_3/2E_3 = dP_3 P_3^2 d\Omega_3/2E_3$ in the frame $R(0, 1, 2)$. Here $x_{03} = m_0 E_3$ gives $dP_3 P_3^2/2E_3 = dx_{03} \{-\Delta_2\}^{\frac{1}{2}}/2m_0^2$, $d\Omega_3$ is obtained directly from equation (II.7.21), and we get

$$\int \frac{d^3 p_3}{2E_3} = \int dx_{03} dx_{13} dx_{23} \{-\Delta_4(p_0, p_1, p_2, p_3)\}^{-\frac{1}{2}}. \quad (8.7)$$

Here one must remember that a set x_{03}, x_{13}, x_{23} corresponds to two values p_3 which are related by a reflection in the p_1, p_2 plane. This has been taken into account by including a factor 2 on the right hand side of equation (8.7). Note also that no Δ_3 appears in equations (8.4–7).

After using equations (8.4–7) the set $x_{ij}, 0 \leq i < j \leq n - 1$, can be directly replaced by the set $x_{ij}, 1 \leq i < j \leq n$, because the Jacobian is unity. Equations (8.3–6) imply for two- and three-particle decays that

$$\begin{aligned} R_2 &= \frac{\pi}{m_0^2} \int dx_{12} (-\Delta_2)^{\frac{1}{2}} \delta(x_{12} - K) \\ &= \frac{\pi}{m_0^2} \{ -\Delta_2(p_0, p_1) \}^{\frac{1}{2}}, \end{aligned} \quad (8.8)$$

$$\begin{aligned} R_3 &= \frac{\pi^2}{m_0^2} \int dx_{12} dx_{23} \\ &= \frac{\pi^2}{4m_0^2} \int ds_{12} ds_{23}, \end{aligned} \quad (8.9)$$

(cf. equations (IV.1.10) and (V.2.10)). The process $1 \rightarrow 4$ involves

$$R_4 = \frac{\pi^2}{m_0^2} \int \prod dx_{ij} (-\Delta_4)^{-\frac{1}{2}} \delta \left(\sum x_{ij} - K \right). \quad (8.10)$$

In going to the five symmetric variables one uses

$$\begin{aligned} s_{34} &= s_{012} \\ &= 2(x_{01} + x_{02} + x_{12}) + \text{masses}, \\ t_{40} &= s_{123} \\ &= 2(x_{12} + x_{13} + x_{23}) + \text{masses}. \end{aligned} \quad (8.11)$$

The Jacobian turns out to be 2^5 and one obtains

$$R_4 = \frac{\pi^2}{32m_0^2} \int \frac{dt_{01} ds_{12} ds_{23} ds_{34} dt_{40}}{(-\Delta_4)^{\frac{1}{2}}}. \quad (8.12)$$

An explicit expression for $-\Delta_4 = \frac{1}{16}B$ is obtained from equations (V.9.4–5) by the replacement $t_1, s_1, s_2, t_2, s \rightarrow t_{01}, s_{12}, s_{23}, s_{34}, t_{40}$.

(b) The case $n > 4$

For $n > 4$ one replaces the index 3 in equation (8.7) by $4, \dots, n - 1$ and substitutes these expressions into equation (8.3) to obtain

$$R_n = \frac{\pi^2}{m_0^2} \int dx_{01} dx_{02} dx_{12} \prod_{i=3}^{n-1} \frac{dx_{0i} dx_{1i} dx_{2i}}{\{ -\Delta_4(p_0, p_1, p_2, p_i) \}^{\frac{1}{2}}} \delta(\xi). \quad (8.13)$$

An equivalent (and trivially related) unsymmetric set of variables was given in equation (7.35) with the corresponding physical region given by equations (7.32 and 34). Replacing p_i , $i = 1, \dots, n$, by linear combinations of the p_s , a large number of different and inequivalent representations are obtained. One way to obtain such formulae is to write the subprocesses of a tree diagram (recursion relation) in terms of purely invariant variables, which then gives a completely invariant parametrization of R_n . An example was mentioned at the end of Section 2, involving the variables t_i, s_i, M_i^2 .

To derive $\rho_n(\Phi)$ for the complete, symmetric set of all x_{ij} , where x_{ij} obey the constraints (7.20), considerably heavier machinery is required. We only quote the relevant results (Byers, 1964, Byckling, 1972b).

The factorization (7.15) implies a corresponding factorization of the differential volume elements of the groups involved. These are the Lorentz group $\{L\}$, the orthogonal group $\{U\}$ and the group $\{B\}$ connected with the 'diagonal' matrices B . Now for $n > 4$, U in equation (7.15) can be replaced by

$$U \rightarrow \begin{bmatrix} I & 0 \\ 0 & V \end{bmatrix} U, \quad (8.14)$$

where I is the 4×4 unit matrix and V is any $(n - 4) \times (n - 4)$ orthogonal matrix, without changing A , because $B_{ij} = 0$ for $j > 4$. Considering all U s related by a transformation (8.14) as equivalent, the number of parameters in the remaining set $\{U'\}$ is $4n - 10$.

The Lorentz group $\{L\}$ involves six parameters, and $\{B\}$ four parameters which can be taken to be $\bar{\Delta}_1, \dots, \bar{\Delta}_4$. Let $d\{U'\}$ and $d\{L\}$ be the volume elements of the set of orthogonal transformations U' and the group of Lorentz transformations L . Then one can prove that

$$\prod_{i=1}^n d^4 p_i = d\{A\} \\ = 2^{-4} \bar{\Delta}_4^{(n-5)/2} d\{U'\} d\{L\} \prod_{i=1}^4 d\bar{\Delta}_i. \quad (8.15)$$

$$= 2^{-4} \prod_{v=1}^{n-4} S_v^{-1} \bar{\Delta}_4^{(n-5)/2} d\{L\} \prod_{0 \leq i \leq j \leq n-1} dx_{ij} \prod_{i=5}^n \delta(\bar{\Delta}_i). \quad (8.16)$$

Here S_v is the surface area of the unit sphere $x_1^2 + \dots + x_v^2 = 1$, see equation (6.14).

Substitution of equation (8.16) into equation (1.2) gives

$$R_n = 2^{-4} \prod_{v=1}^{n-4} S_v^{-1} \int \prod_{i \leq j} dx_{ij} d\{L\} \bar{\Delta}_4^{(n-5)/2} \prod_{i=1}^n \delta(p_i^2 - m_i^2) \\ \times \prod_{i=5}^n \delta(\bar{\Delta}_i) \delta^4(p_0 - \sum p_i).$$

In terms of a Lorentz transformation we can write

$$\delta^4(p_0 - p) = 2m_0^{-2} \delta(m_0^2 - m^2) \delta^3(L_0 - L). \quad (8.18)$$

Factorizing $\{L\}$ into a boost L and 3- and 2-dimensional rotations $\Omega^{(3)}, \Omega^{(2)}$ we get

$$\int dL d\Omega^{(3)} d\Omega^{(2)} \delta^4(p_0 - L \Sigma p_i) = \frac{16\pi^2}{m_0^2} \delta\{m_0^2 - (\Sigma p_i)^2\}. \quad (8.19)$$

Using equation (8.2) and integrating over $p_i^2 = x_{ii}$ we get

$$R_n = \left(\frac{\pi^2}{m_0^2} \prod_{v=1}^{n-4} S_v^{-1} \right) \int \prod_{i < j} dx_{ij} \Delta_4^{(n-5)/2} \prod_{l=5}^n \delta(\Delta_l) \delta(\xi). \quad (8.20)$$

The indices i, j can run either $0, \dots, n-1$ or $1, \dots, n$.

The expression (8.15) can be used to find a representation which is totally invariant, symmetric in particle indices and, instead of $\delta(\Delta_l)$, contains constraints on x_{ii} . Putting equation (8.15) into equation (1.2) and using equation (8.19) we get

$$R_n = \frac{\pi^2}{2m_0^2} \int d\{U'\} \prod_{l=1}^4 d\Delta_l \Delta_4^{(n-5)/2} \prod_{l=1}^n \delta(x_{ii} - m_i^2) \delta(\xi). \quad (8.21)$$

One simple parametrization of $\{U'\}$ is a set of successive rotations $\Omega^{(l)}$, each of which acts in a two-dimensional plane in the l -dimensional space:

$$\{U'\} = (\Omega^{(n)}, \Omega^{(n-1)}, \Omega^{(n-2)}, \Omega^{(n-3)}). \quad (8.22)$$

This set has $4n - 10$ parameters; $\Omega^{(l)}$ needs the specification of the normal to the plane ($l - 2$ parameters) and the angle of rotation.

(c) Collision processes

If one inserts

$$2E_1 \delta^3(\mathbf{p}_1 - \mathbf{p}_a) = \frac{m_b^2}{\pi \lambda^4(s, m_a^2, m_b^2)} \delta\{x_{a1} - \frac{1}{2}(s - m_a^2 - m_b^2)\} \quad (8.23)$$

into equation (1.2) with $p_b \equiv p$ and integrates over \mathbf{p}_1 , the result is exactly $R_{n-1}(p_a, p_b)$ for the process $a + b \rightarrow 2 + \dots + n$. Changing the indices to correspond to the process $a + b \rightarrow 1 + \dots + n$ and integrating over x_{ab} , equations (IV.4.24) and (V.9.2) follow very simply from equations (8.9), (8.12) and (8.23) when $n = 2$ or 3. For $n \geq 4$, equation (8.20) implies

$$R_n(p_a, p_b) = \frac{\frac{1}{2}\pi}{\lambda^4(s, m_a^2, m_b^2)} \prod_{v=1}^{n-3} S_v^{-1} \int dx_{a1} \dots dx_{a,n-1} dx_{b1} \dots dx_{b,n-1} \\ \times \prod_{1 \leq i < j \leq n-1} dx_{ij} \Delta_4^{(n-4)/2} \prod_{l=5}^{n+1} \delta(\Delta_l) \delta(\xi). \quad (8.24)$$

Any one dx in equation (8.24) can be integrated over by using $\delta(\xi)$.

Exercises

- VI.1. Consider a dynamical model according to which the cross section σ_n of an n -particle state is given by

$$\sigma_n(E) = \lambda^n E^{-2} R_n^{\text{ER}}(E),$$

for large CMS total energy E , where R_n^{ER} is given in equation (2.17). Compute

$$(a) \quad \sigma(E) = \sum_{n=2}^{\infty} \sigma_n(E),$$

$$(b) \quad \langle n \rangle = \sum_{n=2}^{\infty} \frac{n\sigma_n(E)}{\sigma(E)}$$

♦

in terms of modified Bessel functions. If the cross section is, instead, defined to be $\sigma_n(E)/\sigma(E)$, show that this implies that the matrix element is effectively such that it exponentially suppresses large three-momenta.

- VI.2. Prove the validity of the non-relativistic form (2.19) of $R_n^{\text{NR}}(M_n^2)$ by replacing M_n in the recursion relation by the kinetic energy $T_n = M_n - \mu_n$.
- VI.3. Show that for $n = 3$ the recursion relation (2.27) is equivalent to equation (V.7.7) so that ϕ_1 can be identified with the Treiman-Yang angle in the 12 rest frame.
- VI.4. What recursion relation is obtained, if one chooses the z axis parallel to the direction of k_{i+2} ($k_{n+1} = p_b$) in the frame $k_{i+1} = 0$ in Figure 2.4 and replaces the polar angle θ_i by the invariant $s_{i+1} = (k_{i+2} - k_i)^2 = (p_{i+2} + p_{i+1})^2$, $p_{n+1} = -p_b$? Show that this relation is equivalent to equation (V.7.8) for $n = 3$.
- VI.5. The minimum of the right hand side of equation (3.49) is obtained when $\cos \omega_j = -1$. From this derive the following condition (Finkelstein, 1968), valid in the multi-Regge limit:

$$\frac{s_1 s_2 \dots s_{n-1}}{s} \leq [\{\sqrt{(-t_1)} + \sqrt{(-t_2)}\}^2 + m_2^2] \dots$$

$$\times [\{\sqrt{(-t_{n-2})} + \sqrt{(-t_{n-1})}\}^2 + m_{n-1}^2].$$

- VI.6. Show that integrating equation (3.50) with $n = 3$ over ω_2 by using the δ function leads to equation (V.11.24) for $d^2\sigma/ds_1 ds_2$.
- VI.7. The boundary of the Chew-Low plot is determined by equation (4.19). Find the slopes of the asymptotes of this curve and show that they are both positive for real particles.

VI.8. Derive the formula

$$R_4 = \frac{1}{2}\pi^2 \int dE_1 dE_2 dE_3 dP_{12} d\phi,$$

where $P_{12} = |\mathbf{p}_1 + \mathbf{p}_2|$ and ϕ is the azimuthal angle of \mathbf{p}_3 with $\mathbf{p}_1 + \mathbf{p}_2$ as axis.

- VI.9. Derive equation (4.29) for the phase space distribution in the cosine of the angle between two CMS momenta in the final state of $p_a + p_b \rightarrow p_1 + \dots + p_n$. What is the result for $n = 3$?
- VI.10. Compute $d^2 R_4/dM_{123}^2 dM_{12}^2$ for a $1 \rightarrow 4$ decay. What is the physical region in the $M_{123} M_{12}$ plane?
- VI.11. What is the physical region in the $M_{1234}^2 M_{3456}^2$ plane of a six-particle final state? What if the final state contains seven particles?
- VI.12. Show that phase space predicts the relation $\langle r_i \rangle = \frac{1}{2}\pi \langle q_i \rangle$ for the expectation values of transverse and CMS longitudinal momenta in a $2 \rightarrow n$ reaction.
- VI.13. Show that the known form of R_2 is obtained if equation (5.12) for L_2 is integrated over \mathbf{r}_1 and \mathbf{r}_2 .
- VI.14. Show by performing an analysis similar to that applied to R_n in Section VI.3 that L_n can be written in the form
- $$L_n(s) = 2^{1-n} \lambda^{\frac{1}{2}}(s, m_a^2, m_b^2) \int dt'_{n-1} \dots dt'_1 \prod_{i=1}^n \lambda^{-\frac{1}{2}}(t'_i, t'_{i-1}, m_i^2) \times \delta\{s - m_a^2 - m_b^2 - 2m_a m_b \cosh(\eta_1 + \dots + \eta_n)\},$$
- where the η_i are given by equation (3.38) generalized in an obvious way to arbitrary n and with t_i replaced by t'_i , $t_n = m_b^2$, $t_0 = m_a^2$.
- VI.15. Prove the validity of the ER limit of L_n given in equation (5.17) by showing that it satisfies equation (5.14).
- VI.16. Evaluate the integrals
- $$I = \int \prod_{i=1}^n \{d^2 r_i f_i(r_i)\} \delta^2(\Sigma \mathbf{r}_i),$$
- where (a) $f_i = \exp(-ar_i)$, (b) $f_i = \exp(-ar_i^2)$.
- VI.17. Verify equation (6.14) giving the area of the unit sphere in m -dimensional Euclidian space.
- VI.18. Determine the regions of LPS populated by the double Regge configurations (equation (V.11.19)) corresponding to the diagrams of Figure 6.3. Is there any overlap?

VII

Inclusive Reactions

1. One-particle distributions

We have so far in this book only treated exclusive reactions. Consider now an inclusive process



where X denotes an unknown system of particles. Experimentally equation (1.1) is realized by having a detection apparatus measuring both the momentum and type of particle c . In this chapter for brevity we omit the index c from variables related to the three-momentum of particle c (E, P, Ω, q, r , etc.), but denote its mass by m_c . One thus measures the quantity

$$\frac{d^3\sigma_c}{d^3p} = \frac{P^{-2} d^3\sigma}{dP d\Omega} \quad (1.2)$$

in the laboratory system. This quantity is a *one-particle distribution* or a *spectrum*. As shown explicitly by equations (III.4.20–22), $d^3\sigma_c/d^3p$ is not Lorentz invariant. Instead we may define the *invariant distribution function*

$$E \frac{d^3\sigma_c}{d^3p} = f(\mathbf{p}; s). \quad (1.3)$$

It is important to realize exactly what the invariance of $f(\mathbf{p}; s)$ means. If $f(\mathbf{p}; s)$ is known in one frame, one can obtain it in another frame in which \mathbf{p} has the value \mathbf{p}' simply by expressing \mathbf{p} as a function of \mathbf{p}' . If E were omitted from the definition (1.3) of f , this procedure would lead to a wrong result unless corrected by a multiplicative Jacobian (equation (III.4.22)).

Processes which contribute to the inclusive cross section $\sigma_c^{incl}(s)$ can produce more than one particle of type c . Defining σ_c^n as the cross-section for producing n particles of type c , we have,

$$\begin{aligned} \sigma_c^{incl}(s) &= \sum_{n=1}^{\infty} n \sigma_c^n(s) \\ &= \langle n_c \rangle \sum_{n=1}^{\infty} \sigma_c^n(s) \\ &= \langle n_c \rangle \sigma_c(s) \end{aligned} \quad (1.4)$$

where $\sigma_c(s)$ is the usual cross-section for producing particle c and $\langle n_c \rangle$ is the average number of particles of type c produced in $a + b \rightarrow c + X$. Thus one event with n particles of type c will contribute n times to the inclusive cross-section: σ_c counts events and σ_c^{incl} particles.

Integrating equation (1.3) over \mathbf{p} gives the following formulae:

$$\begin{aligned} \int d^3 p E^{-1} f(\mathbf{p}; s) &= \int d^3 p \frac{d^3 \sigma_c}{d^3 p} \\ &= \sigma_c^{\text{incl}} \\ &= \langle n_c \rangle \sigma_c(s) \end{aligned} \quad (1.5)$$

$$\begin{aligned} \int d^3 p^* f(\mathbf{p}^*; s) &= \int d^3 p^* E^* \frac{d^3 \sigma_c}{d^3 p^*} \\ &= \eta_c \sqrt{s} \sigma_c(s). \end{aligned} \quad (1.6)$$

In equation (1.6) η_c is the fraction of the total CMS energy \sqrt{s} carried away by particles of the type c and is related to the *inelasticity* of the collision. Equation (1.6) is a special case of a *momentum sum rule* (Exercise VII.13).

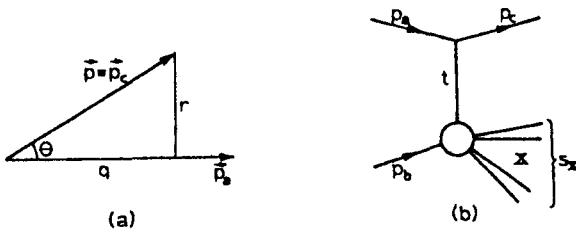


Figure VII.1.1

In experiments with unpolarized incident particles the distribution $f(\mathbf{p}; s)$ does not depend on rotations around the beam axis. It is thus a function of three essential variables. One of these is related to the total energy \sqrt{s} , and for the remaining two variables the following five sets are in general use.

1. P and θ , the absolute value and polar angle of \mathbf{p} (momentum of particle c), see Figure 1.1.
2. q and r , the longitudinal and transverse components of \mathbf{p} .
3. t , the invariant momentum transfer from particle a to particle c, and s_X , the square of the invariant mass of the unobserved system, or *missing mass*:

$$t = (p_a - p_c)^2 \quad (1.7)$$

$$s_X = (p_a + p_b - p_c)^2. \quad (1.8)$$

4. (t) and v, where v is the target system energy of the exchanged object in Figure 1.1(b) and is related to s_x and t by

$$\begin{aligned} v &= E_a^T - E^T \\ &= \frac{s_x - t - m_b^2}{2m_b}. \end{aligned} \quad (1.9)$$

One uses v mainly if particles a and c are identical, in which case v is simply the *energy loss of particle a*. When v is used it is customary to denote $t \equiv -q^2$. (This momentum transfer four-vector q should not be confused with the longitudinal component of p which is also denoted by q .)

5. r and ζ , where ζ is the *longitudinal rapidity* defined by writing in analogy with equation (II.1.9)

$$\begin{aligned} q &= m'_c \sinh \zeta, \\ E &= m'_c \cosh \zeta, \end{aligned} \quad (1.10)$$

where

$$\begin{aligned} m'_c &= (m_c^2 + \mathbf{r}^2)^{\frac{1}{2}} \\ &= (E^2 - q^2)^{\frac{1}{2}} \end{aligned} \quad (1.11)$$

Solving for ζ from equation (1.10) one has equivalently

$$\begin{aligned} \zeta &= \frac{1}{2} \log \frac{E + q}{E - q} \\ &= \log \frac{E + q}{m'_c} \\ &= \log \frac{m'_c}{E - q} \end{aligned} \quad (1.12)$$

These sets are further divided into subsets depending on the frame in which the noncovariant quantities are expressed. In connection with one-particle spectra one normally uses frames related by longitudinal Lorentz transformations, in particular, target, centre-of-momentum and beam systems. Accordingly, we shall distinguish between the variables q^T , q^* and q^B ; ζ^T , ζ^* and ζ^B , etc. One can also modify these sets by carrying out simple transformations of variables, for instance, by using r^2 instead of r .

In Sections 2–4 we shall go through these sets and for each we shall

determine d^3p/E

determine the physical region at fixed s

determine the relation to other variables and investigate curves of constant values of other variables.

The results obtained apply with obvious modifications to one-particle distributions in exclusive reactions also. Since exclusive reactions are more restrictive than inclusive reactions, their physical regions lie within those of inclusive reactions. Also no phase space distribution (Section III.3) is commonly defined for inclusive reactions — one might, however, define it by specifying in an arbitrary manner the relative weights of different multiplicities one sums over when going from exclusive to inclusive reactions.

2. The sets (P, θ) and (q, r)

It is convenient to treat (P, θ) and (q, r) simultaneously, since one pair expresses \mathbf{p} in polar coordinates, the other in Cartesian. To begin with, we have in any frame

$$\begin{aligned} \frac{d^3 p}{2E} &= \pi \frac{P^2 dP d\cos \theta}{E} \\ &= \pi \frac{r dr dq}{E} \\ &= \pi \frac{dr^2 dq}{2E}, \end{aligned} \tag{2.1}$$

so that the invariant function $f(\mathbf{p}) = f(\mathbf{p}, s)$ is given by

$$\begin{aligned} f(\mathbf{p}) &= \frac{E}{P^2} \frac{d^2 \sigma}{dP d\Omega} \\ &= \frac{E}{2\pi P^2} \frac{d^2 \sigma}{dP d\cos \theta} \\ &= \frac{E}{2\pi r} \frac{d^2 \sigma}{dq dr} \\ &= \frac{E}{\pi} \frac{d^2 \sigma}{dq dr^2}. \end{aligned} \tag{2.2}$$

Further transformation properties of f follow from the results of Section III.4.

(a) Boundary of the physical region

We now want to describe the region where events fall in the two dimensional plots in $(P, \cos \theta)$ or (q, r) . In Figure 1.1(b) the system X has the lowest possible invariant mass $m_1 + \dots + m_n$ when its constituents are at rest relative to each other, that is move with the same velocity in any frame.

Among the different allowed channels there is then one that gives the lowest value

$$s_X^{\min} = \min(m_2 + \dots + m_n)^2. \quad (2.3)$$

The value s_X^{\min} is fixed uniquely when the quantum numbers of a , b and c are given. If $a = c$, one usually has $s_X^{\min} = m_b^2$. If $a \neq c$, s_X^{\min} may contain one particle (as in $\pi^- p \rightarrow K^0 X$, $s_X^{\min} = m_A^2$) or more (as in $p p \rightarrow \pi^+ X$, $s_X^{\min} = (m_n + m_p)^2$).

In the CMS the maximum value of P^* is independent of θ and equals

$$P_{\max}^* = \frac{\lambda^{\frac{1}{2}}(s, m_c^2, s_X^{\min})}{2\sqrt{s}}. \quad (2.4)$$

The physical region is given by $0 \leq P^* \leq P_{\max}^*$, $0 \leq \theta^* \leq \pi$. In the $q^* r$ plane the physical region is the circle

$$q^{*2} + r^2 \leq P_{\max}^{*2}. \quad (2.5)$$

This region is called the CMS **Peyrou plot** (Figure 2.1). The function $f(p)$

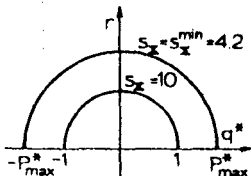


Figure VII.2.1 CMS Peyrou plot, equations (2.4–5), and curves $P^{*2} = q^{*2} + r^2 = \lambda(s, s_X, m_c^2)/4s$ of constant s_X in the $q^* r$ plane. Numbers refer to $p p \rightarrow K X$ at $\sqrt{s} = 4.41$ GeV

in equation (2.2) vanishes outside the Peyrou plot. The value of E^* associated with equation (2.4) is

$$E_{\max}^* = \frac{s + m_c^2 - s_X^{\min}}{2\sqrt{s}}; \quad (2.6)$$

at large s one has

$$\begin{aligned} P_{\max}^* &\approx E_{\max}^* \\ &\approx \frac{1}{2}\sqrt{s}, \\ \frac{P_{\max}^*}{E_{\max}^*} &\approx 1 - \frac{2m_c^2}{s}. \end{aligned} \quad (2.7)$$

The physical region in any other frame is obtained by Lorentz transforming the momentum space sphere (2.4) using techniques described in detail in Sections II.8 and IV.3. The physical region in (P, θ) is obtained from equations (II.8.19–22) and in (q, r) from equations (II.8.14–15). In the

target system the (P, θ) physical region is given by

$$\max \{0, P^T - (\cos \theta^T)\} \leq P^T \leq P^T + (\cos \theta^T) \quad (2.8)$$

where, according to equation (IV.3.8),

$$P^T \pm (\cos \theta^T) = [P_a^T E_{\max}^* \sqrt{s} \cos \theta^T \pm (E_a^T + m_b) \{s(P_{\max}^*)^2 - m_c^2 (P_a^T)^2 \sin^2 \theta^T\}^{\frac{1}{2}}] \\ \times \{s + (P_a^T)^2 \sin^2 \theta^T\}^{-1}. \quad (2.9)$$

The argument of the square root vanishes when

$$\begin{aligned} \sin \theta^T &= \sin \theta_{\max}^T \\ &= \frac{\sqrt{s} P_{\max}^*}{m_c P_a^T} \\ &= \frac{m_b \lambda^{\frac{1}{2}}(s, m_c^2, s_x^{\min})}{m_c \lambda^{\frac{1}{2}}(s, m_a^2, m_b^2)}. \end{aligned} \quad (2.10)$$

If $\sin \theta_{\max}^T > 1$, no θ_{\max}^T exists and particle c can move in any direction in the TS. This holds, for instance, for $p + p \rightarrow \pi + X$. If $\sin \theta_{\max}^T \leq 1$, particle c is emitted into the cone $0 \leq \theta^T \leq \theta_{\max}^T$. For instance, $\theta_{\max}^T = 90^\circ$ for $p + p \rightarrow p + X$. Inserting equation (2.10) into equation (2.9) the value of P^T at θ_{\max}^T is obtained in the form

$$P^T(\cos \theta_{\max}^T) = \left\{ \left(\frac{m_c^2}{m_b} \frac{s + m_b^2 - m_a^2}{s + m_c^2 - s_x^{\min}} \right)^2 - m_c^2 \right\}^{\frac{1}{2}}. \quad (2.11)$$

Examples of the physical region (2.8) will be presented in Section 6; a detailed classification of possible shapes can be found in (Dedrick, 1962).

In the Cartesian coordinates (q^T, r) the TS physical region or TS Peyrou plot is obtained from equations (II.8.14–15) in the form

$$\left(\frac{q^T - \gamma_{CM} v_{CM} E_{\max}^*}{\gamma_{CM} P_{\max}^*} \right)^2 + \left(\frac{r}{P_{\max}^*} \right)^2 = 1, \quad (2.12)$$

where v_{CM} and γ_{CM} are given by equations (II.6.23–24). Equations (2.12) and (2.9) are, of course, different representations of the same curve; it is shown in Figure 2.2.

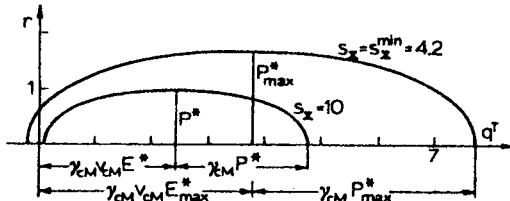


Figure VII.2.2 TS Peyrou plot (equation 2.12) and curves of constant s_x on $q^T r$ plane. This figure is the Lorentz transform of Figure 2.1. Numbers refer to $pp \rightarrow KX$ at $\sqrt{s} = 4.41$ GeV

For the investigation of target fragmentation (Section 5) it is useful to have an approximate form of equation (2.12) valid for $s \rightarrow \infty$ and q^T remaining finite. This is obtained simply by neglecting $(q^T)^2$ in equation (2.12) and expanding v^{CM} and P_{max}^*/E_{max}^* in powers of $1/s$ (equations (II.6.23) and (2.7)). One finds that for $s \rightarrow \infty$ and q^T finite the target system Peyrou plot reduces to the s -independent parabola

$$q^T = \frac{m_c^2 - m_b^2 + r^2}{2m_b}. \quad (2.13)$$

As derived in (Benecke, 1969), this is equivalent to

$$\begin{aligned} E - q^T &= \{(q^T)^2 + r^2 + m_c^2\}^{\frac{1}{2}} - q^T \\ &= m_b. \end{aligned} \quad (2.14)$$

The curve (2.13) is shown later in Figure 5.1.

(b) Constant value contours in the qr plane

As examples of constant-variable curves on Peyrou plots we shall consider curves of constant s_X , t and ζ in the q^*r and q^Tr planes, curves of constant θ^* and P^* in the q^*r plane and curves of constant θ^T and P^T in the q^*r plane. Curves of constant s_X have actually been determined already; they are obtained from equations (2.5) and (2.12) simply by replacing s_X^{min} by s_X in the expression for P_{max}^* . These curves are thus circles in the q^*r plane and ellipses in the q^Tr plane (Figures 2.1 and 2.2). The curves of constant t (Lyons, 1968) are most easily determined by evaluating t in the beam system:

$$\begin{aligned} t &= (p_a - p_c)^2 \\ &= m_a^2 + m_c^2 - 2E^B m_a. \end{aligned} \quad (2.15)$$

In this system curves of constant t are thus the spheres

$$\begin{aligned} (q^B)^2 + r^2 &= (P^B)^2 \\ &= \frac{\lambda(m_a^2, m_c^2, t)}{4m_a^2}. \end{aligned} \quad (2.16)$$

Transforming to the CMS or to the TS the curves of constant t are the ellipses

$$\left(\frac{q - \gamma v E^B}{\gamma P^B} \right)^2 + \left(\frac{r}{P^B} \right)^2 = 1, \quad (2.17)$$

where (equations (II.6.25–28))

$$\begin{aligned} \gamma &= \frac{s + m_a^2 - m_b^2}{2m_a\sqrt{s}} && \text{if } q = q^* \\ \gamma &= \frac{s - m_a^2 - m_b^2}{2m_a m_b} && \text{if } q = q^T. \end{aligned} \quad (2.18)$$

As $\gamma(\text{BS} \rightarrow \text{TS})$ is of the order of s as s grows, the curves of constant t rapidly become very eccentric. Examples of curves of constant t in the q^*r plane are shown in Figure 2.3.

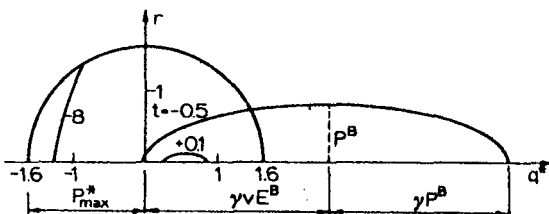


Figure VII.2.3 Curves of constant t (equation (2.17)) on the CMS Peyrou plot ($t = (p_a - p_e)^2$ for $a + b \rightarrow c + X$); E^B , P^B and γ are given in equations (2.15, 16, 18). The numbers refer to $K + p \rightarrow \pi + X$ at $6 \text{ GeV}/c$

Curves of constant θ^* in the q^*r plane are obtained by inserting $q^* = r \cot \theta^*$ in equation (II.8.9) with the result

$$\gamma^{\text{CM}} q^T - \gamma^{\text{CM}} v^{\text{CM}} \{(q^T)^2 + r^2 + m_c^2\}^{\frac{1}{2}} = r \cot \theta^*, \quad (2.19)$$

curves of constant θ^T in the q^*r plane follow similarly from equation (II.8.6):

$$\gamma^{\text{CM}} q^* + \gamma^{\text{CM}} v^{\text{CM}} \{(q^*)^2 + r^2 + m_c^2\}^{\frac{1}{2}} = r \cot \theta^T. \quad (2.20)$$

These curves are branches of a hyperbola. Curves of **constant P^*** in the q^*r plane are **ellipses** obtained from equations (II.8.19–22) or from equation (2.9) by replacing P_{\max}^* by P^* and s_X^{\min} by the associated value $s_X = s + m_c^2 - 2E^* \sqrt{s}$ (see Figure II.8.4). Conversely, **curves of constant P^T** in the q^*r plane are also **ellipses**. The equation defining these ellipses follows by Lorentz transforming the circle

$$(q^T)^2 + r^2 = (P^T)^2 \quad (2.21)$$

from the TS to the CMS with the result

$$\left(\frac{q^* + \gamma^{\text{CM}} v^{\text{CM}} E^T}{\gamma^{\text{CM}} P^T} \right)^2 + \left(\frac{r}{P^T} \right)^2 = 1. \quad (2.22)$$

Figure 2.4 shows examples of the ellipses (2.22).

Finally, to find the **curves of constant ζ** one modifies the definition (1.10–11) to the form

$$\frac{q^2}{\sinh^2 \zeta} - r^2 = m_c^2 \quad (2.23)$$

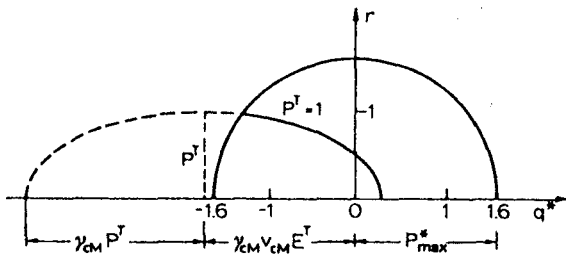


Figure VII.2.4 Curve of constant P^T (equation (2.22)) in the $q^* r$ plane (P^T is the target system momentum of particle c in $a + b \rightarrow c + X$). The numbers refer to $K + p \rightarrow \pi + X$ at 6 GeV/c

with the additional specification that ζ and q have the same sign. These curves are thus hyperbolas, examples of which are shown later in Figures 4.3-4. Note that one need not specify the frame in equation (2.23), and q and ζ may be any of the pairs (q^*, ζ^*) , (q^T, ζ^T) , etc.

(c) Effects of the factor $1/E$ in $d^3\sigma/d^3p$

The presence of the factor E in the definition $d^3\sigma/d^3p = f(\mathbf{p})/E$ of $f(\mathbf{p})$ causes some striking phase space effects. This factor and its consequences are frame-dependent. The function $1/E = (P^2 + m_c^2)^{-\frac{1}{2}}$ has a maximum at $P = 0$, and this peak is particularly pronounced if m_c is small, for instance, if particle c is a pion. Measured distributions presented in a fixed frame will thus present features near $P = 0$ arising from $1/E$ and not from $f(\mathbf{p})$. For example consider the distribution $w(q)$ in longitudinal momentum and the average transverse momentum $\langle r(q) \rangle$ at fixed q . According to equation (2.2) these are computed from

$$w(q) = \frac{\int dr \{r E^{-1} f(q, r)\}}{\int dr dq \{r E^{-1} f(q, r)\}}, \quad (2.24)$$

$$\langle r(q) \rangle = \frac{\int dr \{r^2 E^{-1} f(q, r)\}}{\int dr \{r E^{-1} f(q, r)\}}, \quad (2.25)$$

where the integrals are taken over the Peyrou plot of the frame in question.

The quantities (2.24–25) are presented in Figure 2.5 calculated for the model function

$$f(q, r) = \exp(-1.7|q^*|)r^{0.3} \exp(-6r) \quad (2.26)$$

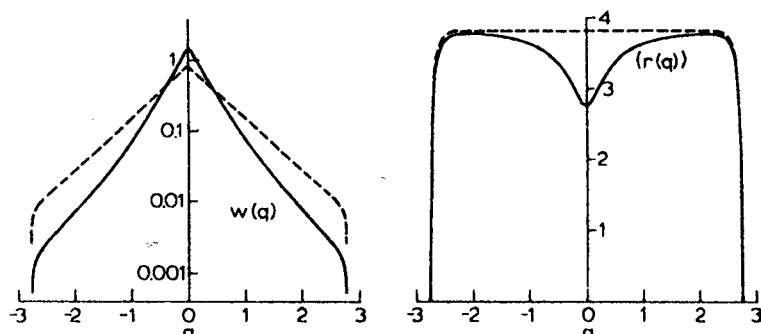


Figure VII.2.5 The quantities $w(q)$ and $\langle r(q) \rangle$ (equations (2.24–25)) computed for the model function in equation (2.26) (solid lines). The dashed lines show the weighted distributions obtained by deleting E^{-1} from equations (2.24–25)

and for the reaction $pp \rightarrow \pi^- X$ at $19 \text{ GeV}/c$. To illustrate the effect of the factor E^{-1} we also show the distributions obtained by deleting the factors E^{-1} from equations (2.24) and (2.25). If equations (2.24) and (2.25) represent directly measured distributions, these latter distributions are obtained by weighting each event by the factor E . The importance of E^{-1} is evident. In particular, the 'Seagull effect' (Bardadin, 1966) or the minimum in $\langle r(q) \rangle$ at small q is quite surprising. The weighting with E eliminates it here completely, although in fact it may appear even then in actual experimental data, because of dynamical effects. Exercises VII.4 and VII.5 contain further examples.

3. The sets (t, s_X) and (t, v)

(a) The variables t, s_X

According to the definitions (1.7–8),

$$t = m_a^2 + m_c^2 - 2E_a^T E^T + 2P_a^T P^T \cos \theta^T \quad (3.1)$$

$$= m_a^2 + m_c^2 - 2E_a^* E^* + 2P_a^* P^* \cos \theta^*, \quad (3.2)$$

$$= m_a^2 + m_c^2 - 2m_a E^B \quad (3.3)$$

$$s_X = s + m_c^2 - 2(E_a^T + m_b)E^T + 2P_a^T P^T \cos \theta^T \quad (3.4)$$

$$= s + m_c^2 - 2\sqrt{s}E^*. \quad (3.5)$$

From these it is possible to rederive by diagonalization the curves of constant

t and s_X in the q^*r and q^Tr planes presented above, but the earlier derivations are much simpler. By replacing dP^* by s_X and $d \cos \theta^*$ by dt in equation (2.1) one finds

$$\begin{aligned}\frac{d^3 p}{2E} &= \frac{\pi}{4\sqrt{s}P_a^*} dt ds_X \\ &= \frac{1}{2}\pi\lambda^{-1}(s, m_a^2, m_b^2) dt ds_X.\end{aligned}\quad (3.6)$$

Thus the invariant function $f(\mathbf{p}) \equiv f(t, s_X)$ is given by

$$f(t, s_X) = \frac{1}{\pi}\lambda^4(s, m_a^2, m_b^2) \frac{d^2\sigma}{dt ds_X}. \quad (3.7)$$

From the results of Sections V.5 and VI.4 one knows that the physical region in the ts_X plane is the Chew-Low plot defined by

$$\begin{aligned}G(s, t, s_X, m_a^2, m_b^2, m_c^2) &\leq 0, \\ s_X &\geq s_X^{\min}.\end{aligned}\quad (3.8)$$

The formulae of Section V.5 can be applied, if one replaces $m_2 + m_3$ by $(s_X^{\min})^{1/2}$.

(b) Constant value contours in the ts_X plane

As examples of constant-variable curves in the ts_X plane we shall discuss curves of constant P^* , θ^* , P^T , q^* , q^T and r . Kinematically the problem is simply that of relating the three-momentum of particle c to t and s_X in a $2 \rightarrow 2$ process with masses $m_a + m_b \rightarrow m_c + \sqrt{s_X}$. Curves of constant P^* are the straight lines defined by equation (3.5). According to equation (IV.5.18), curves of constant θ^* are given by

$$4sG(s, t, s_X, m_a^2, m_b^2, m_c^2) + \sin^2 \theta^* \lambda(s, m_a^2, m_b^2) \lambda(s, m_c^2, s_X) = 0. \quad (3.9)$$

Similarly, using equation (IV.4.13) with $m_b^2 + m_c^2 - u = s + t - s_X - m_a^2$, we see that curves of constant P^T are the straight lines

$$s_X = t + s - m_a^2 - 2m_b E^T \quad (3.10)$$

with slope 1. Curves of constant θ^T are obtained from equation (IV.5.21) with the result

$$4m_b^2 G(s, t, s_X, m_a^2, m_b^2, m_c^2) + \sin^2 \theta^T \lambda(s, m_a^2, m_b^2) \lambda(u, m_b^2, m_c^2) = 0. \quad (3.11)$$

The curves (3.9) and (3.11) are both hyperbolae. To plot them one must use the explicit forms of the G and λ functions. For $\theta^* = 0$ and $\theta^T = 0$ equations

(3.9) and (3.11) reduce to the boundary equation (3.8). Figure 3.1 shows examples of equations (3.10) and (3.11). The t -scale is expanded to show clearly the important small $|t|$ region.

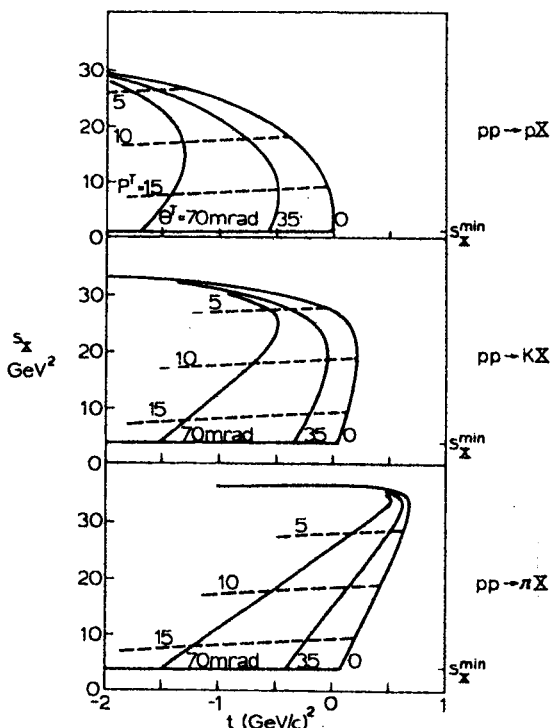


Figure VII.3.1 Contours of fixed laboratory angle and fixed laboratory momentum in the ts_X plane for inclusive pp reactions at $19 \text{ GeV}/c$. The curve $\theta^r = 0$ is the boundary of the physical region

For $r = P^* \sin \theta^* = P^T \sin \theta^T$ one obtains the invariant representation

$$r^2 = -\frac{G(s, t, s_X, m_a^2, m_b^2, m_c^2)}{\lambda(s, m_a^2, m_b^2)} \quad (3.12)$$

from equation (3.8) or (3.11). The curves of constant r in the ts_X plane are thus also branches of a hyperbola, examples of which are shown in Figure 3.2. An important property of these curves is that, at small $|t|$ and for large s , r essentially depends only on t , as is seen from Figure 3.2. This is seen more

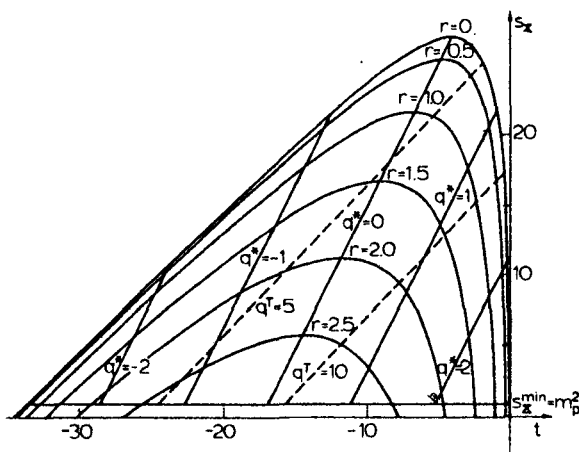


Figure VII.3.2 Curves of constant transverse momentum r and CMS and TS longitudinal momentum q^* , q^T for $p + p \rightarrow p + X$ at 19 GeV/c. This figure shows explicitly that for these masses small $|t|$ implies small r but not vice versa. In general, $t \approx t^+$ (t^+ may be large, see Figure V.5.4) implies small r

quantitatively, if one uses equation (IV.5.29) to write

$$r^2 = -\frac{s(t - t^+)(t - t^-)}{\lambda(s, m_a^2, m_b^2)}, \quad (3.13)$$

where t^\pm are given in equation (IV.5.31), with $m_1^2 = m_c^2$ and with $m_2^2 = s_X$. Near $t \approx t^+$ one has, taking $t^+ - t^-$ from equation (IV.5.31),

$$r^2 \approx \frac{\lambda^{\frac{1}{2}}(s, s_X, m_c^2)}{\lambda^{\frac{1}{2}}(s, m_a^2, m_b^2)}(t^+ - t) = \frac{P^*}{P_a^*}(t^+ - t). \quad (3.14)$$

Still more simply, when $s \gg s_X, m_i^2$ one has $t^+ \approx 0$ and

$$t \approx -r^2. \quad (3.15)$$

Equation (3.15) shows that an exponential in t is approximately a Gaussian in r (see also equation (5.13)).

Finally, according to equation (3.2) the curves of constant q^* are the straight lines

$$t = m_a^2 + m_c^2 - \frac{(s + m_a^2 - m_c^2)(s + m_c^2 - s_X)}{2s} + \frac{q^* \lambda^{\frac{1}{2}}(s, m_a^2, m_b^2)}{\sqrt{s}} \quad (3.16)$$

and according to equations (3.1) and (3.10) the curves of constant q^T are the

straight lines

$$t(s - m_a^2 + m_b^2) = 2m_b^2(m_a^2 + m_c^2) - (s - m_a^2 - m_b^2)(s - m_a^2 - s_x) \\ + 2m_b q^T \lambda^\frac{1}{2}(s, m_a^2, m_b^2). \quad (3.17)$$

Examples of equations (3.16) and (3.17) are shown in Figure 3.2.

(c) The variables t, v

The set (t, v) differs from the set (t, s_x) only by the very simple transformation (1.9),

$$v = E_a^T - E^T \\ = \frac{s_x - t - m_b^2}{2m_b}. \quad (3.18)$$

and there is no need to perform a separate analysis of the set (t, v) . As an example, Figure 3.3 shows the result of transforming the physical region of $pp \rightarrow pX$ at 19 GeV/c (Figure 3.2) to the (t, v) plane. All results concerning the boundary (equation (3.8)) and constant variable curves follow from those presented earlier by replacing s_x by $t + m_b^2 + 2m_b v$.

The most common case in which the set (t, v) is used is *inelastic electron or neutrino scattering from nucleons* (Drell, 1964). There one may set $m_a = m_c$.

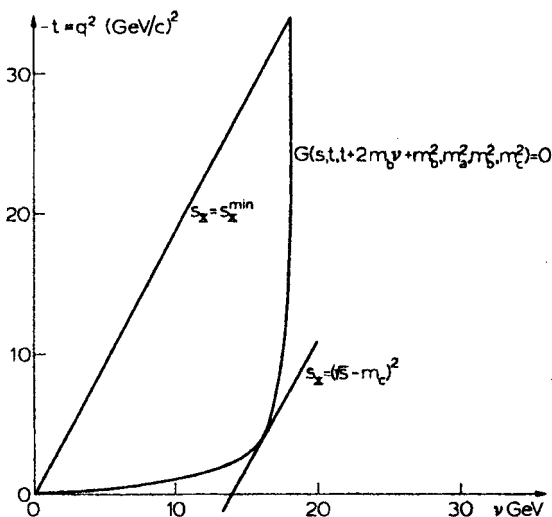


Figure VII.3.3 The physical region for $pp \rightarrow pX$ at 19 GeV/c transformed from Figure 3.2 to the vt plane.

$= 0$ (since in this connection the electron mass is negligible), which implies that the hyperbola (3.8) degenerates to two straight lines given by

$$\begin{aligned}-t \equiv q^2 &= 0, \\ -t \equiv q^2 &= 4E_a^T(E_a^T - v),\end{aligned}\quad (3.19)$$

where

$$E_a^T = \frac{s - m_b^2}{2m_b} \quad (3.20)$$

is the energy of the incident particle in the target system. In this connection it is also customary to use q^2 instead of $-t$. In terms of v the third boundary line $s_X = s_X^{\min} = m_b^2$ is given by

$$v = \frac{q^2}{2m_b}. \quad (3.21)$$

The physical region bounded by equation (3.19–21) is shown in Figure 3.4.

Since $m_e = m_c = 0$ the relation between $-t \equiv q^2$ and the target system scattering angle is simple:

$$\begin{aligned}q^2 &= 2E_a^T E^T (1 - \cos \theta^T) \\ &= 4E_a^T \sin^2 \frac{1}{2}\theta^T (E_a^T - v),\end{aligned}\quad (3.22)$$

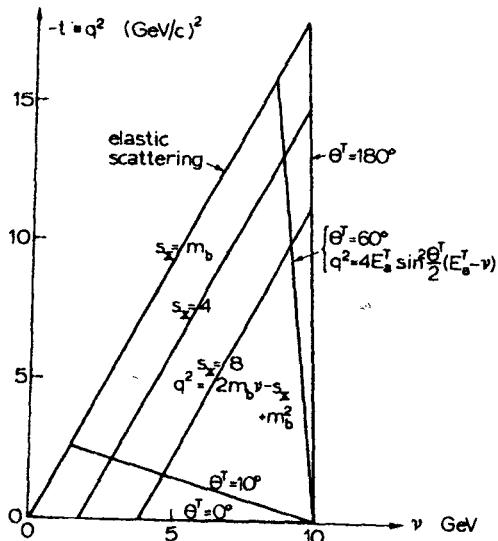


Figure VII.3.4 Physical region in the vt plane for $m_e = m_c = 0$. Numbers refer to $E_a^T = 10$ GeV and $m_b = 0.94$ GeV. Lines of constant θ^T and s_X are given in equations (3.22–23)

where equation (3.18) was used to replace E^T by the energy loss v . Equation (3.22) represents curves of constant θ^T in the $q^2 v$ plane (Figure 3.4), see also Figure 3.1 and equation (3.11). An experiment carried out at fixed incident energy and at fixed target system scattering angle will probe the part of the line (3.22) remaining within the triangle (3.19–21). According to equation (3.18) curves of constant s_X are given by the straight lines

$$q^2 = 2m_b v - s_X + m_b^2. \quad (3.23)$$

4. The set (ζ, r)

According to equations (1.10–11) the relation between ζ , q and r is

$$\begin{aligned} \zeta &= \frac{1}{2} \log \frac{E + q}{E - q} \\ &= \log \frac{E + q}{(m_c^2 + r^2)^{\frac{1}{2}}} \end{aligned} \quad (4.1)$$

or, equivalently

$$\begin{aligned} q &= (r^2 + m_c^2)^{\frac{1}{2}} \sinh \zeta, \\ E &= (r^2 + m_c^2)^{\frac{1}{2}} \cosh \zeta, \end{aligned} \quad (4.2)$$

where $E = (q^2 + r^2 + m_c^2)^{\frac{1}{2}}$. In terms of ζ and r the invariant differential

$$\frac{d^3 p}{E} = \frac{dq \, d^2 r}{E} = d\zeta \, d^2 r = 2\pi \, d\zeta \, r \, dr \quad (4.3)$$

leads to the invariant distribution

$$f(\zeta, r) = \frac{1}{2\pi r} \frac{d^2 \sigma}{d\zeta \, dr} = \frac{1}{\pi} \frac{d^2 \sigma}{d\zeta \, dr^2}. \quad (4.4)$$

As shown in Section II.1, rapidities are additive under collinear Lorentz transformations. Thus longitudinal rapidities ζ and ζ' in two frames related by a longitudinal transformation with parameter γ differ only by an additive constant. This constant is easily identified by inserting $q' = \gamma(q - vE)$, $E' = \gamma(E - vq)$ in equation (4.1):

$$\begin{aligned} \zeta' &= \frac{1}{2} \log \frac{E' + q'}{E' - q'} \\ &\equiv \zeta - \chi, \end{aligned} \quad (4.5)$$

where

$$\begin{aligned} \chi &= \frac{1}{2} \log \frac{1 + v}{1 - v} \\ &= -\log(\gamma - \gamma v) \\ &= \log(\gamma + \gamma v) \\ &= \operatorname{argcosh} \gamma. \end{aligned} \quad (4.6)$$

Here χ is the relative rapidity of the two frames and $\operatorname{argcosh} \gamma = \log \{\gamma + \sqrt{(\gamma^2 - 1)}\}$. For Lorentz transformations of rapidities ζ^T , ζ^* and ζ^B defined in the three standard frames TS, CMS and BS one has, according to equations (II.6.23-28),

$$\begin{aligned}
 \zeta^T &= \zeta^* + \chi^* \\
 &= \zeta^* + \log \frac{E_a^T + m_b + P_a^T}{\sqrt{s}} \\
 &= \zeta^* + \operatorname{argcosh} \frac{s - m_a^2 + m_b^2}{2m_b\sqrt{s}} \\
 &\simeq \zeta^* + \log \frac{\sqrt{s}}{m_b} \\
 \zeta^T &= \zeta^B + \chi^B \\
 &= \zeta^B + \log \frac{E_a^T + P_a^T}{m_a} \\
 &= \zeta^B + \operatorname{argcosh} \frac{s - m_a^2 - m_b^2}{2m_a m_b} \\
 &\simeq \zeta^B + \log \frac{s}{m_a m_b} \\
 \zeta^* &= \zeta^B + \chi^{B*} \\
 &= \zeta^B + \log \frac{E_b^B + m_a + P_b^B}{\sqrt{s}} \\
 &= \zeta^B + \operatorname{argcosh} \frac{s + m_a^2 - m_b^2}{2m_a\sqrt{s}} \\
 &\simeq \zeta^B + \log \frac{\sqrt{s}}{m_a},
 \end{aligned} \tag{4.7}$$

where the approximate forms are valid for $s \gg m_a^2, m_b^2$.

The relation $q = m'_c \sinh \zeta$ between q and ζ is shown in Figure 4.1; both in the CMS and the TS. The slope of the curve is E^{-1} :

$$\frac{d\zeta}{dq} = \frac{1}{E}. \tag{4.8}$$

Thus an interval Δq near $q = 0$ or $E = m'_c$ corresponds to an interval $\Delta\zeta = \Delta q/m'_c$ while near $q = q_{\max}$ (the kinematical upper limit) it corresponds to

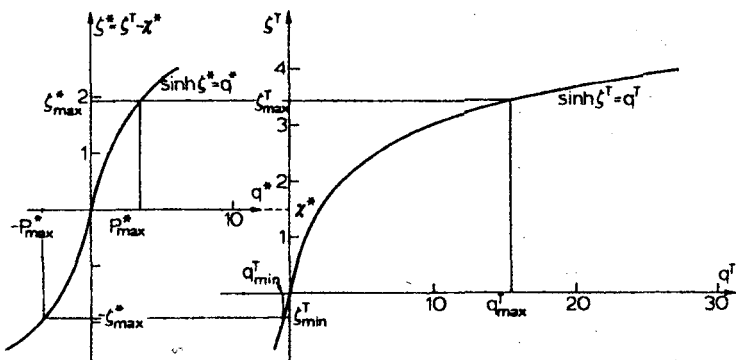


Figure VII.4.1 The relation $q/m'_c = \sinh \zeta$ in the CMS and TS. The origin of the $\zeta^* q^*$ plane is shifted by χ^* to display ζ^* and $\zeta^T = \zeta^* + \chi^*$ at the same height. The numbers apply to $pp \rightarrow KX$ at $P_*^* = 2 \text{ GeV}/c$ ($\sqrt{s} = 4.41 \text{ GeV}$, $\chi^* = 1.5$) for which $\zeta_{\max}^* > \chi^*$, i.e. the K_s can move in any direction in the TS. All momenta are measured in units of m'_c . χ^* is given in equation (4.7) and

$$\zeta_{\max}^* = \operatorname{argcosh} \{(s + m_c^2 - s_X^{\min})/2m_c\sqrt{s}\}$$

$\Delta\zeta \simeq \Delta q/q_{\max}$. This implies that in the limit $s \rightarrow \infty$ the variables q and ζ are complementary in the sense that events near $\zeta = 0$ on a ζ -plot take an almost constant fraction of the ζ -range, while in q plot these cover a diminishing fraction of the whole q -interval. This is illustrated in Figure 4.2, in which the ζ -distribution following from the model function (2.26) is represented (Exercise VII.7). Figure 4.2 should be compared with Figure 2.5.

In order to estimate what numerical values of longitudinal rapidities are met in practice, one notes that according to equations (4.1) and (4.7) the exact

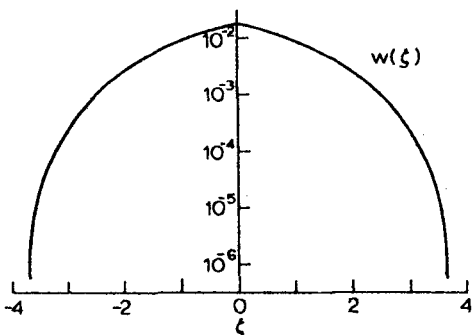


Figure VII.4.2 The q -distribution in Figure 2.5 transformed to longitudinal rapidity ζ

ranges of ζ^* and ζ^T are given by

$$\begin{aligned} |\zeta^*| &\leq \log \left\{ \frac{E_{\max}^* + P_{\max}^*}{m_c} \right\} \\ \log \left(\frac{m_c}{\sqrt{s}} \frac{E_a^T + m_b + P_a^T}{E_{\max}^* + P_{\max}^*} \right) &\leq \zeta^T \leq \log \left\{ \frac{(E_{\max}^* + P_{\max}^*)(E_a^T + m_b + P_a^T)}{m_c \sqrt{s}} \right\} \end{aligned} \quad (4.9)$$

where P_{\max}^* and E_{\max}^* are given by equation (2.4) and by equation (2.6), and ζ^B is similarly bounded (Exercise VII.9). For large s one thus has (correction terms are of order s^{-1})

$$\begin{aligned} -\log \frac{\sqrt{s}}{m_c} &\leq \zeta^* \leq \log \frac{\sqrt{s}}{m_c}, \\ \log \frac{m_c}{m_b} &\leq \zeta^T \leq \log \frac{s}{m_b m_c}, \\ -\log \frac{s}{m_a m_c} &\leq \zeta^B \leq \log \frac{m_a}{m_c}. \end{aligned} \quad (4.10)$$

Note that the limits of ζ^* depend only on m_c and that the total length of the range of any ζ equals $\log(s/m_c^2)$. Thus for incident beams of momenta less than 30 GeV/c one has for $a + p \rightarrow \pi + X$ (a is any projectile)

$$\begin{aligned} -4.0 &\leq \zeta^* \leq 4.0 \\ -1.9 &\leq \zeta^T \leq 6.1 \end{aligned} \quad (4.11)$$

and for $a + p \rightarrow p + X$

$$\begin{aligned} -2.1 &\leq \zeta^* \leq 2.1 \\ 0 &\leq \zeta^T \leq 4.2 \end{aligned} \quad (4.12)$$

The ranges of ζ^B also depend on the projectile a .

The physical region in the $\zeta^* r$ plane is obtained by transforming the curve $P^* = P_{\max}^*$ in equation (2.5). This is a special case of curves of constant P^* in the $\zeta^* r$ plane which are determined by the equation

$$r^2 = \{(P^*)^2 + m_c^2\} (\cosh \zeta^*)^{-2} - m_c^2. \quad (4.13)$$

Examples are given in Figure 4.3. If ζ is expressed in any other frame, the corresponding region is obtained by a parallel displacement with magnitude given by the relative rapidity χ . These figures exhibit clearly the difference between ζ and q in the description of the region $q = 0$.

A variable closely related to rapidity ζ has been used in connection with cosmic ray measurements. In these momenta are difficult to determine and in most experiments only angular distributions of secondaries are obtained.

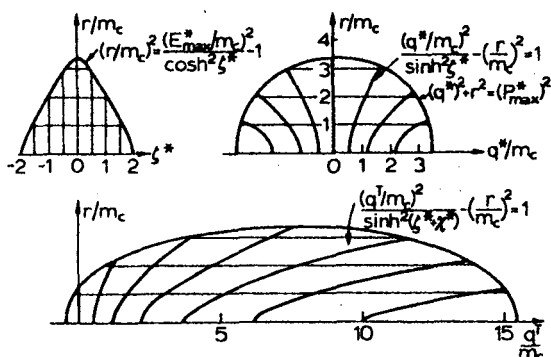


Figure VII.4.3 Transformations of curves of constant ζ^* between the ζ^*r , $q^T r$ and $q^T r$ planes. Numbers refer to $pp \rightarrow \pi X$ at $\sqrt{s} = 4.41 \text{ GeV}/c$, $\chi^* = 1.5$

To present data, it is customary to replace the polar angle θ by a variable which has a simple approximate transformation law from the TS to CMS and which expands the region near $\theta^T = 0$, where most events are concentrated.

According to equation (II.8.30) θ^T and θ^* are related by

$$\tan \theta^T = \frac{v^* \sin \theta^*}{\gamma^{\text{CM}}(v^{\text{CM}} + v^* \cos \theta^*)}, \quad (4.14)$$

where v^* is the CMS velocity of the emitted particle. When v^{CM} and v^* are close to one, one gets

$$\begin{aligned} \tan \theta^T &\simeq \frac{\sin \theta^*}{\gamma^{\text{CM}}(1 + \cos \theta^*)} \\ &= \frac{1}{\gamma^{\text{CM}}} \tan \frac{1}{2}\theta^*. \end{aligned} \quad (4.15)$$

The variables

$$\begin{aligned} u^* &= \log \tan \frac{1}{2}\theta^* \\ u^T &= \log \tan \theta^T \end{aligned} \quad (4.16)$$

are thus related by

$$\begin{aligned} u^T &= u^* - \log \gamma^{\text{CM}} \\ &\simeq u^* - \log \frac{\sqrt{s}}{2m_b} \end{aligned} \quad (4.17)$$

as long as v^* remains sufficiently close to one. The formula (4.17) evidently fails

in the central region shown later in Figure 5.1. Since $du^T = 2(\sin 2\theta^T)^{-1} d\theta^T$ and $du^* = (\sin \theta^*)^{-1} d\theta^*$ it is also clear that u^T and u^* expand the regions of small θ^T and θ^* .

To relate u^T and ζ^T we note that when $m_e \ll r \ll q$

$$\begin{aligned}\zeta &= \log \{(E + q)(m_e^2 + r^2)^{-\frac{1}{2}}\} \\ &\simeq \log \frac{2q}{r} \\ &\simeq -\log \frac{1}{2}\theta \\ &\simeq -\log \tan \frac{1}{2}\theta.\end{aligned}\tag{4.18}$$

One thus finds that

$$\begin{aligned}\zeta^T &= -u^T + \log 2, \\ \zeta^* &= -u^*,\end{aligned}$$

and that the relation (4.17) is equivalent to $\zeta^T = \zeta^* + \log(\sqrt{s}/m_b)$ (equation (4.7)). However, equation (4.7) is exact (in the limit of large s) while equation (4.17) applies only to a limited class of events.

5. Kinematics of scaling and fragmentation

The dynamical concepts of *scaling* (Feynman, 1969) and *fragmentation* (Benecke, 1969) involve essentially some conjectures about the behaviour of $f(q, r; s)$ when $s \rightarrow \infty$. We shall here analyze some relevant kinematical facts, which actually form a significant part of these theories.

Instead of the longitudinal variables q and ζ (expressed in various frames) it is sometimes convenient to *scale* these so that their ranges become essentially constant. No dynamics is involved, since this is always done implicitly when one draws figures on paper of limited size. As we know the exact ranges of q (equations (2.5) and (2.12) and Exercise VII.3) and ζ (equation (4.9) and Exercise VII.9) in all frames it is trivial to introduce new variables with fixed ranges. As the exact limits are rather complicated and as scaled variables are interesting mainly at high s one often simplifies them. Considering longitudinal momenta one may first approximate the exact upper limit of $|q|$ by the incident momentum and define

$$x_p^* = \frac{q^*}{P_p^*}, \quad x_p^T = \frac{q^T}{P_p^T}, \quad x_p^B = \frac{q^B}{P_p^B} \tag{5.1}$$

and then use the approximate values of the momenta at large s to define

$$x^* = \frac{2q^*}{\sqrt{s}}, \quad x^T = \frac{2m_b q^T}{s}, \quad x^B = \frac{2m_b q^B}{s}. \tag{5.2}$$

All different ways of scaling approach (5.2) when $s \rightarrow \infty$ and there the limits become $-1 \leq x^* \leq 1$, $0 \leq x^T \leq 1$ and $-1 \leq x^B \leq 0$. Scaling rapidities is not so interesting since the total range only increases proportionally to $\log(s/m_c^2)$ (equation (4.10)). To scale them it is convenient to use the fact that differences of rapidities are translationally invariant and to write in any frame

$$\xi_{ab} = \frac{\zeta_a - \zeta_b}{\zeta_a + \zeta_b}, \quad (5.3)$$

where ζ_a and ζ_b are the rapidities of particles a and b in this frame, that is,

$$q_a = m_a \sinh \zeta_a, \quad q_b = m_b \sinh \zeta_b. \quad (5.4)$$

For large s we have $\zeta_a - \zeta_b = \log(s/m_a m_b)$ so that, using equation (4.10):

$$\frac{\log(m_c/m_b)}{\log(s/m_a m_b)} \leq \xi_{ab} \leq \frac{\log(s/m_b m_c)}{\log(s/m_a m_b)}. \quad (5.5)$$

Asymptotically $0 \leq \xi_{ab} \leq 1$, although the approach is only logarithmic. The approach to the limits is proportional to s^{-1} if one uses equation (4.10) and writes

$$\xi = \frac{\{\zeta^* + \log(\sqrt{s}/m_c)\}}{\log(s/m_c^2)} \quad (5.6)$$

in analogy to equation (5.2).

Consider then the target fragmentation (TF), central (C) and beam fragmentation (BF) regions defined in Figure 5.1. The theory of limiting fragmentation deals with the limit of the function $f(q, r; s)$ in these three regions for $s \rightarrow \infty$ and r fixed. Choosing as examples the least controversial cases, one conjectures that in the TF and BF regions the function $f(q, r; s)$ approaches

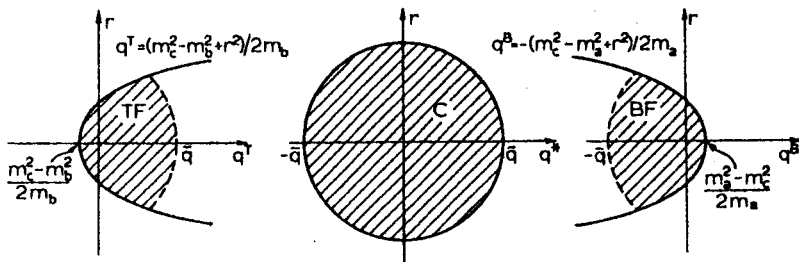


Figure VII.5.1 The target fragmentation (TF), central (C) and beam fragmentation (BF) regions at $s \rightarrow \infty$, \bar{q} being some finite number. The exact form of the regions is irrelevant; one only requires the momenta within the regions to remain finite as $s \rightarrow \infty$. The boundary curves result from equation (2.13)

nonvanishing limits:

$$\begin{aligned} f(q^T, r; s) &\rightarrow f(q^T, r; \infty) > 0, & q^T \text{ in TF region} \\ f(q^B, r; s) &\rightarrow f(q^B, r; \infty) > 0, & q^B \text{ in BF region.} \end{aligned} \quad (5.7)$$

To clarify the interrelations of these regions, in Figure 5.2 we show qualita-

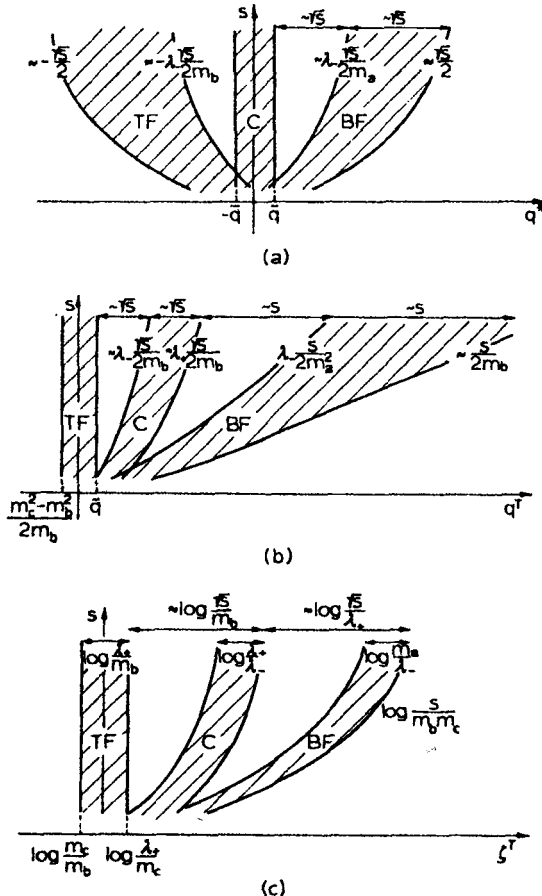


Figure VII.5.2 Qualitative behaviour of the intervals (5.8) or of the TF, C and BF regions (Figure 5.1) as $s \rightarrow \infty$ (a) in the CMS, (b) TS and (c) in terms of the rapidity ζ^T . Here \bar{q} is some finite number and $\lambda_{\pm} = E \pm \bar{q} = (\bar{q}^2 + m_c^2)^{\frac{1}{2}} \pm \bar{q}$. To obtain the exact physical region limits we have chosen $r = 0$, but the same pattern persists for arbitrary fixed r

tively how the intervals

$$\begin{aligned} \frac{m_c^2 - m_b^2}{2m_b} \leq q^T &\leq \bar{q} & (\text{TF}) \\ -\bar{q} \leq q^* &\leq \bar{q} & (\text{C}) \\ -\bar{q} \leq q^B &\leq \frac{m_a^2 - m_c^2}{2m_a} & (\text{BF}) \end{aligned} \quad (5.8)$$

corresponding to $r = 0$ behave in the CMS and TS when $s \rightarrow \infty$. The intervals (5.8) are also plotted against rapidity ζ^T in the same figure. To derive the curves in Figure 5.2, insert the end points in equation (5.8) in the relevant transformation equations (Section II.6), simplified by including only the leading terms in s :

$$\begin{aligned} q^* &\simeq (\sqrt{s}/2m_b)\{q^T - (1 - 2m_b^2/s)E^T\}, \\ q^* &\simeq (\sqrt{s}/2m_a)\{q^B + (1 - 2m_a^2/s)E^B\}, \\ q^T &\simeq (\sqrt{s}/2m_b)(q^* + E^*), \\ q^T &\simeq (s/2m_a m_b)\{q^B + (1 - 2m_a^2 m_b^2/s^2)E^B\}. \end{aligned} \quad (5.9)$$

($E = (q^2 + m_c^2)^{1/2}$, since $r = 0$). Note that the correction terms in some of the velocity parameters are needed to transform points near $q^* = \pm P_{\max}^*$ correctly ($P_{\max}^*/E_{\max}^* \simeq 1 - 2m_c^2/s$). Figure 5.2(c) is obtained simply by applying the relation $\zeta^T = \log \{(E^T + q^T)/m_c\}$ to Figure 5.2(b). One can draw the following conclusions.

In terms of CMS longitudinal momenta, the separation between TF and C and BF regions (the *transition regions*), and the sizes of TF and BF regions grow proportionally to \sqrt{s} .

In terms of target system longitudinal momenta, the separation between TF and C regions and the size of the C region are proportional to \sqrt{s} , and the separation between BF and C regions and the size of BF region are proportional to s .

In terms of rapidity ζ (in TS, CMS or BS) the sizes of TF, C and BF regions are constant while the separations of TF and C and BF and C are proportional to $\log s$.

To express these conclusions in terms of the scaled variables x^* and x^T (equation (5.2)) we choose s large and transform the regions in Figure 5.2(a)-(b) to those in Figure 5.3. Since \bar{q} is any fixed momentum (Figure 5.1) it may

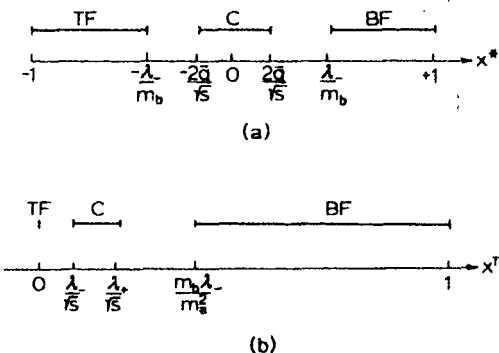


Figure VII.5.3 The TF, C and BF regions at some finite but large s in terms of the scaled variables x^* and x^T . The number \bar{q} defines the regions (Figure 5.1) and $\lambda_{\pm} = (\bar{q}^2 + m_c^2)^{\frac{1}{2}} - \bar{q}$. One can make λ_- arbitrarily small by making \bar{q} large

be chosen large and $\lambda_- = \bar{E} - \bar{q} \approx m_c^2/2\bar{q}$ can be made arbitrarily small. One thus deduces that

In terms of x^* the TF and BF regions are asymptotically the intervals $-1 \leq x^* < 0$ and $0 < x^* \leq 1$, respectively, and the C region shrinks to the point $x^* = 0$.

In terms of x^T the BF region is asymptotically the interval $0 < x^T \leq 1$, while the C and TF regions shrink to the point $x^T = 0$.

If one scales the rapidity variable ζ it is further clear from Figure 5.2(c) that

In terms of ξ_{ab} or ξ (equations (5.3) and (5.6)) the TF, C and BF regions converge to the points $0, \frac{1}{2}$ and 1 , respectively, and the transition regions fill the intervals $0 < \zeta < \frac{1}{2}, \frac{1}{2} < \zeta < 1$.

In terms of the scaled variable $x \equiv x^*$ one has by inserting equation (5.9) in the BF region $0 < x \leq 1$

$$\begin{aligned}
 q^B &= \gamma(q^* - vE^*) \\
 &\simeq \left(\frac{\sqrt{s}}{2m_a}\right) q^* \left\{ 1 - \left(1 - \frac{2m_a^2}{s}\right) \left(1 + \frac{m_c^2}{2q^{*2}}\right) \right\} \\
 &\simeq \left(\frac{x}{2m_a}\right) \left(m_a^2 - \frac{m_c^2}{x^2} \right),
 \end{aligned} \tag{5.10}$$

and in the TF region $-1 \leq x < 0$

$$\begin{aligned} q^T &= \gamma^{\text{CM}}(q^* + v^{\text{CM}}E^*) \\ &\simeq \left(\frac{\sqrt{s}}{2m_b}\right)q^*\left\{1 - \left(1 - \frac{2m_b^2}{s}\right)\left(1 + \frac{m_c^2}{2q^{*2}}\right)\right\} \\ &\simeq \left(\frac{x}{2m_b}\right)\left(m_b^2 - \frac{m_c^2}{x^2}\right). \end{aligned} \quad (5.11)$$

In both regions q^B and q^T are thus functions only of x , that is depend on s only through the combination $2q^*/\sqrt{s}$. Combining this statement with the limiting fragmentation hypothesis (5.7) the latter is seen to imply that in the limit $s \rightarrow \infty$ $f(q, r; s)$ becomes only a function of x :

$$f(q^*, r; s) \rightarrow f(x, r), \quad (5.12)$$

where $-1 \leq x < 0$ or $0 < x \leq 1$. This is the kinematic connection between the target and beam fragmentation hypothesis and the scaling hypothesis equation (5.12). Analysis of what happens in the central region $x = 0$ would necessitate further considerations of a dynamical nature.

We note finally that by writing in equations (3.3) and (3.5) $q^* = P^* \cos \theta^*$, $E_*^* = q_*^* + m_*^2/2q_*^*$, $E^* = q^* + (m_c^2 + r^2)/2q^*$ one can approximate t and s_x by the expressions

$$t = m_a^2 + m_c^2 - (m_c^2/x^* + m_a^2x^*) - r^2/x^*, \quad (5.13)$$

$$s_x = s(1 - x^*). \quad (5.14)$$

These very useful expressions are valid when $x^* \gg 2(m_c^2 + r^2)^{1/2}/\sqrt{s}$. Equation (5.13) is essentially the same as equation (3.14).

6. Missing mass techniques

This section will essentially be an application of the results in Section 2 to missing mass techniques (Maglic, 1965; McLeod, 1969). In these the mass $m_X = \sqrt{s_X}$ of a particle or a system of particles X is calculated from the momenta of the other particles taking part in the interaction, rather than from the kinematic variables of X itself or of its decay products. This method is implicit in kinematic fitting of bubble chamber pictures. In counter experiments it is used to measure mass spectra. For instance, in the inclusive reaction $\pi^- + p \rightarrow p + X^-$ one may detect only the final state proton in order to search for negative boson resonances of high mass.

When in the reaction $a + b \rightarrow c + X$ p_a and p_b are known, p_c determines the four-momentum of X. Usually the azimuthal angle ϕ is irrelevant, and the remaining three variables in p_c determine P_X , θ_X and m_X . In certain configurations the mass m_X is relatively insensitive to one of these three

variables or to a combination of them. It then suffices to identify particle c, measure one variable precisely and one crudely. In the case of triggering spark chamber arrays, this allows simplification in the triggering electronics. A drawback of the 'one variable' methods is that the kinematic region that can be studied is limited. We shall here study two applications of this idea: the **Jacobian peak** and the **zero-degree** methods.

In the target system the missing mass is given by equation (3.4) or, equivalently, by

$$m_X^2 = m_a^2 + m_b^2 + m_c^2 + 2E_a(m_b - E) - 2m_b E + 2P_a P \cos \theta. \quad (6.1)$$

We continue here to omit the index c (apart from m_c); in this section we shall only work in the TS. The rate of change of m_X with P_a , P and θ is given by the derivatives

$$\frac{m_X \partial m_X}{\partial P_a} = \frac{P_a(m_b - E)}{E_a} + P \cos \theta, \quad (6.2)$$

$$\frac{m_X \partial m_X}{\partial P} = -\frac{(E_a + m_b)P}{E} + P_a \cos \theta, \quad (6.3)$$

$$\frac{m_X \partial m_X}{\partial \theta} = -P_a P \sin \theta. \quad (6.4)$$

The situations in which m_X is insensitive to a change in P or in θ are easily visualized by considering the surfaces of constant m_X in p space (Figure 6.1). These are rotational ellipsoids given in terms of q^T and r by equation (2.12). In Figure 6.1(a) the detector acceptance is such that $\partial m_X / \partial P$ is small, in Figure 6.1(b) the detector covers a region where $\partial m_X / \partial \theta$ is small.

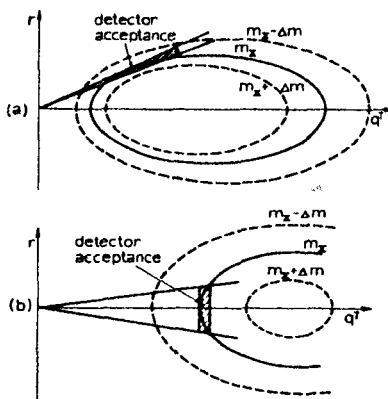


Figure VII.6.1 (a) The Jacobian peak region, and (b) the zero angle region in the missing mass experiment $a + b \rightarrow c + X$ (q^T and r are TS components of the measured momentum p_c)

(a) *The Jacobian peak method*

Consider now fixed s and a fixed m_x in Figure 6.1(a) and plot $\cos \theta$ as a function of P as given by equation (6.1) or, more explicitly, by equation (2.9). Examples are shown in Figure 6.2. The angle θ has a maximum or $\cos \theta$ a

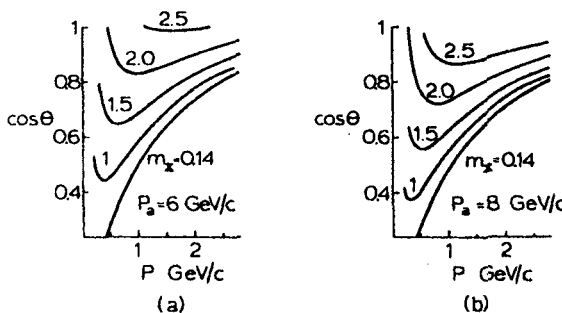


Figure VII.6.2 Dependence of $\cos \theta$ on P for several values of missing mass m_x . The reaction is $\pi^\pm + p \rightarrow p + X^\pm$ (a) at $6 \text{ GeV}/c$ and (b) at $8 \text{ GeV}/c$ (Maglic 1965)

minimum at $\partial \cos \theta / \partial P = 0$, which leads to equation (2.10) for $\sin \theta_{\max}$ and equation (2.11) for the value of P or E at θ_{\max} . Placing a detector at θ_{\max} with acceptance shown in Figure 6.1 will give m_x accurately without precise momentum measurement.

The name Jacobian peak method arises from the fact that the quantity $d \cos \theta^*/d \cos \theta$, which is the Jacobian between $w(\cos \theta)$ and $w(\cos \theta^*)$ (equation (III.4.14.)), is infinite at $\theta = \theta_{\max}$. This is seen explicitly from Figure II.8.4.

Comparison of Figures 6.2(a) and (b) shows that increase in the beam momentum gradually brings heavier masses into the range of the spectrometer without changing θ (and thus the t -range). This makes it possible to scan the mass spectrum under constant conditions. According to equation (6.4), increasing P_a requires improved angular resolution for a given mass resolution.

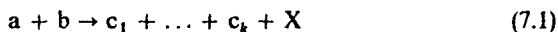
(b) *The zero degree method*

If the detected particle goes nearly forward, m_x depends mainly on P and only to second order on θ (see Figure 6.1(b)). Both the low momentum branch $P^-(\theta)$ and high momentum branch $P^+(\theta)$ (backward resonance production, not shown in Figure 6.1(b)) are of experimental interest. Placing a detector as in Figure 6.1(b) permits one to determine m_x by a momentum measurement

without measuring angles precisely. However, the zero degree method has several disadvantages due to the fact that the detector is near the incident beam direction.

7. Higher order distributions, correlations

Generalizing in an obvious way the contents of Section 1 we may consider the inclusive reaction



and define the associated *k-particle invariant distribution function* f_k by

$$\frac{d^{3n}\sigma}{d^3 p_1 \dots d^3 p_k} = \frac{f_k(p_1, \dots, p_k; s)}{E_1 \dots E_k}. \quad (7.2)$$

If we assume for simplicity that particles c_i in equation (7.1) are all of the same type (type c), we have, corresponding to equations (1.4) and (1.5),

$$\int d^3 p_1 \dots d^3 p_k \frac{f_k(p_1, \dots, p_k; s)}{E_1 \dots E_k} = \sum_{n=k}^{\infty} n(n-1)\dots(n-k+1)\sigma_c^n(s) \\ = \langle n(n-1)\dots(n-k+1) \rangle \sigma_c(s), \quad (7.3)$$

where σ_c^n and σ_c have the same meaning as in equation (1.4) and where $\langle \dots \rangle$, defined by equation (7.3), denotes an expectation value of the quantity inside. In other words, integrals of f_k over all variables are the factorial moments $\langle n \dots (n-k+1) \rangle$ of the multiplicity distribution.

Kinematically the process (7.1) is clearly the same as a $2 \rightarrow k+1$ process, provided that one considers one of the final state masses as the variable invariant mass of system X. For unpolarized initial particles the function f_k is thus a function of $3k-1$ essential variables at fixed s . This number grows rapidly with k and one is here faced with exactly the same problems of choice of variables and methods of presentation as in the study of exclusive reactions.

Considering as an example $a + b \rightarrow c_1 + c_2 + X$ (Figure 7.1), $f_2(p_1, p_2)$ will depend on five variables (at fixed s). For these one may take $2+2$ corresponding to c_1 and c_2 taken separately and add one more to describe

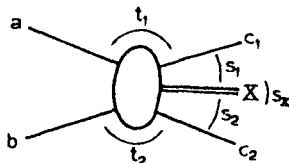


Figure VII.7.1

the coupling of c_1 and c_2 . One thus obtains the following possible sets

$$(P_1, \theta_1, P_2, \theta_2, p_1 \cdot p_2), \quad (7.4)$$

$$(q_1, r_1, q_2, r_2, r_1 \cdot r_2), \quad (7.5)$$

$$(t_1, s_2, t_2, s_1, s_x), \quad (7.6)$$

$$(\zeta_1, r_1, \zeta_2, r_2, r_1 \cdot r_2), \quad (7.7)$$

where the notation for momentum components, rapidities and angles is obvious, and where the variables in equation (7.6) are defined in Figure 7.1. Further sets are obtained by scaling as in Section 5. One could now proceed to analyse physical regions and transformations as was done for one-particle spectra in Sections 2–5, but this will lead to complicated formulas (Exercise VII.14).

In general a k -particle distribution cannot be derived from distributions containing fewer particles. This is due to correlations between particles. These may be analysed by defining correlation functions $c_k(p_1, \dots, p_k)$, which vanish when no correlations are present. The general formalism is taken from the theory of real gases (Huang, 1963) where the interaction between gas molecules gives rise to correlations. One defines

$$f_1(1) = c_1(1), \quad (7.8)$$

$$f_2(1, 2) = c_1(1, 2) + c_1(1)c_2(2), \quad (7.9)$$

$$\begin{aligned} f_3(1, 2, 3) &= c_3(1, 2, 3) + c_2(1, 2)c_1(3) + c_2(1, 3)c_1(2) + c_2(2, 3)c_1(1) \\ &\quad + c_1(1)c_1(2)c_1(3), \end{aligned} \quad (7.10)$$

and so on, where we have written $p_1 = 1, \dots$. It is obvious that if there are no correlations, that is, if

$$f_k(1, \dots, k) = f_1(1) \dots f_1(k), \quad (7.11)$$

then

$$c_k(1, \dots, k) = 0, k \geq 2, \quad (7.12)$$

and vice versa. Nonzero values of c_k thus imply the existence of correlations. This makes the c_k s a convenient tool for correlation analysis. Due to the great number of variables one has, in practice, to consider integrals of c_k .

A type of correlation always present in particle reactions is that due to four-momentum conservation, that is kinematic correlations. Their importance varies from one part of phase space to another. For instance, if in a two-particle inclusive reaction the momenta of the two produced particles are small compared with their maximum values, one is far from the phase space boundary and it is physically obvious that kinematic correlations are insignificant. There is no general rule of separating dynamical and kinematic correlations. In view of this we shall just consider three qualitative examples.

Example 1: Consider first an exclusive reaction $a + b \rightarrow 1 + \dots + n$ and the angles $\phi_{ij}, \cos \phi_{ij} = \mathbf{r}_i \cdot \mathbf{r}_j / r_i r_j$, between transverse momenta. These angles are invariant under longitudinal Lorentz transformations. We want to estimate the expectation value $\langle \cos \phi_{ij} \rangle$ as a function of multiplicity n . Without correlations one evidently has $\langle \cos \phi_{ij} \rangle = 0$. When $n = 2$, $\cos \phi_{12} = -1$ since \mathbf{r}_1 and \mathbf{r}_2 are completely correlated through $\mathbf{r}_1 + \mathbf{r}_2 = 0$. For larger n , taking the expectation value of the square of $\sum \mathbf{r}_i = 0$ leads to

$$\sum_i^n \langle \mathbf{r}_i^2 \rangle + 2 \sum_{i < j} \langle \mathbf{r}_i \cdot \mathbf{r}_j \rangle = 0. \quad (7.13)$$

Assuming that particles are identical this implies

$$\langle \mathbf{r}_i \cdot \mathbf{r}_j \rangle = -\frac{\langle \mathbf{r}_i^2 \rangle}{n-1}. \quad (7.14)$$

If one further assumes that the distributions in the lengths r_i and in $\cos \phi_{ij}$ are independent, then $\langle r_i r_j \cos \phi_{ij} \rangle = \langle r_i \rangle^2 \langle \cos \phi_{ij} \rangle$ by definition of independence and

$$\langle \cos \phi_{ij} \rangle = -\frac{\lambda}{n-1}, \quad (7.15)$$

where $\lambda = \langle \mathbf{r}_i^2 \rangle / \langle r_i \rangle^2 \geq 1$. This result is, of course, very approximate, but it illustrates how correlations arise from kinematics and how they vanish in this case when $n \rightarrow \infty$. These kinematic transverse-momentum correlations are analysed in more detail in (Bertocchi, 1967).

For the inclusive reaction $a + b \rightarrow c_1 + c_2 + X$ the expectation value $\langle \cos \theta_{12} \rangle$ is a weighted sum over n of terms of the form (7.15). It is clear that the kinematic correlation persists.

Example 2: Consider now two longitudinal momenta q_1 and q_2 in an exclusive reaction and take into account the observed limitation in transverse momenta (Section VI.5). For $n = 2$ $q_1 = -q_2$ (in CMS) and the correlation is maximal. For $n = 3$ the analysis of Section VI.6 (Figure VI.6.1) showed that events lie in an essentially one-dimensional region of the $q_1 q_2$ plane, that is correlations are strong but weaker than for $n = 2$. It is clear that this kinematic correlation remains for arbitrary n but gets weaker with increasing n . In any realistic case the situation is greatly complicated by the many various effects seen in longitudinal momentum distributions and the isolation of dynamical effects is difficult.

Example 3: Consider the inclusive reaction $a + b \rightarrow c_1 + c_2 + X$. The physical region in the $q_1^* q_2^*$ plane for s large is shown in Figure 7.2 (Exercise VII.14, see also Figure VI.6.1). The regions A and A' are unphysical and the two-particle f_2 vanishes there identically due to four-momentum conservation. However, it is perfectly possible to form the product $f_1(1)f_1(2)$ corre-

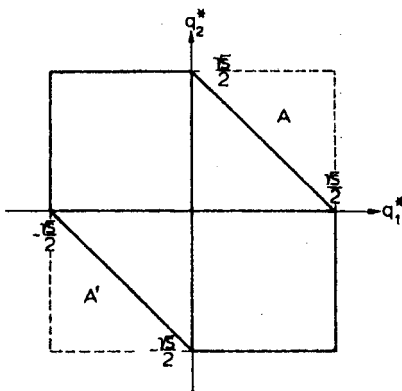


Figure VII.7.2 The limiting form as $s \rightarrow \infty$ of the physical region in the $q_1^* q_2^*$ plane for the inclusive reaction $a + b \rightarrow c_1 + c_2 + X$. The regions A and A' are forbidden by four-momentum conservation: both longitudinal momenta cannot simultaneously be large and parallel

sponding to values of q_1^* and q_2^* within the regions A and A'. Therefore, $c_2(1, 2) = -f_1(1)f_1(2)$ has a nonvanishing negative value in A and A' simply due to a kinematic correlation.

Exercises

- VII.1. Determine the limits of longitudinal momentum q^T in the target system, and study their dependence on s .
- VII.2. When can particle c in $a + b \rightarrow c + X$ move in any direction in the target system ($0 \leq \theta^T \leq 180^\circ$) and when only in a smaller range ($0 \leq \theta^T \leq \theta_{\max}^T$) in the limit $s \rightarrow \infty$? What is θ_{\max}^T ?
- VII.3. What is the beam system Peyrou plot, that is the physical region in the $q^B r$ plane?
- VII.4. Assume that in the CMS $f(q, r) = \exp \{ -b(m_c^2 + q^2 + r^2)^{\frac{1}{2}} \}$ and that P_{\max}^* is so large that the physical region can be assumed to extend to infinity (f decreases rapidly). Show that then

$$w(q) = \frac{\exp(-bE_0)}{\{2m_c K_1(m_c b)\}},$$

$$\langle r(q) \rangle = E_0^2 \exp(bE_0) K_1(bE_0), \quad E_0 = (q^2 + m_c^2)^{\frac{1}{2}}.$$

Determine $\langle r(q) \rangle$ for $q \rightarrow \infty$ and $q \rightarrow 0$ and study the dependence of its shape on m_c .

- VII.5. Calculate $w(q)$ and $\langle r(q) \rangle$ (equations (2.24–25)) if $f(q, r) = 1$ in CMS. Here one has to use the exact physical region.
- VII.6. Consider $a + b \rightarrow c + X$ in terms of the variables t and $u = (p_b - p_c)^2$. Prove that if $s, |t|, |u| \gg m_i^2$, then (a) $tu \approx sm_c^2$, (b) $\zeta = \frac{1}{2} \log(u/t)$.
- VII.7. Derive an expression for $d\sigma/d\zeta$ if $f(q, r)$ is given.
- VII.8. Prove that equations (4.7) are compatible, i.e. $\chi^{B*} = \chi^B - \chi^*$.
- VII.9. What is the exact range of ζ^B , the longitudinal rapidity in the beam system?
- VII.10. Assume the distribution $w(\cos \theta^*)$, where θ^* is the CMS angle between a and c in $a + b \rightarrow c + X$, is isotropic, i.e. $w(\cos \theta^*) = 1$. What is the distribution in CMS longitudinal rapidity ζ^* ?
- VII.11. What is the relation between the angular distributions $w(\cos \theta^T)$ and $w(\cos \theta^*)$ and the distributions in the variables u^* and u^T of equations (4.16)?
- VII.12. In double $O(1, 2)$ expansions of inclusive distributions, the natural variables are the momenta $P_a = m_a \sinh \eta_a$, $P_b = m_b \sinh \eta_b$ and the angle α between p_a and p_b in the frame $p_c = 0$. Show that these are related to variables ζ, r through (Tan, 1971)

$$m_c \cosh \eta_a = (m_c^2 + r^2)^{\frac{1}{4}} \cosh (\zeta^T - \chi^B)$$

$$m_c \cosh \eta_b = (m_c^2 + r^2)^{\frac{1}{4}} \cosh \zeta^T$$

$$m_c \sinh \eta_a \sinh \eta_b \sin \alpha = r \sinh \chi^B$$

where ζ^T is the TS longitudinal rapidity of particle c and χ^B is the relative rapidity of beam and target systems (equation (4.7)).

- VII.13. Prove that

$$\sum_c \int d^3 p E^{-1} p^\mu f_c(p, s) = (p_a + p_b)^\mu \sigma,$$

where f_c is the distribution function for particles of type c produced with momentum p in $a + b \rightarrow c + X$, the sum goes over all types of particles and σ is the total $a + b$ cross-section.

- VII.14. Determine the physical region in the $q_1^* q_2^*$ and $\zeta_1^* \zeta_2^*$ planes for the inclusive reaction $a + b \rightarrow c_1 + c_2 + X$. What is the relation of these regions to the longitudinal phase space plots of Section VI.6?

VIII

Kinematical Reflections

1. General description

The completely differential description of the process $a + b \rightarrow 1 + \dots + n$ in terms of the matrix element squared $T(x_1, x_2, \dots, x_N)$ depends on $N = 3n - 4$ variables. For fixed x_2, \dots, x_n any structure seen in $T(x_1)$ can be unambiguously interpreted as due to variation of the matrix element. For an integrated distribution, say $w(x_1) = \int dx_2 \dots dx_N T$, structure in $w(x_1)$ need not be due to corresponding variation in T . When the data are projected to the x_1 axis, the value $w(x_1)$ depends, of course, also on the ranges of the x_2, \dots, x_n integrations and on the behaviour of T as a function of these variables. In particular, there are situations in which observed structure in some distribution $w(x)$ is totally due to a strong effect in some other kinematic variable y . This phenomenon is called a *kinematical reflection*.

A main reason for watching out for kinematical reflections is that they may cause *fake effects*. Sometimes a conspicuous behaviour of experimental results in some variable x may lead one to conclude that also the matrix element depends strongly on x . However, a close look may reveal that the effect is actually a reflection of a dynamical feature from some other variable. Examples are fake peaks in mass distributions or fake dips, peaks and shoulders in momentum transfer distributions.

Kinematical reflections arise always when an integration over phase space is carried out. The general rule for minimizing their effect is to make the treatment of data as differential as possible. Only a wholly differential treatment is completely free from reflections. If any variables are integrated over, one is trying to determine the integrand (the matrix element squared) from the result of an integration (some distribution), which, of course, is not possible without further assumptions. A wholly differential analysis is feasible only for $2 \rightarrow 2$ and $2 \rightarrow 3$ processes (dimensionality 1 and 4). For more complicated reactions it is hardly thinkable due to limitations both in experimental statistics and in techniques of data analysis; for these a sufficient understanding of kinematical reflections is mandatory.

For practical purposes it is important to know what primary variables are likely to cause strong kinematical reflections. We shall in the following treat (1) reflections due to *cut in transverse momentum* (Section 2), (2) reflections due to *resonances* (Section 3).

2. Effects of cuts in transverse momentum and invariant momentum transfer

The observed cut in transverse momentum (Section VI.5) is a very strong phenomenon relative to pure phase space and it affects all reactions. As the transverse-cut phase space deviates significantly from the entire phase space, also their projections, which are distributions in some variables, are different. To analyse the reflections due to a cut in transverse momentum, we choose the simplest case in which they appear in a fully developed form: $2 \rightarrow 3$ reactions. More complicated reactions will not be considered, since they present qualitatively similar features.

To investigate these reflections in $2 \rightarrow 3$ reactions we distinguish between the following three cases.

1. Cut in transverse momenta:

$$T = \prod_1^3 f_i(r_i), \quad (2.1)$$

2. Singly peripheral cut, for instance ($a > 0$)

$$T = \exp(at_1), \quad (2.2)$$

3. Doubly peripheral cut, for instance ($a, b > 0$)

$$T = \exp(at_1 + bt_2). \quad (2.3)$$

Among these condition (2.3) implies condition (2.1), since if t_1 and t_2 are near their maximum values, r_1 and r_3 are small (Section VII.3 and Figure VII.3.2). By momentum conservation r_2 is small, too. The cut (2.2) is not realistic since it only implies that r_1 is small, but it is nevertheless useful to investigate its consequences. We shall first attempt to determine how the cuts (2.1–3) are reflected on distributions in the invariants s_1 and s_2 .

As explained in detail in Sections VI.5–6, the transverse cut (2.1) implies that the phase space accessible to $2 \rightarrow 3$ reactions is essentially one-dimensional at large s . Any dynamical quantity is thus a function of one variable only (chosen as the angle ω in Section VI.6) and by plotting this quantity versus ω one can immediately see what values are permissible within transverse-cut phase space. For instance, in Figure VI.6.2 s_1, s_2, t_1 and t_2 are plotted versus ω . One sees at once that s_1 and s_2 cannot reach their maximum values simultaneously. In fact, by including also $s_3 = s_{31}$ one sees that

$$s_i s_j \leq \frac{s^2}{4}, \quad i, j = 1, 2, 3. \quad (2.4)$$

This is a fairly weak condition. The same condition is seen to follow if we require t_1 to be near zero (condition (2.2) in addition to condition (2.1)).

However, if we require that t_1 and t_2 are simultaneously near zero (condition (2.3)), this is seen from Figure VI.6.2 to lead to a strong condition on s_1 and s_2 : s_1 large (proportional to s) implies s_2 small. In other words,

$$s_1 s_2 \lesssim \text{constant} \cdot s. \quad (2.5)$$

To put the conditions (2.4–5) in a more quantitative form we have to obtain the distributions in s_1 and s_2 by explicit integrations over t_1 and t_2 . For condition (2.1) this must be done numerically and we shall only consider conditions (2.2) and (2.3), for which the required integrations have already been carried out in Chapter V.

Consider first the singly peripheral cut (2.2). A glance at the $s_2 t_1$ Chew–Low plots in Figures V.5.3–4 gives an idea of how this cut in t_1 is reflected in the distribution of s_2 : giving a large weight to events having t_1 near its maximum possible value will clearly emphasize events with small or large s_2 if the masses are as in Figures V.5.3 or V.5.4, respectively. An exact numerical value of the effect is obtained from $d^2\sigma/ds_1 ds_2$ and $d\sigma/ds_2$, as given by equations (V.11.8) and (V.5.21). Explicit numerical examples of $d\sigma/ds_2$ are given in Figure 2.1; one sees how strongly the effect depends on masses. The

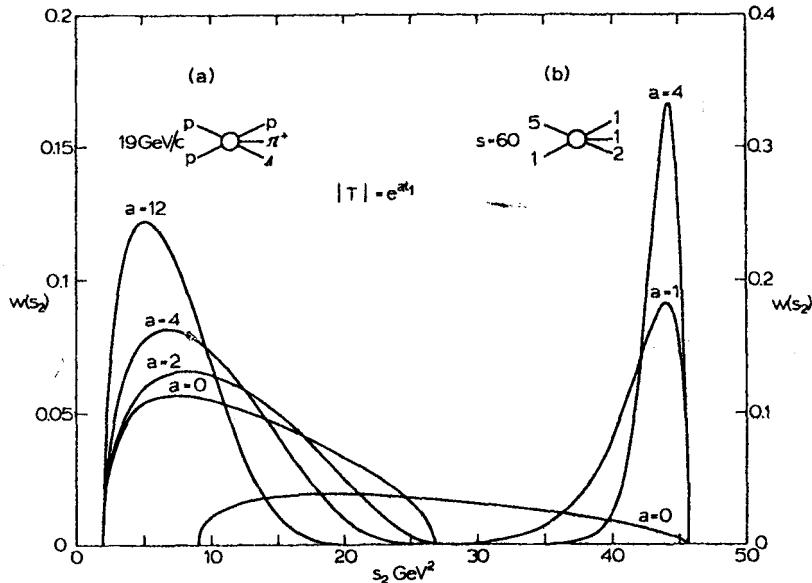


Figure VIII.2.1 The normalized distribution $w(s_2)$ in s_2 arising from the matrix element squared $\exp(at_1)$ and with values of a shown in the figure. The reaction is (a) $pp \rightarrow p\pi\Delta$ at $19 \text{ GeV}/c$ and (b) a reaction with masses $5 + 1 \rightarrow 1 + 1 + 2$ and with $s = 60 \text{ GeV}^2$ (see Figure V.5.4)

effect produces resonance-like peaks but they are either very broad or lie at very large values of s_2 .

To have an approximation for equation (V.5.21) for $d\sigma/ds_2$, assume the reaction has the masses $\mu m_b \rightarrow \mu m_2 m_3$, so that the Chew-Low plot is like that in Figure V.5.3. Then, applying equation (IV.6.6) to a $2 \rightarrow 2$ reaction with masses $\mu m_b \rightarrow \mu \sqrt{s_2}$,

$$t_1^+ \simeq -\frac{\mu^2(s_2 - m_b^2)^2}{s^2},$$

if $s \gg s_2$, $(\text{masses})^2$. Inserting this into equation (V.5.21) and neglecting $\exp(at_1^-)$ one finds

$$\frac{d\sigma}{ds_2} \simeq \exp \left\{ \frac{-a\mu^2(s_2 - m_b^2)^2}{s^2} \right\} \quad (2.6)$$

if $(m_2 + m_3)^2 \ll s_2 \ll s$. Unless s_2 is near the phase space limits, $d\sigma/ds_2$ decreases as a Gaussian (Figure 2.1(a)). However, the parameter $a\mu^2/s^2$ decreases rapidly when $s \rightarrow \infty$, which explains why the peak is so broad in Figure 2.1(a). We conclude that reflections due to a singly peripheral cut can hardly be confused with a resonance.

Turning to the doubly peripheral cut (2.3) the reflections follow from the distribution $d^2\sigma/ds_1 ds_2$ computed in equation (V.11.8). An idea of their general behaviour is simplest to obtain from the form (V.11.25), valid in the double Regge limit (V.11.19). One sees that $d^2\sigma/ds_1 ds_2$ behaves like

$$\frac{d^2\sigma}{ds_1 ds_2} \sim \exp \left\{ \left(\frac{ab}{a+b} \right) \left(m_2^2 - \frac{s_1 s_2}{s} \right) \right\}, \quad (2.7)$$

in other words, it decreases exponentially if the parameter

$$\xi = \frac{s_1 s_2}{s} \quad (2.8)$$

increases. Reflections due to the doubly peripheral cut are thus strong. Note that if the cut is singly peripheral ($ab = 0$), the leading term in the argument of equation (2.7) vanishes and only lower terms, like that in equation (2.6), remain. On $s_1 s_2$ plane curves of constant ξ are hyperbolas symmetric with respect to the line $s_1 = s_2$ and ξ increases when one moves away from the origin (Figure 2.2). As a consequence of the cut (2.3), events will thus populate that part of the Dalitz plot which lies near the origin. Conversely, if events are observed to lie preferably near the origin, this need not imply anything else of the matrix element but that it imposes a cut on transverse momenta. The concentration of events near one corner of the Dalitz plot is a typical kinematical reflection, called the **cornering**

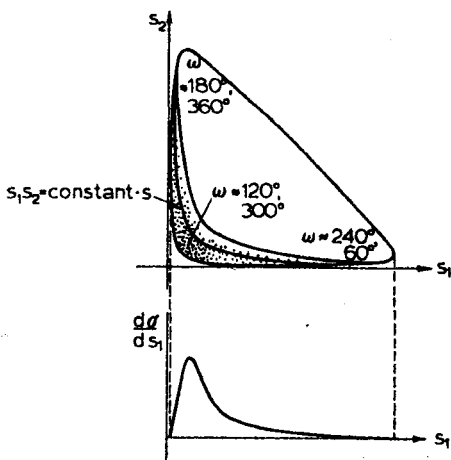


Figure VIII.2.2 Cornering effect on the Dalitz plot (qualitatively) produced by $T = \exp(at_1 + bt_2)$; the projection on s_1 axis exhibits the Deck effect. On LPS plot, this cut populates the region $\omega = 120^\circ$ (Figures VI.6.1 and VI.6.3). Other possible doubly peripheral cuts (Figure VI.6.3) populate the corners denoted by corresponding values of ω

effect (Chan, 1967a). Essentially the same statements hold for exact result (V.11.8). However, one must keep in mind that on experimental Dalitz plots, at least for $s < 100 \text{ GeV}^2$, the cornering effect is masked by effects due to resonances or diffraction dissociation. But this only implies that the matrix element is not $\exp(at_1 + bt_2)$ and is irrelevant for the present argument.

By projecting the distribution in Figure 2.2 on s_1 or s_2 axes one sees that the distributions in s_1 and s_2 will contain sharp resonance-like peaks at small s_1 and s_2 . But here these peaks are reflections of the doubly peripheral matrix element (2.3). In this form the reflection is known as the **Deck effect** (Deck, 1964).

If one instead of the cut (2.3) uses any of the cuts shown in Figure VI.6.3 one sees that if at large $s |t_{ai}|$ and $|t_{bk}|$ ($i \neq k = 1, 2, 3$) are demanded to be small, the distribution on the Dalitz plot is centred in the corner in which s_{ij} and s_{jk} ($j \neq i \neq k$) are simultaneously small and s_{ik} is large (Figure 2.2). In any case the centre of the Dalitz plot remains empty and the **relative width** of the populated region is proportional to $1/\sqrt{s}$ at large s since the size of Dalitz plot is proportional to s and the width of $d^2\sigma/ds_1 ds_2$ to \sqrt{s} . The situation is thus exactly the same as with respect to the LPS plot in

Figure VI.6.1; only when considering the Dalitz plot one loses track of the sign of longitudinal momenta, and thus when one goes once around the LPS (Figure VI.6.1) one has to go twice around the Dalitz plot. These remarks summarize the essence of the mechanism reflecting the cut in transverse momenta to s_1 and s_2 .

Due to the importance of the cornering effect we shall characterize it in still another form. The boundary of the physical region is $\Delta_4 = 0$ (see equation (V.9.3)) and if the transverse momentum components are small equation (II.7.17) implies that Δ_4 is small. Events from transverse cut phase space thus fall near the boundary of the physical region. Turning now to the cut in t_1 and t_2 , and choosing fixed values of t_1 and t_2 , the physically accessible points on $s_1 s_2$ plane are bounded by the curve $\Delta_4 = 0$, expressed as a function of s_1 and s_2 (Section V.9, part (c)). It is easy to see by plotting the curve $\Delta_4 = 0$ (Figure 2.3) that for small values of $|t_1|$ and $|t_2|$ no simultaneously large values of s_1 and s_2 are allowed. In the double Regge limit

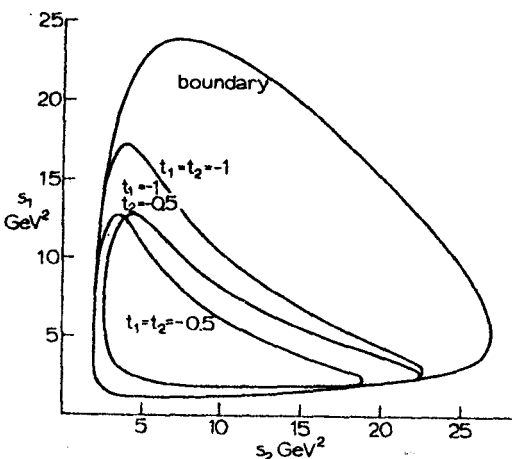


Figure VIII.2.3 The curve $\Delta_4 = 0$ for $pp \rightarrow p\pi\Delta$ at 19 GeV/c plotted for the fixed values of t_1 and t_2 shown in the figure

(V.11.19) one can even put this statement in the quantitative and explicit form (V.11.23). Thus one has again arrived at the cornering effect.

The cut in transverse momentum is also strongly reflected on variables other than invariant masses. We shall consider how the angular variables $(\theta_{b3}^{R23}, \phi_b)$, $(\theta_{13}^{R23}, \lambda_1)$ and ω_2 of Chapter V are modified when a doubly peripheral cut is introduced. Of these all but ω_2 are uniformly distributed

in phase space, ω_2 is strongly peaked at π at large s . The statements will be qualitative and the actual magnitude of the effect increases with the values of the parameters a and b in equation (2.3). One finds that the distribution in

the cosine of the Jackson angle θ_{b3}^{R23} becomes peaked at +1 since according to equation (V.7.5) +1 corresponds to small $|t_2|$,

the Treiman-Yang angle ϕ_b remains uniform since the cut (2.3) contains no s_1 -dependence,

the cosine of the helicity polar angle θ_{13}^{R23} becomes peaked at -1 since according to equation (V.1.8) -1 (+1 for $\cos \theta_{12}^{R23}$) corresponds to small s_1 , and small s_1 dominates due to the cornering effect,

the helicity azimuthal angle λ_1 becomes peaked at 0° since according to equation (V.8.9) $\lambda_1 \approx 0^\circ$ corresponds to small $|t_2|$,

the Toller angle ω_2 becomes less peaked near π .

Note, in particular, that the experimentally observed peaking near π of distributions in the Toller angle is not a reflection of the transverse-cut phase space; the cut in transverse momentum actually weakens the peaking.

3. Effects of resonances

A resonance is characterized by

the Breit-Wigner shape in the dependence on the invariant mass in which the resonance appears,

the angular dependence on decay angles determined by the resonance spin and production mechanism.

These properties may be reflected in other variables as explained above. Since there are only a few prominent and pure resonances, resonance reflections are less important than those due to cut in transverse momentum. As before it is not possible to present an exhaustive analysis covering all types of reflections and we shall, instead, proceed by analysing some typical cases.

(a) Effect of one resonance on another

Consider a $2 \rightarrow 3$ reaction, in which a resonance appears in each of the final state two-particle combinations. An example is $\pi^+ p \rightarrow \pi^+ \pi^0 p$ (Figure 3.1). It is clear that the distribution in any of the s_{ij} will contain contributions from the resonances in the remaining two invariant masses. To disentangle the resonances one must consider the complete Dalitz plot distribution. However, even this is not sufficient, since resonances may overlap. To analyze what happens in the overlap regions one has also to consider the

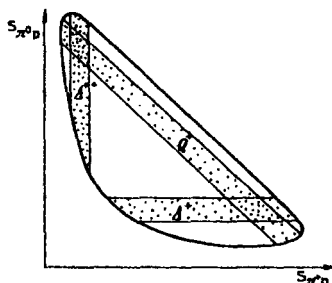


Figure VIII.3.1 Dalitz plot for $\pi^+ p \rightarrow \pi^+ \pi^0 p$ with overlapping resonance bands

two variables t_1 and t_2 integrated over when deriving the Dalitz plot distribution. In other words, one must return to a completely differential treatment in a four-dimensional space. For instance, the subprocesses $\pi^+ p \rightarrow \pi^0 \Delta^{++}$ and $\pi^+ p \rightarrow \rho^+ p$ overlap on the Dalitz plot and a proper method of analyzing them is to add their amplitudes coherently and from this sum derive the Dalitz plot distribution. Trying to separate the channels by using only the Dalitz plot is meaningless.

(b) Effects due to angular distributions of resonances

Resonances are characterized by definite angular distributions, which present more symmetry than expected if the particles in question were not in resonance. For instance, a two-body decay mode may have both a backward and a forward peak in the decay angle distribution, while only the forward peak is expected if the two particles are non-resonant or — which amounts to the same — if there are many overlapping resonances. The backward peak will then by kinematic reflection cause unexpected structure in other distributions (Berger, 1969).

More precisely, assume that there is a resonance in the 13-system of the reaction $a + b \rightarrow 1 + 2 + 3$ and that this resonance decays with strong peaks in the forward and backward directions, i.e. the decay distribution is peaked at $\cos \theta_{b1}^{R31} = \pm 1$, where θ_{b1}^{R31} is the relevant Jackson angle (Section V.6). If this resonance is also peripherally produced, the Jackson and helicity systems are not too different (equation (V.6.1)) and also the distribution in the helicity polar angle will be peaked at 0° and 180° . But this distribution gives directly the distribution on the Dalitz plot (see end of Section V.3) and there will be maxima near both ends of the resonance band (Figure 3.2). It is then clear that the distributions in s_1 and s_2 following from Figure 3.2 will exhibit resonance-like structure. Whether experimentally observed

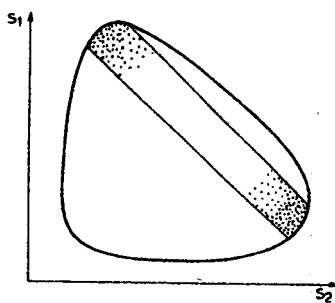


Figure VIII.3.2 A peripherally produced resonance in the 13 system with a Jackson angle distribution peaked at 0° and 180° produces a Dalitz plot distribution with maxima near both ends of the resonance band. When projected on s_1 and s_2 axes, these maxima generate resonance-like structure

resonance-like structure can be explained by this mechanism has to be answered by analysing the data as differentially as possible. For more details we refer to (Berger, 1969).

(c) Effects of resonances on inclusive reactions

In inclusive reactions it is not specified whether the observed particles are decay products of a resonance or, in some sense, directly produced particles. If there are strong resonances present, one certainly expects them to affect inclusive distributions. A striking example of this is the Yen-Berger (Yen, 1970) model for observed sharp forward peaks in one-particle inclusive distributions of transverse momentum. According to this model,

these peaks arise if the observed particle is the decay product of a peripherally produced resonance of small Q value,

the peaks are particularly sharp if the observed particle has a small mass, that is when it is a pion.

The first property guarantees that the decay momenta in the rest frame of the resonance are small, the second that the transverse momentum of a small-mass decay product is small. For a detailed explanation of this effect we refer to (Yen, 1970).

IX

Numerical Methods of Phase Space Integration

1. Introduction

An important numerical problem in particle physics is the computation of the integral

$$I_n = I_n(P) \\ = \int_V \cdots \int \prod_1^n \frac{d^3 p_i}{2E_i} \delta^4(p - p_1 - \dots - p_n) T. \quad (1.1)$$

The matrix element squared, T , is a function of $3n - 4$ independent kinematic variables. The region of integration V is either the whole physical region or part of this. If V is the entire phase space, I_n multiplied by the flux factor gives the total cross-section. Differential cross-sections are obtained by integrating over a subspace of the entire phase space.

As before, it is in practice necessary to eliminate the δ function in the integral (1.1) and to write I_n in the form

$$I_n = \int_V d\Phi \rho_n(\Phi) T(\Phi) \\ = \int d\Phi f_n(\Phi). \quad (1.2)$$

Here Φ stands for the coordinates of a point in the $3n - 4$ dimensional phase space, expressed in terms of any set of kinematical variables — several examples have appeared in previous chapters. The domain of integration V is the domain of integration in equation (1.1) expressed in terms of the phase space variables Φ . The integrand $f_n(\Phi) = \rho_n(\Phi) T(\Phi)$ is a product of the matrix element squared $T(\Phi)$ and the phase space density $\rho_n(\Phi)$, which is the product of certain factors arising from the transformation of variables (the Jacobian), and factors due to integration over the delta function.

The main reason for the complexity of equation (1.1) is, of course, the large number of dimensions to be integrated over. Due to the four-dimensional δ function, which appears very simple, the limits of integration are normally

complicated and interdependent. For $n = 2$ the problem is trivial, but for $n = 3$ there are already four non-trivial variables. Furthermore, the domain V may be such that there exists no set of the variables Φ in terms of which V is simply expressible.

The techniques commonly used to evaluate equation (1.2) fall into the following classes.

1. Direct numerical integration. This is the most straightforward idea and consists essentially of applying to each dimension successively the ordinary techniques of one-dimensional numerical integration (Simpson's rule, Gaussian integration formulas, etc.). Since all these one-dimensional methods are based on evaluating the integrand in a fixed set of points, the multi-dimensional integral (1.2) is also carried out by evaluating $f_n(\Phi)$ in a pre-determined set of points. If the integration interval in each variable is divided into $k - 1$ subintervals, the lattice thus formed in the $3n - 4$ dimensional space contains k^{3n-4} points. Since k is usually required to be a fairly large number (≥ 10), k^{3n-4} grows very rapidly with n . The time required to compute the values of the integrand in the k^{3n-4} points limits the use of direct integration to $n = 2$ or 3, apart from some special cases. A factorizable matrix element is sometimes effectively integrated directly using recursion relations (Section 2).

It is also possible to sample a function in a multidimensional space at a set of points not forming a regular lattice. The optimum choice of these points, which must depend on the type of the function, has not been solved.

The method of direct numerical integration was the first one to be applied to the evaluation of equation (1.2) (Almgren, 1968; Kopylov, 1960; Milburn, 1955; Proriol, 1969), in the special case $T = 1$.

2. The Monte Carlo methods. Since it is not known how the points at which $f_n(\Phi)$ is to be evaluated should be chosen to optimize the efficiency, it appears to be convenient to go to the other extreme and to choose the points at random. This is the Monte Carlo method of integration, which at present is the most efficient, versatile and practical method of evaluating equation (1.2). For this reason our treatment of the Monte Carlo method will be fairly detailed.

The Monte Carlo method is a widely used tool in different branches of applied science, but it also involves many deep problems of purely mathematical nature. For a general description of the method, see the book by Hammersley and Handscomb (Hammersley, 1967) and the review by Halton (Halton, 1970). In particle physics the method was first used in connection with the non-covariant phase space integral by Cerulus and Hagedorn (Cerulus, 1958). Kopylov (Kopylov, 1958, 1960; Komolova, 1965, 1967) was the first one to exploit the covariance properties of equation (1.1). The method in use to-day is essentially the same as Kopylov's.

The Monte Carlo method requires for reasonable accuracy very many random points (at least of the order of 10^3). It rose into full prominence only with the development of fast computers and standard programs simple for the general user. The most extensively used standard Monte Carlo program is FOWL (James, 1968, 1970) written by James on the basis of work done by Lynch and Raubold (Lynch, 1967). The Monte Carlo methods in particle physics have constantly been improved to optimize their efficiency for the problems occurring most frequently in practice (Byckling, 1969a, 1969c; Friedman, 1971a, 1971b; Kittel, 1970; Kopylov, 1962, 1971; Pene, 1969).

3. Statistical methods. When T factorizes,

$$T = g_1(p_1) \dots g_n(p_n), \quad (1.3)$$

some special and very efficient techniques can be used to evaluate equation (1.1). Due to their analogy with certain methods applicable in statistical physics we shall rather loosely call these techniques statistical methods. The name saddle point methods would also be appropriate. The value of equation (1.1) is given by these methods as an expansion in $1/\sqrt{n}$ and the accuracy thus improves with increasing n , in contrast to all other methods.

The factorizability condition includes also the case $T = 1$ to which these statistical methods were first applied (Lepore, 1954; Fialho, 1957; Kolkunov, 1962; Lurçat, 1964; Campbell, 1967). Lurçat and Mazur (Lurçat, 1964) give a particularly elegant interpretation of the method in terms of the central limit theorem of probability theory (Khinchin, 1949). They also calculate the first correction term and show that the resulting values are numerically remarkably accurate. The case in which each g_i in equation (1.3) only depends on the length r_i of the transverse momentum of particle i has been treated by Krzywicki (Krzywicki, 1964, 1965); the longitudinal phase space integral (VI.5.7) is evaluated by this method in (Kajantie, 1972a), the influence of angular momentum conservation is investigated in (Keuk, 1968; Satz, 1963, 1967), the method is applied to integrals in which the integrand is a vector, tensor, etc., in (Kolkunov, 1967a, 1967b, 1969).

2. Direct numerical integration

There are certain cases of phase space integration in which the usual direct methods of numerical integration are applicable. We shall comment on (a) three-particle final states, (b) factorizable matrix elements in connection with recursion relations.

(a) Three particle integrals

Three particle final states involve four essential kinematical variables (in the absence of spin). Calculation of distributions in one or two variables,

which need only three- or two-dimensional integrations, and occasionally also calculation of the total cross-section, are most accurately and economically carried out using multiple Newton-Cotes or Gaussian formulae. There are also special methods for definite integrals in two and three dimensions (Hammer, 1959). A drawback in this approach is that a separate computer program must be written for each problem.

Several choices of kinematical variables for the process $a + b \rightarrow 1 + 2 + 3$ are exhibited in the integral formulae in Chapter V. The choice between such expressions is dictated by the properties of T and by the quantities to be calculated. In this connection we only note that in the expression (V.9.2) involving the variables s_1, s_2, t_1, t_2 , the factor $(-\Delta_4)^{-\frac{1}{2}}$ diverges at the boundaries and the limits of the integration are given by the cumbersome condition $\Delta_4 = 0$. Even if T vanishes sufficiently fast at the boundaries, the latter property makes it preferable to use formulae involving at least one angle and no Δ_4 .

(b) Recursion relations

When the matrix element squared is factorizable in some variables in terms of which the phase space integral can be expressed recursively (Chapter VI), the numerical integration can be carried out so that the number of points grows essentially as $n \cdot k$ (n = number of dimensions, k = number of subdivisions in one dimension) and not like k^n (Pirilä, 1972). This implies an essential improvement in efficiency. As examples we shall briefly treat the cases

$$T = \prod_2^n f(M_i, M_{i-1})$$

and

$$T = \prod_1^{n-1} f(t_i),$$

where the variables have been defined in Chapter VI. Note that the factorization condition here may be different from that in equation (1.3) which allows one to apply statistical methods.

Assuming the matrix element to be unity, equation (VI.2.10) gives $R_n(M_n^2)$ recursively as follows:

$$R_n(M_n^2) = \int_{M_{n-1}}^{M_n - m_r} dM_{n-1} K_n(M_n, M_{n-1}) R_{n-1}(M_{n-1}^2), \quad (2.1)$$

where all variables have been previously defined and the kernel K_n can be read from equation (VI.2.10). To evaluate $R_n(M_n^2)$ by iterating equation (2.1) numerically, one selects a discrete set of k points for each variable of type M_n .

Then R_n is reached from R_2 by $n - 2$ multiplications by a $k \times k$ matrix, which will involve about $(n - 2) \cdot k^2$ multiplications and additions. The matrix elements are products of K_n and coefficients of a suitable integration formula (e.g. Simpson's). This method is applicable in the more general case where the matrix element is of the form $\prod_i f_i(M_i, M_{i-1})$, but this rarely occurs in practice.

When n is large, the statistical methods of Section 6 yield $R_n(M_n^2)$ more rapidly. On the other hand, recursion relations have the property that the distribution in M_{n-1}^2 is obtained with little more effort than the one value $R_{n-1}(M_{n-1}^2)$. In fact, if one starts from $R_2(M_2^2)$ defined in the interval $\mu_2 \leq M_2 \leq M_n - \mu_{n-1}$, then $n - 3$ matrix multiplications give $R_{n-1}(M_{n-1}^2)$ in the whole interval $\mu_{n-1} \leq M_{n-1} \leq M_n - m_n$.

As a second example, consider

$$T = \prod_1^{n-1} f_i(t_i).$$

According to equation (VI.2.26), the integral I_n obtained by integrating T over all phase space can be written recursively as follows:

$$\begin{aligned} I_n(M_n^2, t_n) &= \iint dM_{n-1} dt_{n-1} K_n(M_n, t_n; t_{n-1}) I_{n-1}(M_{n-1}^2, t_{n-1}) \\ K_n &= \frac{\pi}{2} \lambda^{-\frac{1}{2}}(M_n^2, t_n, m_n^2) f_{n-1}(t_{n-1}) \\ I_2(M_2^2, t_2) &= \frac{\pi}{2} \lambda^{-\frac{1}{2}}(M_2^2, t_2, m_2^2) \int f_1(t_1) dt_1, \end{aligned} \quad (2.2)$$

where all variables have been defined previously. The evaluation of equation (2.2) proceeds similarly to that of equation (2.1). A computer program of some complexity carrying this out has been written (Pirilä, 1972). An advantage in this method is that a distribution in s or in the whole *st* Chew-Low plot can be generated efficiently.

3. Principles of Monte Carlo integration

By far the most common way to carry out phase space integrations is the Monte Carlo method. This is due to the following properties of Monte Carlo methods.

- (a) Within the domain of application the rate of convergence is faster than that of other methods. The error decreases proportionally to $1/\sqrt{N}$ or even better, where N is the number of points at which the integrand is evaluated.

- (b) The method is very general in the sense that it can be made reasonably efficient for all matrix elements occurring in practice.
- (c) The method gives many distributions at essentially the same expense as a single distribution; the same events need only be histogrammed in different ways. Also complicated distributions like those in Treiman-Yang angles are easily obtained.
- (d) Monte Carlo computer programs can be made very simple for the general user.
- (e) The Monte Carlo method treats events exactly as they are treated, for example, in bubble chamber physics. The method thus resembles the way in which data are handled in experimental particle physics.

When applying Monte Carlo methods to particle physics one does not evaluate the integrand $f_n(\Phi)$ at a predetermined set of points but rather chooses these points at random. This is done by generating events at random with a known density $g(\Phi)$ in phase space and evaluating $f_n(\Phi)$ at these events. An event here is a set of n momentum vectors $\mathbf{p}_1, \dots, \mathbf{p}_n$ in any given frame satisfying four-momentum conservation and the mass shell conditions $p_i^2 = m_i^2, i = 1, \dots, n$. The density $g(\Phi)$ is defined as a usual probability density, so that the probability that a random event appears in an infinitesimal neighbourhood of a point Φ of the phase space is $g(\Phi) d\Phi$, where $d\Phi$ is the volume element in the phase space. Different sets of $3n - 4$ variables can be used to express the coordinates of the point Φ . We shall use invariants and angles, but one can also use momentum components.

How many events have to be generated to give a reliable result depends on the efficiency of the Monte Carlo method being used. Efficiency can be defined as being inversely proportional to the amount of labour expended to obtain a result with given statistical accuracy. Qualitatively the efficiency is the better the better $g(\Phi)$ approximates the function $f_n(\Phi)$ to be integrated. In the best cases with present Monte Carlo programs a few thousand events are often sufficient.

Notice that, from the point of view of generation of events, there are three different kinds of densities.

- (1) The ideal Monte Carlo generator of events is, of course, a particle reaction. The purpose of most experiments is just to chart with what density in the phase space the particles are produced.
- (2) Any model for a reaction involves the specification of a matrix element or a density of events in the phase space. These matrix elements are often very complicated functions (like those appearing in dual models) and it is not possible to use computers to generate events with these densities.

(3) Monte Carlo programs generate events with certain densities $g(\Phi)$ which mostly are some simple functions of Φ . There is much freedom in the choice of $g(\Phi)$ but one must remember that a $g(\Phi)$ may be good for one problem but inefficient for another. Thus for Monte Carlo programs in general use one has to optimize $g(\Phi)$ so that it is good for as many problems as possible.

Our main goal in the following is to explain how the random generation of events can be carried out and what types of densities $g(\Phi)$ occur in practice. To do this, consider first the simple one-dimensional integral (Figure 3.1)

$$m = \int_0^1 dx f(x). \quad (3.1)$$

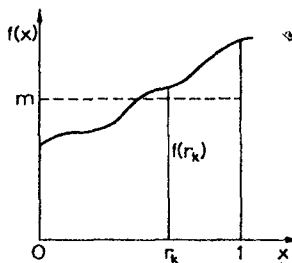


Figure IX.3.1 Monte Carlo integration of a function $f(x)$ over the interval $(0, 1)$: r_k is a random point, m is the exact value of the integral

In practice one would never apply Monte Carlo integration to one-dimensional integrals, since normal numerical methods are much faster and converge more rapidly. We denote the value of the integral by m , since it is clearly the mean value of the function $f(x)$ over the interval $(0, 1)$. Similarly one defines the variance σ^2 of the function $f(x)$:

$$\sigma^2 = \int_0^1 dx \{f(x) - m\}^2. \quad (3.2)$$

The variance measures the fluctuations of $f(x)$ in the interval $(0, 1)$: the larger σ^2 is, the more $f(x)$ fluctuates around its mean value.

Suppose now that we are able to generate random numbers r_k , $0 < r_k < 1$, $k = 1, 2, \dots$, so that each value between 0 and 1 is equally probable, that is the r_k are uniformly distributed within the interval $(0, 1)$. In the following r_k will always denote a random variable of this type. The r_k are basic for any Monte Carlo technique and the problem of how exactly they should be generated in a computer which certainly is not a random device, is a very important one. For this question we refer to the specialized literature mentioned earlier. Let

us now generate N numbers r_1, \dots, r_N and sample the integrand in equation (3.1) at these points. Then m is approximated by the arithmetic mean \bar{m} of the N numbers $f(r_k)$,

$$\bar{m} = \frac{1}{N} \sum_{k=1}^N f(r_k). \quad (3.3)$$

This is a Monte Carlo estimate of the integral (3.1). Applying the terminology of particle physics to the Monte Carlo technique, the generated value r_k is called an 'event' and $f(r_k)$ the 'weight assigned to the event'.

Since the r_k are random variables, \bar{m} is also a random variable, so that if another set of r_k is generated a new value of \bar{m} is obtained. For fixed N , the values of \bar{m} are so distributed that the expectation value of \bar{m} is just the required value m of the integral (3.1). The deviation of \bar{m} from its most probable value is measured by the quantity,

$$\bar{\sigma}^2 = \frac{1}{N-1} \sum_{k=1}^N \{f(r_k) - \bar{m}\}^2, \quad (3.4)$$

which approximates equation (3.2) in the same sense as \bar{m} approximates m . In equation (3.4) one measures the deviation of $f(r_k)$ from the estimated value \bar{m} and not from the true value m . This has the effect of increasing the variance by $N/(N-1)$. One can then show that the quantity $\bar{\sigma}$, defined as in equation (3.4), with $N-1$ in the denominator, will have expectation value equal to σ .

The formal justification of the above statements follows from the central limit theorem of probability theory. Assume that the random variables x_i , $i = 1, \dots, N$, are distributed so that their mean values are m_i and variances σ_i^2 . Under fairly general conditions the distribution of the sum $x = (x_1 + \dots + x_N)/N$ for large N then approaches the normal distribution

$$N(x; m, \sigma) = \frac{1}{\sigma\sqrt{\pi}} e^{-(x-m)^2/2\sigma^2} \quad (3.5)$$

with mean $m = (1/N) \sum_{i=1}^N m_i$ and variance $\sigma^2 = (1/N^2) \sum_{i=1}^N \sigma_i^2$. In the present case the random numbers are the numbers $f_k = f(r_k)$ which are distributed so that their average value is m and variance σ^2 . Thus, for large N , \bar{m} converges to m and the variance of the distribution in \bar{m} is $(1/N)\sigma^2$. The value of σ^2 is not known, of course, but $\bar{\sigma}^2$ in equation (3.4) is an estimate for it. The result of the Monte Carlo integration can thus be expressed as

$$m = \bar{m} \pm \frac{\bar{\sigma}}{\sqrt{N}}. \quad (3.6)$$

It follows from equation (3.5) that for repeated Monte Carlo integrations the probability that the result deviates from the correct value of m , for example, by more than one or two standard deviations σ/\sqrt{N} , is 32 per cent.

or 4.5 per cent., respectively. Note that equation (3.6) tells nothing about the error in a single Monte Carlo integration.

Example: We shall in this example exhibit a simple case for which the probability density $F(\bar{m})$ of \bar{m} can be evaluated explicitly. Assume $f(x) = x$ so that from equations (3.1) and (3.2) $m = \frac{1}{2}$ and $\sigma^2 = \frac{1}{12}$. The Monte Carlo estimate for m , according to equation (3.3), equals

$$m = \frac{1}{N} \sum_{k=1}^N r_k,$$

i.e. N^{-1} times the sum of N random numbers evenly distributed between 0 and 1. The probability density $F(\bar{m})$ of \bar{m} can in this case be calculated by standard methods of probability theory. In fact, $F(\bar{m})$ is the integral

$$F(\bar{m}) = N \int_0^1 dr_1 \dots dr_N g(r_1) \dots g(r_N) \delta(r_1 + \dots + r_N - N\bar{m}) \quad (3.7)$$

where $g(r)$ is one for $0 < r < 1$ and zero elsewhere. Evaluation of the integral by Laplace transforms gives

$$F(\bar{m}) = \frac{N}{(N-1)!} \sum_{k=0}^N (-1)^k \binom{N}{k} \{(Nx - k)_+\}^{N-1}, \quad (3.8)$$

where $(x)_+ = (x + |x|)/2 \equiv x\Theta(x)$. The curve representing $F(\bar{m})$ is drawn for different values of N in Figure 3.2. It consists of segments of N different polynomials of order $N-1$ in the intervals $(0, 1/N), (1/N, 2/N), \dots$, etc. One can clearly see how $F(\bar{m})$ approaches a Gaussian (3.5) peaked at $\frac{1}{2}$ (= the exact value m of the integral) and how the peak becomes narrower when N increases. This gives an idea of how the accuracy of Monte Carlo integration increases when N increases.

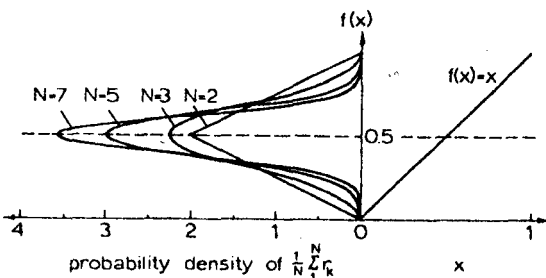


Figure IX.3.2 Illustrating the convergence of Monte Carlo integration. The function to be integrated is $f(x) = x$; the curves show how the normalized probability densities of the Monte Carlo estimates are peaked closer and closer to the correct value 0.5 as N increases

The generalization of equation (3.3) to more dimensions is intuitively obvious:

$$\int_0^1 \dots \int_0^1 dx_1 \dots dx_K f(x_1, \dots, x_K) = \frac{1}{N} \sum_{k=1}^N f(r_1^{(k)}, \dots, r_K^{(k)}) \quad (3.9)$$

where the random points $(r_1^{(k)}, \dots, r_K^{(k)})$ are uniformly distributed in a K -dimensional hypercube. Previously we sampled the integrand within an interval, now we sample it within a hypercube. If the limits of integration are separately dependent on some of the x_i , they can separately be transformed to 0 or 1 and equation (3.9) applied. The error is given by a formula analogous to equation (3.6). In particular, it is proportional to $1/\sqrt{N}$ independent of the dimension K .

4. Reduction of the statistical error

The statistical error of the *crude Monte Carlo* described above depends on two factors, the variance σ^2 of the function to be integrated and the number of random points at which the function is sampled. The simplest way to decrease the error is to increase N . The error is proportional to $1/\sqrt{N}$ so that to decrease the error by ten one has to increase N by 100. The accuracy that can be obtained through increase of N is limited by the computer time available.

There are also numerous more effective ways to decrease the variance of the result of a Monte Carlo integration. Most of these *variance-reducing techniques* can be understood as an application of the following simple ideas: either the original problem with function $f_n(\Phi)$ is modified so that the new function has a smaller variance or the distribution of the random events is changed to be no longer wholly random and uniform. Some techniques, as we shall see, can be formulated in terms of either one of these ideas. We shall describe here some variance reducing techniques which are generally used in particle physics. The art of Monte Carlo techniques has attained considerable sophistication, and if a problem requires going beyond the standard routines presented here, it will pay to consult an expert.

Firstly, it is possible to improve the rate of convergence so that the statistical error may even be proportional to $1/N$ using *quasi-random* numbers. The statement* that the error behaves, in general, like $1/\sqrt{N}$ is based on the assumption that the random numbers used are truly random or, in computers, numbers which 'look random' (*pseudo-random* numbers). With pseudo-random numbers one has no idea of at what points the integrand $f_n(\Phi)$ is sampled. However, one may also use random numbers which on the whole are evenly distributed but which are strongly correlated so that r_{i+1} depends on r_i (*quasi-random* numbers). For instance, the sequence $\frac{1}{2}; \frac{1}{4}, \frac{3}{4}; \frac{1}{8}, \frac{3}{8}, \frac{5}{8}, \frac{7}{8}; \dots$, formed according to an evident rule, would be a sequence of quasi-random numbers. With quasi-random numbers one has some guarantee of

that the integrand is sampled evenly for finite N . In this case one can prove that the error may decrease even as $1/N$. Thus one takes a step from genuine randomness back towards the methods of direct numerical integration, in which the distribution of points is entirely deterministic. The distinction between pseudo- and quasi-random numbers is important in practice and the latter are to be preferred (for instance, FOWL uses them). For more details on this important and only partially understood problem we refer to the references (Hammersley, 1967; Halton, 1970; James, 1968).

A second way to improve the Monte Carlo method is to reduce the variance of the function to be integrated. According to equation (3.2) this is evidently possible by transforming the integral so that the function is as constant as possible. To apply this technique of reducing the variance some information on the behaviour of the integrand is required. Therefore, the methods used in particle physics have been developed specifically to apply to the problems encountered in this field. Their necessity is illustrated by the following example.

Example 1: Consider the integral

$$m = \int_0^1 dx e^{ax} = e^a - 1, \quad (4.1)$$

where a is a constant. Integrals of this type arise in high-energy physics when integrating over an invariant momentum transfer t , since the matrix element is experimentally known to be of the form e^{at} . A simple calculation gives

$$\sigma^2 = \frac{a}{2} \left\{ \left(1 - \frac{2}{a} \right) e^{2a} + \frac{4}{a} e^a - \frac{2}{a} + 1 \right\}. \quad (4.2)$$

Thus for a large a the relative error $\sigma/m\sqrt{N}$ of the Monte Carlo integration increases with a as $\sqrt{(a/2N)}$. The reason is the increasing asymmetry of the integrand $a e^{ax}$. The function is sampled evenly in the interval $(0, 1)$, and at large a the points near 0 have a small weight compared with those near 1. In evaluating the integral the former points are nearly useless. To improve the situation one should somehow generate more points in the region where the integrand is large or sample the integrand only in regions which are most important. In the example this is easy to do by taking $y = e^{+ax}$ as a new variable. This results in

$$m = \int_1^{e^a} dy,$$

which is computed by generating points uniformly in y within the interval $(1, e^a)$. Since the integrand is now a constant, the variance has, in fact, been reduced to zero. Note that a similar transformation is needed if the range of integration in equation (4.1) extends from 0 to ∞ (for $a < 0$).

It is obvious from the example that if $f(x)$ varies considerably the Monte Carlo method becomes more efficient when the random points are generated so that their density is closer to $|f(x)|$. This method is called *importance sampling*. To apply it, we need a way to generate random numbers distributed according to a given density $g(x)$. The density $g(x)$ is defined so that the probability that a value between x and $x + dx$ is obtained is given by $(1/G)g(x) dx$ where $G = G(+\infty)$ and

$$G(x) = \int_{-\infty}^x dt g(t). \quad (4.3)$$

Consider then the integral

$$I = \int_{x^-}^{x^+} dx f(x), \quad (4.4)$$

where arbitrary limits of integration have been introduced for later use. Take as a new variable

$$r = \frac{G(x) - G(x^-)}{G(x^+) - G(x^-)}, \quad (4.5)$$

which varies between 0 and 1 and has the differential

$$dr = \frac{g(x) dx}{G(x^+) - G(x^-)}. \quad (4.6)$$

Equation (4.4) can now be written in the form

$$\begin{aligned} I &= \int_{x^-}^{x^+} dx f(x) \\ &= \int_{x^-}^{x^+} dx g(x) \frac{f(x)}{g(x)} \\ &= \{G(x^+) - G(x^-)\} \int_0^1 dr \frac{f(x)}{g(x)} \end{aligned} \quad (4.7)$$

where

$$x = G^{-1}[G(x^-) + r\{G(x^+) - G(x^-)\}]. \quad (4.8)$$

When equation (3.3) is applied to equation (4.7) we obtain for I

$$\begin{aligned} I &= \int_{x^-}^{x^+} dx f(x) \\ &\approx \bar{I} = \frac{G(x^+) - G(x^-)}{N} \sum_{k=1}^N \frac{f(x_k)}{g(x_k)} \\ &\equiv \frac{1}{N} \sum_{k=1}^N w_k, \end{aligned} \quad (4.9)$$

where x_k is defined in terms of r_k by equation (4.8) and w_k is the weight assigned to the k th event. According to equation (4.6) the random variables x_k are now distributed according to the density $dN(x)/dx = (dN(r)/dr)(dr/dx) = g(x)/\{G(x^+) - G(x^-)\}$ which is normalized to unity over the range of integration.

In the integral over r in equation (4.7) only the ratio f/g appears and thus the variance of f/g is reduced if g approximates f better than a constant. Using equations (3.3), (3.4) and (3.6), the result of the Monte Carlo integration (4.9) can be written in the form

$$I = \bar{I} \pm \delta \bar{I} \quad (4.10)$$

with

$$\begin{aligned} \bar{I} &= \frac{1}{N} \sum_{k=1}^N w_k \\ \delta \bar{I}^2 &= \frac{1}{N(N-1)} \left\{ \sum_{k=1}^N w_k^2 - \frac{1}{N} \left(\sum_{k=1}^N w_k \right)^2 \right\} \\ w_k &= \{G(x^+) - G(x^-)\} \frac{f(x_k)}{g(x_k)} \end{aligned} \quad (4.11)$$

Notice that the transformation of variables carried out above is formally a method of generating random numbers with a density $g(x)$, but need not always be feasible in practice. We list below the conditions under which the method of transforming variables can be used in practice and also describe one different method:

(1) The method of transforming variables is practicable if equation (4.8) is such that there is a simple and fast way of getting from the primary random numbers r_k to the random numbers x_k . Otherwise the increase in labour nullifies the advantage obtained by the decrease in variance. In practice this requires that all the functions $g(x)$, $y = G(x)$ and $x = G^{-1}(y)$ must be elementary functions. In particle physics the two common cases of variations of the integrand resembling the exponential or Breit-Wigner functions can be taken care of by this method. The required transformations are listed in Table IX.1, and can be applied by simply substituting in equation (4.9).

Table IX.1. Densities, integrated densities and inverses to be used in connection with equation (4.9) for importance sampling

Type of Variation	$g(x)$	$G(x)$	$G^{-1}(y)$
Exponential	$a e^{ax}$	e^{ax}	$\frac{1}{a} \log y$
Breit-Wigner	$\frac{b^2}{(x-a)^2 + b^2}$	$\frac{\pi}{2}b + b \operatorname{arctg} \frac{x-a}{b}$	$a + btg \frac{y - (\pi/2)b}{b}$

(2) In addition to the method of variable transformations there are other ways of generating random numbers distributed with a prescribed density $g(x)$. In these cases $g(x)$ must be one of certain special functions but it need not be integrable in closed form. Consider for instance, the case in which $g(x)$ is a Gaussian $g(x) = e^{-x^2/2\sigma^2}$ and the integration goes from $-\infty$ to $+\infty$. This will occur in practice if the peripherality of the matrix element is expressed in terms of transverse momenta. The weight function $g(x)$ is not integrable in closed form, but it is easy to generate random numbers which are normally distributed. For instance, one may apply the central limit theorem to the sum of n rectangularly distributed random numbers. As shown previously, this approaches a Gaussian rapidly and already the density function (3.8) of

$$s = \sigma \left(\sum_{i=1}^{12} r_i - 6 \right) \quad (4.12)$$

is sufficiently close to the limit (3.5) with mean zero and variance σ^2 . Thus, equation (4.9) gives directly

$$\begin{aligned} I &= \int_{-\infty}^{\infty} dx f(x) \\ &\approx \frac{\sigma \sqrt{(2\pi)}}{N} \sum_{i=1}^N f(s_i) e^{+s_i^2/2\sigma^2} \end{aligned} \quad (4.13)$$

where s_i are normally distributed random numbers between $-\infty$ and $+\infty$.

5. Application of the Monte Carlo method to particle physics

In applying the Monte Carlo method to particle physics one should distinguish two sides of the problem : (a) the random generation of the particle events, (b) the treatment of these events. From the practical point of view, the latter, data-handling aspect is as important as the first one and we shall comment on it later. Here we shall first give a reasonably detailed description of event generation.

To evaluate the integral over phase space of equation (1.1), the four-fold δ function must first be eliminated and I_n written explicitly in terms of a set Φ of $3n - 4$ variables as in equation (1.2). The value of Φ defines the event uniquely, so that one can construct the momentum configuration p_1, \dots, p_n when Φ is given.

To be able to generate the events using fast standard computer routines, the integral (1.2) is further transformed until each of the $3n - 4$ variables in Φ has a simple range of variation. In fact, one will find a set

$$\Phi' = (r^{(1)}, \dots, r^{(3n-4)}) \quad (5.1)$$

so that the $3n - 4$ dimensional hypercube V'

$$0 \leq r^{(l)} \leq 1, \quad l = 1, \dots, 3n - 4 \quad (5.2)$$

and the physical region V correspond to each other one-to-one. If now the Jacobian from Φ to Φ' is $\partial\Phi'/\partial\Phi$, the integral (1.2) becomes

$$\begin{aligned} I_n &= \int_{V'} d\Phi' \frac{\rho_n(\Phi(\Phi')) T'(\Phi')}{\partial\Phi'/\partial\Phi} \\ &= \int_{V'} d\Phi' \frac{T'(\Phi')}{g_n(\Phi')} \end{aligned} \quad (5.3)$$

with

$$g_n(\Phi') = \frac{\partial\Phi'/\partial\Phi}{\rho_n(\Phi)}. \quad (5.4)$$

Comparing with equation (4.11) one sees that if the values of Φ'_1, \dots, Φ'_N are generated evenly in the hypercube (5.2), then the Monte Carlo estimate of I_n is

$$\begin{aligned} \bar{I}_n &= \frac{1}{N} \sum_{k=1}^N w_k, \\ w_k &= \frac{T'(\Phi'_k)}{g_n(\Phi'_k)}. \end{aligned} \quad (5.5)$$

The estimate $\delta\bar{I}_n$ of the statistical error is also given by equation (4.11) with w_k from equation (5.5).

There is a limitless number of different ways to choose a set of variables (5.1) which fulfill equation (5.2). From equation (5.3) we see that the density of events is

$$\rho'_n(\Phi') = \frac{1}{g'_n(\Phi')}. \quad (5.6)$$

By a suitable choice of the transformation from Φ to Φ' $g'_n(\Phi')$ can be made to imitate $T(\Phi)$ to exploit importance sampling.

If V is a subspace of the entire phase space, the corresponding I_n is obtained simply by including in the sum in equation (5.5) only those Φ'_k which lie in V . Thus, if the distribution in some variable v or the derivative $\partial I_n / \partial v$ is requested, the range of v is divided in bins of width Δv (not necessarily of equal length). The derivative is then estimated by

$$\frac{\partial I_n}{\partial v} \cong \frac{\Delta \bar{I}_n}{\Delta v}. \quad (5.7)$$

Here $\Delta \bar{I}_n$ is given by equation (5.5) with the restriction that only events with v inside the given bin are included.

We present the method in detail for a particularly simple set of $3n - 4$ variables Φ . Recursion relations allow us to write equation (1.1) in the form of equation (VI.2.14) where μ_i and P_i are defined in equations (VI.2.13, 15). Here the $3n - 4$ variables Φ consist of

$n - 2$ invariant masses $M_i, M_i^2 = k_i^2 = (p_1 + \dots + p_i)^2, i = 2, \dots, n - 1$ defined as the masses of the intermediate decaying particles in Figure VI.2.3.

$2(n - 1)$ angles $\Omega_i = (\cos \theta_i, \phi_i), i = 2, \dots, n$, defining (Figure VI.2.4) the direction of the vector \mathbf{k}_i in the frame $k_{i+1} = p_1 + \dots + p_{i+1} = (M_{i+1}, 0)$, i.e. the rest frame of the intermediate decaying particle.

With these variables the phase space density is

$$\rho_n(\Phi) = \frac{1}{2\sqrt{s}} \prod_{i=2}^n \frac{1}{2} P_i. \quad (5.8)$$

The region of integration in equation (VI.2.14) can be simply transformed to a unit hypercube. We shall consider the angles and masses and the construction of the event separately.

(a) Generation of angles

The angles ϕ_i and θ_i can be generated in the corresponding rest frame $k_{i+1} = (M_{i+1}, 0)$ by writing

$$\phi_i = 2\pi r^{(i)} \quad (5.9)$$

$$\cos \theta_i = (2\tilde{r}^{(i)} - 1), \quad (5.10)$$

where $r^{(i)}$ and $\tilde{r}^{(i)}$ are random numbers between 0 and 1. The transformation (5.9–10) transforms the integral over Ω_i to an integral over a unit square with the Jacobian 4π . The events produced by equations (5.9) and (5.10) are uniformly distributed in ϕ_i and $\cos \theta_i$ and the choice of the polar axis is arbitrary. One may, for instance, use the direction of \mathbf{k}_{i+2} or \mathbf{p}_n . However, when the integrand $T(\Phi)$ is the production amplitude for n particles the events will be collimated along the direction of \mathbf{p}_n and it will be necessary to importance sample in some variable describing this collimation. We shall return to this question soon.

(b) Generation of invariant masses

The invariant masses M_i vary between the limits

$$\mu_i \leq M_i \leq M_{i+1} - m_{i+1}, \quad i = 2, \dots, n - 1. \quad (5.11)$$

When equation (5.11) is satisfied, each two-body decay in Figure VI.2.3 is physical. In the $n - 2$ dimensional space spanned by M_2, \dots, M_{n-1} the inequalities (5.11) define a simplex, which is an interval for $n = 3$, a triangle for $n = 4$ (Figure 5.1), a pyramid for $n = 5$, etc. In the following we give two examples of how to generate the M_i within this simplex.

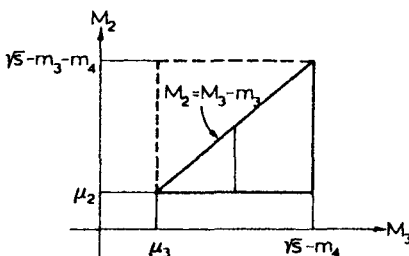


Figure IX.5.1 Domain of integration over the two masses M_3 and M_2 for $n = 4$

(1) The most straightforward method is to transform the simplex to an $n - 2$ dimensional unit hypercube by the linear relation

$$M_i = \mu_i + \tilde{r}^{(i)}(M_{i+1} - \mu_{i+1}), \quad i = 2, \dots, n - 1. \quad (5.12)$$

Each M_i -integration is transformed to an integral over $\tilde{r}^{(i)}$ from 0 to 1. Including the Jacobians arising from equations (5.9), (5.10) and (5.12) the Monte Carlo estimate of the integral I_n can then be written in the form (5.5) with (leaving out the primes)

$$\frac{1}{g_n(\Phi)} = \frac{1}{2\sqrt{s}} \prod_{i=2}^n 2\pi P_i \cdot \prod_{i=3}^n (M_i - \mu_i). \quad (5.13)$$

With this choice of Φ the density $g_n(\Phi)$ of events generated in the phase space is not constant and the statistical error of the estimate (5.5) is larger the more $T(\Phi)$ deviates from $g_n(\Phi)$. In particular, even a constant matrix element involves a definite statistical error. Notice the factors $M_i - \mu_i$ in equation (5.13); the density of points is infinite when this factor vanishes. Why this happens can be clearly seen from Figure 5.1. There M_3 is generated uniformly between μ_3 and $\sqrt{s} - m_4$ while M_2 is generated uniformly on the line between μ_2 and $M_3 - m_3$. The length of this line decreases linearly when M_3 decreases to μ_3 , and thus the density of points increases proportionally to $1/(M_2 - \mu_2)$. The situation is analogous for larger n .

If one wants to generate events which have Breit-Wigner distributions in some of the M_i , the same method of transforming the limits to constants can also be used. The equations (4.5) and (4.6) and Table 1 are immediately applicable and it is easy to write down the resulting density $g(\Phi)$. Note that

this density will not contain pure Breit-Wigner terms but products of these multiplied with factors similar to those in equation (5.13). Near the resonance masses, however, the Breit-Wigner density will dominate. Also not all invariant mass combinations can be given a Breit-Wigner distribution but only those appearing as intermediate states in the cascade-type decay of Figure VI.2.3.

The method can be generalized to include decays in which both decay products may decay further. The intermediate states again allow Breit-Wigner sampling. A program of this type has been described by Friedman (Friedman, 1971a).

(2) Another way of generating the M_i uses the fact that the simplex (5.11) is a part of the $n - 2$ dimensional hypercube

$$\mu_i \leq M_i \leq \sqrt{s} - \mu_n + \mu_i, \quad i = 2, \dots, n - 1. \quad (5.14)$$

Namely, if a further ordering relation is imposed,

$$M_i \leq M_{i+1} - m_{i+1}, \quad i = 2, \dots, n - 1, \quad (5.15)$$

then the resulting region is identical with equation (5.11). One thus generates uniformly in the hypercube (5.14):

$$M_i = \mu_i + \tilde{r}^{(i)}(\sqrt{s} - \mu_n), \quad (5.16)$$

having first ordered the $n - 2$ random numbers $\tilde{r}^{(i)}$:

$$\tilde{r}^{(2)} \leq \tilde{r}^{(3)} \leq \dots \leq \tilde{r}^{(n-1)}.$$

Now the points fall inside the region (5.14–15) because we have

$$M_{i+1} - M_i = (\tilde{r}^{(i+1)} - \tilde{r}^{(i)})(\sqrt{s} - \mu_n) + m_{i+1} \geq m_{i+1}.$$

Referring to Figure 5.1 in the case $n = 4$, one first generates uniformly within the square but if the point generated lies above the diagonal it is by ordering (reflection around the diagonal) transformed so that it lies within the allowed triangle. Since the density is uniform within the hypercube it is also uniform in the simplex, in contrast to the previous manner of transforming the simplex to a hypercube. The density of events in the phase space is now given by

$$\frac{1}{g_n(\Phi)} = \frac{1}{2\sqrt{s}} \prod_{i=2}^n (2\pi P_i) \cdot \frac{1}{(n-2)!} (\sqrt{s} - \mu_n)^{n-2}, \quad (5.17)$$

where the factor $1/(n-2)!$ gives the ratio between the volumes of the simplex and the hypercube.

Notice that in this latter method the $n - 2$ dimensional unit hypercube of the random numbers $\tilde{r}^{(i)}$ is not uniformly populated. The ordering carried out above has as a consequence that the distributions in $\tilde{r}^{(i)}$ are different (Friedman, 1971b).

(c) Construction of the event

When the $n - 2$ masses and $2(n - 1)$ angles have been generated, the random event, that is the momentum configuration $\mathbf{p}_1, \dots, \mathbf{p}_n$, in any given frame, can be constructed. First, in the frame $\mathbf{p}_1 + \mathbf{p}_2 = (M_2, \mathbf{0})$ the length of \mathbf{p}_2 is given by equation (VI.2.15) and its orientation by the generated values of θ_2, ϕ_2 . Thus \mathbf{p}_2 and $\mathbf{p}_1 = -\mathbf{p}_2$ are completely known. Similarly, in the frame $\mathbf{p}_1 + \mathbf{p}_2 + \mathbf{p}_3 = (M_3, \mathbf{0})$, \mathbf{p}_3 is obtained from equation (VI.2.15) and the generated values of θ_3, ϕ_3 . The vectors \mathbf{p}_1 and \mathbf{p}_2 in this frame are then obtained by Lorentz transforming them with a boost along the direction $\mathbf{p}_1 + \mathbf{p}_2 = -\mathbf{p}_3$ from the previous frame $\mathbf{p}_1 + \mathbf{p}_2 = (M_2, \mathbf{0})$. Continuing in this way one obtains finally the required momentum configuration in the CM frame.

The densities of events given by equations (5.13) and (5.17) above are relatively constant. The method is thus effective only if the integrand $T(\Phi)$ also is relatively constant. This is not the case if the total energy is large and $T(\Phi)$ is the production amplitude for not too many particles. Then $T(\Phi)$ is large only if the particle momenta are nearly collimated along the beam axis. At high energy the Monte Carlo method must be modified so that event density is small for large transverse momenta. There are two essentially different methods in use. One can either apply importance sampling in the generation of the angles $\cos \theta_i$ (Byckling, 1969a; Friedman, 1971a) or one can apply it to transverse momenta starting from a completely different set of $3n - 4$ variables Φ (Pene, 1969; Kittel, 1970). Since the first alternative is technically slightly simpler we shall describe it in some detail.

(a') Generation of the angles for peripheral events

In order to carry out importance sampling in some variable describing peripherality, assume that the masses M_k have been generated and choose the direction of \mathbf{p}_n as the z axis in the frame $k_{i+1} = p_1 + \dots + p_{i+1} = (M_{i+1}, \mathbf{0})$. Then θ_i is the angle between \mathbf{k}_i and \mathbf{p}_n in this frame (Figure VI.2.4). Now it would be very simple to importance sample in $\cos \theta_i$ and generate mainly events for small values of θ_i . However, it is more useful to replace $\cos \theta_i$ by the invariant momentum transfer $t_i = (\mathbf{p}_n - \mathbf{k}_i)^2$. The result of replacing $\cos \theta_i$ by t_i in R_n is written in equation (VI.2.27) where $P_n^{(i)}$ is given by equation (VI.2.28).

As shown previously (equations (4.5) and (4.6) and Table IX.1), one can now importance sample in each of the t_i by generating events with the normalized density $a_i e^{\alpha_i t_i} / (e^{\alpha_i t_i} - e^{-\alpha_i t_i})$. Leaving the generation of the ϕ_i and the M_i unchanged and collecting all factors the value of the integral (VI.2.27) can be written in the form (5.5) with

$$\frac{1}{g_n(\Phi)} = \frac{1}{2\sqrt{s}} \prod_{i=1}^{n-1} \left\{ \frac{\pi}{2P_n^{(i+1)}} \frac{e^{\alpha_i t_i} - e^{-\alpha_i t_i}}{a_i e^{\alpha_i t_i}} \right\} \frac{(\sqrt{s} - \mu_n)^{n-2}}{(n-2)!}. \quad (5.18)$$

Here, for definiteness, the masses M_k have been taken to be generated by the ordering method presented above.

One can see that, apart from some more slowly varying mass-dependent factors, the density $g(\Phi)$ of the generated random events in this case behaves as $g(\Phi) = \exp \sum_{i=1}^{n-1} a_i t_i$. It is thus rather efficient in multi-Regge calculations, in which the integrand is roughly of this form.

The construction of the event is carried out as before; now one only has to solve for $\cos \theta_i$ from the generated value of t_i . The dominance of small t_i implies evidently the dominance of small θ_i .

We now have at our disposal a method to generate random events with a number of different phase space densities $g(\Phi)$. For any practical applications the computer routine carrying out the generation must be complemented by a set of routines designed to treat the generated events and to carry out histogramming, estimate statistical errors, and provide other service functions. The complete program needs the following initial data:

- specification of the reaction and the matrix element $T(\Phi)$,
- specification of the density $g(\Phi)$ to be used,
- number of events to be generated,
- details on how the generated events should be histogrammed.

Standard programs like FOWL have been developed to carry out the required tasks. They are very flexible and convenient for the general user, who can use them for many different problems after learning some conventions. For a more detailed description of all practical matters we refer the reader to the long write-up of FOWL (James, 1970).

In order to exhibit the connection between the theory we have given above and a practical example, we show in Fig. 5.2 a histogram printed by FOWL. It contains the following information.

- (a) The histogram gives the distribution in the invariant mass $M_{123} = \{(p_1 + p_2 + p_3)^2\}^{\frac{1}{2}}$ for the reaction $\pi p \rightarrow \pi\pi\pi p$ ($ab \rightarrow 1234$) when the laboratory momentum of the incoming π is 4 GeV/c and the matrix element is $T(\Phi) = \exp(5t_{pp})$. Apart from the normalization, the quantity calculated is thus $\partial I_4 / \partial M_{123}$, where I_4 is defined by equation (1.1).
- (b) The columns denoted by the word INTERVAL give the upper and lower limits of the bins into which the range of M_{123} has been divided by the user.
- (c) The column denoted by the word EVENTS gives the derivative $\partial I_4 / \partial M_{123}$ as estimated by equation (5.7). This distribution is normalized to one. Explicitly the number assigned to each bin is

$$(\text{normalization}) \times \sum w_k, \quad (5.19)$$

where $w_k = T(\Phi)/g(\Phi)$ and the sum includes those events for which the

INTERVAL	EVENTS	ERROR	TOTAL NUMBER OF EVENTS IN PLOT = 2000. EQUIVALENT UNWEIGHTED EVENTS = 1157. SUM OF WEIGHTS = 0.2045E 03
0.40	0.45	0.0000	0.0000
0.45	0.50	0.0002	0.0000
0.50	0.55	0.0007	0.0000
0.55	0.60	0.0014	0.0002
0.60	0.65	0.0027	0.0003
0.65	0.70	0.0041	0.0005
0.70	0.75	0.0062	0.0008
0.75	0.80	0.0083	0.0011
0.80	0.85	0.0112	0.0015
0.85	0.90	0.0151	0.0020
0.90	0.95	0.0191	0.0025
0.95	1.00	0.0229	0.0030
1.00	1.05	0.0292	0.0038
1.05	1.10	0.0396	0.0044
1.10	1.15	0.0383	0.0050
1.15	1.20	0.0478	0.0062
1.20	1.25	0.0507	0.0066
1.25	1.30	0.0568	0.0074
1.30	1.35	0.0656	0.0084
1.35	1.40	0.0640	0.0083
1.40	1.45	0.0639	0.0085
1.45	1.50	0.0660	0.0086
1.50	1.55	0.0678	0.0090
1.55	1.60	0.0651	0.0085
1.60	1.65	0.0608	0.0081
1.65	1.70	0.0555	0.0073
1.70	1.75	0.0500	0.0066
1.75	1.80	0.0401	0.0052
1.80	1.85	0.0278	0.0036
1.85	1.90	0.0174	0.0023
1.90	1.95	0.0065	0.0009
1.95	2.00	0.0004	0.0001

Figure IX.5.2 Example of a distribution printed by the Monte Carlo program FOWL. The histogram is the distribution in M_{123} in the reaction $\pi p \rightarrow \pi\pi\pi p$ at 4 GeV/c with $T = \exp(5t_{pp})$. The numbers are explained in the text

value of M_{123} lies in the bin in question. In the present case, the density $g(\Phi)$ of equation (5.18) was used.

(d) The normalization ($1/\sum w_k$ over all k) is given by SUM OF WEIGHTS = 0.2045×10^3 . Then $N = 2000$ implies that the value of the integral I_4 is $204.5/2000 = 0.10$ according to equation (5.5). The correct numerical value of $\partial I_4 / \partial M_{123}$ is similarly obtained from equation (5.7), although percentage distributions are normally sufficient for comparison with experiment.

(e) The column denoted by the word ERROR gives the statistical error as estimated by equation (5.11). Actually the approximation

$$\frac{1}{N(N-1)} \left\{ \sum w_k^2 - \frac{1}{N} \left(\sum w_k \right)^2 \right\} \approx \frac{1}{N^2} \sum w_k^2$$

has been used, so that the contents of each bin in the ERROR column are

$$(\text{normalization}) \times [\sum w_k^2]^{\frac{1}{2}},$$

where the normalization is the same as in equation (5.19).

(f) The number N' given by EQUIVALENT UNWEIGHTED EVENTS

$= 1157$ is evaluated from the equation

$$\frac{1}{\sqrt{N'}} = \frac{\{\sum w_k^2\}^{1/2}}{\sum w_k},$$

where the sums now go over all the events. It gives thus the statistical error in SUM OF WEIGHTS or in the value of I_4 . In the present case the estimate of this statistical error is $1/\sqrt{1157} = 3$ per cent. The number N' is thus very convenient when one tries to assess the statistical significance of a histogram. If N' is less than 100 the usefulness of a histogram is rather questionable.

6. Statistical methods

In statistical mechanics, the analogue of equation (1.1) is the volume of accessible phase space in the microcanonical ensemble. The four-dimensional δ function in equation (1.1) is there replaced by a single δ function requiring the total energy to be within δE of E . Due to this δ function constraint, calculations are very complicated. The normal way out of the difficulties is to replace the microcanonical ensemble by the canonical ensemble, in which the energy may fluctuate but the temperature is constant. Within a certain approximation, valid in statistical mechanics, the two ensembles give identical results. Basically the same method will now be used to evaluate equation (1.1).

Another distinctive feature of the methods applied in this section is that they treat all particles on an equal footing. All other methods must fix an ordering of the particles and start numerical integration or event generation at some point of a tree diagram. Here the method decouples the correlation between the particles due to four-momentum conservation and only those in T remain. However, the method is useful only if T also does not give correlations between the particles, that is T factorizes.

Assume now that T is factorizable in the coordinates of the particles as shown in equation (1.3). We shall presently see why this condition is necessary. Then the only constraint in equation (1.1) connecting the different particles is the δ function. This constraint may be decoupled by taking the Laplace transform of $I_n(p)$. We define

$$\Phi_n(\alpha) = \int d^4 p e^{-\alpha \cdot p} I_n(p). \quad (6.1)$$

The Laplace transform Φ_n is a function of the timelike four-vector $\alpha = (\alpha_0, \alpha)$. If T is factorizable, $T = \prod_{i=1}^n g_i(p_i)$, then equation (6.1) becomes

$$\begin{aligned} \Phi_n(\alpha) &= \int d^4 p \prod_{i=1}^n \left\{ \frac{d^3 p_i}{2E_i} g_i(p_i) \right\} \delta^4(p - p_1 - \dots - p_n) e^{-\alpha \cdot p} \\ &= \int \prod_{i=1}^n \left\{ \frac{d^3 p_i}{2E_i} g_i(p_i) e^{-\alpha \cdot p_i} \right\}. \end{aligned} \quad (6.2)$$

Thus $\Phi_n(\alpha)$ is a product, $\Phi_n(\alpha) = \prod_i^n \phi_i(\alpha)$, of the Laplace transforms

$$\begin{aligned}\phi_i(\alpha) &= \int \frac{d^3 p_i}{2E_i} g_i(p_i) e^{-\alpha \cdot p_i} \\ &= \int d^4 p_i g_i(p_i) \delta(p_i^2 - m_i^2) e^{-\alpha \cdot p_i}.\end{aligned}\quad (6.3)$$

The function $I_n(p)$ is now given by the inverse Laplace transform

$$I_n(p) = \frac{1}{(2\pi i)^4} \int_C d^4 \alpha e^{\alpha \cdot p} \Phi_n(\alpha), \quad (6.4)$$

and the δ function has disappeared in a symmetric manner. In equation (6.4) the path of integration C in each α_μ goes in the complex α_μ plane from $-i\infty$ to $+i\infty$ so that C is to the right of all the singularities of $\Phi_n(\alpha)$. This equation is exact for the matrix element squared (1.3). The statistical method for evaluating $I_n(p)$ amounts to developing an approximation for the integral (6.4).

We shall first examine the case $T = 1$ in detail, that is evaluate the total phase space volume R_n (Fialho, 1957; Kolkunov, 1962; Lurçat, 1964; Satz, 1965; Campbell, 1967; Kajantie, 1971). For the case in which $g_i(p_i)$ depends on the transverse momentum we refer to (Krzywicki, 1964, 1965; de Groot, 1972; see also Białas, 1965). This is an important case in practice, since then the g_i can describe the experimentally observed limitation of the transverse momenta.

Let us now assume that $T = 1$, so that $I_n(p) = R_n(s)$ is Lorentz-invariant and depends only on $s = p^2$. Then the four-fold Laplace transform (6.1) can be transformed into a single integral. In equation (6.1) everything is invariant and thus $\Phi_n(\alpha)$ can depend only on the length $\beta = |\alpha|$. It can be evaluated most simply in the frame $\alpha = (\beta, 0)$:

$$\begin{aligned}\Phi_n(\beta) &= \int d^4 p e^{-\beta E} R_n(s) \\ &= \int ds \int d^4 p \delta(p^2 - s) e^{-\beta E} R_n(s) \\ &= \int ds \int \frac{d^3 p}{2E} e^{-\beta E} R_n(s) \\ &= \int ds 2\pi \int_{-s}^{\infty} dE (E^2 - s)^{\frac{1}{2}} e^{-\beta E} R_n(s).\end{aligned}\quad (6.5)$$

Using the formula 9.6.23 of (Abramowitz, 1965),

$$K_1(z) = z \int_1^{\infty} dt e^{-zt} (t^2 - 1)^{\frac{1}{2}}, \quad (6.6)$$

where $K_1(z)$ is a modified Bessel function, one finds

$$\Phi_n(\beta) = \frac{2\pi}{\beta} \int_0^\infty ds \sqrt{s} K_1(\beta\sqrt{s}) R_n(s). \quad (6.7)$$

Here $R_n(s)$ vanishes if $s \leq (m_1 + \dots + m_n)^2$, of course. This is a K -transform (Erdelyi, 1953); its inverse is (Kolkunov, 1962; Lurçat, 1964; Campbell, 1967)

$$R_n(s) = \frac{1}{i4\pi^2\sqrt{s}} \int_{c-i\infty}^{c+i\infty} d\beta \beta^2 I_1(\beta\sqrt{s}) \Phi_n(\beta). \quad (6.8)$$

As $T = 1$ we can further evaluate Φ_n in terms of Bessel functions. In the frame $\alpha = (\beta, \mathbf{0})$ we have from equation (6.3):

$$\begin{aligned} \phi_i(\alpha) &= \phi_i(\beta) = \int \frac{d^3 p_i}{2E_i} e^{-\beta E_i} \\ &= 2\pi \int_{m_i}^\infty dE_i (E_i^2 - m_i^2)^{\frac{1}{2}} e^{-\beta E_i} \\ &= \frac{2\pi m_i}{\beta} K_1(\beta m_i). \end{aligned} \quad (6.9)$$

Substitution of $\Phi_n(\beta) = \prod_i^n \phi_i(\beta)$ into equation (6.8) then gives $R_n(s)$ exactly as the value of a complex integral.

The nonrelativistic and extremely relativistic limits of $R_n(s)$ presented in Section VI.2 can be rederived on the basis of equations (6.7–9). The asymptotic form of $K_v(z)$ is (Abramowitz, 1965)

$$K_v(z) \xrightarrow[z \rightarrow \infty]{} \left(\frac{\pi}{2z} \right)^{\frac{1}{2}} e^{-z} \left(1 + \frac{4v^2 - 1}{8z} + \dots \right). \quad (6.10)$$

For $\beta \rightarrow \infty$ only values of $R_n(s)$ near the threshold $\sqrt{s} = \sum_i m_i$ contribute to equation (6.7). Replacing K_1 in equations (6.7) and (6.9) by equation (6.10) one finds ($E^2 \equiv s$)

$$\prod_i \left\{ \left(\frac{2\pi^3 m_i}{\beta^3} \right)^{\frac{1}{2}} e^{-\beta m_i} \right\} = \int_0^\infty dE \left(\frac{2\pi E}{\beta} \right)^{\frac{1}{2}} R_n^{\text{NR}}(E^2) e^{-\beta E}. \quad (6.11)$$

The left side is the Laplace transform of a known function and one obtains directly the result (VI.2.19). For $\beta \rightarrow 0$ large values of \sqrt{s} dominate in equation (6.7). In this case one uses $K_1(z) \rightarrow z^{-1}$ for $z \rightarrow 0$ in equation (6.9) to get

$$(2\pi)^n \beta^{-2n} = \int_0^\infty dE \left(\frac{4\pi E^2}{\beta} \right) K_1(\beta E) R_n^{\text{ER}}(E^2). \quad (6.12)$$

Here β^{-2n} is the K -transform of a known function (Erdeleyi, 1953) and one finds $R_n^{\text{ER}}(s)$ as in equation (VI.2.17).

Let us now see how the exact relation (6.7–9) between $R_n(s)$ and $\Phi_n(s)$ allows a simple approximation when n is large (Kolkunov, 1962; Campbell, 1967). In equation (6.7) $R_n(s)$ increases roughly as s^n and K_1 decreases as $e^{-\beta\sqrt{s}}$. When n is large, the integrand in equation (6.7) has a sharp maximum at a value $\sqrt{s} = \sqrt{\bar{s}}$, Figure 6.1. Then $\Phi_n(\beta)$ depends essentially only on values of $R_n(s)$ near \bar{s} .

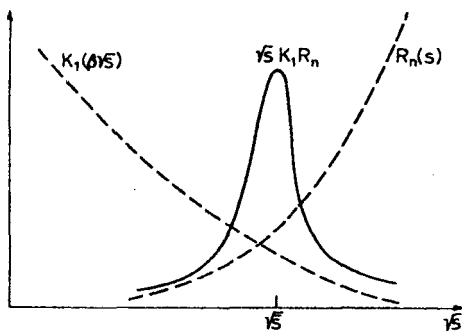


Figure IX.6.1 An example of a situation in which the statistical method is applicable. The integrand $\sqrt{s}K_1(\beta/\sqrt{s})R_n(s)$ of equation (6.7) has a sharp peak at \sqrt{s} and it can be approximated by a Gaussian

Borrowing the terminology of statistical physics (Huang, 1963), one can call the phase space integral $R_n(s)$ at fixed \sqrt{s} the **microcanonical partition function** and the Laplace transform $\Phi_n(\beta)$ at fixed β the **canonical partition function**. It is known from statistical physics that under very general conditions the thermodynamic functions (logarithms of the partition function and its derivatives) become identical in microcanonical and canonical ensembles when the number of degrees of freedom becomes large. In particular this means that, in the present terminology, in the canonical ensemble with fixed β the fluctuations in \sqrt{s} are small (Figure 6.1) and \sqrt{s} is essentially fixed.

Similarly, for large n in the microcanonical ensemble with fixed \sqrt{s} the fluctuations in β are small and one can find a simple approximation to equation (6.8). From equation (6.9) the integrand of equation (6.8) is seen to have a deep minimum on the real β axis, see Figure 6.2. Denoting the integrand by $e^{F(\beta)}$,

$$F(\beta) = \log \left\{ \beta^2 I_1(\beta/\sqrt{s}) \prod_1^n \phi_i(\beta) \right\}, \quad (6.13)$$

the value β at the minimum is determined by $\partial F(\beta)/\partial \beta = 0$. Using the

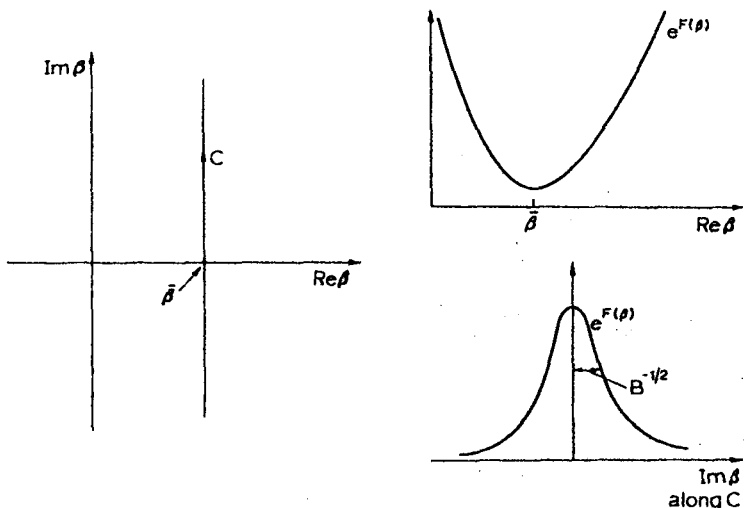


Figure IX.6.2 Motivation of the saddle point method. The integrand of equation (6.8) has a saddle point at $\beta = \bar{\beta}$, i.e. a minimum along real β axis and a maximum in imaginary direction through $\bar{\beta}$. Choosing the contour C going through $\bar{\beta}$, the integrand can be approximated by a Gaussian

properties of I , and K , one finds that this equation is explicitly

$$\sqrt{s} \frac{I_0(\beta\sqrt{s})}{I_1(\beta\sqrt{s})} = \sum_i m_i \frac{K_0(\beta m_i)}{K_1(\beta m_i)} + (2n - 1)\beta^{-1}. \quad (6.14)$$

Solving for $\beta = \bar{\beta} = \bar{\beta}(\sqrt{s}; m_i)$ from equation (6.14) requires numerical computations apart from the limiting cases $\sqrt{s} \rightarrow \sum_i m_i$ and $\sqrt{s} \rightarrow \infty$ (equation (6.22)). It is also inherent to the nature of the problem that for $\sqrt{s} \geq \sum m_i$ equation (6.14) has one and only one solution.

The function $F(\beta)$ is an analytic function of the complex variable β , and thus satisfies Laplace's equation

$$\frac{\partial^2 F}{\partial(\text{Re } \beta)^2} + \frac{\partial^2 F}{\partial(\text{Im } \beta)^2} = 0. \quad (6.15)$$

Because at $\bar{\beta}$ $\partial^2 F / \partial(\text{Re } \beta)^2$ is real, positive and large, $\partial^2 F / \partial(\text{Im } \beta)^2$ is large and negative. The point $\beta = \bar{\beta}$ is a **saddle point** (Morse, 1953). If the path of integration C is taken to pass through $\bar{\beta}$, then $F(\beta)$ has a strong maximum there, Figure 6.2. Writing $\beta - \bar{\beta} = iy$, the first terms of the expansion of $F(\beta)$ at $\bar{\beta}$ will approximate the integrand by a Gaussian:

$$\begin{aligned} e^{F(\beta)} &= e^{F(\bar{\beta}) + \frac{1}{2}B(\beta - \bar{\beta})^2 + \dots} \\ &\approx e^{F(\bar{\beta})} e^{-\frac{1}{2}By^2}. \end{aligned} \quad (6.16)$$

The second derivative B at β from equation (6.13) is given by

$$B = (2n - 2)\beta^{-2} + s \left\{ 1 - \frac{I_0(\beta\sqrt{s})}{I_1(\beta\sqrt{s})} \right\} + 2\beta^{-1} \sum_i^n m_i + \sum_i^n m_i^2 \left\{ 1 + \frac{K_0^2(\beta m_i)}{K_1^2(\beta m_i)} \right\}. \quad (6.17)$$

One always has $B > 0$. Substitution of equation (6.16) in equation (6.8) gives after integration over y

$$R_n(s) \approx \left(\frac{2\pi}{sB} \right)^{\frac{1}{2}} \left(\frac{2\pi}{\beta} \right)^{n-2} I_1(\beta\sqrt{s}) \prod_i^n \{m_i K_1(\beta m_i)\}, \quad (6.18)$$

where β is the solution of equation (6.14) and B is given in equation (6.17). This is the final approximate form.

As it stands, equation (6.18) is not very transparent and the actual dependence on s is hard to see. In order to obtain more insight we consider the behaviour of $\beta = \beta(s)$ and the NR and ER limits.

The product $\beta\sqrt{s}$ grows as n . We then use the first term of

$$I_v(z) \xrightarrow[z \rightarrow \infty]{} (2\pi z)^{-\frac{1}{2}} e^z \left(1 - \frac{4v^2 - 1}{8z} + \dots \right) \quad (6.19)$$

in equation (6.13). In the NR limit $\beta \rightarrow \infty$ one obtains, using also equation (6.10),

$$F(\beta) \propto \beta(\sqrt{s} - \sum m_i) - \frac{3}{2}(n-1) \log \beta, \quad (6.20)$$

and in ER limit $\beta \rightarrow 0$ $K_1(z) \rightarrow z^{-1}$ implies

$$F(\beta) \propto \beta\sqrt{s} - (2n - \frac{3}{2}) \log \beta. \quad (6.21)$$

The condition $\partial F / \partial \beta = 0$ then gives

$$\begin{aligned} \beta^{\text{NR}} &= \frac{\frac{3}{2}n - \frac{3}{2}}{\sqrt{s} - \sum m_i} \\ \beta^{\text{ER}} &= \frac{2n - \frac{3}{2}}{\sqrt{s}}. \end{aligned} \quad (6.22)$$

Equations (6.22) allow the identification of $\beta^{-1} = T$ as 'temperature'. They agree with the well known result that kinetic energy per degree of freedom is $\frac{1}{2}T$.

If one computes the relative width $B^{-\frac{1}{2}}/\beta$ of the peak in Figure 6.2, one obtains in the two cases $1/\sqrt{\{\frac{3}{2}(n-1)\}}$ and $1/\sqrt{(2n-\frac{3}{2})}$. This is an example of the fact that fluctuations in temperature in the microcanonical ensemble go as $N^{-\frac{1}{2}}$ where N is the number of degrees of freedom.

For arbitrary s , β must be found numerically from equation (6.14). The resulting zeroth order approximation (6.18) will have an almost constant

relative error over the whole s range, and the error is approximately proportional to n^{-1} , since the saddle point condition eliminates the term proportional to $n^{-\frac{1}{2}}$. For greater accuracy, one must take higher order terms in equation (6.16). If third and fourth powers of $\beta - \bar{\beta}$ are included, one obtains the correction term proportional to n^{-1} . Then the error is proportional to $n^{-\frac{1}{2}}$ and is below 1 per cent. for $n \geq 6$.

A modification of the preceding method is to regard equation (6.4) as a four-fold integral in the variables $\alpha_0, \dots, \alpha_3$ and find the saddle point in each of them. For $T = 1$ this gives essentially the same results (Lurçat, 1964). The calculations are less transparent but lead to a slightly simpler result. We state here only the leading approximation for reference purposes. One has instead of equation (6.18):

$$R_n(s) \approx \frac{1}{(2\pi)^2} e^{\bar{\beta}\sqrt{s}} \Phi_n(\bar{\beta}) \bar{\beta}^{\frac{n}{2}} \{ \sqrt{s} a(\bar{\beta}) \}^{-\frac{1}{2}} \quad (6.23)$$

where $\bar{\beta}$ is the solution of

$$\sqrt{s} = 2n\bar{\beta}^{-1} + \sum_1^n m_i \frac{K_0(\beta m_i)}{K_1(\beta m_i)}, \quad (6.24)$$

Φ_n is the product of the factors ϕ_i in equation (6.9) and

$$\begin{aligned} a(\bar{\beta}) &= \beta^2 \left. \frac{\partial^2 \log \Phi_n(\beta)}{\partial \beta^2} \right|_{\beta=\bar{\beta}} \\ &= 4n - \bar{\beta}\sqrt{s} + \bar{\beta}^2 \sum_1^n m_i^2 - \sum_1^n \left\{ m_i \bar{\beta} \frac{K_0(m_i \bar{\beta})}{K_1(m_i \bar{\beta})} \right\} \geq 0. \end{aligned} \quad (6.25)$$

We note finally that it is straightforward to extend (de Groot, 1972; Satz, 1965) the statistical method to evaluating inclusive sums of the type

$$I(p, z) = \sum_{n=0}^{\infty} \frac{z^n}{n!} I_n(p), \quad (6.26)$$

where z is a parameter. In statistical terminology (Huang, 1963), this is equivalent to going from the canonical to the grand canonical ensemble.

Appendix A

Gram Determinants

(a) Definitions and properties

The *Gram determinant* of the vectors $p_1, \dots, p_n; q_1, \dots, q_n$ is the determinant of the scalar products $p_i \cdot q_j$:

$$G \begin{pmatrix} p_1, \dots, p_n \\ q_1, \dots, q_n \end{pmatrix} = \det(p_i \cdot q_j) \quad (\text{A.1})$$

$$= \begin{vmatrix} p_1 \cdot q_1 & p_1 \cdot q_2 & \dots & p_1 \cdot q_n \\ \vdots & \vdots & & \vdots \\ p_n \cdot q_1 & p_n \cdot q_2 & \dots & p_n \cdot q_n \end{vmatrix}.$$

A symmetric Gram determinant, $p_i = q_i$, $i = 1, \dots, n$, will be denoted by Δ_n :

$$\Delta_n(p_1, \dots, p_n) = G \begin{pmatrix} p_1, \dots, p_n \\ p_1, \dots, p_n \end{pmatrix} \quad (\text{A.2})$$
$$= \begin{vmatrix} p_1^2 & p_1 \cdot p_2 & \dots & p_1 \cdot p_n \\ \vdots & \vdots & & \vdots \\ p_n \cdot p_1 & p_n \cdot p_2 & \dots & p_n^2 \end{vmatrix}.$$

Any G can be regarded as a minor of a Δ_n , where n is the number of different arguments in G . For example,

$$G \begin{pmatrix} p_1, p_2 \\ p_1, p_3 \end{pmatrix} = \begin{vmatrix} p_1^2 & p_1 \cdot p_3 \\ p_2 \cdot p_1 & p_2 \cdot p_3 \end{vmatrix}$$

is clearly the minor of the element $p_3 \cdot p_2$ in $\Delta_3(p_1, p_2, p_3)$. In this book the arguments p_i are particle four-momenta or linear combinations of these. The elements of G and Δ_n , and thus also G and Δ_n themselves, are thus invariants.

Using the known rules for the behaviour of a determinant when a row or column is multiplied by a constant λ , when one row or column is added to another, or when rows and columns are permuted, we may derive the

following rules for Gram determinants:

$$\begin{aligned} G\left(\begin{matrix} \lambda p_1, p_2, \dots \\ q_1, q_2, \dots \end{matrix}\right) &= G\left(\begin{matrix} p_1, p_2, \dots \\ \lambda q_1, q_2, \dots \end{matrix}\right) \\ &= \lambda G\left(\begin{matrix} p_1, p_2, \dots \\ q_1, q_2, \dots \end{matrix}\right), \end{aligned} \quad (\text{A.3})$$

$$\Delta_n(\lambda p_1, p_2, \dots) = \lambda^2 \Delta_n(p_1, p_2, \dots), \quad (\text{A.4})$$

$$\begin{aligned} G\left(\begin{matrix} p_1, p_2, \dots \\ q_1, q_2, \dots \end{matrix}\right) &= G\left(\begin{matrix} p_1 + \lambda p_2, p_2, \dots \\ q_1, q_2, \dots \end{matrix}\right) \\ &= G\left(\begin{matrix} p_1, p_2, \dots \\ q_1 + \lambda q_2, q_2, \dots \end{matrix}\right), \end{aligned} \quad (\text{A.5})$$

$$\Delta_n(p_1, p_2, \dots) = \Delta_n(p_1 + \lambda p_2, p_2, \dots), \quad (\text{A.6})$$

$$G\left(\begin{matrix} p_1, p_2, \dots \\ q_1, q_2, \dots \end{matrix}\right) = G\left(\begin{matrix} q_1, q_2, \dots \\ p_1, p_2, \dots \end{matrix}\right), \quad (\text{A.7})$$

$$\begin{aligned} G\left(\begin{matrix} p_1, p_2, \dots \\ q_1, q_2, \dots \end{matrix}\right) &= -G\left(\begin{matrix} p_2, p_1, \dots \\ q_1, q_2, \dots \end{matrix}\right) \\ &= -G\left(\begin{matrix} p_1, p_2, \dots \\ q_2, q_1, \dots \end{matrix}\right), \quad \text{etc.} \end{aligned} \quad (\text{A.8})$$

Equations (A.3,5) imply that if the vectors of the set p_1, \dots, p_n (or q_1, \dots, q_n) are linearly dependent, then the Gram determinant (A.1) vanishes. This result can be proven directly as follows. The linear dependence of the vectors p_1, \dots, p_n implies, by definition, that there exists a set of coefficients $\alpha_1, \dots, \alpha_n$ (not all $\alpha_i = 0$) such that

$$\sum_i^n \alpha_i p_i = 0. \quad (\text{A.9})$$

Taking the scalar product of equation (A.9) with q_1 , then with q_2 , etc., to q_n results in n homogeneous linear equations for the invariants $p_i \cdot p_j$. According to equation (A.9) this system has a non-trivial solution $\alpha_1, \dots, \alpha_n$, which is possible only if the determinant formed from the coefficients of the equation vanishes. This determinant is precisely the Gram determinant (A.1). The importance of this result for kinematics follows from the fact that five or more vectors in a four-dimensional space are always linearly dependent.

The elements of the Gram determinants Δ_n are the invariants $p_i \cdot p_j$. In practice, m -particle invariant masses

$$s_{ijk\dots} = (p_i + p_j + p_k + \dots)^2 \quad (\text{A.10})$$

are often more useful. Equation (A.10) is written for outgoing particles, and the momenta of incoming particles occur with a minus sign. To introduce the variables $s_{ijk\dots}$ we note that the Gram determinant Δ_n in p_1, p_j is identical to a *Cayley determinant* of dimension $n + 2$ in $s_{ijk\dots}$. This Cayley determinant is given by the relation (Regge, 1964; Eden, 1966)

$$\Delta_n(p_1, \dots, p_n) = \frac{(-1)^{n+1}}{2^n} \begin{vmatrix} 0 & 1 & 1 & 1 & \cdots & 1 \\ 1 & 0 & p_1^2 & p_2^2 & \cdots & p_n^2 \\ 1 & p_1^2 & 0 & (p_1 - p_2)^2 & \cdots & (p_1 - p_n)^2 \\ 1 & p_2^2 & (p_1 - p_2)^2 & 0 & \cdots & (p_2 - p_n)^2 \\ \vdots & \vdots & \vdots & \vdots & \ddots & \vdots \\ 1 & p_n^2 & (p_1 - p_n)^2 & (p_2 - p_n)^2 & \cdots & 0 \end{vmatrix} \quad (\text{A.11})$$

To prove equation (A.11), one simply subtracts the second row from all the following rows and the second column from all the following columns. To write equation (A.11) in terms of the $s_{ijk\dots}$ one uses the identity

$$\Delta_n(p_1, p_2, \dots, p_n) = \Delta_n(p_1, p_1 + p_2, \dots, p_1 + p_2 + \dots + p_n), \quad (\text{A.12})$$

which follows from equation (A.6). On the right hand side of equation (A.12) the difference squared of two arguments is of the form $s_{i+1,\dots,j}$. Explicitly, Δ_n is then given by

$$\Delta_n(p_1, \dots, p_n) = \frac{(-1)^{n+1}}{2^n} \begin{vmatrix} 0 & 1 & 1 & 1 & \cdots & 1 \\ 1 & 0 & s_1 & s_{12} & \cdots & s_{12\dots n} \\ 1 & s_1 & 0 & s_2 & \cdots & s_{23\dots n} \\ 1 & s_{12} & s_2 & 0 & \cdots & s_{34\dots n} \\ 1 & s_{123} & s_{23} & s_3 & \cdots & s_{45\dots n} \\ \vdots & \vdots & \vdots & \vdots & \ddots & \vdots \\ 1 & s_{12\dots n} & s_{23\dots n} & s_{34\dots n} & \cdots & 0 \end{vmatrix} \quad (\text{A.13})$$

(b) A geometric interpretation

The Gram determinant (A.1) is linear in each p_i and q_i . According to equation (A.7) it is symmetric in the exchange of p_1, \dots, p_n and q_1, \dots, q_n , and according to equation (A.8) it is antisymmetric in permutations inside the two groups. This suggests an interpretation of G . One forms a totally antisymmetric combination of p_1, \dots, p_n and similarly of q_1, \dots, q_n and takes the scalar product of these objects. We show that in this way both the G_s and a geometric interpretation for them are obtained.

To make the interpretation intuitively clear we first work in a three dimensional Euclidean space. Let us introduce the three-dimensional Levi-Civita symbol ϵ_{ijk} ($i = 1, 2, 3$), defined by

$$\epsilon_{123} = \epsilon_{231} = \epsilon_{312} = 1$$

$$\epsilon_{132} = \epsilon_{213} = \epsilon_{321} = -1$$

$$\epsilon_{ijk} = 0 \text{ otherwise.}$$

ϵ_{ijk} is totally antisymmetric, $\epsilon_{ijk} = -\epsilon_{jik}$, etc. Now assume that the three-vectors $\mathbf{p}_1, \mathbf{p}_2, \mathbf{p}_3$, are given and define three tensors b, c and d through the equations

$$b_{jk} = 2^{-\frac{1}{2}} \epsilon_{ijk} p_1^i,$$

$$c_k = \epsilon_{ijk} p_1^i p_2^j,$$

$$d = \epsilon_{ijk} p_1^i p_2^j p_3^k.$$

Summation over repeated indices is everywhere implied. If $\mathbf{p}'_1, \mathbf{p}'_2, \mathbf{p}'_3$ is a second set of three-vectors and a', b', c' are defined in terms of these, one can easily see that

$$\begin{aligned}
 (b, b') &= b_{jk} b'_{jk} \\
 &= \mathbf{p}_1 \cdot \mathbf{p}'_1 \\
 (c, c') &= c_k c'_k \\
 &= (\mathbf{p}_1 \times \mathbf{p}_2) \cdot (\mathbf{p}'_1 \times \mathbf{p}'_2) \\
 &= \begin{vmatrix} \mathbf{p}_1 \cdot \mathbf{p}'_1 & \mathbf{p}_1 \cdot \mathbf{p}'_2 \\ \mathbf{p}_2 \cdot \mathbf{p}'_1 & \mathbf{p}_2 \cdot \mathbf{p}'_2 \end{vmatrix} \\
 (d, d') &= dd' \\
 &= (\mathbf{p}_1 \times \mathbf{p}_2 \cdot \mathbf{p}_3)(\mathbf{p}'_1 \times \mathbf{p}'_2 \cdot \mathbf{p}'_3) \\
 &= \det(p_{ii}) \cdot \det(p'_{ii}) \\
 &= \begin{vmatrix} \mathbf{p}_1 \cdot \mathbf{p}'_1 & \mathbf{p}_1 \cdot \mathbf{p}'_2 & \mathbf{p}_1 \cdot \mathbf{p}'_3 \\ \mathbf{p}_2 \cdot \mathbf{p}'_1 & \mathbf{p}_2 \cdot \mathbf{p}'_2 & \mathbf{p}_2 \cdot \mathbf{p}'_3 \\ \mathbf{p}_3 \cdot \mathbf{p}'_1 & \mathbf{p}_3 \cdot \mathbf{p}'_2 & \mathbf{p}_3 \cdot \mathbf{p}'_3 \end{vmatrix}
 \end{aligned} \tag{A.14}$$

Thus the quantities (b, b') , (c, c') , (d, d') are equal to determinants of the scalar products $\det(\mathbf{p}_i \cdot \mathbf{p}'_j)$. Putting $\mathbf{p}_i = \mathbf{p}'_i$, $i = 1, 2, 3$, the norms squared $|b|^2, |c|^2, |d|^2$ are seen to be equal to the symmetric determinants $\det(\mathbf{p}_i \cdot \mathbf{p}_j)$.

On the other hand, $|d|$ is clearly the volume of the parallelopiped formed by $\mathbf{p}_1, \mathbf{p}_2, \mathbf{p}_3$, $|c|$ equals the area of the parallelogram formed by \mathbf{p}_1 and \mathbf{p}_2 ,

and $|b|$ is the absolute value of \mathbf{p}_1 . These are then also the geometric interpretations of the symmetric determinants $\det(\mathbf{p}_i \cdot \mathbf{p}_j)$. Finally the second unsymmetric determinant has the interpretation

$$\begin{vmatrix} \mathbf{p}_1 \cdot \mathbf{p}'_1 & \mathbf{p}_1 \cdot \mathbf{p}'_2 \\ \mathbf{p}_2 \cdot \mathbf{p}'_1 & \mathbf{p}_2 \cdot \mathbf{p}'_2 \end{vmatrix} = |\mathbf{p}_1 \times \mathbf{p}_2| |\mathbf{p}'_1 \times \mathbf{p}'_2| \cos \phi$$

where ϕ is the angle between the planes $\mathbf{p}_1, \mathbf{p}_2$ and $\mathbf{p}'_1, \mathbf{p}'_2$.

Turning now to the Lorentz space, one defines the four-dimensional Levi-Civita symbol $\epsilon_{\kappa\lambda\mu\nu}$ ($\kappa = 0, 1, 2, 3$; etc.) as follows:

$$\begin{aligned} \epsilon_{\kappa\lambda\mu\nu} \text{ is totally antisymmetric,} \\ \epsilon_{0123} = 1. \end{aligned} \tag{A.15}$$

Antisymmetry implies that if two or more indices are equal, then $\epsilon_{\kappa\lambda\mu\nu} = 0$. The quantity ϵ transforms under Lorentz transformations as a pseudotensor of rank 4. Starting from four four-vectors p_1, p_2, p_3, p_4 one defines the quantities

$$\begin{aligned} a_{\lambda\mu\nu} &= 6^{-\frac{1}{2}} \epsilon_{\kappa\lambda\mu\nu} p_1^\kappa \\ b_{\mu\nu} &= 2^{-\frac{1}{2}} \epsilon_{\kappa\lambda\mu\nu} p_1^\kappa p_2^\lambda \\ c_\nu &= \epsilon_{\kappa\lambda\mu\nu} p_1^\kappa p_2^\lambda p_3^\mu \\ d &= \epsilon_{\kappa\lambda\mu\nu} p_1^\kappa p_2^\lambda p_3^\mu p_4^\nu. \end{aligned} \tag{A.16}$$

Because $\epsilon_{\kappa\lambda\mu\nu}$ is a pseudotensor of rank 4, a, b, c, d are pseudotensors of rank 3, 2, 1, 0. We shall now demonstrate the following properties:

1. If a tensor a, b, c or d is contracted with a similar tensor a', b', c' or d' formed out of another set p'_1, p'_2, p'_3, p'_4 , then the result equals a Gram determinant G (equations (A.17, 20–22)).
2. The absolute values of the tensors are $|a| = \sqrt{(-\Delta_1)}$, $|b| = \sqrt{(-\Delta_2)}$, $|c| = \sqrt{(-\Delta_3)}$, $|d| = \sqrt{(-\Delta_4)}$.
3. As a consequence $\sqrt{(\pm \Delta_i)}$ can be interpreted as the volume of a parallelopiped in $l - 1$ dimensional space, equations (A.24–25)).
4. Further, for one pair of arguments equal, $p_1 = p'_1$, the determinants G have the form $(\pm \Delta_i \Delta'_i)^{\frac{1}{2}} \cos \phi$ if $p_1^2 > 0$ and $(\pm \Delta_i \Delta'_i)^{\frac{1}{2}} \cosh \zeta$ if $p_1^2 < 0$ (equations (A.28–31)).

The scalar product of tensors x and y in the Lorentz metric $g_{\mu\nu}$ is

$$\begin{aligned} (x, y) &= x^{\mu_1 \dots \mu_r} y_{\mu_1 \dots \mu_r} \\ &= g_{\mu_1 \nu_1} \dots g_{\mu_r \nu_r} x^{\mu_1 \dots \mu_r} y^{\nu_1 \dots \nu_r}. \end{aligned}$$

To apply this to equations (A.16) we first note the equality

$$\epsilon^{\mu_1 \dots \mu_4} = g^{\mu_1 v_1} \dots g^{\mu_4 v_4} \epsilon_{v_1 \dots v_4} = -\epsilon_{\mu_1 \dots \mu_4}.$$

This follows simply from the fact that three of the $g^{\mu_i \nu_i}$'s are -1 and one is $+1$. The scalar product of a in equation (A.16) with the similar primed quantity gives

$$\begin{aligned}(a, a') &= \frac{1}{6} \epsilon_{\kappa \lambda \mu \nu} p_1^\kappa \epsilon^{\rho \lambda \mu \nu} p_1'{}_\rho \\ &= -\frac{1}{6} \epsilon_{\kappa \lambda \mu \nu} p_1^\kappa \epsilon_{\rho \lambda \mu \nu} p_1'{}_\rho.\end{aligned}$$

Because $\epsilon_{\kappa \lambda \mu \nu}$ vanishes unless the indices are a permutation of 0123, only the terms with $\kappa = \rho$ contribute. Summing over permutations of $\lambda \mu \nu$ gives in analogy to the first of equations (A.14)

$$\begin{aligned}(a, a') &= -\frac{1}{6} 3! p_1^\kappa p_1'{}_\kappa \\ &= -p_1 \cdot p_1' \\ &= -G \begin{pmatrix} p_1 \\ p_1' \end{pmatrix}.\end{aligned}\tag{A.17}$$

For the second rank tensors b and b' one has similarly

$$\begin{aligned}(b, b') &= \frac{1}{2} \epsilon_{\kappa \lambda \mu \nu} p_1^\kappa p_2^\lambda \epsilon^{\rho \sigma \mu \nu} p_1'{}_\rho p_2'{}_\sigma \\ &= -\frac{1}{2} \epsilon_{\kappa \lambda \mu \nu} p_1^\kappa p_2^\lambda \epsilon_{\rho \sigma \mu \nu} p_1'{}_\rho p_2'{}_\sigma.\end{aligned}\tag{A.18}$$

It is easy to prove the following identity:

$$\epsilon_{\kappa \lambda \mu \nu} \epsilon_{\rho \sigma \mu \nu} = 2! (\delta_{\kappa \rho} \delta_{\lambda \sigma} - \delta_{\kappa \sigma} \delta_{\lambda \rho}).\tag{A.19}$$

Then equation (A.18) becomes

$$\begin{aligned}\hat{\epsilon}(b, b') &= -(p_1 \cdot p_1' - p_2 \cdot p_2' - p_1 \cdot p_2' + p_2 \cdot p_1') \\ &= -G \begin{pmatrix} p_1, p_2 \\ p_1', p_2' \end{pmatrix}.\end{aligned}\tag{A.20}$$

Proceeding in the same manner one finds in analogy with equation (A.14)

$$(c, c') = -G \begin{pmatrix} p_1, p_2, p_3 \\ p_1', p_2', p_3' \end{pmatrix},\tag{A.21}$$

$$\begin{aligned}(d, d') &= -G \begin{pmatrix} p_1, p_2, p_3, p_4 \\ p_1', p_2', p_3', p_4' \end{pmatrix} \\ &= -\{\Delta_4(p_1, p_2, p_3, p_4) - \Delta_4(p_1', p_2', p_3', p_4')\}^{\frac{1}{2}}.\end{aligned}\tag{A.22}$$

As special cases one obtains the norms of the pseudotensors:

$$\begin{aligned}(a, a) &= -\Delta_1, & (b, b) &= -\Delta_2, \\(c, c) &= -\Delta_3, & (d, d) &= -\Delta_4.\end{aligned}\quad (\text{A.23})$$

Turning to the geometric interpretation, the values of $\Delta_1, \dots, \Delta_4$ in the frame $R(p_1)$ for $p_1^2 > 0$ and frame $S(p_1)$ for $p_1^2 < 0$ were computed in Section II.7. In the frame $\mathbf{p}_1 = 0$ we have (see equations (VI.7.31))

$$\begin{aligned}\{\Delta_1(p_1)\}^{\frac{1}{2}} &= m_1 \\ \{-\Delta_2(p_1, p_2)\}^{\frac{1}{2}} &= m_1 P_2 \\ \{\Delta_3(p_1, p_2, p_3)\}^{\frac{1}{2}} &= m_1 |\mathbf{p}_2 \times \mathbf{p}_3| = m_1 P_2 P_3 \sin \theta_{23} \\ \{-\Delta_4(p_1, p_2, p_3, p_4)\}^{\frac{1}{2}} &= m_1 \mathbf{p}_2 \times \mathbf{p}_3 \cdot \mathbf{p}_4 = m_1 P_2 P_3 P_4 \sin \theta_{23} \sin \theta_{24} \sin \phi\end{aligned}\quad (\text{A.24})$$

The angles are defined in Figure II.7.1. In the frame $p_1 = (0, 0, 0, \sqrt{(-t_1)})$ we used the pseudospherical coordinates (II.7.22) with $P_i^2 = p_{i0}^2 - p_{i1}^2 - p_{i2}^2$ and found

$$\begin{aligned}-\Delta_1(p_1) &= \sqrt{(-t_1)} \\ -\Delta_2(p_1, p_2) &= \sqrt{(-t_1)} P_2 \\ -\Delta_3(p_1, p_2, p_3) &= \sqrt{(-t_1)} P_2 P_3 \sinh \zeta_{23} \\ -\Delta_4(p_1, p_2, p_3, p_4) &= \sqrt{(-t_1)} P_2 P_3 P_4 \sinh \zeta_{23} \sinh \zeta_{24} \sin \phi.\end{aligned}\quad (\text{A.25})$$

Here one could use the fact that for $p_{21} = p_{22} = 0$ one has $P_2 = E_2$. Equations (A.24–25) are valid irrespective of the signs of p_2^2, p_3^2 and p_4^2 . Notice the change of sign of Δ_1 and Δ_3 in going from equation (A.24) to equation (A.25). Equations (A.24–25) show that $\sqrt{(\pm \Delta_i)}$ is proportional to the volume of an $l - 1$ -dimensional parallelopiped in the 123-subspace ($p_1^2 > 0$) or in the 012-subspace ($p_1^2 < 0$).

Among the unsymmetric determinants, take first the simplest G with $n = 1$. In the two cases $p_1^2 \geq 0$, one finds

$$\begin{aligned}G\begin{pmatrix} p_1 \\ p_2 \end{pmatrix} &= p_1 \cdot p_2 \\ &= m_1 E_2 \text{ in } R(p_1)\\ &= -\sqrt{(-t_1)} P_2 \text{ in } S(p_1).\end{aligned}\quad (\text{A.26})$$

$$\quad (\text{A.27})$$

For $n = 2$ the determinant (A.1) has a simple interpretation, if two momenta are the same, e.g. $p_1 = p'_1$. Then for timelike p_1 equation (II.7.8) implies in $R(p_1)$

$$G\begin{pmatrix} p_1, p_2 \\ p_1, p_3 \end{pmatrix} = -m_1^2 P_2 P_3 \cos \theta_{23}. \quad (\text{A.28})$$

For $p_1^2 < 0$ one obtains in $S(p_1)$

$$\begin{aligned} \begin{vmatrix} t_1 & -\sqrt{(-t_1)p_{33}} \\ -\sqrt{(-t_1)p_{23}} & p_2 \cdot p_3 \end{vmatrix} &= t_1(p_{20}p_{30} - p_{21}p_{31} - p_{22}p_{32}), \\ G\begin{pmatrix} p_1, p_2 \\ p_1, p_3 \end{pmatrix} &= t_1 P_2 P_3 \cosh \zeta_{23}. \end{aligned} \quad (\text{A.29})$$

The quantity (A.1) for $n = 3$ is according to equation (A.21) the scalar product $(c, c') = c \cdot c'$ of two four-vectors c and c' . Set now two four-momenta equal, say $p_1 = p'_1$, and evaluate G in the standard frame of p_1 . If $p_1^2 > 0$, we see that in $R(p_1)$, c and c' are pure three-vectors. Then $-G = (c, c') = (c, c') = -|c||c'| \cos \phi = -(\Delta_3)^{\frac{1}{2}}(\Delta'_3)^{\frac{1}{2}} \cos \phi$ and equation (A.24) implies

$$G\begin{pmatrix} p_1, p_2, p_3 \\ p_1, p_4, p_5 \end{pmatrix} = m_1^2 P_2 P_3 P_4 P_5 \sin \theta_{23} \sin \theta_{45} \cos \phi, \quad (\text{A.30})$$

where ϕ is the angle between the planes defined by p_2, p_3 and p_4, p_5 in $R(p_1)$. A special case of this is equation (II.7.14).

When p_1 is spacelike, one takes the frame $S(p_1)$ with $p_{13}, p_{20}, p_{23} \neq 0$. Then one finds

$$G\begin{pmatrix} p_1, p_2, p_3 \\ p_1, p_2, p_4 \end{pmatrix} = t_1 P_2^2 P_3 P_4 \sinh \zeta_{23} \sinh \zeta_{24} \cos \phi. \quad (\text{A.31})$$

This follows from $-G = (c, c') = -|c||c'| \cos \phi = (-\Delta_3)^{\frac{1}{2}}(-\Delta'_3)^{\frac{1}{2}} \cos \phi$ and equation (A.25). Again, p_2^2, p_3^2, p_4^2 have either sign without restrictions.

The quantity (d, d') is the product of two pseudoscalars. Thus G with $n = 4$ is simply $(\Delta_4 \Delta'_4)^{\frac{1}{2}}$ (see equation (A.22) and also Exercise II.17).

Both the sine and cosine of the angles θ and ϕ occur in equations (A.24), (A.28) and (A.30). Setting the sum of squares equal to one results in the identities

$$\Delta_2(p_1, p_2)\Delta_2(p_1, p_3) = \Delta_1(p_1)\Delta_3(p_1, p_2, p_3) + G\begin{pmatrix} p_1, p_2 \\ p_1, p_3 \end{pmatrix}^2, \quad (\text{A.32})$$

$$\Delta_3(p_1, p_2, p_3)\Delta_3(p_1, p_2, p_4) = \Delta_2(p_1, p_2)\Delta_4(p_1, p_2, p_3, p_4) + G\begin{pmatrix} p_1, p_2, p_3 \\ p_1, p_2, p_4 \end{pmatrix}^2.$$

Appendix B

Spherical Trigonometry

Formulas of spherical trigonometry are often needed to discuss differential cross-sections and spectrometer apertures. These formulae are easily found in various handbooks, but we shall here derive the basic formulae in a way which emphasizes their symmetry properties.

Consider the spherical triangle with sides a, b, c and angles A, B, C as shown in Figure B.1. Choosing the axes as in Figure B.1, the unit vectors to

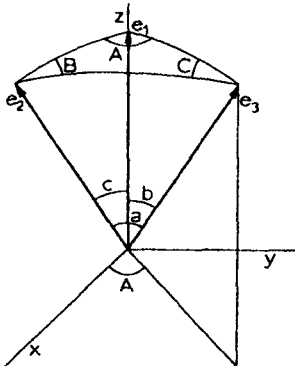


Figure B.1

the corners of the triangle are

$$\begin{aligned}e_1 &= (0, 0, 1) \\e_2 &= (\sin c, 0, \cos c) \\e_3 &= (\sin b \cos A, \sin b \sin A, \cos b).\end{aligned}\tag{B.1}$$

The *law of sines* is obtained by evaluating the volume of the parallelopiped spanned by the e_i :

$$e_1 \cdot e_2 \times e_3 = \sin b \sin c \sin A.\tag{B.2}$$

But by cyclic symmetry this evidently equals $\sin c \sin a \sin B$ or $\sin a \sin b$

$\sin C$, which leads to the law of sines

$$\frac{\sin a}{\sin A} = \frac{\sin b}{\sin B} = \frac{\sin c}{\sin C}. \quad (\text{B.3})$$

The *law of cosines for sides* or the *cosine theorem* is obtained by computing the scalar products between the e_i :

$$\begin{aligned} e_2 \cdot e_3 &= \cos a \\ &= \cos b \cos c + \sin b \sin c \cos A, \end{aligned} \quad (\text{B.4})$$

etc., cyclically.

In order to obtain further formulae in a symmetric fashion one has to consider the spherical triangle generated by the basis vectors \hat{e}_i dual to the e_i :

$$\hat{e}_1 = \frac{e_2 \times e_3}{|e_2 \times e_3|}, \quad \text{etc., cyclically.} \quad (\text{B.5})$$

Explicit computation from equations (B.1) and (B.5) yields

$$\begin{aligned} \hat{e}_1 &= (-\sin B \cos c, -\cos B, \sin B \sin c) \\ \hat{e}_2 &= (\sin A, -\cos A, 0) \\ \hat{e}_3 &= (0, 1, 0). \end{aligned} \quad (\text{B.6})$$

In deriving equation (B.6), the y -component of \hat{e}_1 is obtained most simply from

$$\hat{e}_1 \cdot \hat{e}_3 = -\cos B, \quad \text{etc., cyclically.} \quad (\text{B.7})$$

The volume of the parallellopiped generated by the \hat{e}_i gives again the law of sines, but the scalar products $\hat{e}_i \cdot \hat{e}_j$ give the *law of cosines for angles*:

$$\begin{aligned} -\hat{e}_1 \cdot \hat{e}_2 &= \cos C \\ &= \cos A \cos B - \sin A \sin B \cos c \end{aligned} \quad (\text{B.8})$$

etc., cyclically.

A different set of equations is obtained, if $-\hat{e}_1 \cdot \hat{e}_3$ is evaluated using equations (B.5) and (B.1) for \hat{e}_1 :

$$\begin{aligned} -e_2 \times e_3 \cdot \hat{e}_3 &= \sin a \cos B \\ &= \cos b \sin c - \sin b \cos c \cos A. \end{aligned} \quad (\text{B.9})$$

Replacing $\sin a$ through equation (B.3) reduces the number of variables to four:

$$\sin A \cot B = \cot b \sin c - \cos c \cos A. \quad (\text{B.10})$$

Similar calculation of $e_1 \cdot e_3$ gives

$$\begin{aligned} e_1 \cdot \hat{e}_1 \times \hat{e}_2 &= \cos b \sin C \\ &= \cos c \sin B \cos A + \sin A \cos B. \end{aligned} \quad (\text{B.11})$$

The four variable formula from equations (B.3) and (B.11) is equivalent to equation (B.10).

If one of the angles of the triangle is 90° , the simplified formulas may be summarized in **Napier's rule**. Choosing $C = 90^\circ$ this rule says that, in the diagram of Figure B.2, the cosine of any quantity equals

- (a) the product of cotangents of adjacent quantities,
- (b) the product of sines of non-adjacent quantities.

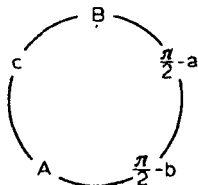


Figure B.2

The solid angle Ω_3 , describing the orientation of e_3 relative to the coordinate system defined by e_1 and e_2 gives now $d\Omega_3 = d \cos b dA$. The previous equations can be used to replace b and A by other pairs of variables in Figure B.1. An important case is that where A is replaced by a . Then

$$d\Omega_3 = \frac{d \cos a d \cos b \theta(K)}{K^4(\cos a, \cos b, \cos c)} \quad (\text{B.12})$$

where

$$K(x, y, z) = 1 - x^2 - y^2 - z^2 + 2xyz \quad (\text{B.13})$$

$$= \begin{vmatrix} 1 & x & y \\ x & 1 & z \\ y & z & 1 \end{vmatrix}$$

Solutions to Exercises

II.1. $(3 \text{ km}) \times \log\left(\frac{E}{m_e}\right) \times m_e/(E - m_e) \simeq 81 \text{ cm}.$

II.2. $\mathbf{x}' = \mathbf{x} + \left\{ \frac{(\gamma - 1)\mathbf{v} \cdot \mathbf{x}}{c^2} \right\} \mathbf{v} - \gamma \mathbf{v} t$

$$t' = \gamma t - \left(\frac{\gamma}{c^2} \right) \mathbf{v} \cdot \mathbf{x}$$

II.3. (a) $\gamma \leq \frac{(1 + \epsilon)}{(1 - \epsilon)}, \quad v \leq 2\sqrt{\epsilon}$

(b) $v \geq \frac{1}{(1 + \epsilon)}, \quad \gamma \geq \frac{1}{\sqrt{2\epsilon}}$.

To an accuracy of 1 per cent, the approximation $E = m + p^2/2m$ can be used if $p \leq 0.2 \text{ m}$, $E = p$ if $p \geq 7 \text{ m}$.

II.4. 10.0 ns, 10.1 ns, 13.7 ns.

II.5. (a) $a = \gamma(c\gamma', \gamma'\mathbf{v} + \gamma\mathbf{v}')$, where $\gamma' = \gamma^3 v v'/c^2$ and the prime denotes a derivative with respect to time,

(b) $a \cdot u = 0$ is obtained by differentiating $u \cdot u = c^2$,

(c) $a \cdot a = \gamma^6/(v')^2$

II.6. $v^{\text{CM}} = 0.952, \quad \gamma^{\text{CM}} = 3.26, \quad p_z^* = -1.46 \text{ GeV}/c,$
 $E^* = 2.65 \text{ GeV}, \quad P^* = 2.48 \text{ GeV}/c.$

II.7. In the target system the momentum vector lies on the hyperboloid $p_x^2 - (\gamma^{\text{CM}} v^{\text{CM}})^2(p_x^2 + p_y^2) = (m_p \gamma^{\text{CM}} v^{\text{CM}})^2$.

The maximum value in the CMS is $P^* \leq \frac{1}{2}\sqrt{(s - 4m^2)}$.

II.9. (a) The plane $q' = \text{constant}$ becomes in the qr plane the hyperbola

$$\frac{(q - \gamma q')^2}{\gamma^2 v^2 (q'^2 + m^2)} - \frac{r^2}{(q'^2 + m^2)} = 1$$

(b) The cylinder $r' = \text{constant}$ remains invariant but within it q and q' are related by $q = \gamma q' - \gamma v(q'^2 + r'^2 + m^2)^{1/2}$.

In qq' plane this is a hyperbola (Figure II.2.1).

II.12. Using equation (II.3.6)

(a) $\tau_q = 2.5 \times 10^{-19} \text{ s}$
(b) $\Gamma_{x^0} = 7.4 \text{ eV}$.

II.13. See (Hagedorn, 1964).

II.14. See equations (II.6.25–26); $v_a^T = v_b^B$.

III.1. (a) GeV^{2-n} ,

(b) GeV^{2n-4} .

III.2. $I(E) = (2\pi m)^{3n/2} E^{3n/2 - 1} / \Gamma(3n/2)$

Hint: use the formulae

$$\begin{aligned}\delta(x) &= \frac{1}{2\pi} \int_{-\infty}^{\infty} dt e^{ixt} \\ \int_0^{\infty} dt t^b e^{-at^2} &= \Gamma\{(b+1)/2\}/2a^{(b+1)/2} \\ \int_{-\infty}^{\infty} dt e^{ixt} \frac{1}{(it)^a} &= \frac{2\pi}{\Gamma(a)} x^{a-1} \cdot \Theta(x)\end{aligned}$$

where Γ is the gamma-function.

III.4. Remember that $0 \leq \theta \leq \frac{1}{2}\pi$.

III.5. Find from equation (III.4.13) that

$$\frac{d\theta^*}{d\theta} = \frac{2}{\gamma(1 - v^2 \cos^2 \theta)}$$

and from equation (II.8.32) that

$$\sin \theta^* = \frac{2 \sin \theta \cos \theta}{\gamma(1 - v^2 \cos^2 \theta)}$$

IV.1. $\sin \frac{\theta_{12}}{2} = \frac{1 - v \cos \theta_1}{\sqrt{(1 - 2v \cos \theta_1 + v^2)}}$.

IV.2. When $\theta_1 = \theta_2$, $E_1 = E_2$ and $\sin \theta_{12}^{\max}/2 = \frac{m}{E} = \frac{1}{\gamma}$ or $\cos \theta_{12}^{\max}/2 = v$.

IV.3. From $P_2^* = \sqrt{\{\lambda(s, m_1^2, m_2^2)\}}/2\sqrt{s} = m_2 \cot \frac{\alpha}{2}$ solve

$$m_2 = \frac{\sqrt{s} - \sqrt{\left(m_1^2 \sin^2 \frac{\alpha}{2} + s \cos^2 \frac{\alpha}{2}\right)}}{\sin \frac{\alpha}{2}}$$

IV.5. $w(r) = r(P^2 - r^2)^{-\frac{1}{2}} w\{(1 - r^2/P^2)^{\frac{1}{2}}\}$, P is the decay momentum.

IV.6. Using equation (III.2.5)

$$\frac{1}{\tau} = \frac{P_1^*}{2m^2} \frac{T_2}{4\pi}$$

where $P_1^* = \sqrt{\{\lambda(m^2, m_1^2, m_2^2)\}}/2m$. T_2 must thus have the dimensions of $(\text{mass})^2 = \text{GeV}^2$.

$$f_K^2/4\pi m_K^2 = 7.4 \times 10^{-14}.$$

$$\text{IV.7. } \frac{1}{\tau_\rho} = \frac{f_{\rho\pi\pi}^2}{4\pi} \frac{2P_\pi^{*3}}{3m_\rho^2} = \frac{f_{\rho\pi\pi}^2}{4\pi} \frac{m_\rho}{12} \left(1 - \frac{4m_\pi^2}{m_\rho^2}\right)^{\frac{3}{2}}$$

$$f_{\rho\pi\pi}^2/4\pi = 2.44.$$

IV.8. See equation (IV.3.8).

IV.9. For equal masses $g_1^* = g_2^* = 1$ and

$$P_1 = \frac{2m(E_a + m)P_a \cos \theta_1}{(E_a + m)^2 - P_a^2 \cos^2 \theta_1}.$$

P_2 is obtained by interchanging 1 and 2.

For $m_a = m_1 = 0$, $m_b = m_2 = m$,

$$E_1 = P_1 = \frac{E_a}{1 + (E_a/m)(1 - \cos \theta_1)},$$

$$E_2 = \frac{(E_a + m)^2 + E_a^2 \cos^2 \theta_2}{(E_a + m)^2 - E_a^2 \cos^2 \theta_2} m,$$

$$P_2 = \frac{2M(E_a + m)E_a \cos \theta_2}{(E_a + m)^2 - E_a^2 \cos^2 \theta_2}.$$

IV.10. (a) $\tan \theta_1 \tan \theta_2 = 1/\gamma^2$, $\gamma = (E_a + m)/\sqrt{s}$.

$$(b) \tan \frac{\theta_1}{2} \tan \theta_2 = 1 - v, \quad v = E_a/(E_a + m).$$

IV.11. (a) $P_1^{\max} = P_a$, $P_1^{\min} = P_a(m^2 - \mu^2)/s$.

$$(b) P_2^{\max} = 2m(E_a + m)P_a/s = \{1 + (m^2 - \mu^2)/s\}P_a, \\ P_2^{\min} = 0.$$

IV.12. The results follow from equations (IV.1.12) and (IV.3.13–14).

IV.14. For elastic scattering masses $\mu m \rightarrow \mu m$.

IV.15. In s channel $t \leq 0$, $u = 4m^2 - s - t \leq 0$; similarly for t and u channels.

IV.17. Assume the tetrahedron is spanned by three vectors $\mathbf{a}_1, \mathbf{a}_2, \mathbf{a}_3$. The volume is $V = 6^{-1} \mathbf{a}_1 \times \mathbf{a}_2 \cdot \mathbf{a}_3$ and $V^2 = 36^{-1} \det(\mathbf{a}_1, \mathbf{a}_2)$. Inserting here $\mathbf{a}_1^2 = u$, $\mathbf{a}_2^2 = x$, $\mathbf{a}_3^2 = w$, $2\mathbf{a}_1 \cdot \mathbf{a}_2 = x + u - v$, $2\mathbf{a}_2 \cdot \mathbf{a}_3 = x + w - z$, $2\mathbf{a}_3 \cdot \mathbf{a}_1 = u + w - y$ leads to the representation of G given in Exercise IV.16 and the answer follows.

IV.18. The result is physically the Lorentz transformation equation transforming \mathbf{p}_2 from CMS to the rest frame of p_b , when all vectors are parallel.

IV.20. The analogue is the part of the hyperbola (IV.5.9) remaining within the half-plane $t > 0$. This region is not physical, of course.

IV.21. (a) $t^+ = -0.00002 (\text{GeV}/c)^2$,

$$(b) t^+ = -0.04 (\text{GeV}/c)^2.$$

IV.22. To leading order in $1/s$ $t = 0$ corresponds to $\theta_{a1}^* = 2s^{-1} \{(m_a^2 - m_1^2)(m_2^2 - m_b^2)\}^{1/2}$. In elastic scattering $\mu m \rightarrow \mu m$ $u = 0$ corresponds to $\theta_{a1}^* = \pi - 2(m^2 - \mu^2)/s \approx 175^\circ$ for $\pi N \rightarrow \pi N$ at $10 \text{ GeV}/c$.

IV.23. Use equations (IV.4.19–22).

IV.24. $\sigma(s) = \beta(s) \{(32\pi a\lambda)\}^{-1} \{1 - \exp(-2a\lambda/s)\}$, $\lambda = \lambda(s, m^2, \mu^2)$.

IV.25. $A = (-0.47 + i)103 e^{-4.5i} (s/1 \text{ GeV}^2)$.

IV.26. Using $t = -4E_a E_1 \sin^2 \frac{1}{2}\theta_1$, where E_1 is given in Exercise IV.9, one finds $d\sigma/dt = (2\pi\alpha^2/t^2) \times \{t^2 + 2st + 2(s - M^2)^2\}(s - M^2)^{-2}$.

IV.27. $(s - 4m^2)(s + t) \sin^2 \theta_{a1}^T + 4m^2 t = 0$.

IV.28. If $t > 0$ then in frame $q = (q^0, \mathbf{0})$ one has $P_a = P_1$ and $P_b = P_2$. Then $(m_a - m_1)(m_b - m_2) \geq 0$ implies $(E_a - E_1)(E_b - E_2) \geq 0$ and $E_a - E_1 = q^0 = E_2 - E_b$ cannot be satisfied.

IV.29. $I_\mu = \pi P_1 E_1 p_\mu / s$,
 $I_{\mu\nu} = (\pi P_1 / 3\sqrt{s}) \{ -P_1^2 g_{\mu\nu} + (P_1^2 + 3E_1^2)p_\mu p_\nu / s \}$,
where $P_1 = \lambda^{\frac{1}{2}}(s, m_1^2, m_2^2)$, $E_1 = (s + m_1^2 - m_2^2)/2\sqrt{s}$, $s = p^2$.

V.1. Compare equations (IV.5.22).

V.2. $I_1 = \log\{\lambda^{\frac{1}{2}}(x, a, b) + x - a - b\}$,
 $I_2 = \lambda^{\frac{1}{2}}(x, a, b) - (a + b)I_1$
 $- |a - b| \log [\{(a - b)^2 - (a + b)x + |a - b|\lambda^{\frac{1}{2}}(x, a, b)\}/x]$
 $I_3 = \frac{1}{2}(x - a - b)\lambda^{\frac{1}{2}}(x, a, b) - abI_1$,
 $K = \pi/\sqrt{(-a)}$.

V.3. $\frac{1}{4}\pi^2\lambda^{-\frac{1}{2}}(s, m_a^2, m_b^2)$.

V.4. Using the results of Exercise V.2. one finds

$$8R_3(s)/\pi^2 s = (s + m_1^2 + m_2^2)/\lambda/s^2$$

$$+ 2s^{-1}|m_1^2 - m_2^2| \log \left\{ \frac{s(m_1^2 + m_2^2) - (m_1^2 - m_2^2)^2 + |m_1^2 - m_2^2|\sqrt{\lambda}}{2m_1 m_2 s} \right\}$$

$$- 2s^{-2}\{s(m_1^2 + m_2^2) - 2m_1^2 m_2^2\} \log \left\{ \frac{s - m_1^2 - m_2^2 + \sqrt{\lambda}}{2m_1 m_2} \right\},$$

where $\lambda = \lambda(s, m_1^2, m_2^2)$.

V.5. Replacing $|A|^2$ by $\sigma_{\pi N}(s_2)$ through equation (IV.4.19) one finds from equation (V.5.16) and equation (III.2.3):

$$d^2\sigma_3/dt_1 ds_2 = \{16\pi^2\lambda(s, m_a^2, m_b^2)\}^{-1}\lambda^{\frac{1}{2}}(s_2, t_1, m_b^2)\sigma_{\pi N}(s_2)F(t_1).$$

V.7. The Jackson-angle distribution is obtained by inserting the integrand $\exp(bt_2)$, where t_2 is given by equation (V.7.5), into equation (V.5.16) and integrating over all variables but $\cos\theta_{b3}^{R23}$. For $m_i = 0$ this leads to the distribution $x\{x - (x + s)e^{-s/x}\}$, $1/x = \sin^2\frac{1}{2}\theta_{b3}^{R23}$.

V.8. Use the properties of equations (A.3–8) of unsymmetric Gram determinants.

V.9. From the Dalitz plot it is seen that $dR_3/dM_{12}^2 = \text{constant}$.

V.10. In the frame $\mathbf{p}_a + \mathbf{p}_b - \mathbf{p}_1 = 0$ the surface is the sphere

$$P^2 = \lambda(s_2, m_2^2, m_3^2)/4s_2 \equiv A^2.$$

This frame is obtained from TS by giving a boost $\gamma = (s_2 - t_1 + m_b^2)/2m_b\sqrt{s_2}$ in the $\mathbf{p}_a - \mathbf{p}_1$ direction in TS. In TS the surface is thus the ellipsoid

$$(\beta p_x - \alpha p_s)^2 + p_y^2 + \gamma^{-2}(\alpha p_x + \beta p_z - h)^2 = A^2$$

where $h^2 = (\gamma^2 - 1)(A^2 + m_3^2)$ and $\alpha = (\mathbf{p}_a - \mathbf{p}_1)_s/|\mathbf{p}_a - \mathbf{p}_1|$, $\beta = (\mathbf{p}_a - \mathbf{p}_1)_z/|\mathbf{p}_a - \mathbf{p}_1|$.

...

- VI.1. Use $I_v(x) = (\frac{1}{4}x)^{\frac{1}{2}} \sum_{k=0}^{\infty} (\frac{1}{4}x^2)^k / k! \Gamma(k + v + 1)$, where I_v is a modified Bessel function, to evaluate

$$\sigma(E) = \frac{\pi\lambda^2}{E^2} \cdot \frac{I_1\{E\sqrt{(2\pi\lambda)}\}}{E\sqrt{(2\pi\lambda)}} \sim \frac{\pi\lambda^2}{E} \frac{e^{E\sqrt{(2\pi\lambda)}}}{2\pi\{E\sqrt{(2\pi\lambda)}\}^{\frac{1}{2}}}$$

$$\langle n \rangle = 1 + \frac{1}{2}E\sqrt{(2\pi\lambda)} \frac{I_0\{E\sqrt{(2\pi\lambda)}\}}{I_1\{E\sqrt{(2\pi\lambda)}\}} \sim \frac{1}{2}E\sqrt{(2\pi\lambda)}$$

If $\sigma_n(E)$ is divided by $\sigma(E)$, one can use $E = \Sigma E_i$ to introduce the factors $\exp\{-E_i\sqrt{(2\pi\lambda)}\}$ in the phase space integration.

- VI.2. In terms of $T_n = M_n - \mu_n$

$$R_n(T_n) = \pi\sqrt{m_n} \left(\frac{2\mu_{n-1}}{\mu_n} \right)^{\frac{1}{2}} \int_0^{T_n} dT_{n-1} (T_n - T_{n-1})^{\frac{1}{2}} R_{n-1}(T_{n-1}).$$

One starts from

$$R_2^{\text{NR}}(T_2) = \pi\sqrt{2} \frac{(m_1 m_2)^{\frac{1}{2}}}{\mu_2^{\frac{1}{2}}} T_2^{\frac{1}{2}},$$

and carries out the integral over T_{n-1} in terms of Euler's beta function.

$$\begin{aligned} \text{VI.4. } R_n &= \frac{\pi}{2\lambda^{\frac{1}{2}}(M_n^2, m_a^2, m_b^2)} \int dM_{n-1}^2 ds_1 \frac{1}{4\lambda^{\frac{1}{2}}(M_n^2, M_{n-1}^2, m_n^2)} d\phi_{n-1} \\ &\quad \times \int dM_2^2 ds_3 \frac{1}{4\lambda^{\frac{1}{2}}(M_3^2, M_2^2, m_3^2)} d\phi_2 \int ds_2 d\phi_1 \end{aligned}$$

where $s_n \equiv t_{bn} = (p_b - p_n)^2$, $s_{n-1} = (p_n + p_{n-1})^2$, etc., and the limits of integration on M_1^2, s_{i+1} plane are given by $G(s_{i+1}, M_{i+1}^2, m_{i+1}^2, M_{i+2}^2, M_i^2, m_{i+2}^2) = 0$ demanding the $2 \rightarrow 2$ process $k_{i+2} - k_i = p_{i+2} + p_{i+1}$ to be physical. This is a form in which the two-particle subenergies of the multiperipheral diagram in Figure 2.7 occur as variables.

- VI.9. Integrate equation (VI.4.27) by measuring the orientation of p_1 relative to an arbitrary axis and that of p_2 relative to p_1 . The angular integrations are then trivial. For $n = 3$ use $R_1(M_{33}^2) = \delta(M_{33}^2 - m_3^2)$.

- VI.10. Use the representation

$$R_4 = \int dM_{123}^2 dM_{12}^2 R_2(s; M_{123}^2, m_4^2) R_2(M_{123}^2; M_{12}^2, m_3^2) R_2(M_{12}^2; m_1^2, m_2^2).$$

The physical region is a triangle.

- VI.11. The physical region on $M_{1234}^2 M_{3456}^2$ plane is obtained by drawing a rectangle around the Dalitz plot for three-particle final state with masses $m_1 + m_2$, $m_3 + m_4$, $m_5 + m_6$ and deleting from this square a region in the corner nearest the origin. For a seven-particle final state the physical region is the entire rectangle.

- VI.12. Use polar coordinates on $r_i q_i$ plane.

- VI.14. Write

$$L_n = \int \prod_i^n d^2 q_{i-1} \delta((q_i - q_{i-1})^2 - m_i^2) \delta^2(q_0 + p_n)$$

and insert $q_i = \{0, \sqrt{(-t_i)}\}$, $q_{i-1} = \sqrt{(-t_{i-1})}(\sinh \eta_i, \cosh \eta_i)$, $d^2 q_i = \frac{1}{2} dt_i d\eta_{i+1}$.

- VI.15. Assume all masses are equal = m' and introduce to equation (VI.5.14) with $n \rightarrow n+1$ a new variable α , $0 \leq \alpha \leq 1$ by writing $M''^2 = \{(\sqrt{s'} - m')^2 - n^2 m'^2\} \alpha + n^2 m'^2 \approx s(\alpha + n^2 x^2)$, $x = m'/\sqrt{s'} \ll 1$. Then $\lambda^4(s', M''^2, m'^2) \approx s(1 + 2x - \alpha)$ and, taking nm' as energy scale,

$$L_{n+1}(s) = \frac{n(n-1)}{2^{n-1}s'} \int_0^1 d\alpha \left(\frac{1}{\alpha + n^2 x^2} + \frac{1}{1+2x-\alpha} \right) \left(\log \frac{\alpha + n^2 x^2}{n^2 x^2} \right)^{n-2}.$$

Both terms produce a $(\log s')^{n-1}$.

- VI.16. Take a Laplace transform.

$$(a) I = (2\pi)^{n-1}/\{(3n-2)a^{2n-2}\},$$

$$(b) I = n^{-1}(\pi/a)^{n-1}.$$

- VI.17. Use

$$\int_0^{\frac{\pi}{2}} dt (\sin t)^a = \frac{1}{2} \sqrt{\pi} \Gamma\{\frac{1}{2}(a+1)\} / \Gamma(\frac{1}{2}a+1).$$

- VI.18. The double Regge regions lie exactly at the values of ω shown in Figure VI.6.3, there is no overlap. Note that the phase space density goes to infinity at these points when $s \rightarrow \infty$.

- VII.1. Use equation (VII.2.12) for $r = 0$.

- VII.2. $\sin \theta_{\max}^T = m_b/m_c$, all directions allowed if $m_b > m_c$, cf. equation (VII.2.10).

- VII.3. Equation (VII.2.12) with v_{CM} replaced by $-v(BS \rightarrow CMS)$ equation (II.6.27).

- VII.4. Use the formula

$$\int_0^\infty dx x^{a-1} (1+x)^{-\frac{1}{2}} \exp\{-b(1+x)^{\frac{1}{2}}\} = 2\pi^{-\frac{1}{2}} (\frac{1}{2}b)^{\frac{1}{2}-a} \Gamma(a) K_{\frac{1}{2}-a} \quad (b)$$

(Gradstein, 1971, equation 3.479) and $K_{\frac{1}{2}}(x) = (\pi/2x)^{\frac{1}{2}} \exp(-x)$.

- VII.5. $w(q) = (E - E_0)[EP - m_c^2 \log\{(P+E)/m\}]^{-1}$
 $\langle r(q) \rangle = [E\rho - E_0^2 \log\{(E+\rho)/E_0\}]/2(E - E_0),$
 $E_0 = (q^2 + m_c^2)^{\frac{1}{2}}, \rho = (P^2 - q^2)^{\frac{1}{2}}, E = E_{\max}^*, P = P_{\max}^*$.

- VII.7. $d\sigma/d\zeta = 2\pi \int_0^{r_{\max}} dr r f\{(m_c^2 + r^2)^{\frac{1}{2}} \sinh \zeta, r\},$

where

$$r_{\max} = \{(P_{\max}^*)^2 + m_c^2\}^{\frac{1}{2}}$$

- VII.9. $-\log(XY/4m_a m_c s) \leq \zeta^B \leq \log(m_a X/m_c Y),$
 $X = s + m_c^2 - s_X^{\min} + \lambda^4(s, m_c^2, s_X^{\min}),$
 $Y = s + m_a^2 - m_b^2 + \lambda^4(s, m_a^2, m_b^2).$

- VII.10. From $\tanh \zeta = P \cos \theta/E$ derive $d \cos \theta/d\zeta = EP^{-1} \cosh^{-2} \zeta$. Thus $w(\cos \theta^*) = 1$ implies $w(\zeta^*) = \text{constant} \cdot \cosh^{-2} \zeta^*$, where the constant contains an integral of the distribution function $f(P)$ over P .

- VII.11. $w(u^*) = w(\cos \theta^*) \sin \theta^* (d\theta^*/du^*) = w(\cos \theta^*) (\cosh u)^{-2}$ since according to equation (VII.4.16) $d\theta^*/du^* = \sin \theta^* = (\cosh u)^{-1}$.
 $w(u^T) = w(\cos \theta^T) \exp 2u^T(1 + \exp 2u^T)^{-\frac{1}{2}}$.

VII.12. Write σ as a sum over exclusive reactions.

VII.14. The equation giving the boundary follows by writing $(p_a + p_b - p_1 - p_2)^2 \geq (\text{minimum value of the missing mass})^2$ in terms of the CMS longitudinal momenta q_1^*, q_2^* or rapidities $\zeta_1^* \zeta_2^*$ for $r_1 = r_2 = 0$:

$$s - 2\sqrt{s(E_1^* + E_2^*)} + m_1^2 + m_2^2 + 2E_1^*E_2^* - 2q_1^*q_2^* \geq (\text{min. missing mass})^2$$

The boundary curve is the same as the $n = 3$ LPS plot boundary curve for a $2 \rightarrow 3$ reaction with masses m_1, m_2 , minimum missing mass, now plotted in Cartesian coordinates q_1^*, q_2^* .

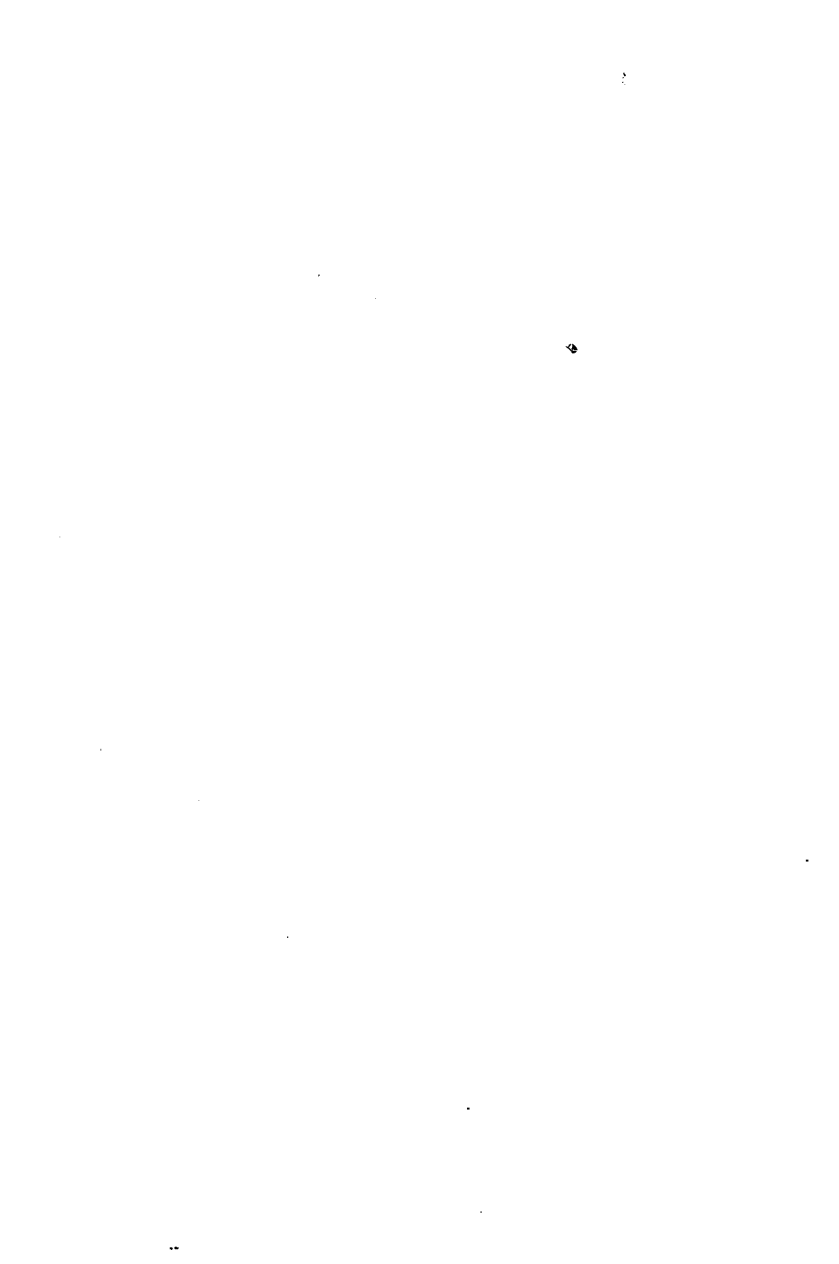
References

- Abramowitz, M., and I. A. Stegun (1965). *Handbook of Mathematical Functions*, Dover Publications, Inc., New York.
- Almgren, B. (1968). *Arkiv för Fysik*, **38**, 161.
- Asribekov, V. E. (1962a). *JETP (USSR)*, **42**, 565. (1962). *Soviet Physics JETP*, **15**, 394.
- Asribekov, V. E. (1962b). *Nucl. Phys.*, **34**, 461.
- Asribekov, V. E. (1962c). *Phys. Letters*, **2**, 284.
- Baldin, A. M., V. I. Goldanskii, and I. L. Rozenthal (1961). *Kinematics of Nuclear Reactions*, Pergamon Press, Oxford.
- Bali, N. F., G. F. Chew, and A. Pignotti (1967a). *Phys. Rev.*, **163**, 1572.
- Bali, N. F., G. F. Chew, and A. Pignotti (1967b). *Phys. Rev. Letters*, **19**, 614.
- Bardadin-Otwinowska, M., L. Michejda, S. Otwinowski, and R. Sosnowski (1966). *Phys. Letters*, **21**, 351.
- Benecke, J., T. T. Chou, C. N. Yang, and E. Yen (1969). *Phys. Rev.*, **188**, 2159.
- Berger, E. L. (1969). *Phys. Rev. Letters*, **23**, 1139.
- Berger, E. L., and A. Krzywicki (1971). *Phys. Letters*, **36B**, 380.
- Bertocchi, L., and K. Zalewski (1967). *Nuovo Cimento*, **49**, 577.
- Bialas, A., and T. Ruijgrok (1965). *Nuovo Cimento*, **39**, 1061.
- Bialkowski, G., and R. Sosnowski (1967). *Phys. Letters*, **25B**, 519.
- Blaton, J. (1950). *Kgl. Danske Vidensk. Selskab. Mat.-Fys. Medd.*, **24**, No. 20.
- Block, M. M. (1956). *Phys. Rev.*, **101**, 796.
- Bubelev, E. G., and N. A. Tšernikov (1964a). *Acta Physica Polonica*, **26**, 155.
- Bubelev, E. G. (1964b). *Acta Physica Polonica*, **26**, 279.
- Byckling, E., and K. Kajantie (1969a). *Nucl. Phys.*, **B9**, 568.
- Byckling, E., and K. Kajantie (1969b). *Nucl. Phys.*, **B14**, 355.
- Byckling, E., M. Kaartinen, K. Kajantie and H. Villanen (1969c). *J. Comp. Phys.*, **4**, 521.
- Byckling, E., and K. Kajantie (1969d). *Phys. Rev.*, **187**, 2008.
- Byckling, E., and P. Pirilä (1972a). *Z. Physik*, **250**, 379.
- Byckling, E., and M. Whippman (1972b). *TFT Preprint*, 8-72.
- Byers, N., and C. N. Yang (1964). *Rev. Mod. Phys.*, **36**, 595.
- Campbell, G. H., J. V. Lepore and R. J. Riddell, Jr. (1967). *J. Math. Phys.*, **8**, 687.
- Cerulus, F., and R. Hagedorn (1958). *Nuovo Cimento Suppl.*, **9**, 646.
- Chan Hong-Mo, K. Kajantie, and G. Ranft (1967a). *Nuovo Cimento*, **49**, 157.
- Chan Hong-Mo, K. Kajantie, G. Ranft, W. Beusch, and E. Flaminio (1967b). *Nuovo Cimento*, **51A**, 696.
- Chew, G. F., and F. E. Low (1959). *Phys. Rev.*, **113**, 1640.
- Chew, G. F., and A. Pignotti (1968). *Phys. Rev.*, **176**, 2112.
- Chew, G. F., and C. de Tar (1969). *Phys. Rev.*, **180**, 1577.
- Czyzewski, O. (1968), in *Methods of Subnuclear Physics*, (ed. M. Nicolic) pp. 129-157, Gordon and Breach, New York.

- Dalitz, R. H. (1953). *Phil. Mag.*, **44**, 1068.
Deck, R. T. (1964). *Phys. Rev. Letters*, **13**, 169.
Dedrick, K. G. (1962). *Rev. Mod. Phys.*, **34**, 429.
Drell, S. D., and J. D. Walecka (1964). *Ann. Phys. (N.Y.)*, **28**, 18.
Eden, R. J., P. V. Landshoff, P. J. Olive, and J. C. Polkinghorne (1966). *The Analytic S-matrix*, pp. 197–204, Cambridge University Press, Cambridge.
Erdelyi, A., W. Magnus, F. Oberhettinger, and F. Tricomi (1953). *Tables of Integral Transforms*, McGraw-Hill Inc., New York.
Fabri, E. (1954). *Nuovo Cimento*, **11**, 479.
Feynman, R. P. (1969). *Phys. Rev. Letters*, **23**, 1415.
Fialho, G. E. A. (1957). *Phys. Rev.*, **105**, 328.
Finkelstein, J., and K. Kajantie (1968). *Nuovo Cimento*, **56A**, 659.
Frenkel, A. (1964). *JETP (USSR)*, **47**, 221; (1965). *Soviet Physics, JETP*, **20**, 149.
Friedman, J. H. (1971a). *J. Comp. Phys.*, **7**, 201.
Friedman, J. H., G. R. Lynch, C. G. Risk and T. A. Zang, Jr. (1971b). *J. Comp. Phys.*, **8**, 144.
Gantmacher, F. R. (1953). *Theory of Matrices*, Moscow.
Goldhaber, G., W. Chinowsky, S. Goldhaber, W. Lee, and T. O'Halloran (1963). *Phys. Letters*, **6**, 62.
Gradstein, I. S., and I. M. Ryshik (1971). *Tables of Integrals, Sums, Series and Products*, Moscow.
de Groot, E. H. (1972). *Nucl. Phys.*, **B48**, 295.
Hagedorn, R. (1964). *Relativistic Kinematics*, W. A. Benjamin, Inc., New York.
Halpern, F. R. (1968). *Special Relativity and Quantum Mechanics*, Prentice-Hall, Inc., Englewood Cliffs.
Halton, J. H. (1970). *SIAM Review*, **12**, 1.
Hammer, P. C. (1959) in *On Numerical Approximation* (ed. R. E. Langer), Madison.
Hammersley, J. M., and D. C. Handscomb (1967). *Monte Carlo Methods*, Methuen & Co., London.
Huang, K. (1963). *Statistical Mechanics*, John Wiley & Sons, Inc., New York.
Huang, K. (1967). *Phys. Rev.*, **156**, 1555.
Jackson, J. D. (1964). *Nuovo Cimento*, **34**, 1644.
Jacobson, D. A. (1966). *Nuovo Cimento*, **45A**, 905.
James, F. (1968). *CERN Yellow Report*, 68-15.
James, F. (1970). *CERN Computer Program Library*, W505 (long write-up).
Kajantie, K. (1968a). *Nuovo Cimento*, **53A**, 424.
Kajantie, K., and P. Lindblom (1968b). *Phys. Rev.*, **175**, 2203.
Kajantie, K., and V. Karimäki (1971). *Comp. Phys. Commun.*, **2**, 207.
Kajantie, K., and V. Karimäki (1972a). *Ann. Acad. Sc. Fennicae, VI, Physica*, **395**.
Kajantie, K., and J. Tuominen (1972b). *Physica Scripta*, **5**, 155.
Källén, G. (1964). *Elementary Particle Physics*, Addison-Wesley Publ. Co., Reading.
van Keuk, G. (1968). 'Zur Anwendung des Statistischen Modells mit Drehimpulserhaltung', *DESY Preprint* 68/10, Hamburg.
Khinchin, A. I. (1949). *Mathematical Foundations of Statistical Mechanics*, Dover Publications, New York.
Kibble, T. W. B. (1960). *Phys. Rev.*, **117**, 1159.
Kittel, W., L. Van Hove, and W. Wojcik (1970). *Comp. Phys. Commun.*, **6**, 425.
Koch, W. (1968) in *Analysis of Scattering and Decay*, (ed. M. Nikolić), Gordon and Breach, New York.
Kolkunov, V. A. (1962). *JETP (USSR)*, **43**, 1448; (1963). *Soviet Physics JETP*, **16**, 1025.

- Kolkunov, V. A., N. N. Meiman, E. S. Nikolaevski, and V. N. Petruhin (1967a). 'Phase Space Integrals' (in Russian), *ITEP Preprint*, 555, Moscow.
- Kolkunov, V. A., N. N. Meiman, E. S. Nikolaevski and V. N. Petruhin (1967b). 'On the Saddle Point Method' (in Russian), *ITEP Preprint*, 561, Moscow.
- Kolkunov, V. A., N. N. Meiman, and E. S. Nikolaevski (1969). *Yadernaya Fizika*, 9, 552; (1969). *Soviet J. of Nuclear Physics*, 9, 316.
- Komolova, V. E., and G. I. Kopylov (1965). *JINR Preprint P-2027*, Dubna.
- Komolova, V. E., and G. I. Kopylov (1967). *JINR Preprint P11-3193*, Dubna.
- Kopylov, G. I. (1958). *JETP (USSR)*, 35, 1426; (1959). *Soviet Physics JETP*, 8, 966.
- Kopylov, G. I. (1960). *JETP (USSR)*, 39, 1091; (1961). *Soviet Physics JETP*, 12, 761.
- Kopylov, G. I. (1962). *Nucl. Phys.*, 36, 425.
- Kopylov, G. I., and V. Komolova (1963). *Nucl. Phys.*, 47, 33.
- Kopylov, G. I. (1970). *Foundations of Kinematics of Resonances* (in Russian), Publishing House 'Nauka', Moscow.
- Kopylov, G. I., V. N. Penev, Yu. V. Tevzadze, and A. I. Shklovskaya (1971). *Nucl. Phys.*, B30, 398.
- Kotanski, A. (1968). *Nuovo Cimento*, 56A, 737.
- Krzywicki, A. (1964). *Nuovo Cimento*, 32, 1067.
- Krzywicki, A. (1965). *J. Math. Phys.*, 6, 485.
- Kumar, R. (1969). *Phys. Rev.*, 185, 1865.
- Kumar, R. (1970). *Phys. Rev.*, D2, 1902.
- Landau, L. (1953). *Izv. Akad. Nauk. SSSR*, 17, 51.
- Lepore, J. V., and R. Stuart (1954). *Phys. Rev.*, 94, 1724.
- Lipes, R. G. (1970). *Nucl. Phys.*, B24, 16.
- Lurçat, F., and P. Mazur (1964). *Nuovo Cimento*, 31, 140.
- Lynch, G. R. (1967). *Alvarez Programming Group Note*, P-162, Berkeley.
- Lyons, L. (1968). *Nucl. Phys.*, B7, 83.
- Lyons, L. (1970). *Nucl. Phys.*, B15, 355.
- Maglić, B., and G. Gosta (1965). *Phys. Letters*, 18, 185.
- McLeod, D. (1969). *Nucl. Instr. Methods*, 72, 333.
- McNeil, R. P., and R. A. Morrow (1969). *J. Math. Phys.*, 10, 2185.
- Michael, C. (1966). *Nuovo Cimento*, 42A, 562.
- Milburn, R. H. (1955). *Rev. Mod. Phys.*, 27, 1.
- Morrow, R. A. (1966). *J. Math. Phys.*, 7, 744.
- Morrow, R. A. (1968). *Phys. Rev.*, 176, 2147.
- Morrow, R. A. (1969). *Nuovo Cimento*, 61A, 215.
- Morrow, R. A. (1970a). *Ann. Phys.*, 57, 333.
- Morrow, R. A. (1970b). *Phys. Rev.*, D1, 2884.
- Morse, P. M., and H. Feshbach (1953). *Methods of Theoretical Physics*, McGraw-Hill Inc., New York.
- Nyborg, P., H. S. Song, W. Kernan, and R. H. Good, Jr. (1965a). *Phys. Rev.*, 140, B914.
- Nyborg, P. (1965b). *Phys. Rev.*, 140, B921.
- Nyborg, P. (1966a). *Physica Norvegica*, 2, 25.
- Nyborg, P. (1966b). *Am. J. Phys.*, 34, 932.
- Nyborg, P., and O. Skjeggestad (1967) in *Kinematics and Multiparticle Systems*, (ed. M. Nikolić), Gordon and Breach, New York.
- Nyborg, P. (1968). *Nuovo Cimento*, 58B, 247.
- Nyborg, P., and A. G. Frodesen (1970a). *Physica Norvegica*, 6, 67.
- Nyborg, P. (1970b). *Nuovo Cimento*, 65A, 544.
- Nyborg, P. (1970c). *Herceg-Novi lectures*.

- Pavlov, V. P. (1963). *JETP (USSR)*, **45**, 1606; (1964). *Soviet Physics JETP*, **18**, 1105.
- Pene, O., and A. Krzywicki (1969). *Nucl. Phys.*, **B12**, 415.
- Pirilä, P., and E. Byckling (1972). *Comp. Phys. Comm.*, **4**, 117.
- Pilkuhn, H. (1967). *The Interaction of Hadrons*, North-Holland Publ. Co., Amsterdam.
- Poon, C. H. (1970). *Nucl. Phys.*, **B20**, 509.
- Proriol, J. (1969). *Nucl. Phys.*, **A126**, 689.
- Regge, T., and G. Barucchi (1964). *Nuovo Cimento*, **34**, 106.
- Rindler, W. (1960). *Special Relativity*, Oliver and Boyd, Edinburgh.
- Rohrlich, F. (1965a). *Nucl. Phys.*, **67**, 659.
- Rohrlich, F. (1965b). *Nuovo Cimento*, **38**, 673.
- Sakmar, I. A., and J. H. Wojtaszek (1967). *Phys. Rev.*, **163**, 1748.
- Satz, H. (1963). *Fortschr. Physik*, **11**, 445.
- Satz, H. (1965). *Nuovo Cimento*, **37**, 1407.
- Satz, H., and G. van Keuk (1967). *Nuovo Cimento*, **50A**, 272.
- Skjeggestad, O. (1964). *CERN Yellow Report*, 64-13, Geneva.
- Srivastava, P. A., and G. Sudarshan (1958). *Phys. Rev.*, **110**, 765.
- Tan, Chung-I (1971). *Phys. Rev.*, **D3**, 790.
- Tarski, J. (1960). *J. Math. Phys.*, **1**, 149.
- Toller, M. (1965). *Nuovo Cimento*, **37**, 631.
- Treiman, S. B., and C. N. Yang (1962). *Phys. Rev. Letters*, **8**, 140.
- Van Hove, L. (1969). *Nucl. Phys.*, **B9**, 331.
- Werbrouck, A. (1968) in *Methods of Subnuclear Physics*, (ed. M. Nicolić), Gordon and Breach, New York.
- Werle, J. (1966). *Relativistic Theory of Reactions*, North-Holland Publ. Co., Amsterdam.
- Wick, G. C. (1962). *Ann. Phys.*, **18**, 65.
- Yen, E., and E. L. Berger (1970). *Phys. Rev. Letters*, **24**, 695.
- Zemach, C. (1965). *Phys. Rev.*, **140**, B97, B109.



List of Symbols

The quantities listed below are defined or explained on the pages indicated.

a	general four-vector, $a = (a^\mu) = (a^0, a^1, a^2, a^3) = (a^0, a_x, a_y, a_z)$	5
\mathbf{a}	space part of a , $\mathbf{a} = (a^1, a^2, a^3)$	5
A	matrix element	50
A	magnitude of \mathbf{a}	8
A	magnitude of the vector with components (a^0, a^1, a^2)	11
B	kinematic function related to Δ_4	137
B, BS	beam (system)	20
c	light velocity	
CB, CBS	colliding beam (system)	20
CM, CMS	centre-of-momentum (system)	19
dg	differential volume element for the group $O(1, 2)$	12
$d\Omega$	element of solid angle	12
D	quantity defined in equation (II.8.21)	40
E	energy	
ER	extremely relativistic limit	111
$f(\mathbf{p}, s)$	invariant distribution function	218
F	flux factor	50
g	metric tensor	5
g^*	$g^* = v/v^*$	40
G	kinematic function related to Δ_3	88-92
$G(p_1, \dots)$	unsymmetric Gram determinant	288
I, I_n	integral over phase space (for n particles)	50
$I_v(x)$	modified Bessel function	283, 303
k_i	$k_i = p_1 + \dots + p_i$	161
K	$K(x, y, z) = 1 - x^2 - y^2 - z^2 + 2xyz$	152, 293
K	$K = \frac{1}{2} \left(m_0^2 - \sum_i m_i^2 \right)$	203
$K_v(x)$	modified Bessel function	282
L	Lorentz transformation	5, 11
L, LS	laboratory (system)	19
L_n	longitudinal phase space integral	189
m, m_i	mass	
m'_i	longitudinal mass	188
m_X	missing mass	219, 243
M_i	invariant mass, $M_i^2 = (p_1 + \dots + p_i)^2$	180
n	multiplicity	
NR	nonrelativistic limit	111
p	four-momentum	14
\mathbf{p}	space part of p , $\mathbf{p} = (p^1, p^2, p^3)$	14

P	magnitude of \mathbf{p}
P	$P^2 = E^2 - p_x^2 - p_y^2 = p_z^2 + m^2$ 34
P^\pm	two values of P at fixed θ 40
q	longitudinal component of \mathbf{p} 36, 188
q, q_i	momentum transfer four-vector, $q_i = p_a - p_1 - \dots - p_i$ 166, 232
r, r'	transverse component of \mathbf{p} 36, 188
$r_k, r^{(i)}, \tilde{r}^{(i)}, \tilde{\tilde{r}}^{(i)}$	random number uniformly distributed within $(0, 1)$ 266
$R(p)$	rest frame of timelike p 8
$R(p_1, p_2, p_3)$	frame defined by p_1, p_2, p_3 for $p_1^2 > 0$ 27
R_{12}	superscript for frame $\mathbf{p}_1 + \mathbf{p}_2 = 0$ 105
$R_n(s)$	phase space integral 54
R_2	two-particle phase space integral 63
R_3	three-particle phase space integral 107, 111, 137
s	total energy squared 21, 76
s_i	two-particle invariant mass squared, $s_i = (p_i + p_{i+1})^2$ 102, 170
s_{ij}	two-particle invariant mass squared, $s_{ij} = (p_i + p_j)^2$ 16
s_X	invariant mass squared of unobserved system X 218
S	Lorentz frame 4
$S(p)$	the standard frame $p = (0, 0, 0, \sqrt{(-p^2)})$ for spacelike p 8
$S(p_1, p_2, p_3)$	frame defined by p_1, p_2, p_3 for $p_1^2 < 0$ 33
S_n	surface area of sphere $x_1^2 + \dots + x_n^2 = 1$ 195
t, t_i	invariant momentum transfer squared 73, 76, 165, 218
t^\pm	values of t in forward and backward directions 92, 97
T	matrix element squared 50
T	kinetic energy 17, 24
T, TS	target (system) 20
u	four-velocity 13
u	invariant variable, $u = (p_a - p_b)^2$ 76
v	velocity three-vector 4
v	magnitude of \mathbf{v} 5
v, v^{CM}	velocity of the CMS in the TS 21, 26, 40
v^B	velocity of the BS in the TS 26
$v^{\text{B, CM}}$	velocity of the BS in the CMS 26
v^{CB}	velocity of the CMS in the CBS 22
v^*	velocity of particle in the CMS 38
w_k	weight in Monte Carlo integration 267, 271
$w(x)$	distribution in variable x 51
x	scaled longitudinal momentum 238
x_{ij}	scalar product, $x_{ij} = p_i \cdot p_j$ 203
X	matrix (x_{ij}) of scalar products 204
γ	Lorentz factor 5
$\delta(x)$	Dirac delta function
Δ_1	symmetric Gram determinant 288
$\bar{\Delta}_t$	signed sum of Δ_t 206
Δ_2	2×2 Gram determinant 29
Δ_3	3×3 Gram determinant 30, 88
Δ_4	4×4 Gram determinant 32, 137
ϵ	totally antisymmetric tensor $\epsilon_{\kappa\lambda\mu\nu}$ 292
ζ, η	rapidities 9, 11, 34, 170
ζ	longitudinal rapidity 220
ζ_{ij}	Toller rapidity variable 146

θ	polar angle
θ_{12}	angle between \mathbf{p}_1 and \mathbf{p}_2 68
θ_{b3}^{R23}	Jackson angle in the rest frame of particles 2 and 3 125
$\Theta(x)$	step function 53
λ_1, λ_3	helicity angle in the rest frame of particles 2 and 3 (particles 1 and 2) 126, 145
$\lambda(x, y, z)$	kinematic function related to Δ_2 23, 29
μ	particle mass 74
μ_i	lower limit of M_i , $\mu_i = m_1 + \dots + m_i$ 162
v	energy loss variable 220
ξ	rapidity 7
ρ	radius vector in LPS plot 194
$\rho_n(\Phi)$	phase space density in variables Φ 53
σ	cross-section 50
τ	lifetime 51
ϕ	azimuthal angle 31, 35
ϕ_b, ϕ_s	Treiman-Yang angle in the rest frame of particles 2 and 3 (particles 1 and 2) 126, 145
Φ	point in phase space 53
χ	relative rapidity of two frames 233
ω, ω_i	Toller angle 146, 171
ω	angle in LPS plot for $n = 3$ 196
Ω	solid angle
*	superscript for CMS quantities 19



Index

- Abramowitz M., 283
Active interpretation of a transformation, 9, 10
Almgren B., 111, 163, 261
Angle,
 between Jackson and helicity frames, 125
 see azimuthal, polar, solid angle
Asribekov V. E., 202, 208, 209
Azimuthal angles, 28, 31, 296
 ambiguities in the
 definition of, 35, 36
 cyclically symmetric
 representation of, 144–146
 in terms of invariants, 32, 134, 136, 145
 Lorentz transformation of, 37
- B* function, 137–143
Backward scattering, 72
Baldin A. M., 2, 37
Bali N. F., 153, 160, 178, 179
Bardadin M., 227
Basic five-particle kinematic function, 137–143
Basic four-particle kinematic function, 88–96
Basic three-particle kinematic function, 29
Beam fragmentation region, 239
Beam system, 20
Benecke J., 238
Berger E. L., 259
Bertocchi L., 248
Bialas A., 282
Bialkowski G., 186
Blaton J., 38
Block M. M., 55, 163
Boost, 6, 10
Box diagram, 151–153
Breit frame, 128
Breit–Wigner function, 124, 272, 276
- Byckling E., 146, 160, 165, 166, 202, 214, 262, 278
Byers N., 202, 205, 206, 214
- Campbell G. H., 262
Cayley determinant, 89, 138, 290
Central limit theorem, 262, 267
Central region,
 in $2 \rightarrow 2$ reactions, 95
 in inclusive reactions, 239
Centre-of-momentum system, 19, 24
Cerulus F., 55, 261
Chan Hong-Mo, 146, 149, 153, 155, 255
Channel, 77
Chew G. F. 120, 124, 167, 178
Chew–Low plot, 120–123, 185, 227–231
Colliding beam system, 20, 25
Cornering effect, 254
Correlation, 247
 correlation function, 245
 kinematic correlation, 188, 247
Crossing, 49, 76, 78
Cross-section, 18
 differential, 51
 inclusive, 218, 219
 total reaction, 50, 82
Cyclic symmetry in $2 \rightarrow 3$ azimuthal angles, 144–146
Cuboctahedron plot, 202
Curves of constant,
 s_x, t in q^*r plane, 224
 t in q^*r plane, 224
 θ^* in q^*r plane, 225
 P^T, θ^T in q^*r plane, 225
 P^* in q^*r plane, 225
 ζ in qr plane, 225
 P^* in ts_x plane, 228
 P^T, θ^T in ts_x plane, 228
 r, q^*, q^T in ts_x plane, 229, 230
 θ^T, s_x in q^*v plane, 233
 P^* in ζ^*r plane, 236

- Cut in transverse momentum, 188–190, 252–257
 Czyzewski O., 2
 Dalitz R. H., 106
 Dalitz plot, 95, 96, 106–111
 Decay,
 angle, 68, 125–128
 channel, 78
 momentum, 64
 plane, 126
 Deck R. T., 255
 Deck effect, 255
 Dedrick K. G., 37
 Density,
 in phase space, 53
 of events, 265, 274
 Density matrix element, 124
 Distribution, 50–52, 218
 in average transverse momentum, 226
 in decay angle, 64
 in decay angles for doubly peripheral processes, 257
 in helicity polar angle, 114
 in longitudinal momentum, 226
 in opening angle, 68–70
 in the Dalitz plot with doubly peripheral matrix element, 149, 150, 254
see also phase space distribution
 Doppler formula, relativistic, 42
 Double Regge limit, 153
 Doubly peripheral, 149, 153, 199, 200
 Drell S. D., 232
 Eden R. J., 290
 Efficiency of Monte Carlo integration, 265, 269
 Elastic scattering,
 kinematics of, 74, 75, 83–85
 Energy,
 as a function of scattering angle, 40–42, 74, 75
 in multi-Regge limit, 178
 in terms of invariants, 23–25, 78, 105, 129
 in Toller variables, 147, 176
 kinetic, 17
 loss, 220, 231–233
 total, 17
 Erdelyi A., 283
 Essential variables, 48, 49
 Event,
 in Monte Carlo, 267, 273
 generation of, 273–281
 Exclusive process, 48
 Fabri E., 106
 Fake effect, 251
 Feynman R. P., 238
 Fialho G. E. A., 262, 282
 Finkelstein J., 178, 218
 Flux factor, 50
 Forward scattering, 72
 Four-acceleration, 44
 Four-momentum, 14–16
 conservation of, 47
 in terms of invariants, 208–209
 Four-vectors, 5–13
 standard forms of, 8
 Four-velocity, 13–14
 FOWL, 262, 270, 279
 Fragmentation, 238–243
 Frenkel A., 202, 208
 Friedman J. H., 262, 277
 $F(t)$ -method, 186
 G function, 88–96
 Goldhaber G., 183
 Goldhaber plot, 183
 Gottfried-Jackson frame, 105
 Gradstein, 304
 Gram determinant, 29–35, 288–295
 conditions, 205, 209
 Groot E. H. de, 191, 282, 287
 Hagedorn R., 2, 5, 56
 Halpern F. R., 1, 2, 67
 Halton J. H., 261, 270
 Hammer P. C., 263
 Hammersley J. M., 261, 270
 Helicity angle, 126–128
 in terms of invariants, 135
 Helicity frame, 125
 Helicity polar angle, 105, 126
 in terms of invariants, 105
 Hexagon plot, 197
 Hyperrotation, 10
 Huang K., 55, 189, 284, 287
 Importance sampling, 271–273
 Inclusive process, 78, 218–249
 Inelasticity, 219
 Invariant, 5, 15, 16

- Invariant distribution function, 218, 246
 Invariant mass, 21
 two particle, 15, 102, 166
 Invariant momentum transfer, 16, 72, 166,
 219, 227
 in forward direction, 96, 97
 Invariant variables.
 for $1 \rightarrow 3$ decay, 102, 103
 for $2 \rightarrow 2$ scattering, 76
 for $1 \rightarrow 4$ decay, 211
 for $2 \rightarrow 3$ scattering, 116–118
 for n particles, 158–188, 203–211
 ISR, 22
 Jackson J. D., 125
 Jackson angle, 125
 in terms of invariations, 129
 Jackson frame, 105, 125
 Jacobian peak method, 245
 Jacobson D. A., 202
 James F., 262, 270, 278
 Kajantie K., 132, 155, 193, 262
 Källen G., 50, 69, 112, 151
 Keuk G. van, 262
 Khinchin A. I., 262
 Kibble T. W. B., 92, 152
 Kinematical reflections, 251–259
 due to peripherality, 252–257
 due to resonances, 257–259
 Kittel W., 262, 278
 Koch W., 2, 124
 Kolkunov V. A., 262, 282, 283
 Komolova V. E., 262
 Kopylov G. I., 2, 111, 163, 181, 261, 262
 Kotanski A., 94
 Krzywicki A., 262, 282
 Kumar R., 202
 Laboratory system, 19
 λ -function, 23, 29, 96
 Landau L., 56
 Laplace transform, 281
 Law,
 of cosines for angles, 297
 of cosines for sides, 32, 297
 of sines, 296
 Lepore J. V., 55, 262
 Levi-Civita symbol,
 four-dimensional, 292
 three-dimensional, 291
 Lifetime, 50
 Light-cone variable, 67
 Lightlike,
 four-vector, 8
 two-particle phase space integral, 66,
 67
 Limiting fragmentation, 239
 Little group, 67
 Longitudinal phase space, 190, 193–202
 integral, 189, 191, 192, 194, 195, 217
 Longitudinal rapidity, 220, 233–238
 Lorentz factor, 5
 Lorentz invariant volume element, 12, 13,
 52, 53
 Lorentz transformations, 4–13
 between centre-of-momentum, target
 and colliding beam systems, 20–23,
 26, 27, 237
 in arbitrary direction, 15, 44, 299
 longitudinal, 188, 220, 241
 of azimuthal angle, 38
 of four-momenta, 15, 36–43
 of one-particle distributions, 57–61
 of polar angle, 42, 43
 of rapidity, 7, 233, 234
 proper orthochronous, 6
 LPS plots, 192–202
 for $n = 3$, 196–200
 for $n = 4$, 200–202
 Lurçat F., 262, 282, 287
 Lynch G. R., 262
 Lyons L., 136, 224
 Maglić B., 243
 McLeod D., 243
 McNeil R. P., 167, 202
 Mean value, 266
 Metric tensor, 6
 Michael C., 202
 Milburn R. H., 163, 261
 Missing mass, 219, 227–231, 243
 Missing mass techniques, 243–246
 Momentum, 17
 as a function of scattering angle, 40, 42,
 74, 75
 in terms of invariants, 23–25, 29, 78–79,
 105
 longitudinal component of, 36, 188,
 219
 transverse component of, 37, 188, 219
 Momentum ellipsoid, 38–42
 Momentum space, 47

- Momentum sum rule, 219, 250
 Monte Carlo method, 261, 262, 264–281
 Morrow R. A., 146, 148, 202
 Morse P. M., 285
 Multiperipheral momentum transfer, 166
 Multiperipherality, 177, 190
 Multi-Regge limit, 177
- Napier's rule, 298
 Normal distribution, 267
 Numerical integration, 261–264
 Numerical methods, 260–287
 Nyborg P., 2, 88, 131, 139, 167, 187
- One-pion exchange model, 124, 156
 Opening angle, 68
 Optical point, 82
 Optical theorem, 82
- Partition function, 55, 284
 Pene O., 262, 278
 Peyrou plot, 222, 249
 Phase space, 47–61
 distribution, 57, 110, 180–188
 longitudinal, 190, 192–202
 transverse cut, 188–192
 Phase space density, 53, 54, 158, 163, 211–215
 Phase space distribution,
 definition of, 54
 for inclusive reactions, 221
 in Chew–Low plot, 123, 156, 186
 in Dalitz plot, 110
 in Goldhaber plot, 183
 in Jackson, Treiman–Yang, helicity
 polar, helicity angles, 127
 in momenta of two particles, 187
 in momentum of one particle, 187
 in one invariant mass, 111, 180, 181
 in one invariant momentum transfer,
 123, 186
 in Toller angle, 148, 257
 in $t_1 t_2$ plot, 133
 in two invariant masses, 182–185
 Phase space integral, 50, 54–56
 extremely relativistic limit of n -particle,
 163, 283
 four-particle, 184, 185, 213, 216, 217
 longitudinal, 189, 191, 195, 217
 multi-Regge limit of n -particle, 179
 non-covariant, 55
- Phase space integral—continued
 non-relativistic limit of n -particle, 163,
 216, 283
 n -particle, in invariant masses and
 angles, 162
 n -particle, in invariant masses and mo-
 mentum transfers, 166
 n -particle, in invariant variables, 213–
 215
 n -particle, in Toller variables, 169, 174,
 175
 numerical evaluation of, 260–287
 splitting relation for, 164, 182
 three-particle, 108, 111, 123, 130, 137
 three-particle, in double Regge limit,
 153–155_a
 three-particle in Toller variables, 148,
 177
 two-particle, 63–67
- Physical region, 53, 115
 of $1 \rightarrow 2$ decay, 67
 of $1 \rightarrow 3$ decay, 106–111
 of $2 \rightarrow 2$ scattering, 82–96
 of $1 \rightarrow 4$ decay, 185, 211
 of $2 \rightarrow 3$ scattering in $t_1 s_2$, 120–123
 of $2 \rightarrow 3$ scattering in $t_1 t_2$, s_1 , 132,
 133
 of $2 \rightarrow 3$ scattering in $t_1 s_1 s_2$, $t_1 s_2 t_2$,
 131, 132
 of $2 \rightarrow 3$ scattering in $t_1 s_2 t_2 s_1$, 137
 in invariants, 203–211
 in (P, θ) or (q, r) , 221–224
 in (t, s_x) , 228
 in (ζ, r) , 236
- Pilkuhn H., 97
 Pirilä P., 262, 264
 Plot, 115
 Polar angle, 28, 30, 296–298
 in invariant form, 30, 31, 144
 Lorentz transformation of, 42, 43
 Poon C. H., 202
 Production plane, 125
 Proriol J., 261
 Pseudo-random number, 269
 Pseudo-spherical coordinates, 8–13, 34
 Pesudothreshold, 24, 67, 93
- Quasi random number, 269
- Random numbers, 266, 269, 270
 normally distributed, 273

- Rapidity, 15, 27
 between TS, CMS, and BS, 234
 longitudinal, 220, 233–238
- Recursion relations
 for longitudinal phase space, 191
 for n -particle phase space, spacelike, 167–175
 for n -particle phase space, timelike, 159–167, 263, 264
- Regge T., 279
- Rest frame, 8
- Rindler W., 1, 4
- Rohrlich F., 202, 208
- Saddle point, 285
- Sakmar I. A., 94
- Satz H., 262, 282
- Scalar product, 5, 203
- Scaling, 238–243
 of longitudinal momenta, 238, 239
 of rapidities, 239
- Scattering,
 angle, 71, 78–80
 inelastic electron, 231
 $2 \rightarrow 2$, 71–97
 $2 \rightarrow 3$, 115–155, 176, 177
- Seagull effect, 226, 227
- Skjeggestad O., 2
- Solid angle, 298
 in terms of invariants, 33
- Spacelike,
 four-vector, 8
 recursion relations, 167–175
 two-particle phase integral, 65–66
- Special relativity, 4–43
- Spherical coordinates, 8, 28, 296–298
- Spherical Trigonometry, 296–298
- Splitting relation, 164, 182
- Srivastava P. A., 160
- Standard,
 form, 8
 frame, 8
- Statistical methods, 55, 56, 262, 281–287
- Step function, 53
- Tan Chung-I, 250
- Target fragmentation region, 239
- Target system, 20, 23, 24
- Tarski J., 202
- Tetrahedron function, 90
- Threshold, 24, 67, 93
- Timelike,
 four-vector, 8
 recursion relations, 150–167
 two-particle phase space integral, 63–65
 t_{\min} , 87
- Toller M., 160
- Toller angle, 146–148, 155, 171
- Toller variable, 146, 160, 167–179
- Transition region, 241
- Transverse cut, 188, 189, 252–257
- Tree diagram, 160
- Triangle function, 23
- Triangular coordinates, 93, 109, 196
- Trieman S. B., 128
- Trieman–Yang angle, 125–128
 in terms of invariants, 134, 135
- Two-particle unitarity relation, 151–153
- Units, 17, 18
- Value of t in the forward direction, 86, 96, 97
- Van Hove L., 193
- Variables,
 number of, 48, 49, 203
- Variance, 266
- Variance-reducing techniques, 269
- Velocity,
 of beam system in centre-of-momentum system, 26
 of beam system in target system, 26
 of centre-of-momentum system in colliding beam system, 22
 of centre-of-momentum system in target system, 21, 26
- Werbrouck A., 2
- Werle J., 2, 8
- Wick G. C., 2
- Yen E., 259
- Zemach C., 2
- Zero-degree method, 245